NOTTINGHAM TRENT UNIVERSITY

Structural Models for the Study of Nucleophile/Electrophile Interactions and Bond Formation

Jonathan Callum Bristow

A thesis submitted in
partial fulfilment of the requirements of
Nottingham Trent University
for the degree of Doctor of Philosophy

January 2020

Declaration

I confirm that this is my own work and the use of all materials from other sources has been properly and fully acknowledged. No part of this thesis has already been, or is being currently submitted for any such degree, diploma or other qualification.

Signed:…… Date:……

Jonathan Callum Bristow

Abstract

This thesis is divided into seven chapters. Chapter 1 gives an introduction to intermolecular interactions, the discovery and development of n-π^* interactions and explores the use of various aromatic backbones (in particular naphthalene) as the scaffold for generating nucleophile/electrophile interactions.

Chapters 2-7 form the results and discussion of the thesis. Chapter 2 reports the first *peri*-interactions between naphtholate oxyanions and electrophilic double bonds in the form of tetramethylguanidine crystalline salts with O---C contacts in the range: 2.558(2)–2.618(2) Å.

Chapters 3-7 are concerned with nitrogen---carbon interactions. Chapter 3 explores the widening of an interaction distance between a dimethylamino nucleophile and a range electrophilic groups, via the use of acenaphthene and fluorene scaffolds. The increase in the contact distance between the two groups allows for cyclisation through an N-methyl group via a *tert*-amino effect reaction in a number of cases. This generates a range of azepine and azocine fused ring systems.

Chapter 4 explores the reduction of an interaction distance between a dimethylamino nucleophile and a range of electrophilic alkenes, via *peri*-repulsion between groups at the opposite *peri*-positions. This repulsion in all cases led to a reduction in the N---C distance, resulting in a short contact of 2.359(2) Å in the ethenedinitrile derivative and the formation of a long N-C bond of 1.672(1) Å when one nitrile was replaced by an ester group.

Chapter 5 introduces a symmetrical system with a set of N---C(alkene) *peri*-interactions at both positions. Generally, the N---C distances increased throughout the series compared to the corresponding systems with just one set of interactions and no second set of *peri* groups. When the alkene terminated in a cyclic diester (from Meldrum's acid) a long N-C bond (1.676(4) Å) formed at one *peri* site and a N---C contact of 2.615(4) Å remained at the other. Further systems demonstrating a *peri* Me_2N^+H---H repulsion were also generated, leading to compounds with N-C bonds in the range of 1.7-2.1 Å. Of particular importance is the ethenedintrile derivative, which undergoes a reversible structural change in the solid-state under cooling, which was carefully mapped by X-ray diffraction. Preliminary variable temperature SSNMR and charge density studies on this system are also reported.

Chapter 6 reports the four structures which demonstrate the Felkin-Anh model for nucleophilic attack of a carbon centre adjacent to a chiral centre. Combining the approaches demonstrated in Chapters 2-4.

Chapter 7 reports structures where a dimethylamino group reacted with a range of stabilised carbocation centres across the *peri*-positions on naphthalene to form long N-C bonds (1.653(2)-1.673(2) Å), and in some cases some interesting fused multi-ringed systems were produced.

Acknowledgements

I would like to thank the following people who have helped me throughout my time at NTU.

Firstly, I would like to thank my supervisor and lifelong friend Prof. John Wallis. Your tireless commitment to both myself and the project has been invaluable. Your love of chemistry is inspiring and infectious. You have taught me a great deal more than chemistry and I will miss our daily catch ups. Enjoy retirement(ish) you deserve it.

A massive thanks to Dr. Warren Cross and Dr. Ray Leslie for initially taking a chance on me, giving me my first taste of academic research chemistry with a summer project and for then sticking by me throughout the PhD. Your discussions, ideas and encouragement have been key, although I'm glad I won't have to hear about carbohydrates for a long while.

Next, I would like to thank Prof. Carole Perry for her consistent support and fresh perspective throughout my PhD which have helped to keep me on track and moving in the right direction.

A special thanks to Dr. Chris Garner for too many things to even begin to list. Good on ya. I will always leave a 4:30pm slot free on Fridays if you need to talk.

The original ERD 117 team of Myles, Brine, Liam and Axel. Pioneers of office sports, champions of the long lunch and the prefect team to pretend to do work with.

The team in CELs of Dr. Patrick Huddleston, Dr. Gareth Cave, Barbara Stevenson, Dr. Songjie Yang, Joe, Subba and last but by not means least Isaac.

To the ISTEC rabble, Omar, BenCLake, Tony and last of all gods gift to synthetic chemistry Ash Holmes. Up the (claret and) Blues.

To David for letting me squat in his office for four months, without which this would have taken a great deal longer to write!

Finally, I would like to thank Megan, who through the course of this thesis has gone from my girlfriend to my wife. Without your support, none of this would have been possible. You've been a constant source of encouragement and positivity, pushing me to persevere even when the crystal gods were not in my favour. I can't thank you enough and I promise once this is done, you'll never have to read my work again!

Abbreviations

Å	Angstroms
br	Broad
BuLi	Butyl Lithium
COSY	Correlation Spectroscopy
^{o}C	Degrees Celsius
^{o}	Degrees
d	Doublet
DCM	Dichloromethane
DMF	Dimethylformamide
DMSO	Dimethylsulfoxide
EDDA	Ethylenediamine Diacetate
Et	Ethyl
EtOAc	Ethyl Acetate
Et_2O	Diethyl Ether
EWG	Electron Withdrawing Group
HMBC	Heteronuclear Multiple Bond Correlation
HMQC	Heteronuclear Multiple Quantum Coherence
in vacuo	Under vacuum (reduced pressure)
IR	Infrared
K	Kelvin
kJ	Kilojoule
m	Multiplet
Me	Methyl
MHz	Megahertz
Mol	Moles
NMR	Nuclear Magnetic Resonance
Ph	Phenyl
ppm	Parts Per Million
s	Singlet
t	Triplet
THF	Tetrahydrofuran
TMG	1,1,3,3-Tetramethylguanidine
TLC	Thin Layer Chromatography

Contents

Chapter 1

Chapter 2

Chapter 3

Chapter 4

Chapter 5

Chapter 6

Chapter 7

Chapter 8

Chapter 1

Introduction

Intermolecular Interactions

The number of non-covalent intermolecular interactions within the chemical world is vast and their importance in dictating molecular conformation, reactivity and function within supramolecular chemistry and biology cannot be overstated.[1–4] Intermolecular interactions provide stability to the molecules they are associated with. Despite the strongest of these interactions having a stabilisation energy of 60+ kJ mol^{-1} (a near ionic hydrogen bond),[5] interactions are easily formed and broken unlike that of covalent bonds, for example C-C bonds which have a bond dissociation constant of 346 kJ mol^{-1}. An example of this is shown in Scheme 1.1 where the folding of a protein, caused by intermolecular interactions, is reversed by heat, causing the proteins secondary structure to decompose but not the peptide chain itself.

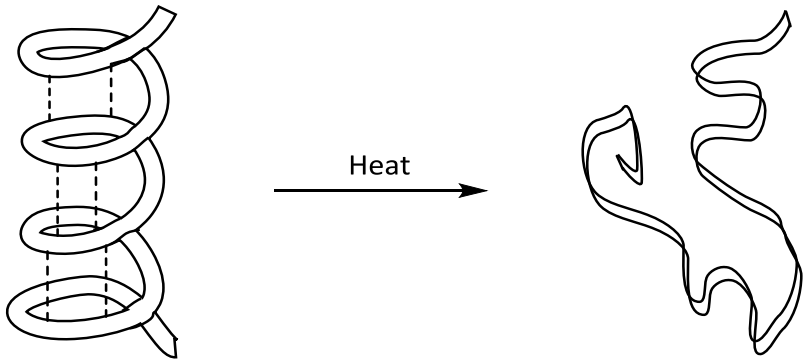

Scheme 1.1. Denaturing of a secondary protein structure by heat, causing the intermolecular interactions to break.

Intermolecular interactions are divided into isotropic and anisotropic forces. Isotropic forces such as van der Waals and π-π interactions are medium range and define the shape, size and close packing of the molecules involved in them. Typically, these are C---C, C---H, and H---H interactions. Anisotropic forces such as hydrogen bonds, halogen bonds and n-π* interactions are directional and electrostatic in nature, involving heteroatoms for example, O-H---O and N-H---O in strong and C-H---O, C-H---N and C-H---X (where X = halogen) in weak hydrogen bonds, causing them to be stronger and therefore referred to as long-range forces.

Isotropic Forces

Van der Waals Interactions

Van der Waals interactions are attractive, dispersive forces, caused by the interaction of a molecule possessing a fluctuating multipole. This subsequently induces a multipole on an adjacent molecule (Figure 1.1). The magnitude of the dispersive forces is proportional to the inverse sixth power of the interatomic separation (r^{-6}) and approximately proportional to the size of the molecule. Consequently, van der Waals forces are only achievable over a short contact distance but are observed between all molecules.[6–8]

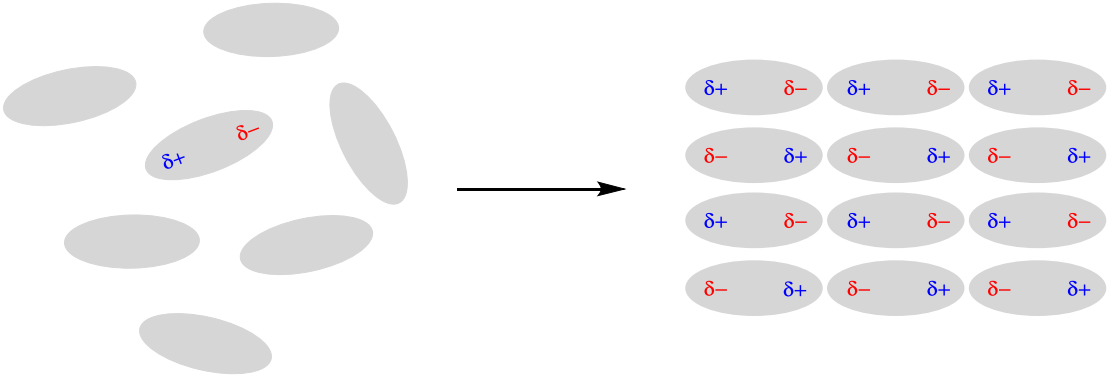

Figure 1.1. Van der Waals induced dipoles represented in idealised non-symmetrical molecules

Van der Waals forces are among the weakest of all of the intermolecular interactions, typically displaying interaction energies of between 0.4–4 kJ mol^{-1}.[8] Despite this, their omnipresence means that their combined effect can outweigh the effect of stronger, less abundant forces. Key to their stabilisation capabilities is therefore how easily they can form between molecules, therefore maximising contacts, so that interactions occur. This can be seen in the three empirically equivalent hydrocarbons, pentane **1.1** (36.0 °C), 2-methyl butane **1.2** (27.9 °C) and 2, 2-dimethyl propane **1.3** (9.5 °C) in Figure 1.2, where their boiling points differ significantly. This is caused by the branching in 2-methyl butane and 2, 2-dimethyl propane, which disrupts the packing of the molecules in solution, reducing the number of van der Waals contacts that

can occur. As the branching becomes greater from **1.1** to **1.3** the energy needed to break the contacts and cause the compound to boil reduces. Furthermore, the maximisation of contacts is demonstrated in crystal packing where molecules will attempt to pack such that they dovetail into the hollows of a neighbouring molecule, increasing the energy of the subsequent lattice.[9] Desiraju and Gavezzotti explain this using a selection of aromatic hydrocarbons, showing that more carbon-rich molecules prefer to adopt 'graphitic' stacking whilst more hydrogen-rich molecules display 'herringbone' geometries. The carbon-hydrogen stoichiometric ratio is therefore a key parameter in how molecules of this type arrange themselves.

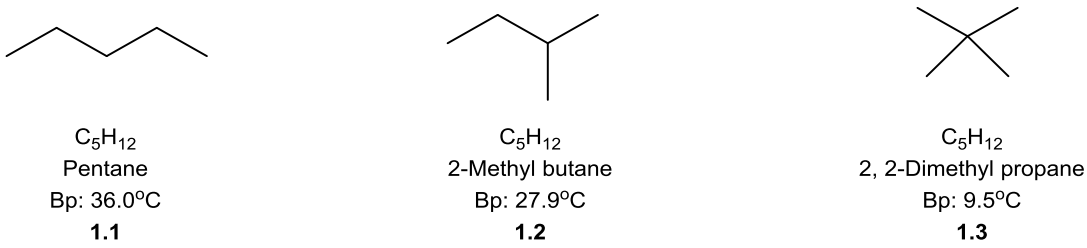

*Figure 1.2. Structures of pentane (**1.1**) and its two structural isomers (**1.2** and **1.3**).*

Van der Waals radii are an expression of the size of bonded atoms, or just atoms for the noble gases. The most commonly used values are those from Bondi,[10] which are derived from the minimum contacts between like atoms in the solid state. These values have been confirmed more recently by Gavezzotti[11] and by Rowland and Taylor[12] using the much greater amount of data available in the Cambridge Structural Database. The sum of van der Waals radii for two atoms indicates their approximate minimum separation unless there are some additional attractive interactions, and this is the context they will be used here. Within this thesis, the following values quantified by Bondi[10] will be used; C: 1.70 Å, H: 1.20 Å, N: 1.55 Å, O: 1.52 Å and I: 1.98 Å.

It is of note that for the elements beyond the first row e.g. S and Cl, bonded atoms do not behave as spheres and for atoms with just one or two bonds may have two radii for distances in line with and perpendicular to the bond(s).[13] Furthermore, there might be some small

variation even for carbon given its many different bonding arrangements, e.g. carbonyl, alkene, alkyne, though these have not been clearly distinguished. More recently van der Waals radii for elements not dealt with by Bondi have been calculated by Truhlar[14] and an alternative approach to determination of such radii have been devised by Alvarez,[15] calculated from contacts from oxygen, and Rahm and Hoffmann[16] have taken an alternative approach based on calculations of the radius at which electron density falls to 0.001 electrons per Bohr.

π-π interactions

The precise nature of the interactions between two π systems (π-π interaction) and between a π-system and another functional group (π-X interaction) have been the subject of significant research. Often these interactions are considered weak, but their extensive occurrence and importance in supramolecular chemistry and biology is well documented and of significant importance.[17–19]

Burley and Petsko[20] first characterised these interactions via a study of the interactions between aromatic side chains in the crystal structures of 33 proteins. They examined the straight-line distance between the centres of the aromatic residues (r), the angle between this line and the normal to the aromatic plane of one of the residues (θ) and the angle between the two aromatic planes (φ) as shown in Figure 1.3. This identified 580 interactions which demonstrated a separation between the two centroids by less than 10.0 Å from which they plotted a histogram of frequency of occurrence as a function of the separation distance. When the centroid separation was less than 3.4 Å, no interaction was observed, due to van der Waals repulsions. Between 3.4 and 6.5 Å the distribution was observed to vary with the separation distance, whilst above 6.5 Å the distribution remained virtually constant.

An analysis of the contacts between 3.4 and 6.5 Å revealed a relationship between the angles θ and φ. When the residues were directly above one another (θ = 0°) or side-by-side (θ = 90°), edge-to-edge or T-shaped geometries were observed respectively. Half-way between these two extremes, the residues were found to be either coplanar or only slightly tilted with respect to each other.

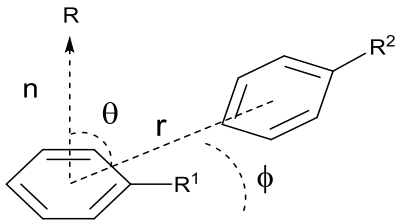

Figure 1.3. Distances and angles examined by Burley and Petsko[20] in their survey of aromatic interactions in proteins; (r) denotes the straight line distance between the centres of the aromatic residues, (θ) denotes the angle between this line and the normal (n) to the aromatic plane of one of the residues and (ϕ) denotes the angle between the two aromatic planes.

Continuing from the work of Burley and Petsko, Hunter *et al.*[19] demonstrated how a simplistic electrostatic model of a π system could be utilised to explain these interactions (Figure 1.4). The model, likened to a simple π-bond, sandwiched a positively charged σ-core between two negatively charged π-clouds, which can be further simplified to a point charge diagram.

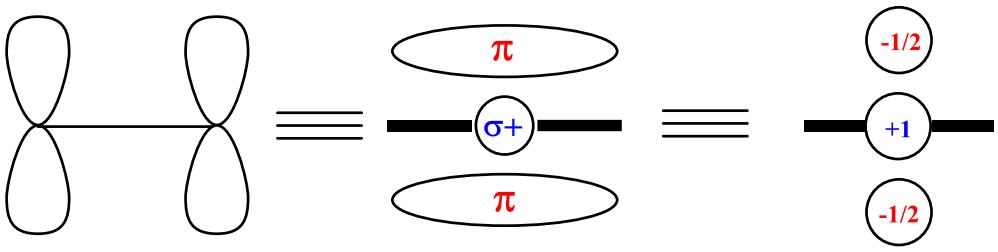

Figure 1.4. Simplification of a π-bond, applying Hunter's point charge system.

Considerable attractive interactions between porphyrins allows them to aggregate in solution and the solid phase. They adopt a co-facial arrangement with their centres offset from each other as shown in Figure 1.5. Geometrically, it can be summarised as the following: (a) the π-systems of two neighbouring porphyrins are parallel, with a 3.4-3.6 Å interplanar separation.

(b) neither of the two porphyrins involved in the π stacking are rotated relative to each other, for example the position of two equivalent nitrogen atoms are parallel to each other or (c) the offset of one porphyrin to the other falls in the range of 3.0-4.0 Å along the same nitrogen-nitrogen axis. Hunter *et al.*[19] used the point charge model to show that by adopting this geometry, the porphyrins maximise the overlap between the attractive σ-core of one ring with the π cloud of a pyrrole ring of another, whilst also minimising the π-π repulsions.

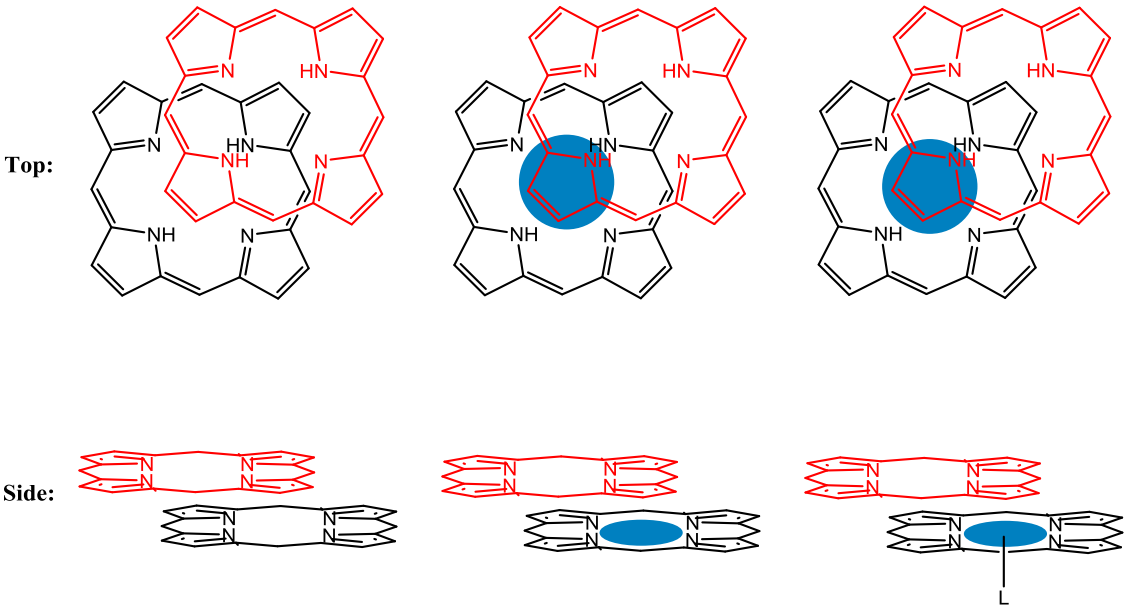

Figure 1.5. Perspectives from both above and the side of two neutral porphyrin rings (left), the same two rings with a chelated metal atom (blue) in the lower ring (middle) and the same chelated system with an electron withdrawing ligand bound to the metal atom (right).

Applying the point charge model again explained why complexation of a metal atom (e.g. zinc) further strengthened the π-π interaction, as the positively charged atom sat directly beneath a negatively charged π-cloud. Whilst the addition of a competing ligand reduced and, in some cases, destroyed the interaction due to the lowering of the stabilisation energy which had resulted from the initial metalation.

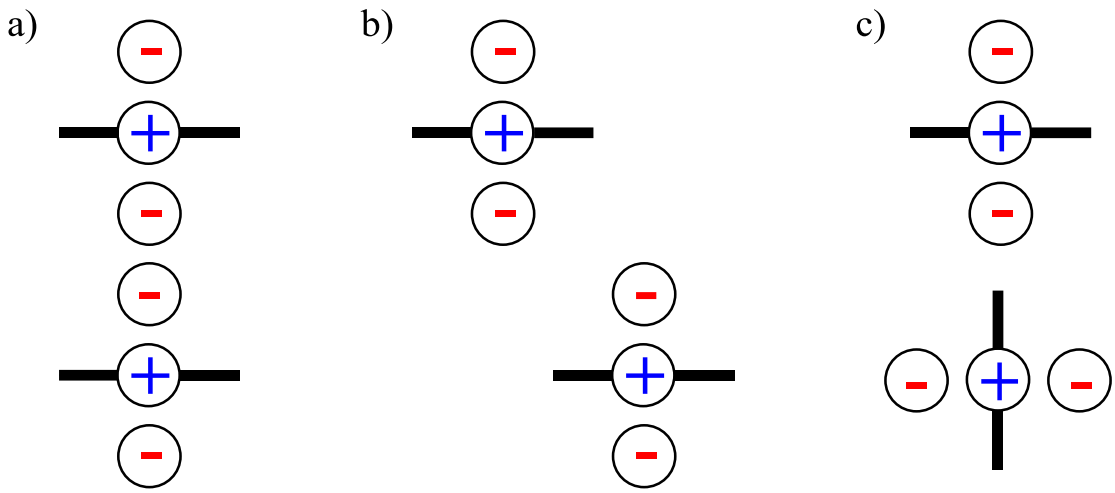

Figure 1.6. Three geometries for π-π stacking.

Hunter *et al.* continued with the point charge system, using it to calculate the energy of a generic interaction between two π-systems for a variety of rotations and displacements relative to each other. From this, the results were simplified to three scenarios that the π-π systems can adopt shown in Figure 1.6. The first is face-to-face stacking (a) whereby the interaction is dominated by π-π repulsions, making it unfavourable. The second (b) is caused by an offsetting of one of the two π-systems by several Angstroms, this allows a π-σ interactions to occur, previously shown between the porphyrins in Figure 1.5. Thirdly (c) the rotation of one of the π-systems by 90° forms an edge-to-face geometry (T-shaped), also dominated by π-σ interactions. The least favoured interaction of the three is found to be (a) face-to-face stacking due to the two overall negative charges of the systems repelling each other.

Anisotropic Interactions

Hydrogen bonds

Following its discovery over 100 years ago, research surrounding hydrogen bonds is vast. This long lasting interest is a result of the sheer importance of hydrogen bonds in the structure, function and dynamics of a vast number of chemical systems, be that in organic, inorganic or biological chemistry. The precise definition of a hydrogen bond has continued to evolve from Pauling[21] describing a hydrogen bond as largely ionic in character and formed only to the most electronegative atoms, with Atkins[22] defining the hydrogen bond as a link formed by a proton lying between two electronegative atoms.

However, it seems only very general and flexible definitions of the term 'hydrogen bond' can do justice to the complex and chemically variable nature of the interaction, including within it the strongest as well as the weakest interactions. An early more inclusive definition was proposed by Pimentel and McClellan[23] who stated that hydrogen bonds exist when there is evidence of a bond and also evidence that this bond sterically involves a hydrogen which is already bound to another atom. This definition leaves the chemical nature of the participants unspecified, allowing for weaker interactions such as C-H---O, C-H---N, O-H---π and C-H---π to be considered. But it also includes pure van der Waals contacts in its definition, which can be involved in the bonding with energies of several tenths of a kcal/mol. It also includes agostic interactions by which electrons of an X-H bond are donated sideways to an electron deficient centre by three-centre two-electron interactions. Thus Steiner[5] states 'An X-H---A interaction is called a "hydrogen bond" if; (1) It constitutes a local bond, and (2) X-H acts as proton donor to A.'.[17,18] The inclusion of point (2) means that pure van der Waals contacts and agostic interactions are excluded, but if taken liberally can also include symmetric hydrogen bonds X-H-X, where donor and acceptor cannot be distinguished. But fundamentally it includes both the classic model of electron density being donated from a lone pair of electrons to a hydrogen

bound to an electronegative atom whilst allowing weaker interactions where π-orbitals can behave as the hydrogen bond acceptor.

Table 1.1. Strong, moderate, and weak hydrogen bonds following the classification of Jeffrey.[24]

	Strong	**Moderate**	**Weak**
Interaction type	Strongly covalent	Mostly electrostatic	Electrostatic/dispersive
H---A (Å)	1.2-1.5	1.5-2.2	> 2.2
Lengthening of X-H (Å)	0.08-0.25	0.02-0.08	< 0.02
X-H versus H---A	X-H ≈ H---A	X-H < H---A	X-H << H---A
X---A (Å)	2.2-2.5	2.5-3.2	> 3.2
Directionality	Strong	Moderate	Weak
Bond angle (º)	170-180	> 130	> 90
Bond energy (kcal/mol)	15-40	4-15	< 4
^{1}H downfield shift	14-22	< 14	-

Hydrogen bonds have a large range of interaction energies depending on their chemical composition. According to the classification of Jeffery[24] (Table 1.1) hydrogen bonds can range from <4 kJ mol^{-1} in weak bonds associated with a π-system acceptor, to 4-15 kJ mol^{-1} for moderate bonds involving electronegative atoms in both cases (e.g. O-H---O) and to 15+ kJ mol^{-1} for strong bonds where the donor and acceptor atoms may be ionic in nature (e.g. -CO_2---H-O-N^+).[5,25] The interaction distance (X---A) of the hydrogen bonds follows a logical trend of decreasing in size as the interaction energy increases; 2.2-2.5 Å (strong interactions), 2.5-3.2 Å (moderate interactions) and >3.2 Å (weak interactions). Furthermore, notable ^{1}H NMR shifts downfield are observed in strong and moderate bonds of 14-22 ppm and <14 ppm respectively.

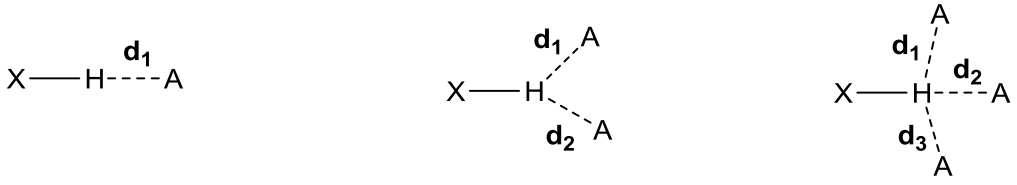

Figure 1.7. Different types of hydrogen bonds; conventional (left), bifurcated (middle), trifurcated (right).

The geometry of the interaction angle X-H---A shifts from almost linear (170-180^{o}) in strong hydrogen bonds to >130^{o} in moderate bonds to >90^{o} in weak hydrogen bonds. As a result, bi- and tri-furcated interactions can arise if the H---A separations are distinctly different, with the shorter of the interactions called the major component and the longest being the minor component (Figure 1.7). This is demonstrated in the work of Anslyn[26] and Grossel [27] in Figure 1.8 for the binding of phosphate by 2, 6-bis(methylguanidinium) pyridine (**1.4**) and sulphate by bis-acylguanidiniums[27–29] (**1.5**).

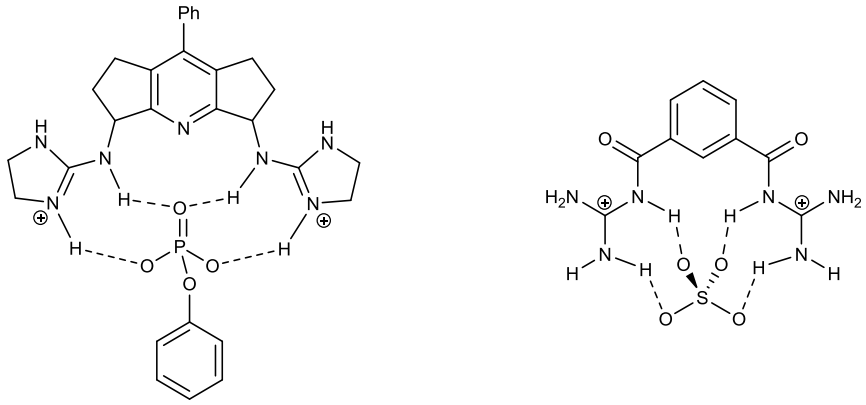

Figure 1.8. Examples of furcated hydrogen bonds by Anslyn and Grossel.[26,27]

Steiner continues to discuss how hydrogen bonds can be tuned depending on the environment of the donor and/or acceptor atoms. This can be justified by considering that hydrogen bonds are made up of several components, including electrostatic, repulsive and dispersive forces. For example, if the polarity of either the donor or the acceptor atom is reduced, the electrostatic contributions to the overall energy in the bond is equally reduced, thus the interaction becomes more van der Waals in nature.

Halogen and Chalcogen Bonds

By IUPAC definition[30] '*A halogen bond occurs when there is evidence of a net attractive interaction between an electrophilic region associated with a halogen atom in a molecular entity and a nucleophilic region in another, or the same, molecular entity*'. In other words, like hydrogen, halogens can accept electrons from electronegative atoms such as N, O and S and thus form directional intermolecular interactions. These interactions occur due to the electron density around a covalently bound halogen atom being anisotropic.[13,31]

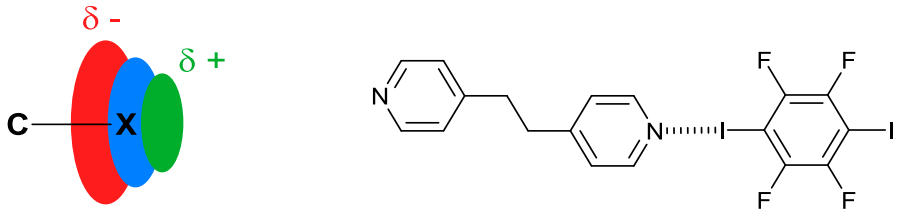

Figure 1.9. The anisotropic distribution of electron density around a halogen atom (X) generating a positive σ-hole, which is shown in green (left) and a structural example of a halogen bond (right).

Clark *et al.*[32] used molecular modelling to suggest that in the R-X bond (X = halogen), the unpaired valence electrons of the halogen form an electron belt around the halogen perpendicular to the axis of the R-X bond. Consequently, the end of the halogen atom furthest from the adjoining atom becomes an electropositive 'σ-hole' (Figure 1.9). This electropositive site now on the end of an R-X bond can therefore accept electrons from an acceptor atom, such as N, O, and S. The magnitude and size of the σ-hole is not uniform and depends on the nature of the halogen; iodine, for example, has notably polarisable valence electrons and the resultant σ-hole is larger and more electropositive than fluorine, which has less polarisable valence electrons. Polarisation due to the group bound to the halogen also plays a role in its halogen bonding capabilities, with more electron withdrawing groups (NO_2, CF_3) being found to induce σ-holes.[33]

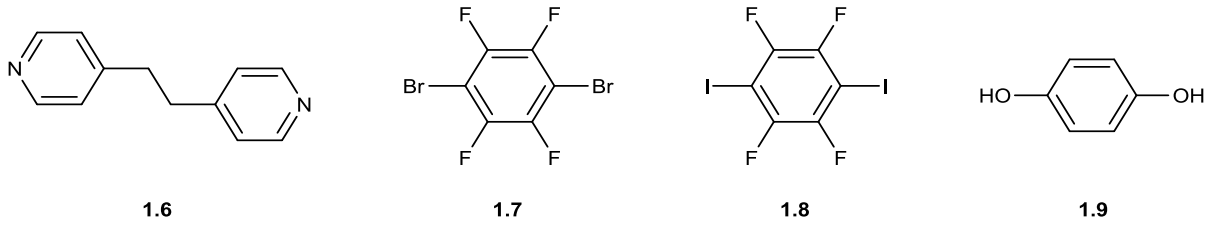

1.6 **1.7** **1.8** **1.9**

Figure 1.10. Compounds used by Metrangolo et al. in their co-crystallisation experiments

The work of Metrangolo *et al.*[34] ranks the halogens in order of strength as halogen bond donors I > Br > Cl > F, with fluorine not being observed forming halogen bonds.[32] A series of co-crystallisation experiments (Figure 1.10) with **1.6**, with either **1.7** or **1.8** revealed that the melting point of **1.6:1.8** had a higher melting point than **1.6:1.7**. Furthermore, a competition co-crystallisation experiment revealed that a 1:1:1 mixture of **1.6**, **1.7** and **1.8** in acetone, gave pure crystals of **1.6:1.8**, showing that iodine is a stronger donor than bromine. Due to the strength of halogen bonds being in the range of 10-200 kJ mol^{-1}, there is experimental evidence of competition with hydrogen bonds. Metrangolo *et al.* demonstrated with a competitive experiment[35] in which **1.6**, **1.8** and **1.9** were dissolved in equimolar amounts in excess acetone and left to crystallise. Co-crystals of **1.6:1.8** were isolated, with TLC and NMR analysis confirming the presence of **1.9** remaining in solution.

The chalcogen atoms of group 16 (O, S, Se, Te etc.) when covalently bonded to electronegative atoms or groups, undergo the same polarisations as discussed for halogen bonds, developing σ-holes at the surface of the atom opposite the binding site.[36–38] These bonds are known are chalcogen bonds. As shown in Figure 1.11, due to the bonding geometry of the chalcogen atoms, two electropositive holes form on the surface of the atom, enabling the formation of two chalcogen bonds with two incoming nucleophiles.[39,40]

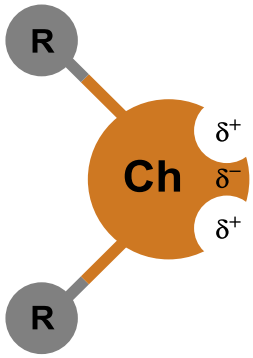

Figure 1.11. Generalised structure of a chalcogen atom (Ch) bound to two electronegative atoms (R), resulting in the formation of two δ^+ holes.

The strength of a chalcogen bond depends on the following: (a) the Lewis basicity of the interacting partner, (b) the nature of the chalcogen atom (Te>Se>O>S), (c) the polarisation of the chalcogen atom (can be dependent on the backbones chosen)[41,42] and (d) the interaction angle between the incoming nucleophile and the R-Ch bond, ideally 180°.[43,44] Despite being known for several decades, chalcogen bonds remain largely un-utilised.[39,45,46] An early example of chalcogen bonding was identified in the complex between diphenyl diselenide and iodine (Figure 1.12).[47] The complex formed a rectangular motif which was held together by two strong halogen bonds ($d_{I\text{-}Se}$ 2.99 Å) along with two chalcogen bonds ($d_{I\text{-}Se}$ 3.59 Å). The chalcogen bonds are shorter than the sum of the van der Waals radii for the two atoms (3.88 Å).[10] This structural example demonstrates the amphiphilic nature of both the halogen and chalcogen atoms.

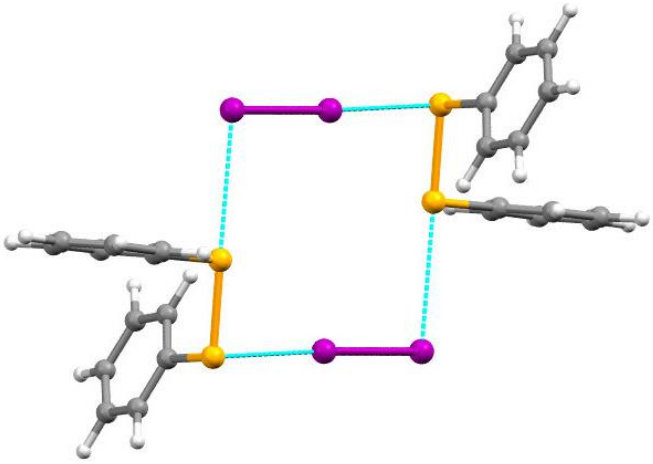

Figure 1.12. Molecular structure the diphenyl diselenide iodine complex, demonstrating both halogen and chalcogen bonds.

A general feature of the interaction between nucleophiles and the positive σ-holes in both halogen and chalcogen bonds is that as the electron withdrawing ability of the residue bound to the chalcogen atom is increased, the interaction between it and the nucleophiles is made more likely.[34] This leads to a decrease in the contact distance as the electrostatic potential at the σ-hole becomes more positive. A combination of 1, 8-disubstituted naphthalenes from a range of studies[48–50] demonstrates this in the distances observed between the dimethylamino nucleophile and a chalcogen atom (Se or Te) substituted with a range of electron withdrawing substituents (Table 1.2).

*Table 1.2. Selection of peri-naphthalenes **1.10**-**1.14** demonstrating a range of nucleophile-chalcogen interactions (d).*

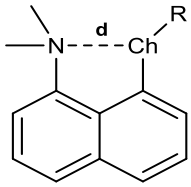

Compound	R	Ch	d (Å)
1.10[48]	Cl	Se	2.174
1.11[49]	Br	Se	2.181
1.12[48]	I	Se	2.241
1.13[50]	Br	Te	2.395
1.14[50]	Ph	Te	2.713

From the examples, a clear trend in both series is shown that as the electron withdrawing capability of the chalcogen substituent (R) is increased, the N---Ch-R contact distance is reduced. The shorter contacts of the selenium atom versus the tellurium atom maybe be a result of either the increase in atom size from Se to Te or the C-Te bond being longer than that of the C-Se bond (2.116 Å (Te) vs. 1.930 Å (Se)).[51]

Quantification of Non-Covalent Interactions

Complex biological molecules allow for the study of non-covalent interactions within a dynamic environment, whereby interactions of multiple molecular contacts and solvent molecules can be observed. The precise geometry of these interactions however is hard to accurately determine, based on the dynamic environment in which they occur. By stripping these complex systems back, synthetic chemistry can be employed to design specific targets which allow for the systematic study of these non-covalent interaction.[52] One approach for this is in the design and synthesis of folding molecules. The conformations of these types of molecules are usually controlled by intramolecular contacts or by interactions with solvent molecules, which when removed generate an alternate conformation of the initial compound. It is in compounds like this that thermodynamic information (ΔG) can be extracted from these conformational changes and the interactions can be quantified. In order to obtain a ΔG measurement, the molecule of interest must have quantifiable populations of each of the distinct conformers; i.e. when using NMR spectroscopy to assess the conformers, a distinct set of signals must be observed in each case. If the signals on the NMR timescale rapidly exchange to give average signals, then quantifiable measurements cannot be achieved.

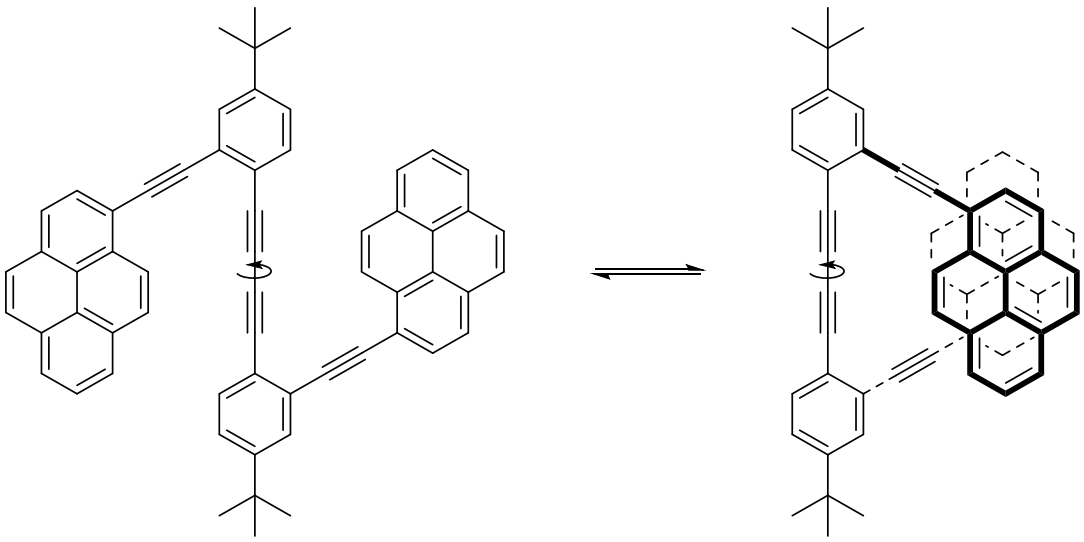

Scheme 1.2. A molecular hinge developed by Sankararaman et al. where the exact position of the equilibrium between the two conformers could not be calculated.[53]

Not all folding molecules are suited to a quantitative study, the molecule shown in Scheme 1.2 is an example of this. The system, designed to investigate aromatic interactions, allows for qualitative information about the preferred geometries to be obtained from spectroscopic studies indicating that at room temperature, the open and closed conformers are in equilibrium, with the data suggesting a closed structure. However, the exact position of the equilibrium cannot be accurately established. Both the open and closed conformers can be observed in the solid-state.[53]

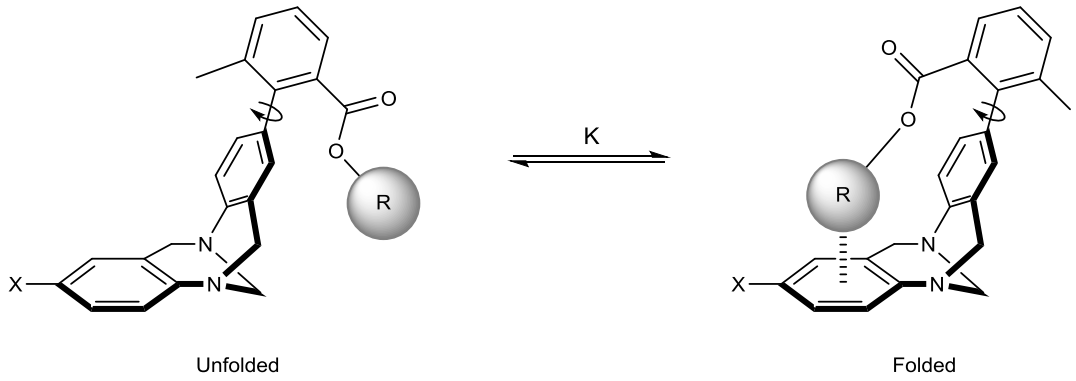

Scheme 1.3. Equilibrium (K) between the two conformations of Wilcox's 'molecular torsion balance'.[54,55]

The first group to coin the phrase 'molecular torsion balance' was that of Wilcox and co-workers based on their investigation into alkyl---arene interactions on the folded molecules shown in Scheme 1.3.[54,55] The folded and unfolded conformations in Wilcox's study displayed visible, distinct signals in the ^{1}H NMR spectrum, with the two conformations stemming from the hindered rotation around the biaryl bond. In the ^{1}H NMR spectrum, a deviation from a 1:1 ratio of the two states indicates the presence of a non-covalent interaction or solvent based effect. Functionalisation of the ester group (R) was pivotal to the interaction taking place. When R= Me, the ester group is too far from the aryl ring for a contact to occur and as a result very little preference for either state in the ^{1}H NMR spectrum is observed.[55] Functionalisation of the ester with R= ^{i}Pr or Ph, resulted in a distinct favourability of the folded conformation in both

$CDCl_3$ and D_2O solutions. The greatest overall degree of folding was shown for the R= ^{i}Pr derivative in D_2O.

The molecular balance shown in Scheme 1.3 was used to further explore aromatic edge-to-face interactions. In order to achieve this, the R-group was varied with a selection of substituted phenyl rings and the X-group altered on the bare aromatic ring. These modifications enabled the effects of substituents on the folding energy to be explored. They found that the introduction of electron-withdrawing groups (NO_2 and CN) in the R-group, shifted the equilibrium towards the folded conformation, as a consequence of the increased strength of the interaction between the more electropositive edge face with the π electron density of the aromatic ring. Substitution at the X group on the base ring surprisingly revealed that folding energies were insensitive to variation. This led to Wilcox *et al.* to propose that dispersion forces, not electrostatic forces, dominate edge-to-face interactions in the system.[55]

*Table 1.3. Peri-disubstituted naphthalenes **1.15-1.20** studied by Cozzi et al.[56] and their respective rotational energy barriers ΔG (kcal/mol) about the aryl-naphthalene bond.*

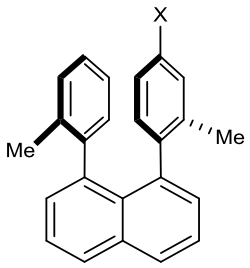

Compound	X	ΔG / kcal/mol
1.15	OMe	13.9
1.16	Me	14.4
1.17	H	14.7
1.18	Cl	15.5
1.19	CO_2Me	16.9
1.20	NO_2	17.3

Based upon the repulsive interaction in face-to-face π-π interactions Hunter *et al.*[19] theorised that polarising atoms may have an effect on the geometry of the interaction and suggested that this may even lead to an ability to stabilise the face-to-face stacking if the π-system becomes electron deficient. Cozzi *et al.*[56] confirmed this theory with a series of molecular balance NMR experiments carried out on 1,8-diphenylnaphthalenes. Steric repulsions, which cause the two *peri*-phenyl groups to arrange themselves perpendicular to the idealised naphthalene plane result in a face-to-face, π-π interaction (Table 1.3). The two competing forces, steric repulsion

and the face-to-face stacking repulsion, have a rotational energy barrier, which if satisfied allows for a 180^{o} rotation of one of the aryl groups. Applying the theory of Hunter *et al.* the strength of the π-π interaction was altered via the introduction of electron donating (**1.15** and **1.16**) and withdrawing groups (**1.18-1.20**) on one of the aryl substituents. ^{1}H NMR spectra of compounds **1.15-1.20** all display clearly resolved signals for the *ortho/ortho'* and *meta/meta'* hydrogens respectively, consistent with the expected perpendicular and restricted rotation aryl groups geometries. Heating of **1.15-1.20** in DMSO-d_6 caused coalescence of both the *ortho/ortho'* and *meta/meta'* hydrogens indicating a rotation of the aryl groups. Line shape analysis allowed for the barrier to rotation for the aryl group of each compound to be determined shown in Table 1.3. From the series, the lowest energy barrier was found to be **1.15** (X = OMe) with ΔG = 13.9 kcal/mol (where the electron donation to the π system is highest) with an increase across the series to **1.20** (X = NO_2) with an energy barrier of ΔG = 17.3 kcal/mol.

n-π* Interactions: Precursors of Bond Formation

Initial Observations, Interpretation and Theories

In 1916, amongst a 213-page article in The Journal of the Chemical Society,[57] W. H. Perkin Jr reported that in order to methylate the tertiary amino group of cryptopine **1.22** (an opium alkaloid, shown in Figure 1.13), the compound had to be treated with methyl iodide in methanol and heated in a sealed tube for two days in a water bath. Similarly, the expected reactions of the keto-carbonyl oxygen with hydroxylamine, semicarbazide or amyl nitrite and ethoxide did not proceed. Perkin justified these two groups' sluggish reactions by both being incorporated in the same ten-membered ring, until that point, unknown in natural alkaloids. Sir Robert Robinson[58] proposed the novel concept that through-space partial bond nucleophile/electrophile interactions between the ring-bound nitrogen and carbonyl carbon, were providing the decrease in reactivity. Roughly three decades later, infrared and ultraviolet spectroscopies provided evidence for this interaction across the nine-membered ring of vomicine.[59,60]

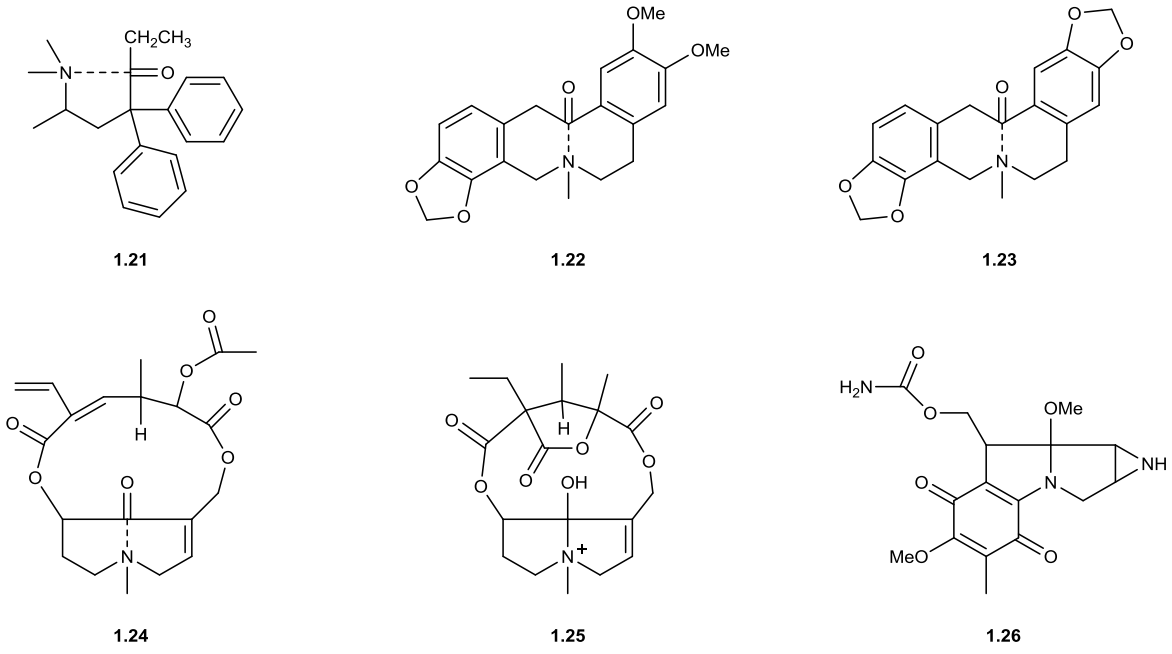

*Figure 1.13. The six alkaloid structures (**1.21**-**1.26**) which provided the basis for the work by Bürgi, Dunitz and Shefter.*[61]

Continued interest in compounds displaying such groups led to several X-ray crystallographic structures in 1971 of related natural products **1.21**-**1.26** (Figure 1.13).[62–67] Structural determination of these compounds confirmed the idea that the nucleophilic nitrogen lone pair was involved in an interaction with the electrophilic carbon of the opposite carbonyl group. The distance between the two interacting atoms was well below the sum of the van der Waals radii for both atoms.[10] Furthermore, the planarity of the carbonyl carbon was removed, with the carbon displaced from the relative plane of its three substituents (pyramidalisation) towards the nitrogen atom (Table 1.4). For example, the 5-azacyclooctanone ring of clivorine **1.24** displays a short 1.993(3) Å N---C=O contact distance, an elongated C=O bond length of 1.258(3) Å and a pyramidalisation of the carbonyl carbon by 0.213 Å from the plane of its pendant atoms. However, in some cases the two groups had instead formed a bond, as in the 5-azabicyclooctanone ring of retusamine **1.25**. In this example the single ring is transformed by protonation into a bicyclic amino alcohol, giving a 1.64 Å C-N bond length which is still significantly longer than standard C-N bonds (1.47 Å).[51] The information gathered on these structures became fully appreciated following the detailed analysis of methadone in its free base form by Bürgi, Dunitz and Shefter in 1973.[61] They proposed that the data of the six structures shown in Figure 1.13, provided an experimental basis for mapping the reaction co-ordinates (minimum energy pathway) for nucleophilic addition to a carbonyl group.[68,69] They believed that each of the structures provided an example of where the reaction had proceeded to a greater or lesser extent and a snap-shot had been captured by the intra- and/or intermolecular constraints imposed by the crystal environment.

*Table 1.4. Selected structural parameters for six alkaloids **1.21**-**1.26**.*

Compound	d^a / Å	e^b / Å	θ^c / °	Δ^d / Å
1.21[61]	2.910	1.214	105.0	0.064
1.22[67]	2.581	1.209	102.2	0.102
1.23[64]	2.555	1.218	101.6	0.115
1.24[65]	1.993	1.258	110.2	0.213
1.25[63]	1.640	1.380	110.9	0.360
1.26[62]	1.490	1.370	113.7	0.420

d[a]: N---C interaction distance; **e**[b]: C=O bond lengths; **θ**[c]: Bürgi-Dunitz angle of approach; **Δ**[d]: pyramidalisation of the electrophilic carbon of the carbonyl.

Analysis of the structural data for compounds **1.21**-**1.26** (Table 1.4) reveals a significant relationship between the N---C=O contact distance (d) and the pyramidalisation of the carbonyl carbon (Δ). As the nitrogen's approach further penetrates the van der Waals radii of the two atoms (3.2 Å[10]), the carbonyl carbon is pulled further from its trigonal plane. The lone pair of the nitrogen overlaps with the carbonyl π* orbital and the former π bond moves to become an sp^2 type oxygen lone pair (Figure 1.14). Consequently, an increase in the C=O bond length is observed as the N---C=O contact distance reduces, indicating the carbonyl group is expressing a higher degree of C-O bond functionality.

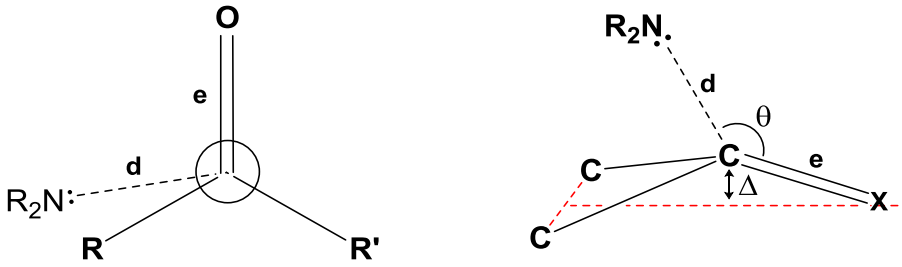

Figure 1.14. Angle of approach (θ) of a nucleophile (R_2N) to an electrophile (C=X), demonstrating the consequential pyramidalisation (Δ) of the electrophile carbon.

Very similar deformations are observed for a nucleophilic neutral oxygen atom's approach to carbonyl groups though not at such short separations as for nitrogen.[69] The library of structures analysed involved oxygen nucleophiles from a range of functionalities (ester, ethers, anhydrides, nitro groups) in a 1, 5 contact with an electrophilic carbon atom. Two examples

(cis-1,2-di-p-chlorobenzoyl-ethylene **1.27**[70] or 1,3,5,7-tetraoxa-9-azacyclodecanon-(10) **1.28**[71]) from this comprehensive study are shown in Figure 1.15 demonstrating oxygen carbonyl (**1.27**) and ether (**1.28**) centres interacting with carbonyl groups. As the O---C contact distance reduces, the pyramidalisation of the electrophilic carbon increases, however, the mean displacement of the carbonyl carbon is found to be three times larger in the nitrogen series over the oxygen series, for similar separations, suggesting that the O---C=O interaction is approximately ten times weaker than that of an N---C=O interaction.[68]

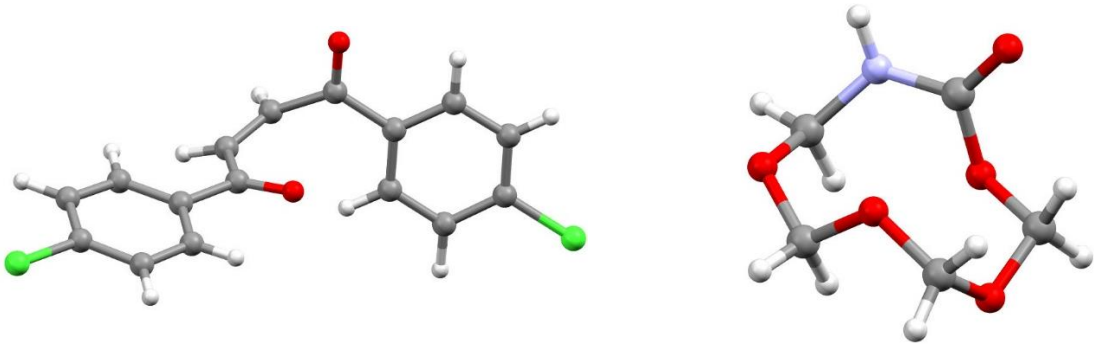

*Figure 1.15. Molecular structures of two O---C=O examples **1.27** (left) and **1.28** (right).*[69]

One of the most influential ideas to stem from these work is that in these nucleophile/electrophile type interactions, the nucleophile approaches the carbonyl group from an angle roughly equal to the tetrahedral valence angle, which stays almost constant along the reaction co-ordinate during the reaction. This optimises the overlap of the incoming lone pair with the π^* orbital. This feature has become widely known as the Bürgi-Dunitz trajectory or 'angle of attack on a carbonyl' which is quoted at approximately 109°.[68] The combination of Bürgi and Dunitz's ideas on the stereoelectronic requirements of reactions inspired the significant works such as 'Baldwin's rules'[72], Liotta's and Burgess's trajectory analysis[73], Seebach's and Eschenmoser's diastereoselection in aldol condensation.[74–76]

Do Carbonyl Groups Interact by n-π* Interactions?

C=O---C=O interactions between two carbonyl groups in the solid state have been recognised for a long time, but their character has been debated. Are these just a result of electrostatic interactions between the polar carbonyl groups, or should they be considered as n-π* interactions? This is of particular importance given that such interactions can occur in proteins and polymers and thus can contribute towards their conformation and stability. Maccallum in 1995 was the first to investigate the role of amide/amide inter-carbonyl interactions in protein structure and favoured optimisation of the Coulombic attraction between the groups to explain the structures of a number of protein motifs, for example the preference for the right handed twisted beta-strand conformation. His calculations suggested stabilisations could be up to –8 kJ mol^{-1}.[77,78] Allen et al. in 1998 used the Cambridge Structural Database to examine carbonyl/carbonyl interactions in crystals of small molecules.[79] Interestingly he identified three main structural motifs: an antiparallel motif, a perpendicular motif and a sheared parallel motif, of which only the latter aligns the molecules close to a Bürgi-Dunitz trajectory for approach of a carbonyl lone pair on the other carbonyl bond. The perpendicular motif orients the oxygen atom, but not its lone pair, into a reasonable approach. Their calculations support the dipolar model of interaction.

However, more recently Raines has made a substantial case in favour of these interactions being n-π* and not electrostatic in nature.[80] Of course, they may be one or the other depending on the relative orientation of groups. Nevertheless, he makes the case for optimisation of the n-π* interaction has a significant role in protein 3D structures as well as in the properties of small molecules. Of note, is that for proteins he shows that the large number of these weak interactions (typically at least 1.1 kJ mol^{-1}) may be as important as hydrogen bonding in determining the conformation. Furthermore, he points to a synergy between the two effects.[81,82] This is because on approach of an oxygen the pyramidalisation of the carbonyl carbon alters

the electron density such that its own oxygen atom becomes more electron rich, increasing its capability as a hydrogen bond acceptor. Alternatively, such a hydrogen bond would make the carbonyl group more susceptible to the n-π* interaction. This leads to the idea that the occurrence of one interaction could potentially generate the existence of the other. Additionally, the "attacking" oxygen in the n-π* interaction could also be involved in a hydrogen bond which would moderate its nucleophilicity.

Raines demonstrated the stabilising effects of these n-π* interactions in the structure of collagen[83] and Wennemers[84] has shown their existence in a crystalline oligo-proline, which contains no hydrogen bonding, where pyramidalisations of carbonyl carbons are observed. α-Helices are also stabilised by 1,5 C=O---C=O interactions, and the attacking O atom is additionally involved in a hydrogen bond also holding the helix together, while similar interactions support the helical conformation of poly(lactic acid) which cannot form hydrogen bonds.[85] In summary Raines has identified several signatures of n-π* interactions in proteins: short O---C contacts oriented at close to the Bürgi-Dunitz angle, lengthening of the carbonyl groups and pyramidalization of attacked carbon along with observed red shifts of the carbonyl stretching frequency, all of which have been observed in high quality measurements. It is now clear that these n-π* interactions have a very important role in the stabilisation and control of protein and polymer structures.

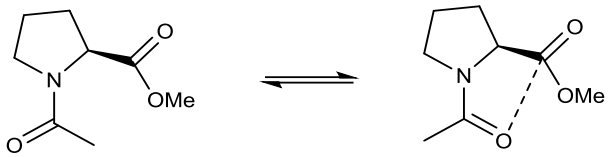

*Scheme 1.4. Equilibrium between the "trans" and "cis" conformations of the N-acetyl proline methyl ester **1.29**.*

Raines used studies on several series of small molecules to support the case for these carbonyl/carbonyl interactions being considered as n-π^*interactions, and not to be due to either electrostatic or dipolar interactions. N-Acetyl proline methyl ester **1.29** has two conformations which interconvert slowly and can be seen in NMR spectra.[86,87] They differ in the orientation of the acetyl group, directing its carbonyl group at or away from the ester group (so called trans and cis conformations (Scheme 1.4)). The equilibrium constant is 4.6 in D_2O at 25 ^oC in favour of the "trans" form. When the acetyl is replaced by thioacetyl, where the S atom carries a lower partial negative charge to oxygen, the equilibrium shifts further in favour of the "trans" conformation (K = 7.6), the opposite of what would be expected if the interaction were driven by charge. The driving force is more likely due the better match in energies between the sulphur lone pair and the carbonyl anti-bonding π^* orbital. Similarly, if the acetyl is retained but the ester replaced by the more polar amide group, the equilibrium shifts towards the cis form (K ~ 3.5), again suggesting charge is not the driving force. Interestingly, if oxygens of both the carbonyl groups of the last compound are both exchanged for sulphur, so that the interaction is between thioamides, which have lower dipoles than amides, then the equilibrium moves further in favour of the "trans" form (K ~ 6.2), contrary to what would be expected for an interaction driven by dipoles. The interaction between the thioamides is calculated to be 3.7 $kJmol^{-1}$ compared with that of 1.1 $kJmol^{-1}$ between the corresponding amides.

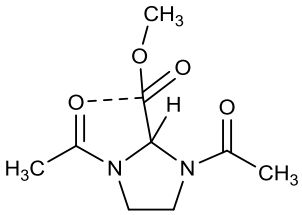

1.30

*Figure 1.16. Structure of **1.30**, where the centre ester carbonyl carbon is pyramidalised towards one of the available amide oxygen atoms.*

Another interesting molecule is **1.30**, in which two equivalent amide carbonyl groups each impinge on an opposite face of an ester group (Figure 1.16).[88] In this case, X-ray crystallography shows that there is an interaction between one pair of groups leading to a pyramidalization of the ester carbonyl carbon atom, changing its chemistry, so that it does not interact from the other side with the waiting amide carbonyl group. The first interaction is shorter than the other (O---C: 2.84 v 3.26 Å), and calculations suggest that the interaction energies are ca 3.0 kJ and 0.04 kJmol^{-1} respectively. If the interactions were driven only by electrostatics then the interactions from either side of the ester plane should have been equivalent.

1.31 **1.32**

*Figure 1.17. Structures of aspirin **1.31** (left) and the acetylsalicylate anion **1.32** (right).*

Raines has also demonstrated further aspects of this type of n-π* interaction in the common pharmaceutical aspirin (Figure 1.17). Both crystallographic[89] and spectroscopic[90] investigations revealed n-π* interactions in low energy conformations of both aspirin **1.31** and its acetylsalicylate anion **1.32**, with the latter demonstrating a shorter O---C contact (2.71 Å) and a closer to optimal Bürgi-Dunitz trajectory (104.6º) than the former (2.83 Å and 96.3º).

This is a result of the more potent oxyanion donor atom in **1.32**. The electron donation from this carboxylate oxyanion into the ester is predicted to shield and disperse the molecules negative charge and thus improve the drugs transportation to its active site through hydrophobic channels. Furthermore, non-planarity of the carboxylate group with respect to the aromatic ring, brought about by the n-π* interaction and not the 'ortho effect', aids in the justification of its anomalously low pK_a (3.48) compared to the similar benzoic acid (4.20) or *o*-methoxybenzoic acid (4.09).[91]

The *Peri*-Naphthalene Skeleton

Why Use the *Peri*-Naphthalene Skeleton for Investigating Interactions?

Naphthalene[92] is the simplest polycyclic aromatic hydrocarbon, possessing three planes of symmetry through the two rings. Unlike benzene, the C-C bond lengths are not identical with C1-C2, C3-C4, C5-C6 and C7-C8 bonds of ~1.37 Å in length and the remaining bonds ~1.42 Å in length. The *exo*-cyclic angle at the point of ring fusion between the two *peri*-hydrogens is found to be 121.7(1)^{o} and results in a H---H *peri*-separation of 2.45 Å (Figure 1.18).[93,94]

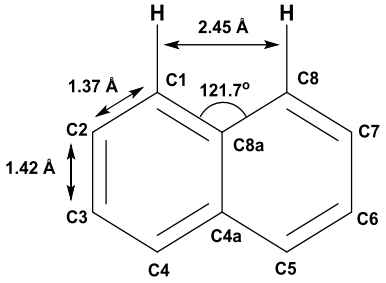

Figure 1.18. Structure of naphthalene labelled with the IUPAC numbering system, bond lengths and angles.[92–94]

Substituents in the *peri*-positions of naphthalene are forced into a close contact, so close in fact that the distance is less than the sums of their non-bonded van der Waals radii.[10] This presents the opportunity to observe interactions between two groups which are locked into close proximity to one another, with the distances maintained by the naphthalene scaffold. Depending on the substituents that are chosen, the interactions at these positions can lead to (a) a distortion of the naphthalene skeleton and its exocyclic angles, (b) bond formation between the two *peri*-substituents if the attractive interaction of the groups is strong enough, or (c) possibly unusual chemical and spectroscopic properties as a result of both (a) and (b).

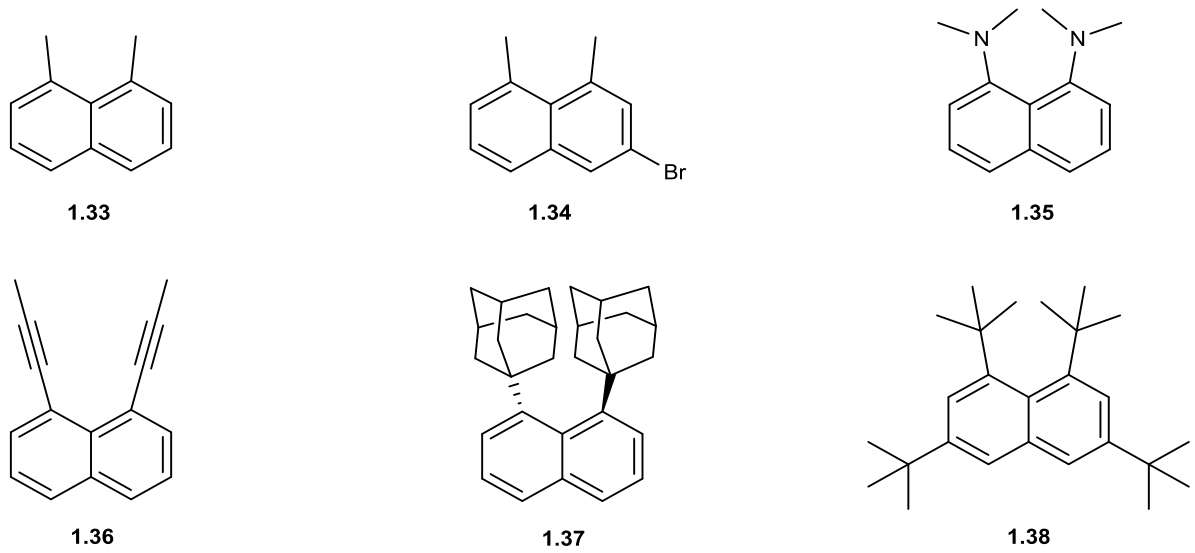

*Figure 1.19. Range of peri-disubstituted naphthalenes **1.33-1.38** displaying varying degrees of 1,8-repulsions.*

The 1, 8-disubstituted naphthalenes (**1.33-1.38**)[95–100] shown in Figure 1.19 demonstrate repulsions between the two *peri*-substituents generating distances in the range of 2.79-3.86 Å between the two *peri*-atoms, significantly increased from that of unsubstituted naphthalene (H---H: 2.45 Å). These repulsions result in the *peri*-groups being displaced in opposite directions to one another along the naphthalene plane, increasing both the contact distance and the *exo*-angle at the point of ring fusion between them. Moreover, the groups are further distanced via displacement to opposite sides of the best naphthalene plane, often causing the naphthalene scaffold itself to twist, clearly demonstrated in the bulkiest examples of **1.37** and **1.38** as shown in Figure 1.20.

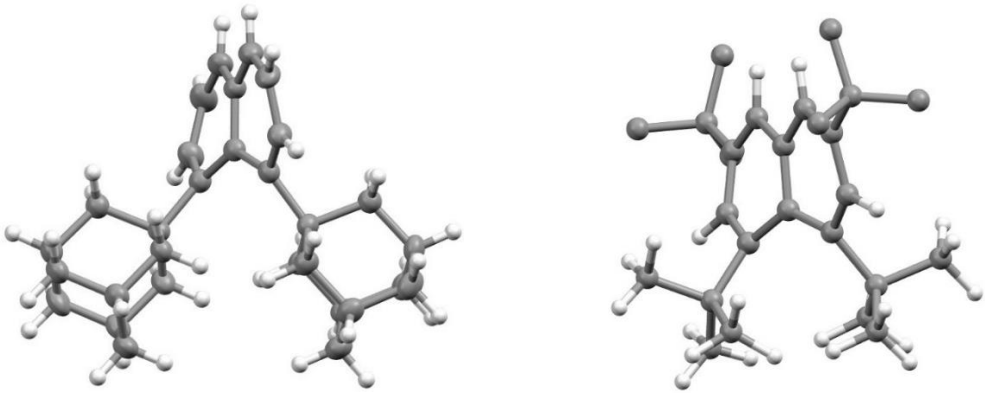

Figure 1.20. Structures of peri-substituted naphthalenes with two adamantly groups (left) and two t-butyl groups (right).

Study of n-π^* Interactions with *Peri*-Naphthalenes

Peri-substituted naphthalenes were first utilised as probes for nucleophile-electrophile interactions by Dunitz *et al.*[101] With naphthalene as the scaffold, the two interacting groups are forced into close contact, well within the sum of their van der Waals radii and thus it was expected that the interactions between the two groups would be strong. The electrophilic groups in all cases were carbonyl groups, present as either carboxylic acids, esters, ketones or amides. The nucleophiles employed were either a hydroxyl or methoxy oxygen group or dimethylamino nitrogen. In total seven molecules were analysed in the series (Table 1.5).

Table 1.5. Summary of nucleophiles and electrophiles in the first peri-naphthalene Dunitz et al. study.[101]

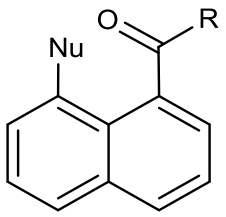

Compound	Nu	R
1.39	NMe_2	Me
1.40	NMe_2	OH
1.41	NMe_2	OMe
1.42	OMe	Me
1.43	OMe	OH
1.44	OMe	NMe_2
1.45	OH	NMe_2

In each of the molecules across the series, the nucleophilic group was displaced in the naphthalene plane toward the electrophilic group which retreated by an almost similar amount. The two displaced groups were also displaced to opposite sides of the best naphthalene plane by small amounts. Overall, the Nu---C=O contact distances were consistent (2.56-2.62 Å) throughout the seven compounds indicating very little change in either the strength of the nucleophile or in the electrophilicity of the carbonyl group. Nevertheless, the contacts all fell well within the sum of the van der Waals radii for the Nu---C=O interaction.[10] The relative strengths of the nucleophiles used is reflected in the degree of pyramidalisation of the carbonyl carbon. In the series, the largest displacements (0.06-0.09 Å) are observed for the stronger dimethylamino group, whilst smaller displacements for the weaker hydroxyl/methoxy group

(0.02-0.05 Å) are seen. The pyramidalisation of the carbonyl carbon also increases as expected with respect to its α-substituent (i.e. COR > COOH~COOR > $CONR_2$). The Bürgi-Dunitz approach angles range from 94-108° across the series positioning the nucleophile optimally for addition to the electrophile. The dimethylamino groups in **1.39**-**1.41**, orientate the N-methyl groups to either side of the naphthalene plane, allowing for the nitrogen lone pair to be positioned optimally for overlap with the π* orbital of the carbonyl group.

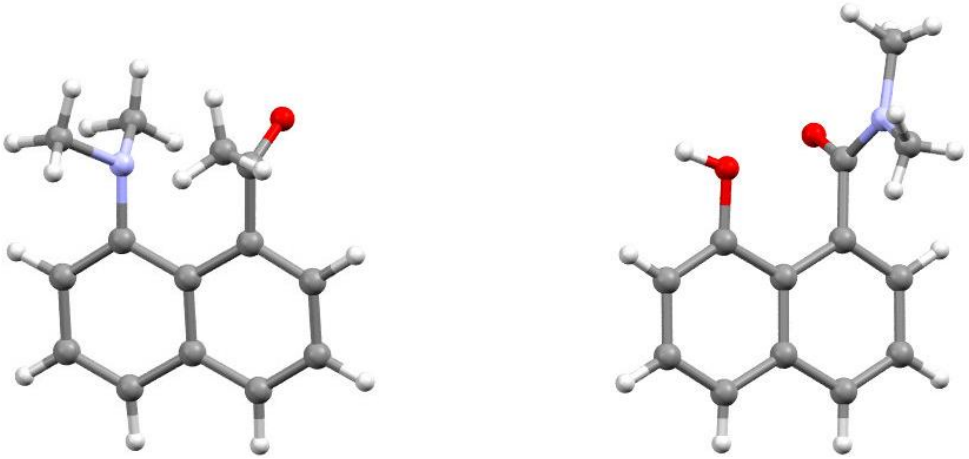

*Figure 1.21. Molecular structures of dimethylamino methyl ketone **1.41** (left) and the hydroxy amide **1.45** (right).*

Since this initial series, significant work has focused on interactions of this type, where a dimethylamino nucleophile is maintained. *Peri*-interactions between a dimethylamino group and elements such as Al,[102] Si,[103,104] Sn,[105] P,[106] Te and Se[48] have been investigated with the functional groups analysed involving these elements including - $AlEt_2$, -$Si(SiMe_3)=C(SiMe_3)_2$, -SiF_3, -$SnPh_3$, -$P(O)(OEt)_2$ and -Se-I. However, the extensive work of primarily Wallis *et al.* has generated a large series of *peri*-naphthalenes which showcase interactions between the dimethylamino nucleophile and a range of electrophilic carbon centres, especially various ketones and electron deficient alkenes (Table 1.6). Collectively these examples provide coordinates at varying points along the reaction pathway for nucleophilic attack of an electrophile. In the most electrophilic of examples, formation of a long, partially formed N-C bond occurs.

*Table 1.6. Selected molecular geometry for a series of peri-naphthalenes **1.46-1.57** in order of increasing Me_2N---C distance and γ angle.*

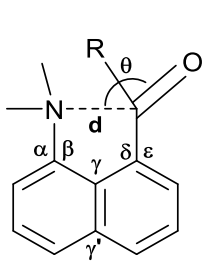

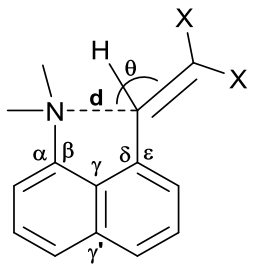

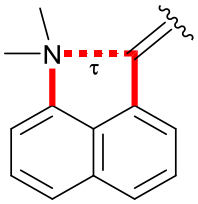

Compound	d / Å	θ / º	α / º	β / º	δ / º	ε / º	γ/γ' / º	τ^a / º
1.46[107]	2.413(3)	112.5(1)	124.3(2)	115.9(2)	120.2(1)	120.3(2)	120.1(4)/122.7(2)	-13.7(1)
1.47[108]	2.422(2)	107.3(1)	124.3(2)	115.3(1)	121.5(1)	118.1(2)	121.2(1)/123.1(2)	1.3(1)
1.48[109]	2.489(6)	113.5(3)	124.3(3)	116.0(4)	122.2(4)	118.5(4)	120.6(3)/121.5(4)	13.4(3)
1.49[110]	2.531(3)	114.4(1)	123.3(2)	116.8(2)	121.7(2)	118.6(2)	122.4(1)/121.3(2)	-6.3(1)
1.50[108]	2.538(2)	107.1(1)	123.8(1)	116.3(1)	123.1(1)	117.2(1)	122.1(1)/122.1(1)	-6.7(1)
1.51[108]	2.613(1)	106.1(2)	123.5(2)	117.0(3)	123.8(3)	116.0(3)	122.3(2)/121.3(3)	-8.7(2)
1.52[111]	2.632(2)	117.7(1)	122.7(2)	117.4(1)	122.0(2)	118.5(2)	123.1(1)/120.9(1)	15.4(1)
1.53[112]	2.642(2)	119.4(1)	123.4(1)	117.3(1)	122.3(1)	118.4(1)	122.9(1)/121.1(1)	-16.0(1)
1.54[112]	2.642(2)	98.9(1)	123.6(1)	116.9(1)	123.2(1)	116.6(1)	123.1(1)/121.5(2)	13.6(1)
1.55[112]	2.674(2)	116.7(1)	122.9(1)	117.5(1)	122.0(1)	118.1(1)	123.5(1)/120.8(1)	18.3(1)
1.56[107]	2.679(2)	118.0(1)	122.3(2)	118.3(2)	122.5(1)	117.6(1)	123.4(2)/121.0(2)	14.8(1)
1.57[113]	2.764(4)	96.7(2)	121.2(3)	118.5(3)	125.4(3)	114.1(3)	125.0(3)/120.3(3)	-0.7(2)

τ^a = torsion angle :C(Ar)-N---C-C(Ar).

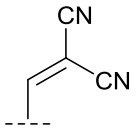

1.46
2.413 Å

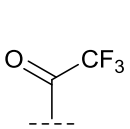

1.47
2.422 Å

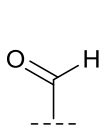

1.48
2.489 Å

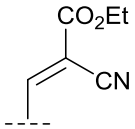

1.49
2.531 Å

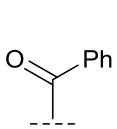

1.50
2.538 Å

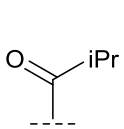

1.51
2.613 Å

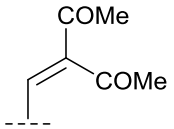

1.52
2.632 Å

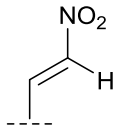

1.53
2.642 Å

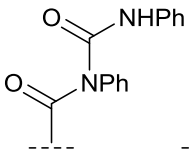

1.54
2.642 Å

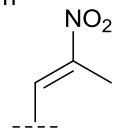

1.55
2.674 Å

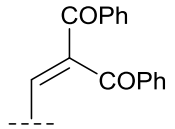

1.56
2.679 Å

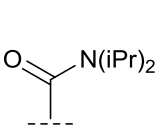

1.57
2.764 Å

The data summarised in Table 1.6 consists of results from several studies over a number of years[107–113] demonstrating the nature of *peri*-interactions in examples where nucleophilic addition by the dimethylamino group to the electrophile did not occur. Compared to the initial series presented by Dunitz *et al.*[101] Table 1.6 displays a much wider spread of electrophilic centres helping to further develop the understanding of several key features of how nucleophile/electrophile interactions of this type proceed along the early stages of the reaction pathway. However, in a situation akin to the chicken and the egg, knowing the order in which these occur is difficult to determine. The first is through the before-mentioned in-plane angular displacements (α, β, δ, ε) of the *peri*-groups. These displacements allow for the nucleophile to approach the electrophilic centre, which on the whole, is displaced in the same direction. Here, the nucleophile is displaced to a higher degree in the most electrophilic examples, with the extent of this displacement reducing as the electrophilicity of the *peri*-group decreases. Similarly, the more electrophilic the *peri*-carbon centre is, the less it is displaced away from the incoming nucleophile due to their greater affinity for the nitrogen lone pair. This is reflected for the shorter contact distances in the most electrophilic alkenes and ketones. Secondly, there is a widening or narrowing of the *exo*-angle (γ) at the point of naphthalene ring fusion between the two *peri*-groups. This angle has a significant influence on the interaction as it can dictate the general direction in which the C(*peri*)-N/C(*peri*)-C bonds are orientated. Looking at the data in Table 1.6, a pattern between the two *exo*-angles (γ and γ') and the interaction distance is observed. The *exo*-angle between the interacting *peri*-groups (γ) is smaller than opposite angle (γ') when the interaction distance is in the region of (or shorter) than the C(*peri*)---C(*peri*) contact distance in unsubstituted naphthalene (2.474(1) Å). Once the contact distance begins to increase above this distance, the difference between the two *exo*-angles begins to decrease, with the two angles even becoming equal in the phenyl ketone derivative **1.50**. As the interaction distance continues to increase, the size of the angles reverse, with the *exo*-angle (γ)

widened with respected to the opposite angle (γ'). Finally, out of plane displacements of the C(*peri*)-N or C(*peri*)-C bonds to either side of the idealised naphthalene plane occur. These displacements typically reduce the steric hinderance between the *peri*-substituents with either each other or the naphthalene ring itself and as a result cause a widening of the contact distance. This displacement is expressed as the torsion angle (τ) between the following atoms C(*peri*)-N($(CH_3)_2$)---C-C(*peri*) in Table 1.6. Overall, as the contact distance between the interacting groups increases upward of 2.6 Å, the groups are more susceptible to larger out of plane displacements. Furthermore, as a consequence of the larger displacements, the Bürgi-Dunitz angles for the nucleophile's approach towards the electrophilic centre become significantly worse. Some examples deviate from this slightly, such as the dinitrile **1.46**. In this case, the larger displacements may be a result of an attempt to reduce the steric repulsions between the two *peri*-groups as a result of their closer proximity or a consequence of crystal packing forces. Crystal packing forces within structural investigations cannot be overlooked, especially when the alterations in a parameter of interest between different structures is small. Although it is not always viable, obtaining several different crystallographic polymorphs of a compound of interest can aid in negating these concerns.

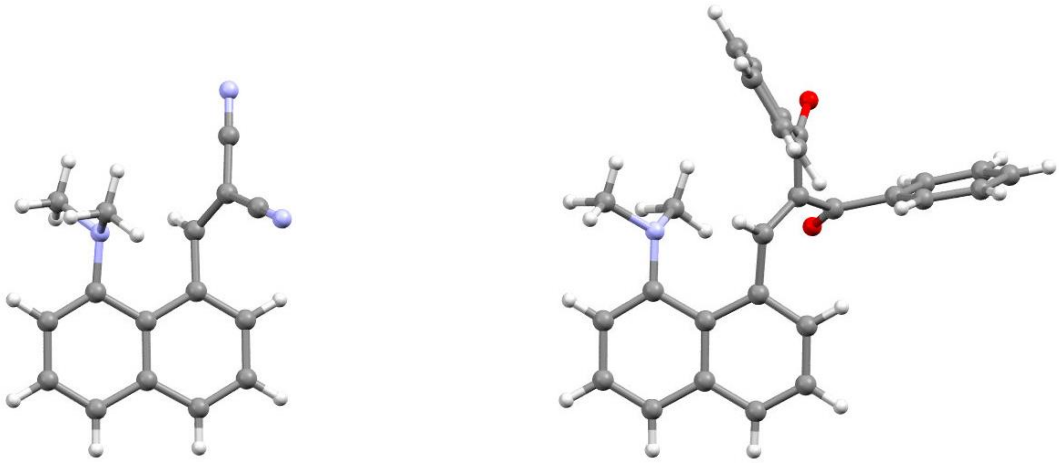

*Figure 1.22. Molecular structure of **1.46** which demonstrate the shortest N---C contact (left) and one of the largest N---C contacts in **1.56** (right).*

Beyond a certain contact distance, the nucleophile/electrophile interaction across the *peri*-positions becomes unfavourable. An example of this can be seen in the dibenzoyl derivative **1.56** (Figure 1.22) which demonstrates an N---C=C distance of 2.679(2) Å. In this example, the nucleophile is still displaced towards the retreating electrophile; however, the N-methyl groups of the nucleophile are no longer evenly distributed to either side of the naphthalene plane. Instead, they are orientated such that the axis of the nitrogen lone pair lies at 30^{o} from the N---C vector, thus poorly overlapping with the π^* orbital of the alkene. The nitrogen lone pair is alternatively conjugated into the aromatic naphthalene system. In this derivative specifically, the electrophilicity of the *peri*-carbon is greatly reduced due to the free rotation of the two benzoyl groups, which reduces the conjugation of the carbonyl groups to the double bond. If the two carbonyl groups of derivatives such as dibenzoyl **1.56** are locked into the same plane, via incorporation into a ringed system, conjugation between them both and the double bond of the alkene is ensured, increasing the electrophilicity of the *peri*-carbon centre greatly. The data summarised in Table 1.7 demonstrates a series of such *peri*-naphthalene derivatives where the nucleophilic dimethylamino group has added to the alkene to give a range of zwitterionic compounds. The carbanionic centre in all case is stabilised by the two cyclic carbonyl groups.

*Table 1.7. Selected molecular geometry for a series of peri-naphthalenes **1.58-1.63** where an N-C bond has formed between the interacting peri-groups.*

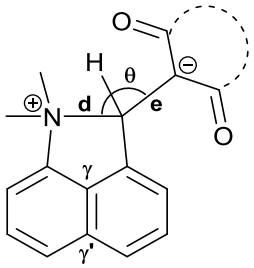

Compound	d / Å	e / Å	N-CH_3 / Å	γ/γ' / °	τ^a / °
1.58[111]	1.654(1)	1.464(2)	1.493(2)/1.498(2)	113.5(1)/127.6(1)	9.6(1)
1.59[107]	1.651(3)	1.471(3)	1.495(3)/1.508(2)	113.3(2)/128.1(2)	17.1(2)
1.60[111]	1.636(4)	1.479(4)	1.500(4)/1.504(3)	113.7(3)/128.7(3)	5.9(2)
1.61[111]	1.631(2)	1.486(2)	1.500(2)/1.502(2)	113.2(1)/128.3(1)	12.1(1)
1.62[111,114]	1.627(2)	1.477(2)	1.496(2)/1.504(2)	113.1(1)/128.2(1)	18.9(2)
1.63[111]	1.626(2)	1.471(3)	1.499(2)/1.502(2)	113.3(2)/128.4(2)	9.7(1)
	1.612(2)	1.478(2)	1.496(2)/1.503(3)	113.0(1)/128.5(2)	23.1(2)

τ^a = torsion angle :C(Ar)-N-C-C(Ar).

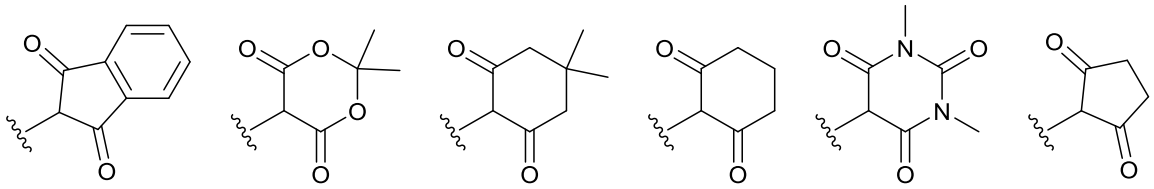

The nature of the cyclic dicarbonyl system has scope for variation i.e. diones[111] (**1.58**, **1.60**, **1.61**, and **1.63**), di-esters[107] (**1.59**) or diamide derivatives[111,114] (**1.62**). In each structure, the N-C bonds lengths (1.612(2)-1.654(1) Å) indicate incomplete bond formation, with the former alkene bond almost broken to give an alkane type bond (1.464(2)-1.486(2) Å).[51] One of the longest N-C bonds occurs in the Meldrum's acid derivative **1.59**, whereby the newly formed five-membered ring adopts a half chair conformation (Figure 1.23). The *bis* enolate group of the cyclic diester is found to be asymmetrical. One fragment of the ring shows a greater degree of enolate character, with a longer C=O bond of 1.236 Å expected as the C=O becomes more C-O^- in nature, and a shorter C-C bond of 1.409 Å, whilst the remaining group displays less enolate character (C=O: 1.224(3) Å and C-C: 1.428(3) Å). In all cases, the N-methyl groups display N-C bond lengths (1.493(2)-1.508(2) Å) consistent with that of a positively charged dimethylammonium group (1.503 Å), as opposed to those observed in a neutral dimethylamino

group (1.469 Å).[115] The formation of the 5-membered ring across the *peri*-positions causes a significant narrowing of the nearby *exo*-angle (γ), with the opposite *exo*-angle (γ') similarly widened. The two *peri*-atoms are displaced by varying degrees from the idealised naphthalene plane.

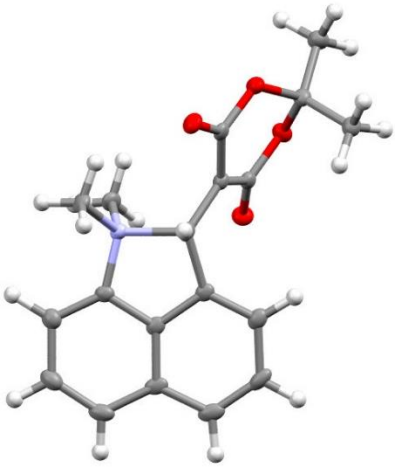

*Figure 1.23. Molecular structure of Meldrum's acid derivative **1.59**.*

Schiemenz *et al.* has proposed two methods for determining the degree of bonding between a $–NMe_2$ group and a *peri* substituent. These are based on (a) the bond angles at the nitrogen atom[116] and (b) the ^{13}C-^{1}H coupling constant of the methyl groups of the NMe_2 nucleophile.[117]

Nucleophiles other than the dimethylamino group have also been studied. Table 1.8 summarises the interactions of the methoxy nucleophile, with a variety of electrophilic double bonds (carbonyls and alkenes).[101,113,118–121]

*Table 1.8. Selected structural details in a series of methoxy naphthalenes **1.64-1.75**.*

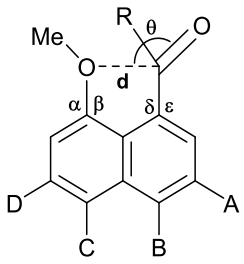

1.64 R=H, A=D=H, B=OMe, C=OTs
1.65 R=H, A=B=D=H, C=OTs
1.66 R=Me, A=B=C=D=H
1.67 R=Me, A=D=H, B=OMe, C=OTs
1.68 R=OH, A=B=C=D=H
1.69 R=OH, A=B=D=H, C=OMe
1.70 R=OH, A=B=H, C=OMe, D=CO_2H
1.71 R=OMe, A=B=D=H, C=OMe
1.72 R=NMe_2, A=B=C=D=H
1.73 R=N^iPr_2, A=B=C=D=H

Compound	d / Å	α / º	β / º	δ / º	ε / º	Δ[a] / Å
1.64[121]	2.628(4)	123.4(2)	115.1(2)	126.4(2)	114.9(2)	0.089(4)
1.65[121]	2.644(4)	123.5(3)	115.3(2)	124.7(3)	115.8(3)	0.072(4)
1.66[101]	2.606(9)	124.4(9)	115.9(8)	125.5(8)	115.3(8)	0.044(10)
1.67[121]	2.579(3)	124.0(2)	114.1(2)	125.5(2)	115.3(2)	0.070(3)
1.68[101]	2.559(4)	124.7(3)	113.2(3)	123.4(3)	115.8(3)	0.022(5)
1.69[118]	2.566(2)	124.7(2)	114.1(2)	124.0(2)	115.0(2)	0.042(2)
1.70[119]	2.526(3)	124.7(2)	114.1(2)	122.1(2)	117.4(2)	0.036(2)
1.71[118]	2.588(3)	125.6(3)	114.3(2)	124.2(2)	115.6(2)	0.037(2)
1.72[101]	2.597(5)	122.7(4)	114.4(4)	124.0(3)	115.1(4)	0.039(4)
1.73[113]	2.623(2)	124.2(2)	114.8(2)	124.2(2)	116.0(2)	0.049(1)

Δ[a]: pyramidalisation of the electrophilic carbon.

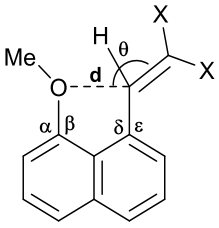

1.74 X=(C(=O)O_2)CMe_2
1.75 X=CN

Compound	d / Å	α / º	β / º	δ / º	ε / º	Δ[a] / Å
1.74[120]	2.550(2)	123.6(2)	115.0(2)	123.2(2)	117.3(2)	0.077(2)
1.75[120]	2.611(1)	124.3(1)	114.9(1)	123.5(1)	117.0(1)	0.029(1)

Δ[a]: pyramidalisation of the electrophilic carbon.

In contrast to the –NMe_2 series, the O---C interaction distances have a much lower range (2.526-2.623 Å), than in the –NMe_2 series (1.651-2.764 Å). This data is consistent with the much lower nucleophilicity of –OMe, compared to –NMe_2, as a result of the oxygen atom conjugating with the naphthalene ring and lowering its nucleophilicity further. An example of

this is observed in the two methoxy aldehyde derivatives **1.64** and **1.65** whereby the aldehyde group is sufficiently small enough to orientate itself close to the naphthalene plane. The two aldehyde groups lie at 30.8° (**1.64**) and 38.5° (**1.65**) to the naphthalene plane, with the methoxy oxygen atom not directed at the face of the carbonyl group. The dimethylamino aldehyde derivative **1.48**, on the other hand, positions the aldehyde at 65.8° to the naphthalene plane, with a short N---C=O contact of 2.489(6) Å observed between the groups. Throughout the methoxy derivatives, hallmarks of the nucleophile/electrophile *peri*-interactions are observed. In all cases the nucleophile is displaced towards the retreating electrophile, with the *peri*-carbon atoms showing varying degrees of pyramidalisation. However, direct comparison between this methoxy series and the parallel dimethylamino series may not be suitable, due to some of the differences observed in the methoxy series being of the same order as those produced by the adoption of different packing arrangements or by different temperatures. In order to accurately compare the two series of results, a greater number of *peri*-methoxy derivatives and polymorphs would need to be investigated to average out the effects of crystal packing. The MeO---C interactions observed in compounds **1.64-1.75** present early stage n-π* interactions. Substitution of the methoxy nucleophile for the more potent dimethylamino nucleophile allows the interaction to develop into bond formation in the most electrophilic examples.

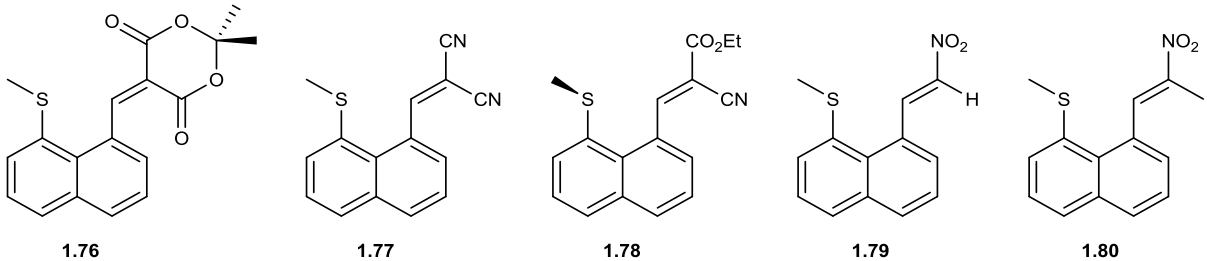

1.76 **1.77** **1.78** **1.79** **1.80**

Figure 1.24. The five peri-naphthalenes in the methylthio study.

The Wallis group further extended the scope of nucleophile/electrophile interactions in a study which investigated the interaction of a nucleophilic methylthio group with a range electron deficient alkenes in *peri*-naphthalenes.[122] New considerations are the increased nucleophilicity

of the larger sulphur atom, issues arising as to which sulphur lone pair is involved in the interaction and the asymmetric effective shape of the bonded sulphur atom. Furthermore, the notably longer C-S bond (vs. C-O or C-N bonds)[51] results in a poorer alignment of the two interaction atoms. In the series, five derivatives (**1.76**-**1.80**) were synthesised via Knoevenagel condensation of 8-(methylthio)-1-naphthaldehyde with a range of active methylene compounds (Figure 1.24). The structures of the five compounds were determined and selected geometric data is summarised in Table 1.9.

*Table 1.9. Selected structural parameters in the methylthio peri-naphthalene series **1.76-1.80**.*

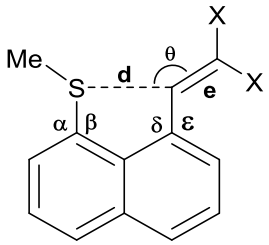

Compound	**d** / Å	**e** / Å	**θ** / °	**α** / °	**β** / °	**δ** / °	**ε** / °	**Δ**[a] / Å
1.76	2.787(2)	1.339(3)	114.6(1)	121.4(2)	119.4(2)	123.9(2)	115.9(2)	0.049(9)
1.77	2.850(3)	1.338(4)	118.2(2)	120.9(2)	119.7(2)	123.5(2)	115.9(2)	0.037(11)
1.78	2.923(1)	1.349(2)	115.9(1)	117.0(1)	122.9(1)	121.7(1)	117.9(2)	0.036(6)
1.79	2.895(2)	1.326(3)	125.9(1)	119.6(2)	120.5(1)	123.0(2)	116.7(2)	0.014(8)
1.80	2.830(2)	1.332(3)	115.6(1)	120.1(2)	120.2(1)	123.4(2)	117.2(2)	0.030(8)

Δ[a]: pyramidalisation of the electrophilic carbon.

The five compounds analysed fall into three groups defined by their participation in the expected interactions: the solid-state structures and the orientations of the two *peri*-groups are controlled by (a) nucleophile/electrophile interactions alone, (b) a combination of this interaction and the optimisation of conjugation between the alkene and the aromatic system or (c) by optimisation of the conjugation alone. The behaviour of Meldrum's acid derivative **1.76**, is dictated solely by nucleophile/electrophile interactions, demonstrating the smallest S---C contact distance (2.787(2) Å). An *ortho*-hydrogen steric interaction (H---H(CH_2S-) aids in the displacement of the methylthio group of 1° towards the alkene, which is in turn displaced by 4° in the same direction. The alkene lies at 57.2(3)° to the mean naphthalene plane, presenting

an interactive face for the methylthio group, resulting in the largest pyramidalisation (Δ = 0.049(9) Å) of the sp^2-C atom in this series (Figure 1.25). The sulphur atom approaches the alkene bond at a Bürgi-Dunitz angle of 114.2(1)°.

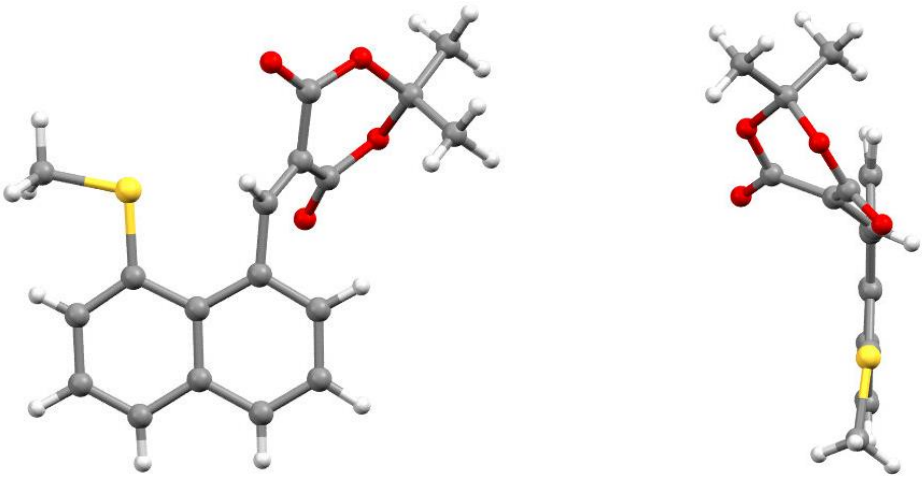

*Figure 1.25. Molecular structures of the Meldrum's acid derivative **1.76** (left) and a bird's-eye view showing the minimal displacement of the peri-groups from the naphthalene plane (right).*

The dinitrile, cyanoester and methylnitro derivatives **1.77**, **1.78** and **1.80** demonstrate a combination of nucleophile/electrophile interactions alongside the optimisation of the sulphur lone pair with both the alkene and the aromatic systems (Figure 1.26). Each of the compounds demonstrates a reduced pyramidalisation of the *peri*-carbon atom and in all cases the alkene moiety lies closer to mean naphthalene plane in order to increase conjugation. Uniquely, the methylthio group of cyanoester **1.78** lies at 109.2(1)° to the naphthalene plane, removing the *ortho*-hydrogen steric repulsion. This allows the methylthio group to be displaced by 2.9° away from the electrophile, which is displaced by only half the distance compared with the similar dinitrile and methylnitro derivatives **1.77** and **1.80**. This additional displacement away from the cyanoester electrophile generates the largest contact distance observed in the series of 2.923(1) Å.

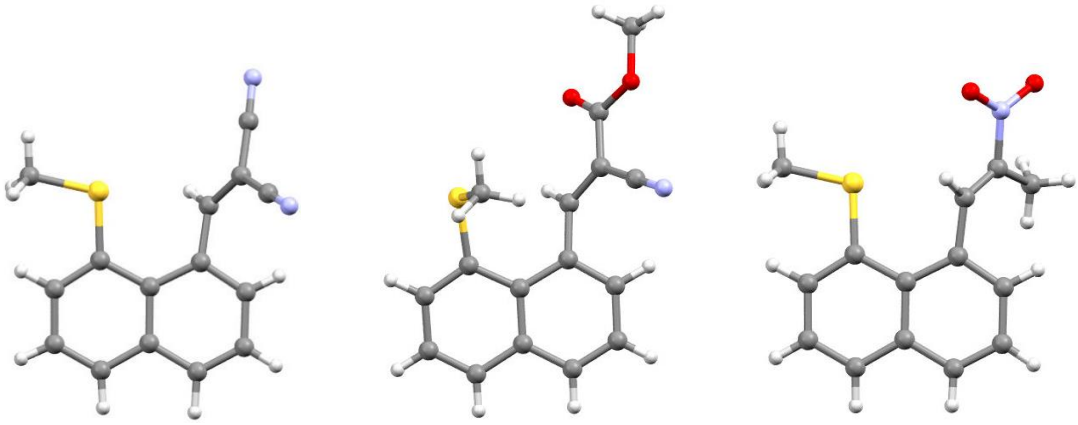

*Figure 1.26. Molecular structures of the dinitrile **1.77** (left), methyl cyanoester **1.78** (middle) and nitromethyl **1.80** (right).*

The final structure in the series is the nitroethenyl derivative **1.79**, which possesses a terminal hydrogen atom on the alkene which lie *cis* to the naphthalene ring (Figure 1.27). The minimum angular orientation between the aromatic system and the alkene in the three derivatives shown in Figure 1.26 is dictated by a steric interaction between the *ortho*-naphthalene proton and the alkene substituent, whereas in the nitro derivative **1.79**, this contact is replaced by a H---H contact. This allows for the alkene group of nitroethenyl derivative **1.79** (36.4(3)^{o}) to lie closer to the naphthalene plane than that of **1.77**, **1.78** and **1.80** (46.7(2)-53.6(3)^{o}). The two *peri*-groups are displaced strongly to either side of the naphthalene plane, with the methylthio group orientated slightly away from the electrophile, which is displaced in the opposite direction. The result of this is the second longest S---C=C contact of the series (2.895(2) Å and the lowest degree of *peri*-carbon pyramidalisation (0.014(8) Å).

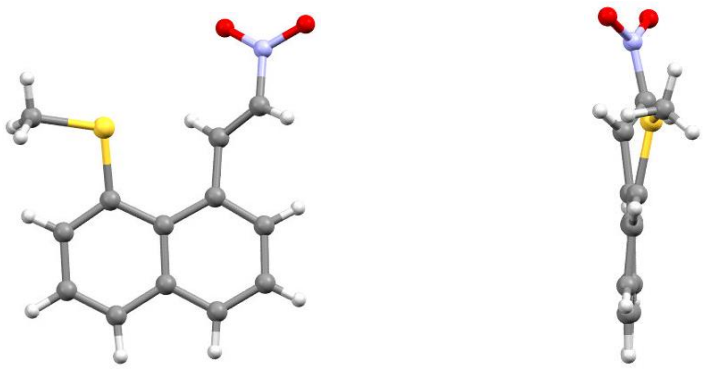

*Figure 1.27. Molecular structure of **1.79** (left) and a view down the naphthalene plane indicating the displacement of each peri-group to either side of the naphthalene plane (right).*

Other Applications for the *Peri*-Naphthalene Scaffold

Peri-naphthalenes have been found to be useful for applications in sulphur chemistry. The work of Grainger *et al.*[123] utilised the *peri*-naphthalene scaffold in the generation of two novel diastereomeric *vic*-disulfoxides, displaying a significantly higher barrier to thermal rearrangement and the shortest (O)S-S(O) bond (2.19 Å) reported for this elusive functionality. The naphthalene scaffold incorporated two *t*-butyl groups in the 2- and 7-positions, causing steric repulsions, which influence the strength of the S-S *peri*-bond (**1.81**). Examples synthesised without the *t*-butyl 'bolsters' did not yield the desired *vic*-disulfoxide with the only isolable product being thio-sulfone **1.82**, shown in Scheme 1.5.

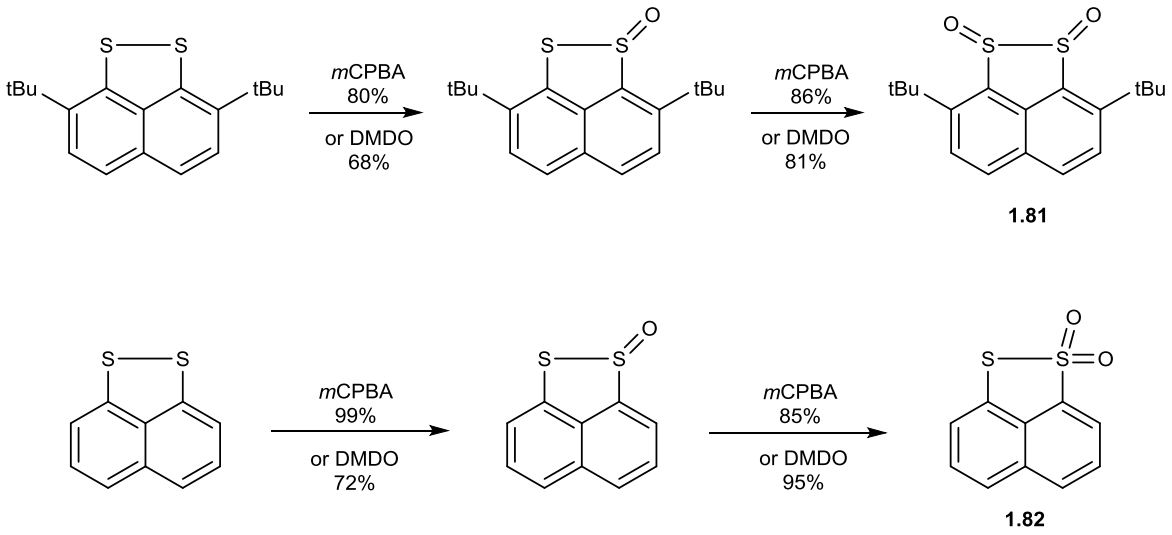

Scheme 1.5. Two synthetic approaches in the oxidation of 1,8-dithianaphthalenes.

Grainger *et al.*[124] further utilised the *peri*-naphthalene scaffold as a means for the generation and transfer of sulphur monoxide to dienes. This is achieved via the synthesis of a strained 1, 2, 3-trithiane-2-oxide ring across the *peri*-positions of naphthalene (Scheme 1.6), which in the solid state adopts a sofa conformation and is evidently strained. Upon heating in the presence of dienes, this ring decomposes, liberating sulphur monoxide which reacts with the diene to give the desired unsaturated cyclic sulfoxides whilst recycling the starting material, 1, 8-

naphthalene disulphide. Similarly, Grainger applied the presence of *ortho* substituents on the naphthalene ring, this time to lower the thermal input required for the degradation of the system by the further destabilisation of the 1, 2, 3-trithiane-2-oxide ring.

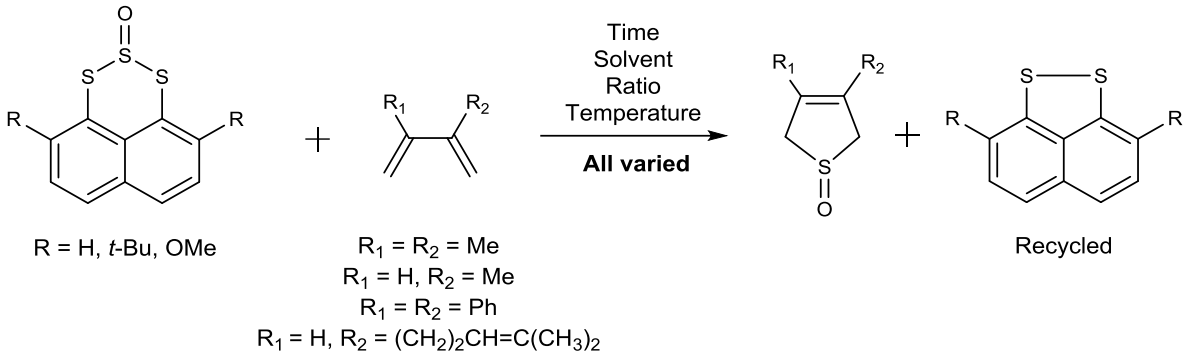

Scheme 1.6. Generalised reaction of the 1, 2, 3-trithiane-2-oxide ring with a variety of dienes, in a range of conditions, giving a variety of sulfoxides, regenerating the 1, 8-dithianaphthalene scaffold.

Peri-Naphthalenes for the Study of Very Long C-C Bonds

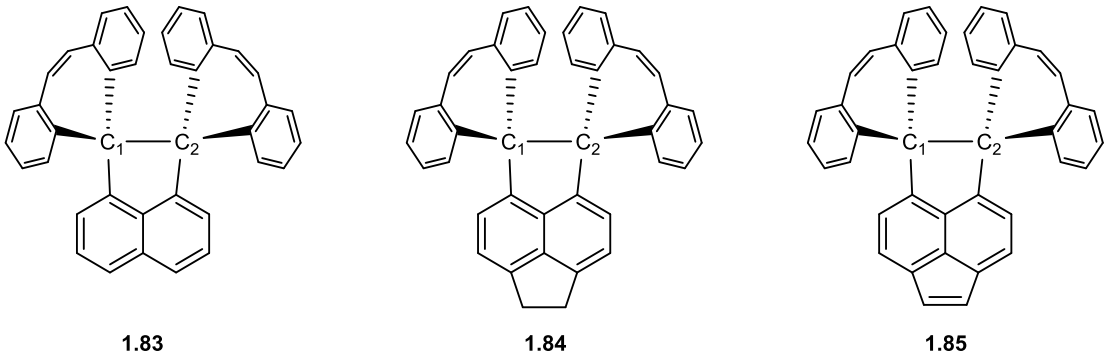

1.83 **1.84** **1.85**

Figure 1.28. The three target structures in Ishigaki's study of long C-C bonds.[128]

The generation of highly elongated and exaggerated C-C bonds has always been an academic challenge. Previous attempts, including the works of Mislow,[125] Herges[126] and Toda[127] have used the molecular skeleton of hexaphenylethane (HPE) in designing their systems. Recently, Suzuki and Ishigaki[128] have employed the *peri*-substituted naphthalene (**1.83**), acenaphthene (**1.84**) and acenaphthylene (**1.85**) scaffolds with dispiro(dibenzocycloheptatriene) groups in the *peri* positions to elongate this bond even further (Figure 1.28). Starting from the respective dihalogenated naphthyl core, the *peri*-substituents were inserted via lithiation and addition of 5-dibenzosuberenone, to give the respective *bis*-alcohol products. Exposure of the diols to acidic conditions in the presence of 1, 1, 1, 3, 3, 3,-hexafluoro-2-propanol (HFIP) gave the dication species, which were reduced with zinc powder to give the desired C-C bonds across the *peri* positions. The two carbon tethers of the acenaphthene and acenaphthylene derivatives pull the base of the fused rings toward each other. This reduction of the exocyclic angle around the 8a-C carbon atom in turn causes the two *peri*-substituents to splay apart slightly broadening the 4a-C exocyclic angle. The exceptionally long C-C bond lengths for the three target compounds thus increase from 1.720(2)-1.742(2) Å (**1.83**) to 1.773 Å (**1.84**) to 1.798(2) Å (**1.85**). It is worth noting that due to the system employed in the generation of the long C-C bonds in **1.83**-**1.85**, if the groups were in fact dissociated, the system could maintain the

appearance of a bond. Despite the C-C bond in **1.85** once holding the title of the longest C-C bond reported, it has since been beaten by the discovery of an even longer 1.93 Å bond in the series of 1,2-diamino-*o*-carboranes developed by Xiao *et al*.[129]

Alternative Skeletons for the Study of Molecular Interactions

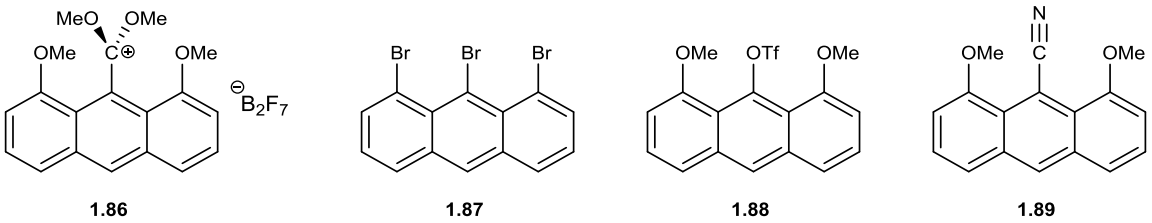

1.86 **1.87** **1.88** **1.89**

*Figure 1.29. The pentacoordinate carbon structure **1.86** and the three comparison structures **1.87-1.89**.*

Naphthalene is not the only skeleton that has been utilised for the study of n-π* interactions. Akiba *et al.* [130–132] have used an anthracene backbone to design and synthesise pentacoordinate (Figure 1.29) and hexacoordinate carbon atoms, stabilised by O---C interactions. The central carbons of the former stabilised systems are trigonal bipyramid (TBP) in nature and are therefore models for the transition state (TS) in S_N2 type reactions. Akiba *et al.*[130] first reported in 1999 carbocation **1.86**, with the unusual counter ion of $B_2F_7^-$. The 1, 8-methoxy groups along with the pentacoordinate C9 carbon are not displaced from the mean plane of the anthracene scaffold, with the pentacoordinate carbon's substituent angles adding up to 360°, confirming no pyramidalisation of the central carbon and that it is sp^2 hybridised. This is in contrast to the findings of Raines *et al.*[88] (Figure 1.16), where the central electrophilic carbon atom of **1.30** displayed pyramidalisation towards one of the two impinging oxygen atoms. Furthermore, the methoxy groups lie entirely in the mean plane of the anthracene scaffold, ensuring the lone pair is directed at the central ester carbon and thus supporting a TBP geometry. The two C---O interaction distances with the 1- and 8-methoxy groups are 2.43(1) and 2.45(1) Å, a distance that is well above the normal covalent C-O bond length (1.43 Å) and below that the sum of the two atoms van der Waals radii (3.25 Å).[10, 94] The group synthesised a selection of comparison compounds (Figure 1.29) to elucidate the properties and the degree of interaction between the central carbon atom and the two oxygen atoms in **1.86**, selected interaction distances are found in Table 1.10.

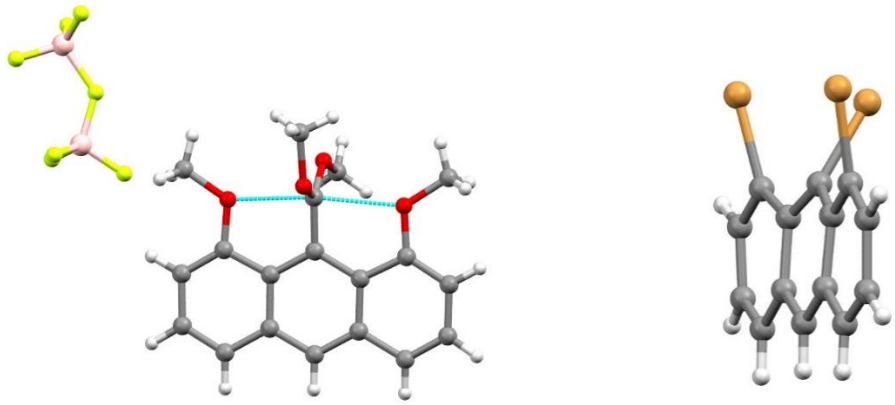

*Figure 1.30. Molecular structure of pentacoordinate carbon structure **1.86** (left) and the tri-bromo anthracene **1.87** (right) showing the displacement of the bromides to opposite sides of the anthracene plane.*

The three bromine or oxygen substituents in the 1-, 8- and 9-positions of anthracenes **1.87** and **1.88**, result in significant steric repulsions between the groups. In order to minimalise these effects, the bulky groups are displaced relative to one another to either side of the idealised anthracene plane (Figure 1.30). These repulsions are not observed in the salt of **1.86**. Furthermore, compound **1.89** with methoxy groups flanking a nitrile group, demonstrates a similar arrangement to **1.86** in that the three groups in the 1-, 8- and 9-positions all remained in the anthracene plane, indicating that the interaction between the two oxygen atoms in **1.86** with the central carbon are attractive and not repulsive in nature. Comparison of the distances between the 1- or 8-substituents (a and a') and the 9-substituent and the distances between the corresponding *ipso* carbons (b and b') also proved useful. In **1.87** and **1.88**, the average a and a' distances (3.2698(6) Å in **1.87**, 2.572(2) Å in **1.88**) are longer than the average of b and b' (2.566(6) Å in **1.87**, 2.550(3) Å in **1.88**). However, in **1.89** the average a and a' and b and b' are comparable with each other (2.531(3) and 2.540(5) Å respectively). In contrast, the same comparison in salt **1.86** finds the averaged a and a' values to be shorter than the averaged b and b' values (2.44(1) and 2.51(2) Å respectively) thus indicating an attractive interaction between the two oxygen atoms and the central carbon.

*Table 1.10. Selected structural parameters for the anthracene derivatives **1.86-1.89**.*

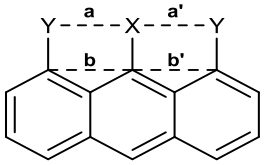

Compound	**a** / Å	**a'** / Å	**b** / Å	**b'** / Å
1.86	3.2658(6)	3.2738(6)	2.564(6)	2.567(6)
1.87	2.572(2)	2.571(2)	2.554(3)	2.545(3)
1.88	2.530(3)	2.531(3)	2.538(6)	2.542(4)
1.89	2.45(1)	2.43(1)	2.49(2)	2.52(2)

Akiba *et al.* continued their work and in 2008 reported the synthesis and structure of a hexacoordinate carbon with 'arguable hypervalence'.[131] To do this they twice exploited the anthracene motif previously used in their work regarding the pentacoordinate carbon. The target dication (**1.91a/1.91b**) was prepared via a demethylation of allene **1.90** affording single crystals of the cation **1.91b** as a borate salt (Figure 1.31).

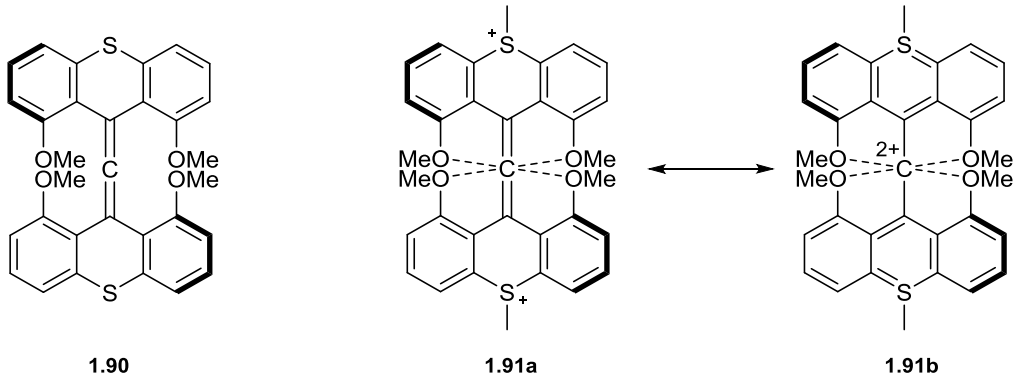

*Figure 1.31. Structures of allene **1.90** (left) and the two resonance structures, **1.91a** and **1.91b**, of the cationic form.*

X-ray data of the neutral and dication structures revealed a significant change in the C---O interaction distances. In the neutral compound **1.90**, the four interactions are split into two larger (2.815 and 2.770 Å) and two smaller contact distances (2.663 and 2.689 Å). However, in the dication **1.91b** the distance between the four distances has reduced (2.641, 2.673, 2.706, 2.750 Å), although a lower degree of variation is observed in the pentacoordinate case. The variations in the C---O distances could be influenced by the severe steric crowding of **1.91b**. Nevertheless, each of the C---O distances fall between the expected covalent C-O bond length

and the sum of the two atom's van der Waals radii. High intensity precision/high resolution X-ray diffraction data of **1.91b** with an alternative borate counter ion was collected using synchrotron radiation. Determination of the charge density distribution data revealed bond paths (of low intensity) between each of the four interacting atoms and the central carbon, indicating that the central carbon may be described as hexacoordinate. Each of the attractive C---O interactions, due to their weakness, is likely to be electrostatic in character, with this data matching that of the pentacoordinate carbon previously described by the team.

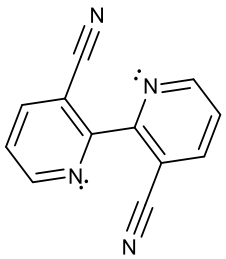

1.92

*Figure 1.32. Structure of the nitrile substituted 2, 2'-bipyridine system **1.92**.*

Wallis *et al.*[133] utilised the 3, 3'-disubstituted 2, 2'-bipyridine system as another useful scaffold for investigating the n-π* interaction between the nucleophilic nitrogen of the pyridine ring and an electrophilic group on the corresponding ring, another potential interaction that can provide information on the early stages corresponding to chemical reactions. A dinitrile group was used as the electrophilic substituent and was prepared via an Ullmann coupling of 2-bromopyridine-3-carbonitrile (Figure 1.32). Structural analysis revealed that the angle between the two pyridine rings of **1.92** is 23.6º, with short N---C attractive interactions occurring between the two pyridine nitrogen's and the two nitrile carbons (Figure 1.33). The contact distances (2.695(2) and 2.740(3) Å) are well within the expected van der Waals for these two atoms (3.2 Å). Both of the nitrile groups (C-C≡N) deviate from linearity by 8.5º such that the *sp*C deviates from the vector through its neighbours towards the adjacent pyridine N atom. Both of the angles

of approach of the pyridine nitrogen's have been optimised rather than the N---C separations, giving two angles (107.6 and 108.0°) which fully adhere to the Bürgi-Dunitz trajectory.

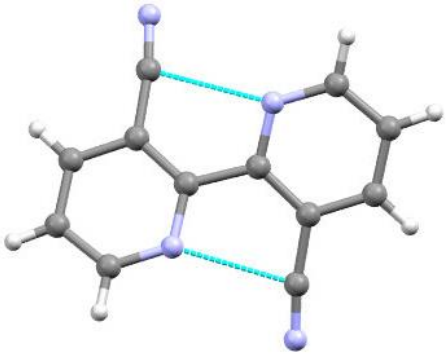

*Figure 1.33. Molecular structure of 2,2'-bipyridine-3,3'-dicarbonitrile **1.92**.*

In a similar vein, biphenyls have been explored by Wallis *et al.* for studying nucleophile/electrophile interactions between the *ortho*-groups of each phenyl ring.[134,135] Using a 2-dimethylaminobiphenyl core, the 2'-position was varied with groups of differing electrophilicities. The biphenyl system has rotational freedom in that the inter-ring bond can allow or deny functional group interaction, as in **1.93**, **1.94**, **1.95** and **1.96** in Figure 1.34.

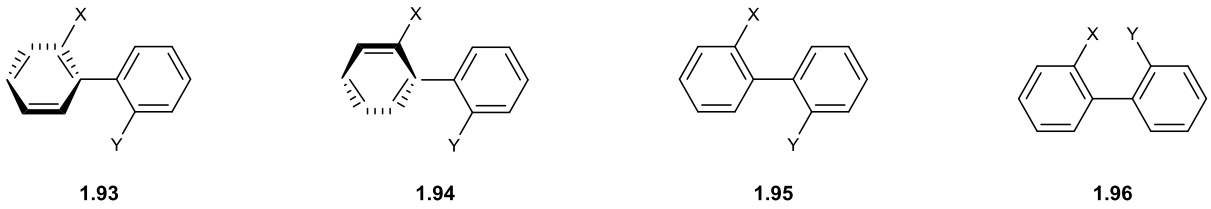

*Figure 1.34. Four of the possible orientations of the biphenyl system, preventing the interaction (**1.93-1.95**) and promoting the interactions (**1.96**).*

Solid-state molecular structures of compounds **1.97-1.101** (Figure 1.35) were obtained and the results are easily divided into two groups. The first, in compounds **1.97-1.99** where the long Me_2N---sp^2C interactions are in the range 2.941(2)-2.981(2) Å, are similar to that of methadone (2.912(3) Å).[61] The second group in compounds **1.100** and **1.101** have formed N-C bonds between the two phenyls, giving zwitterionic structures. Despite the free rotation around the 1, 1'-bond there is no example which displays no interaction between the functional groups. The uncyclised biphenyl examples **1.97-1.99** adopt similar conformations, with the pyramidal

dimethylamino group oriented with N-Me bonds, at *ca.* 112° and 19° to the neighbouring phenyl ring, whilst the carbonyl or alkene lies between 6.2-14.6° to its phenyl ring. In comparison to their *peri*-naphthalene equivalents (where the groups have been forced into closer proximity), a much lower sensitivity in N---C separations is observed, with only a 0.1 Å difference in **1.97-1.99** whilst the aldehyde, cyanoester and nitroalkene display N---C separations of 2.489(5), 2.531(2) and 2.642(2) Å respectively in *peri*-naphthalenes. Furthermore, unlike the *peri*-naphthalene series, the sp^2 carbon involved in these interactions is not significantly pyramidalised. The carbonyl and alkene bond lengths are also shown to be of the expected lengths, thus leading to a reasoning that the interaction between the two groups is either 'open' or 'closed', unlike the *peri*-naphthalenes which demonstrates a range of interactions as electrophilicity is altered.

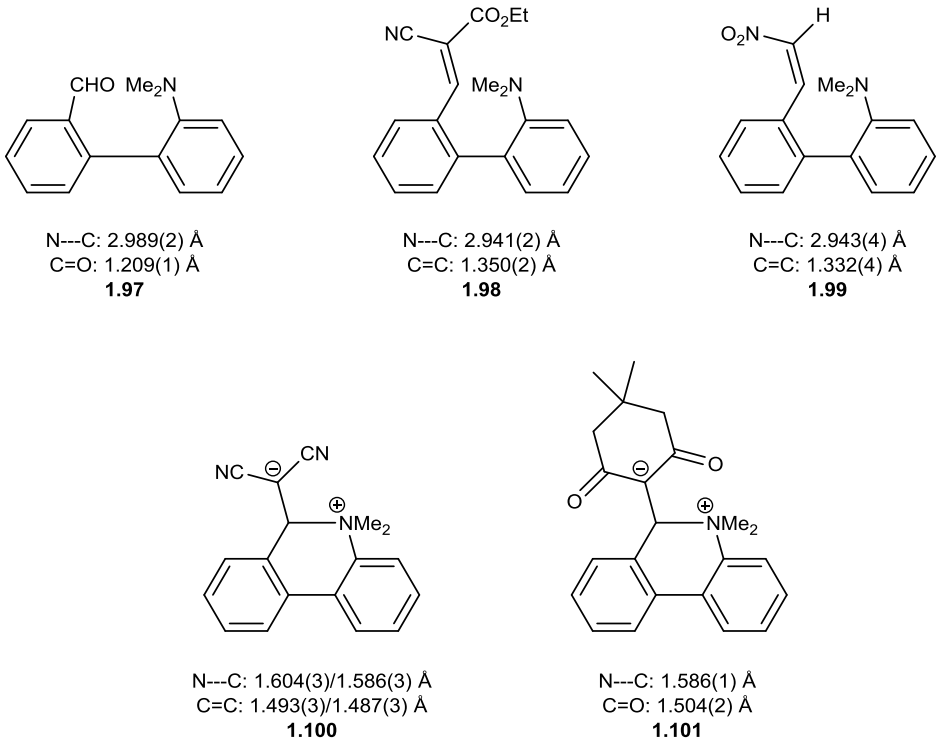

*Figure 1.35. The five biphenyls studied in the Wallis study **1.97-1.101** N---C interaction distances and C=O bond lengths are shown.*

The formation of a long N-C bond in the zwitterionic structures **1.100** and **1.101** generates a new ring which adopts a twisted half chair conformation, similar to 9, 10-

dihydrophenanthrene.[136] In each case, the N-C bond (1.586(1)-1.604(3) Å) is considerably longer than the N-Me bonds already present (1.499(2)-1.513(2) Å). In each case, the negative charge is delocalised through the relevant groups. In **1.101**, the carbonyl bonds are lengthened to 1.254(1) and 1.258(1) Å, while the intervening C-C bonds are shortened to 1.422(2) and 1.427(2) Å displaying some double bond character. In the zwitterion of **1.100**, the delocalisation into the cyano group causes a similar lengthening of the nitrile bonds and a subsequent shortening of the intervening C-C bond. Overall, zwitterions **1.100** and **1.101** provide long N-C bonds formed between a nucleophile and an electrophile (Figure 1.36), whilst the uncyclised structures of **1.97-1.99**, give an insight into molecular interactions between pairs of functional groups more akin to intermolecular interactions, showing attractive forces are utilised in systems where free rotation could easily keep the groups apart.

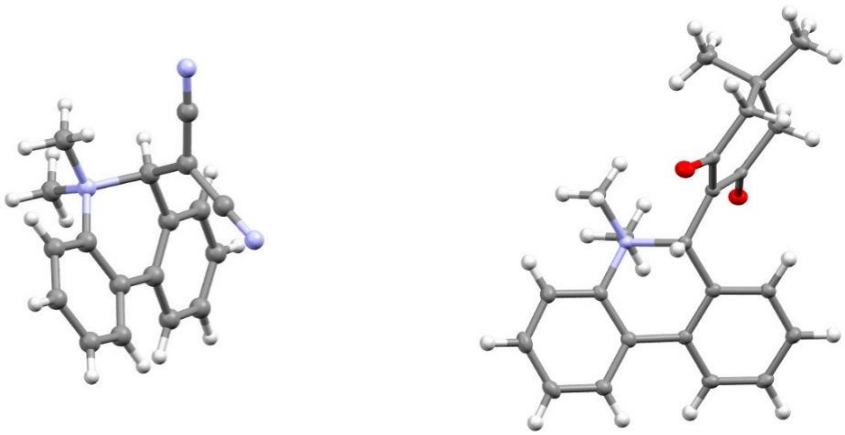

*Figure 1.36. Molecular structures of the dinitrile **1.100** (left) and dimedone **1.101** (right) zwitterionic biphenyl derivatives.*

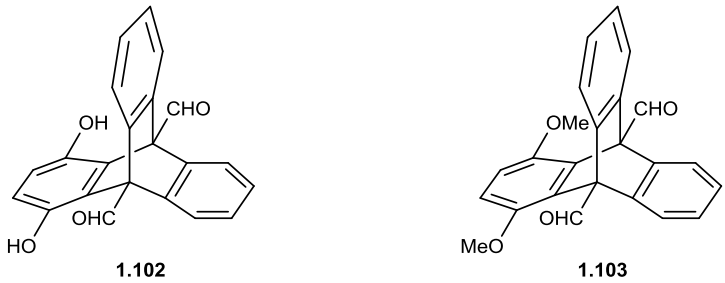

*Figure 1.37. The two triptycene targets, displaying –OH **1.102** (left) and -OMe **1.103** (right) nucleophiles.*

Another interesting scaffold for the analysis of O---C=O interactions is in triptycenes reported by Wallis *et al.*[137] Two triptycene molecules were synthesised to allow for the measurement of 1, 5 interactions between aldehyde groups positioned at sp^3 centres and hydroxyl or methoxy groups, placed at the respective *ortho* positions on the benzene ring as shown in Figure 1.37. Positioning the electrophilic aldehyde at an sp^3 carbon removes the possibility of conjugation to an aromatic system as seen in some previous *peri*-naphthalene examples.

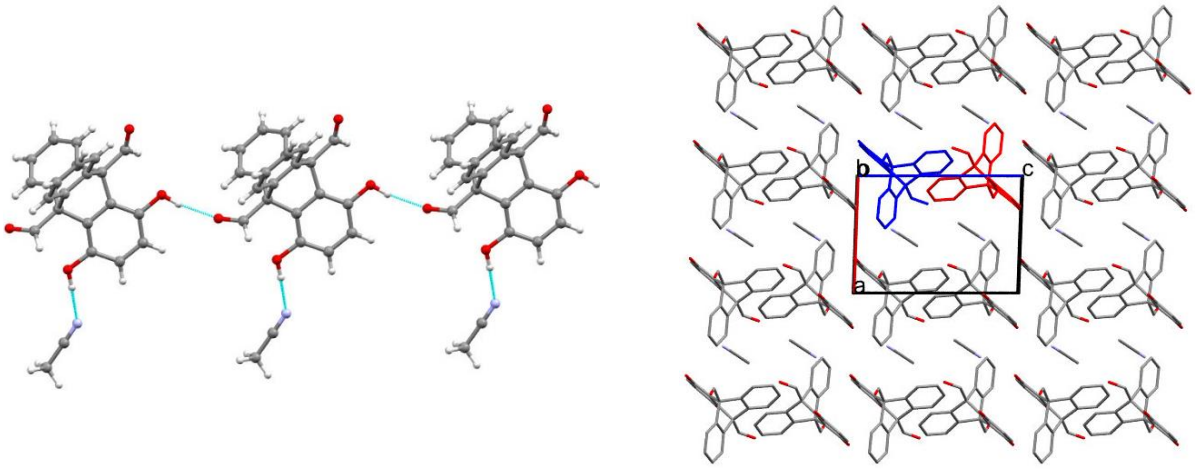

*Figure 1.38. Hydrogen bonding pattern in the crystal structure of **1.102:CH$_3$CN**, in ball and stick model (left) showing the HO---CHO interactions and the crystal packing of **1.102:CH$_3$CN** (right).*

For compound **1.102**, two solvates were isolated with acetonitrile and ethyl acetate and their structures determined via X-ray crystallography at 120 K and 150 K respectively. The acetonitrile solvate was well ordered, however the ethyl acetate solvate contained channels running through the structure, in which the solvent molecules are not well ordered, compared to the rest of the structure. However, the solid-state structure of **1.102:CH$_3$CN** showed that the

OH groups lie in the plane of the benzene ring they are attached too, with their lone pairs pointing in the direction of the aldehyde carbonyl on the bridgehead carbon (Figure 1.38). These contacts lead to O---C interactions of 2.621(2) and 2.679(2) Å, distances that fall below the sum of the two atoms van der Waals radii (3.2 Å).[10] The O---C=O angles of approach for both interactions are 120.1(1)^{o} and 124.7(2)^{o}, which fall close to the expected Bürgi-Dunitz range. Furthermore, both of the hydroxyl groups in each molecule are involved in hydrogen bonds with either a carbonyl group of another molecule or to an acetonitrile molecule.

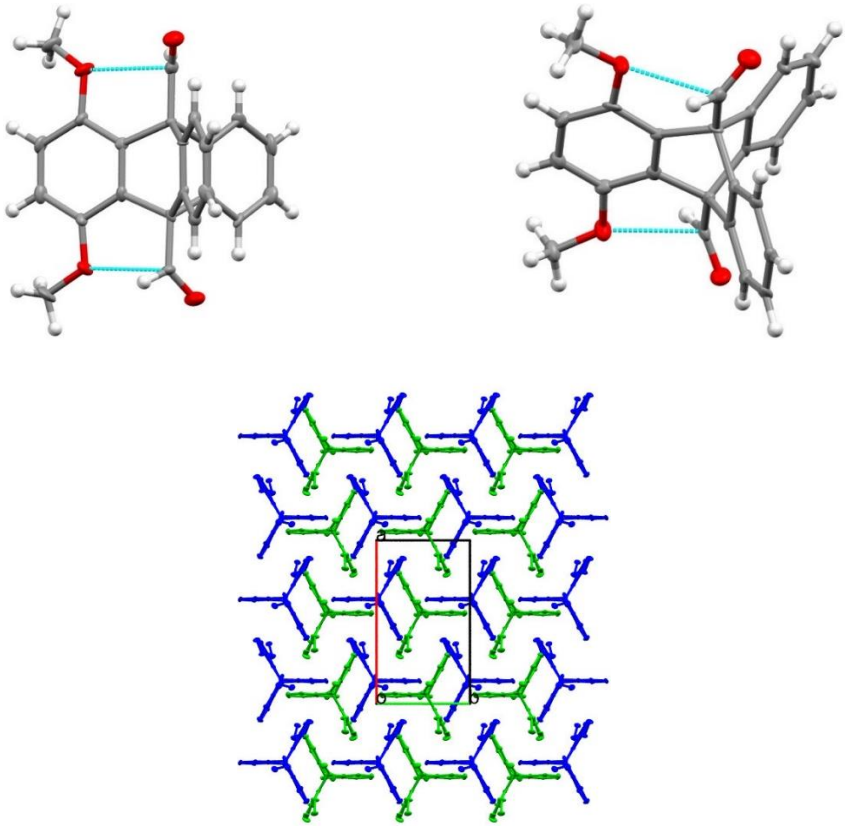

*Figure 1.39. Structures of the two independent molecules of **1.103** (top) and the crystal packing arrangement of **1.103** showing packing of the two independent molecules (blue and green) in layers perpendicular to the c axis (right).*

Structural analysis of the corresponding methoxy compound **1.103**, reveals similar information to **1.102**, however due to two unique molecules in the asymmetric unit, four crystallographically unique O---C=O interactions have been obtained (Figure 1.39). The methoxy groups like the hydroxyl groups lie in the benzene plane and orient their lone pairs toward the carbonyls of the two aldehydes. This allows for angles of approach in the range of

105.2°-114.6°, firmly on the Bürgi-Dunitz trajectory for nucleophilic attack of carbonyls. Furthermore, shorter contacts in the range of 2.528(9)-2.584(9) Å are observed between the methoxy and aldehyde groups. The shorter O---C=O contact distances are a result of the displacement of the methoxy group towards the carbonyl ((aryl)-OMe bond displaced by 3.7-4.5°), due to a steric repulsion between the methyl group and an *ortho* hydrogen. Similarly, each of the carbonyls is involved in an interaction with an *ortho* hydrogen of an unsubstituted benzene ring and the two independent molecules pack in separate layers perpendicular to the *c* axis.

Aims of This Work

The structural data for the compounds summarised in Tables **1.5-1.9**, demonstrate a vast range of interactions between nucleophiles and electrophiles of varying degrees of strength. When the structural data is combined, a series of snap-shot images at different co-ordinates along the reaction pathway for nucleophilic attack of an electrophile are formed. However, the images obtained are heavily focused at either end of the reaction pathway, showing either the moments well before or well after bond formation. For example, using a dimethylamino nucleophile, interactions in *peri*-substituted naphthalenes of short N---C contacts of 2.413(3) Å in dinitrile derivative **1.46** and long N-C bonds of 1.654(1) Å in indandione derivative **1.58** have been observed, with the distances in between remaining inaccessible. Within this thesis, we aim to study new systems based on *peri*-naphthalene to gain structural information on systems with Me_2N---C contacts in the range of 1.65-2.41 Å, in particular by installing substituents at the opposite, unsubstituted second set of *peri*-positions. Furthermore, the first systems with $O^{(-)}$ as a nucleophile will be described.

References

1 K. A. Dill, *Biochemistry*, 1990, **29**, 7133–7155.

2 J. Tomasi and M. Persico, *Chem. Rev.*, 1994, **94**, 2027–2094.

3 C. B. Anfinsen, *Science.*, 1973, **181**, 223–230.

4 C. Bissantz, B. Kuhn and M. Stahl, *J. Med. Chem.*, 2010, **53**, 5061–5084.

5 T. Steiner, *Angew. Chemie - Int. Ed.*, 2002, **41**, 48–76.

6 I. E. Dzyaloshinskii, E. M. Lifshitz and L. P. Pitaevskii, *Adv. Phys.*, 1961, **10**, 165–209.

7 C. A. Hunter, *Angew. Chemie - Int. Ed.*, 2004, **43**, 5310–5324.

8 G. R. Desiraju, *The Crystal as a Supramolecular Entity*, John Wiley & Sons, Chichester, 1996.

9 G. R. Desiraju and A. Gavezzotti, *J. Chem. Soc. Chem. Commun.*, 1989, 621–623.

10 A. Bondi, *J. Phys. Chem.*, 1964, **68**, 441–451.

11 A. Gavezzotti, *J. Am. Chem. Soc.*, 1983, **105**, 5220–5225.

12 R. S. Rowland and R. Taylor, *J. Phys. Chem.*, 1996, **18**, 7384–7391.

13 S. C. Nyburg and C. H. Faerman, *Acta Crystallogr.*, 1985, **41**, 274–279.

14 M. Mantina, A. C. Chamberlin, R. Valero, C. J. Cramer and D. G. Truhlar, *J. Phys. Chem.* 2009, **113**, 5806–5812.

15 S. Alvarez, *Dalton Trans.*, 2013, **42**, 8617–8636.

16 M. Rahm, R. Hoffmann and N. W. Ashcroft, *Chem. Eur. J.*, 2016, **22**, 14625–14632.

17 M. Nishio, Y. Umezawa, M. Hirota and Y. Takeuchi, *Tetrahedron*, 1995, **51**, 8665–8701.

18 M. Nishio, Y. Umezawa, K. Honda, S. Tsuboyama and H. Suezawa, *CrystEngComm*, 2009, **11**, 1757–1788.

19 C. A. Hunter and J. K. M. Sanders, *J. Am. Chem. Soc.*, 1990, **112**, 5525–5534.

20 S. K. Burley and G. A. Petsko, *J. Am. Chem. Soc.*, 1986, **108**, 7995–8001.

21 L. Pauling, *The Nature of the Chemical Bond*, Cornell University Press, New York, 1939.

22 P. Atkin and J. Paula, *Physical Chemistry*, Oxford University Press, Oxford, 8th edn., 2006.

23 G. C. Pimentel and A. L. McClellan, *The Hydrogen Bond*, W. H. Freeman and Company,

London, 1960.

24 G. A. Jeffrey, *An Introduction to Hydrogen Bonding*, Oxford University Press, Oxford, 1997.

25 C. B. Aakeröy and K. R. Seddon, *Chem. Soc. Rev.*, 1993, **22**, 397–407.

26 D. M. Kneeland, K. Ariga, V. M. Lynch, C. Y. Huang and E. V. Anslyn, *J. Am. Chem. Soc.*, 1993, **115**, 10042–10055.

27 M. C. Grossel, D. A. S. Merckel and M. G. Hutchings, *CrystEngComm*, 2003, **5**, 77–81.

28 V. Jubian, R. P. Dixon and A. D. Hamilton, *J. Am. Chem. Soc.*, 1992, **114**, 1120–1121.

29 R. P. Dixon, S. J. Geib and A. D. Hamilton, *J. Am. Chem. Soc.*, 1992, **114**, 365–366.

30 G. R. Desiraju, P. S. Ho, L. Kloo, A. C. Legon, R. Marquardt, P. Metrangolo, P. Politzer, G. Resnati and K. Rissanen, *Pure Appl. Chem.*, 2013, **85**, 1711–1713.

31 T. M. Beale, M. G. Chudzinski, M. G. Sarwar and M. S. Taylor, *Chem. Soc. Rev.*, 2013, **42**, 1667–1680.

32 T. Clark, M. Hennemann, J. S. Murray and P. Politzer, *J. Mol. Model.*, 2007, **13**, 291–296.

33 P. Metrangolo and G. Resnati, *Science.*, 2008, **321**, 918–919.

34 P. Metrangolo and G. Resnati, *Chem. Eur. J.*, 2001, **7**, 2511–2519.

35 E. Corradi, S. V Meille, M. T. Messina, P. Metrangolo and G. Resnati, *Angew. Chemie - Int. Ed.*, 2000, **39**, 1782–1786.

36 J. S. Murray, P. Lane, T. Clark and P. Politzer, *J. Mol. Model.*, 2007, **13**, 1033–1038.

37 L. Vogel, P. Wonner and S. M. Huber, *Angew. Chemie - Int. Ed.*, 2019, **58**, 1880–1891.

38 P. Scilabra, G. Terraneo and G. Resnati, *Acc. Chem. Res.*, 2019, **52**, 1313–1324.

39 R. E. Rosenfield, R. Parthasarathy and J. D. Dunitz, *J. Am. Chem. Soc.*, 1977, **99**, 4860–4862.

40 H. B. Bürgi and J. D. Dunitz, *J. Am. Chem. Soc.*, 1987, **109**, 2924–2926.

41 M. Iwaoka and S. Tomoda, *J. Am. Chem. Soc.*, 1996, **118**, 8077–8084.

42 M. Iwaoka and N. Isozumi, *Molecules*, 2012, **17**, 7266–7283.

43 P. Politzer, J. S. Murray, T. Clark and G. Resnati, *Phys. Chem. Chem. Phys.*, 2017, **19**, 32166–32178.

44 T. N. G. Row and R. Parthasarathy, *J. Am. Chem. Soc.*, 1981, **103**, 477–479.

45 R. Laitinen, R. Steudel and R. Weiss, *Dalton Trans.*, 1986, 1095–1100.

46 R. Weiss, C. Schlierf and K. Schloter, *J. Am. Chem. Soc.*, 1976, **98**, 4668–4669.

47 S. Kubiniok, W.-W. du Mont, S. Pohl and W. Saak, *Angew. Chemie - Int. Ed.*, 1988, **27**, 431–433.

48 A. Panda, G. Mugesh, H. B. Singh and R. J. Butcher, *Organometallics*, 1999, **18**, 1986–1993.

49 P. Rakesh, H. B. Singh and R. J. Butcher, *Organometallics*, 2013, **32**, 7275–7282.

50 S. C. Menon, H. B. Singh, J. M. Jasinski, J. P. Jasinski and R. J. Butcher, *Organometallics*, 1996, **15**, 1707–1712.

51 F. H. Allen, O. Kennard, D. G. Watson, L. Brammer, A. G. Orpen and R. Taylor, *J. Chem. Soc. Perkin Trans. 2*, 1987, 1–19.

52 I. K. Mati and S. L. Cockroft, *Chem. Soc. Rev.*, 2010, **39**, 4195–4205.

53 S. Sankararaman, G. Venkataramana and B. Varghese, *J. Org. Chem.*, 2008, **73**, 2404–2407.

54 S. Paliwal, S. Geib and C. S. Wilcox, *J. Am. Chem. Soc.*, 1994, **116**, 4497–4498.

55 E. I. Kim, S. Paliwal and C. S. Wilcox, *J. Am. Chem. Soc.*, 1998, **120**, 11192–11193.

56 F. Cozzi, M. Cinquini, R. Annunziata, T. Dwyer and J. S. Siegel, *J. Am. Chem. Soc.*, 1992, **114**, 5729–5733.

57 W. H. Perkin, *J. Chem. Soc. Trans.*, 1916, **109**, 815–877.

58 W. O. Kermack and R. Robinson, *J. Chem. Soc. Trans.*, 1922, **121**, 427–440.

59 R. Huisgen, H. Wieland and H. Eder, *Justus Liebigs Ann. Chem.*, 1949, **561**, 193–215.

60 R. Robinson and A. M. Stephens, *Nature*, 1948, **162**, 177–178.

61 H. B. Bürgi, J. D. Dunitz and E. Shefter, *J. Am. Chem. Soc.*, 1973, **95**, 5065–5067.

62 A. Tulinsky and J. H. Van den Hende, *J. Am. Chem. Soc.*, 1967, **89**, 2905–2911.

63 J. A. Wunderlich, *Acta Crystallogr.*, 1967, **23**, 846–855.

64 S. R. Hall, *Acta Crystallogr.*, 1968, **24**, 337–346.

65 K. B. Birnbaum, A. Klásek, P. Sedmera, G. Snatzke, L. F. Johnson and F. Šantavý, *Tetrahedron Lett.*, 1971, **12**, 3421–3424.

66 K. B. Birnbaum, *Acta Crystallogr.*, 1972, **28**, 2825–2833.

67 S. R. Hall and F. R. Ahmed, *Acta Crystallogr.*, 1968, **24**, 346–355.

68 H. B. Bürgi, J. D. Dunitz, J. M. Lehn and G. Wipff, *Tetrahedron*, 1974, **30**, 1563–1572.

69 H. B. Bürgi, J. D. Dunitz and E. Shefter, *Acta Crystallogr.*, 1974, **30**, 1517–1527.

70 D. Rabinovich, G. M. J. Schmidt and Z. Shaked, *J. Chem. Soc. B Phys. Org.*, 1970, 17–24.

71 D. Kobelt and E. F. Paulus, *Acta Crystallogr.*, 1973, **29**, 633–635.

72 J. E. Baldwin, *J. Chem. Soc. Chem. Commun.*, 1976, 734–736.

73 C. L. Liotta, E. M. Burgess and W. H. Eberhardt, *J. Am. Chem. Soc.*, 1984, **106**, 4849–4852.

74 D. Seebach and J. Golinski, *Helv. Chim. Acta*, 1981, **64**, 1413–1423.

75 M. A. Brook and D. Seebach, *Can. J. Chem.*, 1987, **65**, 836–850.

76 E. Wagner, Y. Xiang, K. Baumann, J. Gück and A. Eschenmoser, *Helv. Chim. Acta*, 1990, **73**, 1391–1409.

77 P. H. Maccallum, R. Poet and E. James Milner-White, *J. Mol. Biol.*, 1995, **248**, 361–373.

78 P. H. Maccallum, R. Poet and E. James Milner-White, *J. Mol. Biol.*, 1995, **248**, 374–384.

79 F. H. Allen, C. A. Baalham, J. P. M. Lommerse and P. R. Raithby, *Acta Crystallogr.*, 1998, **54**, 320–329.

80 R. W. Newberry and R. T. Raines, *Acc. Chem. Res.*, 2017, **50**, 1838–1846.

81 G. J. Bartlett, A. Choudhary, R. T. Raines and D. N. Woolfson, *Nat. Chem. Biol.*, 2010, **6**, 615–620.

82 G. J. Bartlett, R. W. Newberry, B. VanVeller, R. T. Raines and D. N. Woolfson, *J. Am. Chem. Soc.*, 2013, **135**, 18682–18688.

83 L. E. Bretscher, C. L. Jenkins, K. M. Taylor, M. L. DeRider and R. T. Raines, *J. Am. Chem. Soc.*, 2001, **123**, 777–778.

84 P. Wilhelm, B. Lewandowski, N. Trapp and H. Wennemers, *J. Am. Chem. Soc.*, 2014, **136**, 15829–15832.

85 Robert W. Newberry and Ronald T. Raines, *Chem. Commun.*, 2013, **49**, 7699-7701.

86 A. Choudhary, D. Gandla, G. R. Krow and R. T. Raines, *J. Am. Chem. Soc.*, 2009, **131**, 7244–7246.

87 R. W. Newberry, B. VanVeller, I. A. Guzei and R. T. Raines, *J. Am. Chem. Soc.*, 2013, **135**, 7843–7846.

88 A. Choudhary, C. G. Fry, K. J. Kamer and R. T. Raines, *Chem. Commun.*, 2013, **49**, 8166–8168.

89 A. Choudhary, K. J. Kamer and R. T. Raines, *J. Org. Chem.*, 2011, **76**, 7933–7937.

90 C. Cabezas, J. L. Alonso, J. C. López and S. Mata, *Angew. Chemie - Int. Ed.*, 2012, **51**, 1375–1378.

91 A. Habibi-Yangjeh and M. Esmailian, *Chinese J. Chem.*, 2008, **26**, 875–885.

92 J. Oddershede and S. Larsen, *J. Phys. Chem.* 2004, **108**, 1057–1063.

93 H. A. Favre and W. H. Powell, *Nomenclature of Organic Chemistry: IUPAC Recommendations and Preferred Names*, Royal Society of Chemistry, Cambridge, 2013.

94 J. A. Dean, *Lange'S Handbook of Chemistry*, McGraw-Hill, Inc, New York, 15th edn., 1999.

95 D. Bright, I. E. Maxwell and J. de Boer, *J. Chem. Soc. Perkin Trans. 2*, 1973, 2101–2105.

96 M. B. Jameson and B. R. Penfold, *J. Chem. Soc.*, 1963, 528–536.

97 A. E. Jungk and G. M. J. Schmidt, *Chem. Ber.*, 1971, **104**, 3272–3288.

98 H. Einspahr, J. B. Robert, R. E. Marsh and J. D. Roberts, *Acta Crystallogr.*, 1973, **29**, 1611–1617.

99 J. Handal, J. G. White, R. W. Franck, Y. H. Yuh and N. L. Allinger, *J. Am. Chem. Soc.*, 1977, **99**, 3345–3349.

100 K. Yamamoto, N. Oyamada, S. Xia, Y. Kobayashi, M. Yamaguchi, H. Maeda, H. Nishihara, T. Uchimaru and E. Kwon, *J. Am. Chem. Soc.*, 2013, **135**, 16526–16532.

101 W. B. Schweizer, G. Procter, M. Kaftory and J. D. Dunitz, *Helv. Chim. Acta*, 1978, **61**, 2783–2808.

102 H. Schumann, S. Dechert, M. Hummert, K. C. H. Lange, S. Schutte, B. C. Wassermann, K. Köhler and J. Eichhorn, *Zeitschrift für Anorg. und Allg. Chemie*, 2004, **630**, 1196–1204.

103 M. Mickoleit, K. Schmohl, R. Kempe and H. Oehme, *Angew. Chemie - Int. Ed.*, 2000, **39**, 1610–1612.

104 F. Carré, R. J. P. Corriu, A. Kpoton, M. Poirier, G. Royo, J. C. Young and C. Belin, *J. Organomet. Chem.*, 1994, **470**, 43–57.

105 J. T. B. H. Jastrzebski, J. Boersma, P. M. Esch and G. Van Koten, *Organometallics*, 1991, **10**, 930–935.

106 F. Carré, C. Chuit, R. J. P. Corriu, P. Monforte, N. K. Nayyar and C. Reyé, *J. Organomet. Chem.*, 1995, **499**, 147–154.

107 P. C. Bell and J. D. Wallis, *Chem. Commun.*, 1999, **2**, 257–258.

108 N. Mercadal, S. P. Day, A. Jarmyn, M. B. Pitak, S. J. Coles, C. Wilson, G. J. Rees, J. V. Hanna and J. D. Wallis, *CrystEngComm*, 2014, **16**, 8363–8374.

109 D. R. W. Hodgson, A. J. Kirby and N. Feeder, *J. Chem. Soc. Perkin Trans. 1*, 1999, 949–954.

110 P. C. Bell, M. Drameh, N. Hanly and J. D. Wallis, *Acta Crystallogr.*, 2000, **56**, 670–

671.

111 A. Lari, M. B. Pitak, S. J. Coles, G. J. Rees, S. P. Day, M. E. Smith, J. V. Hanna and J. D. Wallis, *Org. Biomol. Chem.*, 2012, **10**, 7763–7779.

112 J. O'Leary, X. Formosa, W. Skranc and J. D. Wallis, *Org. Biomol. Chem.*, 2005, **3**, 3273–3283.

113 J. Clayden, C. McCarthy and M. Helliwell, *Chem. Commun.*, 1999, 2059–2060.

114 Á. Földi, K. Ludányi, A. Bényei and P. Mátyus, *Synlett*, 2010, 2109–2113.

115 H. Bock and N. Nagel, *Naturforsch. B.*, 1998, 792–804.

116 G. P. Schiemenz, *Zeitschrift für Naturforsch. B*, 2006, **61**, 535–554.

117 G. P. Schiemenz, S. Petersen and S. Porksen, *Zeitschrift für Naturforsch. B*, 2003, **58b**, 715–724.

118 A. C. Blackburn and R. E. Gerkin, *Acta Crystallogr.*, 1997, **53**, 1077–1080.

119 R. E. Gerkin, *Acta Crystallogr.*, 1997, **53**, 1987–1989.

120 J. O'Leary, P. C. Bell, J. D. Wallis and W. B. Schweizer, *J. Chem. Soc. Perkin Trans. 2*, 2001, 133–139.

121 J. C. Gallucci, D. J. Hart and D. G. J. Young, *Acta Crystallogr.*, 1998, **54**, 73–81.

122 J. O'Leary and J. D. Wallis, *Chem. Eur. J.*, 2006, **12**, 7724–7732.

123 R. S. Grainger, B. Patel and B. M. Kariuki, *Angew. Chemie - Int. Ed.*, 2009, **48**, 4832–4835.

124 R. S. Grainger, B. Patel, B. M. Kariuki, L. Male and N. Spencer, *J. Am. Chem. Soc.*, 2011, **133**, 5843–5852.

125 B. Kahr, D. Van Engen and K. Mislow, *J. Am. Chem. Soc.*, 1986, **108**, 8305–8307.

126 S. Kammermeier, R. Herges and P. G. Jones, *Angew. Chemie - Int. Ed.*, 1997, **36**, 1757–1760.

127 K. Tanaka, N. Takamoto, Y. Tezuka, M. Kato and F. Toda, *Tetrahedron*, 2001, **57**, 3761–3767.

128 Y. Ishigaki, T. Shimajiri, T. Takeda, R. Katoono and T. Suzuki, *Chem*, 2018, **4**, 795–806.

129 J. Li, R. Pang, Z. Li, G. Lai, X.-Q. Xiao and T. Müller, *Angew. Chemie - Int. Ed.*, 2019, **58**, 1397–1401.

130 K. Akiba, M. Yamashita, Y. Yamamoto and S. Nagase, *J. Am. Chem. Soc.*, 1999, **121**, 10644–10645.

131 T. Yamaguchi, Y. Yamamoto, D. Kinoshita, K. Akiba, Y. Zhang, C. A. Reed, D.

Hashizume and F. Iwasaki, *J. Am. Chem. Soc.*, 2008, **130**, 6894–6895.

132 Y. Kikuchi, M. Ishii, K. Akiba and H. Nakai, *Chem. Phys. Lett.*, 2008, **460**, 37–41.

133 P. N. W. Baxter, J. A. Connor, D. C. Povey and J. D. Wallis, *J. Chem. Soc., Chem. Commun.*, 1991, **16**, 1135–1137.

134 J. O'Leary, J. D. Wallis and M. L. Wood, *Acta Crystallogr.*, 2001, **57**, 851–853.

135 J. O'Leary and J. D. Wallis, *Org. Biomol. Chem.*, 2009, **7**, 225–228.

136 R. Cosmo, T. W. Hambley and S. Sternhell, *J. Org. Chem.*, 1987, **52**, 3119–3123.

137 A. Lari, M. B. Pitak, S. J. Coles, E. Bresco, P. Belser, A. Beyeler, M. Pilkington and J. D. Wallis, *CrystEngComm*, 2011, **13**, 6978–6984.

Chapter 2

Structural Models for the Study of Hydroxy/Oxyanion Nucleophiles in *Peri*-Naphthalene Interactions

Single Crystal X-ray Diffraction Overview

X-ray crystallography is a standard technique for determining the molecular structure of materials available as a single crystal. Monochromatic MoKa or CuKa radiation is diffracted by the crystal according to Bragg's law and data collected on an automated diffractometer. This is usually carried out with the crystal cooled to 150 K or 100 K by a stream of cold dry nitrogen gas. The low temperature reduces the thermal motion of the molecules, leads to an improvement in the measurement of bond lengths, and also leads to stronger diffraction so that the weaker diffractions are more accurately measured. After applications of various corrections including absorption by the atoms in the crystal, equivalent reflections are merged, dependant on the crystal system. The electron density is given by the Fourier Transform of the amplitudes of the diffracted waves along with their relative phases. The former is available as the square root of the intensities, but the phases have to be generated by "direct methods", easier for a centrosymmetric structures where there are just two values (0^o or 180^o). Such programs depend in part on relations between the phases of certain sets of reflections. Given a crude electron density map, the user assigns the main peaks of electron density as particular atoms. Refinement involves minimising the difference between the observed and calculated structure factors for all the reflections. This optimises the positions of the assigned atoms, and new atoms are revealed in difference Fourier maps. For organic molecules hydrogen atoms are typically placed in expected positions, unless their location is of particular interest. Initially non-hydrogen atoms are treated as having spherical electron density distributions, but in the later stages of refinement these are changed to anisotropic ellipsoidal shapes to allow for thermal motion of the atoms and, to some degree, the actual distribution of electron density. The intensity of scattering by a particular atom is attenuated by the increased atom motion. A refinement is finalised by applying a weighting scheme which aims to give more weight to the more accurately measured reflections. The final degree of agreement is expressed by two "R-

factors" for unweighted and weighted data. The SHELX suite of programs is commonly used for this[1,2] and is implemented through the XSEED or OLEX[2] software packages.[3,4] Thus for a standard X-ray crystal structure determination, the molecule is really represented by a set of isolated atoms.

Within this thesis, crystals were grown primarily via slow evaporation of solutions in volatile organic solvents. Once crystals were obtained, a general procedure was performed where the crystals were placed onto a microscope slide, an oil (typically silicone) was added and the crystals rotated between crossed polar lenses. Crystals which extinguish the light universally were selected as potential candidates for structure determination. For each structure, several crystals were screened, using shortened exposure times to give an initial assessment of their diffraction and to obtain a preliminary unit cell. Depending on the outcome of this either; the data was collected for that crystal, a new crystal was selected from the existing batch, or the crystals were regrown in order to obtain better quality crystals. If necessary, the crystals were cut to size (typically 0.2–0.3 mm) and the X-ray crystal structures were determined at low temperatures (< 150 K). This methodology applies for each crystal structure obtained within this thesis unless stated otherwise.

Introduction

The *peri*-naphthalene scaffold's unique structure has been ideal for studying the interaction between a nucleophile and an electrophile across the *peri*-positions. Several investigative 1, 8-disubstituted naphthalene series have been constructed which employ different nucleophiles (such as –NMe[5-18], -OMe[6,11,19,20] and –SMe[21]) and electrophiles (such as carbonyls and alkenes). The structural analysis of some of these compounds has revealed 'snap-shot' images, which represent different points along the reaction pathway for nucleophilic addition to an electrophile, expanding the understanding of how bond formation proceeds. Further to this, these 1,8-*peri* naphthalenes give a greater knowledge and understanding of how such interactions in small organic molecules occur, and how they may influence the surround chemical environment. By further developing the understanding of these interactions within small molecules, their contribution toward supramolecular biology and chemistry can be better understood.

Herein lies the investigation into the interactions of the 1-naphthol group and subsequently the expectantly more reactive 1-naphtholate anion, with a variety of adjacent *peri*-electrophilic ketones and alkenes. We aim to assess whether a *peri*-interaction is observed and if so, whether that interaction (in the most electron deficient examples) can lead to bond formation, such as those demonstrated in the series involving the dimethylamino nucleophile.[10,18] An important factor to consider is that the oxygen atom of both the hydroxyl and naphtholate anion can conjugate with the aromatic naphthalene system, which in turn reduces the potency of the oxygen atom as a nucleophile. Deprotonation to generate the oxyanion should dominate this tendency, leading to an increase in the strength of the interaction and a reduction in the contact distance between the *peri*-atoms.

Study of $O^{(-)}$---C=O interactions

The synthetic work centred on reactions of 1, 8-naphtholactone **2.1** which was prepared according to the literature procedure described by Cammidge *et al.*[22] in two steps from 1, 8-naphthalic anhydride, via the respective lactam. This lactone provided a starting material that could be ring opened with a range of organo-lithium reagents, to give the desired hydroxyl ketone derivatives (Scheme 2.1). In each case, the organo-lithium of choice was added to a solution of 1, 8-naphtholactone in anhydrous THF at -78 ^{o}C, with the reaction being allowed to warm to room temperature or held at -78 ^{o}C before quenching with water. Extraction and further washing with organic solvent gave the crude material, which was purified by flash column chromatography. Ring opening of the lactone **2.1** with phenyl lithium gave the desired *peri*-hydroxyl phenyl ketone **2.2**[23] in a 32% yield. There was a notable change in the ^{13}C NMR shift of the lactone carbonyl from 174.4 ppm to 201.7 ppm in **2.2**. Furthermore, the carbonyl stretching frequency in the infrared spectrum shifted from 1774 cm^{-1} for the lactone **2.1** to 1638 cm^{-1} for the ketone **2.2**. As expected, the diphenyl tertiary alcohol **2.3** was also isolated from the reaction along with a small amount of dehydrated diphenyl 1, 8-cyclic naphthalene **2.4** (Scheme 2.1).

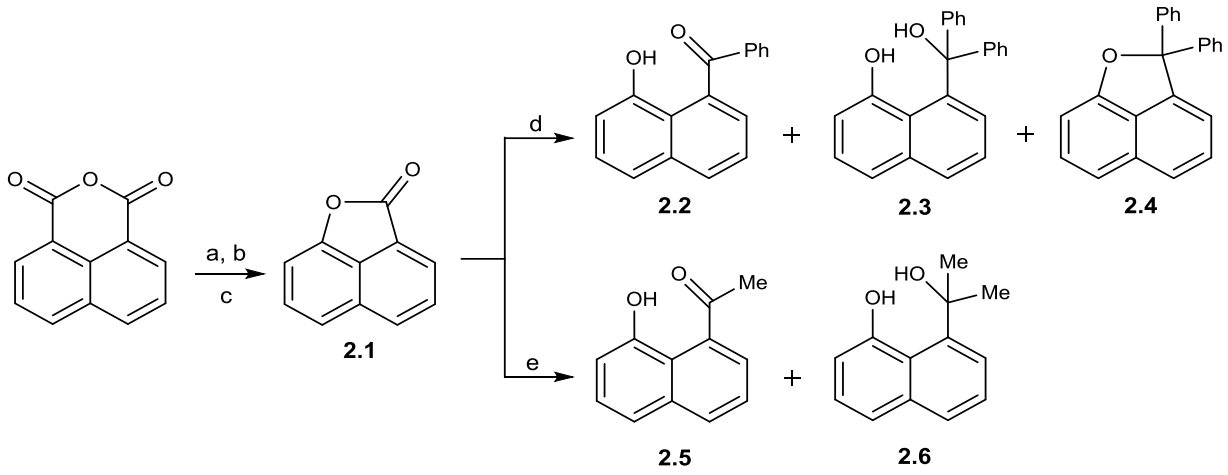

Scheme 2.7. (a) Hydroxylamine hydrochloride, pyridine, reflux followed by p*-toluene sulfonyl chloride* [22] *(b) NaOH, reflux (c) 0 ^{o}C, sodium nitrite, H_2SO_4, 0 ^{o}C to 70 ^{o}C (d) PhLi (1.8M), THF, -78 ^{o}C; (e) MeLi (1.6M), THF, -78 ^{o}C.*

Addition of methyl lithium to lactone **2.1** resulted in the expected *peri*-hydroxyl methyl ketone **2.5** in a 42% yield, with the only other product of note being the di-methyl tertiary alcohol **2.6**, formed by the addition of a further equivalent of methyl lithium to the ketone **2.5** (Scheme 2.1). Synthesis of the methyl ketone **2.5** is supported by the addition of signal in the ^{1}H NMR spectrum at 2.78 ppm for the methyl peak, with the ketone carbonyl signal shifted to 207.3 ppm in the ^{13}C NMR spectrum (lactone carbonyl: 174.4 ppm).

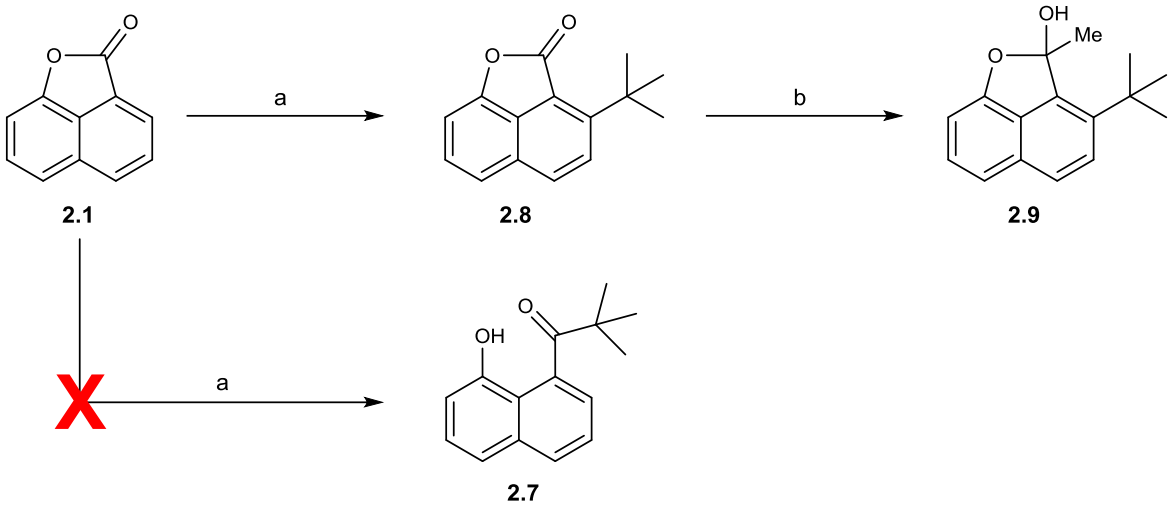

Scheme 2.8. (a) t-BuLi (1.6M), THF, -78 °C; (b) MeLi (1.2M), THF, -78 °C.

Looking to increase the steric bulk of the substituted ketone, *tert*-butyl lithium was employed in the ring opening of lactone **2.1**, but the expected *peri*-hydroxyl *tert*-butyl ketone **2.7** was not isolated (Scheme 2.2). Instead, a *tert*-butyl group had added to the ring carbon *ortho* to the carbonyl group, which after oxidation in the air gave the hindered lactone **2.8** in 14% yield as the only isolable product. Analysis of **2.8** by ^{1}H NMR revealed the loss of one of the aromatic protons, with four doublets and one triplet being observed, and with the *tert*-butyl group signal residing at 1.60 ppm. Signals in the ^{13}C NMR and infrared spectra of 167.1 ppm and 1768 cm^{-1} respectively for the ester carbonyl group represent a retention of the lactone functionality. Crystals of the hindered lactone **2.8** were grown via slow evaporation of a DCM solution, with the X-ray structure of one of these crystals determined at 150 K. As shown in Figure 2.1, the

structure of the hindered lactone **2.8** was confirmed, with the *tert*-butyl group placing two of its methyl groups to either side of the naphthalene plane. The carbonyl and *tert*-butyl groups are splayed apart to reduce steric hindrance. The C-C=O *exo*-cyclic angle between the groups is widened to 136.2(2)°.

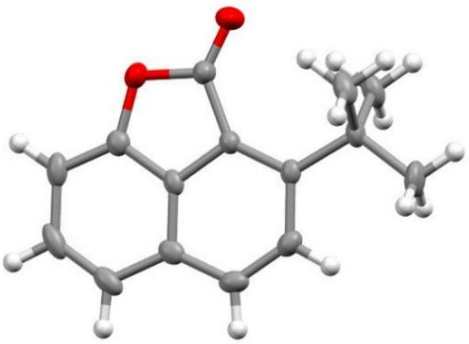

*Figure 2.40. Molecular structures of the hindered lactone **2.8**.*

This hindered lactone **2.8** was ring opened with methyl lithium, resulting in the lactol **2.9**, which was isolated in 75% yield, rather than the ring opened *peri*-hydroxyl methyl ketone. A ^{13}C NMR peak at 114.5 ppm akin to that of a hemi-ketal was observed, with no carbonyl ^{13}C resonance present. This confirms that in a $CDCl_3$ solution, the two *peri*-groups are adopting a lactol structure, likely due to a repulsion between the *peri*-ketone and *tert*-butyl groups in the ring open structure, which allows for a closer contact between the hydroxy and carbonyl moieties and thus addition takes place.

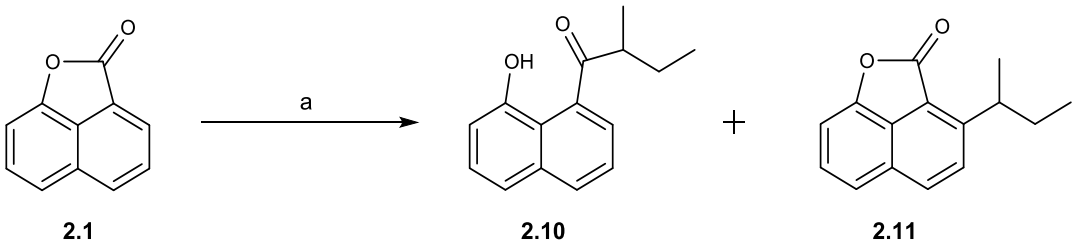

Scheme 2.9. (a) sec-BuLi (1.4M), THF, -78 °C.

Due to its reduced steric bulk when compared to *tert*-butyl lithium, *sec*-butyl lithium was reacted with lactone **2.1**, to give the desired *peri*-hydroxyl *sec*-butyl ketone **2.10** in 24% yield

(Scheme 2.3). The structure of **2.10** was confirmed by the presence of four ^{1}H NMR peaks in the region of 0.97-3.51 ppm, corresponding to a *sec*-butyl moiety. Furthermore, a carbonyl stretching frequency of 1668 cm^{-1} in the infrared spectrum is significantly shifted from that of lactone **2.1** (1774 cm^{-1}) indicating the desired addition. The *ortho*-substituted hindered lactone **2.11** was also isolated in 18% yield. The reduction in steric bulk from a *tert*-butyl to a *sec*-butyl group is significant enough to allow for reaction at the lactone carbonyl. The structure of **2.11** is confirmed by removal of an aromatic proton from the ^{1}H NMR spectrum, with the expected shifts for the *sec*-butyl group observed. A carbonyl signal at 167.3 ppm in the ^{13}C NMR spectrum evidences the retention of the lactone ring.

*Table 2.11. Selected geometric data for naphthols **2.2** and **2.5**.*

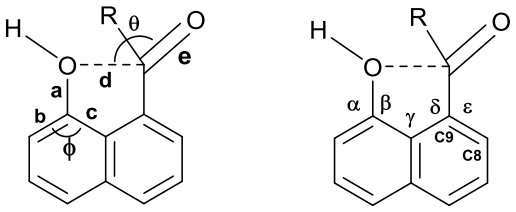

Compound	**a** / Å	**b** / Å	**c** / Å	**ϕ** / °	**d** / Å	**e** / Å	**θ** / °	**Pyr**[a] / Å
2.2	1.346(2)	1.379(2)	1.432(2)	120.5(2)	2.607(3)	1.228(2)	115.8(1)	0.051(2)
2.5	1.367(3)	1.367(3)	1.422(3)	120.8(2)	2.621(3)	1.219(3)	108.3(2)	0.058(2)
	1.364(3)	1.367(3)	1.423(3)	121.3(2)	2.623(3)	1.219(3)	111.9(2)	0.063(2)

Compound	**α** / °	**β** / °	**γ** / °	**δ** / °	**ε** / °	**τ**[b] / °	**Δ**[c] **(O, C)** / Å
2.2	123.7(2)	115.8(2)	122.6(2)	124.8(2)	115.4(2)	62.6(2)	0.059(3), -0.073(3)
2.5	123.1(2)	116.1(2)	122.8(2)	123.5(2)	116.3(2)	65.2(3)	0.153(3), -0.342(3)
	122.7(2)	116.0(2)	123.5(2)	124.0(2)	115.8(2)	67.7(3)	0.104(3), -0.157(3)

[a] pyr = pyramidality, deviation of carbonyl carbon from the plane of the three neighbouring atoms towards the *peri* O atom; **τ**[b] = torsion angle :C8-C9-C=O; **Δ**[c] = deviation from best plane of the naphthalene skeleton.

The *sec*-butyl ketone **2.10**, despite exhaustive attempts, remained an oil under ambient conditions, whereas crystals of the *peri*-hydroxyl ketones **2.2** and **2.5** were grown via slow evaporation of CH_2Cl_2 and EtOAc solutions respectively. The structures of the two ketones **2.2** and **2.5** were determined at 150 K, with selected geometric data summarised in Table **2.1**.

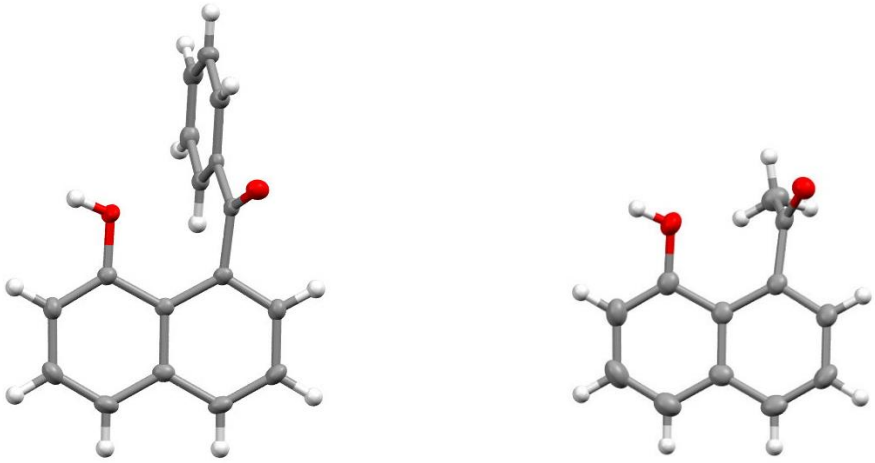

*Figure 2.41. Molecular structures of the peri-hydroxy ketones **2.2** (left) and **2.5** (right).*

The structures of **2.2** and **2.5** as shown in Figure 2.2, demonstrate the expected angular displacements of the two *peri*-groups, with the C-O bond of the nucleophile approaching the retreating carbonyl, in a 'windscreen wiper' type fashion. These displacements result in O---C separations of 2.607(3) Å for the phenyl ketone and 2.621(3) and 2.623(3) Å for the two independent molecules of the methyl ketone. They display O---C=O Bürgi-Dunitz angles of 115.82(14)^{o} for the former and 108.3(2) and 111.9(2)^{o} for the latter. Each of the three molecules displace their *peri*-groups to opposite sides of the naphthalene plane, with the larger displacements observed in the two unique molecules of the methyl ketone **2.5**. Small pyramidalisations of the carbonyl carbons the approaching hydroxyl group of 0.051(2)–0.053(2) Å are observed in each case. Intermolecular hydrogen bonding between the hydroxyl and carbonyl groups link together the molecules in the crystal structures of both **2.2** and **2.5.**

Crystals of the *ortho*-substituted lactol **2.9** were obtained via slow evaporation of a CH_2Cl_2 solution, and the structural analysis confirmed the presence of the lactol functionality in the solid state as well as in solution. The analysis revealed two crystallographically unique molecules of **2.9** are present in the asymmetric unit, with one of the molecules possessing a disordered *tert*-butyl group. Other than this, the two molecules have very similar geometries.

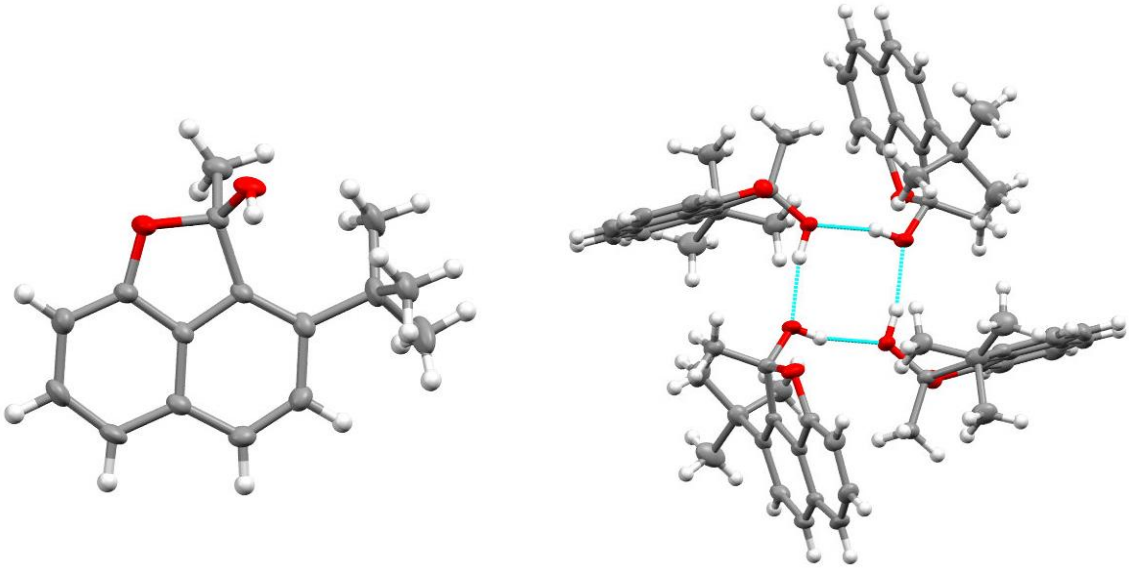

*Figure 2.42. Molecular structure of one of the two crystallographically unique molecules the lactol **2.9** (left) and the crystal packing arrangement for lactol **2.9** (right) in which four molecules are linked together by hydrogen bonds.*

The molecule of **2.9** which displays an ordered *tert*-butyl group orients one of its methyl groups almost perpendicular to the best naphthalene plane, with a torsion angle of 85.6(2)^{o} to the *peri*-naphthalene ring carbon. The remaining two methyl groups are therefore positioned at torsion angles of -36.1(3) and -155.9(2)^{o} to the same ring carbon. The *tert*-butyl groups as a whole are bent away in-plane from the lactol by 4.9 and 5.1^{o}, whilst the lactol is compressed so that the exocyclic angles at the naphthalene skeleton are widened to 136.0 and 136.2^{o}. An anomeric effect between the exocyclic OH group and the ring C-O bond is observed. This results in a shortening of the C-OH bond to 1.394-1.399 Å, whilst the ring O-C bond is lengthened to 1.480-1.485 Å. Furthermore, the C(naphthalene)-C-CH_3 angles at the anomeric centres are widened to 119.4 and 116.3^{o} to reduce the steric interaction between *tert*-butyl and methyl groups. Hydrogen bonding between the lactol hydroxyl groups organises four molecules of **2.9** in the crystal structure into square motifs as shown in Figure 2.3.

The utilisation of a hydroxyl group as the nucleophilic moiety allows for deprotonation to give the oxyanion. Formation of the oxyanion increases the group's nucleophilic potency and should increase the extent to which an interaction occurs between the *peri*-groups. The hydroxyl groups in compounds **2.2**, **2.5**, **2.9** and **2.10** were reacted with a series of bases, ranging in pKa's which would allow for the deprotonation of the hydroxyl group (estimated to be similar to that of a phenolic proton (pKa of 10)). As shown in Figure 2.4 the bases used included: tetramethylguanidine **2.12** (TMG) (pKa 13.6 in DMSO), phosphazine base P_1-tBu **2.13** ($pKBH^+$ 26.9 in H_2O), 4-dimethylaminopyridine **2.14** (DMAP) (pKa 9.2 in H_2O), 1,4-diazabicyclo[2.2.2]octane **2.15** (DABCO) (pKa 8.82 in H_2O) and 1, 8-diazabicyclo[5.4.0]undec-7-ene **2.16** (DBU) (pKa 12 in DMSO).

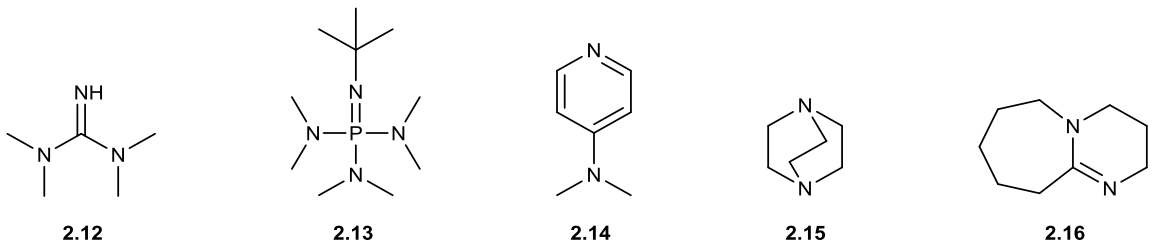

*Figure 2.43. A selection of organic bases used for the deprotonation of the hydroxy-ketones. Left to right: TMG (**2.12**), P_1-tBu (**2.13**), DMAP (**2.14**), DABCO (**2.15**) and DBU (**2.16**).*

Typically, the bases were added to a solution of the target compound in an anhydrous organic solvent (DCM, THF or Et_2O) under nitrogen, stirred for a short period of time and then either left to evaporate in the atmosphere under a slow nitrogen flow. Attempts to obtain crystals from P1-tBu, DABCO and DBU all yielded oils and thus pursuit of these salts was ceased. Reactions of ketones **2.5** and **2.10** and lactol **2.9** with DMAP yielded crystalline products, with suitable crystals obtained via slow evaporation of DCM (**2.5**) or acetone (**2.9**/**2.10**) solutions. The X-ray structures were all determined at 150 K with selected geometric data summarised in Table 2.2. The initial solutions of the three collected structures indicated the formation of salts in each case with a $DMAPH^+$ counter cation, however examination of the difference Fourier

maps, showed that the hydrogen atom was not located on the nitrogen of pyridine but was instead still bound to the oxygen of the hydroxyl group. Compounds **2.5, 2.9** and **2.10**, therefore, all formed DMAP complexes in which the two molecules were linked by a hydrogen bond (Figure 2.5).

*Table 2.12. Selected geometric details of hydroxy ketone **2.5** and DMAP complexes of **2.5**, **2.9** and **2.10**.*

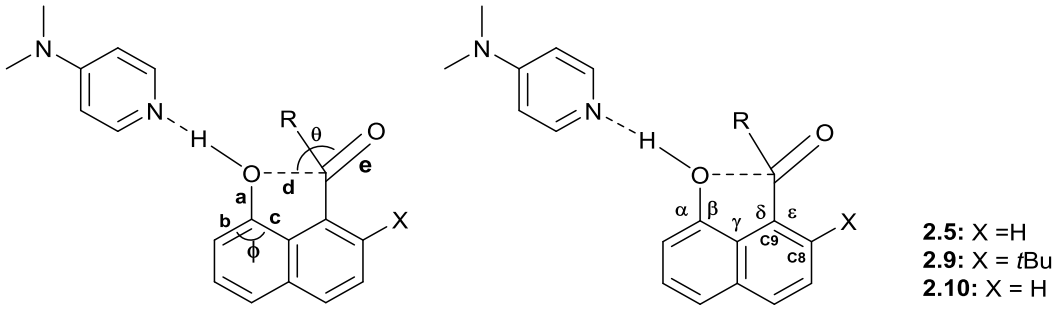

Compound	N---O	a / Å	b / Å	c / Å	ϕ / º	d / Å	e / Å	θ / º
2.5	-	1.367(3)	1.367(3)	1.422(3)	120.8(2)	2.621(3)	1.219(3)	108.3(2)
	-	1.364(3)	1.367(3)	1.423(3)	121.3(2)	2.623(3)	1.219(3)	111.9(2)
2.5.DMAP	2.616(2)	1.356(3)	1.367(3)	1.430(3)	120.1(2)	2.577(3)	1.218(2)	107.5(1)
2.10.DMAP	2.627(3)	1.352(3)	1.376(3)	1.425(3)	120.5(2)	2.603(3)	1.221(3)	112.0(2)
2.9.DMAP	2.580(2)	1.342(2)	1.366(3)	1.432(3)	120.0(2)	2.508(3)	1.206(3)	100.3(2)

Compound	α / º	β / º	γ / º	δ / º	ε / º	τ^a / º	Δ^b (O, C) / Å
2.5	123.1(2)	116.1(2)	122.8(2)	123.5(2)	116.3(2)	65.2(3)	0.153(3), -0.073(3)
	122.7(2)	116.0(2)	123.5(2)	124.0(2)	115.8(2)	67.7(3)	0.104(3), -0.157(3)
2.5.DMAP	123.7(2)	116.2(2)	122.5(2)	123.9(2)	116.6(2)	71.7(3)	0.067(3), -0.032(3)
2.10.DMAP	123.6(2)	115.9(2)	123.0(2)	123.2(2)	116.9(2)	62.7(3)	0.160(3), -0.263(3)
2.9.DMAP	122.5(2)	117.5(2)	122.9(2)	117.4(2)	121.7(2)	73.2(3)	0.260(2), -0.236(3)

τ^a = torsion angle :C8-C9-C=O; Δ^b = deviation from best plane of the naphthalene skeleton.

In the case of lactol **2.9** the complexation with DMAP resulted in an interesting result in that a ^{13}C NMR peak of 115.7 ppm was observed similar to that of the parent lactol (114.5 ppm) for the hemi-ketal, indicating a retention of the lactol structure. However, in the crystal structure of **2.9.DMAP**, the lactol has undergone a ring opening reaction to give the hydroxyl methyl ketone (Figure 2.5), and the DMAP is hydrogen bonded to the hydroxyl proton.

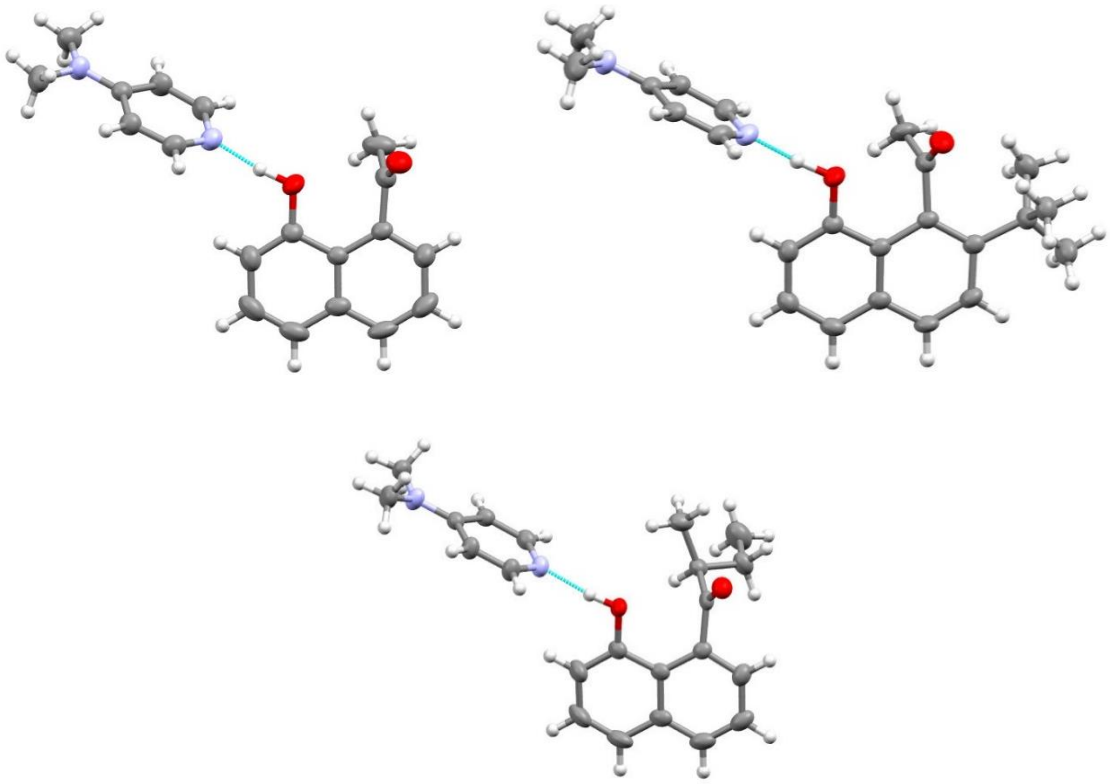

*Figure 2.44. Molecular structures of the hydrogen bonded DMAP complexes of peri-hydroxy methyl ketone **2.5.DMAP** (top left), its ortho-t-butyl substituted derivative **2.9.DMAP** (top right) and the DMAP complex of peri-hydroxy ketone **2.10.DMAP** (bottom).*

The O---C interaction distances for the three DMAP complexes lie in the range of 2.508(3)–2.603(3) Å, all of which are shorter than the non-complexed ketones **2.2** and **2.5** (2.607(3) Å and 2.621(3)/2.623(3) Å respectively). The shortest of the O---C interaction distances occurs in **2.9.DMAP** where a steric interaction with the *ortho tert*-butyl group alters the usual displacement of the *peri*-ketone group. Consequently, the ketone group is now displaced *ca* 2.1^{o} *towards* the naphthol OH group, not away from it as is typically observed in *peri*-interactions of this type. In response, the hydroxyl group's displacement towards the ketone is reduced to 2.5^{o} (from 3.8^{o} in **2.5**) leading to a Bürgi-Dunitz trajectory of 100.3^{o}. In contrast, the other two DMAP complexes display more idealised Bürgi-Dunitz angles of 107.5 and 112.0^{o}, despite the slightly elongated interaction distances compared to **2.9.DMAP**. The O---N distances between the pyridine nitrogen and hydroxyl group in the three complexes lie in the range of 2.580(2)–2.627(3) Å, with the hydrogen bond lying close to a linear geometry. The

assignment **2.5.DMAP**, **2.9.DMAP** and **2.10.DMAP** as hydrogen-bonded complexes is supported by the lengths of the naphthol O-C bonds (1.342(2)–1.356(3) Å) and the size of the corresponding *ipso* angles (120.0(2)–120.5(2)^{o}), which are similar to these in the parent naphthols. Furthermore, the endocyclic angle at the pyridine N atom in DMAP (115.3–115.8^{o}) is consistent with the neutral molecule and not the cation (*ca*. 120.2^{o}).[24] Despite not forming the desired oxyanion, the DMAP complexes demonstrate that even a small increase in the oxygen atom's electron density (via the participation of its hydrogen atom in the hydrogen bond) can result in an increased nucleophilic effect, generating a stronger interaction across the *peri*-positions.

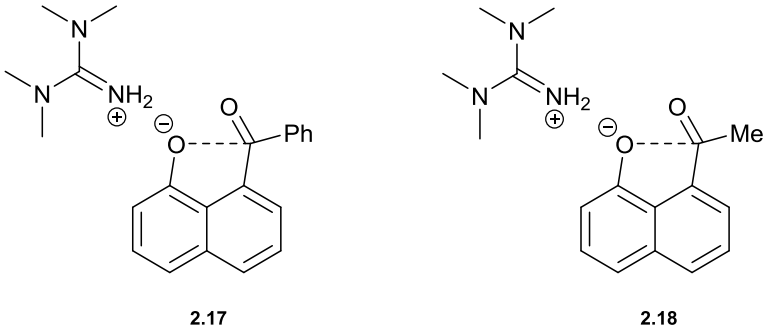

*Figure 2.45. Structures of the TMG-H^{+} salts of the phenyl ketone **2.2** (left) and methyl ketone **2.5** (right).*

Treatment of compounds **2.2** and **2.5** with TMG in CH_2Cl_2, followed by slow evaporation under a positive nitrogen flow, initially yielded two very thick oils. After several weeks under positive nitrogen pressure crystalline products formed. Despite both of the crystalline products degrading under non-nitrogen atmospheres (TMG can react with carbon dioxide to give $TMGH^{+}$ HCO_3^{-}), X-ray structures of the two salts **2.17** and **2.18** (Figure 2.6 and 2.7) were determined at 110 K and 100 K respectively. Selected structural data of the hydroxyl ketone **2.2** and **2.5** along with the TMG salts **2.17** and **2.18** are compared and summarised in Table 2.3.

*Table 2.13. Selected geometric data for naphthols **2.2** and **2.5** and in the TMG salts **2.17** and **2.18**.*

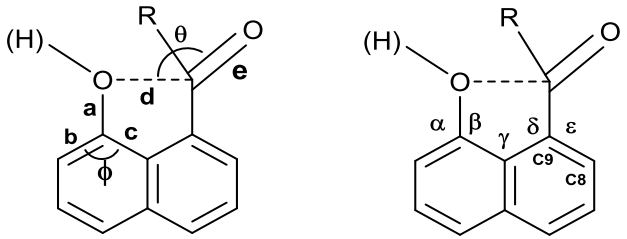

Compound	**a** / Å	**b** / Å	**c** / Å	**ϕ** / º	**d** / Å	**e** / Å	**θ** / º	**Pyr[a]** / Å
2.2	1.346(2)	1.379(2)	1.432(2)	120.5(2)	2.607(3)	1.228(2)	115.8(1)	0.051(2)
2.5	1.367(3)	1.367(3)	1.422(3)	120.8(2)	2.621(3)	1.219(3)	108.3(2)	0.058(2)
	1.364(3)	1.367(3)	1.423(3)	121.3(2)	2.623(3)	1.219(3)	111.9(2)	0.063(2)
2.17	1.306(2)	1.385(3)	1.451(3)	117.2(2)	2.571(2)	1.224(2)	109.3(1)	0.056(2)
	1.299(2)	1.399(3)	1.445(3)	116.8(2)	2.558(2)	1.222(2)	105.6(1)	0.060(2)
2.18	1.306(2)	1.392(3)	1.449(3)	117.2(2)	2.574(3)	1.221(2)	108.4(2)	0.076(3)
	1.304(2)	1.395(3)	1.444(3)	117.0(2)	2.592(2)	1.218(3)	106.9(1)	0.070(2)
	1.293(3)	1.404(3)	1.454(3)	116.0(2)	2.618(2)	1.226(2)	112.5(2)	0.075(2)
	1.307(2)	1.392(3)	1.442(3)	117.2(2)	2.597(2)	1.211(3)	104.3(1)	0.068(2)

Compound	**α** / º	**β** / º	**γ** / º	**δ** / º	**ε** / º	**τ[b]** / º	**Δ[c] (O, C)** / Å
2.2	123.7(2)	115.8(2)	122.6(2)	124.8(2)	115.4(2)	62.6(2)	0.059(3),- 0.073(3)
2.5	123.1(2)	116.1(2)	122.8(2)	123.5(2)	116.3(2)	65.2(3)	0.153(3), -0.342(3)
	122.7(2)	116.0(2)	123.5(2)	124.0(2)	115.8(2)	67.7(3)	0.104(3), -0.157(3)
2.17	124.1(2)	118.7(2)	120.7(2)	123.2(2)	116.2(2)	73.4(2)	0.083(2), -0.161(3)
	124.1(2)	119.1(2)	120.4(2)	122.3(2)	116.8(2)	80.6(2)	0.099(2), -0.236(3)
2.18	123.5(2)	119.4(2)	121.0(2)	122.4(2)	117.2(2)	75.3(3)	0.075(2), -0.030(3)
	123.6(2)	119.5(2)	121.3(2)	121.9(2)	117.2(2)	79.5(2)	0.202(2), -0.145(3)
	123.7(2)	120.3(2)	120.5(2)	123.3(2)	116.9(2)	69.7(3)	0.084(2), -0.041(3)
	123.4(2)	119.3(2)	121.6(2)	121.0(2)	118.0(2)	86.0(2)	0.298(2), -0.246(3)

[a]**pyr** = pyramidality, deviation of carbonyl carbon from the plane of the three neighbouring atoms towards the *peri* O atom; **τ[b]** = torsion angle :C8-C9-C=O; **Δ[c]** = deviation from best plane of the naphthalene skeleton.

There are two crystallographically unique cations and anions for the TMG salt of the phenyl ketone **2.17**, and four unique cations and anions for the salt of the methyl ketone **2.18**, resulting in a total of six examples of naphtholate salt *peri*-interactions. Deprotonation of the hydroxyl group in the phenyl ketone salt **2.17**, opposed to the hydrogen bonding shown in **2.5.DMAP**, **2.9.DMAP** and **2.10.DMAP**, is strongly supported by the shortening of the C-O bond from 1.346(2) to 1.299(2) and 1.306(2) Å. In addition, lengthening of the two nearest aromatic C-C bonds from 1.379(3) and 1.432(2) Å to 1.385(3)/1.399(3) and 1.451(3)/1.445(3) Å, and the compression of the *ispo* bond angle from 120.5(2)^{o} down to 116.8(2) and 117.2(2)^{o} demonstrate a response to the presence of a more electron rich-substituent in the *ispo* position.[25,26] For comparison, the crystal structures of 2-dimethylamino and 2,6-bis(dimethylamino)phenolate show $O^{(-)}$-C bonds in the range of 1.300(5)–1.334(7) Å (average 1.312 Å) and *ipso* bond angles in the range 116.1(4)–117.8(5)^{o} (average 116.8^{o}). Each of the two NH_2-group hydrogen atoms of the TMG-H^+ cation were located in difference Fourier maps and refined with reasonable positions, isotropic displacement parameters (0.020–0.044 $Å^2$) and showed hydrogen bond distances to oxyanions of 1.78–1.99 Å. Hydrogen bonding between TMG-H^+ cations and two anions of **2.2** adopts a square motif as shown in Figure 2.7. Similar features are seen in the four anions of the TMG salt of the methyl ketone, for example the C-O bond and *ipso* angles lie in the ranges 1.293(3)–1.307(2) Å and 116.0(2)–117.2(2)^{o} opposed to 1.367(3)/1.364(3) Å and 120.8(2)/121.3(2)^{o} in the parent ketone.

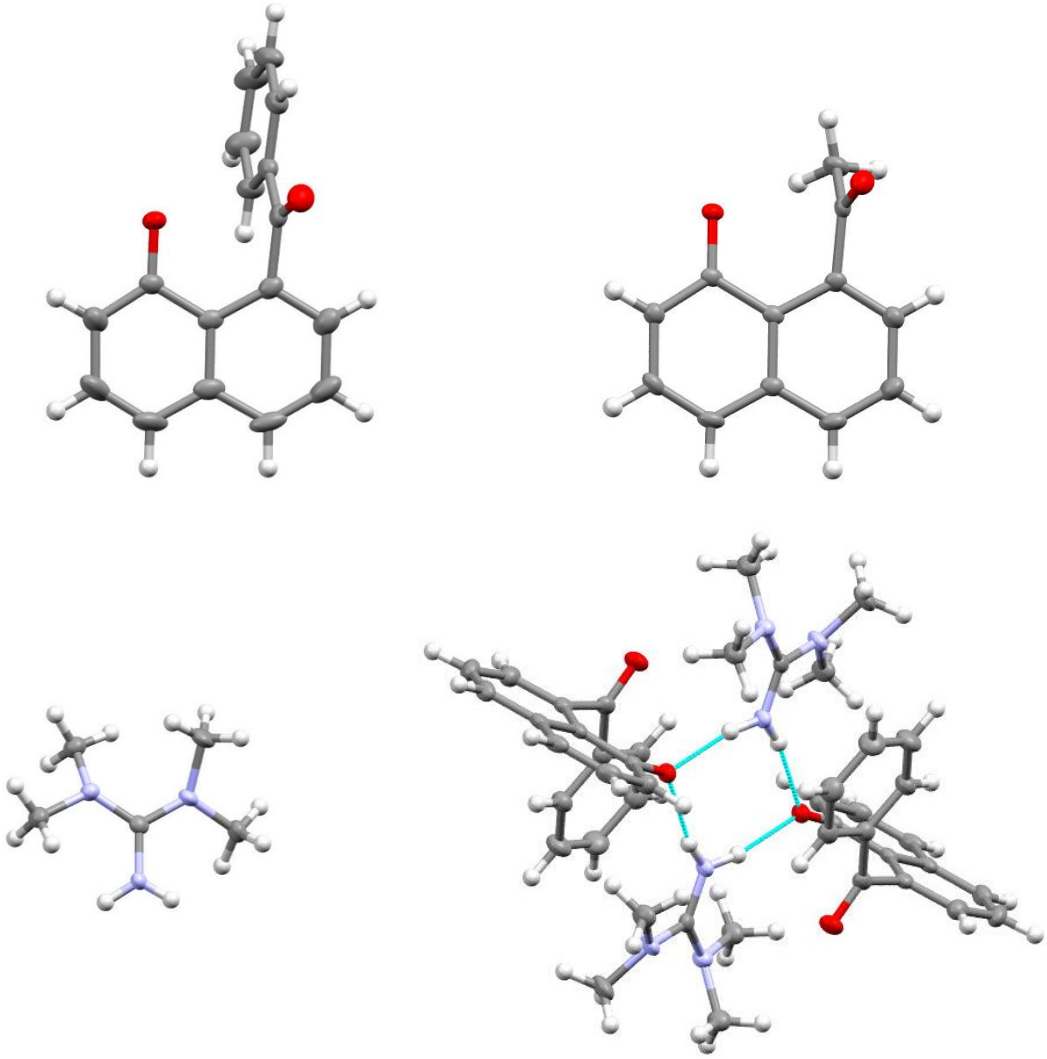

*Figure 2.46. Molecular structures of the anions of **2.17** (top left) and **2.18** (top right), one example of the twisted TMG-H$^+$ cation (bottom left) and the hydrogen bonding arrangement of two TMG-H$^+$ cations and two anions of **2.2** in a square motif (bottom right).*

The O---C interaction distance in the salt **2.17** is decreased on deprotonation from 2.607(3) in naphthol **2.2** to 2.571(2)/2.558(2) Å. The pattern of the in-plane displacements of the *peri*-groups in this naphtholate anion are the same as observed in the parent naphthol **2.2**. Yet the extent of the in-plane displacements are reduced in the anion, resulting in smaller, more favourable Bürgi-Dunitz trajectory angles between the oxyanion and the ketone carbonyl group of 109.3(1) and 105.6(1)^o compared to 115.8(1)^o in parent ketone **2.2**. Small increases in the pyramidalisation of the ketone carbonyls in the anions (average: 0.062(2) Å) are also observed compared to that of the neutral species (0.051(2) Å). Similar trends are followed too for the

four unique anions in the TMG salt of the methyl ketone **2.5**, with O---C interaction distances of 2.574(3)–2.618(2) Å, Bürgi-Dunitz trajectory angles of 104.3(1)–108.4(2)^{o} and small increases in pyramidalisation at the carbonyl carbon (average: 0.072(2) Å) from that of the neutral species (average: 0.058(2) Å). Interestingly, unlike the dimethylamino and methoxy nucleophiles, the oxyanion does not possess a steric contact with the *ortho*-naphthalene ring carbon. This provides structural freedom to the oxyanion which could move in the opposite direction, away from the corresponding *peri*-ketone. However, the group does not and the oxyanion is still displaced towards the *peri*-ketone which supports that a stereoelectronic effect aids in the generation of the optimised Bürgi-Dunitz angle.

Comparison of the solution ^{1}H and ^{13}C NMR spectra of the phenyl ketone **2.2** with those of its TMG-H^{+} and sodium salts in DMSO-d$_6$ indicate a contrasting structure for the TMG-H^{+} salt compared to that of the solid state, whereby only partial deprotonation of the naphthol is observed. The sodium salt of the phenyl ketone **2.2** was prepared by the addition of an excess of sodium hydride (NaH) to a solution of **2.2** in anhydrous THF and stirring until gas evolution ceased. The reaction was then filtered, the solvent was removed and the resultant product was dissolved in DMSO-d$_6$. Utilisation of NaH as the base results in complete irreversible deprotonation as the liberated proton escapes as hydrogen gas. In the fully deprotonated sodium salt, the carbon *ipso* to the naphtholate oxygen resonates at 168.1 ppm, whilst the same carbon in the neutral compound has a resonance of 152.3 ppm. The *ipso* carbon of the TMG-H^{+} salt **2.17** however resonates at 161.4 ppm, midway between these two values. Furthermore, the central carbon of the TMG-H^{+} cation in **2.17** is found at 163.6 ppm, again lying between that of the neutral species (166.3 ppm) and the salt (161.0 – 162.3 ppm in a series of triflate salts[27]). This suggests a rapid exchange of a proton between the TMG-H^{+} and the anion. The TMG salt of the methyl ketone **2.5** also shows similar -^{13}C NMR data. NMR studies of the sodium and

TMG salts of 1-naphthol in THF-d_6 strongly suggest that the equilibrium with TMG lies towards the deprotonated state.

The introduction of an electron-donating oxygen atom *para* to the hydroxyl group on the naphthalene ring could increase the electron density of the *peri*-hydroxyl group. This could result in the more potent nucleophilic oxygen becoming involved in a stronger interaction with the opposite *peri*-electrophile, due to the decreased need for electron donation of an oxygen lone pair into the naphthalene ring. The hydroxy/methoxy substituted derivative **2.21**/**2.22** was thus thought to be an interesting target.

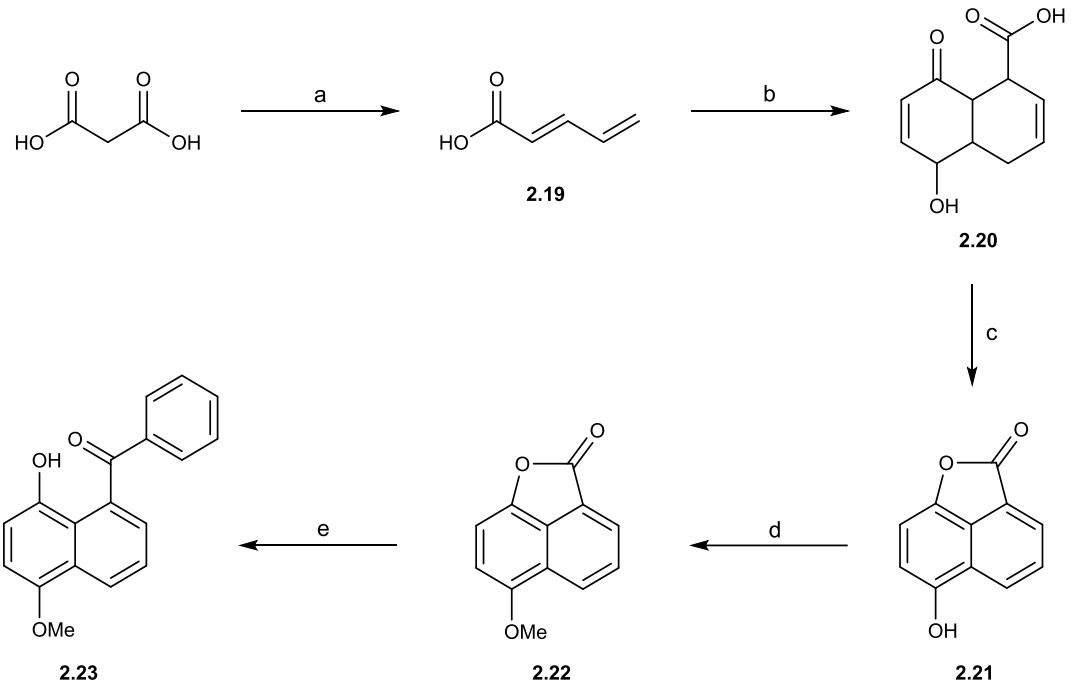

*Scheme 2.10. (a) acrylaldehyde, pyridine, 50 °C;[28] (b) 1,4-benzoquinone, **2.19**, Toluene, 80 °C;[29] (c) Toluene, p-toluenesulfonic acid, Pd/C, reflux;[29] (d) K_2CO_3, DMSO, CH_3I; (e) PhLi (1.9M), THF, -78 °C.*

Following the works of Ferrari *et al.* freshly prepared 2, 4-pentadienoic acid **2.19**[28] was reacted via a Diels-Alder reaction with *p*-benzoquinone to give the bicyclic compound **2.20** (Scheme 2.4).[29] Compound **2.20** was subsequently reacted on with *p*-toluenesulfonic acid and activated palladium on charcoal (10%), to give the desired 5-hydroxy-1,8-naphtholactone **2.21**.[29] Ring opening of lactone **2.21** with phenyl lithium (according to the procedure described for phenyl

ketone **2.2**) allowed for the effects of the hydroxy group to be assessed, via a comparison with the ketone **2.2**. Unfortunately, structural analysis of the product revealed that despite the ring opening of the lactone being successful, the 1,4-dihydroxynaphthalene portion of the molecule had undergone oxidation, resulting in the corresponding naphthoquinone. To avoid this, the *para*-hydroxyl group was O-methylated by the reaction of **2.21** with potassium carbonate in dimethyl sulfoxide (DMSO) followed by the addition of methyl iodide This gave the desired methoxy-lactone **2.22** as a yellow solid in a 37% yield. A signal at 3.27 ppm in the ^{1}H NMR spectrum corresponding to the O-methyl protons confirmed the structure of **2.22**. Ring opening of **2.22** with phenyl lithium this time yielded the desired *para*-methoxy substituted hydroxy phenyl ketone **2.23** as a yellow solid in a 43% yield. Successful addition to the lactone was evidenced by the expected carbonyl ^{13}C NMR shift from 167.7 ppm in the lactone **2.22** to 201.4 ppm in **2.23**. Furthermore, the addition of five aromatic protons is observed in the ^{1}H NMR spectrum.

*Table 2.14. Selected geometric data for naphthols **2.2** and **2.23**.*

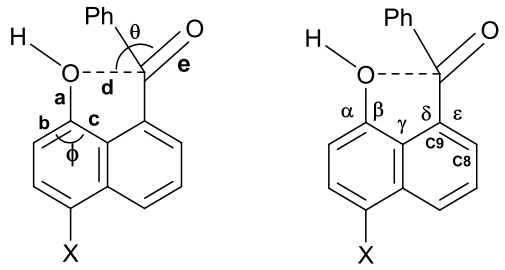

Compound	**a** / Å	**b** / Å	**c** / Å	**ϕ** / °	**d** / Å	**e** / Å	**θ** / °	**Pyr**[a] / Å
2.2 (X=H)	1.346(2)	1.379(2)	1.432(2)	120.5(2)	2.607(3)	1.228(2)	115.8(1)	0.051(2)
2.23 (X=OMe)	1.357(3)	1.361(4)	1.421(4)	120.2(3)	2.566(3)	1.226(3)	108.7(2)	0.050(3)

Compound	**α** / °	**β** / °	**γ** / °	**δ** / °	**ε** / °	**τ**[b] / °	**Δ**[c] **(O, C)** / Å
2.2 (X=H)	123.7(2)	115.8(2)	122.6(2)	124.8(2)	115.4(2)	62.6(2)	0.059(3), -0.073(3)
2.23 (X=OMe)	123.8(2)	116.0(2)	122.3(2)	123.4(2)	115.9(2)	75.6(2)	0.247(4), -0.066(3)

[a]**pyr** = pyramidality, deviation of carbonyl carbon from the plane of the three neighbouring atoms towards the *peri* O atom; **τ**[b] = torsion angle :C8-C9-C=O; **Δ**[c] = deviation from best plane of the naphthalene skeleton.

Crystals of the methoxy-substituted phenyl ketone **2.23** were obtained via slow evaporation of a DCM solution and the crystal structure of one of these was determined at 150 K. Important

geometric data is summarised in Table 2.4 alongside the unsubstituted phenyl ketone **2.2** for comparison. The addition of the *para*-methoxy group (Figure 2.8) in **2.23** results in a small decrease in the HO---C=O interaction distance to 2.566(3) Å compared to 2.607(3) Å in **2.2**. The *peri*-groups of **2.23** display similar displacements to those demonstrated in phenyl ketone **2.2**, except for the ketone moiety itself which is displaced away from the approaching hydroxyl group by 1.4° less than in **2.2**. Furthermore, the carbonyl of the ketone is orientated further from the *ortho*-naphthalene ring carbon, with a torsion angle of 75.6(2)°, larger than those observed in **2.2** and **2.5** (62.6(2)-67.7(3)°). This generates a more favourable Bürgi-Dunitz angle of 108.7(2)°. Despite this, the pyramidalisation of the carbonyl carbon is almost identical to that of the unsubstituted phenyl ketone **2.2**.

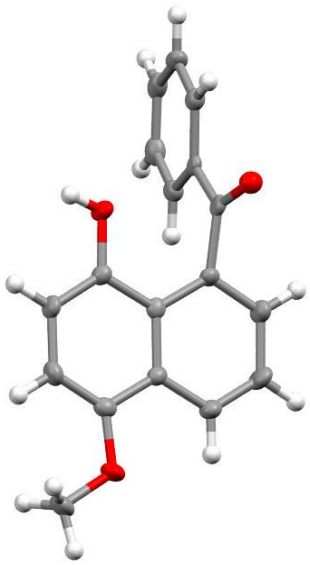

*Figure 2.47. Molecular structure of the para-methoxy peri-hydroxy phenyl ketone **2.23.***

Crystals of the TMG salt of **2.23**, were obtained via the same method as described for the phenyl and methyl TMG salts **2.17** and **2.18** but with THF as the crystallisation solvent. The crystals of **2.24** (Figure 2.9) were even more susceptible to decomposition in a non-nitrogen atmosphere. Despite managing to isolate, mount and collect X-ray diffraction data for several crystals of **2.24**, it was revealed that the crystals were a THF solvate, which was

incommensurate in nature. This meant that there were channels running parallel to the *a* axis filled with THF molecules that are not ordered with respect to the main crystal lattice. The incommensurate structure is evidenced by the random disorder of the diffraction pattern in the Ewald reciprocal space. The cation and anion of the structure appear well ordered, demonstrating an $O^{(-)}$---C=O distance shortening to 2.527(11) Å from that of 2.570(4) Å in the neutral ketone, consistent with the increase in the nucleophilicity of the oxygen atom. The observed decrease in the $O^{(-)}$---C=O distance upon deprotonation in **2.24** appears to be of roughly the same magnitude as that observed for **2.17** and **2.18**. The data related to this structure is unfortunately not completely reliable as a result of the disordered nature of the THF solvate. Therefore, even though it can be concluded that the deprotonation has caused a significant reduction in the contact distance between the *peri*-groups and that the *para*-methoxy group has further aided this, an alternate solvate of the structure, free from the incommensurate THF molecules is required for accurate analysis.

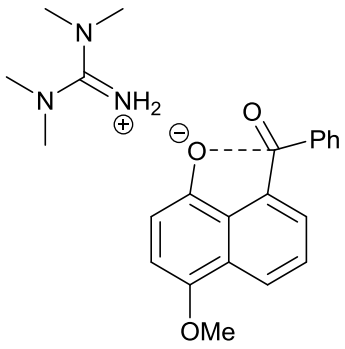

2.24

*Figure 2.48. Structure of the TMG-H$^+$ salt of the para-methoxy peri-hydroxy phenyl ketone **2.23.***

Overall, the substitution of a *para*-electron donating methoxy group has increased the nucleophilicity of the interaction hydroxyl group, reduced the contact distance between the *peri*-groups and optimised the Bürgi-Dunitz angle of approach. The study could be continued by the introduction of a stronger electron donating group (e.g. dimethylamino) to increase this effect further and potentially result in the formation of a long *peri* O-C bond.

Study of $O^{(-)}$---C=C interactions

The study was extended to investigate interactions of *peri*-hydroxy groups, and their anions with polarised alkenes. This began with the reduction of naphtholactone **2.1** with tri-*tert*-butoxyaluminium hydride according to Cammidge *et al*.[22] to give the *peri*-hydroxy aldehyde **2.25**. Condensation of hydroxy aldehyde **2.25** with active methylene compounds ethyl cyanoacetate, malononitrile[30] and Meldrum's acid gave the expected Knoevenagel condensation products, with polarised alkene groups **2.26**-**2.28**, in good yields of 72-86% (Scheme 2.5).

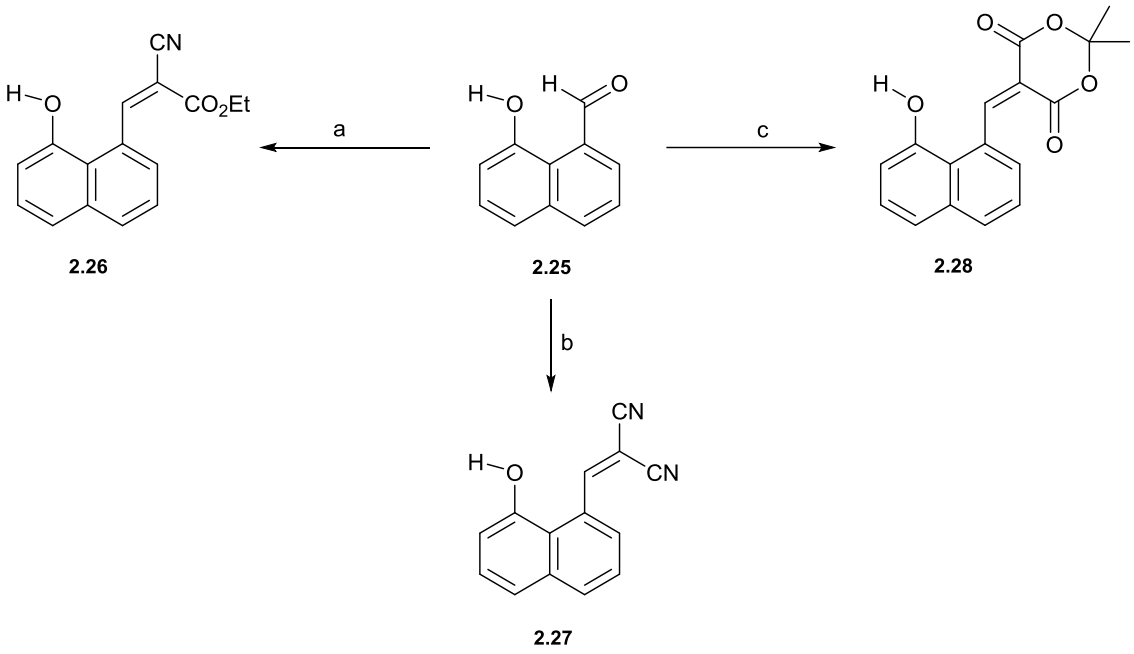

Scheme 2.11. (a) $NCCH_2CO_2Me$, CH_3OH, ($^+NH_3CH_2$-)$_2$(^-OAc)$_2$ (cat.), 65 ^oC; (b) $CH_2(CN)_2$, CH_3OH, 65 ^oC; (c) Meldrum's acid, DMSO, 20 ^oC.

The structure of cyanoester **2.26** is confirmed by peaks in the ^1H NMR spectrum at 1.35 and 4.36 ppm for the ethyl ester group and a peak at 115.8 ppm in the ^{13}C NMR spectrum for the adjacent nitrile group. Similarly, the two nitrile groups of the malononitrile derivative **2.27** are evidenced with peaks in the ^{13}C NMR and infrared spectra at 112.5/113.9 ppm and 2237 cm^{-1}. The structure of the Meldrum's acid derivative **2.28** was confirmed by the ^{13}C NMR peak at 162.9 ppm for the two lactone carbonyls, with the ^1H NMR spectrum possessing a singlet at

1.77 ppm for the two methyl groups. In each of the three Knoevenagel products, the ^{1}H NMR peak at 11.66 ppm for the aldehyde of **2.25** is replaced with peaks at 9.61 ppm (**2.26**), 9.21 ppm (**2.27**) and 9.27 ppm (**2.28**) corresponding to the newly formed vinylic proton.

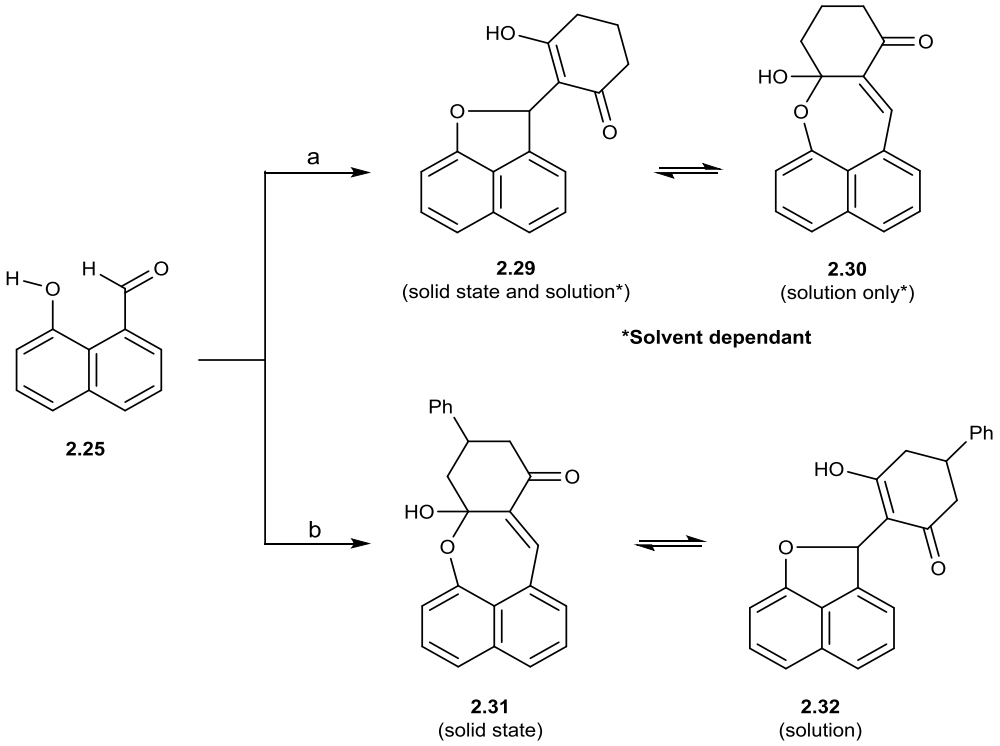

Scheme 2.12. (a) cyclohexa-1,3-dione, CH_3OH, ($^{+}NH_3CH_2$-)$_2$($^{-}$OAc)$_2$ (cat.), 65 ^{o}C; (b) 5-phenylcyclohexa-1,3-dione, DMSO, 20 ^{o}C.

Condensations of aldehyde **2.25** with active methylene compounds cyclohexa-1, 3-dione and 5-phenylcyclohexa-1, 3-dione, on the other hand, did not yield the expected Knoevenagel products (Scheme 2.6). The desired alkenes, which are the most electron deficient of the series, each underwent a further reaction, with the *peri*-hydroxyl group of the naphthalene adding to either the electron deficient *peri*-carbon or to one of the cyclic diketone carbonyl groups (**2.29**-**2.32**). NMR analysis of the product of the condensation with cyclohexane-1, 3-dione revealed that in solution, the cyclised structure **2.29** is present as the major species alongside the minor oxepine species **2.30**. The ratio of the two species differs depending on the solvent, with a 2:1 ratio in acetone-d_6 and a 17:3 ratio in $CDCl_3$. The methine group of the closed form **2.29** resonates in $CDCl_3$ at 7.16 ppm and 87.8 ppm in the ^{1}H and ^{13}C NMR spectra respectively and

at 7.08 ppm and 82.0 ppm in acetone-d_6. The minor isomer is not consistent with that of the un-cyclised form **2.33** despite this being the expected minor species, as is demonstrated by the lack of correlation between the methine ^{1}H and ^{13}C NMR peaks with that of the open chain methylthio analogue **2.34** (^{1}H: 9.11 ppm and ^{13}C: 154.8 ppm) as shown in Figure 2.10.

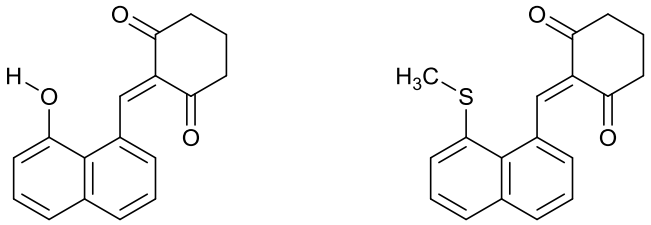

*Figure 2.49. Structures of the uncyclised hydroxy alkene **2.33** (left) and the methylthio analogue **2.34** (right).*

NMR analysis of the product of the 5-phenylcyclohexa-1, 3-dione condensation product in DMSO-d_6, show that only one product is present, unlike that of the cyclohexa-1, 3-dione derivative. The data is consistent with the *peri*-cyclised structure **2.32**, analogous to the solid-state structure of **2.29**, whereby the hydroxyl group has added to the alkene to yield the β-hydroxy unsaturated ketone. The methine CH peaks occur at 7.02 ppm and 81.9 ppm in the ^{1}H and ^{13}C NMR spectra respectively.

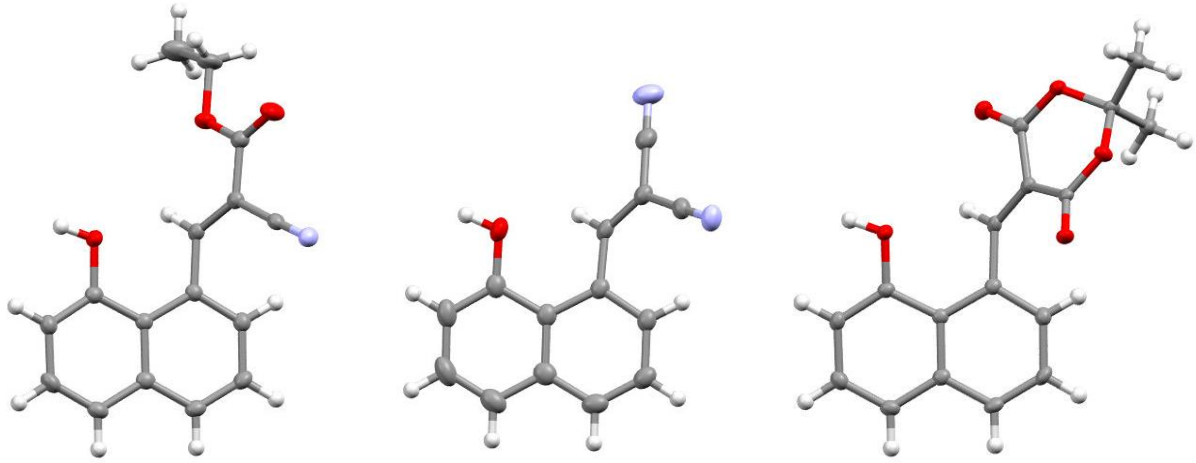

*Figure 2.50. Molecular structures of Knoevenagel product **2.26**, **2.27** and **2.28** (left to right).*

Crystals of the three standard Knoevenagel products **2.26-2.28** were obtained via slow evaporation from a range of solvents. The X-ray structures for compounds **2.26** and **2.27** were determined at 150 K with the Meldrum's acid derivative **2.28** being collected at 100 K (Figure 2.11). Selected geometric data is summarised in Table 2.5. The hydroxyl group of the three examples is involved in intermolecular hydrogen bonding with either a nitrile group in **2.26** and **2.27** or a carbonyl oxygen in **2.28**. The O---C(=C) distances lie in the narrow region 2.615(2)–2.624(2) Å, despite the notable difference in the through-space electron-attracting power of the electrophilic *peri*-substituents. Furthermore, the interaction distances are similar to those observed in the methyl and phenyl ketones **2.2** and **2.3**. Each of the compounds **2.26-2.28** demonstrates the expected in-plane angular displacements of the *peri*-groups, with the hydroxyl group approaching the retreating alkene carbon. The *peri*-alkene groups in each compound are rotated from the best naphthalene plane by less than those of the *peri*-ketone derivative **2.2** and **2.5**, which generates unfavoured Bürgi-Dunitz trajectories (124.7(2)-127.3(2)^{o}). Despite this, the alkene C=C bond demonstrates a slight elongation in **2.26-2.28**, expressing a prearrangement for nucleophilic attack and subsequent transformation to a C-C bond. Overall, a lower degree of sensitivity is observed for the O---C separations than the corresponding N---C separations in the Me_2N---C series (2.531(2) to 1.651(3) Å for the three

equivalent compounds), and a major difference being the lack of *peri*-bond formation in compound **2.28** across the two *peri*-groups, where the dimethylamino analogue is found to form a long bond of 1.651(3) Å.

*Table 2.15. Selected geometry of Knoevenagel product **2.26-2.28** and the ring closed product **2.29***

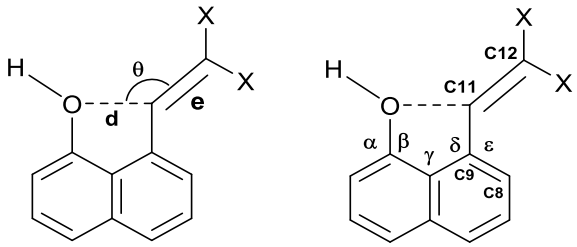

Compound	d / Å	e / Å	θ / °	α / °	β / °	γ / °	δ / °	ε / °	τ[a] / °
2.26	2.615(2)	1.343(2)	124.7(2)	122.4(2)	116.8(1)	123.4(1)	122.9(1)	117.7(1)	48.8(2)
2.27	2.624(2)	1.351(2)	127.3(2)	122.4(2)	116.8(1)	123.4(2)	122.0(1)	118.7(1)	41.1(2)
2.28	2.623(2)	1.350(3)	125.1(2)	121.3(2)	117.4(2)	124.2(2)	120.7(2)	119.4(2)	45.6(1)
2.29	1.521(3)	1.500(3)	-	130.6(3)	110.7(2)	109.5(2)	108.2(2)	134.7(2)	60.6(4)
	1.508(3)	1.496(3)	-	128.7(3)	110.9(2)	110.0(2)	107.3(2)	134.0(2)	53.3(4)

τ[a] = torsion angle :C12-C11-C9-C8.

Crystals of the equilibrating cyclohexa-1, 3-dione derivative **2.29**/**2.30** were obtained via slow evaporation of an ethyl acetate solution. X-ray structure determination at 100 K revealed that in the crystals obtained, the compound resided purely as the peri-cyclised form **2.29** (Figure 2.12), in which the hydroxyl group has added to the polarised alkene, forming a hydroxycyclohexanone group. Selected geometric data can be found in Table 2.5.

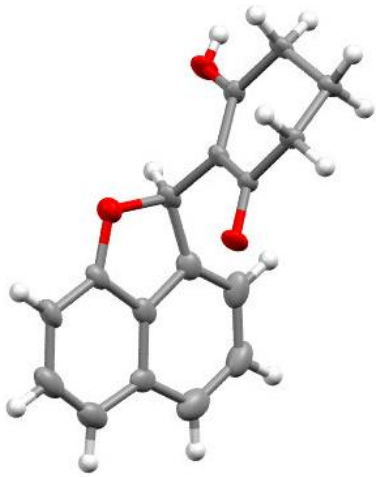

*Figure 2.51. The cyclised molecular structure of one molecule of Knoevenagel product **2.29.***

Two crystallographically unique molecules of **2.29** are found in the asymmetric unit which display surprisingly long (aryl)O-CHC_2 bonds of 1.508(3) and 1.521(3) Å, considerably larger than that of the average (1.447 Å) for this type of bond.[31] These bonds can be viewed as representing two points in the later stages of formation of an O-C bond. The shorter *peri* O-C bond in this pair is associated with a longer bond from *peri*-oxygen to the aromatic ring, 1.364(3) *cf.* 1.350(3) Å, and consequentially a longer bond from the *peri*-carbon to the aromatic ring, 1.506(4) *cf.* 1.493(4) Å. The bonding *peri*-atoms in each molecule lie in the best naphthalene plane, with little to no strain placed on the naphthalene scaffold itself. In the cyclohexenone ring, the bond lengths along the chain HO-C=C-C=O indicate the strong conjugation from the hydroxyl group into the carbonyl group: (H)O-C: 1.325(3)/1.322(3), C=C: 1.368(3)/1.373(3), C-C(=O) 1.439(3)/1.436(3) and C=O 1.249(3)/1.248(3) Å.

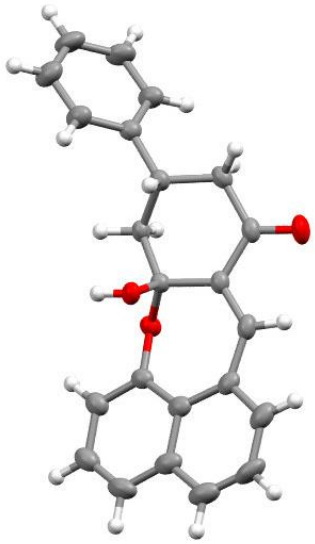

*Figure 2.52. The cyclised molecular structure of the Knoevenagel product **2.31.***

Crystals of the 5-phenylcyclohexadione derivative **2.31**/**2.32** were grown via slow evaporation of an ethyl acetate solution. The structure, determined at 150 K, revealed that the hydroxyl group had added to a carbonyl ring carbon, adopting the lactol form and forming a seven-membered oxepine ring, which is fused to both the naphthalene and cyclohexyl rings to give the tetracyclic structure **2.31** as shown in Figure 2.13. The two *peri*-atoms bound into the

oxepine ring are displaced very slightly to either side of the idealised naphthalene plane (C: 0.020 Å, O: 0.157 Å), with the two cyclohexane carbons displaced to the same side of the naphthalene plane. The naphthalene scaffold itself remains planar, unaffected by the oxepine ring formation. The widest bond angle in the oxepine ring is at the alkene methine carbon atom (131.0(2)^{o}) and the smallest at the lactol carbon (108.6(2)^{o}). To form the ring the bonds from naphthalene to the *peri* atoms are necessarily splayed apart, widening the naphthalene *exo*-angle between the benzene rings to 125.0(2)^{o}. The lactol group shows the expected anomeric interaction with a short HO-C bond of 1.399(2) Å and the ring C-O bond lengthened to 1.457(2) Å.

In the same fashion as the hydroxy ketones, the Knoevenagel products **2.27-2.29** and **2.31** were reacted with either two organic bases DMAP and DABCO or sodium hydride in order to form the desired oxyanion nucleophile. Despite exhaustive attempts, isolation of any crystalline materials from these reactions was not possible, instead a series of 'crispy foams' or gels were obtained.

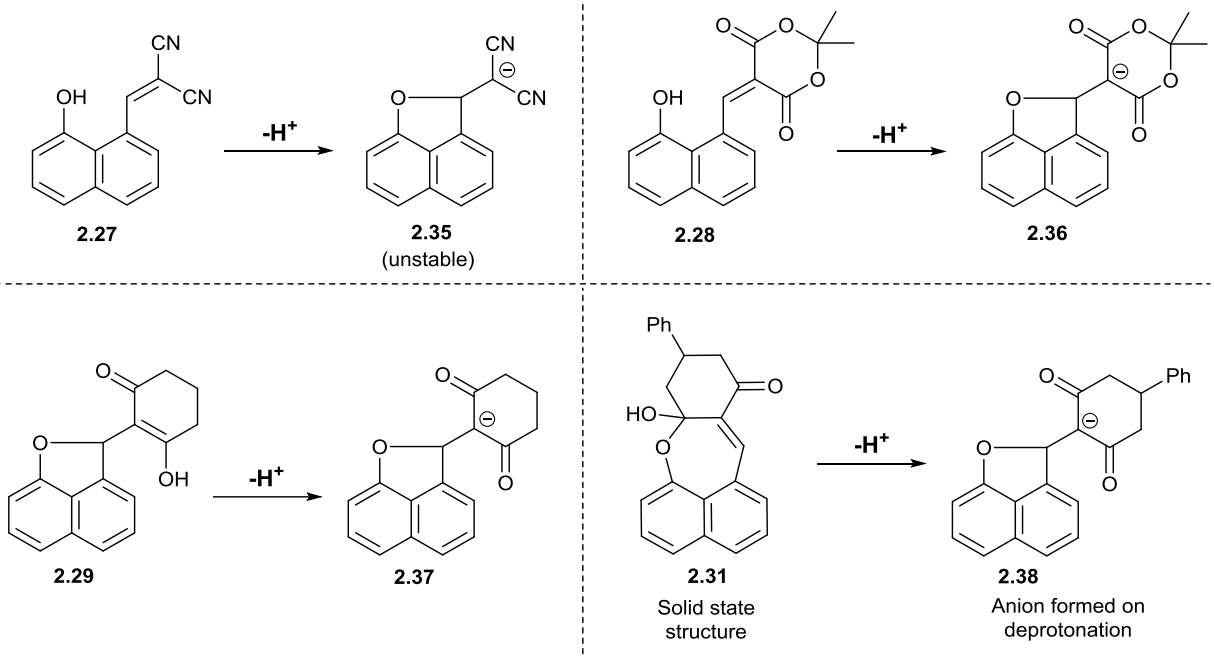

*Scheme 2.13. Anions **2.35-2.38** produced by deprotonation of Knoevenagel products **2.27-2.29** and **2.31**.*

The Knoevenagel products **2.28, 2.29** and **2.31,** which have the most electrophilic alkenes activated by two in-plane carbonyl groups, were deprotonated with mild organic bases DMAP and DABCO, giving stable anions **2.36-2.38** (Scheme 2.7). Upon deprotonation, each oxyanion has added to the adjacent *peri*-alkene forming an O-C bond, with the negative charge stabilised by the two carbonyl groups (similar to the reaction shown in the structural analysis of **2.29**). The structure of each anion is strongly evidenced by the methine CH peaks in the ^{1}H and ^{13}C NMR spectra. On the other hand, the less electrophilic ethenedinitrile group of **2.27**, like ketones **2.2** and **2.3,** could not be deprotonated to give the desired oxyanion with DMAP and DABCO. However, the use of the stronger guanidine base TMG or sodium hydride did result in the deprotonation of the hydroxyl group. The resultant deep purple anion **2.35** possessed poor stability, decomposing after only several hours at room temperature in a range of solvents. The behaviour of these anions follows the alkene reactivity found in the corresponding series of *peri*-dimethylamino derivatives.

An example of a stable anion is seen when Meldrum's derivative **2.28** is treated with DABCO, to give the cyclic anion **2.36**. NMR analysis reveals that the methine group of the anion **2.36** is found with peaks at 7.00 ppm and 89.7 ppm in the ^{1}H and ^{13}C NMR spectra respectively, compared to 9.27 ppm and 163.5 ppm in neutral compound **2.28**. The carbanionic centre has a ^{13}C NMR shift of 75.6 ppm, with only one carbonyl peak at 167.1 ppm being observed, since the 1, 3-dioxanedione ring now has rotational freedom. Despite the formation of the *peri*-bond, the naphthyl hydrogen *ortho* to the oxygen is shifted up field by 0.38 ppm to 6.50 ppm. Equally, in the 13C spectra the *ortho* carbon is also shifted up field by 10.8 ppm to 100.1 ppm and the *ipso* carbon is shifted downfield by 8.5 ppm to 162.8 ppm. Together these shifts suggest some degree of delocalisation of charge into the naphthalene ring. The closely related anions **2.37** and **2.38** show similar characteristics in their NMR spectra. Despite great difficulty due to the rate of decomposition of the anion **2.35** from the dinitrile derivative, NMR spectra of the TMG

and sodium salt were collected. The sodium salt of **2.35** shows a methine group at 101.8 and a $^{(-)}C(CN)_2$ carbanion at 23.2 ppm.[32] In contrast, the TMG salt of **2.35** shows an equilibrium between the neutral dinitrile and its anion with two broad peaks in the ^{13}C NMR at 158.4 and 69.2 ppm for the alkene carbons.

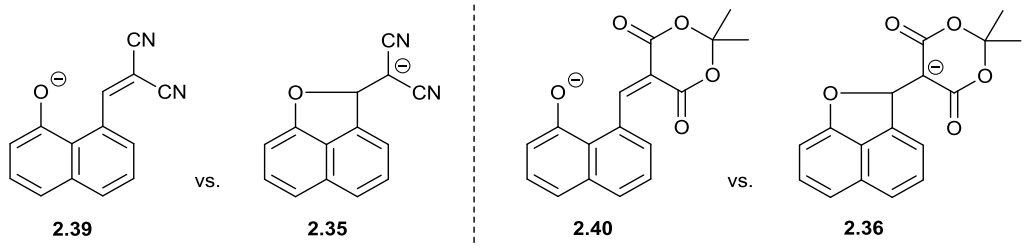

*Scheme 2.14. Open and closed forms for the anions of naphthols **2.27** and **2.28** explored in the DFT calculations.*

In view of the lack of experimental structural data, the structures of the anions formed from *peri*-naphthols **2.27** and **2.28** were calculated by density functional theory (DFT) by Dr. M. A. Addicoat. 1D potential energy surfaces (PES), with different *peri* O···C separations were calculated using B3LYP/6-31++gIJd,p) in order to identify the relative energies and structures of the open and closed forms: **2.39** vs. **2.35**, and **2.40** vs. **2.36**, for the two naphtholates (Scheme 2.8). For the anion of the Meldrum's acid derivative **2.28**, the closed form **2.36**, with a *peri* O–C bond length of 1.540 Å was the only minimum identified, consistent with NMR studies. In contrast, for the anion of dinitrile **2.27** both the open form **2.39** (O(−)···C: 2.362 Å) and the closed form **2.35** (O···C: 1.622 Å) were found to be of similar energy, $\Delta E = 0.33$ kJ mol^{-1}, and separated by a low energy barrier of 2.35 kJ mol^{-1}. This is in contrast to the NMR studies of the sodium salt which support the short-lived closed structure. However, the calculations refer to the isolated anion *in vacuo*, and so do not include effects of cations or solvent. It is notable that the O–C bond length predicted for the closed form **2.35** is comparable to the longest O–C bond reported (1.622 Å)[33] which was observed in a strained oxonium system embedded in an oxatriquinane and so the low stability of this anion is not surprising.

To conclude, a series of naphthols have been synthesised that demonstrate an interaction between the nucleophilic hydroxyl group and a *peri*-electrophilic centre (ketone or alkene). The neutral ketones **2.2** and **2.5** as well as the Knoevenagel products **2.26-2.28** demonstrate O---C contacts well within the Van der Waals radii for the interacting atoms, with the alkenes **2.26-2.28** demonstrating a reactivity series parallel to that of the dimethylamino series. Substitution of the alkenes with the cyclic diketones in examples **2.29** and **2.31** generated two interesting structures, whereby the solution and solid state structures differed. In the case of the cyclohexadione derivative **2.29**, long O-C bonds of 1.508(3) and 1.521(3) Å were observed in the cyclised neutral species. Complexation of the *peri*-hydroxy ketone derivatives with DMAP results in a hydrogen bonded complex between the pyridine nitrogen and the hydroxyl proton. This leads to a small increase in the nucleophilicity of the oxygen atom and in turn reduces the O---C=O contact distance. Further extending this, the first 1-naphtholates of *peri*-benzoyl- (**2.17**) and acetyl-naphthols (**2.18**) as TMG salts were synthesised, showing $O^{(-)}$---C=O distances of 2.558(2)-2.618(2) Å. A small increase in the pyramidalities of the carbonyl groups compared to the neutral compounds are observed as a result of the increased nucleophilicity of the oxyanion. The corresponding anions where a polarised alkene replaces the carbonyl (**2.35-2.38**) could only be detected by NMR but showed in all cases addition of the oxyanion to the alkene. Calculations on the anions of the malononitrile and Meldrum's acid naphthol derivatives **2.27** and **2.28** revealed remarkably long O-C bonds (1.622 and 1.540 Å respectively), suggesting that very long bonds could be found and studied in similar derivatives, however adaptations would be required in order to increase the crystallinity of the products. Modifications to the naphthalene scaffold were also performed in an attempt to increase the potency of the oxygen nucleophile via installation of a *para*-methoxy group in the ketone **2.23**. This modification caused a decrease of 0.041(3) Å in the O---C=O contact distance in the neutral species compared to its unsubstituted analogue, with a more favourable Bürgi-Dunitz

angle of approach (108.7(2)^{o}) being observed. Deprotonation of oxyanion **2.23** with TMG results in the oxyanion salt **2.24**, however the structure was found to incommensurate. Nevertheless, preliminary structural data suggested a further decrease in the $O^{(-)}$---C=O contact distance when compared to the neutral species **2.23** or the equivalent unsubstituted analogue **2.17**.

Experimental

General. Solution NMR spectra were measured on a Jeol ECLIPSE ECX or ECZ 400 spectrometer at 400 MHz for ^{1}H and at 100.6 MHz for ^{13}C using $CDCl_3$ as solvent and tetramethylsilane (TMS) as standard unless otherwise stated, and measured in p.p.m. downfield from TMS with coupling constants reported in Hz. IR spectra were recorded on a Perkin Elmer Spectrum 100 FT-IR Spectrometer using Attenuated Total Reflection sampling on solids or oils and are reported in cm^{-1}. Mass spectra were recorded at the EPSRC Mass Spectrometry Centre at the University of Swansea. Chemical analysis data were obtained from Mr Stephen Boyer, London Metropolitan University.

Preparation of 1,8-Naphtholactam.

1,8-Naphthalic anhydride 1 (10.00 g, 0.05 mol) and hydroxylamine hydrochloride (3.51 g, 0.05 mol) were heated under reflux in dry pyridine (50 mL) for 1 h. p-Toluene sulfonyl chloride (20.90g, 0.11 mol) was carefully added in portions to cause controlled boiling. Reflux was continued for a further 1 h. The mixture was poured onto water (300 mL) and the crystalline precipitate collected by filtration and washed with 0.5N NaOH and water to remove N-hydroxynaphthalimide. The crystals were stirred in refluxing water (150 mL) and ethanol (50 mL) containing NaOH (10 g) for 2 h. After this time ethanol was removed *in vacuo*. The resulting mixture was cooled to room temperature, acidified with concentrated HCl (30 mL) and the crude product allowed to precipitate overnight. The solid was collected by filtration, washed with water and dried at under reduced pressure. The crude yellow solid was purified by flash column chromatography (4:1 EtOAc/petrol 40-60), to give 1,8-naphtholactam as a yellow solid (6.65 g, 79%). Data for the product obtained was consistent with the literature sources.[22]

Preparation of 1,8-Naphtholactone, 2.1.

1,8-Naphtholactam (1.50 g, 18 mmol) was added to 0.5 N NaOH (150 mL) and the mixture was heated until complete solubility was achieved. This mixture was cooled to 0 °C and sodium nitrite (0.84 g, 20 mmol) added. This solution was then added (over 15 min) to sulfuric acid (10 mL conc. H_2SO_4 in 200 mL ice/water). The mixture was warmed slowly and when the temperature reached 40 °C crystals started to appear. Heating was stopped when the temperature reached 70 °C. The mixture was then cooled to 0 °C and the solid collected. The crude yellow solid was purified by flash column chromatography (2:3 EtOAc/petrol 40-60), to give 1,8-naphtholactone as a pale yellow solid (0.98 g, 64%). Data for the product obtained was consistent with the literature sources [22]

NMR of Naphth-1-ol and its Sodium Salt.

Naphth-1-ol: δH (400 MHz, THF-d_8, 24 °C): 8.98 (1H, s, O*H*), 8.27 (1H, m, 8-*H*), 7.77 (1H, m, 5-*H*), 7.39-7.46 (2H, m, 6-,7-*H*), 7.34 (1H, d, J = 7.3 Hz, 4-*H*), 7.27 (1H, t, J = 7.3 Hz, 3-*H*), 6.77 (1H, dd, J = 7.3, 0.9 Hz, 2-*H*); δC (100 MHz, THF-d_8, 24 °C): 154.9 (1-*C*), 136.5 (4a-*C*), 128.6 (5-*C*), 127.3 (3-*C*), 127.2 (6-*C*), 126.6 (8a-*C*), 125.5 (7-*C*), 123.6 (8-*C*), 120.1 (4-*C*), 109.1 (2-*C*). Naphth-1-ol, dissolved in THF-d_8, was treated with excess sodium hydride, stirred for 10 min and filtered. δH (400 MHz, THF-d_8, 24 °C): 8.48 (1H, d, J = 8.2 Hz, 8-*H*), 7.63 (1H, d, J = 8.2 Hz, 5-*H*), 7.22 (1H, t, J = 8.0 Hz, 6-*H*), 7.18 (1H, t, J = 8.0 Hz, 3-*H*), 7.09 (1H, t, J = 6.9 Hz, 7-*H*), 6.81 (1H, d, J = 7.8 Hz, 4-*H*), 6.61 (1H, d, J = 8.2 Hz, J = 7.8 Hz, 2-*H*); δC (100 MHz, THF-d_8, 24 °C): 168.8 (1-*C*), 138.0 (4a-*C*), 132.0 (8a-*C*), 129.4 (3-*C*), 128.8 (5-*C*), 125.8 (6-*C*), 124.2 (8-*C*), 123.2 (7-*C*), 111.7 (4-*C*), 110.9 (2-*C*).

Reaction of Naphth-1-ol with 1,1,3,3-Tetramethylguanidine.

Naphth-1-ol (35 mg), dissolved in THF-d_8, was treated with TMG (28 mg), δH (400 MHz, THF-d_8, 24 °C): 8.40 (2H, br, 1-O*H*, TMG: N*H*), 8.29 (1H, d, J = 7.2 Hz, 8-*H*), 7.66 (1H, d, J = 7.3 Hz, 5-*H*), 7.26-7.34 (2H, m, 6-,7-*H*), 7.11-7.18 (2H, m, 3-,4-*H*), 6.85 (1H, dd, J = 6.9, 1.4 Hz, 2-*H*), 2.69 (12H, s, TMG: 4 x CH_3); δC (100 MHz, THF-d_8, 24 °C): 167.4 (TMG: -*C*=NH), 157.5 (1-*C*), 136.2 (4a-*C*), 127.9 (5-*C*), 127.5 (8a-*C*), 127.2 (3-*C*), 126.1 (6-*C*), 124.0 (7-*C*), 123.9 (8-*C*), 117.1 (4-*C*), 108.8 (2-*C*), 39.4 (TMG-H^+: 4 x CH_3), corresponds to *ca*. 20% deprotonation of naphthol by TMG.

Preparation of 8-Benzoylnaphth-1-ol, 2.2.

Lactone **2.1** (1.00 g, 5.88 mmol) was dissolved in anhydrous THF (15 mL) under nitrogen and cooled to -78℃. Phenyl lithium (1.8M in dibutyl ether, 2.61 mL, 4.71 mmol) was steadily added and the bright orange solution was allowed to warm to room temperature overnight. After 16 h. the resulting dark yellow solution was quenched with EtOAc (10 mL) and H_2O added. The aqueous solution was washed with DCM (3 x 40 mL) and the combined organic layers washed with H_2O (2 x 40 mL), brine (1 x 40 mL) and dried over $MgSO_4$. The solvent was removed *in vacuo* to give a crude oil which was purified by flash column chromatography (1:4 EtOAc/petrol 40-60), to give **2.2** as a brown solid (370 mg, 32%) m.p. 183-185℃ (lit.[23] 184-187 ºC). δH (400 MHz, $CDCl_3$, 24 °C): 8.01 (1H, d, J = 7.8 Hz, 7-*H*), 7.81 (2H, d, J = 8.2 Hz, 2'-,6'-*H*), 7.58 (1H, t, J = 8.7 Hz, 4'-*H*), 7.50 - 7.55 (2H, m, 4-,5-*H*), 7.38 - 7.49 (4H, m, 3-,6-,3'-,5'-*H*), 7.12 (1H, br s, O*H*), 6.99 (1H, d, J = 7.8 Hz, 2-*H*); δC (100 MHz, $CDCl_3$, 24 °C): 201.7 (C=O), 152.3 (1-*C*), 138.5 (1'-*C*), 135.6, 134.6 (Ar-C_2), 133.1 (4'-*C*), 132.4 (Ar-

C$_1$), 130.5 (2'-,6'-*C*), 129.9 (Ar-*C*$_1$), 128.3 (3'-,5'-*C*), 127.4, 124.2, 122.0, 121.5 (Ar-*C*$_4$), 113.7 (2-*C*); ν_{max}/cm^{-1} 3050 (OH), 1638 (C=O), 1574, 1432, 1345, 1270; *HRMS* (ESI) calcd for $C_{17}H_{13}O_2$ ($[M+H]^+$): 249.0910, found: 249.0912.

Preparation of Sodium 8-benzoylnaphth-1-olate.

8-Benzoylnaphth-1-ol (25 mg) was dissolved in THF (3 mL) and the solution treated with sodium hydride (60% dispersion in oil, *ca*. 4 mg) until there was no more effervescence. After stirring for a further 5 min. the solution was evaporated *in vacuo*, DMSO-d$_6$ (1 ml) was added, and the solution was filtered, and the NMR spectra were recorded. δH (400 MHz, DMSO-d$_6$, 24 °C): 7.49 (1H, d, J = 7.3 Hz, 5-*H*), 7.45 (2H, d, J = 7.6 Hz, 2'-, 6'-*H*), 7.35 (1H, t, J = 6.0 Hz, 4'-*H*), 7.28 (2H, t, J = 7.3 Hz, 3'-,5'-*H*), 7.14 (1H, t, J = 7.0 Hz, 6-*H*), 6.99 (1H, t, J = 8.0 Hz, 3-*H*), 6.65 (1H, dd, J = 6.9, 0.9 Hz, 7-*H*), 6.39 (1H, d, J = 7.3 Hz, 4-*H*), 5.79 (1H, dd, J = 7.8, 0.9 Hz, 2-*H*); δC (100 MHz, DMSO-d$_6$, 24 °C): 197.8 (*C*=O), 168.3 (1-*C*), 140.6 (1'-*C*), 139.5 (8-*C*), 136.3(4a-*C*), 130.1 (4'-*C*), 129.7 (3-*C*), 129.5 (8a-*C*), 127.5 & 127.4 (2'-,3'-,5'-,6'-*C*), 126.7 (5-*C*), 123.8 (6-*C*), 118.1 (7-*C*), 108.1 (2-*C*), 103.7 (4-*C*).

Preparation of 1,1,3,3-Tetramethylguanidium 8-benzoylnaphth-1-olate, 2.17.

8-Benzoylnaphth-1-ol **2.2** (100 mg, 0.42 mmol) was dissolved in chloroform (2 mL) and TMG (0.05 mL, 0.42 mmol) was added. The solvent was removed *in vacuo* and the solid was dissolved in DCM. Nitrogen was passed over the surface of the solution, yielding yellow crystals of the salt **2.17**, m.p. 100-103℃. δH (400 MHz, DMSO-d$_6$ 24 °C): 7.53 (1H, d, J = 8.2

Hz, 5-*H*), 7.38 (2H, d, J = 7.8 Hz, 2'-,6'-*H*), 7.30 (1H, t, J = 6.8 Hz, 4'-*H*), 7.20 (2H, t, J = 6. Hz, 3'-,5'-*H*), 7.15 (1H, t, J = 7.8 Hz, 6-*H*), 6.81 (1H, t, J = 7.8 Hz, 3-*H*), 6.77 (1H, d, J = 6.9 Hz, 7-*H*), 6.70 (1H, d, J = 8.2 Hz, 4-*H*), 5.67 (1H, d, J = 7.3 Hz, 2-*H*), 2.66 (12H, s, TMG-H^+: 4 x CH_3); δC (100 MHz, $CDCl_3$, 24 °C): 197.9 (*C*=O), 163.6 (TMG-H^+: *C*=NH_2^+), 161.4 (1-*C*), 139.8 (1'-*C*), 138.3 (8-*C*), 135.4 (4a-*C*), 131.5 (4'-*C*), 128.6 (3-*C*), 128.4 (2'-,6'-*C*), 128.1 (3'-,5'-*C*), 128.0 (5-*C*), 125.6 (8a-*C*), 124.4 (6-*C*), 120.9 (7-*C*), 111.3 (4-*C*), 108.7 (2-*C*), 39.3 (TMG-H^+: 4 x *C*H_3); ν_{max}/cm^{-1} 3083, 3083, 2891, 1654 (C=O), 1594, 1568, 1491, 1442, 1385, 1318, 1270, 1106; *HRMS* (ESI): calcd for $C_{17}H_{11}O_2$ ([M-H]$^-$): 247.0765, found: 247.0771.

Preparation of 8-(3'-Methylbutanoyl)naphth-1-ol, 2.10.

Lactone **2.1** (1.00 g, 5.88 mmol) was dissolved in anhydrous THF (15 mL) under nitrogen and cooled to -78℃. *Sec*-BuLi (1.4M in cyclohexane, 4.20 mL, 5.88 mmol) was steadily added, and the bright orange solution was allowed to warm to room temperature overnight. After 16 h. the resulting dark yellow solution was quenched with EtOAc (10 mL) and H_2O was added. The aqueous solution was washed with DCM (3 x 40 mL) and the combined organic layers were washed with H_2O (2 x 40 mL), brine (1 x 40 mL) and dried over $MgSO_4$. The solvent was removed *in vacuo* to give a crude oil which was purified by flash column chromatography (1:19 EtOAc/petrol 40-60), to give **2.10** as a yellow solid (320 mg, 24%), m.p. 71-74℃. δH (400 MHz, $CDCl_3$, 24 °C): 8.19 (1H, s, O*H*), 8.00 (1H, dd, J = 8.2, 1.4 Hz, 7-*H*), 7.83 (1H, dd, J = 7.3, 0.9 Hz, 5-*H*), 7.42 - 7.52 (3H, m, 3-,4-,6-*H*), 7.11 (1H, dd, J = 7.3, 1.8 Hz, 2-*H*), 3.51 (1H, sxt, J = 6.9 Hz, 2'-*H*), 1.89 (1H, m, 3'-H_α), 1.56 (1H, m, 3'-H_β), 1.28 (3H, d, J = 6.9 Hz, 2'-CH_3), 0.97 (3H, t, J = 7.3 Hz, 4'-H_3); δC (100 MHz, $CDCl_3$, 24 °C): 215.0 (*C*=O), 152.9 (1-*C*), 136.0, 135.7 (Ar-C_2), 134.0 (7-*C*), 129.1, 127.6, 124.0, 121.5, 121.4 (Ar-C_5), 114.9 (2-*C*), 47.0

(2'-*C*), 27.1 (3'-*C*), 17.1 (2'-*C*H_3), 11.8 (4'-*C*); ν_{max}/cm^{-1} 3131 (OH), 3047, 2967, 2931, 1668 (C=O), 1620, 1577, 1523, 1439, 1346, 1239; *HRMS* (ESI): calcd for $C_{15}H_{17}O_2$ ($[M+H]^+$): 229.1223, found: 229.1223. A preceding fraction yielded a small amount (120 mg, 18%) of *3-(sec-butyl)-2H-naphtho[1,8-bc]furan-2-one* ***2.11***, δH (400 MHz, $CDCl_3$, 24 °C): 8.02 (1H, d, J = 8.5 Hz, Ar-*H*), 7.62 (1H, d, J = 8.4 Hz, Ar-*H*), 7.56 (1H, d, J = 8.4 Hz, Ar-*H*), 7.43 (1H, dd, J = 8.4, 7.2 Hz, 7-*H*), 7.06 (1H, d, J = 7.3 Hz, 8-*H*), 3.74 (1H, sxt, J = 7.2 Hz, 2'-*H*), 1.72 (1H, quin, J = 7.4 Hz *3'*-H_2), 1.32 (3H, d, J = 7.0 Hz, 2'-CH_3), 0.79 (3H, t, J = 7.3 Hz, 4'-H_3); δC (100 MHz, $CDCl_3$, 24 °C): 167.3 (*C*=O), 151.8 (8a-*C*), 149.5, 132.4, 129.1, 128.2, 128.1, 128.0, 120.5, 117.3, 105.8 (Ar-C_9), 36.3 (2'-*C*), 30.2 (3'-*C*), 20.8 (2'-*C*H_3), 12.1 (4'-*C*).

Preparation of 8-(3'-Methylbutanoyl)naphth-1-ol . 4-Dimethylaminopyridine Molecular Complex, 2.10.DMAP.

Ketone **2.10** (63 mg, 0.28 mmol) was dissolved in THF (5 mL), DMAP (33 mg, 0.28 mmol) was added and the reaction was stirred for 30 min. at room temperature. The solvent was removed *in vacuo* and the solid was dissolved in acetone. The solution was left to evaporate slowly, yielding **2.10.DMAP** as a brown crystalline solid, m.p. 83-86℃. δH (400 MHz, $CDCl_3$, 24 °C): 8.17 (2H, dd, J = 5.0, 1.4 Hz, DMAP: 2-,6-*H*), 7.80 (1H, d, J = 8.2 Hz, 7-*H*), 7.40 (1H, t, J = 6.9 Hz, 6-*H*), 7.22 - 7.36 (3H, m, 3-,4-,5-*H*), 6.91 (1H, dd, J = 6.9, 1.8 Hz, 2-*H*), 6.49 (2H, dd, J = 5.5, 1.4 Hz, DMAP: 3-,5-*H*), 3.11 - 3.21 (1H, m, 2'-*H*), 2.99 (6H, s, DMAP: N(CH_3)$_2$), 1.77 - 1.90 (1H, m, 3'-H_α), 1.38 - 1.53 (1H, m, 3'-H_β), 1.21 (3H, d, J = 6.9 Hz, 2'-H_3), 0.90 (3H, t, J = 7.3 Hz, 4'-H_3); δC (100 MHz, $CDCl_3$, 24 °C): 212.3 (*C*=O), 154.7 & 154.4 (1-*C*, DMAP: 4-*C*) 148.3 (DMAP: 2-,6-*C*), 138.5, 135.5 (Ar-C_2), 129.5 (7-*C*), 127.2, 124.9, 124.1, 122.5, 118.8 (Ar-C_5), 110.4 (2-*C*), 106.7 (DMAP: 3-,5-*C*), 48.4 (2-*C*), 39.2 (DMAP,

N(CH_3)$_2$), 25.8 (3'-*C*), 15.6 (2'-*C*H_3), 11.6 (4'-*C*); ν_{max}/cm^{-1} 2913, 2450, 1681 (C=O), 1602, 1526, 1445, 1343, 1223.

Preparation of 8-Acetylnaphth-1-ol, 2.5.

Lactone **2.1** (1.00 g, 5.88 mmol) was dissolved in anhydrous THF (15 mL) under nitrogen and cooled to -78℃. MeLi (1.6M in diethyl ether, 2.94 mL, 4.71 mmol) was steadily added, and the bright orange solution was kept at -78 ºC for 1 h. The resulting yellow solution was quenched with saturated ammonium chloride (10 mL) and acidified with 1M aqueous hydrochloric acid. The aqueous solution was washed with ethyl acetate (3 x 40 mL) and the combined organic layers were washed with H_2O (2 x 40 mL), brine (1 x 40 mL) and dried over $MgSO_4$. The solvent was removed *in vacuo* to give a crude oil which was purified by flash column chromatography (1:9 EtOAc/petrol 40-60), to give **2.5** as a yellow solid (460 mg, 42%), %), m.p. 82-84 ºC (lit.[23] 81-83 ºC). δH (400 MHz, $CDCl_3$, 24 °C): 9.67 (1H, s, O*H*), 8.00 (1H, dd, J = 8.2, 0.9 Hz, 5-*H*) 7.96 (1H, dd, J = 7.3, 0.9 Hz, 7-*H*), 7.41 - 7.45 (3H, m, 3-,4-,6-*H*), 7.10 (1H, dd, J = 6.0, 2.7 Hz, 2-*H*), 2.78 (3H, s, C*H*$_3$)*;* δC (100 MHz, $CDCl_3$, 24 °C): 207.3 (*C*=O), 153.3 (1-*C*), 136.1 (4a-*C*), 135.4 (5-*C*), 135.0 (8-*C*), 131.3 (7-*C*), 127.9 & 124.0 (3-,6-*C*), 121.3 (8a-*C*), 121.1 (4-*C*), 115.0 (2-*C*), 30.5 (*C*H_3); ν_{max}/cm^{-1} 3114 br, 3056, 2959, 1671 (C=O), 1620, 1577, 1522, 1438, 1346, 1292, 1257, 1189, 1165, 1142, 1091, 946, 821, 790. Found: C, 77.48; H, 5.47. Calc. for $C_{12}H_{10}O_2$: C, 77.40; H, 5.41%.

Preparation of Sodium 8-acetylnaphth-1-olate.

8-Acetylnaphth-1-ol **2.5** (20 mg) was dissolved in THF (4 ml) and the solution treated with sodium hydride (60% dispersion in oil, *ca*. 4.5 mg) until there was no more effervescence. After stirring for a further 5 min. the solution was evaporated i*n vacuo*, THF-d_8 (1 ml) added, and the solution filtered, and the NMR spectra recorded. δH (400 MHz, THF-d_8, 24 °C): 7.49 (1H, d, J = 8.2 Hz, 5-*H*), 7.06 (1H, t, J = 7.8 Hz, 3-*H*), 7.09 (1H, t, J = 7.3 Hz, 6-*H*), 6.71 (1H, d, J = 6.9 Hz, 7-*H*), 6.63 (1H, d, J = 8.2 Hz, 4-*H*), 6.29 (1H, d, J = 7.8 Hz, 2-*H*), 2.54 (3H, s, C*H*$_3$); δC (100 MHz, THF-d_8, 24 °C): 213.5 (*C*=O), 168.2 (1-*C*), 142.7 (8-*C*), 137.6 (4a-*C*), 129.9 (3-*C*), 128.3 (5-*C*), 128.2 (8a-*C*), 124.2 (6-*C*), 117.1 (7-*C*), 110.7 (2-*C*), 109.0 (4-*C*), 33.6 (*C*H$_3$).

Preparation of 8-Acetylnaphth-1-ol . 4-Dimethylaminopyridine Molecular Complex, 2.5.DMAP.

8-Acetylnaphth-1-ol **2.5** (32 mg, 0.17 mmol) was dissolved in THF (3 mL), DMAP (22 mg, 0.17 mmol) was added and the reaction was stirred for 30 min. at room temperature. The solvent was removed *in vacuo* and the solid was dissolved in DCM. The solution was left to evaporate slowly, yielding **2.5.DMAP** as a brown crystalline solid, m.p. 110-112℃. δH (400 MHz, $CDCl_3$, 24 °C): 8.08 (2H, dd, J = 5.0, 1.4 Hz, DMAP: 2-,6-*H*), 7.75 (1H, m, 7-*H*), 7.29-7.34 (2H, m, 5-,6-*H*), 7.22 - 7.27 (2H, m, 3-,4-*H*), 7.17 (1H, br s, O), 6.87 (1H, dd, J = 5.5, 2.7 Hz, 2-*H*), 6.40 (2H, dd, J = 5.0, 1.4 Hz, DMAP: 3-,5-*H*), 2.90 (6H, s, DMAP: N(C*H*$_3$)$_2$), 2.58 (3H, s, C*H*$_3$); δC (100 MHz, $CDCl_3$, 24 °C): 206.0 (*C*=O), 154.6 & 154.2 (1-*C*, DMAP-H$^+$: 4-*C*), 148.0 (DMAP: 2-,6-*C*), 135.4, 138.6 (Ar-*C*$_2$), 130.6 (7-*C*), 127.4, 124.8, 124.2, 121.8, 118.9

(Ar-C_5), 111.1 (2-*C*), 106.6 (DMAP: 3-,5-*C*), 39.0 (DMAP: N(CH_3)$_2$), 31.8 (CH_3); ν_{max}/cm^{-1} 2921, 2345 br, 1687 (C=O), 1604, 1567, 1528, 1437, 1345, 1255, 1223, 1186, 1062, 1001, 808, 781, 750.

Preparation of 1,1,3,3-Tetramethylguanidinium 8-acetylnaphth-1-olate, 2.18.

8-Acetylnaphth-1-ol **2.5** (250 mg, 1.34 mmol) was dissolved in THF (5 mL) and 1, 1, 3, 3-tetramethylguanidine (0.17 mL, 1.34 mmol) was added. Nitrogen was passed over the surface of the solution, yielding a bright yellow oil. Maintenance of the oil under nitrogen eventually yielded yellow crystals of the salt, **2.18**, m.p. 88-90 ºC. δH (400 MHz, $CDCl_3$, 24 °C): 7.64-7.74 (3H, m (d + br s), 7-*H*, TMG-H$^+$: NH_2), 7.25-7.31 (2H, m, 3-,6-*H*), 7.08 (1H, d, J = 7.3 Hz), & 7.00 (1H, dd, J = 6.9, 1.4 Hz) (4-,5-*H*), 6.80 (1H, dd, J = 7.3, 0.9 Hz, 2-*H*), 2.70 (12H, s, TMG-H$^+$: 4 x CH_3), 2.57 (3H, s, CH_3); δC (100 MHz, $CDCl_3$, 24 °C): 208.6 (*C*=O), 166.1 (TMG-H$^+$: *C*=N), 158.8 (1-*C*), 140.6, 135.5 (Ar-C_2), 128.5 (7-*C*), 128.1, 128.0, 124.5, 120.0, 114.4 (Ar-C_5), 110.2 (2-*C*), 39.2 (TMG-H$^+$: 4 x CH_3), 32.9 (-CH_3); ν_{max}/cm^{-1} 3319, 3020, 2940 br, 2906, 1676 (C=O), 1594, 1560, 1445, 1407, 1379, 1348, 1315, 1259, 1093, 1061, 1033, 944, 821, 760.

Preparation of 3-(*t*-Butyl)-2H-naphtho[1,8-bc]furan-2-one, 2.8.

Lactone **2.1** (0.75 g, 4.41 mmol) was dissolved in anhydrous THF (15 mL) under nitrogen and cooled to -78℃ (CO_2/acetone bath). *t*-BuLi (1.6M in pentane, 2.75 mL, 4.41 mmol) was steadily added, and the bright orange solution was allowed to warm to room temperature. After

72 h. the resulting dark brown solution was quenched with EtOAc (10 mL) and H_2O (5 mL) added. The aqueous solution was washed with DCM (3 x 40 mL) and the combined organic layers were washed with H_2O (2 x 40 mL), brine (1 x 40 mL) and dried over $MgSO_4$. The solvent was removed *in vacuo* to give a crude oil which was purified by flash column chromatography (1:49 EtOAc/petrol 40-60), to give **2.8** as a light brown solid (140 mg, 14%) m.p. 106-109℃. δH (400 MHz, $CDCl_3$, 24 °C): 8.08 (1H, d, J = 8.6 Hz, 4-*H*), 7.83 (1H, d, J = 8.6 Hz, 5-*H*), 7.61 (1H, d, J = 8.4 Hz, 6-*H*), 7.49 (1H, dd, J = 8.4, 7.3 Hz, 7-*H*), 7.12 (1H, d, J = 7.3 Hz, 8-*H*), 1.60 (9H, s, 3 x CH_3); δC (100 MHz, $CDCl_3$, 24 °C): 167.1 (*C*=O), 155.8 (8a-*C*), 149.7 (Ar-C_1), 132.7 (4-*C*), 130.4, 128.5 (Ar-C_2), 127.9 (5-,7-*C*), 120.5 (6-*C*), 117.8 (Ar-C_1), 105.4 (8-*C*), 36.3 (*C*(CH_3)$_3$), 29.6 (C(*C*H_3)$_3$); ν_{max}/cm^{-1} 2958, 2870, 1768 (C=O), 1748, 1461, 1361. Found: C, 79.84; H, 6.33. Calc. for $C_{15}H_{14}O_2$: C, 79.62; H, 6.24%.

Preparation of 3-(*tert*-Butyl)-2-methyl-2H-naphtho[1,8-bc]furan-2-ol, 2.9.

Ortho-substituted lactone **2.8** (75 mg, 0.33 mmol) was dissolved in anhydrous THF (5 mL) under nitrogen and cooled to -78℃. MeLi (1.2M in diethyl ether, 0.33 mL, 0.39 mmol) was steadily added, and the reaction was allowed to warm to room temperature overnight. After 24 h. the resulting solution was quenched with EtOAc (10 mL) and H_2O (5 mL) added. The aqueous solution was washed with DCM (3 x 40 mL) and the combined organic layers were then washed with H_2O (2 x 40 mL), brine (1 x 40 mL) and dried over $MgSO_4$. The solvent was removed *in vacuo* to give a crude oil which was purified by flash column chromatography (1:19 EtOAc/petrol 40-60) to give a pink oil. The oil was heated to 50℃ under a high vacuum for 4 h. and cooled to -20℃ to give **2.9** as a pink solid (60 mg, 75%), m.p. 108-110℃. δH (400 MHz, $CDCl_3$, 24 °C): 7.67 - 7.75 (2H, m, 4-,5-*H*), 7.36 (1H, t, J = 7.8 Hz, 7-*H*), 7.25 (1H, d, J = 8.2

Hz, 6-*H*), 6.67 (1H, d, J = 7.3 Hz, 8-*H*), 3.65 (1H, br s, O*H*), 2.12 (3H, s, CH_3), 1.55 (9H, s, (CH_3)$_3$); *δC* (100 MHz, $CDCl_3$, 24 °C): 156.4 (8a-*C*), 144.2, 136.2, 130.2 (Ar-C_3), 129.4 (4- or 5-*C*), 128.6 (7-*C*), 127.2 (Ar-C_1), 126.3 (4- or 5-*C*), 115.5 (6-*C*), 114.5 (2-*C*), 101.1 (8-*C*), 36.8 (3-*C*(CH$_3$)$_3$), 33.0 (3-C(*C*H$_3$)$_3$), 28.4 (2-*C*H$_3$); ν_{max}/cm^{-1} 3350 (OH), 2957, 2919, 1688 (w), 1571, 1457, 1364, 1215, 1197, 1161, 1139, 1051, 939, 821, 749; Found: C, 79.16; H, 7.54. Calc. for $C_{16}H_{18}O_2$: C, 79.31; H, 7.49%.

Preparation of 3-(*tert*-Butyl)-2-methyl-2H-naphtho[1,8-bc]furan-2-ol. 4-Dimethylamino-pyridine Molecular Complex, 2.9.DMAP.

Lactol **2.9** (28 mg, 0.12 mmol) was dissolved in DCM (3 mL), DMAP (14 mg, 0.12 mmol) was added and the reaction stirred for 30 min. at room temperature. The solvent was removed *in vacuo* and the residual oil was dissolved in acetone. The solution was cooled to -78℃ in a CO_2/acetone bath and a stream of nitrogen blown over it, resulting in **2.9.DMAP** a pink crystalline solid, m.p. 93-96℃. This material exists as the DMAP complex with the hindered lactol in $CDCl_3$ solution, but as the DMAP complex of the hydroxyl ketone in the crystalline state. δH (400 MHz, $CDCl_3$, 24 °C): 7.86 - 7.99 (2H, m, DMAP: 2-,6-*H*), 7.62 - 7.71 (2H, AB system, J = 8.7 Hz, 4-,5-*H*), 7.31 (1H, t, J = 8.2 Hz, 7-*H*), 7.21 (1H, d, J = 7.8 Hz, 6-*H*), 6.69 (1H, d, J = 6.9 Hz, 8-*H*), 6.38 (2H, d, J = 6.4 Hz, DMAP: 3-,5-*H*), 2.95 (6H, s, DMAP: N(C*H*$_3$)$_2$), 2.23 (3H, s, C*H*$_3$), 1.50 (9H, s, 3-C(C*H*$_3$)$_3$); δC (100 MHz, $CDCl_3$, 24 °C): 156.3 (8a-*C*), 154.5 (DMAP: 4-*C*), 148.6 (DMAP: 2-,6-*C*), 143.4, 136.9, 130.9 (Ar-C_3), 128.7 (4- or 5-*C*), 128.1 (7-*C*), 126.5 (Ar-C_1), 126.3 (4- or 5-*C*), 115.7 (2-,6-*C*), 106.5 (DMAP: 3-,5-*C*), 102.6 (8-*C*), 39.1 (DMAP: N(*C*H$_3$)$_2$), 36.8 (3-*C*(CH$_3$)$_3$), 32.9 (3-C(*C*H$_3$)$_3$), 30.0 (2-*C*H$_3$); ν_{max}/cm^{-1} (solid state) 2962, 2410, 1700 (C=O), 1604, 1536, 1380, 1362, 1216.

Preparation of 6-Methoxy-2H-naphtho[1,8-bc]furan-2-one, 2.22.

6-Hydroxy-2H-naphtho[1,8-bc]furan-2-one **2.21** (265 mg, 1.42 mmol) was dissolved in anhydrous DMSO (10 mL) and stirred whilst anhydrous K_2CO_3 (393 mg, 2.85 mmol) was added, resulting in a colour change from orange to dark purple. After 2 h, iodomethane (0.27 mL, 4.26 mmol) was added and stirring continued for a further 3 h. The reaction was quenched with H_2O (20 mL) and the reaction was extracted with EtOAc (3 x 20 mL). The combined organics were washed with brine (20 mL), dried over $MgSO_4$, filtered and concentrated *in vacuo* to give a dark oil residue. The residue was purified by flash column chromatography (1:9 EtOAc/petrol 40-60), to give the methoxy-lactone **2.22** as a yellow solid (100 mg, 35%) m.p. 142-145℃ (lit. [34]146-147 ºC). δH (400 MHz, $CDCl_3$, 24 °C): 8.26 (1H, d, J = 8.2 Hz, 4-*H*), 8.07 (1H, d, J = 7 Hz, 2-*H*), 7.71 (1H, dd, J = 8.1, 1.0 Hz, 3-*H*), 6.97 (1H, d, J = 7.9 Hz, 7-*H*), 6.67 (1H, d, J = 8.0 Hz, 6-*H*), 3.27 (1H, s, C*H*$_3$); δC (100 MHz, $CDCl_3$, *24* °C): 167.7 (C=O), 152.1 (5-*C*), 143.4 (8-*C*), 129.9 (1-*C*), 128.6 (3-*C*), 128.2 (4-*C*), 126.7 (2-*C*), 122.8 (4a-*C*), 121.1 (8a-*C*), 106.3 (7-*C*), 105.2 (6-*C*), 55.9 (CH_3); ν_{max}/cm^{-1} 3096, 2935, 2835, 2111, 1890, 1765, 1730, 1634, 1600, 1458, 1431, 1367, 1251, 1220, 1130, 1070, 1013, 942, 852, 814, 737, 674, 634, 598.

Preparation of 8-Benzoyl-4-methoxynaphth-1-ol, 2.23.

6-Methoxy-2H-naphtho[1,8-bc]furan-2-one **2.22** (150 mg, 0.75 mmol) was dissolved in anhydrous THF (10 mL) under nitrogen and cooled to -78℃ (CO_2/acetone bath). Phenyl lithium (1.9M in dibutyl ether, 0.43 mL, 0.83 mmol) was steadily added and the bright yellow solution slowly became orange and then brown. After 2 h at -78℃ the solution was quenched

with saturated NH_3.HCl (10 mL) and stirred for 10 mins before 1M HCl (10 mL) was added. The solution was extracted with EtOAc (3 x 20 mL) and the combined organics were washed with H_2O (20 mL) and brine (20 mL). The organics were subsequently dried over $MgSO_4$, filtered and concentrated *in vacuo* to give an orange oil, which crystallised when left in the freezer overnight. The orange solid was purified by flash column chromatography (1:9 EtOAc/hexane), to give **2.23** as a yellow solid (90 mg, 43%) m.p. decomp >130℃. δH (400 MHz, $CDCl_3$, 24 °C): 8.47 (1H, dd, J = 8.2, 1.8 Hz, 4-*H*), 7.77-7.83 (2H, m, 2', 6'-*H*), 7.37-7.60 (5H, m, 2-,3-,3'-,4'-,5'-*H*), 6.91 (1H, d, J = 8.7 Hz, 7-*H*), 6.77 (1H, d, J = 8.2 Hz, 6-*H*), 3.98 (1H, s, C*H*$_3$); δC (100 MHz, $CDCl_3$, *24* °C): 201.4 (C=O), 150.0 (Ar-*C*$_5$), 145.3, 138.4, 134.4, 133.1, 130.5 (2',6'-*C*), 129.8 (Ar-*C*$_4$), 128.3, 128.0, 126.8, 126.1 (4-*C*), 123.7 (Ar-*C*$_1$), 113.3 (7-*C*), 105.2 (6-*C*), 55.9 (CH_3); ν_{max}/cm^{-1} 3247, 2927, 1655, 1620, 1587, 1474, 1447, 1405, 1375, 1339, 1317, 1262, 1134, 1032, 946, 810, 767, 732, 713, 684, 661, 451;

Preparation of Ethyl (*E*)-2-cyano-3-(8'-hydroxynaphthalen-1'-yl)propenoate, 2.26.

1-Hydroxy-8-naphthaldehyde **2.25** (250 mg, 1.45 mmol) was dissolved in anhydrous MeOH (20 mL) under nitrogen. Ethyl cyanoacetate (197 mg, 1.74 mmol) and ethylenediamine diacetate (39 mg, 0.22 mmol) were added and the reaction was heated to reflux for 6h. The solvent was removed *in vacuo* to give **2.26** as a crude yellow solid which was purified by flash column chromatography (1:9 EtOAc:petrol 40-60), to give a yellow solid (224 mg, 72%) m.p. 189-192 ℃; δH (400 MHz, $(CD_3)_2CO$, 24 °C): 9.61 (1H, s, O*H*), 9.55 (1H, s, 1-*H*), 8.03 (1H, d, J = 8.2 Hz, 7'-*H*), 7.80 (1H, d, J = 6.9 Hz, 5'-*H*), 7.58 (1H, t, J = 7.3 Hz, 6'-*H*), 7.48 (1H, d, J = 8.2 Hz, 4'-*H*), 7.40 (1H, d, J = 7.3 Hz, 3'-*H*), 7.06 (1H, dd, J = 7.8, 0.9 Hz, 2'-*H*), 4.36 (2H, q, J = 7.3 Hz, C*H*$_2$CH$_3$), (3H, t, J = 7.3 Hz, CH$_2$C*H*$_3$); δC (100 MHz, $(CD_3)_2CO$, 24 °C): 162.9

(*C*=O), 161.9 (1-*C*), 154.6 (1'-*C*), 136.7 (4a'-*C*), 132.8 (7'-*C*), 130.2 (8'-*C*), 128.4 (5'-*C*), 128.0 (3'-*C*), 126.3 (6'-*C*), 123.1 (8a'-*C*), 121.1 (4'-*C*), 115.8 (*C*≡N), 112.1 (2'-*C*), 104.6 (2-*C*), 62.8 (CH_2CH_3), 14.4 (CH_2CH_3); ν_{max}/cm^{-1} 3251, 3071, 2253 (C ≡N), 1708, 1600, 1436, 1370, 1344, 1263, 1240, 1088, 1084, 1013, 830, 770, 748; Found: C, 71.67; N, 5.25; H, 4.95. Calc. for $C_{16}H_{13}NO_3$: C, 71.90; N, 5.24; H, 4.90%.

Preparation of 2-Cyano-3-(8'-hydroxynaphthalen-1'-yl)propenenitrile, 2.27.

1-Hydroxy-8-naphthaldehyde **2.25** (150 mg, 0.87 mmol) was dissolved in anhydrous MeOH (10 mL) under nitrogen and malononitrile (70 mg, 1.05 mmol) was added, and the deep orange solution was heated to reflux. After 2 h. the solvent was removed *in vacuo* to give a crude yellow solid which was purified by flash column chromatography (1:9 EtOAc:petrol 40-60), to give **2.27**[30] as a yellow solid (140 mg, 73%), m.p. 145-148℃. δH (400 MHz, $CDCl_3$, 24 °C): 9.21 (1H, s, 3-*H*), 7.98 (1H, d, J = 7.9 Hz, 2'-*H*), 7.81 (1H, d, J = 7.3 Hz, 4'-*H*), 7.49-7.58 (2H, m, 3'-,5'-*H*), 7.41 (1H, t, J = 7.6 Hz, 6'-*H*), 6.92 (1H, dd, J = 7.4, 0.8 Hz, 7'-*H*), 5.85 (1H, br s, O*H*); δC (100 MHz, $CDCl_3$, 24 °C): 166.0 (3-*C*), 151.8 (8'-*C*), 135.7 (4a'-*C*), 133.5 (2'-*C*), 128.5 (4'-*C*), 127.8 (1'-*C*), 127.1 (6'-*C*), 125.7 (3'-*C*), 121.9 (8a'-*C*), 121.4 (5'-*C*), 113.9 & 112.5 (2 x *C*≡N), 112.1 (7'-*C*), 83.3 (2-*C*); ν_{max}/cm^{-1} 3374, 3068, 2237 (C≡N), 1582, 1562, 1368, 1244; Found: C, 76.31; N, 12.54; H, 3.53. Calc. for $C_{14}H_8N_2O$: C, 76.35; N, 12.72; H, 3.66%.

Preparation of Sodium Dicyano-(2-(2*H*-naphtho(1,8-bc)furan-2'-yl)methanide, 2.35.Na$^+$.

Dinitrile **2.27** (35 mg, 0.05 mmol) was dissolved in THF (4 mL) under nitrogen and excess sodium hydride (10 mg, 60% dispersion in oil) was added to give an immediate red-brown colour. The mixture was stirred for 5 min, the solvent was evaporated *in vacuo* and THF-d_8 (*ca*. 0.4 ml) added to the purple residue followed by sufficient DMSO-d_6 to completely dissolve the product. δH (400 MHz, THF-d_8 and DMSO-d_6, 24 °C): 7.54 (1H, d, J = 8.2 Hz, 3'-*H*), 7.44 (1H, t, J = 7.8 Hz, 4'-*H*), 7.25 (1H, t, J = 7.8 Hz, 7'-*H*), 7.15 (1H, d, J = 6.9 Hz, 5'-*H*), 7.04 (1H, d, J = 8.2 Hz, 6'-*H*), 6.67 (1H, s, 2'-*H*), 6.41 (1H, d, J = 7.3 Hz, 8'-*H*); δC (100 MHz, THF-d_8 and DMSO-d_6, 24 °C): 162.3 (8a'-*C*), 141.6 (2a'-*C*), 132.8 (5a'-*C*), 131.6 (8b'-*C*), 130.3 (7'-*C*), 129.1 (4'-*C*), 128.0 (2 x *C*≡N), 123.9 (3'-*C*), 118.3 (5'-*C*), 114.0 (6'-*C*), 101.8 (2'-*C*), 100.7 (8'-*C*), 23.2 (2-*C*).

Reaction of 21 with 1-,1'-,3'-,3'-Tetramethylguanidine, 2.35.TMG.

Dinitrile **2.27** (35 mg) dissolved in THF-d_6 (0.6 ml) was treated with TMG (18 mg) to give an instant dark brown solution whose NMR spectra were recorded immediately and indicated a dynamic partial deprotonation of the naphthol with the equilibrium strongly towards the naphthol form. δH (400 MHz, THF-d_8, 24 °C): 9.31 (1H, s, 3-*H*), 7.73 (1H, d, J = 7.8 Hz, 4'-*H*), 7.37 (1H, d, J = 7.3 Hz, 2'-*H*), 7.30 (1H, t, J = 7.6 Hz, 3'-*H*), 7.20 (1H, t, J = 7.8 Hz, 6'-*H*), 6.91 (1H, d, J = 8.2 Hz, 5'-*H*), 6.68 (1H, d, J = 7.8 Hz, 7'-*H*), 2.74 (6H, s, TMG: 4 x C*H*$_3$); δC (100 MHz, THF-d_8, 24 °C): 164.3 (8'-*C*), 164.0 (TMG: *C*=N), 158.4 (br, 3-*C*), 136.7 (4a'-*C*), 133.1 (2'-*C*), 131.7 (4'-*C*), 129.7 (6'-*C*), 127.9 (8a'-C), 125.4 (3'-*C*), 124.0 (2'-*C*), 117.4 (2 x *C*N), 113.2 (5'-*C*), 110.8 (7'-*C*), 68.9 (br, 2-*C*), 39.7 (TMG: 4 x *CH*$_3$).

Preparation of 5-((8'-Hydroxynaphthalen-1'-yl)methylidene)-2,2-dimethyl-1,3-dioxane-4,6-dione, 2.28.

1-Hydroxy-8-naphthaldehyde **2.25** (800 mg, 4.65 mmol) was dissolved in anhydrous DMSO (25 mL) under nitrogen and Meldrum's acid (804 mg, 5.58 mmol) added and the deep orange solution was stirred at room temperature. After 7 days, H_2O (100 mL) was added producing an orange precipitate. The precipitate was dissolved by the addition of DCM (30 mL) and the organic layer was separated. The aqueous solution was extracted further with DCM (3 x 30 mL) and the combined organic fractions were washed with H_2O (30 mL) and brine (30 mL), dried over $MgSO_4$ and filtered. The solvent was removed *in vacuo* to give a crude orange solid which was purified by flash column chromatography (1:9 EtOAc:petrol 40-60), to give **2.28** as an orange solid (1.19 g, 86%), m.p. 169-172℃. δH (400 MHz, DMSO-d_6, 24 °C): 10.58 (1H, s, O*H*), 9.27 (1H, s, 5-=C*H*), 7.89 (1H, d, J = 8.2 Hz, 2'-*H*), 7.28 - 7.47 (4H, m, 3'-, 4'-,5'-,6'-*H*), 6.88 (1H, d, J = 8.7 Hz, 7'-*H*), 1.77 (6H, s, 2 x -CH_3); δC (100 MHz, DMSO-d_6, 24 °C): 163.5 (5-=*C*H), 162.9, 159.9 (2 x *C*=O), 154.3 (8'-*C*), 135.5 (Ar-C_1), 131.1 (2'-*C*), 130.3, 127.5, 127.4, 125.6, 122.5, 119.8 (Ar-C_6), 114.4 (5-*C*), 110.9 (7'-C), 105.2 (*C*$(CH_3)_2$), 27.7 (2 x *C*H_3); ν_{max}/cm^{-1} 3276 (OH), 1697 (C=O), 1594, 1372, 1292, 1200; Found: C, 68.50; H, 4.64. Calc. for $C_{17}H_{14}O_5$: C, 68.45; H, 4.73%.

Preparation of Sodium 2,2-dimethyl-5-(2H-naphtho[1,8-bc]furan-2'-yl)-4,6-dioxo-1,3-dioxan-5-ide, 2.36.Na^+.

Knoevenagel product **2.28** (30 mg) was dissolved in THF (4 ml) and the solution was treated with sodium hydride (60% dispersion in oil, *ca*. 4 mg) until the solution turned from yellow to

colourless. After stirring for a further 5 min., the solution was evaporated i*n vacuo*. CD_3CN (1 ml) was added, the solution filtered, and the NMR spectra recorded. δH (400 MHz, CD_3CN, 24 °C): 7.51 (1H, d, J = 8.2 Hz, 3'-*H*), 7.41 (1H, t, J = 7.6 Hz, 4'-*H*), 7.30 (1H, t, J = 7.8 Hz, 7'-*H*), 7.13 (1H, d, J = 8.2 Hz, 6'-*H*), 7.04 (1H, d, partially obscured, 5'-*H*), 7.00 (1H, s, 2'-*H*), 6.48 (1H, d, J = 7.3 Hz, 8'-*H*), 1.59 (6H, s, 2 x 2-CH_3); δC (100 MHz, CD_3CN, 24 °C): 166.8 (2 x *C*=O), 162.8 (8a-*C*), 145.4, 132.6, 130.4 (Ar-C_3), 130.1 (7'-*C*), 129.4 (4'-*C*), 122.3 (3'-*C*), 115.5 (5'-*C*), 114.7 (6'-*C*), 101.6 (2-*C*), 99.9 (8'-*C*), 89.6 (2'-*C*), 74.7 (5-C^-), 26.2 (2 x 2-*C*H_3).

Preparation of 1,4-Diazabicyclo[2.2.2]octan-1-ium 2,2-Dimethyl-5-(2H-naphtho[1,8-bc]furan-2-yl)-4,6-dioxo-1,3-dioxan-5-ide, 2.36.DABCO.

Knoevenagel product **2.28** (20 mg, 0.067 mmol) was dissolved in CD_3CN (2 mL), 1,4-diazabicyclo- [2.2.2]octane (7.5 mg, 0.067 mmol) was added and the reaction was stirred for 30 min. at room temperature. The yellow solution became paler upon addition. Removal of the solvent resulted in the formation of a solidified foam, δH (400 MHz, CD_3CN, 24 °C): 7.53 (1H, d, J = 7.7 Hz, 3'-*H*), 7.42 (1H, t, J = 6.8 Hz, 4'-*H*), 7.30 (1H, t, J = 8.2 Hz, 7'-*H*), 7.13 (1H, d, J = 8.2 Hz, 6'-*H*), 7.04 (1H, d, J = 8.2 Hz, 5'-*H*), 7.00 (1H, s, 2'-*H*), 6.50 (1H, d, J = 7.3 Hz, 8'-*H*), 6.14 (1H, br s, DABCO-H^+ N*H*), 2.88 (12H, s, DABCO-H^+: 6 x NCH_2), 1.63 (6H, s, 2 x 2-CH_3); δC (100 MHz, CD_3CN, 24 °C): 167.1 (2 x *C*=O), 162.8 (8a'-*C*), 145.2, 132.7, 130.4 (Ar-C_3), 130.2 (7'-*C*), 129.5 (4'-*C*), 122.5 (3'-*C*), 115.6 (5'-*C*), 114.8 (6'-*C*), 102.1 (2-*C*), 100.1 (8'-*C*), 89.7 (2'-*C*), 75.7 (5-C^-),45.4 (DABCO-H^+: 6 x NCH_2), 26.2 (2 x 2-*C*H_3); ν_{max}/cm^{-1} 2943, 2881, 2258, 1765, 1709, 1615, 1591, 1369, 1054; *HRMS* (ESI): calcd for $C_{17}H_{13}O_5$ ([M-H]$^-$): 297.0768, found: 297.0844.

Preparation of 3-Hydroxy-2-(2'H-naphtho[1,8-bc]furan-2'-yl)cyclohex-2-en-1-one, 2.29.

1-Hydroxy-8-naphthaldehyde **2.25** (250 mg, 1.45 mmol) was dissolved in anhydrous MeOH (20 mL) under nitrogen. 1, 3-Cyclohexandione (195 mg, 1.74 mmol) and ethylenediamine diacetate (26 mg, 0.15 mmol) were added and the reaction was heated to reflux for 6h. The solvent was removed *in vacuo* to give a crude yellow solid which was purified by flash column chromatography (3:1 EtOAc:Pet 40-60), to give **2.29** as a brown solid (200 mg, 52%), m.p. 186-189℃; in solution it exists in two forms: ring closed **2.29** and a minor component in *ca*. 17:3 ratio. δH (400 MHz, ($CDCl_3$, 24 °C): main component (ring closed) 85%: 9.11 (1H, br, O*H*), 7.62 (1H, d, J = 7.8 Hz, 3'-*H*), 7.49 (1H, t, J = 7.8 Hz, 4'-*H*), 7.33-7.41 (2H, m, 6'-,7'-*H*), 7.29 (1H, dd, J = 6.9, 1.4 Hz, 5'-*H*), 7.16 (1H, s, 2'-*H*), 6.82 (1H, d, J = 6.9 Hz, 8'-*H*), 2.25-2.52 (4H, m, 4-, 6-H_2), 1.85-2.00 (2H, m, 5-H_2), minor component, 15%, spectrum obscured apart from: 7.96 (1H, s), 7.91 (1H, d, J = 7.7 Hz), 7.72 (1H, d, J = 7.3 Hz); δC (100 MHz, ($CDCl_3$, 24 °C): 197.5 br (*C*=O), 174.2 br (3-*C*), 158.4 (8a'-*C*), 140.5, 131.6 (Ar-C_2), 129.4 (4'-*C*), 128.9 (7'-*C*), 127.6 (Ar-C_1), 123.4 (3'-*C*), 117.9 (5'-*C*), 117.2 (6'-*C*), 112.2 (2-*C*), 101.8 (8'-*C*), 87.8 (2'-*C*), 36.8 br (6-*C*), 29.5 br (4-*C*), 20.3 (5-*C*); ν_{max}/cm^{-1} 2917 (OH), 2849, 1622 (C=O), 1574, 1465, 1414, 1360, 1282. Found: C, 76.47; H, 5.37. Calc. for $C_{17}H_{14}O_3$: C, 76.68; H, 5.30%.

Preparation of 4-(Dimethylamino)pyridin-1-ium 1-(2H-naphtho[1,8-bc]furan-2-yl)-2,6-dioxocyclohexan-1-ide, 2.37.DMAP.

Cyclohexenone derivative **2.29** (40 mg, 0.16 mmol) was dissolved in CD_3CN (2 mL), DMAP (18 mg, 0.16 mmol) was added and the reaction was stirred for 30 min. at room temperature. The brown solution became paler upon addition. Removal of the solvent resulted in the formation of a solidified foam, δH (400 MHz, CD_3CN, 24 °C): 10.61 (1H, br s, DMAP-H^+: N*H*), 7.80 (2H, d, J = 6.9 Hz, DMAP-H^+: 2-,6-*H*), 7.45 (1H, d, J = 8.2 Hz, 3'-*H*), 7.34 (1H, t, J = 6.9 Hz, 4'-*H*), 7.27 (1H, t, J = 7.8 Hz, 7'-*H*), 7.13 (1H, s, 2'-*H*), 7.09 (1H, d, J = 8.2 Hz, 6'-*H*), 6.86 (1H, dd, J = 8.2, 1.4 Hz, 5'-*H*), 6.56 (2H, d, J = 7.3 Hz, DMAP-H^+: 3-,5-*H*), 6.46 (1H, d, J = 7.3 Hz, 8'-*H*), 2.98 (6H, s, DMAP-H^+: N(CH_3)$_2$), 2.12 (4H, t, J = 6.0, 1.4 Hz, 3-,5-H_2), 1.89 - 1.94 (2H, m, 4-H_2); δC (100 MHz, CD_3CN, 24 °C): 192.0 (2 x *C*=O), 163.3 (8a'-*C*), 156.8 (DMAP-H^+: 4-*C*), 146.2 (Ar-C_1), 144.8 (DMAP-H^+: 2-,6-*C*), 132.6, 130.6 (Ar-C_2), 130.1 (7'-*C*), 129.4 (4'-*C*), 122.0 (3'-*C*), 114.8 (5'-*C*), 114.7 (6'-*C*), 111.1 (1-*C*), 107.5 (DMAP-H^+: 3-,5-*C*), 100.0 (8'-*C*), 85.7 (2'-*C*), 39.8 (DMAP-H^+: N(*C*H_3)$_2$), 35.9 (3-,5-*C*), 22.0 (4-*C*); ν_{max}/cm^{-1} 2930, 1644, 1598, 1557, 1471, 1401, 1342, 1219, 1182, 1129; *HRMS* (ESI): calcd for $C_{17}H_{13}O_3$ ([M-H]$^-$): 265.0870, found: 265.0869.

Preparation of 1,4-Diazabicyclo[2.2.2]octan-1-ium 1-(2H-naphtho[1,8-bc]furan-2-yl)-2,6-dioxocyclohexan-1-ide, 2.37.DABCO.

Cyclohexenone derivative **2.29** (40 mg, 0.16 mmol) was dissolved in CD_3CN (2 mL), 1,4-diazabicyclo-[2.2.2]octane (17 mg, 0.16 mmol) was added and the reaction was stirred for 30 min. at room temperature. The brown solution became paler upon addition. Removal of the

solvent resulted in the formation of a solidified foam, δH (400 MHz, CD_3CN, 24 °C): 9.25 (1H, br s, DABCO-H^+: N*H*), 7.54 (1H, d, J = 8.2 Hz, 3'-*H*), 7.42 (1H, t, J = 6.9 Hz, 4'-*H*), 7.35 (1H, t, J = 8.2 Hz, 7'-*H*), 7.17 (1H, d, partially obscured, 6'-*H*), 7.19 (1H, s, 2'-*H*), 6.93 (1H, dd, J = 6.8, 1.4 Hz, 5'-*H*), 6.53 (1H, d, J = 7.3 Hz, 8'-*H*), 2.71 (12H, s, DABCO-H^+: 6 x NCH_2), 2.18 (4H, t, J = 6.3 Hz, 3-,5-H_2), 1.84 - 1.92 (2H, quin, J = 6.3 Hz, 4-CH_2); δC (100 MHz, CD_3CN, 24 °C): 192.4 (2 x *C*=O), 163.5 (8a-*C*), 146.7, 132.6, 130.8 (Ar-C_3), 130.1 (7'-*C*), 129.4 (4'-*C*), 121.8 (3'-*C*), 114.6 (5'-,6'-*C*), 110.8 (1-*C*), 99.9 (8'-*C*), 86.1 (2'-*C*), 45.8 (DABCO-H^+: 6 x NCH_2), 36.8 (3-,5-*C*), 22.2 (4-*C*); ν_{max}/cm^{-1} 3044, 2938, 2882, 2471, 1619, 1593, 1488, 1460, 1372; *HRMS* (ESI): calcd for $C_{17}H_{13}O_3$ ($[M-H]^-$): 265.0870, found: 265.0863.

Preparation of 7a-Hydroxy-9-phenyl-7a,8,9,10-tetrahydro-11H-benzo[f]naphtho[1,8-bc]oxepin-11-one, 2.31 (solid form) /3-Hydroxy- 2-(2'H-naphtho[1,8-bc]furan-2'-yl)-5-phenyl-cyclohex-2-en-1-one, 2.32 (solution form).

1-Hydroxy-8-naphthaldehyde **2.25** (100 mg, 0.58 mmol) was dissolved in anhydrous DMSO (25 mL) under nitrogen and 5-phenyl-1,3-cyclohexandione (120 mg, 0.64 mmol) was then added. The deep orange solution was stirred at room temperature. After 5 days, H_2O (100 mL) was added to produce a yellow precipitate. The precipitate was dissolved by the addition of DCM (30 mL) and the organic layer was separated. The aqueous solution was extracted further with DCM (3 x 30 mL). The combined organics were washed with H_2O (30 mL) and brine (30 mL), dried over $MgSO_4$ and filtered. The solvent was removed *in vacuo* to give a crude yellow solid which was purified by flash column chromatography (1:4 EtOAc:petrol 40-60), to give **2.31** as a yellow solid (150 mg, 75%), m.p. 172-175℃. This compound exists as the fused oxepine **2.31** in the solid state but as the naphthofuran **2.32** in solution in DMSO-d_6. δH (400

MHz, DMSO-d_6, 24 °C): 7.57 (1H, d, J = 8.2 Hz, 3'-*H*), 7.41 (1H, t, J = 6.9 Hz, 4'-*H*), 7.28 - 7.35 (5H, m, 7'-*H*, 2 x *ortho*-Ph-*H*, 2 x *meta*-Ph-*H*), 7.15 - 7.24 (2H, m, 6'-*H*, *para*-Ph-*H*), 7.02 (1H, s, 2'-*H*), 6.98 (2H, br d, J = 6.4 Hz, 5'-*H*), 6.56 (1H, br d, J = 6.9 Hz, 8'-*H*), 3.16 - 3.51 (1H, m, 5-*H*), 2.65 - 2.85 (2H, m, 6-H_2), 2.48 - 2.57 (1H, m, 4-H_2); δC (100 MHz, DMSO, 24 °C): 197.1 (*C*=O), 162.0 (3-*C*), 151.8 (8a'-*C*), 143.7 & 143.3 (*ipso*-Ph-*C*, Ar-C_1), 131.6 (Ar-C_1), 129.8 (7'-*C*), 129.1 (4'-*C*), 129.1 (2 x *meta*-Ph-*C*), 127.5 (2 x *ortho*-Ph-*C*), 127.2 (*para*-Ph-*C*), 122.4 (3'-*C*), 115.0 (6'-*C*), 114.9 (5'-*C*), 112.3 (Ar-C_1), 101.1 (2-*C*), 100.2 (8'-*C*), 81.9 (2'-*C*), 47.0 (6-*C*), 40.2 (4-*C*), 38.4 (5-*C*); ν_{max}/cm^{-1} 3395 (OH), 3067, 3040, 2950, 1676 (C=O), 1592, 1581, 1388, 1227; Found: C, 80.63; H, 5.16. Calc. for $C_{17}H_{14}O_5$: C, 80.68; H, 5.30%.

Preparation of Sodium 1-(2H-naphtho[1,8-bc]furan-2-yl)-2,6-dioxo-4-phenylcyclohexan-1-ide, 2.38.Na^+.

The fused oxepine **2.31** (20 mg) was dissolved in THF (4 ml) and the solution was treated with sodium hydride (60% dispersion in oil, *ca*. 4 mg) until the solution turned from yellow to colourless. After stirring for a further 5 min., the solution was evaporated i*n vacuo*. THF-d_8 (1 ml) was added, the solution was filtered, and the NMR spectra recorded. δH (400 MHz, THF-d_8, 24 °C): 7.27 (1H, d, J = 8.2 Hz, 3'-*H*), 7.01 - 7.20 (7H, m, 4'-,7'-*H*, -C_6H_5), 7.20 (1H, s, 2'-*H*), 6.91 (1H, d, J = 8.2 Hz, 6'-*H*), 6.74 (1H, dd, J = 8.2, 1.5 Hz, 5'-*H*), 6.31 (1H, d, J = 6.8 Hz, 8'-*H*), 3.06 - 3.26 (1H, m, 4-*H*), 2.14 - 2.34 (4H, m, 3-,5-H_2); δC (100 MHz, THF-d_8, 24 °C): 191.7 (*C*=O), 163.7 (8a'-*C*), 147.3 (*ipso*-Ph-C and Ar-C_1), 146.8, 132.7 (Ar-C_2), 131.0, 129.5 (4'- or 7'-*C*), 129.0 (2 x *meta*-Ph-*C*), 128.8 (4'- or 7'-*C*), 127.7 (2 x *ortho*-Ph-*C*), 126.5 (*para*-Ph-*C*), 121.1 (3'-*C*), 114.4 (5'-*C*), 114.0 (6'-*C*), 108.4 (1-C^-),99.5 (8'-*C*), 87.6 (2'-*C*), 44.6 (3-,5-*C*), 40.6 (4-*C*).

Preparation of 4-(Dimethylamino)pyridin-1-ium 1-(2H-naphtho[1,8-bc]furan-2-yl)-2,6-dioxo-4-phenylcyclohexan-1-ide, 2.38.DMAP.

The fused oxepine **2.31** (10 mg, 0.029 mmol) was dissolved in CD_3CN (2 mL), 4-dimethylaminopyridine (3.6 mg, 0.029 mmol) was added and the reaction was stirred for 30 min. at room temperature. The yellow solution became paler upon addition. Removal of the solvent resulted in the formation of a solidified foam, δH (400 MHz, CD_3CN, 24 °C): 7.71 (2 H, d, J = 7.3 Hz, DMAP-H^+: 2-,6-*H*), 7.38 (1 H, d, J = 8.2 Hz, 3'-*H*), 7.16-7.34 (7H, m, C_6H_5, 4'-,7'-*H*), 7.15 (1H, s, 2'-*H*), 7.05 (1H, d, J = 8.2 Hz, 6'-*H*), 6.83 (1H, dd, J = 6.9, 1.8 Hz, 5'-*H*), 6.53 (2H, d, J = 7.3 Hz, DMAP-H^+: 3-,5-*H*), 6.42 (1H, d, J = 7.3 Hz, 8'-*H*), 3.25 - 3.33 (1H, m, 4-*H*), 2.97 (6H, s, DMAP-H^+: N(CH_3)$_2$), 2.49 (2H, dd, J = 16.5, 11.4 Hz , 3-H_α, 5-H_α), 2.37 (2H, dd, J = 16.5, 4.6 Hz, 3-H_β, 5-H_β); δC (100 MHz, CD_3CN, 24 °C): 190.8 (2 x *C*=O), 163.3 (8a'-*C*), 157.0 (DMAP-H^+: 4-*C*), 146.1 and 145.8 (*ipso*-Ph-*C*, Ar-C_1), 143.7 (DMAP-H^+: 2-,6-*C*), 132.5, 130.6, 130.1, 129.4 (2 x *meta*-Ph-*C* & Ar-C_1), 128.0 (2 x *ortho*-Ph-*C*), 127.3 (*para*-Ph-*C*), 122.0 (3'-*C*), 114.8 (6'-*C*), 114.7 (5'-*C*), 110.6 (1-*C*), 107.5 (DMAP-H^+: 3-,5-*C*), 100.0 (8'-*C*), 85.7 (2'-*C*), 43.4 (3-,5-*C*), 40.0 (DMAP-H^+: N(CH_3)$_2$), 39.9 (4-*C*); ν_{max}/cm^{-1} 3394, 3067, 3040, 2950, 1679, 1617, 1593, 1581, 1388, 1267, 1202; *HRMS* (ESI): calcd for $C_{23}H_{17}O_3$ ([M-H]$^-$): 341.1183, found: 341.1180.

Preparation of 1,4-Diazabicyclo[2.2.2]octan-1-ium 1-(2H-naphtho[1,8-bc]furan-2-yl)-2,6-dioxo-4-phenylcyclohexan-1-ide, 2.38.DABCO.

The fused oxepine **2.31** (20 mg, 0.058 mmol) was dissolved in CD_3CN (2 mL), 1,4-diazabicyclo- [2.2.2]octane (6.5 mg, 0.058 mmol) was added and the reaction was stirred for

30 min. at room temperature. The yellow solution became paler upon addition. Removal of the solvent resulted in the formation of a solidified foam, δH (400 MHz, CD_3CN, 24 °C): 7.36 (1H, d, J = 8.7 Hz, 3'-*H*), 7.14 - 7.29 (6H, m, 4'-,7'-*H*, 2 x *ortho*-Ph-*H*, 2 x *meta*-Ph-*H*), 7.08 - 7.14 (1H, m, *para*-Ph-*H*), 7.05 (1H, s, 2'-*H*), 7.01 (1H, d, J = 8.2 Hz, 6'-*H*), 6.77 (1H, dd, J = 8.2, 1.5 Hz, 5'-*H*), 6.37 (1H, d, J = 7.3 Hz, 8'-*H*), 3.16 - 3.27 (1H, m, 4-*H*), 2.55 (12H, s, DABCO-H^+: 6 x NCH_2), 2.18 - 2.45 (4H, m, 3-,5-H_2); δC (100 MHz, CD_3CN, 24 °C): 191.2 (*C*=O), 163.3 (8a'-*C*), 146.7 and 146.1 (*ipso*-Ph-*C*, Ar-C_1), 132.7, 130.8 (Ar-C_2), 130.1 (4'-*C*), 129.5 (7'-*C*), 129.4 (2 x *meta*-Ph-*C*), 128.0 (2 x *ortho*-Ph-*C*), 127.3 (*para*-Ph-*C*), 121.8 (3'-C), 114.6 (5'-,6'-*C*), 110.3 (1-C^-), 99.9 (8'-*C*), 86.1 (2'-*C*), 45.6 (DABCO-H^+: 6 x NCH_2), 44.2 (3-,5-*C*), 40.2 (4-*C*); ν_{max}/cm^{-1} 3300 (NH), 3028 , 2939, 2887, 2479, 1620 (C=O), 1593, 1489, 1372, 1247; *HRMS* (ESI): calcd for $C_{23}H_{17}O_3$ ($[M-H]^-$): 341.1183, found: 341.1176.

Preparation of 2-((8-(methylthio)naphthalen-1-yl)methylene)cyclohexane-1,3-dione, 2.34.

1-methylthio-8-naphthaldehyde (250 mg, 1.21 mmol) was dissolved in anhydrous MeOH (15 mL) under nitrogen. 1, 3-Cyclohexandione (166 mg, 1.45 mmol) and ethylenediamine diacetate (26 mg, 0.15 mmol) were added and the reaction was heated to reflux for 24h. The reaction was quenched with H_2O (30 mL) and the solution was extracted with EtOAc (3 x 20 mL). The combined organics were washed with H_2O (20 mL) and brine (20 mL) and the organics were subsequently dried over $MgSO_4$, filtered and concentrated *in vacuo* to give a dark brown oil which was purified by flash column chromatography (EtOAc), to give **2.34** as an orange oil (200 mg, 66%), δH (400 MHz, ($CDCl_3$, 24 °C): 9.11 (1H, s, 3-*H*), 7.82 (1H, d, J

= 8.2 Hz, 4'-*H*), 7.79 (1H, dd, J = 8.2, 1.0 Hz, 5'-*H*), 7.71 (1H, dd, J = 7.2, 1.3 Hz, 7'-*H*), 7.36-7.43 (2H, m, 3', 6'-*H*), 7.25 (1H, m, 2'-*H*), 2.60-2.70 (4H, br m, 4-, 6-H_2), 2.28 (3H, s, S(CH_3)), 2.04-2.13 (2H, m, 5-H_2); δC (100 MHz, ($CDCl_3$, 24 °C): 198.0 (*C*=O), 154.8 (3-*C*), 134.8, 134.5, 133.7 (Ar-C_3), 133.3 (8a'-*C*), 132.3 (7'-*C*), 130.2 (4'-*C*), 129.1 (5'-*C*), 127.2 (2'-*C*), 125.9 & 125.4 (3'-, 6'-*C*), 39.7 (4-, 6-*C*), 21.8 (S(*C*H_3)), 18.2 (5-*C*); ν_{max}/cm^{-1} 3052, 2919, 1658, 1616, 1561, 1496, 1453, 1423, 1363, 1330, 1188, 1168, 1075, 907, 820, 764, 724, 646, 555, 532; *HRMS* (ESI): calcd for $C_{18}H_{17}SO_2$ ($[M+H]^+$): 297.0949, found: 297.0967.

Crystal data

*Table 2.16. Crystallographic data for ketones, **2.2**, **2.5** and **2.23**, salts **2.17** and **2.18**, lactone **2.8** and lactol **2.9**.*

	2.2	**2.5**	**2.23**	**2.17**	**2.18**	**2.8**	**2.9**
Formula	$C_{17}H_{12}O_2$	$C_{12}H_{10}O_2$	$C_{18}H_{14}O_3$	$C_5H_{14}N_3$. $C_{17}H_{11}O_2$. 0.05 H_2O	$C_5H_{14}N_3$. $C_{12}H_9O_2$	$C_{15}H_{14}O_2$	$C_{16}H_{18}O_2$
Formula weight	248.27	186.20	278.29	364.35	301.38	226.26	242.30
Crystal system	Orthorhombic	Orthorhombic	Orthorhombic	Triclinic	Triclinic	Orthorhombic	Monoclinic
Space group	*Iba*2	$P2_12_12_1$	$Pna2_1$	*P*-1	*P*-1	*Pnma*	$P2_1/c$
***a*[Å]**	17.3065(5)	9.9122(2)	19.0379(13)	8.2578(4)	15.1117(6)	14.0730(6)	12.4248(5)
***b*[Å]**	17.6303(4)	13.8433(3)	9.4268(4)	10.5748(5)	15.6707(7)	6.8273(4)	22.9673(7)
***c*[Å]**	8.0817(2)	13.9018(3)	7.7089(3)	23.1819(12)	16.4672(7)	12.0491(7)	9.8566(4)
***α*[°]**	90	90	90	99.596(4)	80.552(4)	90	90
β [°]	90	90	90	91.720(4)	69.591(4)	90	112.446(5)
***γ*[°]**	90	90	90	104.122(4)	61.179(4)	90	90
***V* [Å^3]**	2465.88(11)	1907.57(7)	1383.49(12)	1930.40(17)	3202.1(3)	1157.68(11)	2599.63(19)
Z	4	8	4	4	8	4	8
***ρ* [g cm^{-3}]**	1.34	1.297	1.336	1.25	1.250	1.298	1.238
***T* [*K*]**	110(2)	150.01(10)	150.01(10)	110(2)	100.01(10)	150(2)	110(2)
***λ* (Å)**	0.71073	0.71073	0.71073	0.71073	0.71073	0.71073	0.71073
***μ* (mm^{-1})**	0.087	0.088	0.091	0.082	0.083	0.085	0.080
unique refl.	3039	4651	5786	9106	11729	1484	5334
Refl, I > 2σI	2920	4090	2731	6926	8260	1268	4107
***R*$_1$**	0.033	0.0418	0.0456	0.067	0.0555	0.0538	0.0611
***wR*$_2$**	0.079	0.0953	0.0873	0.126	0.1291	0.1437	0.1450
Δ*ρ*(r) [e Å^{-3}]	0.210/-0.194	0.210/-0.232	0.170/-0.180	0.236/-0.235	0.345/-0.226	0.330/-0.257	0.267/-0.228
Crystallisation Solvent	CH_2Cl_2	EtOAc	CH_2Cl_2	CH_2Cl_2	CH_2Cl_2	CH_2Cl_2	$(CH_3)_2CO$

*Table 2.17. Crystallographic data for DMAP complexes of **2.5**, **2.10** and **2.9**.*

	2.5.DMAP	**2.10.DMAP**	**2.9.DMAP**
Formula	$C_7H_{10}N_2$. $C_{12}H_{10}O_2$	$C_7H_{10}N_2$. $C_{15}H_{16}O_2$	$C_7H_{10}N_2$. $C_{16}H_{18}O_2$
Formula weight	308.37	350.45	364.47
Crystal system	Monoclinic	Monoclinic	Monoclinic
Space group	*C*2/*c*	$P2_1/c$	$P2_1/c$
***a*[Å]**	27.588(4)	8.4313(5)	10.1265(11)
***b*[Å]**	8.2227(4)	26.5593(11)	25.804(3)
***c*[Å]**	19.874(3)	9.5945(5)	7.9261(7)
α[°]	90	90	90
β [°]	132.66(3)	114.586(7)	105.497(10)
γ[°]	90	90	90
***V* [Å^3]**	3315.6(13)	1953.7(2)	1995.9(4)
Z	8	4	4
ρ [g cm^{-3}]	1.236	1.191	1.213
***T* [*K*]**	149.97(12)	150.01(10)	150.00(10)
λ (Å)	0.71073	0.71073	0.71073
μ (mm^{-1})	0.081	0.076	0.077
unique refl.	3819	4523	4601
Refl, I > 2σI	2427	3146	2813
***R*$_1$**	0.0723	0.0738	0.0691
***wR*$_2$**	0.1398	0.1790	0.1364
$\Delta\rho$(r) [e Å^{-3}]	0.166/-0.229	0.437/-0.292	0.203/-0.185
Crystallisation Solvent	CH_2Cl_2	$(CH_3)_2CO$	$(CH_3)_2CO$

*Table 2.18. Crystallographic data for Knoevenagel products and **2.26-2.29** and **2.31**.*

	2.26	**2.27**	**2.28**	**2.29**	**2.31**
Formula	$C_{16}H_{13}NO_3$	$C_{14}H_8N_2O$	$C_{17}H_{14}O_5$	$C_{17}H_{14}O_3$	$C_{23}H_{18}O_3$
Formula weight	267.27	220.22	298.28	266.28	342.37
Crystal system	Monoclinic	Monoclinic	Monoclinic	Monoclinic	Triclinic
Space group	$P2_1/c$	$P2_1/c$	$P2_1/c$	$P2_1/c$	P-1
***a*[Å]**	10.8607(7)	9.9169(5)	7.3963(3)	13.4588(5)	6.9441(4)
***b*[Å]**	8.0882(5)	7.4879(2)	14.2452(4)	9.4421(3)	8.8146(4)
***c*[Å]**	15.3629(9)	15.8768(6)	13.5274(5)	20.9855(9)	14.8418(8)
α[°]	90	90	90	90	77.773(4)
β [°]	100.510(5)	108.096(5)	105.187(4)	95.122(4)	78.744(4)
γ[°]	90	90	90	90	76.371(4)
***V* [Å^3]**	1326.89(14)	1120.64(8)	1375.49(9)	2656.17(17)	852.70(8)
Z	4	4	4	8	2
ρ [g cm^{-3}]	1.338	1.305	1.440	1.332	1.333
***T* [*K*]**	150(2)	150.00(10)	100(2)	100(2)	150.01(10)
λ (Å)	0.71073	0.71073	0.71073	0.71073	0.71073
μ (mm^{-1})	0.093	0.085	0.107	0.091	0.088
unique refl.	3097	2465	3198	6253	3941
Refl, I > 2σI	2604	1936	2640	4538	3040
***R*$_1$**	0.0553	0.0527	0.0573	0.0763	0.0690
***wR*$_2$**	0.1235	0.1102	0.1198	0.2046	0.1519
$\Delta\rho$(r) [e Å^{-3}]	0.273/-0.230	0.208/-0.171	0.304/-0.216	1.007/-0.301	0.323/-0.178
Crystallisation Solvent	$(CH_3)_2CO$	EtOAc	$CH_2Cl_2/(CH_3)_2CO$	EtOAc	EtOAc

References

1 G. M. Sheldrick, *Acta Crystallogr.*, 2008, **64**, 112–122.

2 G. M. Sheldrick, *Acta Crystallogr.*, 2015, **71**, 3–8.

3 L. J. Barbour, *J. Supramol. Chem.*, 2001, **1**, 189–191.

4 O. V. Dolomanov, L. J. Bourhis, R. J. Gildea, J. A. K. Howard and H. Puschmann, *J. Appl. Crystallogr.*, 2009, **42**, 339–341.

5 N. Mercadal, S. P. Day, A. Jarmyn, M. B. Pitak, S. J. Coles, C. Wilson, G. J. Rees, J. V. Hanna and J. D. Wallis, *CrystEngComm*, 2014, **16**, 8363–8374.

6 W. B. Schweizer, G. Procter, M. Kaftory and J. D. Dunitz, *Helv. Chim. Acta*, 1978, **61**, 2783–2808.

7 J. T. B. H. Jastrzebski, J. Boersma, P. M. Esch and G. Van Koten, *Organometallics*, 1991, **10**, 930–935.

8 F. Carré, C. Chuit, R. J. P. Corriu, P. Monforte, N. K. Nayyar and C. Reyé, *J. Organomet. Chem.*, 1995, **499**, 147–154.

9 A. Panda, G. Mugesh, H. B. Singh and R. J. Butcher, *Organometallics*, 1999, **18**, 1986–1993.

10 P. C. Bell and J. D. Wallis, *Chem. Commun.*, 1999, **2**, 257–258.

11 J. Clayden, C. McCarthy and M. Helliwell, *Chem. Commun.*, 1999, 2059–2060.

12 D. R. W. Hodgson, A. J. Kirby and N. Feeder, *J. Chem. Soc. Perkin Trans. 1*, 1999, 949–954.

13 P. C. Bell, M. Drameh, N. Hanly and J. D. Wallis, *Acta Crystallogr.*, 2000, **56**, 670–671.

14 J. O'Leary, P. C. Bell, J. D. Wallis and W. B. Schweizer, *J. Chem. Soc. Perkin Trans. 2*, 2001, 133–139.

15 P. C. Bell, W. Skranc, X. Formosa, J. O'Leary and J. D. Wallis, *J. Chem. Soc. Perkin Trans. 2*, 2002, 878–886.

16 J. O'Leary, X. Formosa, W. Skranc and J. D. Wallis, *Org. Biomol. Chem.*, 2005, **3**, 3273–3283.

17 A. Wannebroucq, A. P. Jarmyn, M. B. Pitak, S. J. Coles and J. D. Wallis, *Pure Appl. Chem.*, 2016, **88**, 317–331.

18 A. Lari, M. B. Pitak, S. J. Coles, G. J. Rees, S. P. Day, M. E. Smith, J. V. Hanna and J. D. Wallis, *Org. Biomol. Chem.*, 2012, **10**, 7763–7779.

19 A. C. Blackburn and R. E. Gerkin, *Acta Crystallogr.*, 1997, **53**, 1077–1080.

20 R. E. Gerkin, *Acta Crystallogr.*, 1997, **53**, 1987–1989.

21 J. O'Leary and J. D. Wallis, *Chem. Eur. J.*, 2006, **12**, 7724–7732.

22 A. N. Cammidge and O. Öztürk, *J. Org. Chem.*, 2002, **67**, 7457–7464.

23 R. J. Packer and D. C. C. Smith, *J. Chem. Soc. C Org.*, 1967, 2194–2201.

24 G. Saritemur, L. Nomen Miralles, D. Husson, M. B. Pitak, S. J. Coles and J. D. Wallis, *CrystEngComm*, 2016, **18**, 948–961.

25 M. P. Hogerheide, S. N. Ringelberg, M. D. Janssen, J. Boersma, A. L. Spek and G. van Koten, *Inorg. Chem.*, 1996, **35**, 1195–1200.

26 A. Domenicano and P. Murray-Rust, *Tetrahedron Lett.*, 1979, **20**, 2283–2286.

27 A. W. T. King, J. Asikkala, I. Mutikainen, P. Järvi and I. Kilpeläinen, *Angew. Chemie - Int. Ed.*, 2011, **50**, 6301–6305.

28 G. A. M. Jardim, E. N. da Silva Júnior and J. F. Bower, *Chem. Sci.*, 2016, **7**, 3780–3784.

29 S. Ferrari, S. Calò, R. Leone, R. Luciani, L. Costantino, S. Sammak, F. Di Pisa, C. Pozzi, S. Mangani and M. P. Costi, *J. Med. Chem.*, 2013, **56**, 9356–9360.

30 V. V Tkachenko, N. G. Tregub, A. P. Knyazev and V. V. Mezheritskii, *Zh. Org. Khim.*, 1990, **26**, 638–649.

31 F. H. Allen, O. Kennard, D. G. Watson, L. Brammer, A. G. Orpen and R. Taylor, *J. Chem. Soc. Perkin Trans. 2*, 1987, 1–19.

32 J. O'Leary and J. D. Wallis, *Org. Biomol. Chem.*, 2009, **7**, 225–228.

33 G. Gunbas, N. Hafezi, W. L. Sheppard, M. M. Olmstead, I. V. Stoyanova, F. S. Tham, M. P. Meyer and M. Mascal, *Nat. Chem.*, 2012, **4**, 1018–1023.

34 J. Cai, Y. Li, J. Chen, P. Wang and M. Ji, *Res. Chem. Intermed.*, 2015, **41**, 1–9.

Chapter 3

Structural Modifications to the Biphenyl and Naphthalene Scaffolds to Investigate the Effect of Small Linker Bridges on *Peri*-Interactions

Introduction

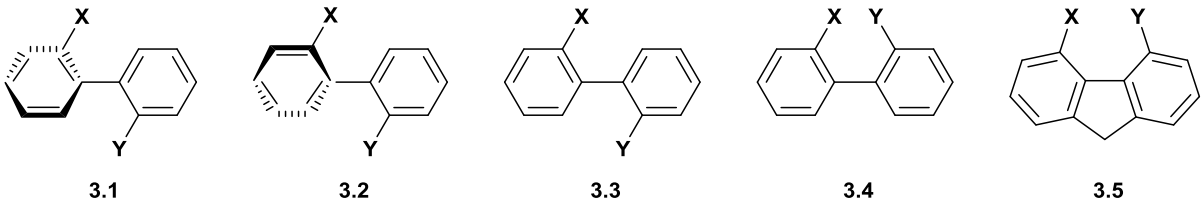

*Figure 3.53. Possible orientations of the ortho-substituted benzene rings of biphenyl **3.1**-**3.4** and the locked conformation of fluorene **3.5**.*

Biphenyls of the type shown in Figure 3.1 (**3.1**-**3.4**) possess free rotation around the inter-ring carbon-carbon bond leading to orientations which can either promote or prevent the interaction of the *ortho*-substituents (X and Y). Removal of this free rotation via the installation of a methylene bridge between the unsubstituted *ortho*-carbons from each ring (to give a fluorene derivative) locks the conformation into that of **3.5**, akin to conformation **3.4**.

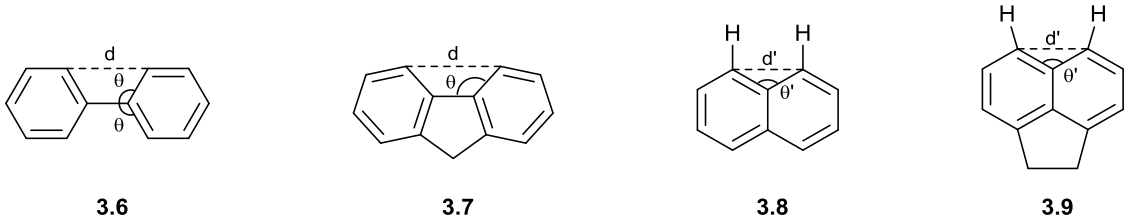

*Figure 3.54. Structures of biphenyl[1] **3.6**, fluorene[2] **3.7**, naphthalene[3] **3.8** and acenaphthene[4] **3.9**.*

The addition of the methylene bridge to give the 5-membered ring in fluorene[2] has a large impact on the *exo*-cyclic angle between the benzene ring and inter-ring bond to unsubstituted biphenyl[1] **3.6** (Figure 3.2). This angle (θ) widens from an average of 121.1(1)^{o} in biphenyl **3.6** to 130.1(1)^{o} in fluorene **3.7**. Furthermore, there is an increase in the distance (d) between the unsubstituted *ortho*-carbons of the rings from 2.937(6) in biphenyl **3.6** to 3.293(3) Å in fluorene **3.7**. A similar effect is demonstrated by the introduction of an ethylene bridge at one set of *peri*-positions on naphthalene,[3] resulting in acenaphthene[4]. In this structural adjustment, the *exo*-angle (θ') and distance (d') of naphthalene **3.8** at each side of the molecule become unsymmetrical as a result of the 5-membered ring formed by the ethylene bridge. This results

in the carbon-carbon distance between the opposite *peri*-carbons being lengthened from 2.475 Å in naphthalene **3.8** to an average of 2.541 Å in acenaphthene **3.9**, with the *exo*-angle between these two *peri*-positions widened from 121.7º (**3.8**) to an average of 126.8º (**3.9**). Consequently, the *peri*-hydrogen H---H separation has increased from 2.45 Å in naphthalene to 2.67 Å in acenaphthene.

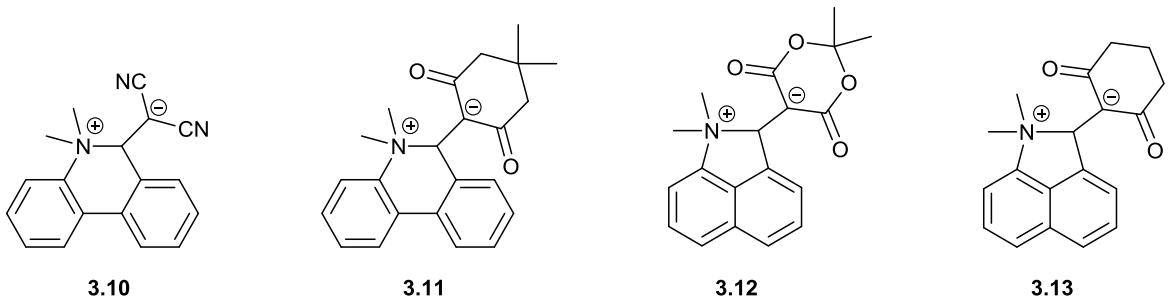

3.10 **3.11** **3.12** **3.13**

*Figure 3.55. Examples of nucleophile/electrophile interactions in two biphenyl[5] (**3.10** and **3.11**) and two naphthalene[6,7] (**3.12** and **3.13**) derivatives which have undergone nucleophilic addition.*

The unsubstituted backbones **3.6** and **3.8** have been previously discussed in Chapter 1 with regards to their use as a scaffold to study nucleophile/electrophile interactions.[5–7] Figure 3.3 demonstrates four examples from these studies where the attractive interaction between the two groups has led to the formation of long N-C bonds. In the biphenyl dinitrile and dimedone derivatives **3.10** and **3.11** (Figure 3.4), the newly formed six-membered ring adopts a twisted half chair conformation, similar to that of 9, 10-dihydrophenanthrene.[8] This creates an average angle between the two benzene rings' best planes of 25.7º, with the distance between the substituted *ortho*-positions found to be 2.887(3)/2.891(3) Å for the two independent molecules of **3.10** and 2.891(2) Å for **3.11**. Similarly, the Meldrum's acid and cyclohexanedione (Figure 3.4) *peri*-substituted naphthalene derivatives **3.12** and **3.13** demonstrate *peri*-carbon separations of 2.323 (3) Å and 2.338(2) Å respectively. In all four examples the distance between the ring carbons of the interacting groups is found to be lower than that of the equivalent separation in fluorene (**3.7**) or acenaphthene (**3.9**) molecules, whereby the bridging atoms have influenced the interaction.

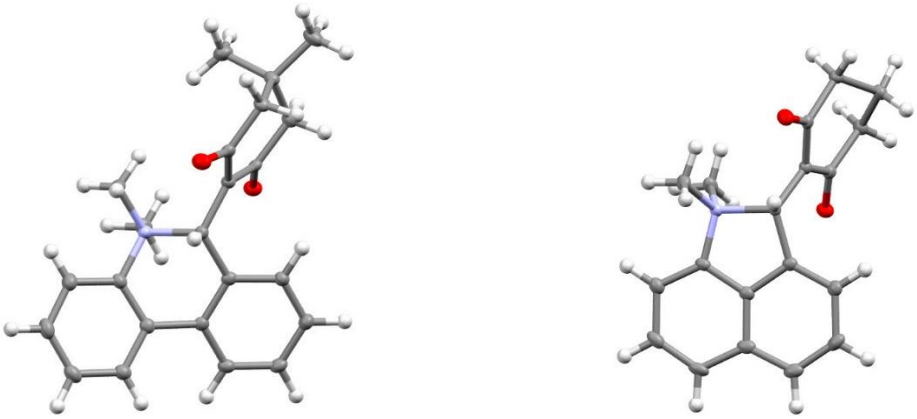

Figure 3.56. Molecular structures of biphenyl zwitterion ***3.11***[5] *and naphthalene zwitterion* ***3.13***.[7]

To this end, an investigation was proposed to explore the effect that the widening of the *exo*-angle opposite to the added bridging moiety, and thus increased carbon/carbon separation, has on the long N-C bonds in zwitterionic examples (such as those in Figure 3.3). In particular it was important to assess whether the bond can be further elongated or if the increased distance prevents bond formation altogether. In order to do this, a series of 4, 5-disubstituted fluorenes and 5, 6-disubstituted acenaphthenes were designed. The two series would utilise the same nucleophilic dimethylamino group and a similar range of electrophilic alkenes as those that formed zwitterionic bonds in the relevant prior studies. In each case the molecular structure determined by single crystal X-ray diffraction will be used to observe the effect of the increased separation between functional groups, and in the fluorene examples to determine the effect of restricting the relative orientation of the *ortho*-groups.

Investigation of 4, 5-disubstituted fluorenes

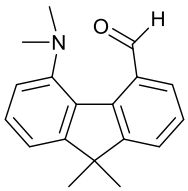

3.14

*Figure 3.57. Structure of the target dimethylamino aldehyde **3.14**.*

To begin the fluorene series, the synthesis of dimethylamino aldehyde **3.14** was targeted (Figure 3.5). This structure provides a base from which the desired series of compounds can be synthesised by Knoevenagel condensations with a range of active methylene compounds.

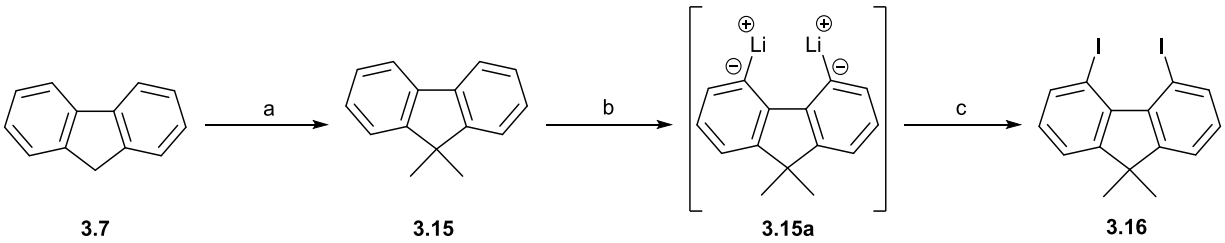

3.7 **3.15** **3.15a** **3.16**

Scheme 3.15. (a) ^{t}BuOK, THF, CH_3I, 25 ^{o}C;[9] (b) n-BuLi, TMEDA, 60 ^{o}C;[10] (c) -78 ^{o}C, I_2, RT.

Following the literature procedure described by Lardiès *et al.*[9] 9H-fluorene (**3.7**) was dimethylated to give 9, 9-dimethylfluorene **3.15** (Scheme 3.1). Aided by the works of Bonifácio *et al.*[10] this alkylated fluorene **3.15** underwent a two-fold *ortho*-lithiation at 60 ^{o}C with *n*-BuLi/TMEDA. A large excess of iodine (I_2) was subsequently added to the lithiated salt **3.15a** at -78 ^{o}C and the reaction left to warm to room temperature, and the *di*-iodo fluorene **3.16** isolated as a pale yellow solid in 25% yield. The loss of a signal worth two aromatic protons in the ^{1}H NMR spectrum and the appearance of a peak at 87.3 ppm in the ^{13}C NMR spectrum, corresponding to the C-I bonds, indicated a successful *di*-iodination. The compound, however, proved too unstable when left for longer than several days at ambient temperature or when

heated to temperatures in excess of 60 °C. As a result, neither mass spectroscopy or elemental analysis data was obtained for this new compound.

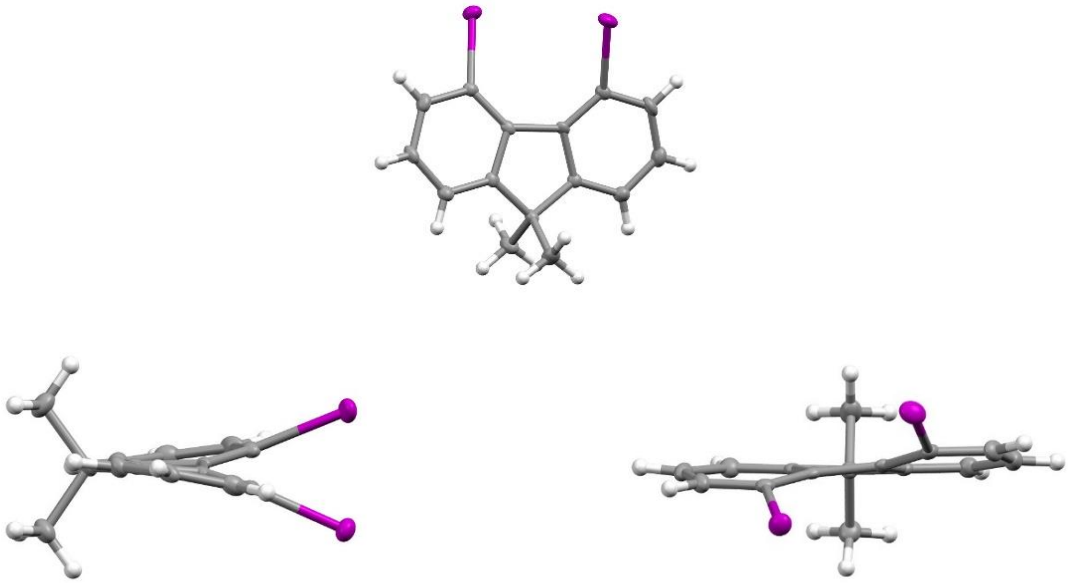

*Figure 3.58. Molecular structure of di-iodo fluorene **3.16** (top), demonstrating the displacement of the iodine atoms to either side of the fluorene plane due to their steric interaction (bottom).*

However, crystals of **3.16** suitable for X-ray crystal structure determination were obtained via slow evaporation of an ethyl acetate/petrol solution and the structure determined at 150 K (Figure 3.6). The structure demonstrates the extent to which the larger steric bulk of the iodine atoms causes the fluorene skeleton to twist well out of its desired planar conformation. The iodine atoms lie 1.126(3) and 1.128(3) Å from the plane of the relatively planar central 5-membered ring. The I---I contact distance of 3.639(1) Å lies well within the sum of the van der Waals radii for this type of contact[11] (4.0 Å), further demonstrating the strain upon the system and hence the lability of the C-I bonds.

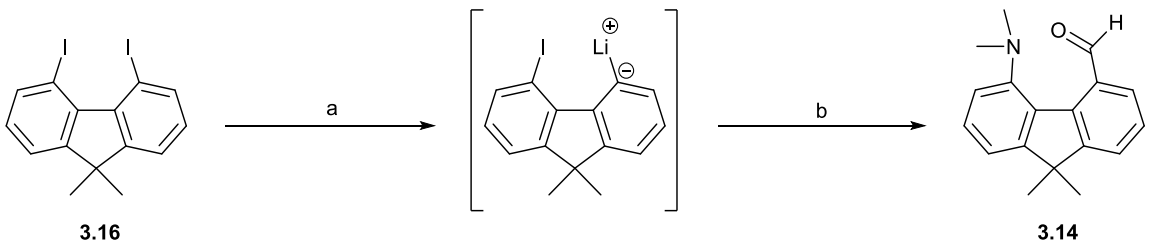

Scheme 3.16. (a) n-BuLi, Et_2O, -78 °C; (b) DMF, -78 °C to RT.

Initially, a series of attempts at electrophilic amination were performed in order to install the desired dimethylamino functionality at one of the *ortho*-carbons, e.g. via a Buchwald-Hartwig amination, but with no success. Alternatively, installation of the aldehyde group was tried (Scheme 3.2). *Di*-iodofluorene **3.16** was *mono*-lithiated with *n*-BuLi at -78 ^{o}C for 2 hours, an excess of DMF added and the reaction left to warm to room temperature overnight. However, the main compound isolated from the reaction was not the expected iodo-aldehyde, but instead the dimethylamino aldehyde **3.14** in 42% yield. The structure of **3.14** was supported by the introduction of ^{1}H NMR shifts at 2.63 and 10.86 ppm and ^{13}C NMR shifts at 43.5 and 192.5 ppm for the dimethylamino and aldehyde groups respectively. The ^{13}C signal corresponding to a C-I bond (previously observed in **3.16** at 87.3 ppm) was not present. Furthermore, a strong peak at 1677 cm^{-1} was observed in the infrared spectrum for the C=O stretch.

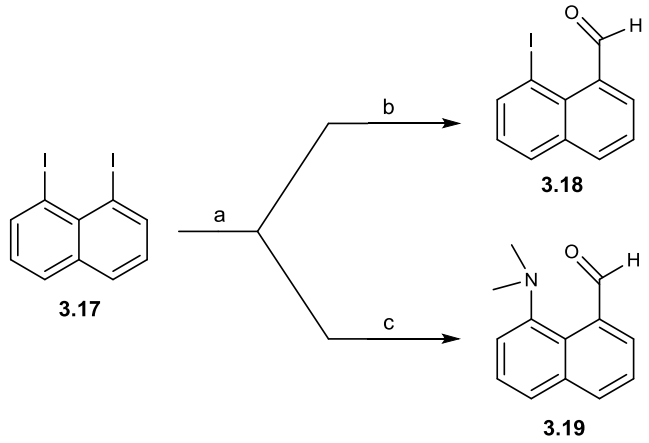

Scheme 3.17. (a) n-BuLi, Et_2O, -78 ^{o}C to -30 ^{o}C; (b) DMF, held at -30 ^{o}C; (c) DMF, -30 ^{o}C to RT.[12]

Upon further investigation, it was found that a reaction of this type was reported by Grudzein *et al.*[12] in which they reacted the *mono*-lithiated derivative of 1, 8-diiodonaphthalene (**3.17**) with DMF to give the dimethylamino aldehyde **3.19** in a one step, one pot synthesis with a 74% yield (Scheme 3.3). Interestingly, they reported that when the reaction was held at -30 ^{o}C and not allowed to warm to ambient temperature before being quenched, the subsequent addition

of the dimethylamino anion does not occur, instead giving the expected iodo-aldehyde **3.18**. Consistent with this, we observed no iodo-aldehyde in our synthesis of **3.14**.

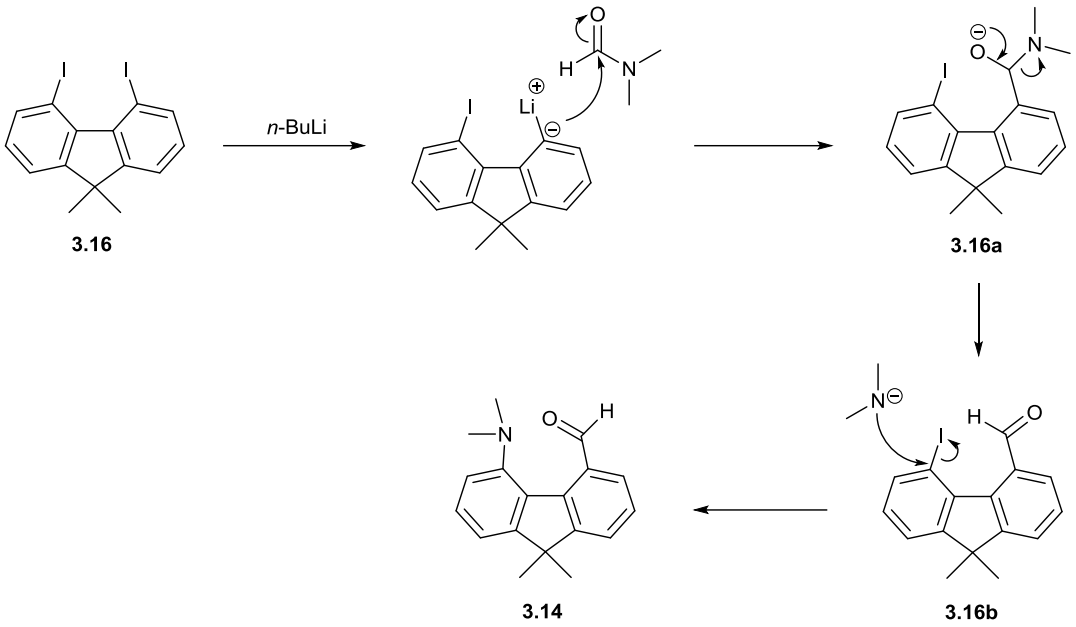

*Scheme 3.18. Proposed intermolecular mechanism for the synthesis of dimethylamino aldehyde **3.14**.*

The proposed intermolecular mechanism for the synthesis of **3.14** is shown in Scheme 3.4. Key to the reaction mechanism is the intermediate **3.16a**, which possess the bulky iodine and tetrahedral aminal anion as substituents. As shown in the molecular structure of **3.16** in Figure 3.6, the fluorene skeleton can only undergo limited twisting to minimise contacts between bulky *ortho*-substituents. As a result, a dimethylamine anion is released via the collapse of the oxyanion, allowing this nucleophilic anion to perform an S_NAr type reaction (**3.16b**) at the adjacent *ortho*-carbon, liberating an iodide anion in the process giving the dimethylamino aldehyde **3.14**.

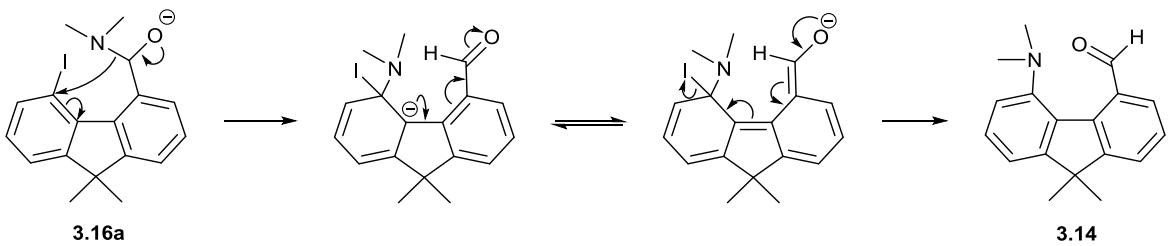

*Scheme 3.19. Proposed intramolecular mechanism for the synthesis of dimethylamino aldehyde **3.14**.*

Alternatively, the reaction could proceed via an intramolecular mechanism as shown in Scheme 3.5. In this route, the dimethylamino group of **3.16a** migrates as a result of the aminal collapse to the adjacent *ortho* carbon. The negative charge of the stabilised carbanion can thus resonate in the aromatic system before eliminating the labile iodide group to give the dimethylamino aldehyde **3.14**.

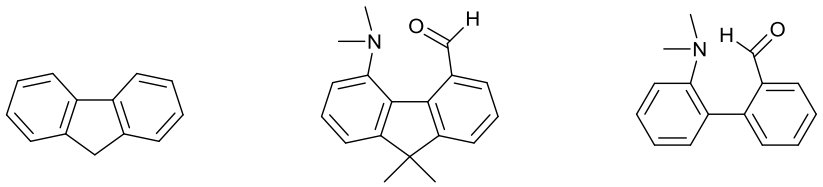

3.7 **3.14** **3.20**

*Figure 3.59. Structures of fluorene[2] **3.7**, fluorene dimethylamino aldehyde **3.14** and biphenyl dimethylamino aldehyde[13] **3.20**.*

Suitable crystals of aldehyde **3.14** were obtained via slow evaporation of a DCM/hexane solution, and the X-ray crystal structure determined at 150 K (Figure 3.8). Unusually for an organic system, the crystal system was tetragonal (space group $I4_1cd$). The relevant molecular geometries of **3.14** are summarised in Table 3.1. The locked conformation of the fluorene backbone, results in a torsion angle between the two *ortho*-substituted carbons of 11.6(4)^o as opposed to 0^o in unsubstituted fluorene **7** and 58.9(1)^o in the biphenyl substituted dimethylamino aldehyde[13] **3.20** (Figure 3.7). This reorientation allows for the much shorter Me_2N---C contact distance of 2.691(3) Å (compared to 2.989(2) Å in biphenyl **3.20**), whilst the twisting from the idealised planar conformation results in an increase of the *ortho*-carbon C---C distance to 3.332(3) Å in aldehyde **3.14** from 3.293(3) Å in unsubstituted fluorene **3.7**.

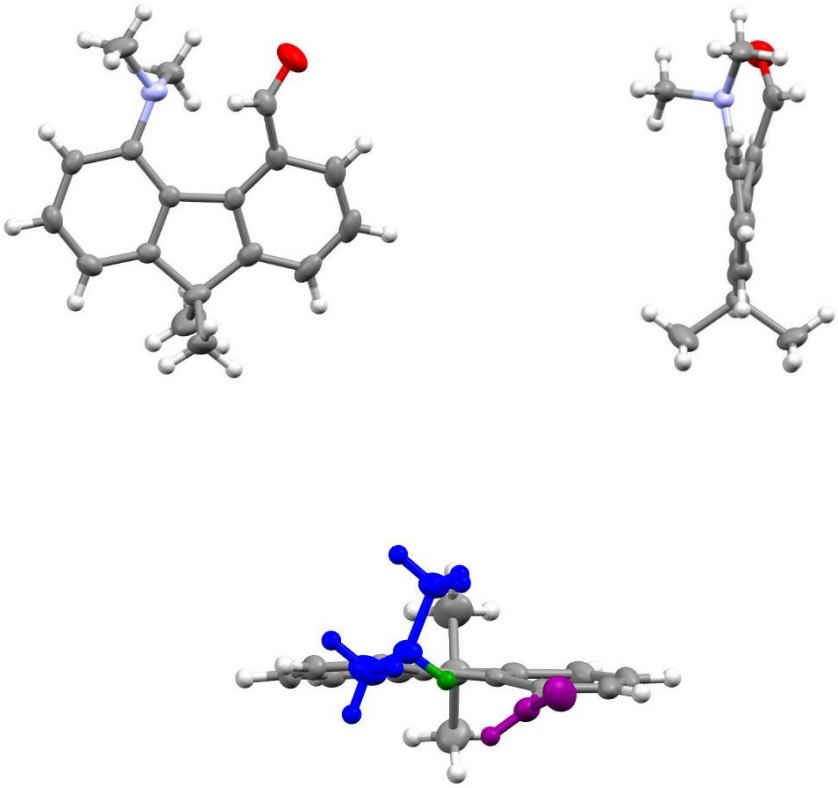

*Figure 3.60. Molecular structure of dimethylamino aldehyde **3.14** (left), with a view along the fluorene plane (right) to indicate the displacement of two ortho-substituents to either side of the plane. The bird's eye view (bottom) demonstrates the angle of approach for the dimethylamino (blue) nitrogen lone pair (green) toward the π* orbital of the aldehyde (pink) group.*

Removal of the free rotation around the C-C bond connecting the two phenyl rings results in large displacements of the dimethylamino (0.188 Å) and aldehyde (0.313 Å) groups from the planes of their respective benzene rings. The dimethylamino group adopts a pyramidal geometry (Σ N bond angles = 340.98º) with (H_3)C-N-C-C(H) torsion angles of -105.6(2) and 25.4(3)º. This results in the axis of the nucleophilic nitrogen lone pair lying at an angle of 11.6º to the N---C=O vector, with the carbonyl group positioned at an angle (O=C-C-C(H)) of 40.6(3)º to its benzene ring. The approach of the dimethylamino group to the carbonyl group generates a Bürgi-Dunitz angle (N---C=O) of 111.0(2)º.

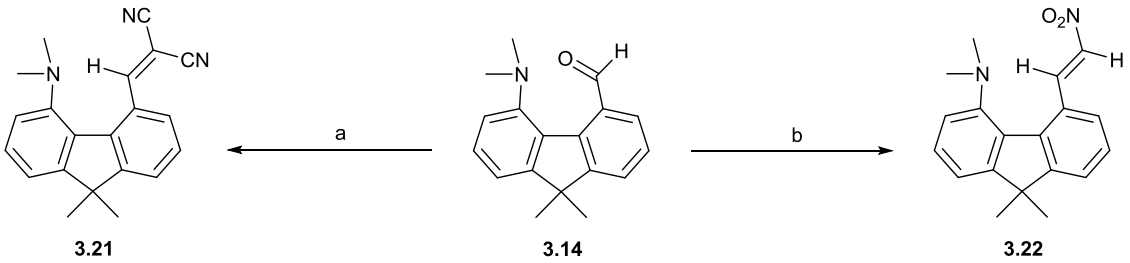

Scheme 3.20. (a) $CH_2(CN)_2$, CH_3OH, $(^+NH_3CH_2\text{-})_2(^-OAc)_2$ (cat.), 65 °C; (b) NO_2CH_3, CH_3OH, $(^+NH_3CH_2\text{-})_2(^-OAc)_2$ (cat.), 65 °C.

Condensation of dimethylamino aldehyde **3.14** with active methylene compounds malononitrile and nitromethane gave the expected Knoevenagel condensation products **3.21** and **3.22** (Scheme 3.6). In each case the aldehyde **3.14**, the appropriate methylene compound and ethylenediamine diacetate (EDDA) as the catalyst were refluxed together in methanol, producing **3.21** and **3.22** in 59% and 63% yields respectively. The structure of **3.21** was confirmed by the ^{1}H NMR shift of the vinylic proton to 9.07 ppm whilst the addition of the nitrile groups was shown by peaks of 114.6 ppm and 2223 cm^{-1} in the ^{13}C NMR and infrared spectrum respectively. The structure of **3.22** was similarly confirmed by the ^{1}H NMR shifts of the two *trans* coupled vinylic protons at 9.93 and 7.50 ppm. The loss of the aldehyde signal (192.5 ppm) in the ^{13}C NMR spectrum for **3.21** and **3.22** further supported their synthesis.

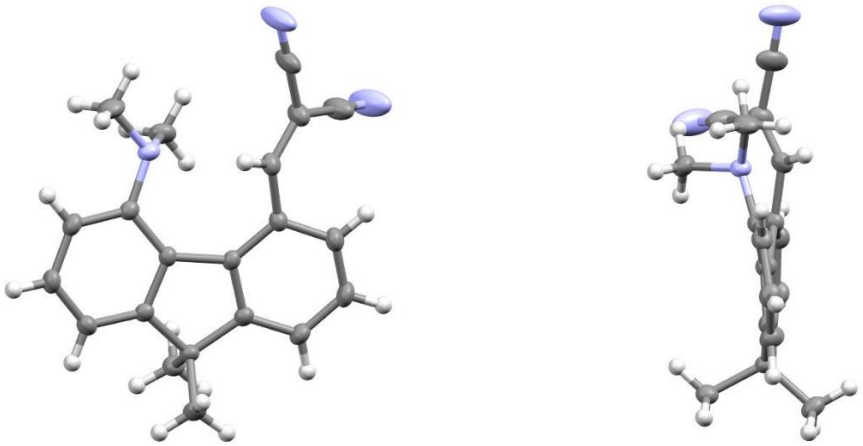

*Figure 3.61. Molecular structure of the dinitrile derivative **3.21** (left), with a view along the fluorene plane (right) to indicate the displacement of two ortho-substituents to either side of the plane.*

Exhaustive attempted to crystallise nitro condensation product **3.22** from a range of different solvent mixtures resulted in amorphous powders or very small unsuitable crystals. However, orange crystals of the dinitrile **3.21** were successfully grown from a $CDCl_3$/hexane solution and the X-ray crystal structure was determined at 150 K (Figure 3.9). When compared to its biphenyl equivalent **3.23**, the stand out difference is that dinitrile **3.21** no longer forms a long Me_2N-C bond between the interacting *ortho*-substituents, instead displaying a particularly long Me_2N---C contact distance of 2.830(2) Å which is also longer than the Me_2N---C contact distance in aldehyde **3.14**. There is a -10.2(2)^o torsional rotation in dinitrile **3.21** between the two *ortho*-substituted carbons, similar to the ring rotation of 11.6(4)^o in aldehyde **3.14** and larger than 24.2(3)-24.4(2)^o in the biphenyl **3.23**. Furthermore, the displacements of the dimethylamino nitrogen (0.261 Å) and vinylic alkene carbon (0.173 Å) groups from the planes of their respective benzene rings are similar to those shown in aldehyde **3.14**. However, an increase in the *ortho*-carbon C---C separation distance from 3.332(3) Å in aldehyde **3.14** to 3.441(2) Å in dinitrile **3.21**, could play a role in the overall increase of the Me_2N---C distance.

*Table 3.19. Selected geometric data for aldehyde and dinitrile derivatives **3.14**, **3.20**, **3.21** and **3.23**.*

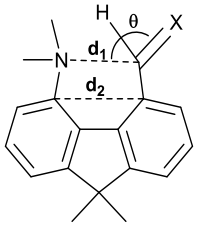

3.14: X = O
3.21: X = $C(CN)_2$

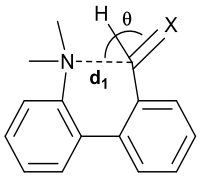

3.20: X = O
3.23: X = $C(CN)_2$

Compound	d_1 / Å	d_2 / Å	θ / ^{o}	τ^a / ^{o}	τ^b / ^{o}	τ^c / ^{o}	Σ^d / ^{o}
3.14	2.691(3)	3.332(3)	111.0(2)	11.6(4)	25.4(3)/-105.6(2)	40.6(3)	341.0(3)
3.20[13]	2.989(2)	-	126.5(1)	58.9(1)	-14.9(2)/116.5(1)	6.2(2)	341.8(3)
3.21	2.830(2)	3.441(2)	110.8(1)	-10.2(2)	-15.84(2)/111.7(1)	-42.5(2)	338.0(3)
3.23[5]	1.604(3)	-	112.62(2)	-24.2(3)	-16.4(2)/103.9(2)	101.1(2)	-
	1.586(3)	-	113.4(1)	24.4(2)	16.6(2)/-103.5(2)	-96.7(2)	-

τ^a = torsion angle: (*ortho*)C-C-C-C(*ortho*), τ^b = torsion angle: 2 x (H_3)C-N-C(Ar)-C(H), τ^c = torsion angle: X=C-C(Ar)-C(H), Σ^d = Sum of bond angles at dimethylamino nitrogen (NMe_2).

The dimethylamino group maintains a pyramidal geometry, with the sum of the bond angles of nitrogen adding up to 338.0^o, with (H_3)C-N-C-C(H) torsion angles of 111.7(1) and -15.8(2)^o. The lone pair of electrons of the nitrogen atom lie at an angle of 24.4^o to the N---C=C vector

demonstrating a poorer alignment at this elongated interaction distance. The alkene moiety is orientated at an angle ($(CN_2)C=C(H)-C-C(H)$) of -42.5(2)^o to its benzene ring, which allows for a Bürgi-Dunitz angle (N---C=O) of 110.8(1)^o, almost identical to the angle generated in aldehyde **3.14**. The short intramolecular contact between the carbon of the nitrile group nearest the aromatic ring and an aromatic proton (2.547 Å) could limit the orientational freedom of the alkene group with respect to its benzene ring, as reducing the torsion angle (τ^c) will result in an increased repulsion due to this interaction. Meanwhile, the shortest intermolecular contacts are observed between an aromatic proton and a nitrile nitrogen atom (2.735 Å) and an aromatic proton and the protons of the methyl groups (2.358 Å).

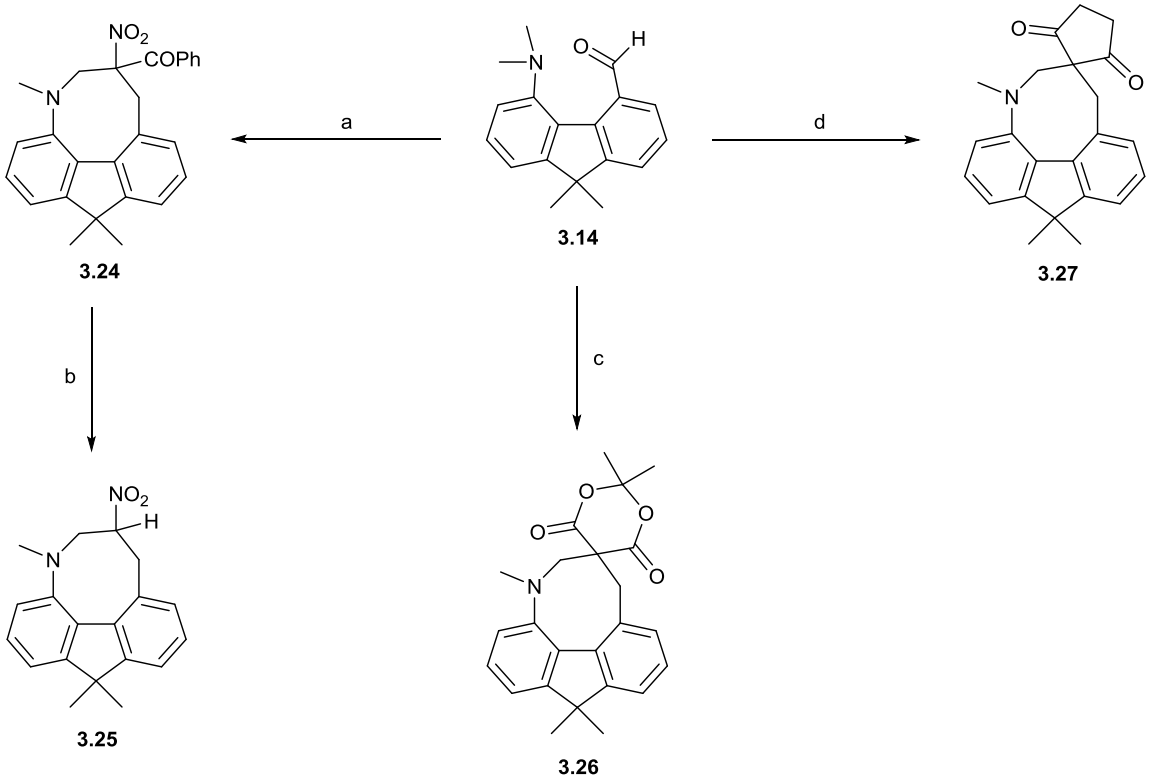

Scheme 3.21. (a) Benzoylnitromethane, CH_3OH, ($^+NH_3CH_2$-)$_2$(^-OAc)$_2$ (cat.), 65 ^oC; (b) Recrystallisation from a DCM/hexane solution; (c) Meldrum's acid, CH_3OH, ($^+NH_3CH_2$-)$_2$(^-OAc)$_2$ (cat.), 65 ^oC; (d) Cyclopenta-1,3-dione, DMSO, RT.

The condensations of dimethylamino aldehyde **3.14** with active methylene compounds benzoylnitromethane, Meldrum's acid and cyclopenta-1,3-dione did not yield the expected

Knoevenagel condensation products **3.28**-**3.30** (Figure 3.10). Instead, the only isolated products were found to be **3.24**, **3.26** and **3.27**, whereby following the desired Knoevenagel condensation, the *ortho* N-methyl and alkene groups have further reacted together forming an eight-membered azocine ring (Scheme 3.7). Modification to the reaction conditions of **3.24**, **3.26** and **3.27** were made by either 1) changing the solvent, 2) removal of the catalyst or 3) stirring the reaction at ambient temperature. Unfortunately, any change (or combination of changes) led only to the same products being formed but with a lower overall yield or no reaction taking place. Optimal yields of 76% and 71% for **3.24** and **3.26** were achieved by refluxing aldehyde **3.14**, EDDA and the relevant methylene compound in MeOH. In contrast, the cyclic diketone derivative **3.27** was best synthesised by stirring the aldehyde **3.14** and 1,3-cyclopentanedione in DMSO at ambient temperature, isolating the product in a 41% yield. In all cases isolation of the desired Knoevenagel intermediates **3.28**-**3.30** was not achieved.

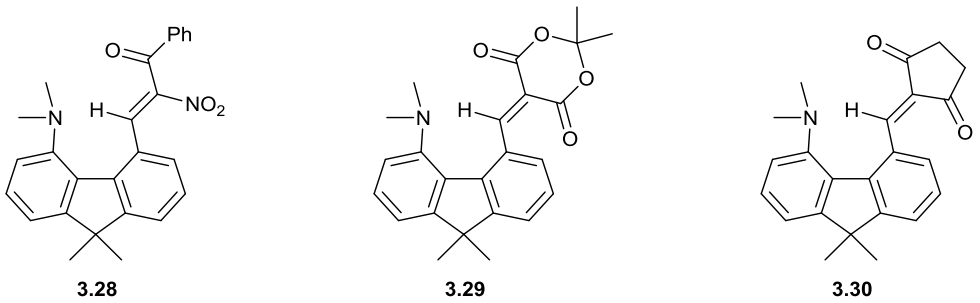

3.28 **3.29** **3.30**

*Figure 3.62. Structures of the three expected and desired Knoevenagel products **3.28**-**3.30**.*

The structure of **3.24** is confirmed not only by the absence of a vinylic proton, but by the presence of four doublets between 3.60-4.89 ppm and the singlet at 2.81 ppm in the ^{1}H NMR spectrum. These peaks correspond to the two methylene groups flanking the new quaternary carbon and one N-methyl group respectively. Similar sets of shifts of 3.04-4.51 ppm and 2.57-4.26 ppm for the methylene groups and 2.96 ppm and 3.02 ppm for the N-methyl protons are observed in the ^{1}H NMR spectra of **3.26** and **3.27**. The different substitution of each of the chosen methylene derivatives at the quaternary carbon in the azocine ring was evidenced by

the signals from the carbonyl groups in the ^{13}C NMR and infrared spectra; 189.4 ppm and 1686 cm^{-1} for the ketone **3.24**, 168.9/166.2 ppm and 1735 cm^{-1} for the cyclic diester **3.26** and 215.3/212.0 ppm and 1714 $cm^{-1}$for the cyclic diketone **3.27**.

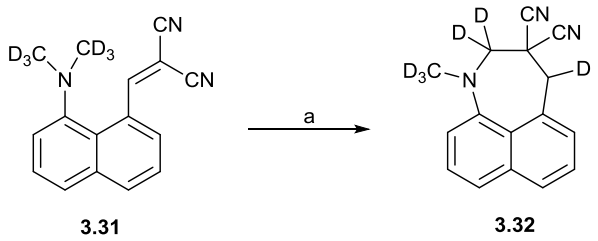

3.31 **3.32**

Scheme 3.22. (a) DMSO-d_6, 100 ^oC.

The work of Mátyus *et al.*[14,15] demonstrated the synthesis of a range of azepine and azocine rings on a series of *ortho/ortho* disubstituted biphenyls and *peri*-naphthalenes. In each case, the *ortho* or *peri* substituents consisted of a nucleophilic amine and a Knoevenagel-derived electrophilic alkene which, when heated in DMSO, underwent a rearrangement to give the appropriate azepine/azocine system. The nature of the rearrangement was confirmed by the synthesis of the hexadeuterated dimethyl analogue in the *peri*-naphthalene derivative **3.31**.[14] Monitoring of the reaction of **3.31** in d_6-DMSO at 100 ^oC revealed that no deuterium loss occurred in the reaction (Scheme 3.8), confirming the azepine ring **3.32** was synthesised via an intramolecular pathway. A proposed mechanism for the rearrangement is shown in Scheme 3.9 for the synthesis of the eight-membered azocine ring **3.27**. As discussed, the desired Knoevenagel product is initially synthesised, but in our cases not isolated. Two factors then subsequently play an important role in the reaction not stopping at this Knoevenagel product with a second reaction instead proceeding. Firstly, the increased distance between the *ortho*-carbons allows for a larger degree of rotation around the N-C(aromatic) bond. Secondly, the three alkene products in **3.28**-**3.30** are more electrophilic than those in **3.14** and **3.21**. This facilitates the optimised orientation and donation of an *N*-methyl hydride ion via a 1, 5 sigmatropic shift, to the electrophilic alkene (**3.14a**), an example of a type 2 *tert*-amino effect

reaction.[14–17] This forms an iminium cation and a stabilised carbanion (**3.14c**) which subsequently react together to form the azocine ring **3.27**. The examples of both azepine and azocine synthesised by Matyus *et al.* require heating of the selected Knoevenagel product in DMSO, whereas the azocine derivatives **3.24**, **3.26** and **3.27** of this study do not. This indicates that the wider C---C distance between the *ortho*-substituents and locked conformation of the *ortho*-groups allows for the type 2 *tert*-amino effect reaction to proceed via a lower energy pathway.

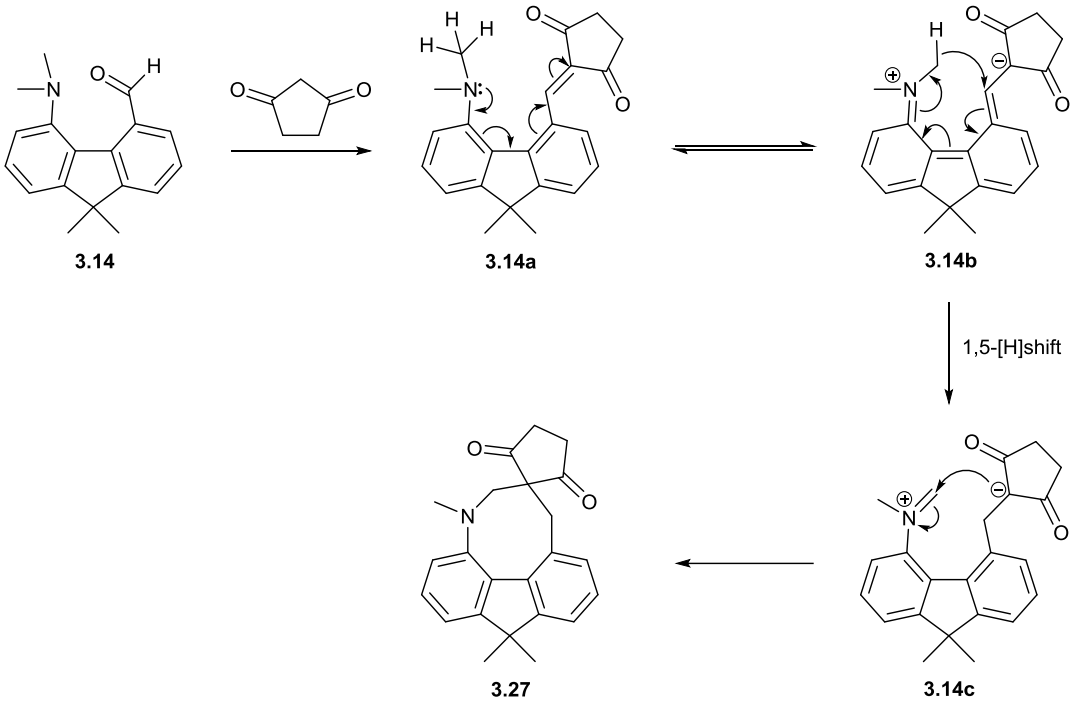

*Scheme 3.23. Proposed synthesis of the azocine **3.27** proceeding via a type 2 tert-amino effect reaction.*

Suitable crystals of azocine **3.24** were grown via slow evaporation of a DCM/hexane solution. The X-ray crystal structure of the resultant yellow plates was determined at 150 K. Whilst confirming the structure, one of the two crystallographically unique molecules in the symmetric unit has significant disorder relating to the azocine ring, making the accuracy of the solution poor. Thus, attempts to grow better quality crystals were made. However, upon recrystallisation from the same solvent mixture, a different 'set' of crystals appeared in the vessel alongside the

expected yellow plates, differing in colour, shape and size. The two crystal systems were separated under a microscope, analysed by ^{1}H and ^{13}C NMR, infrared and mass spectroscopy and suitable crystals screened for structural determination. Spectroscopic data of the yellow plates revealed they were the expected azocine **3.24**. Whereas, spectroscopic data for the alternate colourless needles did not match the data for azocine **3.24**, thus proving they were not a crystallographic polymorph. Determination of the crystal structure at 150 K in fact revealed the material to be a decomposition product caused by the cleavage of the benzoyl group from the quaternary carbon, likely due to the action of water to give nitro-azocine **3.25** (Figure 3.11). Spectroscopically, the structure of **3.25** is confirmed by the loss of the ^{13}C NMR and infrared peaks of 189.4 ppm and 1686 cm^{-1}, corresponding to that of the benzoyl ketone and its replacement with a ^{1}H NMR triplet at 4.38 ppm for the tertiary proton.

*Table 3.20. Selected geometric details for the nitro and Meldrum's azocine derivatives **3.25** and **3.26**.*

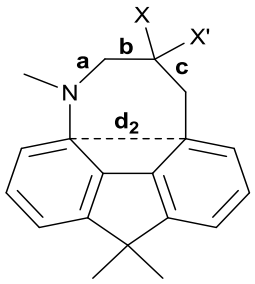

3.25: X = H, X' = NO_2

3.26: X, X' = $(C(=O)O)_2CMe_2$

Compound	d_2 / Å	a / Å	b / Å	c / Å	τ^a / º	Σ^b / º
3.25	3.448(4)	1.460(4)	1.525(4)	1.506(4)	-11.5(5)	348.9(3)
3.26	3.447(2)	1.454(2)	1.565(2)	1.561(2)	-10.3(3)	350.6(3)

τ^a = torsion angle: (*ortho*)C-C-C-C(*ortho*), Σ^b = Sum of bond angles at nitrogen.

Crystals of azocine **3.26** were grown via slow evaporation from an acetone solution, whilst azocine **3.27** unfortunately failed to crystallise. The X-ray crystal structure of **3.26** was determined at 150 K. The molecular structures and selected geometric information for **3.25** and **3.26** are shown in Figure 3.11 and Table 3.2. Both of the eight-membered azocine rings of **3.25** and **3.26** show signs of strain in their non-aromatic portions which extend from the fluorene backbone. The more highly substituted azocine **3.26** has two long bonds to the quaternary

carbon of 1.565(2) and 1.561(2) Å, whilst the less substituted derivative **3.25** displays slightly shorter lengths of 1.525(4) and 1.506(4) for the same bonds. The bonding geometry of the nitrogen atom in **3.25** and **3.26** is almost planar with it positioned marginally on the same side of the fluorene plane as the sp^3 carbons α and β to it. Torsion angles of -11.5(5)/-10.3(3)º and C---C distances of 3.448(4)/3.447(2) Å for **3.25** and **3.26** respectively between the two *ortho*-substituted carbons of the fluorene skeleton are similar to those of the Knoevenagel product **3.21**.

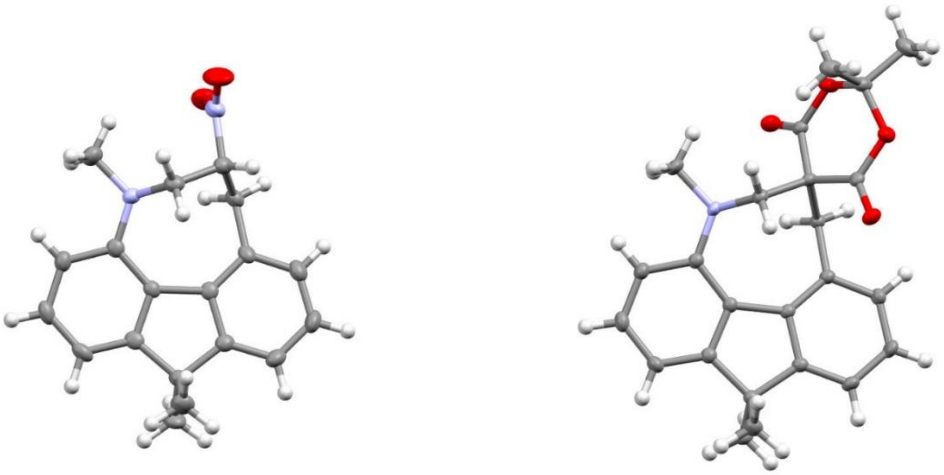

*Figure 3.63. Molecular structures of the decomposition nitro azocine product **3.25** and the Meldrum's acid azocine **3.26**.*

Investigation of 5, 6-disubstituted acenaphthenes

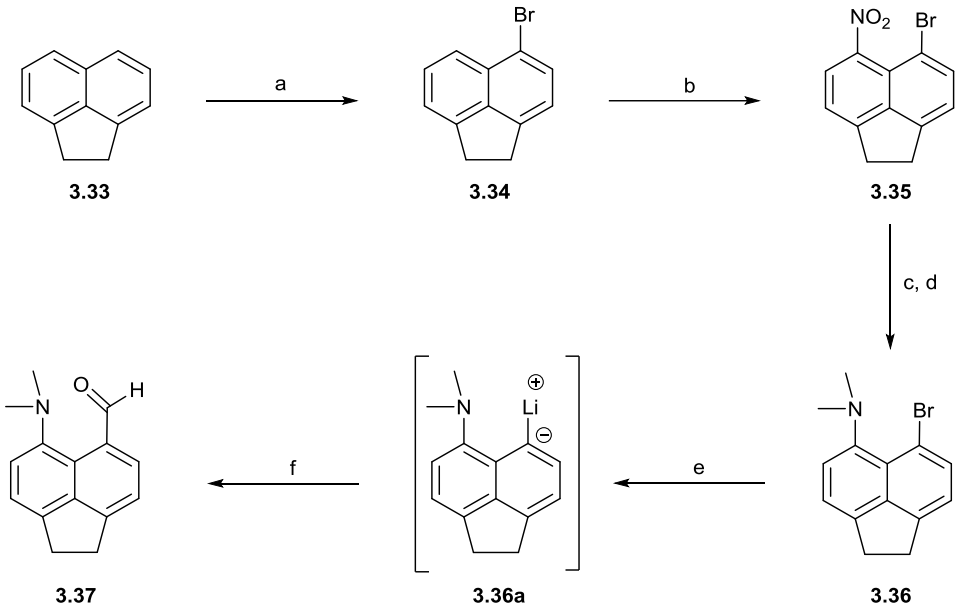

Scheme 3.24. (a) NBS, DMF, 25 °C;[18] (b) Fuming HNO_3, AcOH, 25 °C;[18] (c) Fe, $FeCl_3$, AcOH, EtOH, 100 °C;[19] (d) MeI, K_2CO_3, CH_3CN, 50 °C;[19] (e) n-BuLi (1.6M), THF, -78 °C; (f) DMF, -78 to 25 °C.

Acenaphthalene **3.36** which contains an ethylene bridge *para* to the dimethylamino and bromo *peri*-groups was prepared according to known literature procedures[18,19] (Scheme 3.10). To begin, acenaphthene **3.33** was *mono*-brominated at the *5*-position *para* to the ethylene bridge with *N*-bromosuccinimide (NBS) giving **3.34**,[18] before being *peri*-nitrated via the addition of excess fuming nitric acid in acetic acid to give **3.35**.[18] Following the methods described by Pla *et al.*[19] the nitro group was reduced with iron(III) chloride and iron powder resulting in the amino compound, which was *N*-dimethylated *in situ* with potassium carbonate and iodomethane to give **3.36**. Lithium-halogen exchange of bromoamine **3.36** with *n*-BuLi at -78 °C over 3h, resulted in a deep red solution of the *peri*-lithiated compound **3.36a**. A two-fold excess of DMF was added and the reaction was allowed to warm to room temperature, resulting in the isolation of the desired dimethylamino aldehyde **3.37** as an orange solid in 55% yield. The successful addition of the aldehyde group is evidenced by signals at 11.38 and 195.7 ppm in the ^{1}H and ^{13}C NMR spectra. A carbonyl stretching frequency of 1660 cm^{-1} is observed in the infrared spectrum.

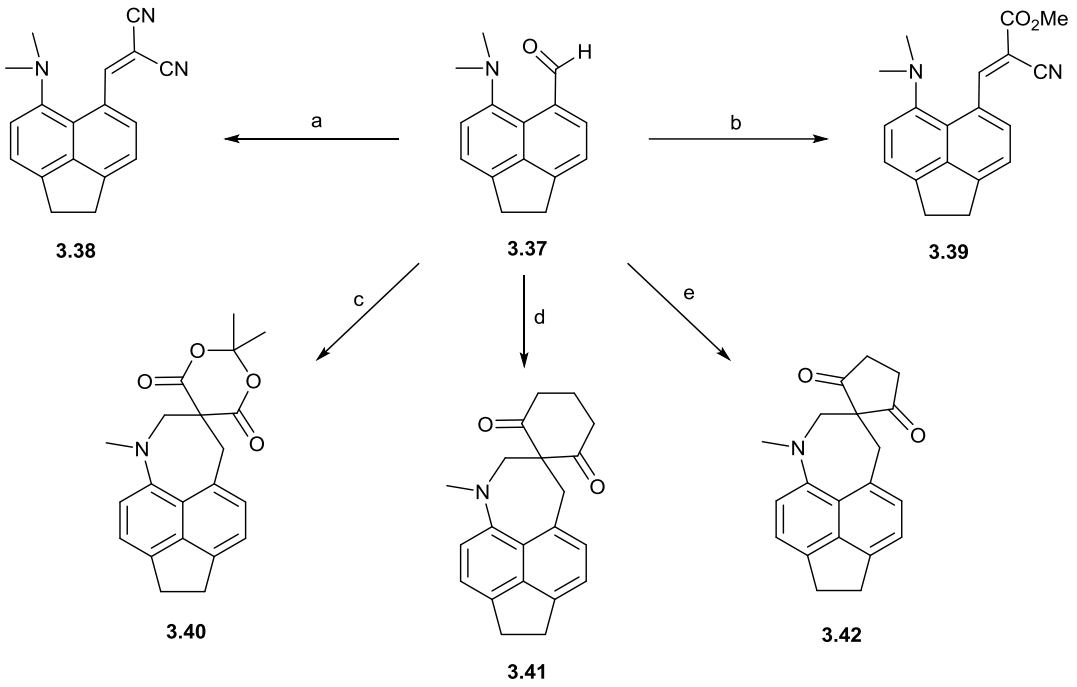

Scheme 3.25. (a) $CH_2(CN)_2$, CH_3OH, $(^+NH_3CH_2\text{-})_2(^-OAc)_2$ (cat.), 65 °C; (b) $CH_2(CN)(CO_2Me)$, CH_3OH, $(^+NH_3CH_2\text{-})_2(^-OAc)_2$ (cat.), 65 °C; (c) Meldrum's acid, DMSO, RT; (d) Cyclohexa-1,3-dione, DMSO, RT; (e) Cyclopenta-1,3-dione, DMSO, RT.

Condensation of aldehyde **3.37**, with the active methylene compounds malononitrile and methyl cyanoacetate (Scheme 3.11) yielded the expected Knoevenagel condensation products **3.38** and **3.39** in good yields of 91% and 88% respectively. In both cases, the aldehyde **3.37**, the appropriate methylene compound and an ethylenediamine diacetate (EDDA) catalyst were refluxed in methanol. The structures of the both compounds **3.38** and **3.39** demonstrated the expected vinyl proton ^{1}H NMR signals at 9.43 and 9.31 ppm. The ^{13}C NMR for **3.38** shows signals for the nitrile carbons at 113.0 and 114.4 ppm, whilst for **3.39** the nitrile carbon is found at 116.1 ppm with the ester carbonyl at 163.9 ppm. The infrared spectra for **3.38** and **3.39**, demonstrate peaks at 2221 and 2223 cm^{-1} respectively corresponding to the nitrile stretching frequencies, with the carbonyl ester stretching of **3.39** observed at 1727 cm^{-1}.

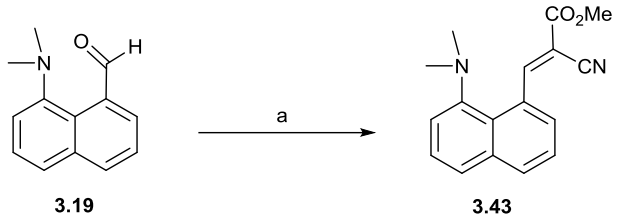

3.19 **3.43**

Scheme 3.26. (a) $CH_2(CN)(CO_2Me)$, CH_3OH, $(^+NH_3CH_2\text{-})_2(^-OAc)_2$ (cat.), 65 ^oC.

In order to achieve an accurate comparison, data for the unsubstituted naphthalene analogues of the aldehyde **3.37** and of the Knoevenagel products **3.38** and **3.39** were required. The data for the aldehyde and dinitrile derivatives has been previously reported[6,20] whereas the corresponding methyl cyanoester **3.43** had to be prepared and its crystal structure measured. Following the method described by Wallis *et al.*[6] dimethylamino aldehyde **3.19** was refluxed with methyl cyanoacetate and EDDA catalyst in methanol, to give the Knoevenagel condensation product **3.43** as a yellow solid in a 53% yield (Scheme 3.12). The structure of **3.43** was confirmed by the expected vinyl proton ^{1}H NMR signal at 9.21 ppm. Moreover, the nitrile carbon is found at 116.1 ppm with the ester carbonyl at 163.9 ppm in the ^{13}C NMR spectrum. Crystals of **3.43** were grown via slow evaporation of an ether solution and its structure determined at 150 K.

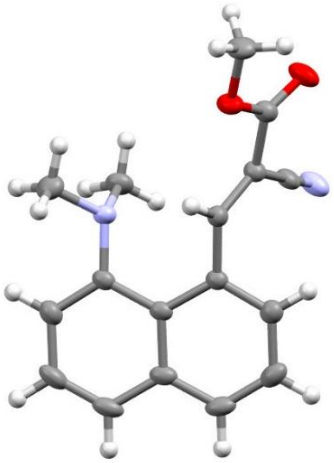

*Figure 3.64. Molecular structure of the methyl cyanoester derivative **3.43**.*

The stereochemistry around the alkene double bond of **3.43** places the bulkier methyl ester *trans* to the naphthalene ring (Figure 3.12), with the alkene rotated from the naphthalene by 55.2(2)°. The *peri*-groups show the expected angular displacements, with the C-N bond of the nucleophile orientated slightly (~1°) towards the alkene, which is retreating in the same direction (~4°) (Table 3.3). Interestingly, despite the attractive interaction across the *peri*-positions, the *exo*-angle between them is larger than the opposite *exo*-angle (122.6(1) vs 121.4(1). The two *peri*-bonded atoms are displaced to either side of the idealised naphthalene plane by 0.18 Å (for the dimethylamino nitrogen) and 0.31 Å (for the alkene C-H). These displacements result in a Me_2N---C separation of 2.595(2) Å *ca.* 0.6 Å within the Van der Waals radii of C and N atoms. This gives a Bürgi-Dunitz angle of 116.2(1)° which is in accordance with a series of previously studied compounds.[6,7,20–22]

*Table 3.21. Selected geometric details for the acenaphthene (**3.37-3.39**) and naphthalene (**3.42-3.44**) aldehyde, dinitrile and cyanoester derivatives.*

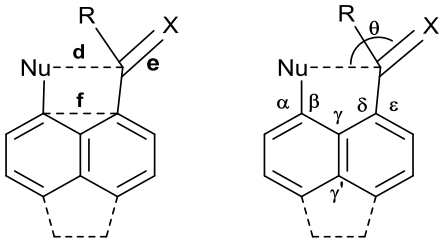

3.37, 3.19: X = O

3.38, 3.44: X = $C(CN)_2$

3.39, 3.43: X = $C(CN)(CO_2Me)$

Compound	**d** / Å	**e** / Å	**f** / Å	**θ** / °	**τ^a** / °	**τ^b** / °
3.37	2.953(2)	1.217(2)	2.602(2)	149.7(1)	18.8(2)/-111.3(2)	17.4(2)
3.19[20]	2.489(6)	1.213(5)	2.479(6)	113.5(3)	44.5(5)/-85.2(5)	57.3(5)
3.38a	2.846(3)	1.348(3)	2.595(3)	133.0(2)	27.5(3)/-100.8(2)	35.9(3)
3.38b	2.755(3)	1.343(3)	2.562(3)	122.7(1)	-45.8(3)/82.1(2)	-51.9(3)
3.44[6]	2.413(2)	1.354(2)	2.463(3)	112.1(1)	-49.7(2)/81.5(2)	-56.5(2)
3.39	2.843(2)	1.340(2)	2.592(2)	129.3(1)	-27.5(2)/100.0(2)	-40.8(2)
3.43	2.595(2)	1.349(2)	2.503(2)	116.2(1)	34.5(2)/-93.8(2)	55.2(2)

Compound	**α** / °	**β** / °	**δ** / °	**ε** / °	**γ / γ'** / °
3.37	121.7(1)	119.3(1)	124.1(1)	116.1(1)	129.5(1)/111.4(1)
3.19[20]	124.3(4)	116.0(3)	122.2(4)	119.2(3)	120.6(3)/121.5(4)
3.38a	121.8(2)	119.6(2)	121.3(2)	119.9(2)	128.5(2)/111.3(2)
3.38b	122.8(2)	118.2(2)	121.9(2)	119.5(2)	127.3(2)/111.7(2)
3.44[6]	124.3(2)	115.9(1)	120.2(1)	120.3(2)	120.4(1)/122.6(2)
3.39	121.8(1)	119.5(1)	121.4(1)	119.7(1)	128.6(1)/111.5(1)
3.43	123.2(1)	116.8(1)	122.5(1)	117.9(1)	122.6(1)/121.4(1)

τ^a = torsion angle: 2 x (H_3)C-N-C-C(H), **τ^b** = torsion angle: X=C-C-C(H).

Suitable crystals of the bridged aldehyde **3.37** were obtained via crystallisation from a $CDCl_3$ NMR sample solution, whereas crystals of the Knoevenagel condensation products **3.38** and **3.39** were grown via slow evaporation of methanol and DCM/hexane solutions respectively. X-ray crystal structures for the three compounds were determined at 150 K, with selected molecular geometry information summarised in Table 3.3. The Me_2N---C=O contact distance in the bridged aldehyde **3.37** has widened to 2.953(2) Å, compared to 2.489(6) Å in the unsubstituted analogue **3.19**. Moreover, a difference of 18.1(1)^o in the *exo*-angles at the ring fusions between the two *peri*-positions (γ/γ') shows how the short ethylene bridge has compressed the distance between one set of *peri*-ring carbon atoms and widened the other (129.5(1)^o vs 111.4(1)^o) compared to naphthaldehyde **3.19** which does not possess the ethylene bridge (120.6(3)^o vs 121.5(4)^o). This widening causes an increase in the C---C distance between the *peri*-naphthalene ring carbons to 2.602(2) Å in **3.37** from 2.479(6) Å in **3.19**. The extent of the angular displacement for the *peri*-dimethylamino group towards the electrophile (α/β) is much smaller in bridged aldehyde **3.37** than in the naphthaldehyde **3.19**, whereas the opposite is true for the angular displacement of the *peri*-aldehyde group (δ/ε) away from the dimethylamino group. As a result of the larger contact distance, torsional angles (τ^a) of 18.8(2)/-111.3(2)^o for the N-methyl groups with respect to the *ortho*-ring carbon display a preference for conjugation of the nitrogen lone pair into the naphthalene ring. This allows the aldehyde group to rotate to lie in almost the same plane as the naphthalene ring (O=C-C-C(H) torsion angle (τ^b) of 17.4(2)^o), giving a N---H-C=O contact distance of 2.37 Å. This generates a highly unfavourable angle of approach of the dimethylamino group to the carbonyl group of 149.7(1)^o along way from the idealised Bürgi-Dunitz angle of 109^o or that shown in the aldehyde **3.19** (113.5(3)^o). All in all, these orientations indicate a preference for conjugation into the ring over a Me_2N---C=O interaction as a direct result of widening the distance between the groups. As shown in Figure 3.13, the molecules of bridged aldehyde **3.37** pack in π-stacked

centrosymmetric pairs, which are oriented perpendicular to each other in layers in the *b*, *c* plane. Neighbouring layers are related by a [100] translation in *a*.

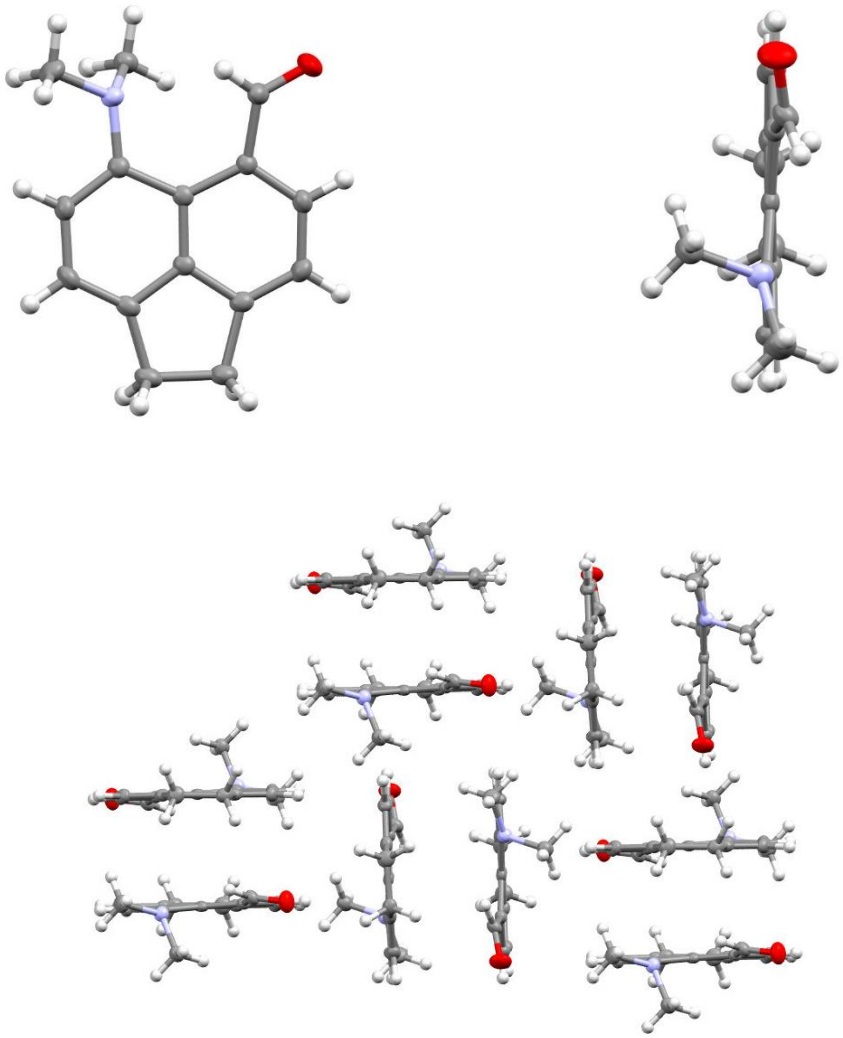

*Figure 3.65. Molecular structure of the acenaphthene aldehyde **3.37** (top left), a bird's-eye view (right), showing the twisting and displacements of the peri-substituents and the packing arrangement (bottom).*

The bridged dinitrile **38** displays Me_2N---CH=$C(CN)_2$ distances in its two crystallographically unique molecules of 2.846(3) (**3.38a**) and 2.755(3) Å (**3.38b**), compared to 2.413(2) Å in the unsubstituted analogue **3.44** (Figure 3.14). A 16-17º difference in the *exo*-angles, similar to that of the bridged aldehyde **3.37**, is observed as a consequence of the ethylene bridge, resulting in a widening of the C---C distance between the *peri*-carbons from 2.463(3) Å in the unsubstituted dinitrile **3.44** to 2.595(3) Å (**3.38a**) and 2.562(3) Å (**3.38b**). The conformations of the two molecules **3.38a** and **3.38b** are significantly different from one another, with **3.38a**

presenting similar features to the bridged aldehyde **3.37**, whilst **3.38b** demonstrates numerous similarities to the unsubstituted dinitrile analogue **3.44**. In **3.38a** the increased separation and thus reduced interaction between the *peri*-groups allows for the ethenedinitrile group to rotate further from the naphthalene plane (τ^b of 35.9(3)^o vs 17.4(2)^o in **3.37**). The orientation of the dimethylamino groups of the two compounds (**3.38a** and **3.37**) are also similar with torsion angles of 27.5(3)/-100.8(2)^o in **3.38a** and 18.8(2)/-111.3(2)^o in **3.37**. This positions the axis of the nucleophilic nitrogen lone pair at an angle of 36.1^o to the N---C vector, showing poor overlap between the nucleophile and the anti-bonding π* orbital of the *peri*-carbon. These rotations thus result in an increase in the conjugation of the alkene moiety and nitrogen lone pair with the aromatic system and an unfavoured Bürgi-Dunitz angle of 133.0(2)^o.

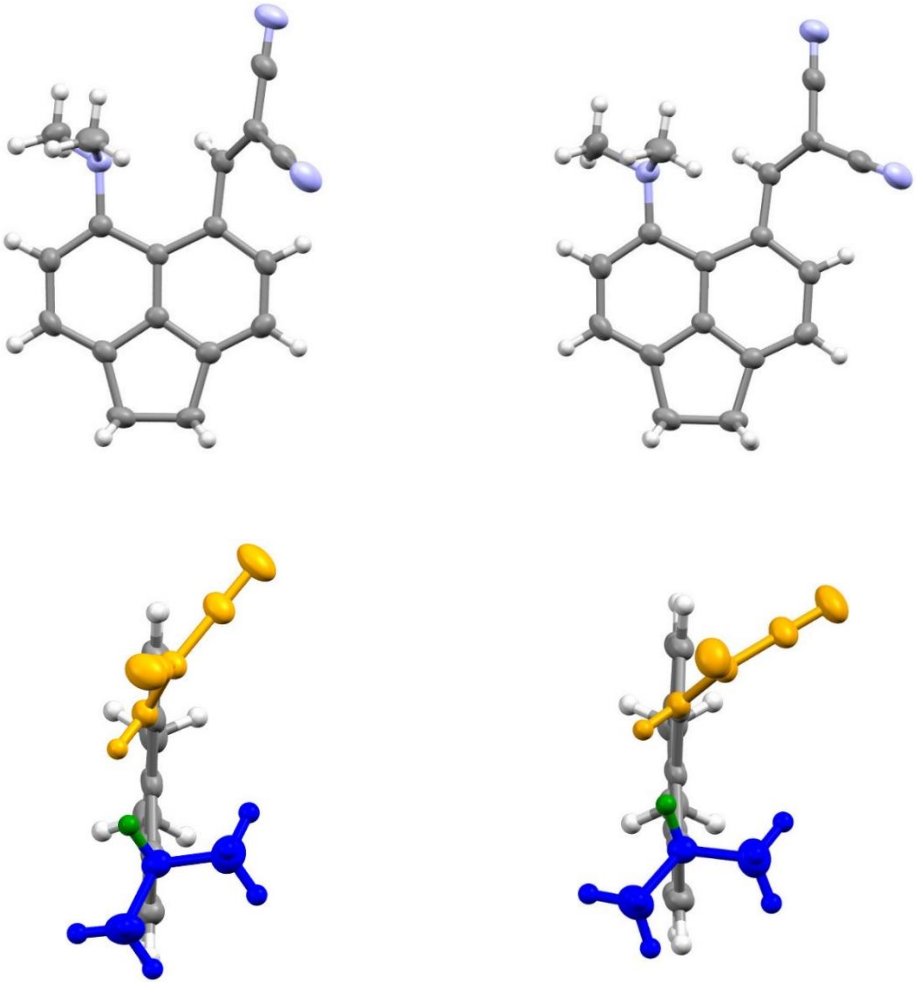

*Figure 3.66. Molecular structures of the two crystallographically unique molecules of dinitrile derivative **3.38a** (top left) and **38b** (top right). The two bird's eye views of **3.38a** (bottom left) and **3.38b** (bottom right) demonstrate the angle of approach for the dimethylamino (blue) nitrogen lone pair (green) toward the π* orbital of the alkene (orange).*

The unique molecule **3.38b** on the other hand, demonstrates a slightly shorter contact distance (2.755(3) Å) and thus a slightly stronger interaction between the *peri*-groups. This is evidenced by the less severe rotation of the nitrogen lone pair which is placed at an angle of 25.2° to the N---C vector and a greater torsion angle between the alkene moiety from the best naphthalene plane. Both of these are remarkably similar to the orientation observed in the unsubstituted dinitrile **3.44**. However, a less than ideal Bürgi-Dunitz angle of 122.7(1)° is still observed in **3.38b** compared to that of **3.44** (112.1(1)°). The in-plane angular displacement of the dimethylamino groups in **3.38a** and **3.38b** is greater for the molecule which possesses ad shorter interaction distance, whilst in both molecules the displacement of the ethenedinitrile group remains similar.

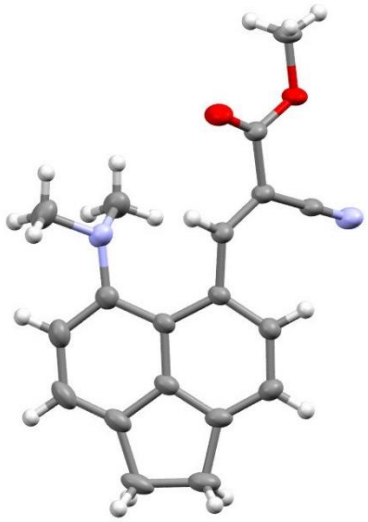

*Figure 3.67. Molecular structure of methyl cyano ester **3.43**.*

Bridged cyanoester **3.43** demonstrates a very similar structural profile to that of the bridged dinitrile **3.38a** (Figure 3.15). It possesses a Me_2N---C=C contact distance of 2.843(2) Å (2.846(3) Å in **3.38a**), a C---C distance between *peri*-naphthalene ring carbons of 2.592(2) Å (2.595(3) Å in **3.38a**), *exo*-angle differences of 17.1(1)° (17.2(2)° in **3.38a**), torsional rotations τ^a and τ^b of -27.5(2)/100.0(2)° and -40.8(2)° (27.5(3)/-100.8(2)° and 35.9(3)° in **3.38a**) and a Bürgi-Dunitz angle of approach of 129.3(1)° (133.0(2)° in **3.38a**).

The condensations of the bridged aldehyde **3.37** with the active methylene compounds, Meldrum's acid, 1, 3-cyclohexanedione and 1, 3-cyclopentanedione did not yield the expected Knoevenagel condensation products **3.45**-**3.47** (Figure 3.16). Instead, the only isolated products were found to be **3.40**-**3.42**, similar to fuse azocine systems **3.24**-**3.27** in the fluorene series. The reaction similarly began with synthesis of the desired Knoevenagel products, with the *peri*-N methyl and alkene groups reacting together via a type 2 *tert*-amino effect reaction[14–17], to give the seven-membered azepine ring. The naphtho-azepines **3.40**-**3.42** were isolated in 80%, 59% and 40% yields respectively. In all cases, we observed no trace of the Knoevenagel condensation products.

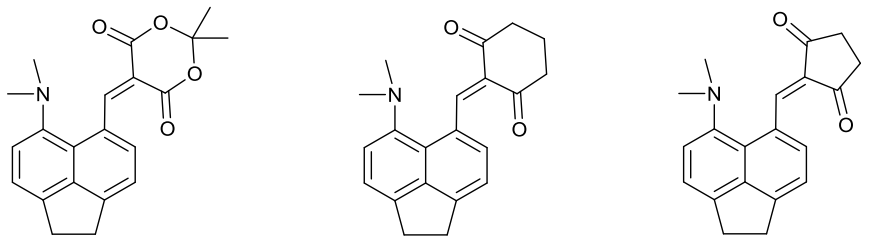

*Figure 3.68. Structures of the three expected and desired Knoevenagel products **3.45**-**3.47**.*

The structures of each of the azepines **3.40**-**3.42** were confirmed not only by the absence of a vinylic proton, but by the presence of four protons corresponding to the two methylene groups α the new quaternary carbon in the ^{1}H NMR spectra (3.70-3.90 ppm in **3.40**, 3.63-3.72 ppm in **3.41** and 3.35-3.45 ppm in **3.42**). Furthermore, a singlet corresponding to the N-methyl protons in the ^{1}H NMR spectra at 3.08, 3.03 and 3.04 ppm in **3.40**, **3.41** and **3.42** respectively is observed. Peaks in the infrared spectra at 1735 cm^{-1} (**3.40**), 1684 cm^{-1} (**3.41**) and 1707 cm^{-1} (**3.42**) correspond to the carbonyl stretching frequencies of the expected cyclic diester or cyclic diketone groups.

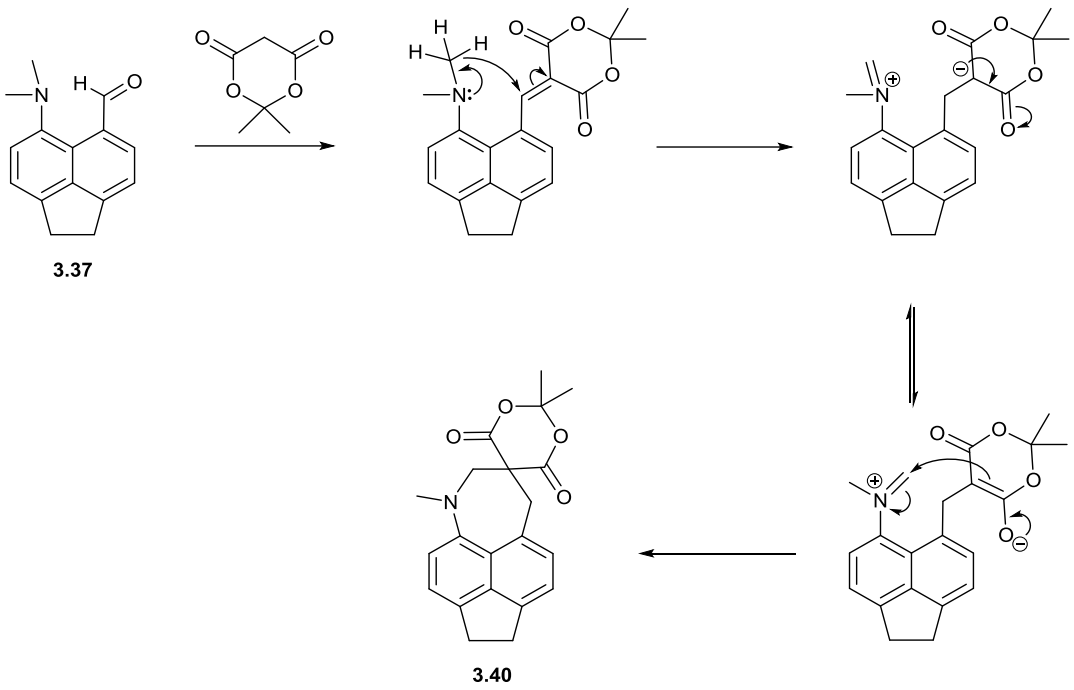

*Scheme 3.27. Proposed synthesis of the azepine **3.40** proceeding via a type 2 tert-amino effect reaction.*

The synthesis of naphtho-azepines has previously been reported by the groups of Wallis[7] and Matyus,[14,15] who proposed a mechanism for their synthesis, as shown in Scheme 3.13 using **3.40** as an example. The mechanism follows the same pathway as that shown in Scheme 3.9 where an azocine ring is formed in **3.27**.

*Table 3.22. Selected geometric details for the three azepines **3.40**-**3.42**.*

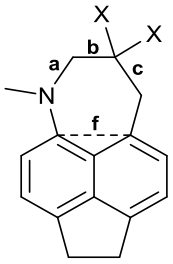

3.40: X, X = $(C(=O)O)_2CMe_2$

3.41: X, X = $(C(=O)C)_2CH_2$

3.42: X, X = $(C(=O)CH_2)_2$

Compound	**f** / Å	**a** / Å	**b** / Å	**c** / Å	Σ^a / º	τ^b / º
3.40	2.569(2)	1.456(2)	1.549(2)	1.560(2)	349.6(3)	19.1(1)
3.41	2.565(2)	1.470(2)	1.525(2)	1.562(2)	343.6(3)	14.8(1)
3.42	2.576(4)	1.453(4)	1.551(4)	1.529(4)	346.9(9)	17.5(3)
	2.572(5)	1.447(5)	1.551(5)	1.520(5)	348.3(9)	-17.5(3)

Σ^a = Sum of bond angles at nitrogen, τ^b = N-C(*peri*)-C(*peri)*-C(H_2).

Suitable crystals of the naphtho-azepines **3.40**-**3.42** were all grown via slow evaporation of DCM/hexane solutions and their X-ray crystal structures determined at 150 K (Table 3.4). Each of the structures are well resolved, but it should be noted that the -O-C(CH_3)$_2$-O portion of the Meldrum's acid ring is disordered across two positions. The molecular structures are similar, in each case the azepine ring demonstrates elongated carbon-carbon bonds to the quaternary centre, for example 1.549(2) and 1.560(2) in the Meldrum's derivative **3.40**. Interestingly, compared to the series described by Wallis *et al.*[7] in which the naphthalene skeleton was unsubstituted, the ethylene bridged acenaphthene backbone results in a lower degree of a torsional strain related to the twisting of the *peri*-groups from the naphthalene plane (τ^b). This could be a result of the increased distance between the *peri*-groups, thus allowing for a greater area in which to accommodate the 7-membered azepine ring. Within the azepine ring, the carbon atoms α and β to the nitrogen atom are displaced to the same side of the naphthalene plane, with the remaining carbon displaced to the opposite side (Figure 3.17 bottom right). The α-carbon in each case is displaced further from the naphthalene plane than the β-carbon and the nitrogen atom, with the nitrogen being the least shifted (e.g. N: 0.21 Å, α-C: 1.31 Å and β-C: 0.87 Å from the idealised naphthalene plane in **3.41**). The bonding geometry of the nitrogen atoms in **3.40**-**3.42** suggests an almost pyramidal arrangement, with the sum of the nitrogen angles ranging from 343.6-349.6^o.

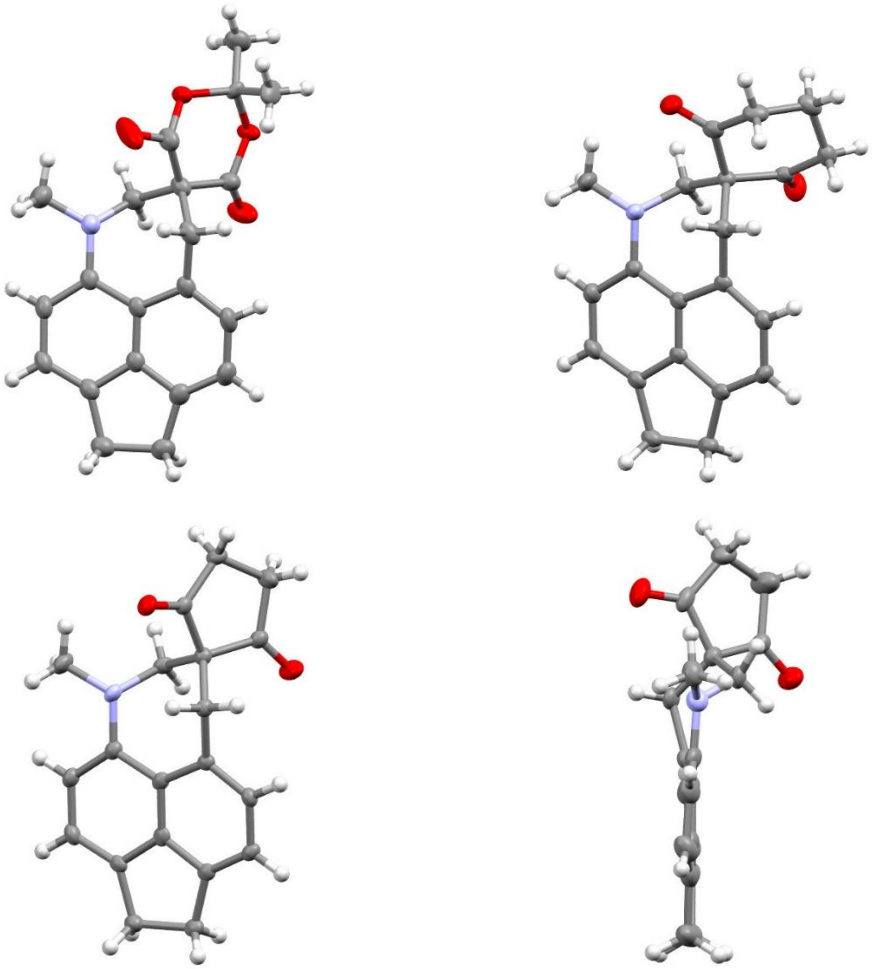

*Figure 3.69. Molecular structures of the three azepines **3.40-3.42** (top left, top right and bottom left) with a view down the acenaphthene plane of azepine **3.42** (bottom right) demonstrating the orientation of the azepine ring.*

Dehydrogenation of the ethylene bridge in the acenaphthene aldehyde **3.37** and dinitrile **3.38** derivatives was attempted using the oxidant 2,3-dichloro-5,6-dicyano-1,4-benzoquinone (DDQ). Unfortunately, despite using a variety of reaction conditions, the crude materials isolated from the reaction mixtures of each derivative indicated that the desired dehydrogenation had not occurred.

To conclude, a series of 4, 5-disubstituted fluorenes and 5, 6-disubstituted acenaphthenes have been synthesised yielding some unexpected results. With the exception of the fluorene aldehyde derivative **3.14**, the installation of carbon bridges between the two rings of the two backbones generated a larger interaction between the interacting *ortho* or *peri*-groups compared to respective biphenyl and naphthalene derivatives. The closer contact of the

fluorene aldehyde **3.14** is observed as a result of the locked planar conformation of the two rings, with the non-bridged derivative **3.20** possessing the rotational capability to generate a longer contact. In each series, the milder electrophilic groups (dinitrile/cyanoester alkenes and aldehyde) resulted in larger nucleophile/electrophile interaction distances, compared to those in the biphenyl/naphthalene series. The increased distance between the groups allows for a greater degree of rotational freedom for the electrophilic moiety with respect to the idealised plane of its scaffold, with examples such as the dimethylamino aldehyde **3.37** and dinitrile **3.38a** acenaphthene derivatives demonstrating reduced torsion angles compared to their non-bridged equivalents. Increased rotational freedom is also observed in the dimethylamino moiety, whereby the group rotates one of its N-methyl groups further toward to the electrophilic moiety in order to optimise conjugation of its lone pair into the aromatic system. A correlation is observed between the increasing contact distance and the extent to which the nucleophile prioritises nitrogen lone pair delocalisation into the aromatic system. Further increase of the electrophilicity of the alkene bond resulted not in a shortening of the observed contact distance, but instead in a type 2 *tert*-amino effect reaction. This occurred as a result of the increased rotational freedom of the dimethylamino nucleophile and the close to planar relationship between the two groups. This reaction led to a series of multi-ringed azocines and azepines, functionalised with the methylene reagent of choice. In all cases, the widening of the interaction distance facilitates the reaction to a point in which the desired Knoevenagel intermediate was not observed or isolated. In the cases of the azepines **3.40**-**3.42** the reaction proceeded under milder conditions than the equivalent reaction upon a naphthalene scaffold.

Experimental

General. Solution NMR spectra were measured on a Jeol ECLIPSE ECZ or ECX 400 spectrometer at 400 MHz for ^{1}H and at 100.6 MHz for ^{13}C using $CDCl_3$ as solvent and tetramethylsilane (TMS) as standard unless otherwise stated, and measured in p.p.m. downfield from TMS with coupling constants reported in Hz. IR spectra were recorded on a Perkin Elmer Spectrum 100 FT-IR Spectrometer using Attenuated Total Reflection sampling on solids or oils and are reported in cm^{-1}. Mass spectra were recorded at the EPSRC Mass Spectrometry Centre at the University of Swansea. Chemical analysis data were obtained from Mr Stephen Boyer, London Metropolitan University.

Preparation of 4, 5-diiodo-9, 9-dimethyl-9H-fluorene, 3.16.

9, 9-Dimethylfluorene **3.14** (1.00 g, 5.15 mmol) was stirred in anhydrous TMEDA (3.09 mL, 20.62 mmol) whilst *n*-BuLi (1.6M in hexanes, 12.89 mL, 20.62 mmol) was steadily added, producing an orange solution which was heated to 60℃ for 5h. The deep brown solution was diluted with anhydrous THF (100 mL), cooled to -78℃ and iodine (13.09 g, 51.50 mmol) was added. The reaction was allowed to warm to room temperature and stirred for 16h. The deep brown solution was quenched with sat. sodium thiosulfate solution (150 mL) and stirred for 10mins. The aqueous layer was washed with EtOAc (3 x 40 mL) and the combined organic layers were washed with sat. sodium thiosulfate solution (3 x 40 mL), H_2O (40 mL), brine (40 mL) and dried over $MgSO_4$. The solvent was removed *in vacuo* to give a crude thick brown oil which was purified by flash column chromatography (hexanes), to give **3.16** as a pale yellow (570 mg, 25%), m.p. 50-53℃. δH (400 MHz, $CDCl_3$, 24 °C): 7.93 (2H, d, J = 7.8 Hz, 3, 6-*H*), 7.40 (2H, d, J = 7.2 Hz, 1, 8-*H*), 7.04 (2H, t, J = 7.7 Hz, 2, 7-*H*), 1.43 (6H, s, 9-(CH_3)$_2$); δC (100 MHz, $CDCl_3$, 24 °C): 156.9, 142.7 (Ar-C_4), 140.8 (3, 6-*C*), 128.9 (2, 7-*C*), 121.5 (1, 8-

C), 87.3 (4, 5-*C*), 47.1 (9-C), 27.7 (9-(*C*H_3)$_2$); ν_{max}/cm^{-1} 2957, 2920, 2857, 1442, 1392, 1075, 931, 779, 762, 732, 661.

Preparation of 4-(dimethylamino)-9, 9-dimethyl-9H-fluorene-5-carbaldehyde, 3.14.

The *di*-iodo-fluorene **3.16** (0.4 g, 0.90 mmol) was dissolved in anhydrous Et_2O (15 mL) under nitrogen and cooled to -78℃. *n*-BuLi (1.6M in hexanes, 0.62 mL, 0.99 mmol) was steadily added, and the orange solution was stirred at -78℃ for 2h. Anhydrous DMF (0.36 mL, 4.63 mmol) was added and the reaction was allowed to warm to room temperature. After 16 h. the resulting green/yellow solution was quenched with H_2O (10 mL) and stirred for 10min. The aqueous solution was washed with Et_2O (3 x 30 mL) and the combined organic layers were washed with H_2O (40 mL), brine (40 mL) and dried over $MgSO_4$. The solvent was removed *in vacuo* to give a yellow/green oil which was purified by flash column chromatography (5:95 EtOAc/petrol 40-60), to give **3.14** as a yellow solid (100 mg, 42%), m.p. 80-83℃. δH (400 MHz, $CDCl_3$, 24 °C): 10.86 (1H, s, C*H*O), 7.61 (1H, dd, J = 7.3, 0.9 Hz, 6-*H*), 7.52 (1H, dd, J = 7.3, 0.9 Hz, 8-*H*), 7.34 (2H, m, 2, 7-*H*), 7.17 (1H, d, J = 7.3 Hz, 1-*H*), 7.12 (1H, d, J = 7.8 Hz, 3-*H*), 2.63 (6H, s, N(C*H*$_3$)$_2$), 1.47 (6H, s, 9-(C*H*$_3$)$_2$); δC (100 MHz, $CDCl_3$, 24 °C): 192.5 (*C*=O), 156.1, 154.0 (Ar-*C*$_2$), 150.1 (4-*C*), 138.1 (Ar-*C*$_1$), 133.5 (5-*C*), 131.8 (Ar-*C*$_1$), 129.5 & 127.1 (2, 7-*C*), 126.3 (6-*C*), 125.8 (8-*C*), 118.3 (3-*C*), 118.1 (1-*C*), 47.0 (9-*C*), 43.5 (N(*C*H_3)$_2$), 27.4 (9-(*C*H_3)$_2$); ν_{max}/cm^{-1} 2950, 2834, 2786, 1677 (C=O), 1581, 1481, 1455, 1381, 1317, 1289, 1224, 1200 1181, 1118, 985, 795, 764, 726; *HRMS* (ESI) calcd for $C_{18}H_{20}NO$ ($[M+H]^+$): 266.1545, found: 266.1538.

Preparation of 2-cyano-2-((4'-(dimethylamino)-9', 9'-dimethyl-9H-fluoren-5'-yl) propenenitrile, 3.21.

Dimethylamino aldehyde **3.14** (100 mg, 0.38 mmol) was dissolved in anhydrous MeOH (15 mL). Malononitrile (30 mg, 0.45 mmol) and ethylenediamine diacetate (10 mg, 0.06 mmol) were added and the solution was heated to reflux for 2h. The solvent was removed *in vacuo* to yield a crude orange solid which was purified by flash column chromatography (3:97 EtOAc:petrol 40-60), to give **3.21** as an orange solid (70 mg, 59%), m.p. 122-125℃. δH (400 MHz, $CDCl_3$, 24 °C): 9.07 (1H, s, C*H*), 7.67 (1H, dd, J = 7.8, 0.9 Hz, 6'-*H*), 7.56 (1H, d, J = 7.3 Hz, 8'-*H*), 7.39 (2H, m, 2'-, 7'-*H*), 7.22 (1H, d, J = 7.8 Hz, 1'-*H*), 7.19 (1H, d, J = 7.8 Hz, 3'-*H*), 2.68 (6H, s, N(CH_3)$_2$), 1.48 (6H, s, 9'-(CH_3)$_2$); δC (100 MHz, $CDCl_3$, 24 °C): 163.8 (*C*H), 156.1, 154.6, 149.1, 138.3, 131.6 (Ar-C_5), 129.9 (2'-, 7'-*C*), 127.8 (6'-*C*), 127.4 (2'-, 7'-*C*), 126.3 (Ar-C_1), 126.1 (8'-*C*), 118.9 (3'-*C*), 118.8 (1'-*C*), 114.6 (*C*≡N), 112.9 (*C*(CN)$_2$), 46.9 (9'-*C*), 44.2 (N(*C*H_3)$_2$), 27.1 (9'-(*C*H_3)$_2$); ν_{max}/cm^{-1} 2942, 2862, 2223 (C≡N), 1582, 1481, 1459, 1314, 1183, 1043, 984, 879, 797, 764, 730; Found: C, 80.27; H, 6.23; N, 13.36%. Calc. for $C_{21}H_{19}N_3$: C, 80.41; H, 6.06; N, 13.40%.

Preparation of E-2-((4'-(Dimethylamino)-9',9'-dimethyl-9H-fluorene-5'-yl)-2-nitroethene, 3.22.

Dimethylamino aldehyde **3.14** (55 mg, 0.21 mmol) was dissolved in anhydrous MeOH (5 mL). Nitromethane (0.03 mL, 0.56 mmol) and ethylenediamine diacetate (5 mg, 0.03 mmol) were added and the solution was heated to reflux for 24h. The solvent was removed *in vacuo* to yield a crude orange solid which was purified by flash column chromatography (5:95 EtOAc:petrol

40-60), to give **3.22** as an orange solid (40 mg, 63%), m.p. 99-102℃. δH (400 MHz, $CDCl_3$, 24 °C): 9.93 (1H, d, J = 13.7, 1'-*H*), 7.45-7.52 (3H, m, 2', 6, 8-*H*), 7.29-7.39 (2H, m, 2, 7-*H*), 7.10-7.18 (2H, m, 1, 3-*H*), 2.72 (6H, s, N(CH_3)$_2$), 1.46 (6H, s, 9-(CH_3)$_2$); δC (100 MHz, $CDCl_3$, 24 °C): 156.7, 155.2, 150.1 (Ar-C_3), 141.7 (*C*H), 135.0, 131.1 (Ar-C_2), 129.5 & 127.0 (2, 7-*C*), 126.6, 126.2, 125.1 (Ar-C_3), 117.9 & 117.2 (1, 3-*C*), 46.3 (9-*H*), 43.8 (N(CH_3)$_2$), 27.7 (9-(CH_3)$_2$); ν_{max}/cm^{-1} 2957, 2860, 1623, 1582, 1545, 1500, 1481, 1332, 1259, 1090, 985, 969, 799, 732; *HRMS* (ESI) calcd for $C_{19}H_{21}N_2O_2$ ($[M+H]^+$): 309.1603, found: 309.1594.

Preparation of 3-Benzoyl-3-nitro-1,2,3,4-tetrahydro-1,8,8-trimethyl-8H-fluoreno[4,5-bcd]azocine, 3.24.

Dimethylamino aldehyde **3.14** (55 mg, 0.21 mmol) was dissolved in anhydrous MeOH (10 mL). Benzoyl nitromethane (69 mg, 0.42 mmol) and ethylenediamine diacetate (5 mg, 0.03 mmol) were added and the solution was refluxed for 4h. The solvent was removed *in vacuo* to yield a crude yellow oil which was purified by flash column chromatography (5:95 EtOAc:petrol 40-60), to give **3.24** as an orange solid (65 mg, 76%), m.p. 172-175℃. δH (400 MHz, $CDCl_3$, 24 °C): 7.87 (2H, dd, J = 8.2, 0.91 Hz, *ortho*-Ph-*H*), 7.65 (1H, t, J = 7.8 Hz, *para*-Ph-*H*), 7.51 (2H, t, J = 7.8 Hz, *meta*-Ph-*H*), 7.20-7.30 (2H, m, 7-, 10-*H*), 6.98 (1H, dd, J = 7.3, 0.9 Hz, Ar-*H*), 6.95 (1H, t, J = 7.3 Hz, 6-*H*), 6.83 (1H, d, J = 8.2 Hz, Ar-*H*), 6.30 (1H, dd, J = 7.8, 0.9 Hz, 5-*H*), 4.89 (1H, d, J = 13.3 Hz, 2-*H*), 4.60 (1H, d, J = 16.0 Hz, 4-*H*), 3.90 (1H, dd, J = 16.0, 2.3 Hz, 4-*H*), 3.60 (1H, dd, J = 13.3, 2.3 Hz, 2-*H*), 2.81 (3H, s, NCH_3), 1.44 (3H, s, 8-C(CH_3)), 1.40 (3H, s, 8-C(CH_3)); δC (100 MHz, $CDCl_3$, 24 °C): 189.4 (C=O), 156.8 (8a-*C*), 153.5 (7a-*C*), 148.4 (11a-*C*), 139.9 (Ar-C_1), 134.1 (*p*-Ph-*C*), 129.7 (6-*C*), 129.2 (*m*-Ph-*C*), 128.7 (Ar-C_1), 128.6 (*o*-Ph-*C*), 128.5 (Ar-C_1), 126.5 (6-*C*), 126.4, 126.0, 120.0, 114.3, 112.3

(Ar-*C*$_5$), 94.0 (3-*C*), 62.6 (2-*C*), 46.4 (8-*C*), 39.7 (N*C*H$_3$), 38.2 (4-*C*), 28.1 & 27.5 (8-C(*C*H$_3$)$_2$); ν_{max}/cm^{-1} 2980, 2821, 1686 (C=O), 1533, 1485, 1444, 1425, 1321, 1269, 1241, 1200, 1179, 1159, 1000, 922, 786, 728, 695; *HRMS* (ESI) calcd for $C_{26}H_{25}N_2O_3$ ([M+H]$^+$): 413.1865, found: 413.1854.

Preparation of 3-Nitro-1,2,3,4-tetrahydro-1,8,8-trimethyl-8H-fluoreno[4,5-bcd]azocine, 3.25.

Recrystallisation of the fused azocine **3.24** from a DCM/hexanes solution gave two separate crystal types. Separation of the two crystal systems under a microscope gave two samples; the first the starting azocine **3.24** and the second a decomposition product **3.25** as pale yellow plates, m.p. 115-118℃. δH (400 MHz, $CDCl_3$, 24 °C): 7.33 (1H, d, J = 7.1 Hz, Ar-*H*$_1$), 7.25 (1H, t, J = 7.8 Hz, Ar-*H*$_1$), 7.21 (1H, t, J = 7.6 Hz, Ar-*H*$_1$), 7.08 (1H, d, J = 6.8 Hz, Ar-*H*$_1$), 6.96 (1H, dd, J = 7.3, 0.9 Hz, Ar-*H*$_1$), 6.81 (1H, d, J = 7.9 Hz, Ar-*H*$_1$), 4.60-4.70 (1H, m, 4-*H*), 4.38 (1H, t, J = 12.6 Hz, 3-*H*), 3.85-4.08 (2H, m, 2-*H*$_2$), 3.10-3.16 (1H, m, 4-*H*), 2.86 (3H, s, NCH$_3$), 1.44 (6H, d, J = 8.6 Hz, 8-C(C*H*$_3$)$_2$); δC (100 MHz, $CDCl_3$, 24 °C): 156.8, 153.6 (Ar-*C*$_2$), 148.6 (11a-*C*), 139.8, 129.9, 128.6, 128.5, 126.8, 121.8, 121.7, 114.1, 112.4 (Ar-*C*$_9$), 83.0 (3-*C*), 57.9 (2-*C*), 46.4 (8-*C*), 39.8 (N*C*H$_3$), 34.2 (4-*C*), 28.2 & 27.5 (9-C(*C*H$_3$)$_2$); ν_{max}/cm^{-1} 2957, 2862, 1584, 1537, 1474, 1454, 1438, 1358, 1269, 1177, 984, 793, 730; *HRMS* (ESI) calcd for $C_{19}H_{21}N_2O_2$ ([M+H]$^+$): 309.1603, found: 309.1595.

Preparation of 1',2,2,8',8'-Pentamethyl-1',2',3',4'-tetrahydro-8'H-spiro[1,3-dioxane-5,3'-fluoreno[4,5-bcd]azocine]-4,6-dione, 3.26.

Dimethylamino aldehyde **3.14** (143 mg, 0.54 mmol) was dissolved in anhydrous MeOH (10 mL). Meldrum's acid (109 mg, 0.76 mmol) and ethylenediamine diacetate (9 mg, 0.05 mmol) were added and the reaction was heated to reflux for 5h, with a precipitate forming after 15mins. The precipitate was filtered, washed with cold MeOH and dried *in vacuo* to give **3.26** as a pale yellow solid (150 mg, 71%), m.p. 204-207℃. δH (400 MHz, ACETONE-d_6, 24 °C): 7.34 (1H, d, J = 7.8 Hz, 7'-*H*), 7.20 (1H,t, J = 8.2 Hz, 10'-*H*), 7.12 (1H, t, J = 7.8 Hz, 6'-*H*), 7.00 (1H, d, J = 7.3 Hz, 9'-*H*), 6.94 (1H, d, J = 7.3 Hz, 5'-*H*), 6.87 (1H, d, J = 8.2 Hz, 11'-*H*), 4.51 (1H, d, J = 13.3 Hz, 4'-*H*), 4.12 (1H, d, J = 15.1 Hz, 2'-*H*), 3.71 (1H, d, J = 15.6 Hz, 4'-*H*), 3.04 (1H, d, J = 13.7 Hz, 2'-*H*), 2.96 (3H, s, NCH_3), 1.81 (6H, m, 2-(CH_3)$_2$), 1.39 (6H, m, 8-(CH_3)$_2$); δC (100 MHz, ACETONE-d_6, 24 °C): 168.9 & 166.2 (C=O), 156.6, 152.9, 148.9, 139.4 (Ar-C_4), 131.5 (5'-*C*), 129.7 (Ar-C_1), 128.4 (10'-*C*), 126.2 (Ar-C_1), 126.1 (6'-*C*), 121.4 (7'-*C*), 114.0 (9'-*C*), 112.7 (11'-*C*), 105.0 (3'-*C*), 60.8 (2'-*C*), 50.1 (2-*C*), 45.8 (8'-*C*), 40.3 (N*C*H$_3$), 39.1 (4'-*C*), 28.6 & 28.3 (2-(*C*H$_3$)$_2$), 27.8 & 27.0 (8'-(*C*H$_3$)$_2$); ν_{max}/cm^{-1} 2965, 2868, 1778, 1735 (C=O), 1571, 1477, 1436, 1379, 1278, 1258, 1198, 1026, 948, 795, 740; Found: C, 73.49; H, 6.36; N, 3.86%. Calc. for $C_{24}H_{25}NO_4$: C, 73.57; H, 6.39; N, 3.58%.

Preparation of 1',2,2,8',8'-Pentamethyl-1',2',3',4'-tetrahydro-8'H-spiro[cyclopentane-1,3'-fluoreno[4,5-bcd]azocine]-2,5-dione, 3.27.

Dimethylamino aldehyde **3.14** (100 mg, 0.38 mmol) was dissolved in anhydrous DMSO (10 mL) under nitrogen and 1,3-cyclopentandione (44 mg, 0.45 mmol) was added. The deep orange

solution was stirred at room temperature. After 24h, the solution was diluted with water (15 mL) and extracted with EtOAc (3 x 20 mL). The combined organics were washed with brine (1 x 20 mL), dried over $MgSO_4$ and filtered. The solvent was removed *in vacuo* to yield a crude brown oil which was purified by flash column chromatography (10:90 EtOAc:petrol 40-60), to give **3.27** as an orange solid (53 mg, 41%), m.p. 60-63℃. δH (400 MHz, $CDCl_3$, 24 °C): 7.30 (1H, d, J = 7.3 Hz, 7'-*H*), 7.23 (1H,t, J = 7.8 Hz, 10'-*H*), 7.12 (1H, t, J = 7.3 Hz, 6'-*H*), 6.95 (1H, d, J = 7.8 Hz, 9'-*H*), 6.85 (1H, d, J = 8.2 Hz, 5'-*H*), 6.77 (1H, d, J = 7.3 Hz, 11'-*H*), 4.26 (1H, d, J = 13.7 Hz, 4-*H*), 3.86 (1H, d, J = 15.1 Hz, 2-*H*), 3.16 (1H, dd, J = 13.1, 1.4 Hz, 4-*H*), 3.02 (3H, s, NCH_3), 2.75-2.90 (4H, m, 3-, 4-H_2), 2.57 (1H, d, J = 13.7, 1.9 Hz, 2-*H*), 1.47 (3H, s, 8-C(CH_3)), 1.40 (3H, s, 8-C(CH_3)); δC (100 MHz, $CDCl_3$, 24 °C): 215.3 & 212.0 (C=O), 156.7, 153.3, 148.7, 139.8 (Ar-C_4), 130.7 (5'-*C*), 128.9 (Ar-C_1), 128.3 (10'-*C*), 126.7 (Ar-C_1), 126.1 (6'-*C*), 121.6 (7'-*C*), 113.8 (9'-*C*), 112.6 (11'-*C*), 57.8 (3'-*C*), 57.1 (2'-*C*), 46.2 (8'-*C*), 40.4 (N*C*H_3), 37.7 (4'-*C*), 36.1 & 35.1 (3-, 4-*C*), 28.2 & 27.7 (9-(*C*H_3)$_2$); ν_{max}/cm^{-1} 2957, 2920, 2862, 1714 (C=O), 1584, 1485, 1442, 1420, 1280, 1168, 1153, 1129, 987, 907, 790, 728; Found: C, 71.91; H, 6.30; N, 3.67%. Calc. for $C_{23}H_{23}NO_2$: C, 79.94; H, 6.66; N, 4.06%.

Preparation of 6-(dimethylamino)-1,2-dihydroacenaphthylene-5-carbaldehyde, 3.37.

Bromo amine **3.36** (0.5 g, 1.81 mmol) was dissolved in anhydrous THF (15 mL) under nitrogen and cooled to -78℃. *n*-BuLi (1.6M in hexanes, 1.7 mL, 2.72 mmol) was steadily added, and the deep red solution was stirred at -78℃ for 3h. Anhydrous DMF (0.28 mL, 3.62 mmol) was added and the reaction was allowed to warm to room temperature. After 16 h. the resulting orange solution was quenched with H_2O (10 mL) and stirred for 10 min. The aqueous solution was washed with EtOAc (3 x 30 mL) and the combined organic layers were washed with H_2O

(40 mL), brine (40 mL) and dried over $MgSO_4$. The solvent was removed *in vacuo* to give a crude deep orange oil which was purified by flash column chromatography (5:95 EtOAc/petrol 40-60), to give **3.37** as an orange solid (226 mg, 55%), m.p. 96-99℃. δH (400 MHz, $CDCl_3$, 24 °C): 11.38 (1H, s, CHO), 8.06 (1H, d, J = 7.3 Hz, 4-*H*), 7.32 (1H, d, J = 7.3 Hz, 3-*H*), 7.24-7.28 (2H, m, 7-, 8-*H*), 3.34-3.38 (4H, m, 1-, 2-*H*), 2.76 (6H, s, $N(CH_3)_2$); δC (100 MHz, $CDCl_3$, 24 °C): 195.7 (C=O), 153.6, 148.1, 141.9, 141.4, 131.3 (Ar-C_5), 129.2 (4-*C*), 126.5, 120.2, 119.7, 119.4 (Ar-C_4), 45.1 ($N(CH_3)_2$), 31.1 & 29.8 (1, 2-*C*); ν_{max}/cm^{-1} 2819, 2773, 1660 (C=O), 1600, 1578, 1500, 1444, 1392, 1332, 1308, 1205, 1185, 1144, 1114, 1049, 961, 840, 821, 773, 657; Found: C, 79.85; H, 6.79; N, 6.18%. Calc. for $C_{15}H_{15}NO$: C, 79.97; H, 6.71; N, 6.22%

Preparation of 3-cyano-(6'-(dimethylamino)-1',2'-dihydroacenaphthylen-5'-yl)propenenitrile, 3.38.

Dimethylamino aldehyde **3.37** (100 mg, 0.44 mmol) was dissolved in anhydrous MeOH (15 mL). Malononitrile (44 mg, 0.67 mmol) and ethylenediamine diacetate (8 mg, 0.04 mmol) were added and the deep orange solution was heated to reflux for 2h. The solvent was removed *in vacuo* to yield a crude dark orange solid which was purified by flash column chromatography (1:4 EtOAc:petrol 40-60), to give **3.38** as an orange solid (110 mg, 91%), m.p. 123-126℃. δH (400 MHz, $CDCl_3$, 24 °C): 9.43 (1H, s, 1-*H*), 7.85 (1H, d, J = 7.3 Hz, 4'-*H*), 7.28 - 7.37 (3H, m, 3'-, 7'-, 8'-*H*), 3.36-3.42 (4H, m, 1'-, 2'-*H*), 2.71 (6H, s, $N(CH_3)_2$); δC (100 MHz, $CDCl_3$, 24 °C): 164.6 (1-*C*), 153.4, 147.6, 142.7, 140.9 (Ar-C_4), 130.0 (4'-*C*), 126.1, 124.3, 121.2, 120.8, 119.3 (Ar-C_5), 114.4 & 113.0 (2 x *C*≡N), 79.5 (2-C), 45.4 ($N(CH_3)_2$), 31.0 & 29.7 (1'-, 2'-*C*); ν_{max}/cm^{-1} 2827, 2786, 2221 (C≡N), 1553, 1496, 1474, 1438, 1416, 1362, 1319, 1297,

1274, 1218, 1151, 1088, 1041, 961, 890, 840, 777, 752; Found: C, 78.82; H, 5.70; N, 15.37%. Calc. for $C_{18}H_{15}N_3$: C, 79.10; H, 5.53; N, 15.37%.

Preparation of methyl (E)-2-cyano-3-(6'-(dimethylamino)-1',2'-dihydroacenaphthylen-5'-yl)propenoate, 3.39.

Dimethylamino aldehyde **3.37** (100 mg, 0.44 mmol) was dissolved in anhydrous MeOH (10 mL). Methyl cyanoacetate (0.12 mL, 1.33 mmol) and ethylenediamine diacetate (8 mg, 0.04 mmol) were added and the deep orange solution was heated to reflux for 16h. The solvent was removed *in vacuo* to yield a crude dark orange solid which was purified by flash column chromatography (1:4 EtOAc:petrol 40-60), to give **3.39** as an orange solid (120 mg, 88%), m.p. 82-85℃. δH (400 MHz, $CDCl_3$, 24 °C): 9.31 (1H, s, 1-*H*), 7.93 (1H, d, J = 7.3, 0.7 Hz, 4'-*H*), 7.30 (1H, d, J = 7.3 Hz, 3'-*H*), 7.25-7.28 (2H, m, 7'-, 8'-*H*), 3.95 (3H, s, OCH_3), 3.35-3.45 (4H, m, 1'-, 2'-*H*), 2.70 (6H, s, N(CH_3)$_2$); δC (100 MHz, $CDCl_3$, 24 °C): 163.9 (*C*=O), 160.7 (1-*C*), 152.1 (2a'-*C*), 148.2 (6'-*C*), 142.5 (8a'-*C*), 141.2 (5'-*C*), 130.0 (4'-*C*), 127.0 (5a'-*C*), 125.4 (2a''-*C*), 120.7 & 120.6 (7'-, 8'-*C*), 119.5 (3'-*C*), 116.1 (*C*≡N), 100.3 (2-C), 53.1 (O*C*H_3), 45.8 (N(*C*H_3)$_2$), 31.0 & 29.9 (1'-, 2'-*C*); ν_{max}/cm^{-1} 2922, 2849, 2825, 2786, 2223 (C≡N), 1727 (C=O), 1589, 1436, 1263, 1246, 1209, 1088, 957, 842, 829, 764, 751; *HRMS* (ESI) calcd for $C_{19}H_{19}N_2O_2$ ([M+H]$^+$): 307.1440, found: 307.1447.

Preparation of 1',2',3',4'-Tetrahydro-1',2,2-trimethyl-spiro[1,3-dioxane-5,3'-acenaphth[5,6-bc]azepine]-4,6-dione, 3.40.

Dimethylamino aldehyde **3.37** (120 mg, 0.53 mmol) was dissolved in anhydrous DMSO (10 mL) under nitrogen and Meldrum's acid (115 mg, 0.8 mmol) was added. The deep orange solution was stirred at room temperature. After 24h, a precipitate had formed which was collected via filtration and dried under vacuum to give **3.40** as a yellow solid (150 mg, 80%), m.p. 198-201℃. δH (400 MHz, $CDCl_3$, 24 °C): 7.08-7.14 (2H, m, 6'-, 9'-*H*), 6.99 (1H, d, J = 6.9 Hz, 5'-*H*), 6.75 (1H, d, J = 7.3 Hz, 10'-*H*), 3.70-3.90 (4H, m, 2'-, 4'-H_2), 3.25-3.35 (4H, m, 8'-, 7'-H_2), 3.08 (3H, s, NCH_3), 1.86 (3H, s, 2-CH_3), 1.75 (3H, s, 2-CH_3); δC (100 MHz, $CDCl_3$, *24* °C): 169.0 (C=O), 148.4, 145.5, 141.2, 137.9, 129.0 (Ar-C_5), 128.2 (5'-*C*), 124.7 (Ar-C_1), 119.5 & 119.1 (6'-, 9'-*C*), 110.3 (10'-*C*), 104.9 (2-*C*), 63.6 (3'-*C*), 55.3 (2'-*C*), 41.5 (4'-*C*), 40.8 (N*C*H_3), 30.5 & 29.6 (7'-,8'-*C*), 29.4 & 29.0 (2-*C*H_3); ν_{max}/cm^{-1} 1772, 1735 (C=O), 1589, 1502, 1472, 1448, 1422, 1388, 1295, 1276, 1239, 1176, 1151, 1129, 1101, 1082, 1030, 941, 913, 820, 777; Found: C, 71.65; H, 5.99; N, 4.05%. Calc. for $C_{21}H_{21}NO_4$: C, 71.72; H, 5.98; N, 3.98%.

Preparation of 1',2',3',4'-Tetrahydro-1',2,2-trimethyl-spiro[cyclohexan-1,3'-acenaphth[5,6-bc]azepine]-2,6-dione, 3.41.

Dimethylamino aldehyde **3.37** (100 mg, 0.44 mmol) was dissolved in anhydrous DMSO (10 mL) under nitrogen and 1,3-cyclohexanedione (88 mg, 0.79 mmol) was added, and the deep orange solution was stirred at room temperature. After 24h, H_2O (20 mL) was added to produce a pale orange precipitate. The precipitate was collected via filtration and dried under vacuum

to give **3.41** as a pale orange solid (84 mg, 59%), m.p. Decomp, > 155℃. δH (400 MHz, $CDCl_3$, 24 °C): 7.08 (1H, d, J = 7.8 Hz, 9'-*H*), 7.04 (1H, d, J = 6.9 Hz, 6'-*H*), 6.94 (1H, d, J = 6.9 Hz, 5'-*H*), 6.78 (1H, d, J = 7.8 Hz, 10'-*H*), 3.63-3.72 (4H, m, 2'-, 4'-H_2), 3.22-3.33 (4H, m, 7'-, 8'-H_2), 3.03 (3H, s, NCH_3), 2.62-3.00 (4H, m, 3-, 5-H_2), 2.10-2.25 (1H, m, 4-*H*), 1.75-1.89 (1H, m, 4-*H*); δC (100 MHz, $CDCl_3$, 24 °C): 207.5 (C=O), 149.6, 145.4, 141.2, 137.1, 129.4 (Ar-C_5), 127.0 (5'-*C*), 125.3 (Ar-C_1), 119.4 & 119.3 (6'-, 9'-*C*), 109.9 (10'-*C*), 73.7 (3'-*C*), 57.8 (2'-*C*), 40.8 (4'-*C*), 40.6 (NCH_3), 37.9 (3-, 5-*C*), 30.7 & 29.7 (7', 8'-*C*), 18.5 (4-*C*); ν_{max}/cm^{-1} 1718, 1684 (C=O), 1593, 1504, 1470, 1431, 1317, 1272, 1190, 1108, 1079, 1004, 834, 767; Found: C, 78.90; H, 6.65; N, 4.37%. Calc. for $C_{21}H_{21}NO_2$: C, 78.90; H, 6.58; N, 4.38%.

Preparation of 1',2',3',4'-Tetrahydro-1',2,2-trimethyl-spiro[cyclopentan-1,3'-acenaphth[5,6-bc]azepine]-2,5-dione, 3.42.

Dimethylamino aldehyde **3.37** (100 mg, 0.44 mmol) was dissolved in anhydrous DMSO (10 mL) under nitrogen and 1,3-cyclopentanedione (65 mg, 0.67 mmol) was added. The deep orange solution was stirred at room temperature. After 24h, H_2O (20 mL) was added to produce a pale orange precipitate. The precipitate was dissolved by the addition of DCM (30 mL) and the organic layer separated. The aqueous solution was extracted further with DCM (2 x 30 mL). The combined organics were washed with H_2O (30 mL) and brine (30 mL), dried over $MgSO_4$ and filtered. The solvent was removed *in vacuo* to give a crude orange solid which was purified by flash column chromatography (1:2 EtOAc:petrol 40-60), to give **3.42** as an off-white solid (54 mg, 40%), m.p. 180-183℃. δH (400 MHz, $CDCl_3$, 24 °C): 7.06-7.10 (2H, m, 6'-, 9'-*H*), 6.91 (1H, d, J = 6.9 Hz, 5'-*H*), 6.72 (1H, d, J = 7.3 Hz, 10'-*H*), 3.35-3.45 (4H, m, 2'-, 4'-H_2), 3.25-3.34 (4H, m, 7'-, 8'-*H*), 3.04 (3H, s, NCH_3), 2.90-2.98 (2H, m, 3-, 4-H_2), 2.68-2.76 (2H,

m, 3-, 4-*H*$_2$); δC (100 MHz, $CDCl_3$, 24 °C): 213.7 (C=O), 148.8, 145.5, 141.3, 137.7, 129.0 (Ar-*C*$_5$), 127.8 (5'-*C*), 125.1 (Ar-*C*$_1$), 119.4 & 119.3 (6'-, 9'-*C*), 110.5 (10'-*C*), 63.7 (3'-*C*), 59.2 (2'-*C*), 41.3 (N*C*H_3), 39.1 (4'-*C*), 34.9 (3-, 4-*C*), 30.7 & 29.7 (7'-, 8'-*C*) ; ν_{max}/cm^{-1} 2917, 1707 (C=O), 1591, 1502, 1470, 1416, 1285, 1271, 1149, 1101, 1077, 1037, 1000, 943, 834, 805, 766; *HRMS* (ESI) calcd for $C_{20}H_{20}NO_2$ ($[M+H]^+$): 306.1494, found: 306.1486.

Preparation of methyl (E)-2-cyano-3-(8'-(dimethylamino)naphthalen-1'-yl)propenoate, 3.43.

1-Dimethylamino-8-naphthaldehyde **3.19** (400 mg, 2.01 mmol), methyl cyanoacetate (0.35 mL, 4.02 mmol) and ethylenediamine diacetate (18 mg, 0.10 mmol) were dissolved in anhydrous methanol (10 mL) under nitrogen and refluxed for 16h. The solvent was removed *in vacuo* and the residual crude oil was triturated with diethyl ether, giving a yellow precipitate. The solid was collected by filtration and washed with diethyl ether (3 x 20 mL) and dried to give **3.43** as a yellow solid (300 mg, 53%), m.p. 100-103℃. δH (400 MHz, $CDCl_3$, 24 °C): 9.21 (1H, s, 1-*H*), 7.90 (1H, dd, J = 6.9, 2.7 Hz, Ar-*H*$_1$), 7.67 (1H, d, J = 7.8 Hz, Ar-*H*$_1$), 7.45-7.55 (3H, m, Ar-*H*$_3$), 7.35 (1H, d, J = 7.3 Hz, Ar-*H*$_1$), 3.94 (3H, s, OC*H*$_3$), 2.63 (6H, s, N(C*H*$_3$)$_2$); δC (100 MHz, $CDCl_3$, 24 °C): 164.3 (*C*=O), 161.7 (1-*C*), 150.2 (8'-*C*), 135.3, 130.9, 130.3, 129.9 (Ar-*C*$_4$), 127.3 (2'-*C*), 126.9, 126.1, 125.5, 119.7 (Ar-*C*$_4$), 115.9 (C≡N), 96.1 (2-*C*), 53.0 (O*C*H_3), 45.4 (N(*C*H_3)$_2$); ν_{max}/cm^{-1} 3047, 2994, 2950, 2857, 2829, 2788, 2223 (C≡N), 1718 (C=O), 1574, 1438, 1403, 1377, 1340, 1256, 1205, 1185, 1155, 1086, 1045, 1019, 890, 833, 769, 739; *HRMS* (ESI) calcd for $C_{17}H_{17}N_2O_2$ ($[M+H]^+$): 281.1290, found: 281.1284.

Crystal Data

*Table 3.23. Crystallographic data for the fluorene derivatives **3.16**, **3.14**, **3.21**, **3.25** and **3.26**.*

	3.16	**3.14**	**3.21**	**3.25**	**3.26**
Formula	$C_{15}H_{12}I_2$	$C_{18}H_{19}NO$	$C_{21}H_{19}N_3$	$C_{19}H_{20}N_2O_2$	$C_{24}H_{25}NO_4$
Formula weight	446.05	265.34	313.39	308.37	391.45
Crystal system	Monoclinic	Tetragonal	Monoclinic	Monoclinic	Monoclinic
Space group	$P2_1/c$	$I4_1cd$	$I2/a$	$P2_1$	$P2_1/n$
***a*[Å]**	8.4109(2)	24.7956(1)	18.4256(4)	9.7431(3)	10.9539(3)
***b*[Å]**	9.6735(3)	24.7956(1)	11.2921(3)	6.9459(2)	9.5493(3)
***c*[Å]**	17.0655(5)	9.4744(1)	16.4939(4)	12.1403(4)	19.3902(6)
α[°]	90	90	90	90	90
β [°]	90.496(2)	90	99.223(2)	105.257(4)	104.652(3)
γ[°]	90	90	90	90	90
***V* [Å^3]**	1388.45(7)	5825.07(8)	3387.42(14)	792.63(4)	1962.30(11)
Z	4	16	8	2	4
ρ [g cm^{-3}]	2.134	1.210	1.229	1.292	1.325
***T* [*K*]**	150.01(10)	149.99(10)	150.00(10)	150.01(10)	150.00(10)
λ (Å)	0.71073	1.54184	0.71073	0.71073	0.71073
μ (mm^{-1})	4.506	0.579	0.074	0.085	0.090
unique refl.	6967	13777	8045	8479	9504
Refl, I > 2σI	2837	2152	3936	3165	4532
***R*$_1$**	0.0289	0.0314	0.0478	0.0462	0.0510
***wR*$_2$**	0.0646	0.0796	0.1108	0.0935	0.1030
$\Delta\rho$(r) [e Å^{-3}]	0.96/-0.53	0.13/-0.17	0.29/-0.23	0.20/-0.20	0.28/-0.23
Crystallisation Solvent	EtOAc/Petrol (40-60)	CH_2Cl_2/*n*-hexane	$CDCl_3$/*n*-hexane	CH_2Cl_2/*n*-hexane	$(CH_3)_2CO$

*Table 3.24. Crystallographic data for the acenaphthene derivatives **3.37**, **3.38**, **3.39**, **3.40**, **3.41**, **3.42** and **3.44**.*

	3.37	**3.38**	**3.39**	**3.40**	**3.41**	**3.42**	**3.43**
Formula	$C_{15}H_{15}NO$	$C_{18}H_{15}N_3$	$C_{19}H_{18}N_2O_2$	$C_{21}H_{21}NO_4$	$C_{21}H_{21}NO_2$	$C_{20}H_{19}NO_2$	$C_{17}H_{16}N_2O_2$
Formula weight	225.28	273.33	306.35	351.39	319.39	305.36	280.32
Crystal system	Monoclinic	Triclinic	Triclinic	Monoclinic	Monoclinic	Monoclinic	Triclinic
Space group	$P2_1/c$	P-1	P-1	$P2_1/n$	$P2_1/c$	$P2_1/c$	P-1
***a*[Å]**	9.1836(6)	9.8149(4)	8.7457(5)	10.4254(3)	15.2740(6)	10.7625(5)	8.6964(8)
***b*[Å]**	9.4806(5)	9.9853(4)	9.3638(7)	8.8249(2)	10.3218(4)	32.3176(10)	9.2214(7)
***c*[Å]**	13.2584(8)	15.1587(6)	11.2739(7)	18.7794(6)	10.2175(3)	8.6130(3)	10.4886(8)
α[°]	90	84.234(3)	108.887(6)	90	90	90	102.971(7)
β [°]	99.767(7)	78.977(4)	91.171(5)	101.547(3)	93.356(3)	98.945(4)	101.832(7)
γ[°]	90	80.518(3)	113.671(6)	90	90	90	113.041(8)
***V* [Å^3]**	1137.62(12)	1434.64(10)	787.91(10)	1692.79(8)	1608.08(10)	2959.3(2)	712.90(11)
Z	4	4	2	4	4	8	2
ρ [g cm^{-3}]	1.315	1.265	1.291	1.379	1.319	1.371	1.306
***T* [*K*]**	150.01(10)	150.00(10)	150.01(10)	150.01(10)	150.00(10)	150.01(10)	150.01(10)
λ (Å)	0.71073	0.71073	0.71073	0.71073	0.71073	0.71073	0.71073
μ (mm^{-1})	0.082	0.077	0.085	0.096	0.084	0.088	0.087
unique refl.	4702	11593	7276	7469	6553	14496	8910
Refl, I > 2σI	2341	5911	3915	3498	3311	6829	3523
***R*$_1$**	0.0487	0.0575	0.0506	0.0478	0.0514	0.1040	0.0472
***wR*$_2$**	0.1057	0.1157	0.1229	0.0956	0.1005	0.1877	0.1024
$\Delta\rho$(r) [e Å^{-3}]	0.21/-0.21	0.23/-0.25	0.30/-0.21	0.21/-0.21	0.18/-0.26	0.53/-0.29	0.27/-0.22
Crystallisation Solvent	$CDCl_3$	CH_3OH	CH_2Cl_2/*n*-hexane	CH_2Cl_2/*n*-hexane	CH_2Cl_2/*n*-hexane	CH_2Cl_2/*n*-hexane	Et_2O

References

1 G. Charbonneau and Y. Delugeard, *Acta Crystallogr.*, 1976, **32**, 1420–1423.

2 R. E. Gerkin, A. P. Lundstedt and W. J. Reppart, *Acta Crystallogr.*, 1984, **40**, 1892–1894.

3 J. Oddershede and S. Larsen, *J. Phys. Chem.* 2004, **108**, 1057–1063.

4 A. C. Hazell, R. G. Hazell and L. Norskov-Lauritsen, *Acta Crystallogr.*, 1986, **42**, 690–693.

5 J. O'Leary and J. D. Wallis, *Org. Biomol. Chem.*, 2009, **7**, 225–228.

6 P. C. Bell and J. D. Wallis, *Chem. Commun.*, 1999, **2**, 257–258.

7 A. Lari, M. B. Pitak, S. J. Coles, G. J. Rees, S. P. Day, M. E. Smith, J. V. Hanna and J. D. Wallis, *Org. Biomol. Chem.*, 2012, **10**, 7763–7779.

8 R. Cosmo, T. W. Hambley and S. Sternhell, *J. Org. Chem.*, 1987, **52**, 3119–3123.

9 N. Lardiés, I. Romeo, E. Cerrada, M. Laguna and P. J. Skabara, *Dalton Trans.*, 2007, 5329–5338.

10 V. D. B. Bonifácio, J. Morgado and U. Scherf, *Synlett*, 2010, 1333–1336.

11 A. Bondi, *J. Phys. Chem.*, 1964, **68**, 441–451.

12 K. Grudzień, K. Żukowska, M. Malińska, K. Woźniak and M. Barbasiewicz, *Chem. A Eur. J.*, 2014, **20**, 2819–2828.

13 J. O'Leary, J. D. Wallis and M. L. Wood, *Acta Crystallogr.*, 2001, **57**, 851–853.

14 Á. Földi, K. Ludányi, A. Bényei and P. Mátyus, *Synlett*, 2010, 2109–2113.

15 Á. Polonka-Bálint, C. Saraceno, K. Ludányi, A. Bényei and P. Mátyus, *Synlett*, 2008, 2846–2850.

16 P. Mátyus, O. Éliás, P. Tapolcsányi, Á. Polonka-Bálint and B. Halász-Dajka, *Synthesis*, 2006, 2625–2639.

17 A. Y. Platonova, T. V. Glukhareva, O. A. Zimovets and Y. Y. Morzherin, *Chem. Heterocycl. Compd.*, 2013, **49**, 357–385.

18 L. Liu, C. Zhang and J. Zhao, *Dalton Trans.*, 2014, **43**, 13434–13444.

19 D. Pla, O. Sadek, S. Cadet, B. Mestre-Voegtlé and E. Gras, *Dalton Trans.*, 2015, **44**, 18340–18346.

20 D. R. W. Hodgson, A. J. Kirby and N. Feeder, *J. Chem. Soc. Perkin Trans. 1*, 1999, 949–954.

21 P. C. Bell, M. Drameh, N. Hanly and J. D. Wallis, *Acta Crystallogr.*, 2000, **56**, 670–671.

22 J. O'Leary, X. Formosa, W. Skranc and J. D. Wallis, *Org. Biomol. Chem.*, 2005, **3**, 3273–3283.

Chapter 4

Structural Models to Investigate the Effect of *Peri*-repulsions on the Opposing *Peri*-interaction in a Series of Naphthalenes

Introduction

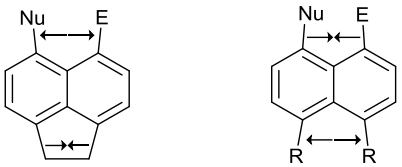

Figure 4.70.Generalised structures demonstrating the pulling (left) and pushing (right) capabilities of peri-substituents.

Previously (Chapter 3), the installation of a short ethylene bridge between the second set of *peri*-positions on a naphthalene scaffold, has been shown to impose a large effect on the interaction that occurs between a nucleophile (NMe_2) and an electrophilic centre (e.g. aldehyde, electron deficient alkenes) at the opposing *peri*-positions (Figure 4.1). In short, the ethylene bridge causes a widening of the opposite *exo*-angle and increases the distance between the interacting groups. If the ethylene bridge is substituted for two sterically bulky substituents the opposite effect should be observed as a result of a *peri*-steric repulsion between them. However, considerations of which substituents are chosen must be made. Figure 4.2 shows naphthalene (**4.1**)[1] and four *peri*-disubstituted derivatives (**4.2-4.5**)[2,3] which possess either aliphatic or aromatic substituents. Each structure was obtained from the Cambridge Structural Database (CSD) and some key geometric features have been summarised in Table 4.1.

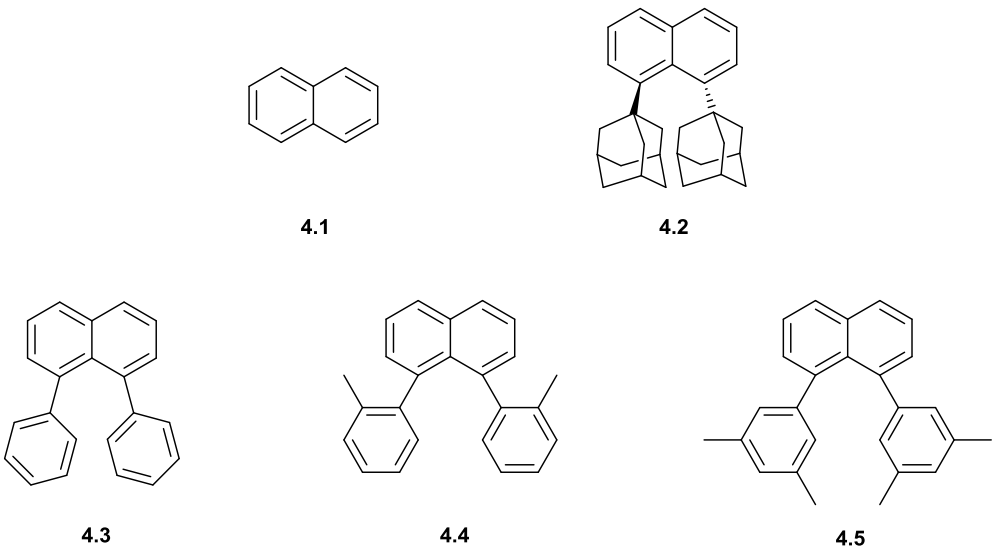

*Figure 4.71. Naphthalene **4.1**[1] and four examples of peri-disubstituted naphthalenes **4.2-4.5**.[2,3]*

*Table 4.25. Selected geometric details for the five naphthalene derivatives **4.1-4.5***

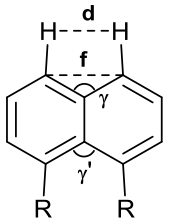

Compound	**d** / Å	**f** / Å	**γ / γ' / º**	**τ[a] / º**
4.1	2.446	2.475	121.7/121.7	-
4.2	2.460	2.458(4)	120.9(2)/129.0(2)	71.6(2)
4.3	2.420	2.447(5)	119.6(3)/125.6(3)	3.4(3)
4.4	2.409	2.439(6)	119.0(3)/125.6(2)	0.3(2)
4.5	2.402	2.439(2)	118.7(1)/125.9(1)	10.9(1)

τ[a] = torsion angle: C-C(*peri*)-C(*peri*)-C.

Naphthalene (as discussed in Chapter 1) as a control molecule, displays a *peri*-naphthalene C---C distance of 2.475 Å, an *exo*-cyclic angle at the point of ring fusion (γ/γ') of 121.7º and a *peri*-hydrogen H---H separation of 2.446 Å. Substitution at one set of the *peri*-groups with very bulky adamantane substituents (**4.2**) results in a very large repulsion. Unfortunately, instead of repelling each other whilst remaining in a plane close to that of the naphthalene scaffold, the groups swing like pendulums in opposite directions perpendicular to it (Figure 4.3). This displacement of the groups to either side of the plane results in a highly distorted naphthalene ring, with a C-C(*peri*)-C(*peri*)-C torsion angle (τ^a) of 71.6(2)º. Despite the significantly widened *exo*-cyclic angle between the substituents (129.0(2)º) the expected narrowing at the opposite angle (120.9(2)º) is not observed as a result of the naphthalene plane distortion. Thus, *peri* C---C and H---H separations are found to be 2.458(4) and 2.460 Å respectively, only marginally shorter than naphthalene **4.1** itself. The groups to be chosen are therefore required to partially reduce the steric repulsions by in-plane displacements, which was not possible with adamantane as a result of its consistent uniform spatial diameter.

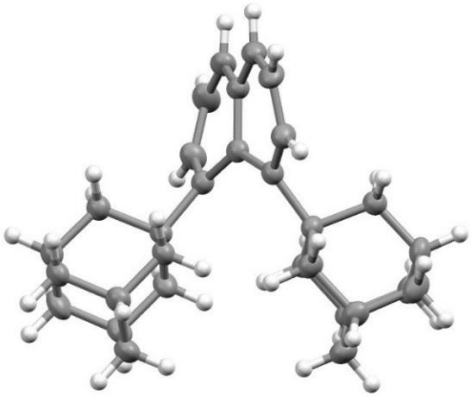

*Figure 4.72. Molecular structure of the di(1-adamantyl)naphthalene **4.2**.[3]*

Flat aromatic groups, such as those observed in **4.3-4.5,** can fulfil this whilst also possessing significant steric bulk to cause a repulsion. The diphenyl substituted naphthalene **4.3** demonstrates an *exo*-cyclic angle adjacent to the phenyl rings of 125.6(5)^{o}, causing a narrowing of the opposite *exo*-angle to 119.6(3)^{o}. This results in shorter *peri* H---H and C---C contacts of 2.420 and 2.447(5) Å with the naphthalene backbone remaining very close to planar, unlike the adamantane derivative **4.2**. The phenyl rings are rotated to lie at 67-68^{o} to the idealised naphthalene plane in order to maximise the π-π stacking between the two rings. The closest contact between the rings is the *ipso* C---C contact of 2.977(5) Å, with the rings gradually pulled further and further apart due to the widened *exo*-cyclic angle between them. The two rings are not rotated in order to minimalise the H---H between the *ortho*-naphthalene and *ortho*-phenyl protons. The use of aromatic rings also allows modifications to be made at varying positions as demonstrated in **4.4** and **4.5**, where methyl groups are present at one of the *ortho*-positions (**4.4**) and the two *meta*-positions (**4.5**) of each phenyl ring. The *ortho*-substituted naphthalene **4.4** crystallises in the *syn*-conformer with the same cofacial stacking and rotation observed between the two phenyl rings. The presence of the *ortho*-methyl groups results in a marginal increase in the *exo*-cyclic angle between the rings leading to decreased contact distances between the opposite *peri*-hydrogen and carbon atoms. The same effect is observed for the *meta*-substituted derivative **4.5**, however despite the further increase in steric repulsion

between the two rings, the *exo*-angle is only marginally increased (125.9(1)^{o}). This is due to the naphthalene skeleton twisting from its planar conformation like the adamantane derivative **4.2**, however to a much lesser extent, with a torsion angle (τ^{a}) of 10.9(1)^{o}. Negation of the steric repulsion in this fashion leads to the opposite *peri*-carbon and hydrogen atoms displaying contact distances similar to the *ortho*-substituted derivative **4.4**. Overall, substitution of one set of *peri*-positions with aromatic systems, causes a significant reduction in the contact distances observed in the opposite *peri*-positions. Increasing the steric bulk of these aromatic systems extends this effect to a critical point, at which the naphthalene skeleton begins to distort, negating the desired effect.

We herein describe the design and synthesis of a series of 4, 5-diphenyl-1, 8-disubstituted naphthalenes. Throughout, the nucleophile will remain constant (dimethylamino), whilst the electron deficient substituent will be varied from an aldehyde to a range of electron deficient alkenes. In each case, the molecular structure, determined by single crystal X-ray diffraction, will be utilised to analyse the effect of the repulsion between the *peri*-phenyl rings and to determine whether a reduction in the interaction distance has occurred and whether it can lead to the formation of long N-C bonds in alkene derivatives where previously, only N---C interactions were observed.

Synthesis and Structural Discussion of 4,5-Diphenyl-1,8-disubstituted Naphthalenes

In order to explore these desired effects, the dimethylamino aldehyde **4.10** was prepared in four steps (Scheme 4.1). From this aldehyde a series of Knoevenagel condensation products could be synthesised to give a range alkenes of differing electrophilicities. Following a literature procedure, a double Suzuki-Miyaura coupling of 1, 8-dibromonaphthalene **4.6** with phenyl boronic acid[4] was performed to give the fluorescent diphenylnaphthalene **4.7**. The stirring of **4.7** in a concentrated nitric acid/DCM solution resulted in the *mono*-nitrated diphenylnaphthalene **4.8** as described by House *et al.*[5] Following the general methods described by Pla *et al*,[6] the nitrated naphthalene **4.8** was reduced using Fe/$FeCl_3$ in acetic acid and subsequently *N*-dimethylated *in situ* to give the desired 1-dimethylamino 4, 5-diphenylnaphthalene **4.9** as a pale brown solid in 89% yield.

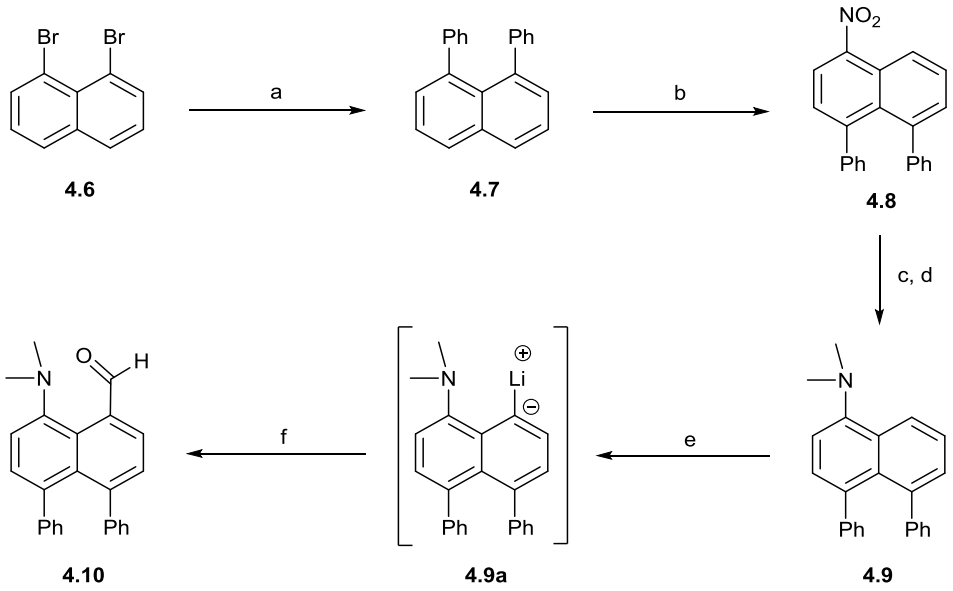

Scheme 4.28.(a) Phenyl boronic acid, $Pd(OAc)_2$ (10 mol%), K_2CO_3, H_2O, DMF, 100 °C;[4] (b) Conc. HNO_3, DCM, 25 °C;[5] (c) Fe, $FeCl_3$, AcOH, EtOH, 100 °C;[6] (d) MeI, K_2CO_3, CH_3CN, 50 °C;[6] (e) n-BuLi (2.5M), THF, 80 °C; (f) DMF, THF, -78 to 25 °C.

The structure of dimethylamino derivative **4.9** was confirmed by the introduction of a six proton singlet at 2.99 ppm in the ^1H NMR and a corresponding ^{13}C NMR peak at 45.5 ppm. Furthermore, crystals of **4.9** were obtained by slow evaporation of a hexane solution and the

X-ray structure determined at 150 K. As shown in Figure 4.4 and Table 4.2, the two phenyl rings of the amine **4.9** are twisted in the same direction at angles of 56.7(2) and 60.2(2)^{o} to the idealised naphthalene plane but are splayed apart by *ca.* 10^{o}. A repulsion between the rings results in a widening of the nearby *exo*-angle (γ') at the fusion of the naphthalene rings to 124.8(1)^{o}, with the opposite *exo*-angle (γ) narrowing to 119.4(2)^{o}. This generates a C---C distance between the latter *peri*-naphthalene carbons to either side of the *exo*-angle (γ) of 2.464(2) Å. In addition, the naphthalene plane itself is twisted slightly from its preferred planar conformation, with a torsion angle of 13.8(1)^{o} between the *ipso*-C---*peri*-C bonds. In order to maximise conjugation of the nitrogen lone pair into the aromatic ring, the *N*-methyl groups are positioned at -23.9(2) and 105.1(2)^{o} with respect to the C1-C2 naphthalene ring bond. The theoretical axis of the lone pair of the nitrogen atom is positioned at an angle of 41.7^{o} to the N---H vector across the *peri*-positions.

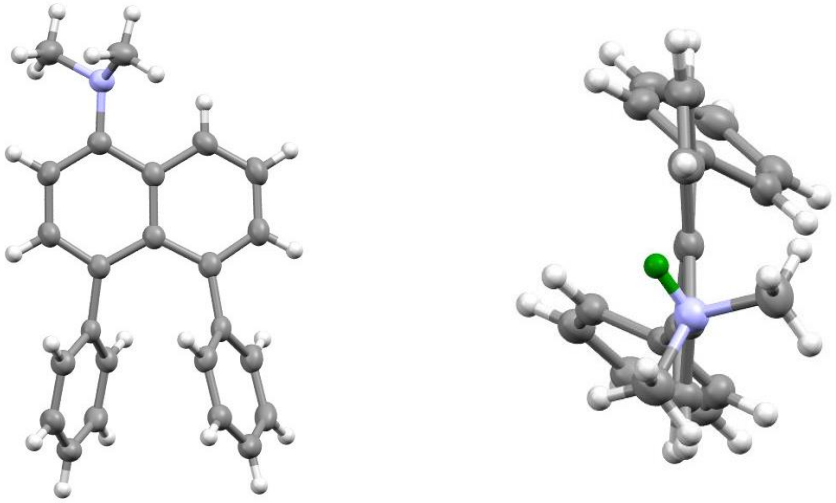

*Figure 4.73. Molecular structures of dimethylamino naphthalene **4.9** (left) and the orientation of the nitrogen lone pair (green) relative to the peri N---H vector (right).*

The dimethylamino naphthalene **4.9** was successfully *peri*-lithiated with an excess of *n*-butyl lithium in refluxing *n*-hexane, which over the course of several days resulted in the formation of a grey precipitate of the lithiated salt **4.9a.** The supernatant, including excess *n*-butyl lithium, was removed by syringe and the reaction diluted with THF and cooled to -78 ^{o}C before an

excess of DMF was added. This resulted in the desired dimethylamino aldehyde **4.10** in a 34% yield as an off-white solid. The synthesis of dimethylamino aldehyde **4.10** was evidenced by the aldehyde peaks at 10.38 ppm, 186.7 ppm and 1638 cm^{-1} in the ^{1}H NMR, ^{13}C NMR and infrared spectra respectively. Slow evaporation from an ethyl acetate solution resulted in suitable 'fin' shaped crystals of aldehyde **4.10**, and their X-ray structure was determined at 150 K (Figure 4.5). Selected geometric data are shown in Table 4.2.

*Table 4.26. Selected geometric details of dimethylamino naphthalene **4.9** and naphthaldehydes **4.10** and **4.11**.[7]*

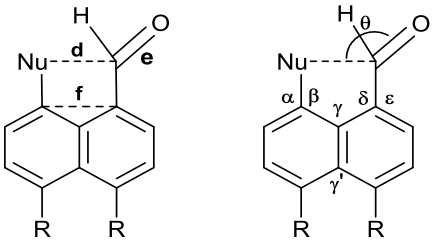

Compound	**d** / Å	**e** / Å	**f** / Å	**θ** / º	**τ^a / º**	**τ^b / º**
4.9	-	-	2.464(2)	-	-23.9(2)/105.1(2)	-
4.10 (R = Ph)	2.309(3)	1.216(3)	2.434(4)	112.6(2)	-51.6(3)/78.0(3)	-58.9(3)
4.11[7] **(R = H)**	2.489(6)	1.213(5)	2.479(6)	113.5(3)	44.5(5)/-85.2(5)	57.3(5)

Compound	**α** / º	**β** / º	**δ** / º	**ε** / º	**γ / γ' / º**
4.9	123.2(1)	117.7(1)	-[c]	-[c]	119.4(2)/124.8(1)
4.10 (R = Ph)	124.8(2)	114.8(2)	121.7(2)	118.1(2)	117.5(2)/126.1(2)
4.11[7] **(R = H)**	124.3(4)	116.0(3)	122.2(4)	119.2(3)	120.6(3)/121.5(4)

τ^a = torsion angle: 2 x (H_3)C-N-C-C(H), **τ^b** = torsion angle: O=C-C-C(H).
[c]Note: no bond angles for C-C-H due to riding model.

The two *peri*-phenyl rings in aldehyde **4.10** are tilted at 54.1(3) and 59.0(3)º in the same sense from the best naphthalene plane. The groups are splayed apart by *ca.* 9º at each phenyl group. As expected, the nearby *exo*-angle is widened to 126.1(2)º with the opposing *exo*-angle narrowing to 117.5(2)º, making the difference between the angles 3.2º larger than that observed in the dimethylamino diphenylnaphthalene **4.9** and 7.7º larger than that in the corresponding naphthalene derivative with no phenyl substituents **4.11**. Similarly, a decrease in the C---C distance between the interacting *peri*-naphthalene carbons is observed, from 2.479(6) Å and 2.464(2) Å in **4.11** and **4.9** to 2.434(4) Å in **4.10**. The decrease in C---C distance and *exo*-angle in the dimethylamino-diphenylnaphthalene **4.9** compared to the dimethylamino aldehyde **4.10**,

is assisted by the Me_2N---CHO attractive interaction between the two *peri*-groups. This results in an Me_2N---C=O contact distance of 2.309(3) Å, significantly shorter than in the corresponding compound without phenyl groups **4.9** (2.489(6) Å) and well within the sum of the two atoms' Van der Waals radii (3.2 Å).[8] Despite the shorter contact, the orientation of the aldehyde carbonyl and N-methyl groups with respect to the naphthalene plane (τ^a and τ^b) and the angle of approach of the dimethylamino group towards the aldehyde carbonyl (θ) remain similar to the analogue without the phenyl groups **4.11**. Furthermore, even with a 0.18 Å reduction in the N---C contact distance, the length of the carbonyl bond remains almost identical to that of the unsubstituted analogue **4.11**. It is notable too that the aldehyde group in **4.10** has a notably lower carbonyl stretching frequency (1638 cm^{-1}) than in **4.11** (1658 cm^{-1}). The interacting *peri*-atoms of **4.10** deviate to opposite side of the idealised naphthalene plane by 0.06 Å (NMe_2) and 0.20 Å (CHO). The main cause of the decreased Me_2N---C=O separation is the change in the *exo*-cyclic angle between the groups. The pattern of in-plane displacements of the *peri*-groups in **4.10** and **4.11** are very similar.

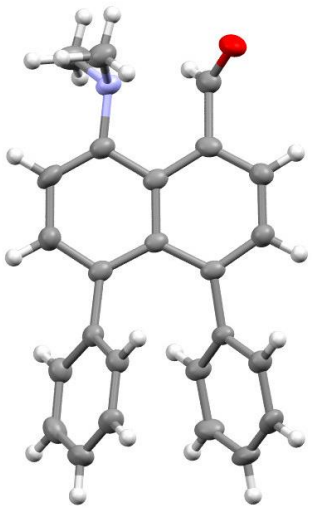

*Figure 4.74. Molecular structure of dimethylamino aldehyde **4.10**.*

Previously, Wallis *et al.*[9] have demonstrated how 8-(dimethylamino)-1-naphthaldehyde **4.11** can undergo O-protonation or acylation to form long N-C bonds between the *peri*-substituents, resulting in a salt. In order to determine the effect of the two phenyl substituents on such N-C bonds, the methodology of Wallis *et al.* was applied to aldehyde **4.10**.

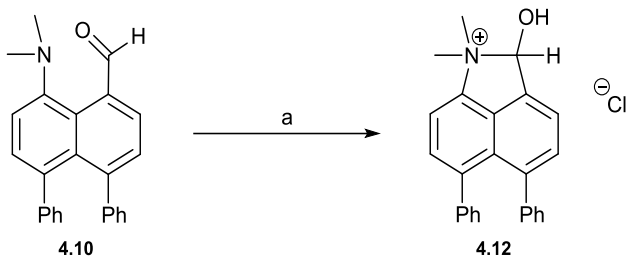

4.10 **4.12**

Scheme 4.29. (a) Ethereal HCl (1M), Et_2O, RT.

The chloride salt **4.12** was generated via the careful addition of a 1M ethereal HCl solution to a stirred solution of diphenyl aldehyde **4.10** in diethyl ether (Scheme 4.2). Immediately, an off-white precipitate formed which was collected via filtration under a nitrogen stream, due to the hygroscopic nature of the salt, in 74% yield. The structure of the closed chloride salt **4.12** was confirmed by the shift of the former aldehyde signals in the ^{1}H and ^{13}C NMR spectra to 7.31 and 110.5 ppm. Moreover, a splitting of the N-methyl protons into two singlets for three protons each confirms the N-C bond formation and removal of the free rotation for the NMe_2 group. This unusual chemistry is similar to the chemistry of a carboxylic amide, however, the electron density required by the carbonyl group is obtained via a 'through space' rather than a 'through bond' donation from the *peri*-dimethylamino group. Despite the hygroscopic nature of **4.12**, crystals for structural determination were grown via slow evaporation from a DCM solution and structural data determined for the DCM solvate at 150 K (Figure 4.7).

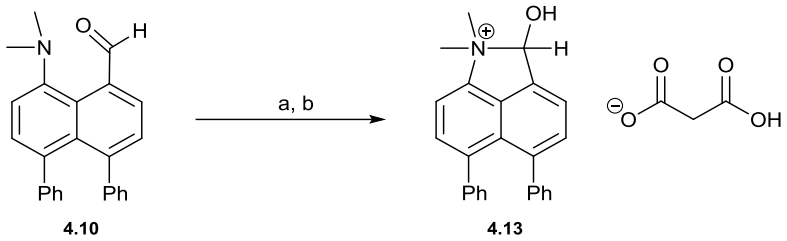

Scheme 4.30. (a) Meldrum's acid, MeOH; (b) Et_2O.

Fortuitously, another salt of the cation **4.13** was also isolated when attempting to perform a Knoevenagel condensation of diphenyl aldehyde **4.10** with Meldrum's acid (Scheme 4.3). Initially, the reaction appeared to have proceeded as expected, with an off-white precipitate collected from the reaction, however NMR analysis confirmed no peaks corresponding to either the two methyl groups of the Meldrum's acid or the expected vinylic proton. Slow evaporation of an EtOAc/DCM solution of the precipitate afforded crystals of **4.13**. X-ray crystal structure determination at 150 K of one of these crystals revealed that instead of forming the expected alkene derivative, the acidic protons of the methylene group had protonated the aldehyde. This resulted in the formation of a long N-C bond, with the counterion being identified as 2-carboxy acetate, a decomposition product of Meldrum's acid (Figure 4.7). Selected geometric data for both aminal salts **4.12** and **4.13** are shown in Table 4.3.

*Table 4.27. Selected geometric details of naphthaldehyde **4.10** and aminal salts **4.12-4.14**.*

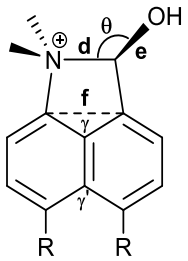

Compound	**d** / Å	**e** / Å	**f** / Å	**N-CH$_3$** / Å	**θ** / °	**γ / γ' / º**	**τ^a / º**
4.10	2.309(3)	1.216(3)	2.434(4)	1.459(3)/1.464(3)	112.6(2)	117.5(2)/126.1(2)	-9.8(2)
4.12 (R = Ph)	1.617(5)	1.360(4)	2.311(6)	1.491(5)/1.499(5)	111.3(3)	111.6(3)/130.0(3)	7.7(4)
4.13 (R = Ph)	1.621(2)	1.363(2)	2.317(3)	1.487(3)/1.499(2)	110.9(2)	112.1(3)/130.3(4)	12.0(2)
4.14[9] **(R = H)**	1.638(2)	1.353(2)	2.332(2)	1.497(2)/1.498(2)	111.6(1)	113.9(2)/128.3(2)	7.1(2)

τ^a = torsion angle: C(Ar)-N(+)-C-C(Ar).

For the diphenyl substituted chloride salt **4.12** an N-C bond of 1.617(5) Å has formed between the *peri*-groups. The aminal C-O bond of 1.360(4) Å, lies as an intermediate between the expected lengths of a carbonyl group (1.20 Å) and a C-O bond of this type (1.43 Å).[10] Similarly, the 2-carboxy acetate salt **4.13** demonstrates an N-C bond length of 1.621(2) Å and a C-O bond length of 1.363(2) Å. Torsional twists of the *peri*-naphthalene carbons about the N-C bond (τ^a) of 7.7(4)^o and 12.0(2)^o are observed for the two salts **4.12** and **4.13** respectively, a result of the *peri*-atoms displacements to either side of the naphthalene plane. In comparison to Wallis's salt **4.14**, it is clear that the repulsions of the *peri*-phenyl rings in **4.12** and **4.13**, have made for a slightly shorter N-C bond and thus a longer, more established, C-O bond. This is evidenced through the reduced *peri*-naphthalene C---C distances (2.311(6)/2.317(3) Å in **4.12**/**4.13** compared to 2.332(2) Å in **4.14**) and the observable difference in the *exo*-angles of **4.12** and **4.13** compared to those in **4.14**. These structures therefore represent a position further along the nucleophilic attack reaction pathway as a direct consequence of the *peri*-repulsion introduced by the phenyl rings.

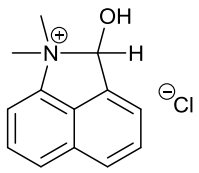

4.14

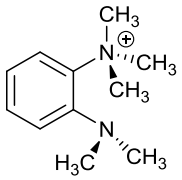

4.15

*Figure 4.75. Structure of aminal chloride salt **4.14**[9] and 1-trimethylamonium-2-dimethylaminobenzene cation **4.15**.[11]*

Salts **4.12** and **4.13** both display N-CH_3 bond lengths in the range of 1.487(3)-1.499(5) Å, very similar not only to the N-CH_3 bonds in Wallis' salt **4.14** (1.497(2)/1.498(2) Å) but also to the $N^+(CH_3)_3$ group of cation **4.15**[11] (1.500 Å) rather than the neutral dimethylamino group (1.465 Å) (Figure 4.6). The hydroxyl group of the diphenyl chloride salt **4.12** is hydrogen bonded to the chloride ion (O---Cl distance: 2.924(4) Å, O-H---Cl angle: 164.7(4)^o). Of the remaining contacts to the chloride, the shortest is to a proton of the DCM solvate. Likewise, in the 2-carboxy acetate salt **4.13**, one carboxylate group is hydrogen bonded intermolecularly to the

hydroxyl group of an aminal moiety (O---O distance: 2.592(2) Å, O-H---O angle: 175.5(4)º). The same carboxylate group also forms an intramolecular hydrogen bond to the well-established carboxylic acid functionality (C=O: 1.204(3) C-O(H): 1.315(3) Å) at the alternate end of the anion (O---O distance: 2.485(2) Å).

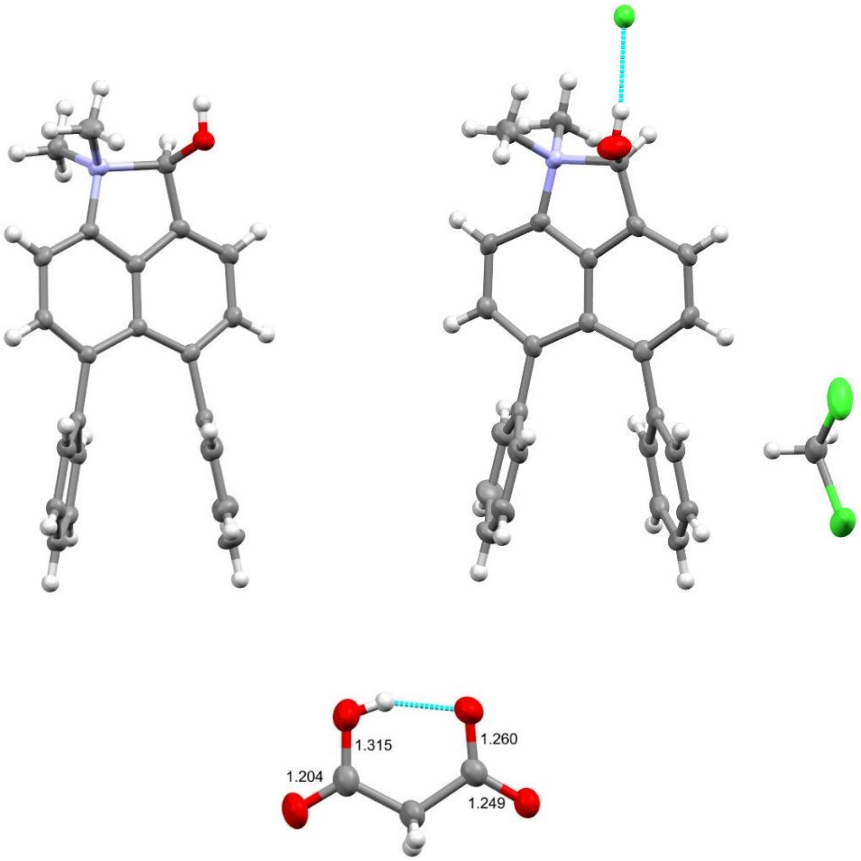

*Figure 4.76. Molecular structure of cation **4.13** (left), the DCM solvate of the chloride salt **4.12** (right) and the 2-carboxy acetate anion (middle) with the different bond lengths labelled.*

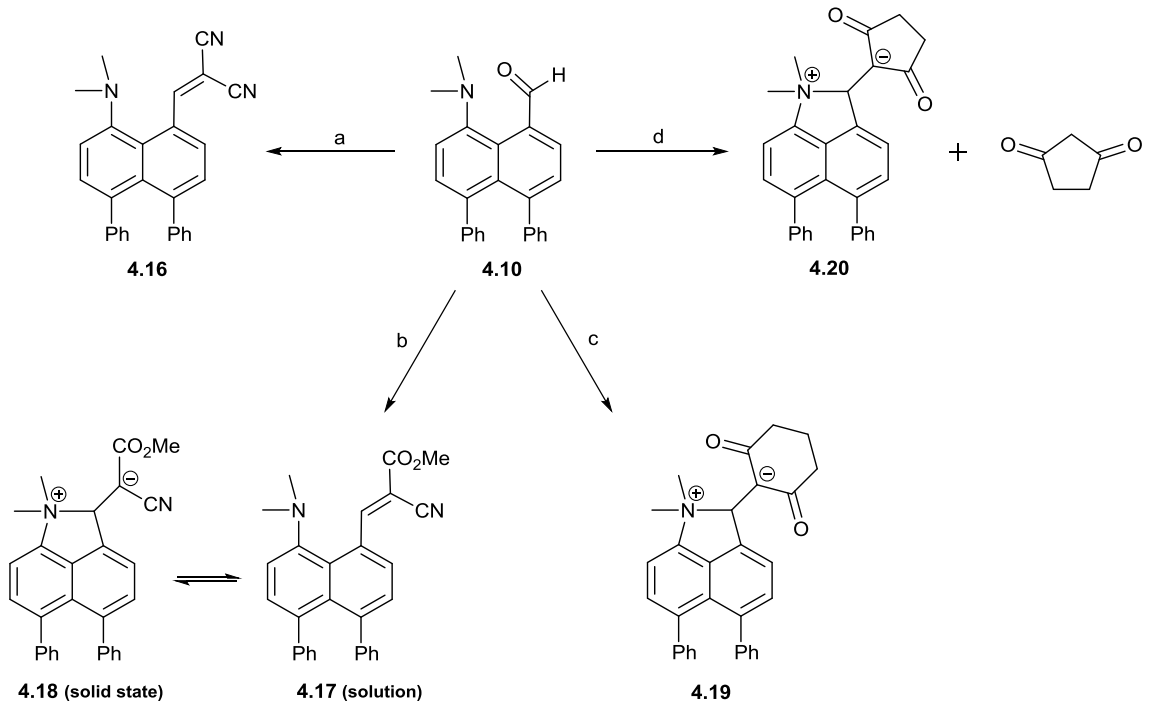

Scheme 4.31. (a) $CH_2(CN)_2$, ($^+NH_3CH_2$-)$_2$($^-OAc)_2$ (cat.), CH_3OH, 65 ^oC; (b) $NCCH_2CO_2Me$, CH_3OH, ($^+NH_3CH_2$-)$_2$($^-OAc)_2$ (cat.), 65 ^oC; (c) Cyclohexa-1,3-dione, CH_3OH, ($^+NH_3CH_2$-)$_2$($^-OAc)_2$ (cat.), 65 ^oC; (d) Cyclopentan-1,3-dione, CH_3OH, ($^+NH_3CH_2$-)$_2$($^-OAc)_2$ (cat.), 65 ^oC

Condensation of the diphenyl dimethylamino aldehyde **4.10** with active methylene compounds malononitrile, methyl cyanoacetate and cyclohexan-1,3-dione (Scheme 4) yielded the expected Knoevenagel condensation products **4.16**, **4.17** and **4.19**. In each case, aldehyde **4.10**, the chosen methylene compound and EDDA (catalyst) were refluxed in methanol for 24 hours, with the alkenes **4.16** and **4.17** being isolated via flash column chromatography, whilst **4.19** was isolated via trituration of the crude product with diethyl ether. Moderate yields of 31% and 53% were observed for **4.19** and **4.16** whilst **4.17** was isolated in a respectable 87% yield. Cyclopentan-1,3-dione performed the expected Knoevenagel condensation under the same conditions (Scheme 4.4) to give product **4.20**, however upon trituration with diethyl ether the desired compound precipitated alongside unreacted cylopentan-1,3-dione. It is important to note that the purification of zwitterionic species, such as **4.19** and **4.20**, cannot be performed via conventional flash column chromatography do to their highly polar nature. Thus, titration with a non-polar solvent (usually diethyl ether or *n*-hexanes) is used. In some cases, trituration

also causes precipitation of unreacted starting materials (especially if they are polar) which results in the mixture observed in Scheme 4.4. Even when the molar ratio of aldehyde **4.10** was increased, making it the limiting reagent, unreacted dione was still present in the precipitate. Moreover, the compound which began as a fine powder, was found to be hygroscopic, quickly becoming an oil under atmospheric conditions. Due to its structural similarity to the cyclohexan-1, 3-dione, the compound was excluded from the investigation.

The 'open-form' structure of dinitrile derivative **4.16** was supported by the ^{1}H NMR signals for the dimethylamino and vinylic protons of 2.82 and 8.45 ppm respectively. ^{13}C NMR shows the expected nitrile signals of 114.6/116.2 ppm, with the alkene carbons residing at 65.5 and 161.3 ppm. The nitrile groups are further evidenced by a peak of 2220 cm^{-1} in the infrared spectrum. Likewise, the 'open-form' structure of methyl cyanoester **4.17** was confirmed by ^{1}H NMR peaks of 2.77 ppm (dimethylamino) and 8.95 ppm (vinyl), ^{13}C NMR peaks of 161.8 ppm (carbonyl), 87.5/156.7 ppm (alkene), 117.4 ppm (nitrile) and 52.7 ppm (methoxy) and infrared peaks of 2167 cm^{-1} (nitrile) and 1638 cm^{-1} (ester carbonyl). As expected, the derivative **4.19** which possesses the most electrophilic alkene of the group, a result of the two in-plane ketones of the cyclohexanedione group, resides in the 'closed-form'. This is validated by the upfield shift of the vinylic proton to 7.13 ppm whilst the dimethylamino protons have shifted downfield to 3.23 and 3.62 ppm in the ^{1}H NMR spectrum. Splitting of the methyl groups of the nucleophile is caused by the fixing of their positions due to the N-C bond formation, with each methyl group now occupying a set and slightly different from each other position on either side of the naphthalene plane. The ^{13}C NMR signal of the N(+)-C bonded carbon is now shifted significantly upfield to 89.8 ppm,[9] whilst the inequivalent ketones of the dione reside at 195.4 and 193.4 ppm.

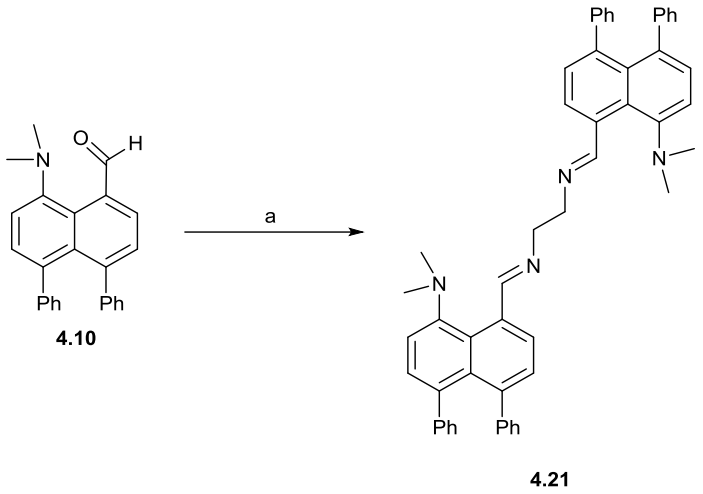

Scheme 4.32. (a) NO_2CH_3, ($^+NH_3CH_2$-)$_2$($^-$OAc)$_2$ (cat.), CH_3OH, RT.

Reaction of the aldehyde **4.10** with active methylene compounds nitromethane, benzoyl nitromethane, dimethyl malonate and dibenzoyl methane (using the same reaction conditions as described for **4.16**-**4.20**) did not yield the expected Knoevenagel products. Both dimethyl malonate and benzoyl nitromethane underwent no observable reaction, with TLC and NMR analysis of the reaction mixture indicating only unreacted starting materials. The addition of extra portions of catalyst and longer heating times still resulted in no reaction. Reactions with nitromethane and dibenzoyl methane in each case demonstrated a faint 'new' spot when analysed via TLC, so the solvent was removed, and the crude mixtures of each reaction triturated with ether yielding a light coloured yellow precipitate in both cases (Scheme 4.5). Isolation of the precipitate via filtration found the yield to be poor with respect to the amount of aldehyde used (e.g. 22 mg from 100 mg of **4.21**) whilst ^{1}H and ^{13}C NMR spectrometry revealed the products to be identical despite the use of different methylene compounds. Crystals of the product **4.21** were obtained from a DCM/hexane solution and the structure determined at 150 K (Figure 4.8). It revealed that the ethylenediamine of the catalyst had reacted with the aldehydes of two separate molecules, forming a bridge capped by two imines (or Schiff bases). This accounted for the low reaction yield, which when recalculated based

upon the moles of catalyst used is found to be 69%. This justified the ^{1}H NMR peaks at 9.27 and 4.05 ppm as the imine and methylene protons of the bridge.

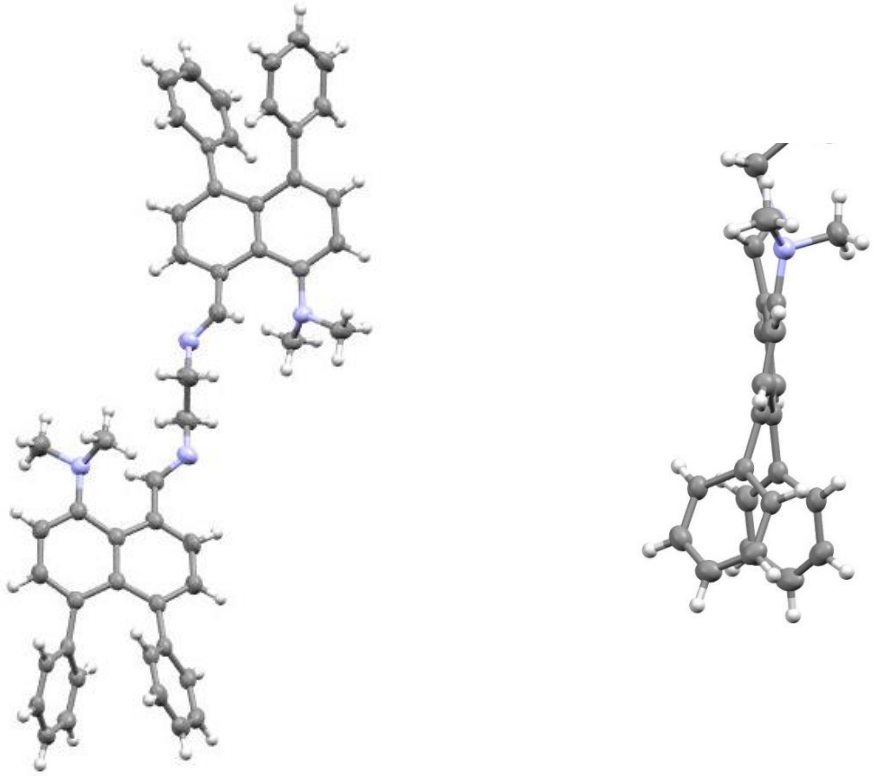

*Figure 4.77. Molecular structure of the bridged di-imine **4.21** (left) and a view demonstrating the peri-bond displacements which twist the naphthalene plane (right).*

The weaker attractive interaction of a dimethylamino group with an imine is displayed by the long N-C contacts of 2.677(3) and 2.711(3) Å in the bridged compound **4.21**. In order to generate this large contact, the groups cannot simply move apart in the plane of the naphthalene ring. If they were to do this, the *exo*-angle between them would widen and consequently cause the opposite *exo*-angle between the opposite two *peri*-phenyl rings to narrow. The steric repulsion between the two rings prevents this, and as a result the naphthalene skeletons are both severely twisted from their idealised planar conformation, splaying the two *peri*-phenyl groups and interacting *peri*-substituents to either side of the naphthalene plane (Figure 4.8). Furthermore, the extent of the distortion to the naphthalene rings is so severe, that the repulsions between the *peri*-phenyl rings are almost negated, with *exo*-angles between the

interacting *peri*-carbons widened slightly to 121.6(2) and 122.0(2)^{o} instead of being forced into closer proximity.

*Table 4.28. Selected geometric details for the substituted dinitrile **4.16** and the unsubstituted analogue **4.22**.*[12]

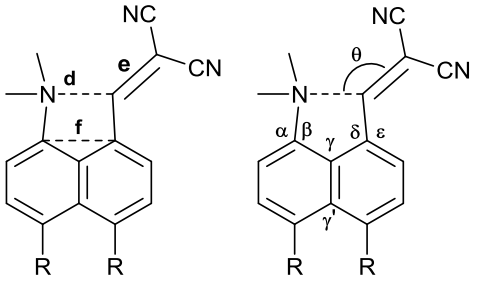

Compound	**d** / Å	**e** / Å	**f** / Å	**θ** / ^{o}	**τ^{a}** / ^{o}	**τ^{b}** / ^{o}
4.16 (R = Ph)	2.359(2)	1.360(3)	2.439(3)	113.8(1)	37.0(3)/-94.9(2)	51.2(3)
4.22[12] **(R = H)**	2.413(2)	1.354(2)	2.463(3)	112.1(1)	-49.7(2)/81.5(2)	-56.5(2)

Compound	**α** / ^{o}	**β** / ^{o}	**δ** / ^{o}	**ε** / ^{o}	**γ / γ'** / ^{o}
4.16 (R = Ph)	124.5(2)	115.4(2)	119.4(2)	119.9(2)	117.7(2)/126.3(2)
4.22[12] **(R = H)**	124.3(2)	115.9(1)	120.2(1)	120.3(2)	120.4(1)/122.6(2)

τ^{a} = torsion angle: 2 x (H_3)C-N-C-C(H), **τ^{b}** = torsion angle: (H)C=C-C(Ar)-C(H).

Slow evaporation of a solution of dinitrile **4.16** in toluene resulting in suitable crystals for X-ray structure determination, which was performed at 100 K (Figure 4.9). Some of the structural features of **4.16** and also the unsubstituted dinitrile derivative **4.22** are shown together in Table 4.4. The crystal grown was found to be a toluene solvate, with a well ordered toluene molecule for every molecule of the dinitrile **4.16** in the asymmetric unit. The *peri*-phenyl rings of **4.16** are rotated, in the same direction, at angles of 61.0(3) and 62.3(2) to the idealised naphthalene plane. This causes the nearby *exo*-angle at the naphthalene ring fusion carbon to widen to 126.3(2)^{o}, with the opposite *exo*-angle narrowing to 117.7(2)^{o}, a difference of 8.6^{o} compared to 2.2^{o} in the equivalent angles of unsubstituted dinitrile **4.22**. The narrowing of the upper *exo*-cyclic angle causes a shortening in the C---C distance between the *peri*-carbons to 2.439(3) Å which in turn contributes to the reduced Me_2N---C contact distance of 2.359(2) Å (compared to C---C 2.463(3) Å and Me_2N---C 2.413(2) Å distances in **4.22**). Within the packing lattice, short contacts between the toluene solvate and dinitrile derivative **4.16** occur, with the shortest

occurring between the 4-*H* proton of the toluene and the nitrogen atom of the *trans* nitrile group (2.64 Å).

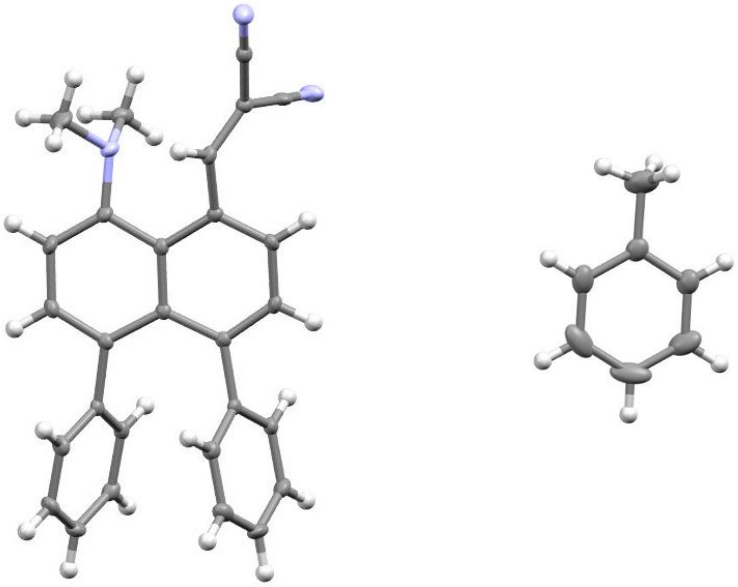

*Figure 4.78. Molecular structure of dinitrile **4.16** (left) and the well order toluene solvate (right).*

The in-plane angular displacements of the dimethylamino group in **4.16** and **4.22** fall within three standard deviations of each other, whilst the displacement of the C-C bond to the *peri*-carbon is more interesting. Conventionally, as the nucleophile approaches the electrophile, the C-C bond is displaced in the same direction, away from the nucleophile. In diphenyl dinitrile **4.16**, the alkene is angled slightly *towards* the dimethylamino group by 0.2° from the symmetrical orientation angle, with the only other example of this shown in the *peri*-hydroxy methyl ketone series where a *t*-butyl bolster *ortho* to the ketone is employed.[13] Unlike the *t*-butyl bolster example, the alkene moiety is not forced into this angle by reducing a steric interaction, indicating the strength of the interaction has increased significantly as the distance has decreased. The two *peri*-substituents of **4.16** deviate to either side of the best naphthalene plane by large distances of 0.250 Å (NMe_2) and 0.495 Å (alkene) compared to that of the unsubstituted dinitrile **4.22** of 0.166 Å (NMe_2) and 0.270 Å (alkene). The alkene is rotated by 51.2(3)° from the naphthalene plane, similar to that in the unsubstituted dinitrile **4.22** (-

56.5(2)°). The N-methyl groups of the nucleophile straddle either side of the naphthalene plane unevenly with torsion angles of 37.0(3) and -94.9(2)° with the ring HC=C bond which causes the axis of the nitrogen lone pair to lie at an angle of 14.2° to the N---C vector, well aligned with the *peri*-carbon of the alkene.

*Table 4.29. Selected geometric details for the ring closed derivatives **4.18** and **4.19**, and the unsubstituted analogues **4.23** and **4.24**.*[9]

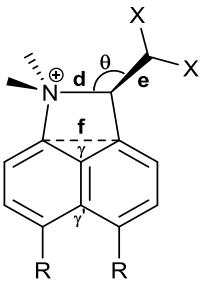

4.18 X = CO_2Me, CN; R = Ph

4.23 X = CO_2Me, CN; R = H

4.19 X = $(C(=O)O)_2CH_2$; R = Ph

4.24 X = $(C(=O)O)_2CH_2$; R = H

Compound	**d** / Å	**e** / Å	**f** / Å	**N-CH$_3$** / Å	**θ** / °	**γ / γ'** / °	**τ^a** / °
4.18	1.672(1)	1.454(1)	2.324(2)	1.490(2)/1.493(2)	115.9(1)	112.3(1)/129.9(1)	18.5(1)
4.23	2.595(2)	1.349(2)	2.503(2)	1.459(2)/1.464(2)	116.2(1)	122.6(1)/121.4(1)	14.1(1)
4.19	1.620(4)	1.484(4)	2.309(5)	1.503(4)/1.496(4)	116.0(3)	111.6(3)/130.0(3)	-12.8(3)
4.24[9]	1.631(2)	1.486(2)	2.338(2)	1.500(2)/1.502(2)	114.0(1)	113.2(1)/128.3(1)	12.1(1)

τ^a = torsion angle: C(Ar)-N(+)-C-C(Ar).

Crystals of the diphenyl methylcyanoester **4.18** were grown by slow evaporation of ethyl acetate solution and the X-ray structure determined at 150 K. The molecular structure of cyanoester **4.18** in the solid state was found in fact to reside in the 'closed-form', despite being in the 'open-form' in solution (Figure 4.10). This was an unexpected result as previously dinitrile alkene derivatives[12] have shown shorter N---C contacts than cyanoester derivatives[14,15], with the only recorded N-C bond formation for either the dinitrile or cyanoester being for the dinitrile derivative in the biphenyl series.[14] The alkene is orientated such that the cyano moiety is *cis* to the naphthalene, as is observed in the unsubstituted 'open-form' structure **4.23**. As expected, the *peri*-phenyl rings of **4.18** are rotated at 61.2(1) and 59.2(1)° in the same direction from the naphthalene plane, with the repulsion between them generating a nearby *exo*-angle of 129.9(1)°. The size of this *exo*-angle is aided somewhat by the formation of the long Me_2N-C bond at the other *peri* position, which gives a strained five-membered ring,

further narrowing the opposite *exo*-cyclic angle to 112.3(1)°. The N-C bond of 1.672(1) Å formed in this case is among the longest observed in studies of this kind, representing a relatively early point during bond formation. The longer N-C bond in **4.18** results in a lower degree of strain in the five-membered ring, thus making the pair of *exo*-angles at the naphthalene deviate the least from their favoured angles (Table 4.5). For example: the shorter N-C bond of cation **4.12** (1.617(5) Å), formed by the protonation of aldehyde **4.10**, displays *exo*-angles of 111.6(3)/130.0(3)° a 0.8° increase in their difference from **4.18**. The lower degree of formation in the N-C bond also causes a C-C bond length of the former alkene bond to sit intermediately between that of an alkane (~1.52 Å) and alkene (~1.34 Å) at a length of 1.454(1) Å. This may be indicative of some donation of electron density from the carbanion back into the anti-bonding orbital of the N-C bond. Both of the H_3C-N bond lengths (1.490(2)/1.493(2) Å) in cyanoester **4.18** are consistent with the $(CH_3)_3N^+$ group[11] in **4.15** rather than the neutral dimethylamino group N-CH_3.

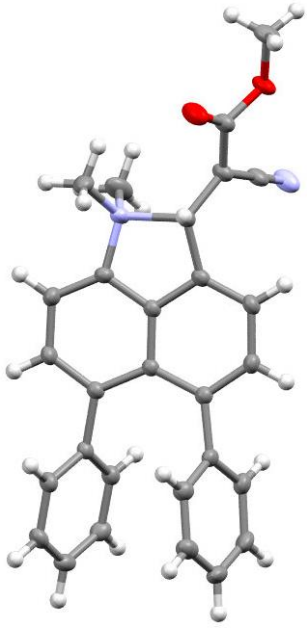

*Figure 4.79. Molecular structure of the ring closed methylcyanoester **4.18**.*

Crystals of the cyclohexanedione derivative **4.19** were grown by slow evaporation of a chloroform solution and the X-ray structure determined at 150 K. The molecular structure of

cyclohexanedione **4.19** is in line with the expected closed form (Figure 4.11). The *peri*-phenyl rings are consistent with the previous examples discussed, displaying rotations of 57.8(5) and 51.6(5)^{o} with respect to the best naphthalene plane, with a resultant nearby *exo*-angle of 130.0(3)^{o}. The long N-C bond formed (1.620(4) Å) at the opposite set of *peri*-positions gives a nearby *exo*-angle of 111.6(3)^{o}, which is smaller than the equivalent angle of the cyanoester **4.18**, further evidencing the relationship between the length of the N-C bond and the resultant strain forced upon the five-membered ring.

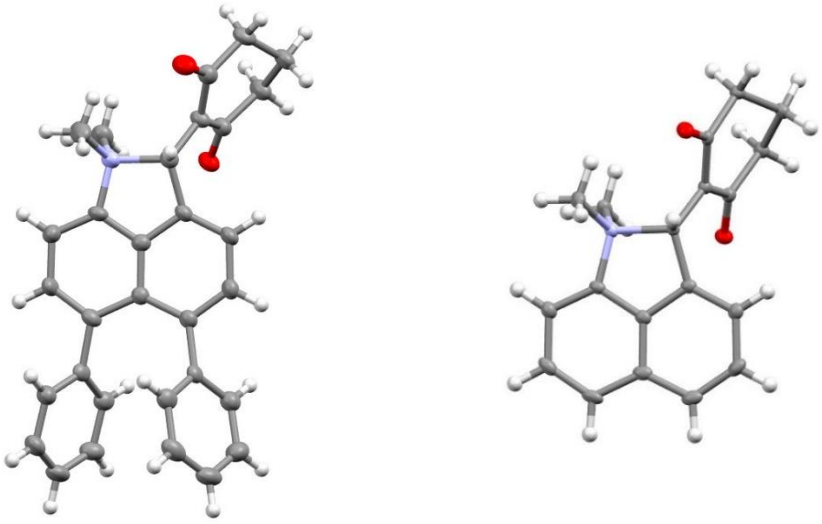

*Figure 4.80. Molecular structures of the phenyl substituted **4.19** (left) and unsubstituted **4.24**[9] (right) ring closed compounds.*

Structurally, the differences between the diphenyl substituted derivative **4.19** and the corresponding unsubstituted compound **4.24** are small, but nevertheless significant and a direct result of the *peri*-phenyl repulsions. For example: the N-C bond has shortened from 1.631(2) Å to 1.620(4) Å in accordance with the noticeable increase in the difference between the *exo*-cyclic angles of the two molecules (18.4^{o} in **4.19** compared to 15.1^{o} in **4.24**) and a noticeable difference in the C---C distance between the *peri*-carbons of the interaction groups (2.309(5) Å in **4.19** vs. 2.338(2) Å in **4.24**) is also observed. Compared to the cyanoester derivative **4.18**, the N-C bond is shorter (1.620(4) Å **4.19** vs. 1.672(1) Å **4.18**) and the C-C bond to the

carbanionic centre longer, in accord with a greater degree of N-C bond formation and π bond breaking.

To conclude, a series of 4, 5-diphenyl-1, 8-disubstituted naphthalenes have been synthesised that yielded some expected and unexpected results. The phenyl repulsion in all cases allowed for a marked increase in the difference between naphthalene *exo*-angles, a decrease in the *peri*-naphthalene C---C distance and a reduction in the contact distance between the nucleophilic dimethylamino group and the electrophilic substituent. The significantly long N-C bond formed in the cyanoester **4.18** demonstrates all of the above, producing a structure which represents an early point during bond formation following nucleophilic attack. The partially formed bond in **4.18** is also demonstrated in the aldehyde salts **4.12** and **4.13** and the cyclohexanedione derivative **4.19**, which all show N-C bonds that are long in comparison to a fully formed bond of its type[10], but slightly shorter than their equivalents without the two phenyl rings. Substitution of the phenyl rings for more sterically hindered derivatives, such as those shown in **4.4** and **4.5**, could further demonstrate the influence that a *peri*-repulsion can have on the opposite set of *peri*-positions, potentially forming long N-C bonds in examples where we have demonstrated significantly short contacts (2.309(3) Å and 2.359(2) Å in aldehyde and dinitrile derivatives **4.10** and **4.16**).

Experimental

General. Solution NMR spectra were measured on a Jeol ECLIPSE 400 ECX or ECZ spectrometer at 400 MHz for ^{1}H and at 100.6 MHz for ^{13}C using $CDCl_3$ as solvent and tetramethylsilane (TMS) as standard unless otherwise stated, and measured in p.p.m. downfield from TMS with coupling constants reported in Hz. IR spectra were recorded on a Perkin Elmer Spectrum 100 FT-IR Spectrometer using Attenuated Total Reflection sampling on solids or oils and are reported in cm^{-1}. Mass spectra were recorded at the EPSRC Mass Spectrometry Centre at the University of Swansea. Chemical analysis data were obtained from Mr Stephen Boyer, London Metropolitan University.

Preparation of N,N-dimethyl-4,5-diphenylnaphthalen-1-amine, 4.9.

The following method is adapted from the works of Pla *et al.* [6]

1-Nitro-4,5-diphenylnaphthalene **4.8**[5] (1.00 g, 3.08 mmol), was dissolved in ethanol (100 mL), acetic acid (10 mL) added and the reaction was heated to 100 ^{o}C. Iron powder (1.98 g, 35.38 mmol) and iron chloride (0.40 g, 2.46 mmol) were added and the reaction heated at 100 ^{o}C for a further 3h. The reaction was cooled, the solvent was removed *in vacuo* and the resultant brown oil was dissolved in DMF (100 mL). The solution was stirred for 10min before being filtered through Celite and concentrated *in vacuo* to give a crude brown oil. Acetonitrile (100 mL) and potassium carbonate (2.55 g, 18.46 mmol) were added to the crude oil and the reaction was heated to 50 ^{o}C for 1h. Iodomethane (1.15 mL, 18.46 mmol) was added and heating was continued for 16h. The reaction was cooled, diluted with Et_2O (100 mL) and filtered through a small plug of silica gel, eluting with further portions of Et_2O. The solvent was removed *in*

vacuo yielding a crude brown oil which was purified by flash column chromatography (40:1 hexane:diethyl ether) to give product **4.9** as a pale brown solid (0.89 g, 89%), m.p. 51-54 ^{o}C. δH (400 MHz, $CDCl_3$, 24 °C): 8.44 (1H, dd, J = 8.5, 1.3 Hz, 8-*H*), 7.55 (1H, dd, J = 8.5, 7.0 Hz, 7-*H*), 7.42 (1H, dd, J = 7.0, 1.5 Hz, 6-*H*), 7.34 (1H, d, J = 7.8 Hz, 3-*H*), 7.21 (1H, d, J = 7.8 Hz, 2-*H*), 6.83-7.05 (10H, m, Ar-H_{10}), 2.99 (6H, s, N(CH_3)$_2$); δC (100 MHz, $CDCl_3$, 24 °C): 150.7 (1-*C*), 143.5, 143.4, 140.7, 135.3 (Ar-C_4), 130.9 & 130.8 (3-, 6-*C*), 130.6, 130.4 (Ar-C_2), 130.0, 129.8, 127.1, 127.0 (Meta/Ortho-C_4), 125.6, 125.3 (Para-C_2), 124.4 (7-*C*), 124.1 (8-*C*), 113.7 (2-*C*), 45.5 (N(CH_3)$_2$); ν_{max}/cm^{-1} 3055, 3023, 2937, 1570, 1491, 1441, 1401, 1319, 1193, 1168, 1139, 1072, 952, 908, 826, 773, 695; Found: C, 89.02; H, 6.58; N, 4.39%. Calc. for $C_{24}H_{21}N$: C, 89.12; H, 6.54; N, 4.33%.

Preparation of 8-(dimethylamino)-4,5-diphenyl-1-naphthaldehyde, 4.10.

Dimethylamino naphthalene **4.9** (700 mg, 2.17 mmol), dry hexane (20 mL) and *n*-BuLi (2.5M in hexanes, 3.50 mL, 8.68 mmol) were stirred heated to 80 ^{o}C and the mixture refluxed for 72 h, resulting in the formation of a grey precipitate. The precipitate was cooled to room temperature, allowed to settle and the supernatant removed. Tetrahydrofuran (20 mL) was added and the reaction mixture was cooled to -78 ^{o}C before anhydrous DMF (1.34 mL, 17.36 mmol) was added dropwise. The reaction was stirred for a further 18 h at room temperature. The reaction was quenched with a few drops of methanol, diluted with water (100 ml) and extracted with dichloromethane (3 x 50 mL). The combined organic layer was washed with brine (50 mL), dried over anhydrous $MgSO_4$, filtered and concentrated *in vacuo*. The crude oil was purified by flash column chromatography (ethyl acetate) to give **4.10** as an off white solid

(260 mg, 34%), m.p. 177-179 ^{o}C. δ_H (400 MHz, $CDCl_3$, 24 °C): 10.38 (1H, s, C*H*O), 7.55 (1H, d, J = 6.9 Hz, 2-*H*), 7.39-7.47 (3H, m, 3-, 6-, 7-*H*), 6.89-7.00 (10H, m, Ar-H_{10}), 2.77 (6H, N(CH_3)$_2$); δ_C (100 MHz, $CDCl_3$, 24 °C): 186.7 (*C*HO), 149.0 (8-*C*), 142.6, 142.4, 142.1, 137.7, 137.6, 131.6, 131.4, 131.1, 130.3 (Ar-C_9), 129.8, 129.7, 127.2 (*m*-,*o*-*C*) 126.1 & 125.9 (*p*-*C*), 123.9 (2-*C*), 117.6 (Ar-C_1), 44.8 (N(*C*H$_3$)$_2$); ν_{max}/cm^{-1} 3030, 2986, 2943, 2865, 2831, 1638 (C=O), 1582, 1510, 1491, 1441, 1400, 1364, 1316, 1195, 118, 1154, 1122, 1074, 1042, 1010, 962, 870, 840, 764, 697; Found: C, 85.16; H, 5.79; N, 4.08%. Calc. for $C_{25}H_{21}NO$: C, 85.44; H, 6.02; N, 3.99%.

Preparation of 2-hydroxy-1,1-dimethyl-5,6-diphenyl-1,2-dihydrobenzo[cd]indol-1-ium chloride, 4.12.

Dimethylamino aldehyde **4.10** (75 mg, 0.21 mmol) was dissolved in anhydrous diethyl ether (5 mL) and ethereal hydrochloric acid (1M, 0.32 mL, 0.32 mmol) was added dropwise with immediate formation of a white precipitate. The solution was stirred for a further 1 h. before the solid was collected by careful filtration under a flow of nitrogen. The solid was washed with cold anhydrous diethyl ether and dried under vacuum to give **4.12** as an off-white solid (61 mg, 74%), m.p. decomp > 150 ^{o}C. δ_H (400 MHz, $CDCl_3$, 24 °C): 7.81 (1H, dd, J = 7.3, 0.9 Hz, 3-*H*), 7.70 (1H, d, J = 7.3 Hz, 4-*H*), 7.56-7.66 (2H, m, 7-, 8-*H*), 7.31 (1H, s, 2-*H*), 6.86-7.03 (10H, m, Ar-H_{10}), 3.84 (3H, s, N$^{(+)}$(CH_3)), 3.43 (3H, s, N$^{(+)}$(CH_3)); δ_C (100 MHz, $CDCl_3$, 24 °C): 144.0 (8a-*C*), 142.1, 141.6, 140.0, 139.9 (Ar-C_4), 134.3 (4-*C*), 131.7 (7-*C*), 131.3, 129.4, 129.1, 127.4, 126.9, 126.7 (Ar-C_9), 122.7 (3-*C*), 113.7 (8-*C*), 110.5 (2-*C*), 53.5 & 48.7 (N$^{(+)}$(*C*H$_3$)$_2$); ν_{max}/cm^{-1} 3050, 2957, 1492, 1466, 1442, 1291, 1176, 1133, 1105, 930, 861, 842,

821, 762, 697; Found: C, 77.20; H, 5.58; N, 3.58%. Calc. for $C_{25}H_{22}NOCl$: C, 77.41; H, 5.72; N, 3.61%.

Preparation of 2-hydroxy-1,1-dimethyl-5,6-diphenyl-1,2-dihydrobenzo[cd]indol-1-ium 2-carboxyacetate, 4.13.

Dimethylamino aldehyde **4.10** (100 mg, 0.28 mmol) and Meldrum's acid (82 mg, 0.56 mmol) were dissolved in anhydrous methanol (10 mL) under nitrogen and stirred at room temperature for 24h. The solvent was removed *in vacuo* and the crude oil was titrated with Et_2O, yielding a precipitate which was isolated and recrystallised from ethyl acetate to give **4.13** as an off-white solid (63 mg, 49%), m.p. 168-171 ºC. δ_H (400 MHz, $CDCl_3$, 24 °C): 7.80 (1H, d, J = 7.3 Hz, 3-*H*), 7.72 (1H, br s, 2-*H*), 7.70 (1H, d, J = 6.9 Hz, 4-*H*), 7.58 (2H, m, 7-, 8-*H*), 6.86-7.06 (10H, m, Ar-H_{10}), 3.50 (6H, s, $N^{(+)}(CH_3)_2$), 3.31 (2H, s, CH_2); δ_C (100 MHz, $CDCl_3$, 24 °C): 173.4 (*C*=O), 144.4 (8a-*C*), 141.9, 141.8, 140.0, 139.8 (Ar-C_4), 134.1 (4-*C*), 132.3 (Ar-C_1), 131.5 (7-*C*), 129.4, 129.3, 127.7, 127.4, 127.3, 126.9, 126.7 (Ar-C_9), 123.1 (3-*C*), 113.7 (8-*C*), 49.6 ($N^{(+)}(CH_3)_2$), 38.8 (CH_2); ν_{max}/cm^{-1} 3050, 2415, 2117, 1889, 1723 (C=O), 1587, 1464, 1440, 1407, 1366, 1259, 1179, 1138, 1097, 985, 930, 821, 752, 711, 695; Found: C, 73.50; H, 5.27; N, 2.87%. Calc. for $C_{28}H_{25}NO_5$: C, 73.88; H, 5.53; N, 3.08%.

Preparation of 3-cyano-3-((8'-(dimethylamino)-4',5'-diphenylnaphthalen-1'-yl)propenenitrile, 4.16.

Dimethylamino aldehyde **4.10** (100 mg, 0.28 mmol), malononitrile (60 mg, 0.91 mmol) and ethylenediamine diacetate (10 mg, 0.06 mmol) were dissolved in anhydrous methanol (10 mL) under nitrogen and refluxed for 24 h. The solvent was removed *in vacuo* and the crude product was purified by flash column chromatography (4:1 hexane: ethyl acetate) to give **4.16** as a yellow solid (100 mg, 53%), m.p. 138-140 ^{o}C. δH (400 MHz, $CDCl_3$, 24 °C): 8.45 (1H, d, J = 1.0 Hz, 3-*H*), 7.44-7.56 (4H, m, 2'-,3'-,6'-,7'-*H*), 6.89-6.96 (10H, m, Ar-H_{10}), 2.82 (6H, s, 8'-N(CH_3)$_2$); δC (100 MHz, $CDCl_3$, 24 °C): 161.3 (3-*C*), 147.5 (8'-*C*), 143.9, 141.9, 141.6, 139.4, 132.4, 131.9, 131.5, 130.5, 129.8, 129.7, 128.3, 127.5, 126.6, 126.5, 126.3, 119.2 (Ar-C_{17}), 116.2 & 114.6 (br 2 x C≡N), 65.5 (2-*C*), 45.5 (N(CH_3)$_2$); ν_{max}/cm^{-1} 3027, 2980, 2939, 2868, 2834, 2792, 2220 (C≡N), 2207, 1653, 1547, 1508, 1491, 1441, 1388, 1318 (C-N), 1183, 1154, 1126, 1074, 1034, 1016, 999, 926, 908, 841, 753, 695; Found: C, 83.92; H, 5.26; N, 10.74%. Calc. for $C_{28}H_{21}N_3$: C, 84.18; H, 5.30; N, 10.52%.

Preparation of methyl (E)-2-cyano-3-(8'-(dimethylamino)-4',5'-diphenylnaphthalen-1'-yl)propenoate, 4.17.

Dimethylamino aldehyde **4.10** (75 mg, 0.21 mmol), methyl cyanoacetate (0.075 mL, 0.85 mmol) and ethylenediamine diacetate (6 mg, 0.03 mmol) were dissolved in anhydrous methanol (10 mL) under nitrogen and refluxed for 24 h. The solvent was removed *in vacuo* and the crude product was purified by flash column chromatography (4:1 hexane: ethyl acetate) to

give **4.17** as a yellow solid (80 mg, 87%), m.p. 165-168 ºC. δH (400 MHz, $CDCl_3$, 24 °C): 8.95 (1H, s, 3-*H*), 7.58 (1H, d, J = 7.3 Hz, Ar-H_1), 7.39-7.51 (3H, m, Ar-H_3), 6.87-6.97 (10H, m, Ar-H_{10}), 3.94 (3H, s, OCH_3), 2.77 (6H, s, 8'-N(CH_3)$_2$); δC (100 MHz, $CDCl_3$, 24 °C): 161.8 (*C*=O), 156.7 (3-*C*), 148.4 (8'-*C*), 142.9, 142.3, 142.0, 138.9, 132.6, 131.6, 131.5, 130.5, 129.9, 129.8, 127.9, 126.4, 126.2, 126.1, 118.7 (Ar-C_{17}), 117.4 (*C*N), 87.5 (2-*C*), 52.7 (O*C*H$_3$), 45.7 (N(*C*H$_3$)$_2$); ν_{max}/cm^{-1} 2167 (C≡N), 1638 (C=O), 1433, 1371, 1345, 1276, 1250, 1189, 1095, 918, 849, 756, 695; Found: C, 80.53; H, 5.70; N, 6.57%. Calc. for $C_{29}H_{24}N_2O_2$: C, 80.53; H, 5.59; N, 6.48%.

Preparation of 1-(1',1'-dimethyl-5',6'-diphenyl-1',2'-dihydrobenzo[cd]indol-1'-ium-2'-yl)-2,6-dioxocyclohexan-1-ide, 4.19.

Dimethylamino aldehyde **4.10** (100 mg, 0.28 mmol), 1, 3-cyclohexandione (28 mg, 0.25 mmol) and ethylenediamine diacetate (5 mg, 0.03 mmol) were dissolved in anhydrous methanol (10 mL) under nitrogen and refluxed for 24 h. The solvent was removed *in vacuo* and the crude oil was titrated with Et_2O, yielding a precipitate which was isolated give **4.19** as a yellow solid (35 mg, 31%), m.p. decomp, > 150 ºC. δH (400 MHz, $CDCl_3$, 24 °C): 7.53 (1H, d, J = 7.3 Hz, 8'-*H*), 7.47-7.51 (2H, m, 4'-, 7'-*H*), 7.23 (1H, dd, J = 7.3, 1.4 Hz, 3'-*H*), 7.13 (1H, d, J = 1.4 Hz, 2'-*H*), 6.85-7.04 (10H, m, Ar-H_{10}), 3.62 (3H, s, $N^{(+)}CH_3$), 3.23 (3H, s, $N^{(+)}CH_3$), 2.44-2.50 (2H, m, CH_2CH_2CH_2), 2.17-2.32 (2H, m, CH_2CH_2CH_2), 1.90-2.05 (2H, m, CH_2CH_2CH_2); δC (100 MHz, $CDCl_3$, 24 °C): 195.4 & 193.4 (*C*=O), 146.8 (8a'-*C*), 141.4, 140.9, 140.6, 137.6, 137.5, 134.1, 130.8, 130.1, 129.6, 127.5, 127.3, 126.5, 126.1 (Ar-C_{15}), 119.0 (3'-*C*), 112.2 (8'-*C*), 101.3 (Ar-C_1), 89.8 (2-*C*), 55.5 & 50.2 ($N^{(+)}$(CH_3)$_2$), 37.7 & 36.7 (3, 5-*C*), 21.5 (4-*C*);

ν_{max}/cm^{-1} 3028, 2965, 2927, 2868, 1587, 1522 (C=O), 1444, 1431, 1401, 1384, 1349, 1179, 1120, 1073, 998, 982, 941, 844, 754, 726, 697; *HRMS* (ESI) calcd for $C_{31}H_{28}NO_2$ ($[M+H]^+$): 446.2120, found: 446.2137.

Preparation of N, N-Bis(4',5'-diphenyl-8'-dimethylamino naphth-1'-methylidene)-1,2-ethanediamine, 4.21.

Dimethylamino aldehyde **4.10** (100 mg, 0.28 mmol), nitromethane (0.05 mL, 0.85 mmol) and ethylenediamine diacetate (8 mg, 0.04 mmol) were dissolved in anhydrous methanol (10 mL) under nitrogen and stirred at room temperature for 24 h. The solvent was removed *in vacuo* and the crude oil was titrated with Et_2O, the resultant precipitate **4.21** was isolated as a yellow solid (22 mg, 69%), m.p. 218-221 ^oC. δH (400 MHz, CD_2Cl_2, 24 °C): 9.27 (2H, s, C*H*), 7.69 (2H, d, J = 7.3 Hz, 2'-*H*), 7.30-7.37 (4H, m, 3'-, 6'-*H*), 7.25 (2H, d, J = 7.8 Hz, 7'-*H*), 6.87-6.97 (20H, m, Ar-H_{10}), 4.05 (4H, s, CH_2), 2.78 (12H, s, 8-, 8'-N(CH_3)$_2$); δC (100 MHz, $CDCl_3$, 24 °C): 163.6 (*C*H), 150.7 (8'-*C*), 143.4, 143.2, 141.7, 135.8, 134.7, 131.4, 130.9, 130.4, 130.3, 130.0, 129.9, 127.3 (Ar-C_{13}), 125.9 (2'-*C*), 125.8, 125.5 (Ar-C_2), 115.6 (7'-*C*), 62.3 (*C*H_2), 44.9 (N(*C*H_3)$_2$); ν_{max}/cm^{-1} 3075, 2865, 1632, 1492, 1440, 1390, 1354, 1276, 1183, 1146, 1114, 1036, 928, 833, 758, 695; *HRMS* (ESI) calcd for $C_{52}H_{47}N_4$ ($[M+H]^+$): 727.3800, found: 727.3771.

Crystal data

*Table 4.30. Crystallographic data for dimethylamino naphthalene **4.9**, aldehyde **4.10**, Knoevenagel products **4.16**, **4.18**, **4.19** and bridged di-imine **4.21**.*

	4.9	**4.10**	**4.12**	**4.13**	**4.16**	**4.18**	**4.19**	**4.21**
Formula	$C_{24}H_{21}N$	$C_{25}H_{21}NO$	$C_{25}H_{22}NO.Cl.CH_2Cl_2$	$C_{25}H_{22}NO.C_3H_3O_4$	$C_{28}H_{21}N_3.C_7H_8$	$C_{29}H_{24}N_2O_2$	$C_{31}H_{27}NO_2.CHCl_3$	$C_{52}H_{46}N_4$
Formula weight	323.42	351.43	472.81	455.49	491.61	432.50	564.90	726.93
Crystal system	Monoclinic	Monoclinic	Orthorhombic	Triclinic	Triclinic	Monoclinic	Monoclinic	Orthorhombic
Space group	*C*2/*c*	$P2_1/n$	$P2_12_12_1$	*P*-1	*P*-1	$P2_1/n$	*I*2/*a*	*Pbca*
***a*[Å]**	22.0584(7)	12.6676(5)	6.1138(3)	6.0395(3)	8.6923(3)	10.6932(3)	19.4622(12)	9.8042(2)
***b*[Å]**	9.7183(2)	9.9541(3)	11.1707(5)	13.8019(8)	12.6464(5)	8.4601(3)	9.9340(8)	15.4073(4)
***c*[Å]**	16.5596(4)	15.1783(6)	33.8350(17)	14.6137(9)	12.8192(5)	25.0272(8)	29.6756(15)	52.7317(11)
***α*[°]**	90	90	90	67.400(5)	81.716(3)	90	90	90
β [°]	99.142(3)	108.164(4)	90	86.108(4)	77.638(3)	101.328(3)	93.325(5)	90
***γ*[°]**	90	90	90	81.742(4)	78.624(3)	90	90	90
***V* [Å^3]**	3504.78(16)	1818.53(12)	2310.78(19)	1112.84(12)	1341.80(9)	2219.99(13)	5727.7(6)	7965.5(3)
Z	8	4	4	2	2	4	8	8
***ρ* [g cm^{-3}]**	1.226	1.284	1.359	1.359	1.217	1.294	1.310	1.212
***T* [*K*]**	150.01(10)	150.00(10)	150.01(10)	150.01(10)	100.00(10)	150.01(10)	150.01(10)	150.01(10)
***λ* (Å)**	0.71073	0.71073	0.71073	0.71073	0.71073	0.71073	0.71073	1.54184
***μ* (mm^{-1})**	0.070	0.078	0.415	0.093	0.071	0.082	0.350	0.542
unique refl.	35872	19390	15877	23808	43402	20457	20831	20439
Refl, I > 2σI	3568	3708	5702	6361	6656	5513	5880	7645
***R*$_1$**	0.0476	0.0721	0.0594	0.0644	0.0727	0.0399	0.0805	0.0524
***wR*$_2$**	0.1015	0.1890	0.1074	0.1326	0.1296	0.1027	0.1354	0.1278
Δρ(r) [e Å^{-3}]	0.15/-0.17	0.67/-0.32	0.49/-0.64	0.44/-0.29	0.35/-0.34	0.31/-0.23	0.40/-0.37	0.21/-0.19
Crystallisation Solvent	*n*-hexane	EtOAc	CH_2Cl_2	EtOAc/CH_2Cl_2	Toluene	EtOAc	$CHCl_3$	CH_2Cl_2/*n*-hexane

References

1 J. Oddershede and S. Larsen, *J. Phys. Chem.* 2004, **108**, 1057–1063.

2 G. Pieters, V. Terrasson, A. Gaucher, D. Prim and J. Marrot, *European J. Org. Chem.*, 2010, 5800–5806.

3 K. Yamamoto, N. Oyamada, S. Xia, Y. Kobayashi, M. Yamaguchi, H. Maeda, H. Nishihara, T. Uchimaru and E. Kwon, *J. Am. Chem. Soc.*, 2013, **135**, 16526–16532.

4 C. F. R. A. C. Lima, J. E. Rodriguez-Borges and L. M. N. B. F. Santos, *Tetrahedron*, 2011, **67**, 689–697.

5 H. O. House and R. W. Bashe, *J. Org. Chem.*, 1967, **32**, 784–791.

6 D. Pla, O. Sadek, S. Cadet, B. Mestre-Voegtlé and E. Gras, *Dalton Trans.*, 2015, **44**, 18340–18346.

7 D. R. W. Hodgson, A. J. Kirby and N. Feeder, *J. Chem. Soc. Perkin Trans. 1*, 1999, 949–954.

8 A. Bondi, *J. Phys. Chem.*, 1964, **68**, 441–451.

9 A. Lari, M. B. Pitak, S. J. Coles, G. J. Rees, S. P. Day, M. E. Smith, J. V. Hanna and J. D. Wallis, *Org. Biomol. Chem.*, 2012, **10**, 7763–7779.

10 F. H. Allen, O. Kennard, D. G. Watson, L. Brammer, A. G. Orpen and R. Taylor, *J. Chem. Soc. Perkin Trans. 2*, 1987, 1–19.

11 H. Bock and N. Nagel, *Naturforsch. B.*, 1998, 792–804.

12 P. C. Bell and J. D. Wallis, *Chem. Commun.*, 1999, **2**, 257–258.

13 J. C. Bristow, M. A. Addicoat and J. D. Wallis, *CrystEngComm*, 2019, **21**, 1009–1018.

14 J. O'Leary and J. D. Wallis, *Org. Biomol. Chem.*, 2009, **7**, 225–228.

15 P. C. Bell, M. Drameh, N. Hanly and J. D. Wallis, *Acta Crystallogr.*, 2000, **56**, 670–671.

Chapter 5

Synthesis of Symmetrical Naphthalene Systems to Investigate the Effect of Competing *P*eri-Interactions

Introduction

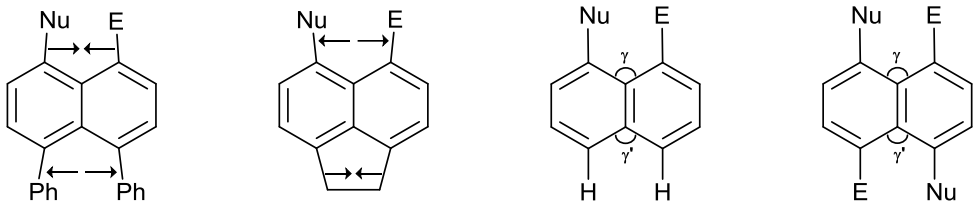

5.1 **5.2** **5.3** **5.4**

*Figure 5.81. Generalised nucleophile/electrophile interactions in peri-naphthalenes whereby the second set of peri-positions demonstrate; a Ph---Ph repulsion **5.1**, an ethylene bridge **5.2**, no substitution **5.3** and the equivalent nucleophile/electrophile interaction **5.4**.*

Throughout our work, modifications have been made to the naphthalene scaffold (see Chapters 3 and 4) in order to explore how an interaction between a nucleophile and an electrophile across the *peri*-positions is affected (Figure 5.1). For example; the two bulky phenyl groups in Chapter 4 allowed for the interacting *peri*-groups to be forced into closer proximity (**5.1**), whereas the installation of a 4, 5-ethylene bridge in Chapter 3 results in the groups being forced apart (**5.2**). Building upon this, we set out to explore what effect the addition of a competing symmetrical interaction, at the opposite *peri*-positions, has on the original interaction, investigating whether the interactions will co-exist or compete within the same molecule. As discussed in Chapter 1, a clear trend is observed in the size of the two *exo*-angles at the point of naphthalene ring fusion (γ/γ') in molecules of the general structure **5.3** (Figure 5.1). The trend follows that at interaction distances less than ~2.5 Å, *exo*-angle (γ) is smaller than the opposite (γ'), with the reverse observed when the interaction distance increases above ~2.5 Å. In the proposed *bis*-system **5.4**, where the two interactions occurring across the *peri*-positions are chemically equivalent, three questions arise:

1) Will the two *exo*-cyclic angles be identical and thus generate a symmetrical molecule expressing two identical interactions?

2) Will one *peri*-interaction be favoured over the other, resulting in a non-symmetrical structure demonstrating two unique interactions?
3) In the case of the most electrophilic groups, will the interaction result in the formation of a long N-C bond at one or both sets of *peri*-positions?

In order to investigate these questions, we herein report the design and synthesis of a range of naphthalenes bearing a dimethylamino group and an electrophile at both sets of *peri*-positions. The electrophilic group will be varied, utilising an aldehyde, ketone or substituted alkenes of differing electrophilicities. The molecular structure of each target will be determined by single crystal X-ray diffraction, in order to assess the effect of the particular *peri*-interaction, with comparisons being drawn throughout to the previously reported dimethylamino naphthalene reactivity series.[1–7]

Investigation into Symmetrical Systems with Two Me2N---C Interactions

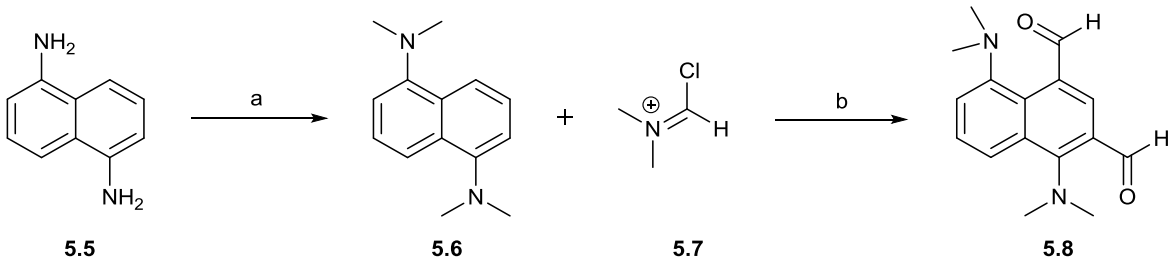

Scheme 5.33. (a) KOH, MeI, DMSO, RT; (b) DMF, RT to 35 °C.

Our initial target was to synthesis a naphthalene demonstrating two sets of *peri*-interacting dimethylamino and aldehyde groups. The first approach involved the use of electrophilic formylation (Scheme 5.1). To start 1,5-diaminonaphthalene[8] **5.5** was fully N-methylated to give *bis*-naphthylamine **5.6** with a Vilsmeier-Haack reaction then employed in order to *bis*-formylate the vacant *peri*-positions. Reaction of *bis*-naphthylamine **5.6**, with two equivalents of the reactive chloroiminium cation[9] **5.7**, resulted in the substitution of two formyl groups on the naphthalene ring. Despite the dimethylamino groups being expected to direct the substitution to their opposite *para*-positions, the only isolated product was found to be the *bis*-formylated naphthalene **5.8** in 21% as a deep yellow solid. The structure of the product **5.8** was confirmed by the two sets of aldehyde peaks in the ^{1}H and ^{13}C NMR spectra of 10.42/10.34 ppm and 191.1/189.8 ppm. An aromatic singlet peak of 7.85 ppm in ^{1}H NMR spectrum indicated that the formylation had occurred at the *ortho* and *para* positions on one side of the naphthalene ring system. The X-ray structure of *bis*-aldehyde **5.8** was determined at 150 K using a crystal grown from a DCM solution. To crystallographically unique molecules are found in the asymmetric unit for *bis*-aldehyde **5.8**, with the two molecules displaying very similar group orientation. As shown in Figure 5.2, an intermolecular hydrogen bond is formed across the *peri*-positions with N---H-C(=O) angles of 89.2/89.7° and distances of

2.549(2)/2.534(3) Å for the two molecules. Alternatively, no such bond is formed between the remaining dimethylamino group and the *ortho*-aldehyde group in each case.

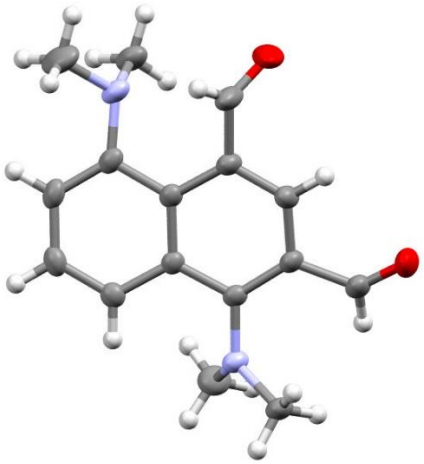

*Figure 5.82. Molecular structure of **5.8**.*

Formylation of the *ortho* and *para* positions on one side of the naphthalene ring is justified when the additions are looked at in a stepwise fashion (Scheme 5.2). Before addition, the electron donating capabilities of the dimethylamino groups mean that the *para*-positions (and thus the two C-H *peri*-positions) are the most activated sites for substitution. However, following the first formylation to give **5.9**, the desired interaction across the *peri*-positions occurs, generating an Me_2N---C=O contact involving the nitrogen lone pair. This results in a significant reduction in the electron donation of this dimethylamino nitrogen to the *para*-position. Consequently, the favoured site of attack for the second formylation becomes *ortho* to the dimethylamino group which is not involved in the attractive *peri*-interaction (**5.8**), as opposed to the deactivated *para*-position (**5.10**).

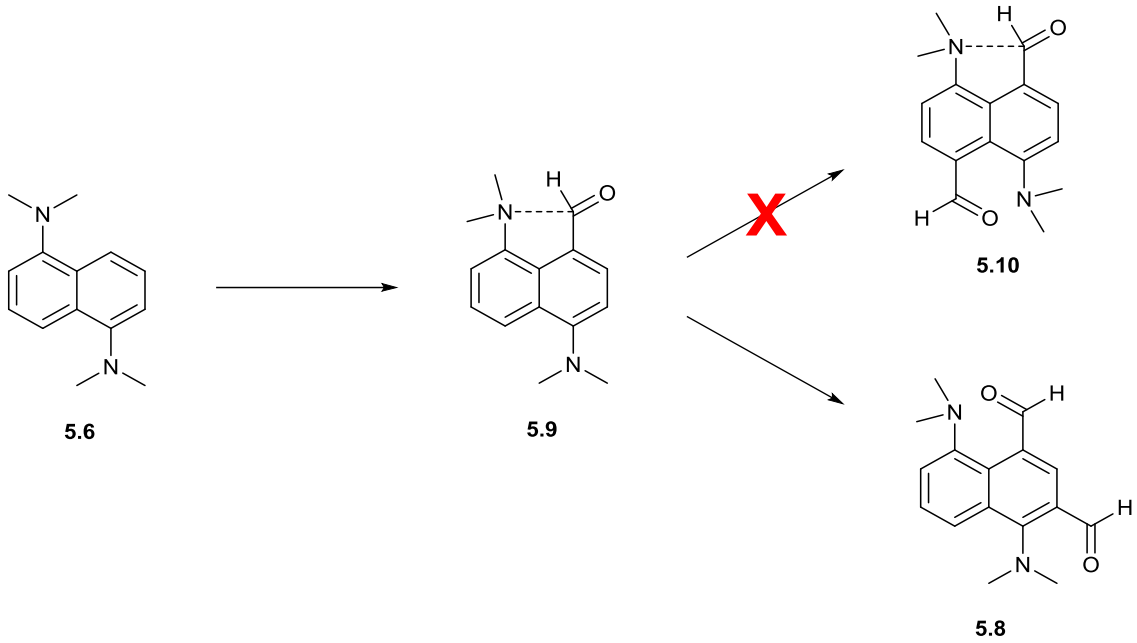

*Scheme 5.34. In the formylation of **5.8**, addition of the first aldehyde group (**5.9**) deactivates the remaining para-position, giving **5.8** instead.*

In an alternate approach, 1,5-*bis*(dimethylamino)naphthalene **5.6** was lithiated with *n*-butyl lithium in refluxing hexane, precipitating the *bis*-lithiated compound **5.6a** after three days.[10] Reaction of lithiated salt **5.6a** with DMF at 0 ^{o}C resulting in the isolation of *bis*-aldehyde **5.10** in 40% yield as a dark yellow solid (Scheme 5.3). The *mono*-aldehyde **5.11** was also isolated from the reaction as an orange solid in 19% yield. The introduction of peaks at 10.66 ppm and 191.0 ppm in the ^{1}H and ^{13}C NMR spectra along with the loss of two aromatic proton peaks to leave just two doublet signals confirmed the structure of the *bis*-aldehyde **5.10**. Similarly, the structure of the *mono*-aldehyde **5.11** was confirmed by peaks at 10.62 ppm and 191.6 ppm in the ^{1}H and ^{13}C NMR spectra for the newly added aldehyde group.

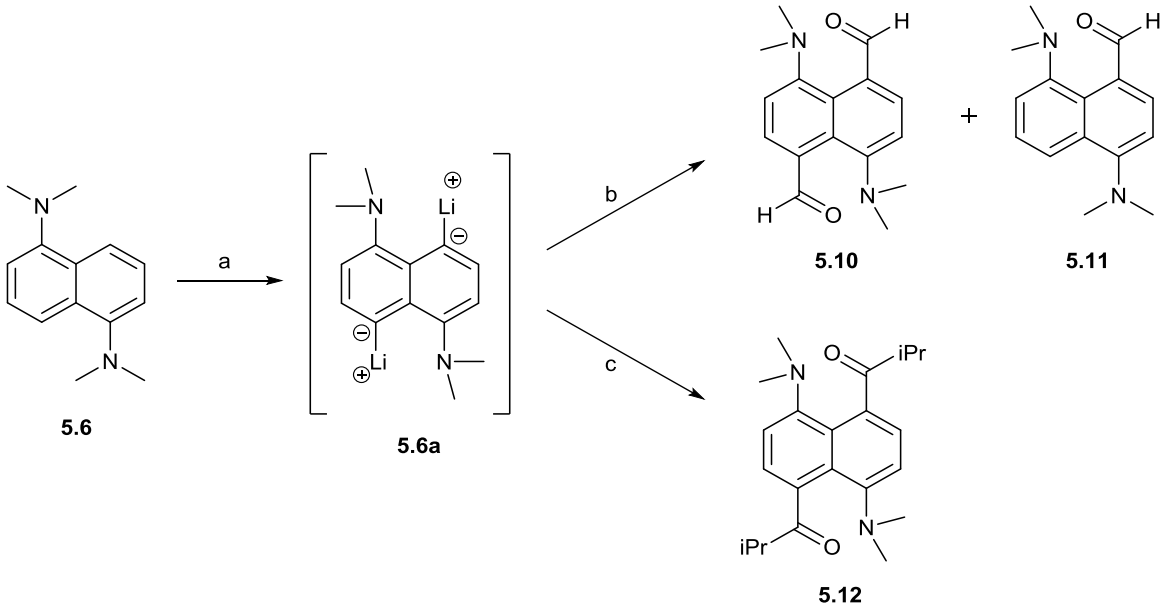

Scheme 5.35. (a) n-BuLi, hexane, reflux; (b) DMF, THF, 0 °C to RT; (c) Isobutyric anhydride, THF, 0 °C to RT.

Treatment of the *bis*-lithiated salt **5.6a** with isobutyric anhydride in a similar fashion gave the *bis*-isopropyl ketone **5.12** as a brown solid in 29% yield. The successful addition of the two isopropyl ketone groups is evidenced by peaks of 209.1 ppm and 1673 cm^{-1} for the carbonyl groups in the ^{13}C and Infrared spectra, with the isopropyl protons accounted for with peaks at 1.90-2.00 and 0.80-1.35 ppm in the ^{1}H NMR spectrum.

*Table 5.31. Selected geometric data for symmetrical naphthalenes **5.10**, **5.12a** and **5.12b** and the mono-substituted analogues **5.13** (R=H) and **5.14** (R=^{i}Pr).*

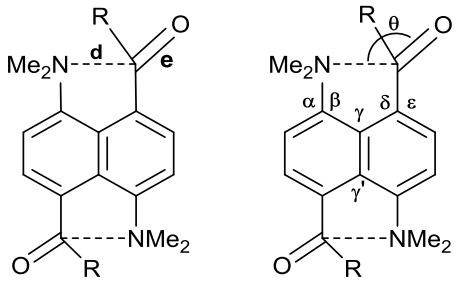

Compound	**d** / Å	**e** / Å	**θ** / º	**τ^{a}** / º	**τ^{b}** / º
5.10 (R = H)	2.566(2)	1.213(2)	119.1(1)	37.7(2)/-91.1(2)	-50.1(2)
5.13[3]	2.489(6)	1.213(5)	113.5(3)	44.5(5)/-85.2(5)	57.3(5)
5.12a (R = ^{i}Pr)	2.604(2)	1.221(2)	108.3(1)	-30.8(2)/96.7(2)	-63.1(2)
	2.640(2)	1.216(2)	109.0(1)	-29.8(2)/97.6(1)	-61.8(2)
5.12b (R = ^{i}Pr)	2.559(2)	1.217(2)	105.4(1)	-42.3(2)/84.3(2)	-70.9(2)
	2.547(2)	1.220(2)	104.3(1)	-52.1(2)/74.6(2)	-75.9(2)
5.14[2]	2.613(6)	1.213(4)	106.1(2)	-35.6(3)/92.1(3)	-70.3(3)

Compound	**α** / º	**β** / º	**δ** / º	**ε** / º	**γ / γ'** / º
5.10 (R = H)	123.7(1)	116.2(1)	122.6(1)	117.7(1)	121.6(1)^{c}
5.13[3]	124.3(4)	116.0(3)	122.2(4)	119.2(3)	120.6(3)/121.5(4)
5.12a (R = ^{i}Pr)	123.8(1)	116.6(1)	123.7(1)	116.7(1)	121.5(1)^{c}
	123.5(1)	116.8(1)	123.7(1)	116.2(1)	121.7(1)^{c}
5.12b (R = ^{i}Pr)	123.3(1)	116.9(1)	123.9(1)	117.0(1)	121.4(1)^{c}
	122.7(1)	117.3(1)	123.3(1)	117.2(1)	121.5(1)^{c}
5.14[2]	123.5(2)	117.0(3)	123.8(3)	116.0(3)	122.3(2)/121.3(3)

τ^{a} = torsion angle: 2 x (H_3)C-N-C(Ar)-C(H), **τ^{b}** = torsion angle: O=C-C(Ar)-C(H), ^{c} = plane of symmetry in the structure.

Crystals of the *bis*-aldehyde **5.10** were grown via slow evaporation of a DCM solution and the X-ray structure of one of these crystals determined at 150 K. Interestingly, for *bis*-isopropyl ketone **5.12** two different crystal polymorphs were obtained via slow evaporation of either a DCM/hexane (**5.12a**) or EtOAc/hexane (**5.12b**) solution. The structures for each of the polymorphs were determined at 150 K. Selected geometric data for the compounds **5.10**, **5.12a** and **5.12b** are shown in Table 5.1, alongside their equivalent *mono*-substituted analogues (aldehyde **5.13** and isopropyl ketone **5.14**).

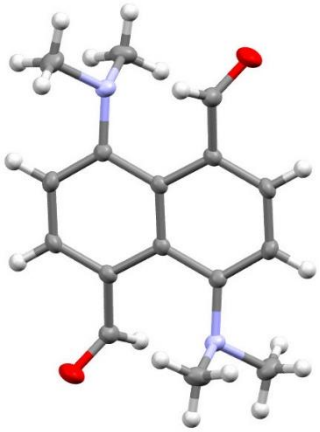

*Figure 5.83. Molecular structure of the symmetrical bis-aldehyde **5.10**.*

The *bis*-aldehyde **5.10** (Figure 5.3) is located on a centre of symmetry and thus the molecule possesses two identical sets of *peri*-interactions, showing that the interaction between the *peri*-groups are working in tandem and not competing with one another. As a result of the increased symmetry of the structure, the *exo*-angle at the point of naphthalene ring fusion has increased to 121.6(1)°. This causes an increase in the Me_2N---C=O contact distance of **5.10** to 2.566(2) Å compared to 2.489(6) Å in the equivalent *mono*-substituted naphthalene. An increase in the Bürgi-Dunitz angles between the interacting groups is observed from 113.5(3)° (**5.13**) to 119.1(1)° (**5.10**). Furthermore, the aldehyde group itself is rotated closer to the best naphthalene plane by 7.2° in compared to the *mono*-analogue, likely due to the increased contact distance and thus reduced steric influence from the approaching dimethylamino group. With regards to the in-plane angular displacements of the *peri*-substituents, there is very little difference, except that the aldehyde group in **5.10** is displaced further towards the *ortho*-carbon of the naphthalene ring, again contributing to the increase contact distance. The aldehyde groups in both **5.10** and **5.13** are displaced by equal amounts to one side of the naphthalene plane, whilst the dimethylamino groups is displaced to the other side, however by an increased extent in the *bis*-aldehyde.

The two polymorphs of *bis*-isopropyl ketone **5.12** (Figure 5.4), one triclinic (**5.12a**) and the other monoclinic (**5.12b**), each possess two crystallographically unique molecules in their asymmetric unit. Furthermore, as found in the *bis*-aldehyde **5.10** each of the four molecules sits on a centre of symmetry and presents two identical sets of *peri*-interactions. As a result, four examples of a N---C=O interaction in the *bis*-isopropyl ketone **5.12** are available for comparison against the naphthalene equivalent possessing one set of *peri*-interactions **5.14**.

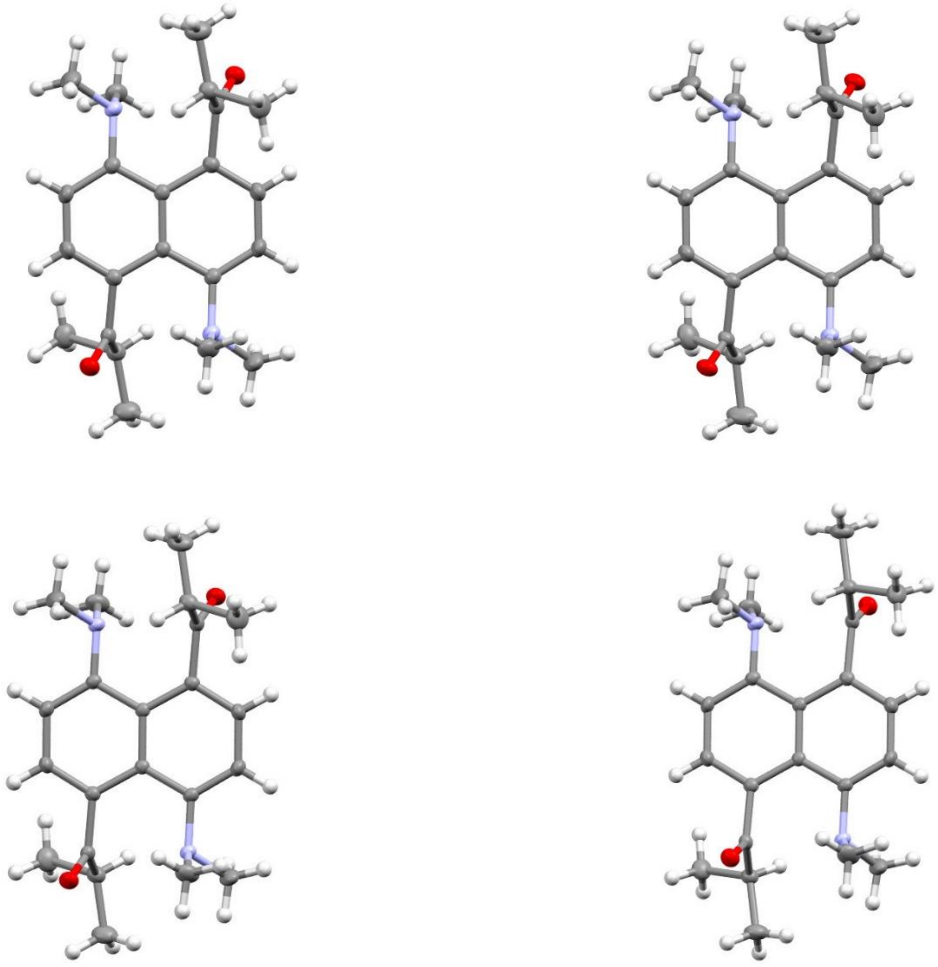

*Figure 5.84. Molecular structures of the four crystallographically unique molecules of **5.12**. The triclinic system **5.12a** (top row) and the monoclinic system **5.12b** (bottom row).*

Despite being structurally identical, the four molecules of *bis*-ketone **5.12** display a range of Me_2N---C=O contact distances, with three out of the four molecules displaying a contact shorter than the *mono*-analogue **5.14**. All four molecules show close structural similarity with respect to the Bürgi-Dunitz angle of approach, the carbonyl bond length and the angular

displacements of the two interacting *peri*-groups. The two molecules of polymorph **5.12a** possesses N---C=O separations of 2.604(2) and 2.640(2) Å whereas the molecules of polymorph **5.12b** demonstrate separations of 2.547(2) and 2.559(2) Å. A distinct trend is observed in the displacements of the *peri*-groups to either side of the naphthalene plane. As the contact distance lengthens the extent to which they are displaced increases, for example; in **5.12a**, the contact of 2.640(2) Å displays deviations of 0.285 and -0.363 Å for the dimethylamino and ketone groups respectively. Whereas in **5.12b**, displacements of 0.113 and -0.114 Å are observed for the contact of 2.547(2) Å. The N-methyl groups of the nucleophile are therefore displaced more evenly to either side of the naphthalene plane in the polymorph **5.12b** which displays shorter contacts and lesser out of plane displacements, optimising the nitrogen lone pair overlap with the antibonding orbital of the carbonyl group. The *peri*-ketone group rotates further from the idealised naphthalene plane as the contact distance decreases, likely due to the steric interference of the approaching nucleophile and in order to optimise the angle of its approach. Despite the relatively larger deviations in the contact distances, the *exo*-angle at the point of naphthalene ring fusion is almost constant (*ca.* 121.5^{o}) in all four molecules, with the *bis*-aldehyde **5.10** showing a similar angle (121.6(1)^{o}).

The two polymorphs **5.12a** and **5.12b** are an excellent example of how the crystal packing environment of the compound in question can influence the result obtained and how in all cases demonstrated throughout this thesis, that the results discussed are specific to that crystal structure. Nevertheless, the results obtained are accurate and important, but if possible, all attempts should be made to obtain different polymorphs of the compounds in question, so that the interaction of interest can be fully explored.

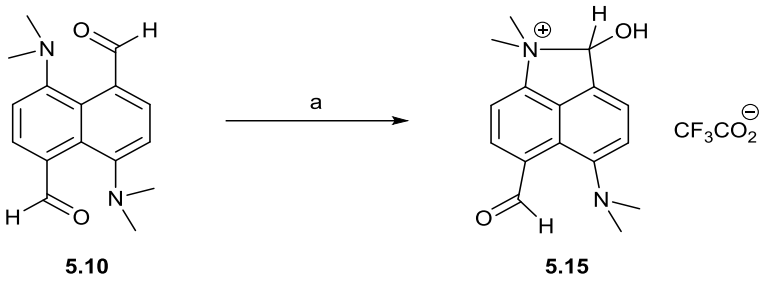

Scheme 5.36. (a) TFA, Et_2O, RT.

Reaction of the *bis*-aldehyde **5.10** with one equivalent of trifluoroacetic acid (TFA) in Et_2O resulted the precipitation of the *mono*-hemi-aminal salt **5.15** as a yellow solid in an 84% yield (Scheme 5.4). NMR analysis of hemiaminal **5.15** in DMSO-d_6 shows an averaged structure corresponding to the reversible protonation of both sets of *peri*-groups with a very broad peak in the ^{1}H NMR at 9.21 ppm for the two aldehyde protons. Furthermore, the two dimethylamino groups are represented as a sharp singlet, opposed to the expected two peaks of the NMe_2 and $N(+)Me_2$ groups, again suggesting an averaged structure. Peaks at -73.93 ppm and 159.5 ppm in the ^{19}F and ^{13}C NMR spectra confirm the presence of the trifluoroacetate counterion.

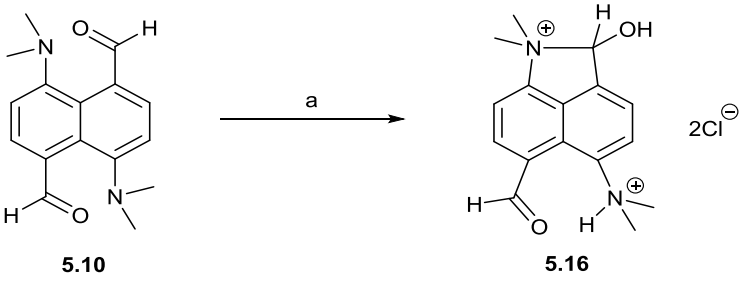

Scheme 5.37. (a) Ethereal HCl, DCM, RT.

The reaction was repeated, using an excess of TFA in order to protonate both of the aldehyde groups, however the same *mono*-hemiaminal **5.15** was obtained following the addition of approximately one equivalent. This is due to the low polarity of diethyl ether, which prevents the second protonation from occurring due to the *mono*-hemi-aminal salt **5.15** precipitating from the solution. In order to achieve the desired double protonation, the product must remain

soluble following the first initial protonation and therefore a more polar solvent is required. The solvent was replaced with DCM and the acid of choice altered to ethereal HCl. This led to the precipitation of the desired *bis*-chloride salt **5.16** as a pale yellow solid in 79% yield, following the addition of well over two equivalents of acid. Despite its low solubility, ^{1}H and ^{13}C NMR spectra were obtained in d_3-methanol for the chloride salt **5.17**.

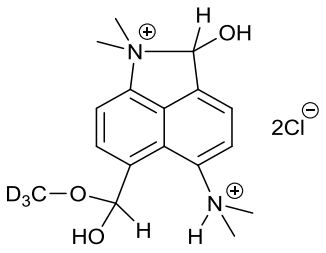

5.17

*Figure 5.85. NMR structure of bis-chloride salt **5.16** when dissolved in d-MeOH (**5.17**).*

Analysis of the NMR spectra indicated that a second protonation had occurred along with addition of CD_3OD from the NMR solvent (Figure 5.5). The N-methyl protons were all shifted upward of 3.52 ppm, indicating two positively charged dimethylamino groups, to give four singlet peaks corresponding to three protons in the range of 3.52-3.91 ppm. The ^{1}H and ^{13}C NMR data suggests that two different interactions are present in the compound, the first a bond formation reaction to give the hemi-aminal group with signals for the sp^3-C-H group of 7.14 and 115.0 ppm. While the other is due to the CD_3OD solvent adding to aldehyde, with ^{1}H and ^{13}C NMR signals at 5.86 and 109.1 ppm respectively. Addition of the solvent is likely due to the formation of the opposite hemi-aminal, which widens the *exo*-angle between the unreacted *peri*-groups and prevents the formation of a second hemi-aminal group. Alternatively, the dimethylammonium groups forms a hydrogen bond to the aldehyde oxygen, catalysing the addition of the slightly nucleophilic CD_3OD solvent.

*Table 5.32. Selected geometric data for mono (**5.15**) and bis (**5.16**) TFA and chloride salts of bis-aldehyde **5.10** and the unsubstituted analogue TFA salt **5.18**.*

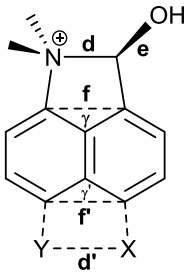

5.15: X = NMe_2 Y = CHO

5.16: X = $^{+}NHMe_2$ Y = CHO

5.18: X = Y = H

Compound	**d** / Å	**d'** / Å	**f** / Å	**f'** / Å	**e** / Å
5.15	1.645(2)	2.918(2)	2.325(2)	2.602(2)	1.349(2)
5.16	1.603(5)	3.170(5)	2.317(5)	2.630(5)	1.363(4)
5.18[5]	1.628(5)	-	2.332(5)	2.565(5)	1.362(4)
	1.624(5)	-	2.331(5)	2.559(5)	1.352(4)

Compound	[a]**N-CH$_3$** / Å	[b]**N-CH$_3$** / Å	**γ / γ'** / °	**τ**[c] / °
5.15	1.492(2)/ 1.500(2)	1.461(3)/1.459(2)	112.7(2)/129.4(2)	0.7(2)
5.16	1.499(4)/1.507(4)	1.492(5)/1.486(5)	112.2(3)/132.5(3)	6.1(3)
5.18[5]	1.501(4)/1.496(4)	-	113.4(4)/128.8(4)	11.6(3)
	1.500(5)/1.499(4)	-	113.4(4)/129.3(4)	18.6(3)

[a] = aminal N-CH_3 bond lengths, [b] = other dimethylamino N-CH_3 bond lengths, **τ**[c] = torsion angle: C(Ar)-N(+)-C-C(Ar).

Suitable crystals of the *bis*-aldehyde *mono*- and *bis*-salts **5.15** and **5.16** were grown via slow evaporation of acetonitrile and acetonitrile/methanol solutions respectively. The X-ray structures of both salts were determined at 150 K, with geometric data for each compound summarised in Table 5.2, along with same data for the corresponding aminal salt **5.18** with just one set of *peri*-interactions.

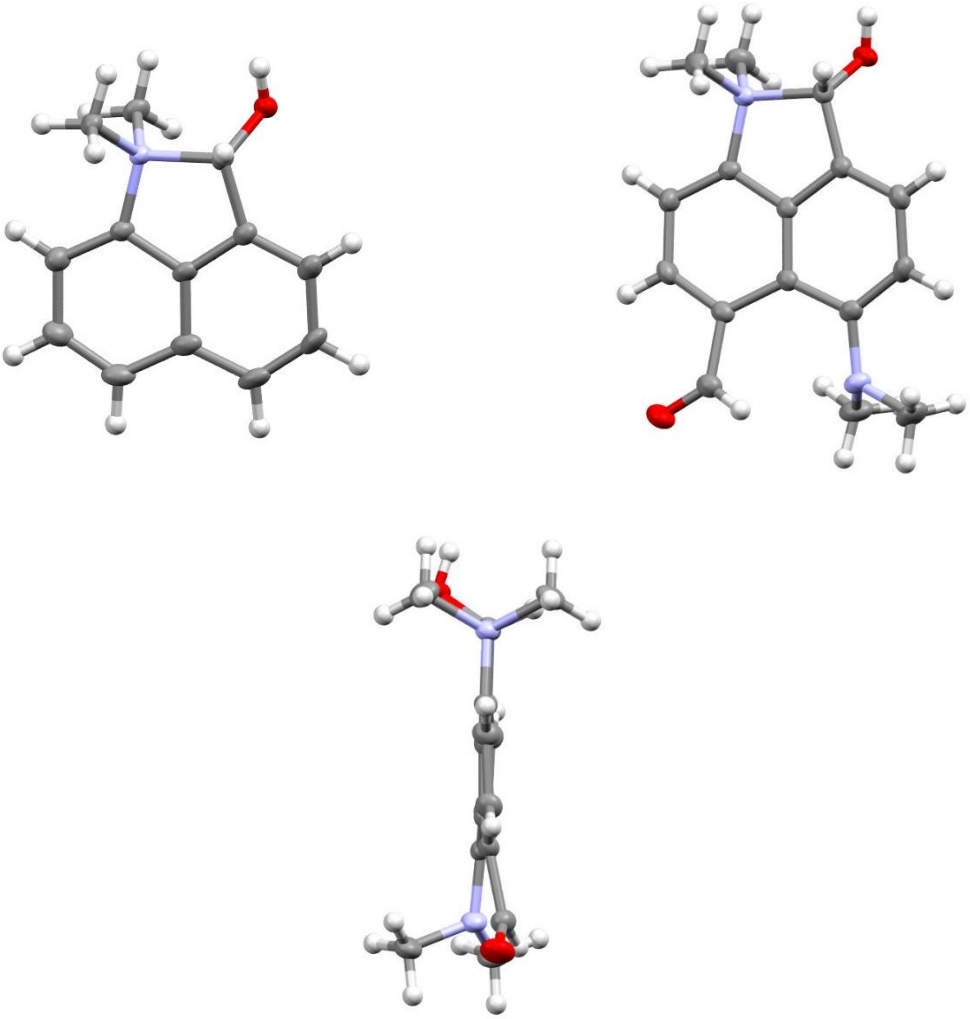

Figure 5.86. Molecular structures of cations 5.18[5] (top left) and 5.15 (top right). The view along the naphthalene plane of cation 5.15 is shown (bottom) demonstrating the displacements of the two unreacted peri-substituents.

In the *bis*-aldehyde *mono*-salt **5.15** one dimethylamino group has added to a carbonyl group which has protonated, and demonstrates a slightly elongated long N-C bond of 1.645(2) Å compared to the *mono*-aldehyde salt **5.18** (1.624(5)/1.628(5) Å) as shown in Figure 5.6. A slight decrease is also observed in the aminal C-OH bond length, evidencing that a lower degree of N-C bond formation results in the C-O bond possessing marginally more C=O character. The bonded *peri*-groups lie almost exactly in the naphthalene plane, generating a C(Ar)-N(+)-C(OH)-C(Ar) torsion angle of just 0.7(2)º. Formation of the aminal between the first set of *peri*-groups causes a widening of the opposite *exo*-angle at the point of the naphthalene ring fusion (γ') to 129.4º. This results in the distance between the second set of *peri*-groups

(2.918(2) Å) being too large for a Me_2N---C=O interaction to occur. Consequently, the aldehyde group is rotated, positioning its proton towards the nucleophilic nitrogen in order to generate a hydrogen bond of 2.35 Å, and the dimethylamino nitrogen continues to lie in the idealised naphthalene plane, the aldehyde group is displaced from it by 0.408 Å.

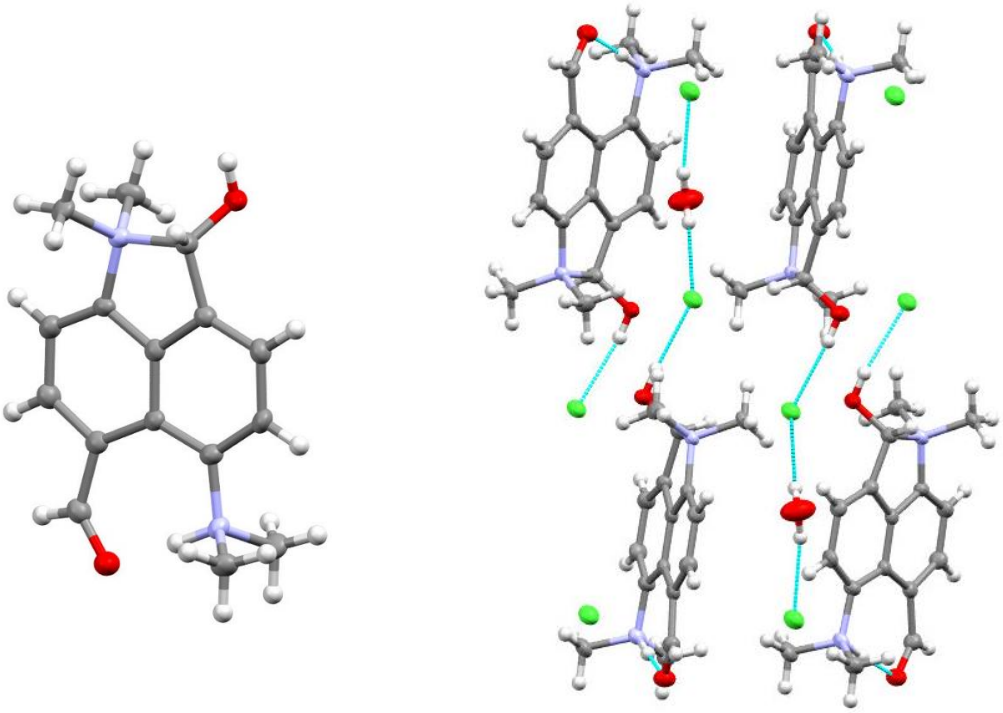

*Figure 5.87. Molecular structures of the di-cation **5.16** (left) and a demonstration of how this salt is packed within the crystal lattice (right), looking down the b axis.*

Protonation of the remaining free dimethylamino group in the *bis*-aldehyde *bis*-chloride salt **5.16** does not result in the formation of an aminal at the second set of *peri*-positions. Instead, the protonation of nitrogen results in a reversal of the hydrogen bond observed in the TFA salt **5.15**, in which the aldehyde group is rotated so that there is a short C=O---H-$N^{(+)}$ interaction of 1.63 Å (Figure 5.7). In order to allow this contact, the two *peri*-groups are splayed even further apart, generating a significantly widened *exo*-angle of 132.5(3)^o. As a consequence of this, akin to the *peri*-phenyl repulsion study of Chapter 4, the N-C aminal bond at the opposite *peri*-positions is shortened by 0.042 Å to 1.603(5) Å in length and *exo*-angle (γ) is narrowed to

112.2(3)º. A molecule of water, which hydrogen bonds to the two chloride ions, is present in the asymmetric unit displaying O---$Cl^{(-)}$ contacts of 3.223 and 3.217 Å.

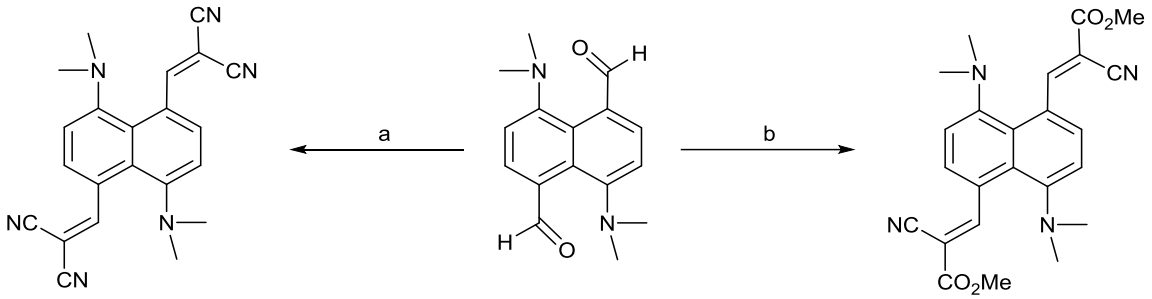

5.19 **5.10** **5.20**

Scheme 5.38. (a) $CH_2(CN)_2$, ($^+NH_3CH_2$-)$_2$($^-$OAc)$_2$ (cat.), CH_3OH, 65 ºC; (b) $NCCH_2CO_2Me$, CH_3OH, ($^+NH_3CH_2$-)$_2$($^-$OAc)$_2$ (cat.), 65 ºC

Condensation of *bis*-aldehyde **5.10** with active methylene compounds malononitrile and methyl cyanoacetate (Scheme 5.6) yielded the expected Knoevenagel condensation products **5.19** and **5.20**. In both cases, aldehyde **5.10**, the chosen methylene compound and EDDA (catalyst) were refluxed in methanol. Once cooled, the reactions yielded orange precipitates of alkenes **5.19** and **5.20** in 68% and 78% yields respectively. The structure of the *bis*-dinitrile **5.19** was confirmed by the ^{1}H NMR peak at 8.69 ppm for the vinylic protons, with signals for the nitrile groups observed at 114.1 ppm and 2227 cm^{-1} in the ^{13}C NMR and infrared spectra. Similarly, the structure of the *bis*-cyanoester **5.20** demonstrates a ^{1}H NMR signal at 9.27 ppm corresponding to the vinylic proton as well as a peak at 3.94 ppm for the methoxy ester moieties. The ^{13}C NMR spectrum evidenced the presence of the nitrile groups with a peak at 115.8 ppm, and signals at 164.0 and 53.1 ppm confirming the methoxy ester group. In both alkenes **5.19** and **5.20**, the 'open form' structure is observed, as shown by the neutral dimethylamino group shifts (**5.19**: 2.72 ppm, **5.20**: 2.66 ppm).

*Table 5.33. Selected geometric data for the bis dinitrile (**5.19**) and methyl cyanoester (**5.20**) and their mono-substituted analogues **5.21** and **5.22**.*

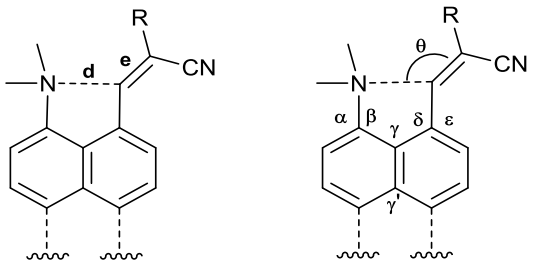

Compound	**d** / Å	**e** / Å	**θ** / °	**τ**[a] / °	**τ**[b] / °
5.19 (R = CN)	2.507(2)	1.350(2)	115.6(1)	-44.0(2)/87.4(1)	53.9(2)
5.21 (R = CN)[1]	2.413(2)	1.354(2)	112.1(1)	-49.7(2)/81.5(2)	-56.5(2)
5.20 (R = CO_2Me)	2.445(2)	1.352(2)	110.7(1)	-46.9(2)/85.4(2)	61.3(2)
5.22 (R = CO_2Me)	2.595(2)	1.349(2)	116.2(1)	34.5(2)/-93.8(2)	55.2(2)

Compound	**α** / °	**β** / °	**δ** / °	**ε** / °	**γ / γ'** / °
5.19 (R = CN)	123.8(1)	116.3(1)	121.0(1)	119.3(1)	121.3(1)[c]
5.21 (R = CN)[1]	124.3(2)	115.9(1)	120.2(1)	120.3(2)	120.4(1)/122.6(2)
5.20 (R = CO_2Me)	123.9(1)	116.0(1)	120.4(1)	120.2(1)	121.2(1)[c]
5.22 (R = CO_2Me)	123.2(1)	116.8(1)	122.5(1)	117.9(1)	122.6(1)/121.4(1)

τ[a] = torsion angle: 2 x (H_3)C-N-C(Ar)-C(H), **τ**[b] = torsion angle: C=C-C(Ar)-C(H), [c] = plane of symmetry in the structure.

Crystals of the *bis*-dinitrile and -cyanoester **5.19** and **5.20** were obtained via slow evaporation of DCM/hexane solutions. The X-ray structure of each was determined at 150 K (Figure 5.8) with selected geometric data summarised in Table 5.3. Data for the equivalent analogues containing one set of *peri*-interactions are also shown. Both *bis*-alkenes **5.19** and **5.20** are located on a centre of symmetry and thus each molecule possesses two identical sets of *peri*-interactions.

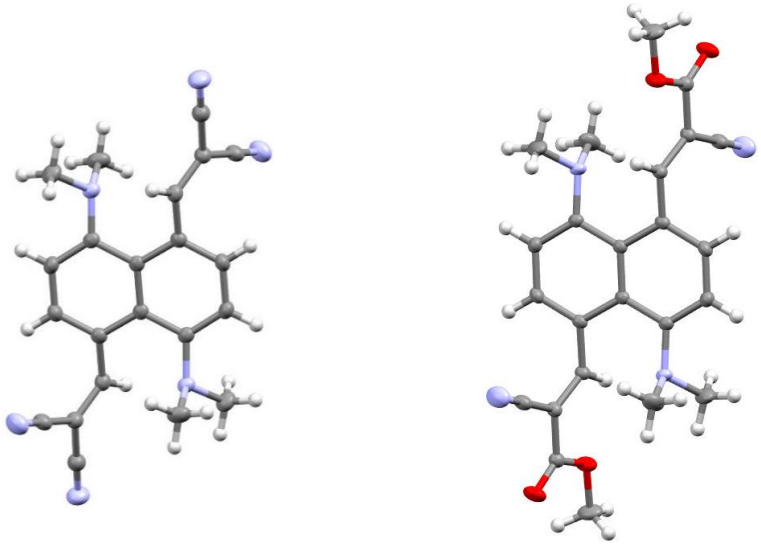

*Figure 5.88. Molecular structure of the bis-dinitrile **5.19** (left) and bis-methyl cyanoester **5.20** (right).*

Across the three *bis*-interaction examples (**5.10**, **5.19** and **5.20**) the Me_2N---C contact distance reduces from 2.566(2) Å in the *bis*-aldehyde **5.10** to 2.507(2) Å in the *bis*-dinitrile **5.19** to 2.455(2) Å in the *bis*-cyanoester **5.20**. The dimethylamino group is displaced towards the electrophile in the plane of the naphthalene by a similar amount in all three cases, while the electrophile is displaced away from the dimethylamino group by a decreasing amount across the series. As the Me_2N---C distance decreases, the distribution of the N-methyl groups of the nucleophile with respect to the naphthalene plane becomes more even, allowing for a more optimal orientation of the nitrogen lone pair in the direction of the electrophile. This trend is matched by the electrophilic moiety, which rotates further from the idealised naphthalene plane as the contact distance decreases. The notable consistency of the *exo*-angles of the symmetrical *bis*-interaction compounds is continued as both **5.19** and **5.20** demonstrate angles of 121.3(1) and 121.2(1)^o respectively, an average of the *exo*-angles observed in their *mono*-interaction analogues.

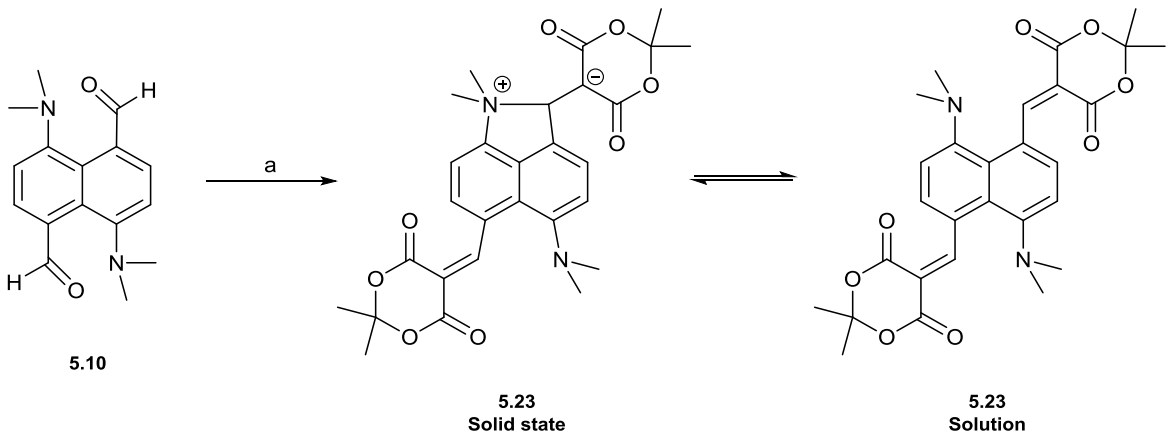

Scheme 5.39. (a) Meldrum's acid, CH_3OH, RT

Conditions for the condensation of *bis*-aldehyde **5.10** with Meldrum's acid (Scheme 5.7) were altered slightly, with the catalyst removed and the reaction stirred at room temperature. This is due to the increased acidity of Meldrum's acid, which was found to decompose under heat in the presence of the EDDA catalyst. The reaction after 24 hours yielded an orange precipitate which was isolated in a 49% yield. NMR analysis of the product confirmed that the *bis*-condensation had occurred with a peak in the ^{1}H NMR spectrum at 8.24 ppm for the vinylic protons. Maintenance of the Meldrum's acid cyclic diester structure is confirmed by the ^{1}H and ^{13}C NMR spectra with peaks of 1.85 ppm and 165.6/162.7 ppm for the ring methyl and carbonyl groups respectively. The downfield shift of the vinylic protons (similar to alkenes **5.19** and **5.20**) supports that compound is in the 'open form' in solution. However, the infrared spectrum however, taken of the recrystallised product, suggests that in the solid state the two cyclic diester rings are not equivalent, with two significantly different carbonyl stretching frequencies observed at 1729 and 1636 cm^{-1}.

*Table 5.34. Selected geometric data for the bis-Meldrum's acid derivative **5.23** and the mono-analogue **5.24**.*

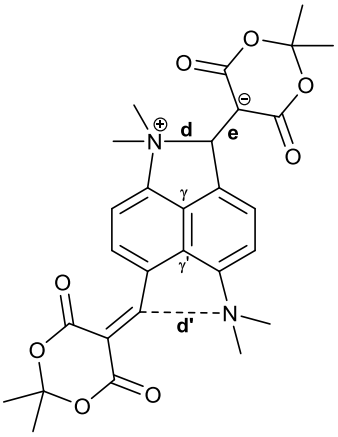

Compound	**d** / Å	**e** / Å	**d** / Å	[a]**N-CH$_3$** / Å	[b]**N-CH$_3$** / Å	**γ / γ'** / °	**τ^c** / °
5.23	1.676(4)	1.465(4)	2.615(4)	1.497(4)/1.500(4)	1.455(4)/1.458(5)	113.7(3)/126.4(3)	0.5(3)
5.24[1]	1.651(3)	1.471(3)	-	1.495(3)/1.508(2)	-	113.3(2)/128.1(2)	17.1(2)

[a] = N^+-CH_3 bond lengths, [b] = other dimethylamino N-CH_3 bond lengths, **τ^c** = torsion angle: C(Ar)-N(+)-C-C(Ar).

Crystals of the *bis*-Meldrum's alkene **5.23** were obtained via slow evaporation of a DCM solution, with the X-ray structure of one of those crystals determined at 150 K (Figure 5.9). Selected data from the structure of the *bis*-Meldrum's derivative **5.23** and the *mono*-Meldrum's acid analogue **5.24** are summarised in Table 5.4.

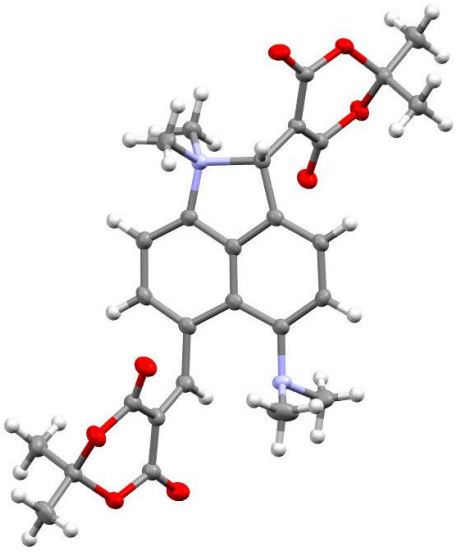

*Figure 5.89. Molecular structure of zwitterion **5.23**, showing the two different interactions between the same groups.*

Whilst NMR evidence indicates that the *bis*-Meldrum's derivative **5.23** exists in the 'open form' in solution, the structural analysis revealed that in the solid state, the 'closed form' is adopted, with a very long 1.676(4) Å N-C bond between *one* of the two sets of *peri*-positions. There's a Me_2N---C contact of 2.615(4) Å between the second pair of groups. This molecule thus demonstrates two different interactions between the same pair of groups. The N-C *peri* bond, which is 0.025 Å longer than the *mono*-substituted analogue, represents a slightly earlier point in bond formation (than the *mono*-analogue), resulting in a slightly shorter and therefore less broken alkene bond. The *exo*-angle between the bonded *peri*-groups is slightly wider in the *bis*-derivative **5.23** than the *mono*-analogue **5.24**, with the opposite *exo*-angle demonstrating the reverse, with the *bis*-analogue angle being significantly narrower. This is likely a result of the attractive interaction between the second set of *peri*-groups, which is evidenced by the angular displacement of the dimethylamino group towards the only slightly retreating electrophile, with a Bürgi-Dunitz angle of 111.3(3)^o. The strength of this attractive interaction leads to a Me_2N---C contact of 2.616(4) Å, which behaves as a very weak mimic of the ethylene bridge of the acenaphthene derivatives discussed in Chapter 3, restricting the extent to which the opposite long *peri* N-C bond can form. The difference between the two dimethylamino groups is shown clearly by the longer N-CH_3 bonds in the zwitterionic group (1.497(4) and 1.500(4) Å) compared to the neutral dimethylamino group (1.455(4) and 1.458(5) Å). The bonded dimethylamino group positions its N-methyl groups evenly to either side of the naphthalene plane, with the vector of the long N-C bond parallel to that of the idealised naphthalene plane. The opposite non-bonded dimethylamino group displays a slight rotation of the N-methyl groups, generating torsion angles of -72.2(4)/57.4(4)^o to the *ortho*-naphthalene ring carbon. This rotation results in the axis of the nitrogen lone pair lying at 15.6^o to N---C=C vector. Each of the four *peri*-substituents across the molecule lie very closely to the idealised naphthalene plane, minimising the strain on the backbone system.

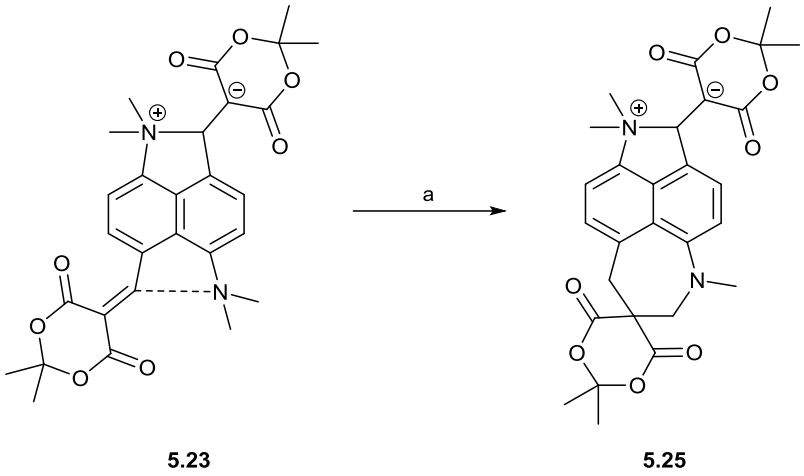

Scheme 5.40. (a) MeOH, RT.

When dissolved in a range of organic solvents (e.g. DCM, MeOH and CH_3CN), the *bis*-Meldrum's acid derivative **5.23** demonstrates a deep orange coloured solution. Over the course of a week, the colour of an NMR solution of **5.23** in d_4-MeOH changed dramatically, with the orange colour fading completely to give a colourless solution with a colourless crystalline material in the base of the tube (Scheme 5.8). The NMR sample was analysed again no signals corresponding to the Meldrum's acid derivative **5.23** observed. The crystals were isolated from the solution to reveal a 95% yield and their structure determined at 150 K, with selected data given in Table 5.5. As shown in Scheme 5.8 and Figure 5.10, the new colourless material was found to be azepine **5.25**, which crystallised alongside a disordered methanol molecule, which is split over four possible positions. NMR analysis of the crystalline solid confirmed the azepine ring formation with the ^{1}H NMR peaks at 3.75-3.85 and 3.11 ppm for the two methylene groups and N-methyl group respectively. Shifts of 6.92 and 3.33 ppm for the vinylic proton and dimethylamino group of the opposite N-C bonded *peri*-groups in the ^{1}H NMR spectrum were all observed.

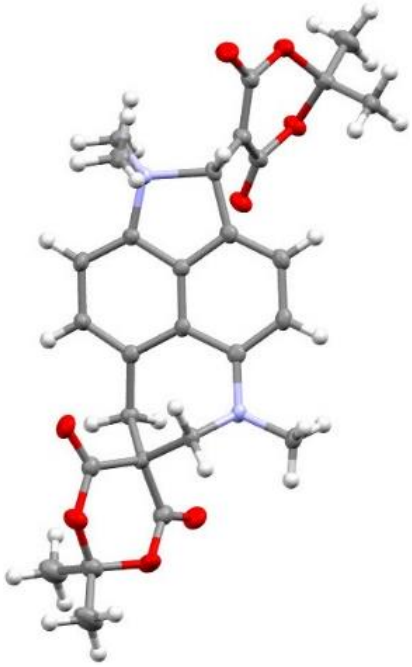

*Figure 5.90. Molecular structure of the **5.25** caused by a reaction between the interacting peri-groups to form an azepine ring.*

Previously, the formation of azepine ring systems has been demonstrated and discussed in acenaphthene derivative in Chapter 3. In these examples, as shown in the mechanism in Scheme 5.9, the azepine ring is formed due to the donation of an N-methyl hydride ion to the electrophilic alkene, demonstrating a type 2 *tert*-amino effect reaction. The resultant iminium cation **5.26** and stabilised carbanion **5.27** subsequently react to form the azepine ring **5.25**. The *bis*-Meldrum's derivative **5.25** is akin to the acenaphthene derivatives in Chapter 3, with the ethylene bridge replaced by the newly formed N-C bond at the opposite *peri*-interactions. This allows for a higher degree of rotation for the free dimethylamino group, allowing for optimal orientation for the *tert*-amino reaction to proceed. In a similar vein to similar reactions demonstrated by Matyus *et al*. the reaction requires a polar media in which to perform the rearrangement, with the reaction in this case requiring milder conditions than the similar reactions reported which require heating.

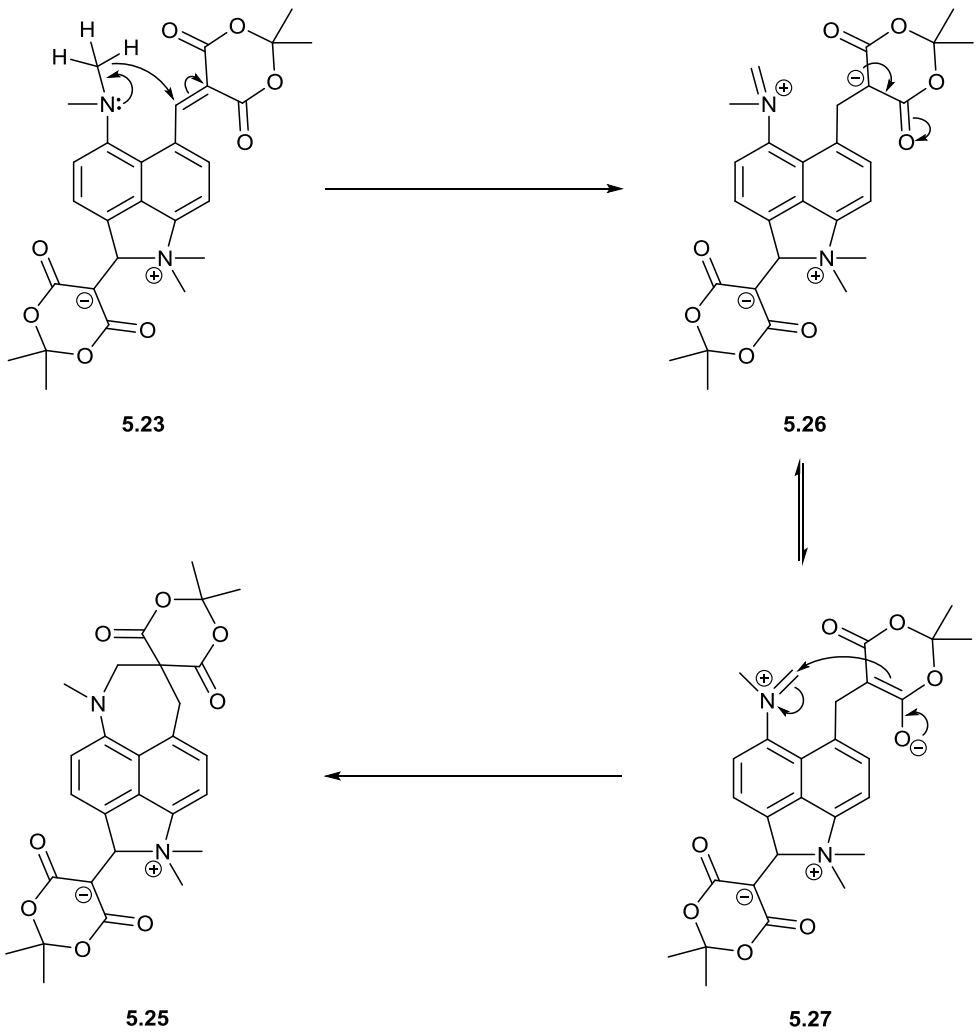

*Scheme 5.41. Proposed mechanism for the formation of the azepine ring in **5.25** via a type 2 tert-amino effect reaction.*

Formation of the azepine ring in **5.25** results in a widening of the *exo*-angle at the point of naphthalene ring fusion from 126.4(3)º in **5.23** to 127.8(3)º in **5.25**. This widening is complimented with a narrowing of the equivalent angle between the N-C bond *peri*-groups from 113.7(3)º in **5.23** to 113.0(3)º in **5.25**. As a result of this, the long N-C bond is shortened by 0.024 Å to 1.652(4) Å, almost the same length as in the *mono*-analogue **5.24** (1.651(3) Å). The azepine ring also introduces a degree of strain into the naphthalene scaffold, with the *peri*-methylene and nitrogen groups displaced from the idealised naphthalene plane by 0.409 and -0.346 Å respectively to opposite sides of the naphthalene plane. This introduces a torsional twist along between the Me_2N^+-C bond and the *peri*-naphthalene carbons (τ^a) of -9.1(3)º

compared to the almost planar orientation of 0.5(3)^{o} in **5.23**. Azepine **5.25** demonstrates very similar ring bonds lengths (**a, b** and **c**) as the acenaphthene equivalent **3.40**-**3.42**.

*Table 5.35. Selected geometric data for azepine **5.25**.*

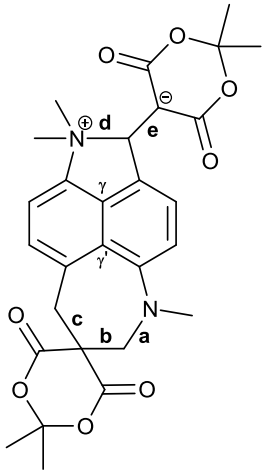

Compound	**d** / Å	**e** / Å	**γ / γ'** / ^{o}	**a** / Å	**b** / Å	**c** / Å	τ^{a} / ^{o}
5.25	1.652(4)	1.467(5)	113.0(3)/127.8(3)	1.454(4)	1.565(5)	1.541(4)	-9.1(3)

τ^{a} = torsion angle: C(Ar)-N(+)-C-C(Ar).

To conclude, we have demonstrated that the introduction of an identical nucleophile/electrophile interaction at the opposite set of *peri*-positions on a naphthalene backbone, has a notable impact on the interaction observed. For moderately weak interactions, such as those in **5.10**, **5.12**, **5.19** and **5.20** the two interactions form symmetrical structures. In the *bis*-aldehyde (**5.10**), -dinitrile (**5.19**) and -isopropyl ketone (**5.12a**) derivatives the introduction of the second set of interactions resulted in an increase in the observed Me_2N---C contact distance, whilst in the remaining *bis*-isopropyl ketone (**5.12b**) and -cyanoester (**5.20**) derivatives a decrease in the contact distance was observed. Most notable in all cases was the consistency of the *exo*-angles across the series, with all the examples falling in the range of 121.2-121.7^{o}, whereas the *mono*-analogues can deviate by up to 2.6^{o} for example in the *mono*-dinitrile analogue. When the attraction between the groups became stronger in the *bis*-Meldrum's derivative **5.23**, one set of *peri*-substituents took precedent, forming a very long N-C bond (1.676(4) Å), whilst the opposite *peri*-substituents formed an Me_2N---C=C interaction

(2.616(4) Å). The strong electrophilicity of the free polarised alkene resulted in the transfer of a hydride anion from one of the N-methyl groups, leading to the synthesis of azepine **5.25**. Azepine **5.25** demonstrates a shorter, but nevertheless long *peri* N-C bond (1.652(4) Å) as a result of the strained *para*-azepine ring system. Protonation of the *bis*-aldehyde takes place on the oxygen atom, resulting the formation of a long (1.645(2) Å) aminal N-C bond. Further protonation takes place on the opposite dimethylamino group forming a C=O---H-$N^{(+)}$ hydrogen bond, resulting in a shortened N-C aminal bond (1.603(5) at the other side of the molecule.

Investigation into Unsymmetrical Systems with One Me_2N---C Interactions

One of the by-products in the synthesis of *bis*-aldehyde **5.10** was found to be the *mono*-aldehyde **5.11**, which could have formed either as a result of incomplete lithiation or incomplete reaction with DMF. *Mono*-aldehyde **5.11** presents only one set of *peri*-interactions, but also boasts a free *para*-dimethylamino group that not only has an electron donating capability but could cause a minor Me_2N---H repulsion with the *peri*-naphthalene hydrogen atom. Consequently, the conditions for the synthesis of the *mono*-aldehyde **5.11** were adjusted in order to maximise its yield (Scheme 5.10).

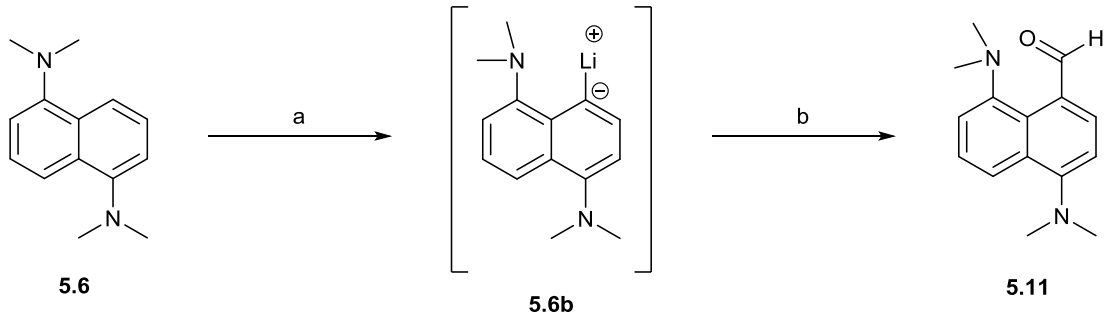

Scheme 5.42. (a) n-BuLi, hexane, reflux; (b) DMF, THF, 0 °C to RT.

In order to maximise the yield of the *mono*-aldehyde **5.11**, the equivalents of lithiating agent used was dropped, giving a 1:1 ratio of 1,5-*bis*(dimethylamino)naphthalene **5.6** and *n*-BuLi (Scheme 5.10). Previously, the precipitate formed during the reaction was isolated, with the supernatant removed and quenched. In this case, the supernatant could contain the *mono*-lithiated compound **5.6b** and thus the supernatant was kept. Finally, the equivalents of DMF added following the lithiation were reduced in order to reduce the chances of double addition in molecules where the undesired *bis*-lithiation had occurred. As a result of these changes, the desired *mono*-aldehyde **5.11** was isolated in an increased 35% yield as a low melting orange

solid. Despite numerous combinations of solvents and growing conditions, crystals of **5.11** suitable for X-ray structure determination were not obtained.

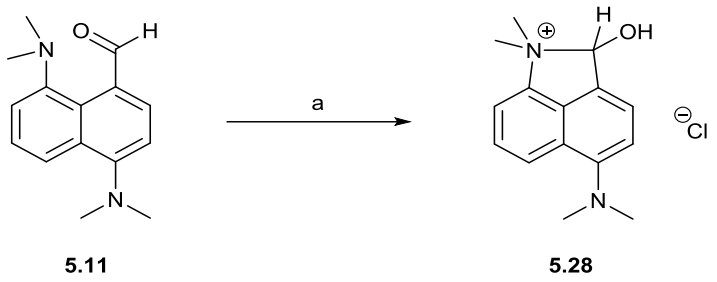

5.11 **5.28**

Scheme 5.43. (a) HCl, Et_2O, RT.

Reaction of *mono*-aldehyde **5.11** with one equivalent of ethereal hydrochloric acid in diethyl ether (Scheme 5.11), resulted in protonation of the aldehyde oxygen atom to give the aminal derivative **5.28**, which was isolated from the reaction as a beige solid in 87% yield. NMR analysis of the product confirmed the formation of the aminal structure with peaks in the ^{1}H and ^{13}C NMR spectra of 7.18 ppm and 109.1 ppm respectively for the methine group. The infrared spectrum also confirms addition to give the aminal form with no carbonyl stretching frequency observed. Unfortunately, the aminal salt **5.28** displayed a degree of hygroscopicity, with most attempts at crystallisation resulting in the formation of oils or very fine oily powders thus a structure was not obtained.

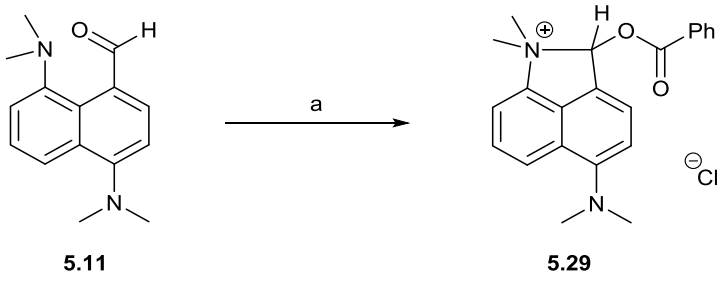

5.11 **5.29**

Scheme 5.44. (a) Benzoyl chloride, Et_2O, RT.

Benzoylated salt **5.29** was generated by the careful dropwise addition of 1M benzoyl chloride to a solution of *mono*-aldehyde **5.11** in diethyl ether (Scheme 5.12). Immediately, an orange

precipitate formed, which was collected via filtration under a nitrogen stream, due to the hygroscopic nature of the salt, in a 63% yield. The structure of the benzoylated chloride salt **5.29** was evidenced by peaks in the ^{1}H and ^{13}C NMR spectra for the methine group of 7.15 ppm and 115.7 ppm respectively. Furthermore, distinct downfield shifted resonances of 4.21/3.89 ppm and 56.9/49.4 ppm are shown in the ^{1}H and ^{13}C spectra corresponding to the aminal dimethylamino group. A carbonyl stretching frequency of 1606 cm^{-1} is observed in the infrared spectrum.

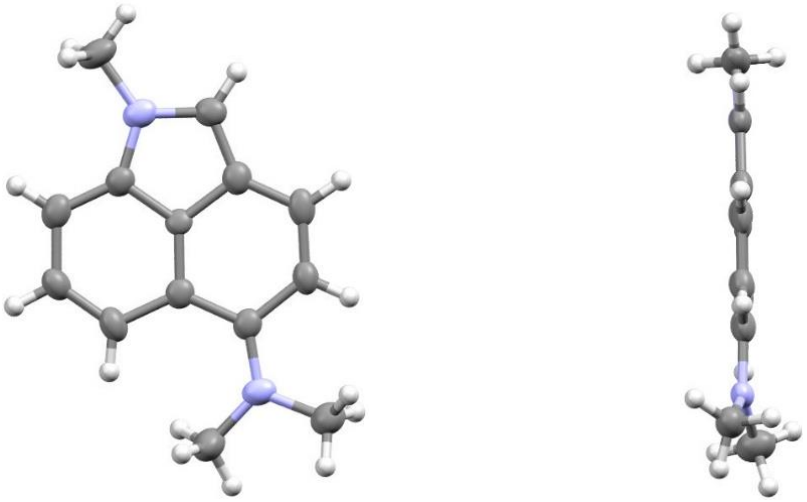

*Figure 5.91. Molecular structure of the decomposition product **5.32** (left) and a demonstration of the planar conformation of the free dimethylamino group (right).*

Crystals of the benzoylated salt **5.29** were obtained when the sample was dissolved and left in DCM over the course of a week. The thin orange needles were found to be extremely hygroscopic once removed from solution, thus the crystals were placed in a sample of silicon oil. The structure of one of these crystals was determined at 150 K (Figure 5.11) to reveal that the initial benzoylated product **5.29** had decomposed, resulting in the formation of fused ring chloride salt **5.32** (Scheme 5.12). Elimination of the benzoate to give the decomposition product **5.32**, may have resulted from the donation of the *para*-nitrogen lone pair through the naphthalene ring system, resulting in a temporary dication **5.30** (Scheme 5.13). Cleavage of an N-methyl group (**5.31**) from the *peri*-bonded dimethylamino group frees the nitrogen lone pair,

which can form a *peri* N=C double bond, restoring aromaticity to the aromatic ring. The free dimethylamino group of **5.32** remains conjugated with the N=C double bond as evidenced by its planar geometry, with the sum of the angles around the nitrogen atom adding up to 359.9º.

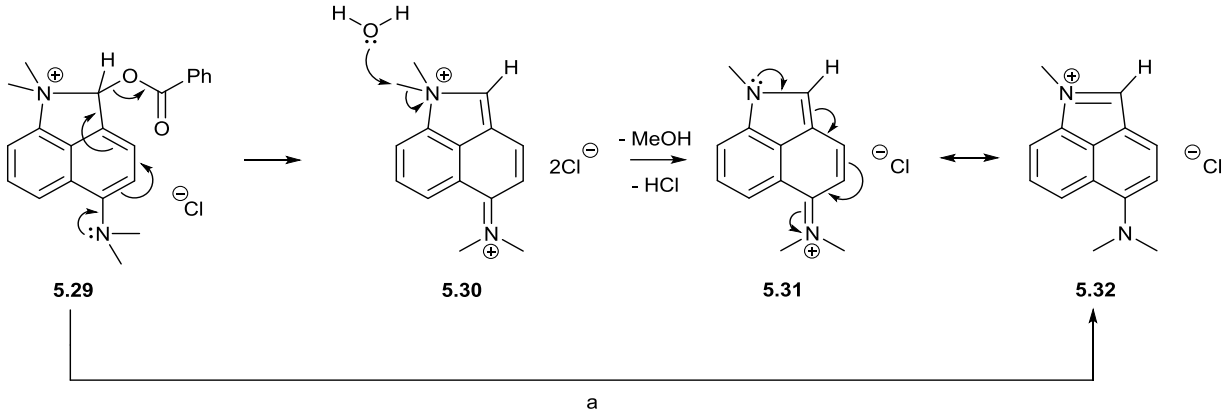

*Scheme 5.45. Proposed mechanism for the decomposition of benzoylated salt **5.29** to give the fused ring system **5.32**.*

Condensation of *mono*-aldehyde **5.11** with active methylene compounds malononitrile, methyl cyanoacetate and dimethyl malonate (Scheme 5.14) yielded the expected Knoevenagel condensation products **5.33-5.35**. In each case, aldehyde **5.11**, the chosen methylene compound and EDDA (catalyst) were refluxed in methanol, cooled, the solvent was removed, and the resultant crude orange oils were purified via flash column chromatography. Moderate yields of 72, 42 and 69% were obtained for the dinitrile **5.33**, cyanoester **5.34** and diester **5.35** derivatives respectively.

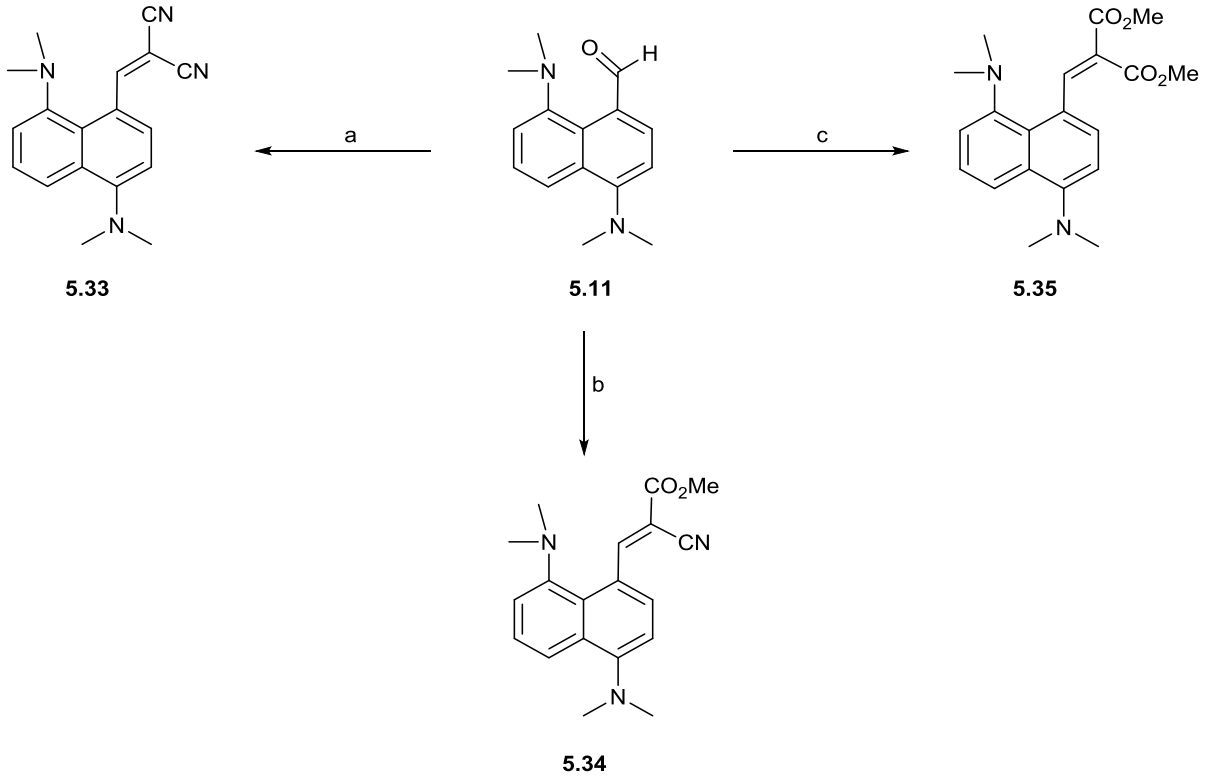

Scheme 5.46. (a) $CH_2(CN)_2$, CH_3OH, $(^+NH_3CH_2\text{-})_2(^-OAc)_2$ (cat.), 65 °C; (b) $NCCH_2CO_2Me$, CH_3OH, $(^+NH_3CH_2\text{-})_2(^-OAc)_2$ (cat.), 65 °C; (c) $CH_2(CO_2Me)_2$, CH_3OH, $(^+NH_3CH_2\text{-})_2(^-OAc)_2$ (cat.), 65 °C.

The structure of the dinitrile derivative **5.33** was confirmed by the peak in the ^1H NMR spectrum at 8.69 ppm for the vinylic proton. Furthermore, the ^{13}C NMR spectrum revealed peaks at 165.8 ppm and 115.4/114.0 ppm for the vinylic carbon and nitrile groups respectively, while a nitrile stretching frequency of 2218 cm^{-1} is observed in the infrared spectrum. Similarly, the structure of cyanoester derivative **5.34** is evidenced by resonances in the ^1H and ^{13}C NMR

spectra for the vinylic (9.16 ppm and 161.7 ppm), methoxy (3.92 ppm and 52.8 ppm) and nitrile (116.5 ppm) groups. Infrared peaks for the nitrile (2219 cm^{-1}) and ester (1718 cm^{-1}) stretching frequencies are also observed. For the diester **5.35**, the vinylic group was evidenced with peaks of 8.77 ppm and 150.8 ppm in the ^{1}H and ^{13}C NMR spectra, whilst the methyl ester groups reside at 3.85/3.61 ppm (^{1}H) and 52.7/52.1 ppm (^{13}C). A carbonyl stretching frequency of 1727 cm^{-1} is shown in the infrared spectrum for the two ester groups. In all three examples, the dimethylamino groups resonate at less than 2.93 ppm in the ^{1}H NMR, indicating further that they exist in the neutral form.

*Table 5.36. Selected geometric data for dinitrile, methyl cyanoester and methyl diester derivatives **5.33-5.35** and the unsubstituted dinitrile and methyl cyanoester analogues **5.21** and **5.22**.*

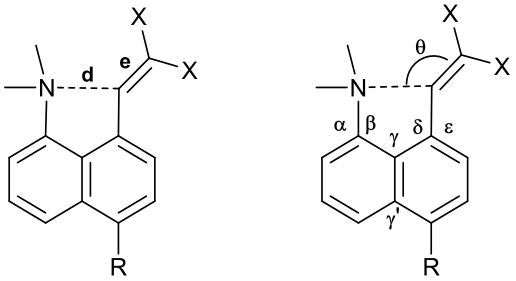

Compound	**d** / Å	**e** / Å	**θ** / º	τ^{a} / º	τ^{b} / º	τ^{c} / º
5.33a (R = NMe_2)	2.455(2)	1.356(2)	116.3(1)	54.9(3)/-77.8(2)	-10.4(2)/121.7(2)	53.1(2)
5.33b (R = NMe_2)	2.512(2)	1.350(2)	117.2(1)	43.0(3)/-90.5(2)	17.7(3)/-113.0(2)	49.9(2)
5.21 (R = H)[1]	2.413(2)	1.354(2)	112.1(1)	-49.7(2)/81.5(2)	-	-56.5(2)
5.34 (R = NMe_2)	2.482(2)	1.342(2)	110.0(1)	34.1(2)/-96.7(2)	14.4(2)/-113.4(2)	58.8(2)
5.22 (R = H)	2.595(2)	1.349(2)	116.2(1)	34.5(2)/-93.8(2)	-	55.2(2)
5.35 (R = NMe_2)	2.674(3)	1.348(3)	121.6(2)	-28.0(3)/99.8(3)	19.0(3)/-110.1(3)	-47.6(3)

Compound	**α** / º	**β** / º	**δ** / º	**ε** / º	**γ / γ'** / º
5.33a (R = NMe_2)	123.5(2)	115.8(2)	122.2(1)	119.4(2)	120.3(2)/122.7(2)
5.33b (R = NMe_2)	123.8(2)	116.1(1)	121.4(1)	119.6(2)	120.8(2)/122.8(2)
5.21 (R = H)[1]	124.3(2)	115.9(1)	120.2(1)	120.3(2)	120.4(1)/122.6(2)
5.34 (R = NMe_2)	124.0(1)	115.8(1)	120.8(1)	120.1(2)	120.7(1)/123.3(1)
5.22 (R = H)	123.2(1)	116.8(1)	122.5(1)	117.9(1)	122.6(1)/121.4(1)
5.35 (R = NMe_2)	121.5(2)	118.1(2)	122.0(2)	118.9(2)	123.7(2)/120.4(2)

τ^{a} = torsion angle interacting NMe_2: 2 x (H_3)C-N-C(Ar)-C(H), τ^{b} = torsion angle for free NMe_2: 2 x (H_3)C-N-C(Ar)-C(H), τ^{c} = torsion angle: C=C-C(Ar)-C(H).

Crystals of three Knoevenagel products **5.33**, **5.34** and **5.35** were grown via the slow evaporation of DCM, DCM/hexanes and $CHCl_3$ solutions respectively. In each case the structure of a suitable crystal was determined at 150 K, with a summary of selected geometric

data for the three Knoevenagel products **5.33**-**5.35** and their *mono*-substituted analogues (where applicable) are shown in Table 5.6. The dinitrile derivative **5.33** contains two crystallographically unique molecules in the asymmetric unit which present quite different Me_2N---C=C contacts of 2.455(2) (**5.33a**) and 2.512(2) Å (**5.33b**), both of which are a little larger than the *mono*-analogue. The former, demonstrates rotations of the dimethylamino and alkene groups (τ^a and τ^c) akin to that of the even shorter *mono*-analogue (2.413(2) Å), whilst the longer distance of the latter is accompanied with a less even distribution of the N-methyl groups to either side of the naphthalene plane, suggesting a greater degree of donation from the lone pair into the aromatic system. The *peri*-carbon of the electrophile and the *para*-dimethylamino group of **5.33a** are displaced to the same side of the idealised naphthalene plane by 0.247 and 0.129 Å respectively, whilst the interacting dimethylamino group lies directly in the naphthalene best plane. On the other hand, the *peri*-carbon in **5.33b** is displaced even further from the idealised plane (0.402 Å), with the *para* and *peri*-dimethylamino groups displaced to the opposite side by 0.144 and 0.279 Å respectively. The in-plane angular displacements of both molecules are similar to those of the *mono*-analogue, with a larger *exo*-angle (γ) observed in **5.33b** (120.8(2)^o) as a result of the increased contact distance.

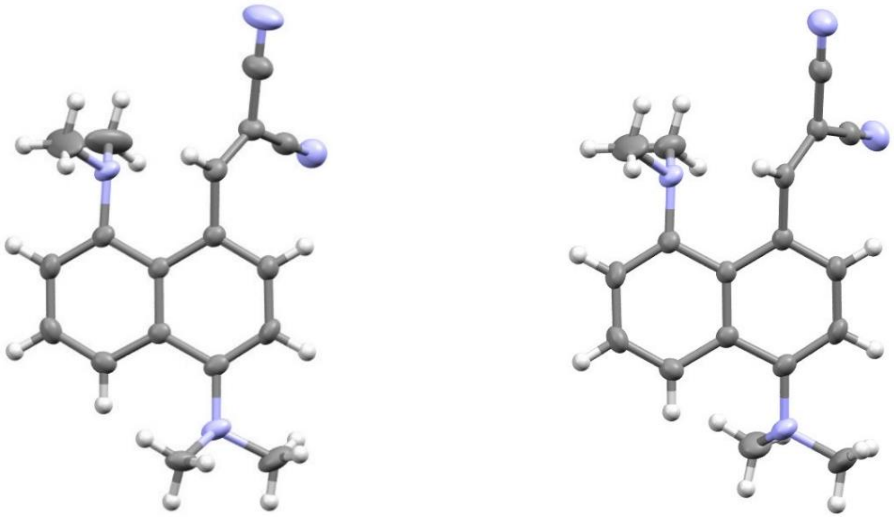

*Figure 5.92. Molecular structures of the two crystallographically unique molecules of dinitrile **5.33** (**5.33a** left and **5.33b** right).*

In contrast, the cyanoester derivative **5.34** demonstrates a reduction in the Me_2N---C=C contact distance to 2.482(2) Å from 2.595(2) Å in the *mono*-analogue (Figure 5.13). The naphthalene scaffold demonstrates a high degree of strain around its two central fusion carbons, with a torsion angle for the N-C(*peri*)-C(*peri*)-C atoms of 18.8(2)°. With respect to which ring of the naphthalene system they are substituted, the two dimethylamino groups remain close to planar, whilst the electrophile is displaced significantly. These twists and displacements result in the orientations of the N-methyl groups of the nucleophile and the alkene of the electrophile remaining very similar to their *mono*-analogue, with a more favourable Bürgi-Dunitz angle observed (110.0(1)° vs 116.2(1)°). Notable changes are observed in the angular displacements of the interacting *peri*-substituents, whereby the dimethylamino group is displaced at a larger angle toward the electrophile which shows close to no displacement. This is in stark contrast to the *mono*-analogue which shows a strong displacement of the both the nucleophile and electrophile in the same direction. Furthermore, the *exo*-angles in **5.34** have reversed with respect to those of the *mono*-analogue, as a consequence of the short contact distance.

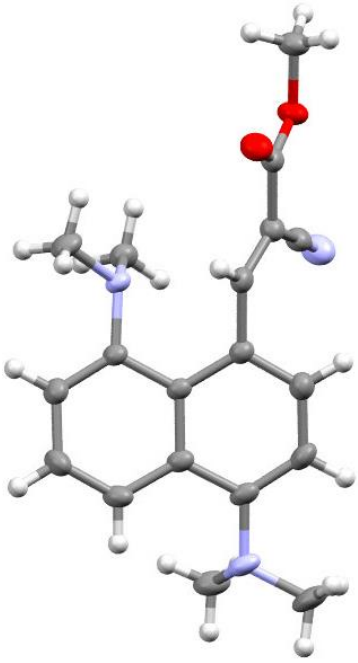

*Figure 5.93. Molecular structure of the methyl cyano ester derivative **5.34**.*

The diester derivative **5.35** demonstrates a long Me_2N---C=C contact distance of 2.674(3) Å (Figure 5.14). Consequently, the interacting dimethylamino group is rotated such that the lone pair is split between donation toward the electrophilic alkene and into the aromatic naphthalene system (τ^a). The interacting *peri*-groups shows the lowest combined angular displacement, with *exo*-angles that match the increased contact distance. The naphthalene scaffold remains planar unlike that of **5.34**, with the two dimethylamino groups displaced marginally (0.115 and -0.173 Å) to opposite sides, whereas the bulkier electrophile is displaced more significantly by 0.299 Å, a factor that contributes to the larger contact distance observed.

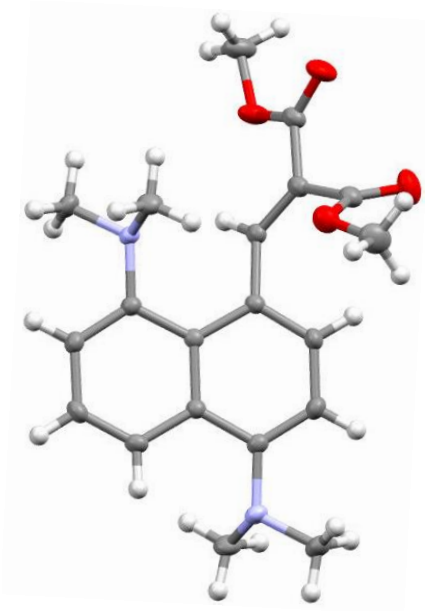

*Figure 5.94. Molecular structure of the methyl diester derivative **5.35**.*

Between all three structures, a clear trend is seen in the orientation of the free *para*-dimethylamino group. The shorter the N---C contact between the interacting *peri*-groups, the larger the angle between the nitrogen lone pair and the *peri* N---H vector; **5.33a**: 52.9°, **5.34**: 49.3°, **5.33b**: 48.1°, **5.35**: 44.4°. This results in a greater donation of nitrogen lone pair into the naphthalene ring system. Furthermore, in each case example, the nitrogen substituents are orientated in order to position the nitrogen lone pair closest to the *peri*-hydrogen atom, minimalising steric contacts between the atoms. Utilising this information, we proposed that if

the free dimethylamino group was protonated, a steric repulsion between the dimethylammonium hydrogen and the *peri*-hydrogen atoms will occur. This repulsion could result in a widening of the *exo*-angle between the two groups, akin to that of the phenyl groups studied in Chapter 4, causing the angle between the interacting *peri*-groups to become narrower.

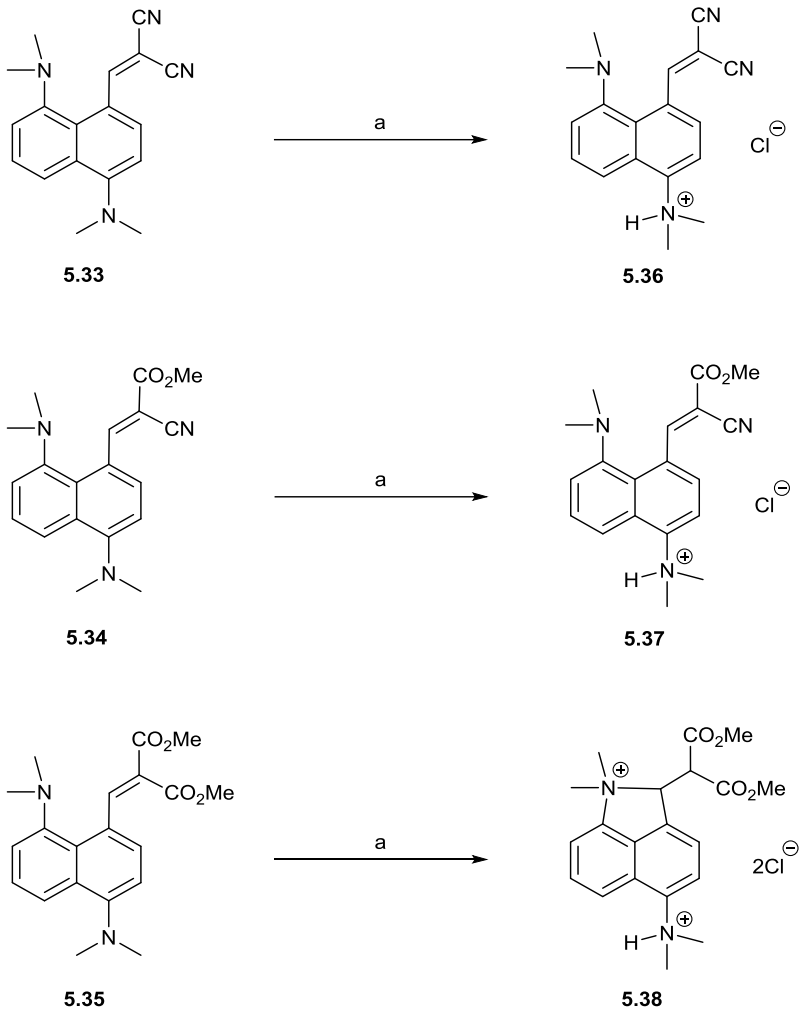

Scheme 5.47. (a) Ethereal HCl, Et_2O, RT.

In order to explore whether or not protonation would occur on the free *para*-dimethylamino group, one equivalent of ethereal HCl was added to a solution each of the three Knoevenagel products **5.33-5.35** in diethyl ether to give salts **5.36-5.38** (Scheme 5.15). Each reaction, upon addition of the acid yielded a precipitate, with each being isolated under a flow of nitrogen due

to the materials demonstrating a degree of hygroscopicity. Analysis of the products isolated from the reactions of dinitrile and cyano ester derivatives **5.33** and **5.34** were found to the desired protonated salts **5.36** and **5.37**, with the protonation occurring on the free dimethylamino group, confirmed by peaks in the ^{1}H NMR of 3.33 ppm (**5.36**) and 3.34 ppm (**5.37**). The *peri*-interaction remains in the 'open form' in both cases, with the neutral dimethylamino shifts of 2.71 and 2.64 ppm in the ^{1}H NMR spectra observed for **5.33** and **5.34** respectively. The vinylic protons and *peri*-alkene carbon are identified by peaks at 8.56/163.1 ppm (**5.33**) and 2.64/158.5 (**5.34**) in the ^{1}H and ^{13}C NMR spectra. For the diester derivative **5.35**, analysis of the isolated orange solid revealed the product to be that of the dichloride salt **5.38,** where not only the free dimethylamino group has been protonated, but so too has the former alkene carbon between the two ester moieties. As evidenced by the ^{1}H NMR peaks of 5.25 and 6.23 ppm for the methine protons and downfield resonances of 3.76 and 3.01 ppm for the $N^{(+)}$-methyl protons. The ester groups are retained as peaks in the ^{13}C NMR and infrared spectra of 167.0/166.0 ppm and 1723 cm^{-1} are observed.

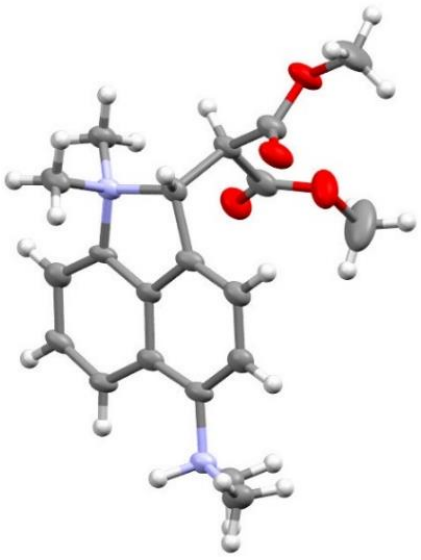

*Figure 5.95. Molecular structure of the methyl diester di-cation **5.38**.*

Rhombus shaped crystals of the dichloride salt **5.38** were isolated from an acetonitrile solution and the structure of one determined at 150 K (Figure 5.15). As suggested by the NMR data,

protonation of the free dimethylamino group has occurred as well as the formation of an N-C bond between the two *peri*-groups, with the resultant carbanion undergoing protonation. The effect of the $N^{(+)}$-H---H repulsion is difficult to assess and quantify using this example as the exo-angle contraction caused by the *para*-fully formed N-C bond naturally causes a widening of the opposite *exo*-angle between the two repelling atoms.

*Table 5.37. Selected geometric data for dinitrile derivatives **5.21**, **5.33**, **5.39**, **5.40** and **5.36** shown in Figure 5.16. Compound **5.36** has been measured at various temperatures between 90-200 K.*

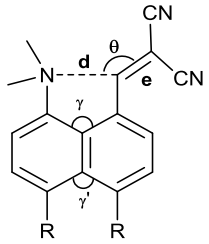

Compound	T / K	d / Å	e / Å	θ / °	γ/γ' / °	N-CH$_3$[a] / Å	N-H---H[b] / Å	τ^c / °	τ^d / °	τ^e / °
5.21[1]	150	2.413(2)	1.354(2)	112.1(1)	120.4(1)/122.6(2)	1.455(2)/1.464(2)	-	-49.7(2)/81.5(2)	-	-56.5(2)
5.33	150	2.455(2)	1.356(2)	116.3(1)	120.3(2)/122.7(2)	1.445(3)/1.451(3)	-	54.9(3)/-77.8(2)	-10.4(2)/121.7(2)	53.1(2)
		2.512(2)	1.350(2)	117.2(1)	120.8(2)/122.8(2)	1.455(2)/1.456(2)	-	43.0(3)/-90.5(2)	17.7(3)/-113.0(2)	49.9(2)
5.39	150	2.846(3)	1.348(3)	133.0(2)	128.5(2)/111.3(2)	1.460(3)/1.460(3)	-	27.5(3)/-100.8(2)	-	35.9(3)
		2.755(3)	1.343(3)	122.7(1)	127.3(2)/111.7(2)	1.455(3)/1.461(2)	-	-45.8(3)/82.1(2)	-	-51.9(3)
5.40	100	2.359(2)	1.360(3)	113.8(1)	117.7(2)/126.3(2)	1.465(3)/1.466(2)	-	37.0(3)/-94.9(2)	-	51.2(3)
5.36	200	2.167(5)	1.369(4)	113.2(2)	117.8(2)/126.5(3)	1.462(5)/1.476(4)	2.07	-48.9(5)/82.3(4)	-28.7(4)/98.2(4)	-53.0(4)
5.36	180	2.151(4)	1.374(4)	113.5(2)	117.8(2)/126.7(2)	1.460(4)/1.476(4)	2.08	-49.5(4)/81.5(4)	-29.0(4)/98.2(3)	-52.1(4)
5.36	160	2.120(4)	1.375(4)	113.5(2)	117.3(2)/126.7(2)	1.463(4)/1.477(4)	2.08	-49.2(4)/81.3(3)	-29.0(4)/97.6(3)	-51.9(4)
5.36	150	2.098(4)	1.378(4)	113.4(2)	117.1(2)/127.1(2)	1.465(4)/1.475(3)	2.09	-49.1(4)/81.0(3)	-29.1(3)/97.8(3)	-51.4(4)
5.36	140	2.046(4)	1.381(4)	114.0(2)	116.8(2)/127.4(2)	1.463(4)/1.477(3)	2.09	-49.7(4)/80.1(3)	-29.3(3)/97.4(3)	-49.8(4)
5.36	138	2.021(4)	1.384(4)	114.3(2)	116.7(2)/127.5(2)	1.468(4)/1.474(3)	2.09	-49.5(4)/79.9(3)	-29.4(3)/97.1(3)	-48.7(4)
5.36	136	1.981(4)	1.391(4)	114.6(2)	116.4(2)/127.6(2)	1.468(4)/1.476(3)	2.10	-49.5(4)/79.3(3)	-29.8(3)/97.2(3)	-47.8(4)
5.36	134	1.932(4)	1.401(4)	115.0(2)	116.0(2)/128.1(2)	1.472(4)/1.480(3)	2.11	-49.6(4)/78.6(3)	-30.3(3)/96.7(3)	-46.6(4)
5.36	132	1.888(4)	1.408(4)	115.2(2)	115.6(2)/128.4(2)	1.472(4)/1.481(3)	2.12	-49.2(4)/78.2(3)	-30.7(3)/96.2(3)	-45.6(4)
5.36	130	1.855(4)	1.415(4)	115.3(2)	115.4(2)/128.6(2)	1.478(4)/1.482(3)	2.13	-49.1(4)/77.7(3)	-30.9(3)/96.1(3)	-44.7(4)
5.36	120	1.793(4)	1.424(4)	115.8(2)	114.7(2)/129.2(2)	1.486(3)/1.487(3)	2.14	-48.2(4)/77.1(3)	-31.7(3)/95.6(3)	-43.0(4)
5.36	110	1.762(4)	1.431(3)	115.8(2)	114.5(2)/129.1(2)	1.486(3)/1.490(3)	2.14	-48.3(3)/76.8(3)	-32.0(3)/95.1(3)	-42.2(4)
5.36	100	1.749(3)	1.431(3)	115.9(2)	114.3(2)/129.3(2)	1.486(3)/1.490(3)	2.14	-48.0(3)/76.4(3)	-31.9(3)/95.2(3)	-42.0(4)
5.36	90	1.734(3)	1.437(3)	115.9(2)	114.1(2)/129.5(2)	1.489(3)/1.493(3)	2.14	-47.8(3)/76.5(3)	-32.3(3)/94.8(3)	-41.8(4)

[a] N-CH$_3$ bond lengths in the interacting dimethylamino group; [b] each hydrogen assigned via a riding model, thus the bond lengths are fixed, N-H: 0.98Å and C(Ar)-H: 0.93Å τ^c = torsion angle: 2 x C(H$_3$)-N-C(*peri*)-C(*ortho*); τ^d = torsion angle: 2 x C(H$_3$)-N(H)-C(*peri*)-C(*ortho*); τ^e = torsion angle: C=C-C(*peri*)-C(*ortho*).

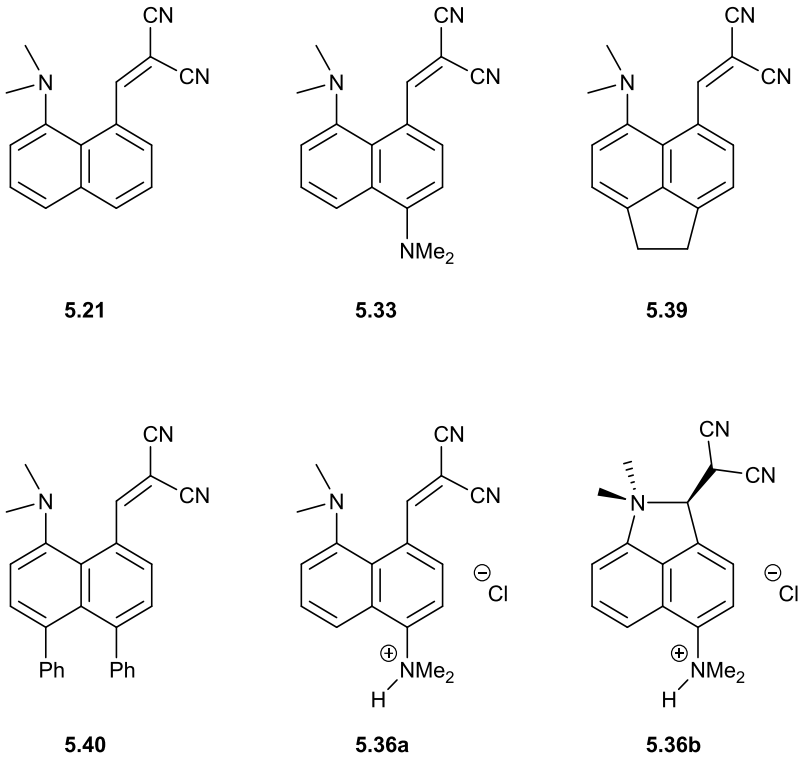

Figure 5.96. Structures of a variety of dinitrile derivatives ***5.21****,*[1] ***5.33****,* ***5.39****,* ***5.40****,* ***5.36a*** *(150 K) and* ***5.36b*** *(100 K).*

Crystals of the dimethylammonium dinitrile salt **5.36** were successfully grown via the slow evaporation of an acetonitrile solution. The salt crystallised in the orthorhombic space group *Fdd*2 with one molecule of water per two cations and two chloride anions. The crystal structure, which was determined at 150 K, demonstrates a surprisingly short Me_2N---C=C contact distance of 2.098(4) Å (Table 5.7), the results of a much more significant repulsion between the dimethylammonium group and the *peri*-hydrogen atom. This interaction lies *ca.* 1 Å within the sum of the van der Waals radii for the two interacting atoms.[11] Furthermore, this interaction is 0.31 Å shorter than the same interaction in the unsubstituted analogue **5.21** (Figure 5.16), which possess *peri*-hydrogen atoms at the opposite set of *peri*-positions. The interacting dimethylamino group is twisted, displacing its N-methyl groups unevenly relatively to the idealised naphthalene plane. This orientation is a direct consequence of the out-of-plane displacements of both the dimethylamino (0.206 Å) and dicyanoethenyl (-0.242 Å) groups from the idealised naphthalene plane. As a result, the axis of the nitrogen lone pair lies at an

angle of 7.3^{o} to the N-C vector, with a Bürgi-Dunitz approach angle (N---C=C) of 113.4(2)^{o} optimal for overlap of the nitrogen lone pair with the antibonding π^* orbital of the alkene. The N-C bond lengths of the N-methyl groups show slight elongation (1.462(5)/1.476(4)) compared to the equivalent bonds in a molecule with a larger contact distance (e.g. **5.21**: 1.455(2)/1.464(2) Å). Moreover, the alkene bond is lengthened by 0.024 Å compared to the unsubstituted equivalent **5.21**, which is measured at the same temperature, suggesting that the salt **5.36a** represents a point further along the reaction pathway for the addition of the tertiary amine to the alkene. The dimethylammonium group of **5.36a** is similarly positioned to the equivalent (unprotonated) group in **5.33**, however now the N-H proton is involved in a van der Waals contact with the *peri*-hydrogen, whereas the nitrogen lone pair in **5.33** was not. Meanwhile, the N-methyl groups have rotated slightly compared to those in **5.33**, in order to minimise steric interactions with the *ortho*-naphthalene ring proton. The *peri* N^{+}-H---H repulsion (2.09 Å) results in a widening of the *exo*-angle between the groups to 127.1(2)^{o}, with the opposite *exo*-angle narrowed to 117.1(2)^{o}, a large contribution factor to the reduced distance between the opposite *peri*-amine and alkene. The dimethylammonium group forms a hydrogen bond to the chloride anion (N---Cl distance: 3.02 Å), with a water molecule bridging two chloride anions. (Figure 5.17).

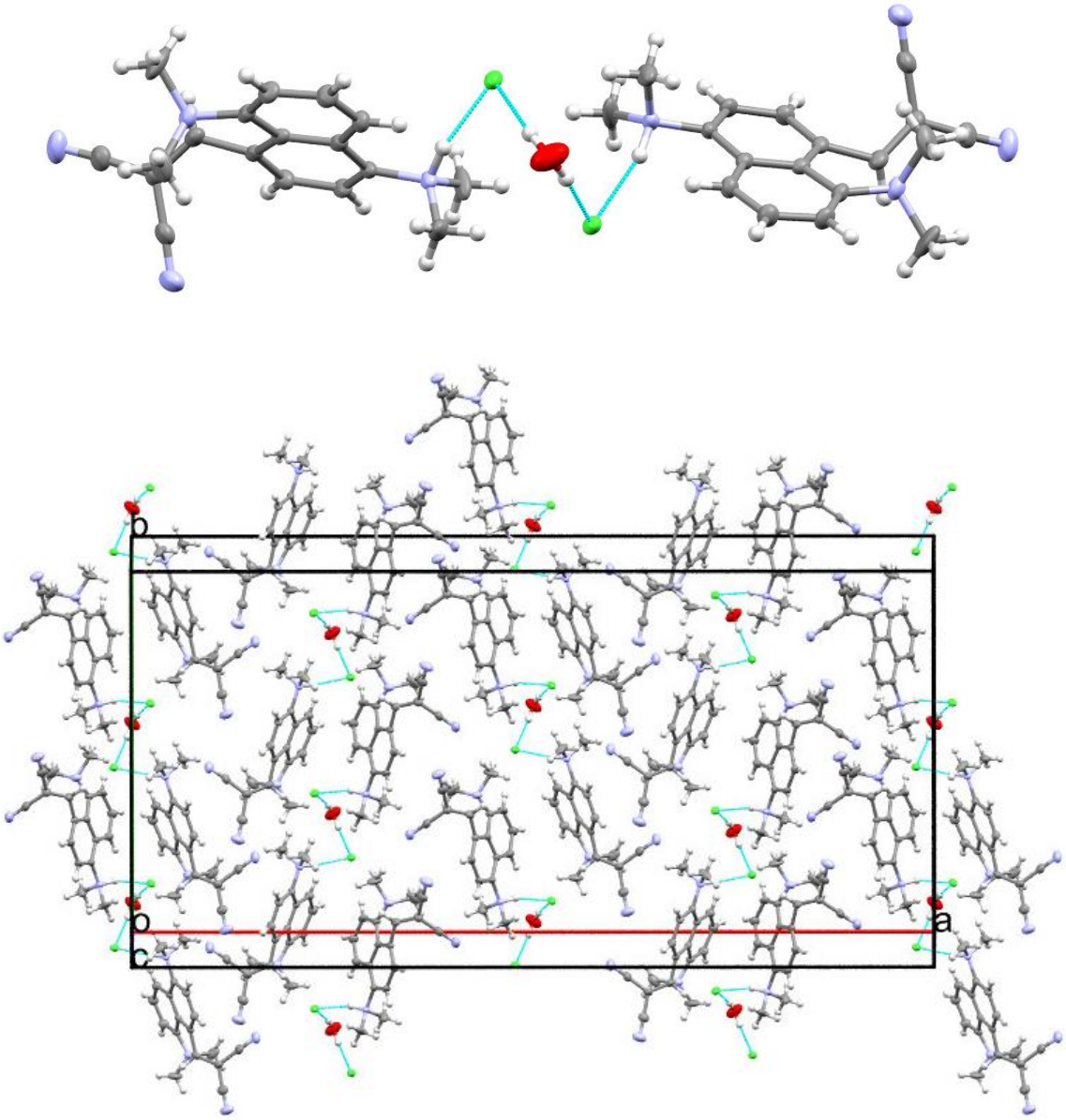

*Figure 5.97. Crystal packing for the salt **5.36a** at 150 K: a pair of chloride anions bridged by a water molecule and each forming a hydrogen bond to a **5.36a** cation (above); full crystal packing arrangement (below).*

The temperature at which the crystal structure of **5.36** was determined was lowered to 100 K, resulting in a significant change in the structure of the cation. Naturally upon cooling, the crystal lattice contracts, the contraction in this example applied significant enough pressure to the cation such that the dimethylamino and dicyanoethenyl groups were forced into even closer proximity. This enabled the two groups to react to together to form the zwitterion **5.36b**, in which the nitrogen atom is positively charged and the carbanion is stabilised by the two nitrile

groups. At 100 K, the N-methyl bonds have lengthened in response to the positive charge on the nitrogen atom, increasing from 1.465(4) and 1.475(3) Å at 150 K to 1.486(3) and 1.490(3) Å at 100 K, however they remain shorter than the dimethylammonium N-methyl bond lengths of 1.495(3) and 1.500(4) Å. The former elongated alkene bond in **5.36a** (1.378(4) Å) has broken to give a noticeably short carbon-carbon single bond (1.431(3) Å) in **5.36b** suggesting that the bond in question still maintains a degree of double bond character. A very long N-C bond has formed between the two *peri*-substituents (1.749(3) Å) which is 0.349 Å shorter than in the structure at 150 K, this bond is aligned approximately along the *c* axis of the unit cell. Contraction of the cell upon cooling (from 150 K to 100 K) does not occur in a isotropic fashion, with the most notable contraction occurring along the *c* axis by *ca.* 2.4%, smaller changes on the *a* axis (+0.7%) and the *b* axis (-0.4%) are observed. The overall packing arrangement observed at 150 K (Figure 5.17) is maintained in the structure at 100 K. As shown by the overlay of the open (150 K) and closed (100 K) forms in Figure 5.18, despite the significant alteration of the now bonded *peri*-groups, the remainder of the backbone and their relative orientations remain very similar.

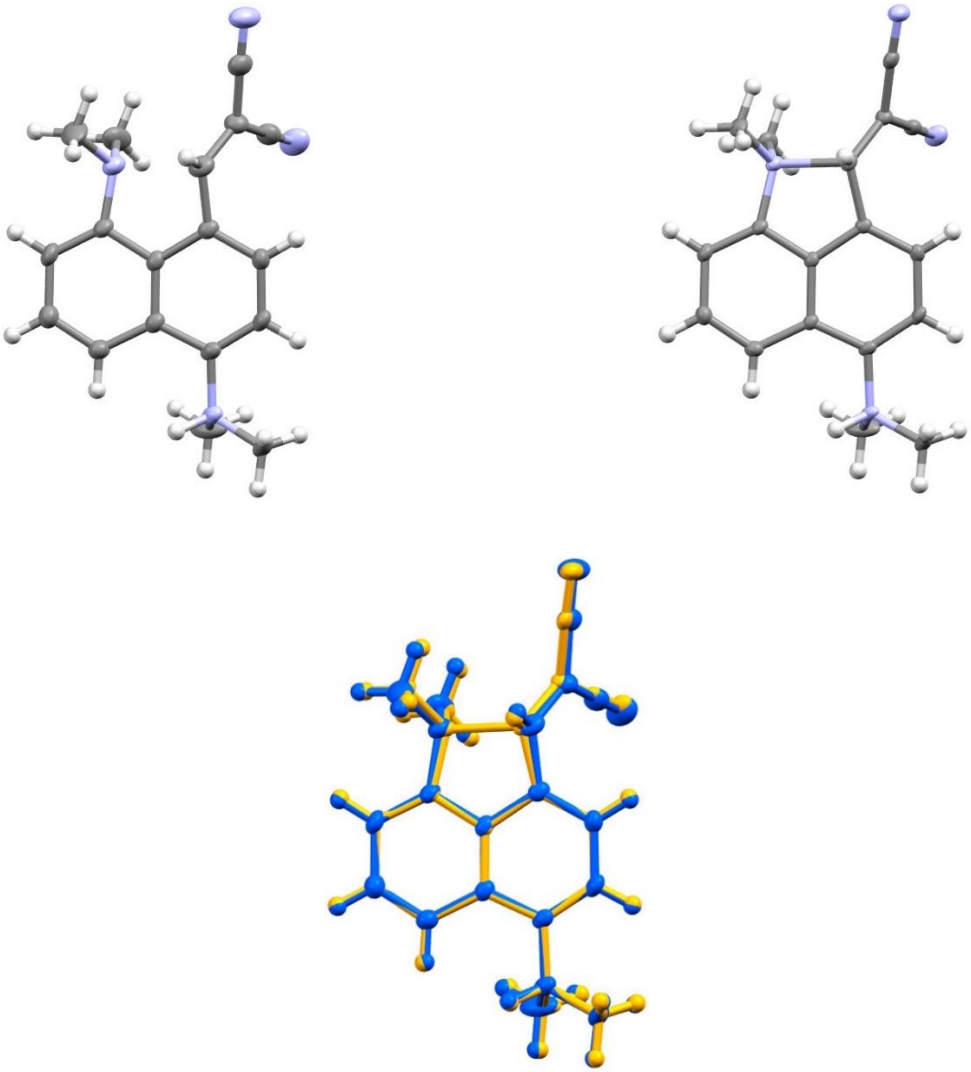

*Figure 5.98. The molecular structure of the protonated cation **5.36** at 150 K (left) and 100 K (right). An overlay of the two structures at 150 K (blue) and 100 K (yellow) demonstrates the changes in the overall skeleton (bottom).*

The data collected at 150 K and 100 K evidences the change in the *peri*-interaction but does not shed light on the nature of this conversion as the temperature is lowered. It may be that as the temperature is lowered and the cell begins to contract, the conversion may not occur until a critical pressure is applied, meaning that at a certain temperature the reaction will proceed. Or perhaps, as the cell contracts at increasingly lower temperatures, the *peri*-interaction could become narrower, with each molecule adjusting appropriately in tandem with each other. Alternatively, the structure observed could represent an average of two forms (open and closed), which at different temperatures are present in varying ratios. In order to further explore

this, the crystal structure of **5.36** was determined at a set of additional intermediate temperatures above and below the already obtained 150 K and 100 K temperatures. It is worth noting that the structural changes from the open form **5.36a** to the zwitterionic form **5.36b** are reversible, and after cooling to 100 K and warming up to 150 K the structure reverts back to **5.36a**. The most notable structural changes took place between 130 K and 140 K, so this region was explored in greater detail via smaller temperature increments of 2 K. Within these increments, a test for hysteresis was performed in that after the ramping from 140 K to 130 K, the crystal was heated back up in the same increments and recollected at each temperature. The data summarised in Table 5.8 and in the graphs in Figure 5.19 demonstrates no significant differences were observed in the crystal structure at the same temperature after the temperature variants and thus no hysteresis was observed. In the temperatures above (200-150K) and below (120-90K) this key region, the rate of change in the *peri*-interacting/bonded atoms are relatively similar and significantly smaller. From 140 to 130 K there is a sharp increase in the contact distance reduction of almost 0.2 Å, with a complimentary sharp increase is observed for the adjacent carbon-carbon bond of the alkene/alkane (Figure 5.19). This indicates that within this region lies the transition from two chemical reagents (amine and alkene) to a single bonded moiety.

*Table 5.38. Selected geometric data for dinitrile **5.36** as the temperature is increases from 130 K to 138 K.*

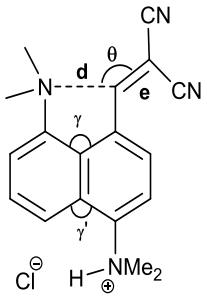

Compound	T / K	d / Å	e / Å	θ / °	γ/γ' / °	N-CH$_3$[a] / Å	N-H---H[b] / Å	τ^c / °	τ^d / °	τ^e / °
5.36	138	2.018(4)	1.392(4)	114.1(2)	116.5(2)/127.4(2)	1.468(4)/1.473(3)	2.10	-49.3(4)/79.9(3)	-29.6(3)/97.2(3)	-49.5(4)
5.36	136	1.983(4)	1.396(4)	114.4(2)	116.2(2)/127.5(2)	1.467(3)/1.478(3)	2.10	-49.4(4)/79.2(3)	-29.6(3)/97.5(3)	-48.0(4)
5.36	134	1.938(4)	1.400(4)	114.7(2)	116.0(2)/128.0(2)	1.480(3)/1.475(3)	2.11	-49.4(4)/78.5(3)	-30.2(3)/97.0(3)	-46.9(4)
5.36	132	1.894(4)	1.411(4)	115.2(2)	115.6(2)/128.2(2)	1.479(4)/1.480(3)	2.12	-48.7(4)/78.4(3)	-30.6(3)/96.8(3)	-45.6(4)
5.36	130	1.856(4)	1.416(3)	115.3(2)	115.3(2)/128.6(2)	1.478(3)/1.481(3)	2.13	-49.2(4)/77.4(3)	-30.7(3)/96.2(3)	-44.9(4)

[a] N-CH$_3$ bond lengths in the interacting dimethylamino group; [b] each hydrogen assigned via a riding model, thus the bond lengths are fixed, N-H: 0.98Å and C(Ar)-H: 0.93Å τ^c = torsion angle: 2 x C(H$_3$)-N-C(*peri*)-C(*ortho*); τ^d = torsion angle: 2 x C(H$_3$)-N(H)-C(*peri*)-C(*ortho*); τ^e = torsion angle: C=C-C(*peri*)-C(*ortho*).

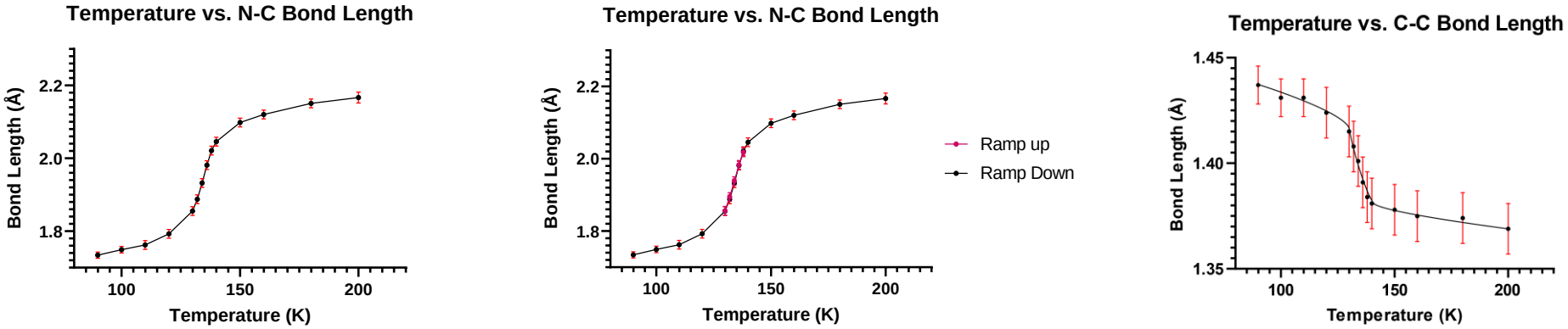

*Figure 5.99. Three graphs indicating the changes in N-C (left and middle) and C-C (right) bond lengths in dinitrile derivative **5.36** between 90-200 K.*

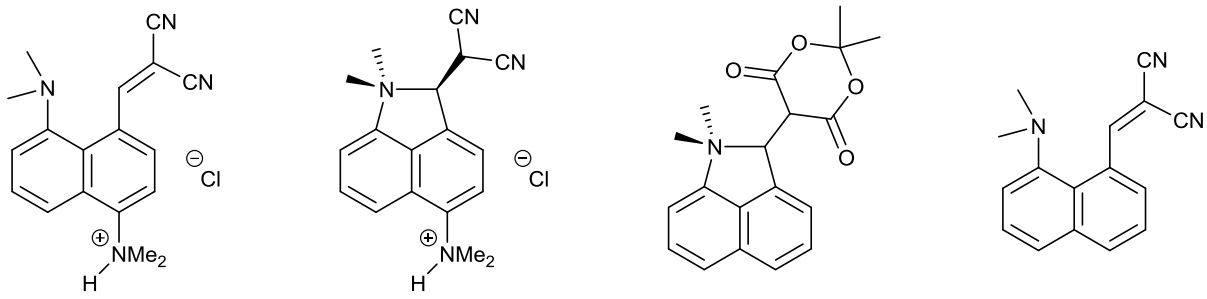

Figure 5.100. Four structures which were analysed in a charge density studies.

To explore the distribution of bonding electron density further two changes are made to the standard crystallographic procedure. First of all, great care is taken to collect as much data as possible and as accurately as possible. Secondly, after establishing the molecular structure, the electronic distributions around each atom are modelled by a series of multipolar functions, carried out with the program suite MoPro.[12] Two particular results come from this. The first is a deformation map which is the difference between this model and that obtained with just isolated atoms and so shows the accumulations and depletions of charge on the formation of bonds. Secondly the topology of the 3D total charge density map is examined as proposed by Bader.[13] A so-called (3, -1) critical point is found between bonded atoms, which are linked by a bond path which is a line of maximum electron density. The critical point is point of zero gradient in the total charge density, but combines two maxima (perpendicular to the bond) and one minimum along the bond. This point is used as a characterisation point, where the total charge density can be recorded. Furthermore, the second derivative of the charge density i.e. the rate of change of the density, known as the Laplacian, is measured. This value is typically strongly negative for bonding regions, but positive for weak interactions. Thus, in unpublished work from the Wallis/Coles groups the charge densities of several naphthalenes with *peri*-interactions or bonds between Me_2N group and an electrophilic double bond have been determined, with only negative Laplacians for the compounds with Me2N-C < 1.65 Ang (Tables 5.9 and 5.10). What is lacking is an exploration of the region 1.65-2.41 Å, for this

reason the charge density distributions for the chloride salt **5.36**, was determined at 150 and 100 K, in collaboration with Dr. Wim Klooster at the National Crystallographic Service at the University of Southampton.

*Table 5.39. Charge density parameters at the N---C (3, -1) critical point for compounds **5.36a**, **5.36b**, **5.24** and **5.21**.*

Compound	**T** / K	**d** /Å	**ρ** / eÅ^{-3}	**Laplacian** / eÅ^{-5}
5.36a	150	2.098(4)	0.403	+3.771
5.36b	100	1.749(3)	0.866	+0.859
5.24	100	1.6467(5)	1.195	-2.924
5.21	100	2.416(2)	0.213	+2.199

*Table 5.40. Charge density parameters at the alkene/alkane C-C (3, -1) critical point for compounds **5.36a**, **5.36b**, **5.24** and **5.21**.*

Compound	**T** / K	**d** /Å	**ρ** / eÅ^{-3}	**Laplacian** / eÅ^{-5}
5.36a	150	1.378(4)	2.346	-23.633
5.36b	100	1.431(3)	2.030	-15.677
5.24	100	1.4703(5)	1.812	-13.019
5.21	100	1.3659(2)	2.250	-20.098

Data at the (3, -1) critical points found for the N---C and C-C(CN)$_2$ interactions/bonds in **5.36** at 100 and 150 K are given in Tables 5.9 and 5.10 along with the corresponding data from the charge density determination, at 100 K, of Meldrum's acid and dinitrile derivatives **5.24** and **5.21** (Figure 5.20). The charge density data for **5.24** and **5.21** was measured earlier by Dr. Mateus Pitak in collaboration with the Wallis group and will be published soon. For the N---C interaction, on cooling from 150 to 100 K, the charge density has increased from 0.403 to 0.866 eÅ^{-3} an intermediate amount of bond formation between the dinitrile **5.21** (0.213 eÅ^{-3}) and the Meldrum's derivative **5.24** (1.195 eÅ^{-3}). There is also a decrease in the size of the Laplacian, consistent with greater degree of bond formation. Further data for Meldrum's derivative **5.24** suggests a fully formed N^{+}-C(H$_3$) bond has a charge density about 1.6 eÅ^{-3} and a Laplacian of -8.5 eÅ^{-5}. For the C-C alkene/alkane bond, the charge density decreases on cooling, with the weakening of the bond and the Laplacian increases. These values fit nicely in between the corresponding values for the dinitrile and Meldrum's derivatives **5.21** and **5.24**, with longer and short N-C interactions respectively.

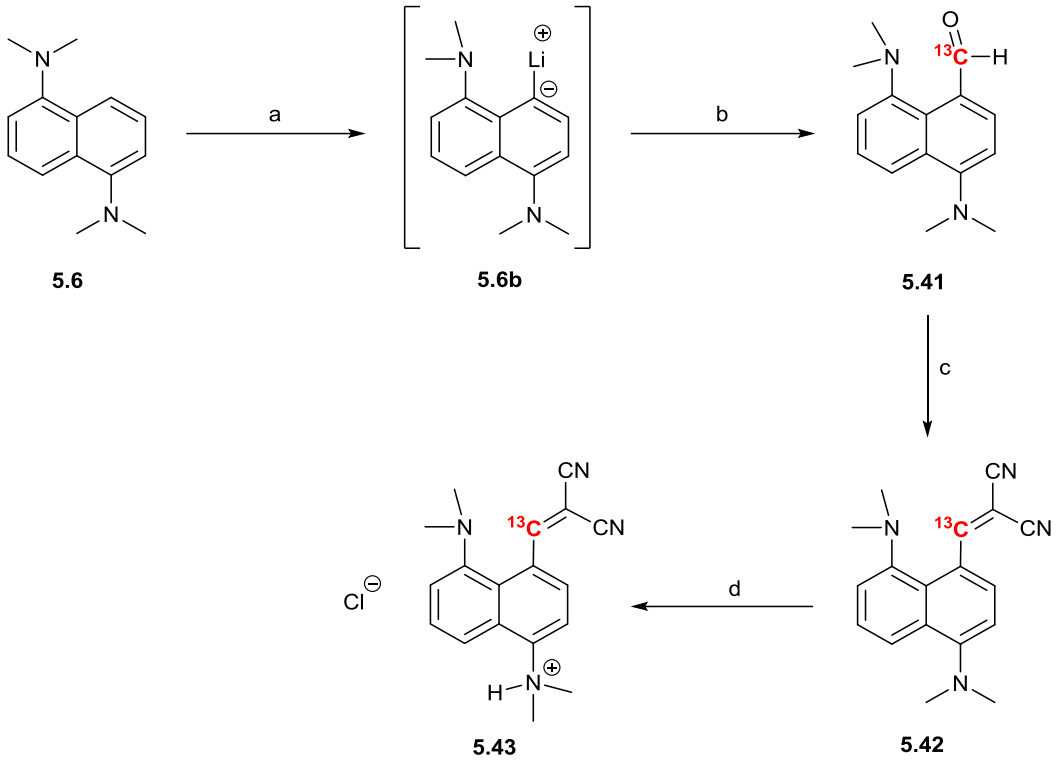

Scheme 5.48. (a) n-BuLi, hexane, reflux; (b) Carbonyl-^{13}C DMF, THF, 0 °C to RT; (c) $CH_2(CN)_2$, CH_3OH, $(^+NH_3CH_2)_2(OAc)_2$ (cat.), 65 °C; (d) Ethereal HCl, Et_2O, RT.

The data obtained across the temperature range for compound **5.36** confirmed that as the temperature was reduced, the molecules in the unit cell proceeded along the reaction pathway for the Michael addition of a nucleophile to a *peri*-electrophile. However, the structural data does not confirm whether the molecules are all partaking in the same structural changes at once, or whether the structure observed is an average of the two forms **5.36a** and **5.36b** in varying ratios. To solve this problem, we sought to conduct solid state NMR (SSNMR) analysis on the crystals of **5.36** with a particular focus on the *peri*-carbon atom of the alkene. We chose to monitor this atom due to its significant and notable shift during the structural transformation from **5.36a** to **5.36b**, as the vinylic proton (*ca.* 160 ppm) is converted to the methine group (*ca.* 100 ppm). Due to the low natural abundance of ^{13}C (1%), the synthetic pathway for the synthesis of **5.36** was adapted in order to enrich this carbon in ^{13}C (Scheme 5.16). Following the *mono*-lithiation of **5.6**, N,N-dimethylformamide-(carbonyl-^{13}C 99 atom %) was added to

the lithiated salt **5.6b** with the ^{13}C enriched aldehyde **5.41** isolated as an orange solid in a 35% yield. A small portion of the ^{13}C enriched *bis*-aldehyde was also isolated in a 10% yield. The successful addition of the desired carbonyl was confirmed by a peak in the ^{1}H NMR at 10.41-10.88 ppm for the aldehyde proton with a large ^{1}H-^{13}C coupling constant of 186.4 Hz. The most dominant peak in the ^{13}C NMR spectrum of 191.5 ppm corresponds to the enriched carbon atom of interest. Condensation of the aldehyde **5.41** with malononitrile under the same conditions as described for **5.33** yielded the desired enriched dinitrile derivative **5.42** as an orange solid in a 64% yield. The vinylic proton of **5.42** in the ^{1}H NMR is identified as a doublet peak at 8.50-8.93 ppm with a large ^{1}H-^{13}C coupling constant of 172.8 Hz. The transformation from an aldehyde to an alkene causes the ^{13}C NMR peak to shift from 191.5 ppm to 165.3 ppm. Finally, the enriched dinitrile **5.42** was protonated via the addition of ethereal HCl yielding a yellow precipitate **5.43**, which was isolated in a 60% yield. The structure of the hygroscopic solid, which was isolated under a flow of nitrogen, was confirmed by a broad doublet at 8.90 ppm in the ^{1}H NMR spectrum which matched that of the non-enriched compound **5.36**. The vinylic ^{13}C atom was found to resonate at 162.5 ppm in the ^{13}C NMR spectrum. Crystals of **5.43** were obtained via slow evaporation of an acetonitrile solution, which eventually yielded yellow needles of the desired salt **5.43**. These crystals were screened via X-ray crystallography to ensure that the crystals obtained were of the same polymorph as those investigated in the previous temperature variant study, which they were.

Preliminary results have been obtained by Dr. Ivo Heinmaa at the National Institute of Chemical Physics and Biophysics in Tallinn, Estonia by recording a CPMAS (Magic Angle Spinning) spectrum at 90 MHz at different temperatures, which are shown in Figure 5.21.

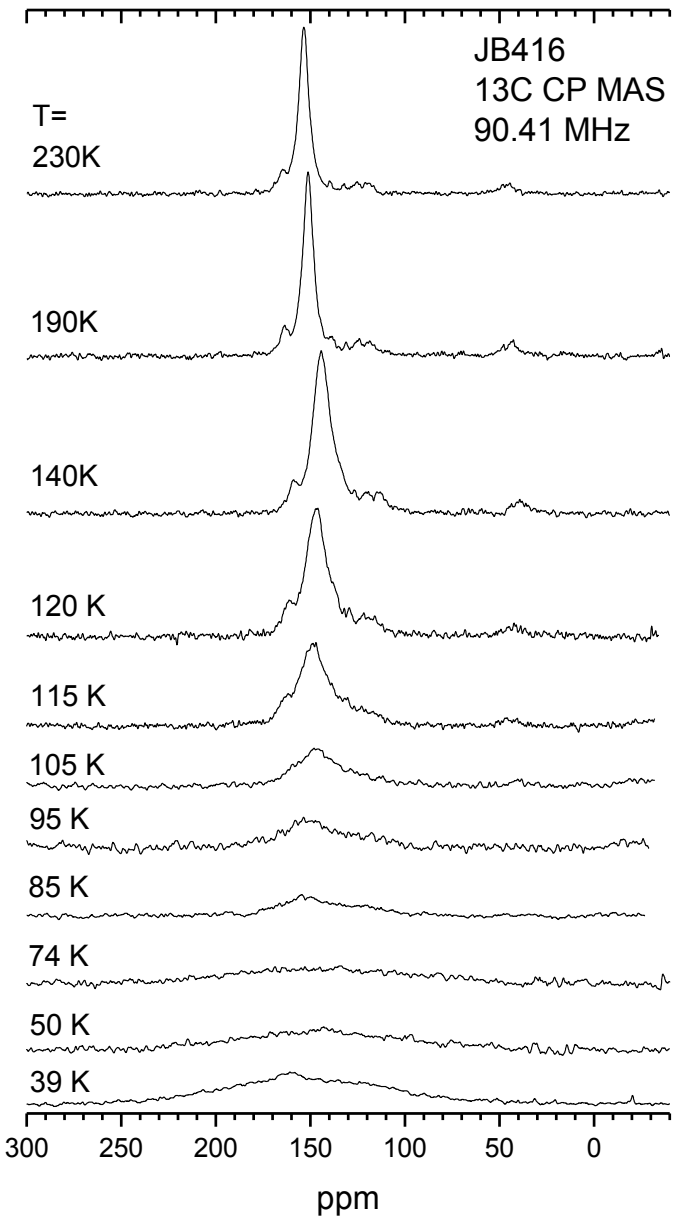

*Figure 5.101. CPMAS spectrum at 90 MHz for the carbon enriched dinitrile derivative **5.43** over a range of temperatures 39-230 K.*

At 230 K, the labelled carbon appears at *ca.* 154 ppm and as temperature decreases this peak shifts upfield slightly reaching *ca.* 146 ppm at 140 K. By 120 K this peak starts to shift downfield, and at temperatures lower than this, the signal collapses, with barely any signal

observed at 74 K and on further cooling a very broad signal is seen at 39 K. At 120 K the measured bond length is 1.793(4) Å and the solid state NMR results suggest that this bond is still only partially formed since for the known Meldrum's derivative **5.24**, with a N-C bond of 1.651(3) Å (150 K), the SSNMR at room temperature shows a clear sp^3-C signal at 94 ppm. In summary the charge density and SSNMR data suggest that even at low temperature, the N-C bond is only partially formed and the alkene only partially broken.

*Table 5.41. Selected geometric data for methyl cyanoester **5.34** at 150 K and its chloride salt **5.37** at 260, 150 and 100 K.*

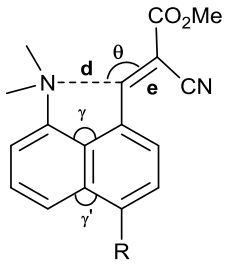

Compound	T / K	d / Å	e / Å	θ / º	γ/γ' / º
5.34	150	2.482(2)	1.342(2)	110.0(1)	120.7(1)/123.3(1)
5.37	260	1.753(6)	1.443(5)	115.5(3)	114.1(3)/128.9(4)
5.37	150	1.705(3)	1.452(3)	115.2(2)	113.7(2)/129.0(2)
5.37	100	1.697(4)	1.453(4)	115.3(2)	113.7(2)/129.4(2)

Compound	N-CH_3[a] /Å	N-H---H[b] / Å	τ^c / º	τ^d / º	τ^e / º
5.34	1.461(2)/1.462(2)	-	34.1(2)/-96.7(2)	14.4(2)/-113.4(2)	58.8(2)
5.37	1.485(4)/1.489(5)	1.97	-56.2(5)/67.1(5)	-37.0(5)/89.7(5)	-46.4(6)
5.37	1.490(3)/1.497(3)	2.14	-55.7(3)/66.7(3)	-36.5(3)/89.7(3)	-45.7(3)
5.37	1.489(3)/1.496(3)	2.15	-55.7(4)/66.7(3)	-36.3(3)/89.5(3)	-45.3(4)

[a] N-CH_3 bond lengths in the interacting dimethylamino group; [b] each hydrogen assigned via a riding model, thus the bond lengths are fixed, N-H: 0.98Å and C(Ar)-H: 0.93Å τ^c = torsion angle: 2 x C(H_3)-N-C(*peri*)-C(*ortho*); τ^d = torsion angle: 2 x C(H_3)-N(H)-C(*peri*)-C(*ortho*); τ^e = torsion angle: C=C-C(*peri*)-C(*ortho).*

Crystals of the dimethylammonium cyanoester salt **5.37** were also grown via slow evaporation of an acetonitrile solution. Surprisingly, the salt crystallised in the same orthorhombic space group as the dinitrile equivalent **5.36** (*Fdd*2) with one molecule of water per two cations and two chloride anions. In addition to this, the unit cells of both of the compounds **5.36** (**a**: 44.36 Å, **b**: 22.77 Å, **c**: 7.04 Å) and **5.37** (**a**: 48.25 Å, **b**: 22.79 Å, **c**: 6.67 Å) are remarkably similar to one another, with the most notable difference shown in the *a* axis. Consequently, the molecules of **5.37** pack in a very similar manner to that of **5.36** (Figure 5.22), with the major difference in the asymmetric unit being the substitution of the *trans*-nitrile moiety for the methoxy ester.

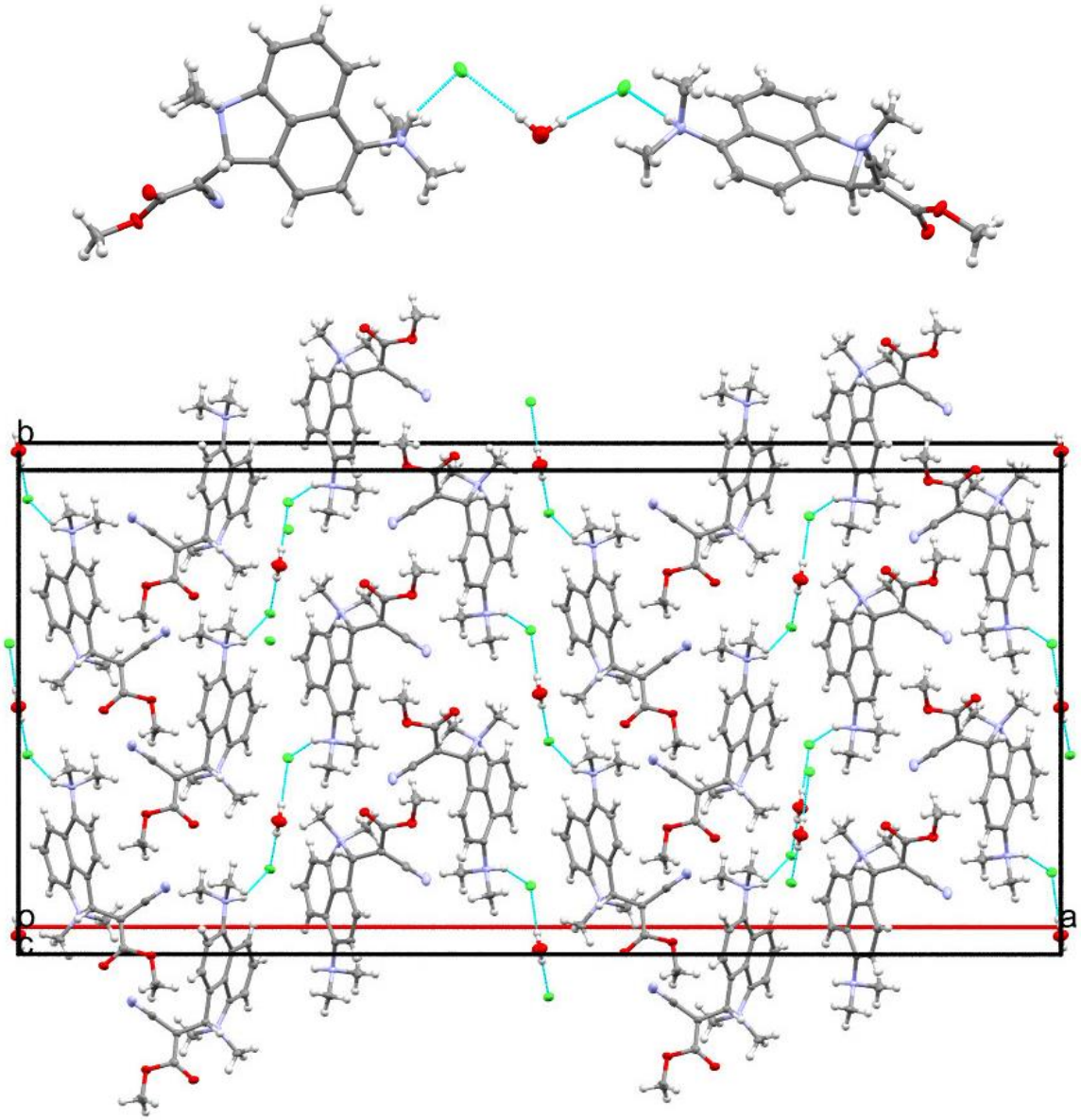

*Figure 5.102. Crystal packing for the salt **5.37** at 150 K: a pair of chloride anions bridged by a water molecule and each forming a hydrogen bond to a **5.37** cation (above); full crystal packing arrangement (below).*

Initially, the structure of cyanoester **5.37** was determined at 150 K (Table 5.11) and despite the similarities with the dinitrile salt **5.36**, the structure was found to reside in the closed form (Figure 5.23). The structure exhibits a long N-C bond of 1.705(3) Å, with the adjacent former alkene bond elongated to 1.452(3) Å. The *exo*-angle between the now bonded *peri*-groups has narrowed (113.7(2)^{o}) resulting in a widening of the opposite *exo*-angle to 129.0(2)^{o}, increasing the contact distance between the dimethylammonium hydrogen atom and the *peri*-hydrogen, with a N-H---H contact distance of 2.14 Å.

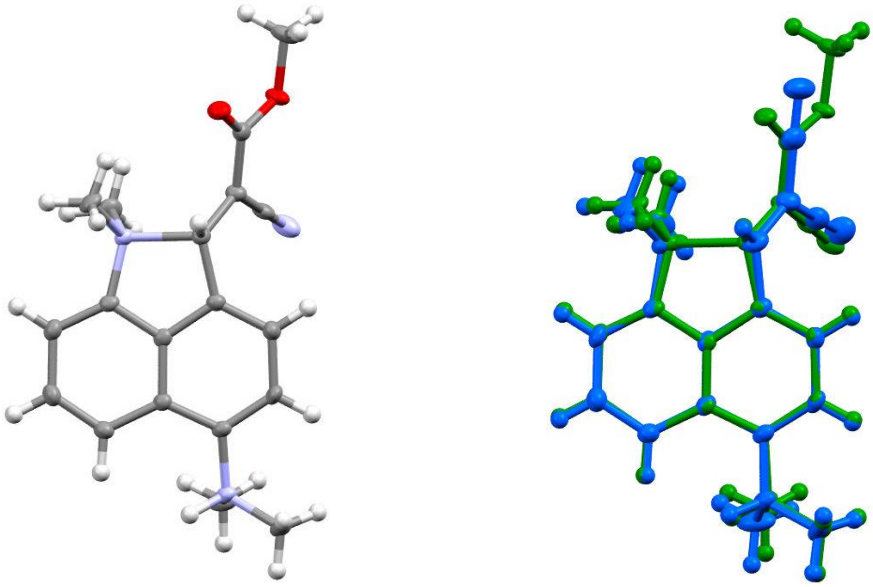

*Figure 5.103. The molecular structure of the methyl cyanoester cation **5.37** at 150 K (left). An overlay of the methyl cyano ester **5.37** (green) and the dinitrile **5.36** (blue) cations at 150 K (right) demonstrates the similarities between the two molecules.*

The structure of cyanoester **5.37** was also determined at 260 and 100 K in order to assess whether the crystal underwent the same transformations as that of the dinitrile salt **5.36**. A contraction (albeit minor) was observed on the unit cell but only in the *a* (-0.7%) and *c* (-0.2%) axes, with no change occurring in the *b* axis when the crystal was cooled from 260 to 100 K. The zwitterionic N-C bonded structure of **5.37** was maintained when the crystal was warmed to 260 K, with an elongation of 0.048 Å and a reduction of 0.009 Å observed for the N-C and C-C bonds of the zwitterion respectively. Further to this and in alignment with the data obtained for **5.36** across a larger temperature range, the elongation of the N-C bond allows for a widening of the *exo*-angle between the *peri*-bonded atoms, narrowing the opposite *exo*-angle. Consequently, there is an increase in the steric repulsion between the *peri* and dimethylammonium hydrogen atoms, due to a shorter N-H---H contact (1.97 Å). Cooling of the crystal from 150 to 100 K has very little impact on the observed structural data, unlike in the same 50 K range for the dinitrile salt **5.36**. This compound is a potential candidate for SSNMR studies for comparison with the previous described work on dinitrile derivative **5.36** but having a shorter N-C bond which shows a lower sensitivity to temperature.

*Table 5.42. Selected geometric data for a range of dinitrile (**1.100**, **3.21**, **3.38b**, **4.16**, **5.21**, **5.33a/b** and **5.36a/b**) and the cyanoester (**1.98**, **4.18**, **5.22** and **5.37**).*

Compound	**T** / K	**d** / Å	**e** / Å
1.98[14]	150	2.941	1.350
3.21	150	2.830	1.340
3.38b	150	2.755	1.343
5.22	150	2.595	1.349
5.33b	150	2.512	1.350
5.33a	150	2.455	1.356
5.21[1]	150	2.413	1.354
4.16	100	2.359	1.360
5.36a	150	2.089	1.378
5.37	260	1.753	1.443
5.36b	100	1.749	1.431
5.37	100	1.697	1.453
4.18	150	1.672	1.454
1.100[14]	150	1.604	1.493
1.100[14]	150	1.586	1.487

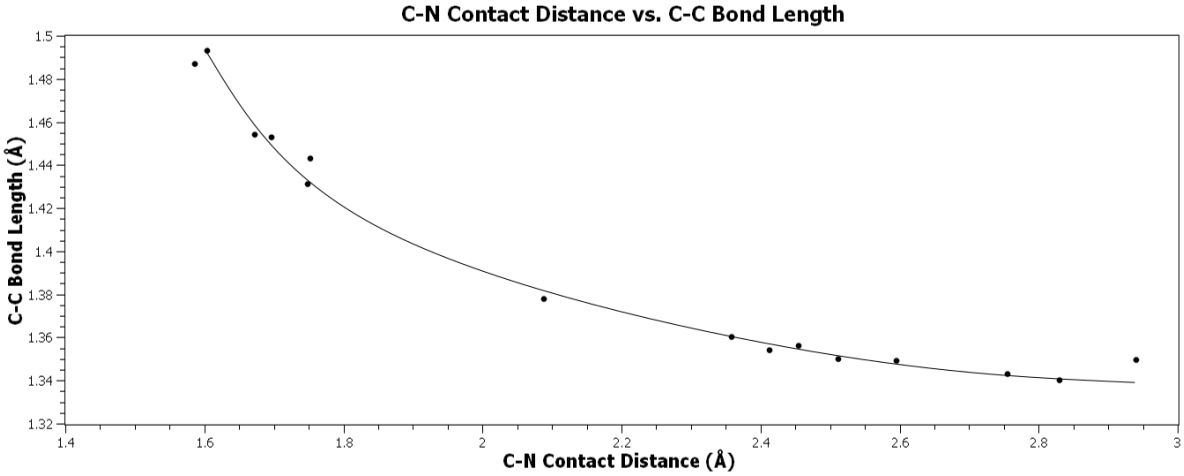

Figure 5.104. Graph demonstrating the correlation between a decrease in the N---C contact distances and an increase in the adjacent C=C/C-C bond length.

The structural data relating to N-C bond formation and C=C breaking obtained both by Wallis *et al.*[1,14] and in this thesis for the interactions of a dimethylamino group with either a dinitrile or cyanoester terminally substituted alkene is summarised in Table 5.12. The data for ethenedinitriles and ethencyanoesters are combined since their interactions in a given system are reasonably similar. The data (plotted in the graph in Figure 5.24) demonstrates a clear trend that as the N---C contact distance (d) reduces, eventually forming a bond, the length of the corresponding alkene bond (e) increases. This increase is indicative of the breaking of the

alkene bond to give an alkane bond as the N-C bond is formed. The dinitrile and cyanoester chloride salts **5.36** and **5.37** are examples of structures with N---C distances in the range 2.3-1.7 Å are of significant importance as lengths in this range have not been observed before. Further work in this area to extend the diversity of structures in the least explored range relating to compounds **5.36** and **5.37** could include making salts with alternative anions, seeking out alternative polymorphs and making small structural modifications to the naphthalene scaffold. Further structures in this region will help complete a map of the reaction coordinate for the Michael addition of an amine to a polarised alkene, and studies of their charge density distributions may help identify the position of the transition state for such a reaction.

Experimental

General. Solution NMR spectra were measured on a Jeol ECLIPSE 400 spectrometer at 400 MHz for ^{1}H and at 100.6 MHz for ^{13}C using $CDCl_3$ as solvent and tetramethylsilane (TMS) as standard unless otherwise stated, and measured in p.p.m. downfield from TMS with coupling constants reported in Hz. IR spectra were recorded on a Perkin Elmer Spectrum 100 FT-IR Spectrometer using Attenuated Total Reflection sampling on solids or oils and are reported in cm^{-1}. Mass spectra were recorded at the EPSRC Mass Spectrometry Centre at the University of Swansea. Chemical analysis data were obtained from Mr Stephen Boyer, London Metropolitan University.

Carbon ^{13}C CP MAS NMR spectra were recorded on Bruker AVANCE-II spectrometer at 8.5 T magnetic field, with ^{13}C resonance frequency 90.41 MHz using a cryoMAS NMR probe for 1.8 mm od Si_3N_4 rotors and a He-flow cryostat from Janis Research Inc. The temperature was controlled by a LakeShore '332' temperature controller and Cernox temperature sensors. According to earlier calibrations the temperature of rotating sample was 5% higher than the read-out temperature of the controller and was corrected correspondingly.

Spin-lattice relaxation times of carbons were measured in a 14.1 T magnetic field with 4 mm sample. It turned out, that the relaxation of carbons is very slow, T_1^{13C} = 170 s, whereas the relaxation of protons is conveniently fast: T_1^{1H} = 0.94 s at 300 K and 13 s at 39 K (at 360 MHz, 8.5 T field). It was not possible to record ^{13}C MAS NMR spectrum at 8.5 T with cryoMAS probe with simple one pulse excitation, despite the ^{13}C enriched sample. Therefore, in all cryoMAS experiments a 2 ms cross polarization (CP) was used. The sample spinning speed in cryoMAS experiment was 22.5 kHz. At that high spinning speed the proton decoupling at comparatively low power level was not effective and the resolution in cryoMAS spectra is lower than that in the spectrum recorded at 14.1 T field. In a N2 atmosphere, the RF amplitudes

at CP were approximately 78 and 55 kHz for ^{1}H and ^{13}C, respectively. Due to the arcing of long CP pulses in a He atmosphere, the RF power was turned down to 32 and 18 kHz, respectively. At CP low power levels the signal was about 1.5 times smaller. The spectrum in figure 5.21 was recorded in N2 atmosphere down to 85 K, and below that, in He atmosphere. The intensities are normalized by the number of scans.

Preparation of 4,8-Bis(dimethylamino)naphthalene-1,3-dicarbaldehyde, 5.8.

To an ice cold solution of anhydrous DMF (3 mL), phosphoryl chloride (1.56 mL, 16.82 mmol) was added and stirred for 30mins.[9] 1,5-*Bis*(dimethylamino)naphthalene[8] **5.6** (1.50g, 7.01 mmol) in anhydrous DMF (7 mL) was added dropwise and the solution was stirred for a further 30mins before being heated to 35ºC for 1h. The reaction was cooled and poured onto a mixture of ice/NaOH solution (37% w/v). The solution was extracted with EtOAc (3 x 30 mL) and the combined organics were washed with water (1 x 30 mL), 10% LiCl solution (2 x 30 mL), brine (1 x 30 mL), dried over $MgSO_4$ and filtered. The solvent was removed *in vacuo* to give a yellow/green oil which was purified by flash column chromatography (1:1 EtOAc/petrol 40-60), to give **5.8** as a yellow solid (0.40 g, 21%), m.p. 95-98℃. δH (400 MHz, $CDCl_3$, 24 °C): 10.42 & 10.34 (2H, s, 1, 3-C*H*O), 7.94 (1H, d, J = 8.5 Hz, 5-*H*), 7.85 (1H, s, 2-*H*), 7.49 (1H, t, J = 8.1 Hz, 6-*H*), 7.37 (1H, d, J = 7.4 Hz, 7-*H*), 3.22 (6H, s, 4-N(CH_3)$_2$), 2.65 (6H, s, 8-N(CH_3)$_2$); δC (100 MHz, $CDCl_3$, 24 °C): 191.1 & 189.8 (1-, 3-*C*HO), 157.3 (8-*C*), 150.9 (4-*C*), 133.6, 133.5, 133.4, 128.4 (Ar-C_4), 127.0 (6-*C*), 124.4 (2-*C*), 122.5 (5-*C*), 120.7 (7-*C*), 46.3 & 44.9 (4, 8-N(*C*H_3)$_2$); ν_{max}/cm^{-1} 2862, 2832, 2791, 1664 (C=O), 1600, 1581, 1559, 1507, 1449, 1382, 1360, 1315, 1177, 1157, 1053, 1038, 1012, 972, 952, 814, 775; Found: C, 71.27; H, 6.74; N, 10.20%. Calc. for $C_{16}H_{18}N_2O_2$: C, 71.02; H, 6.66; N, 10.36%.

Preparation of 4,8-Bis(dimethylamino)naphthalene-1,5-dicarbaldehyde, 5.10.

In a three-neck flask, 1,5-*bis*(dimethylamino)naphthalene **5.6** (4.00 g, 18.69 mmol) was dissolved in anhydrous hexanes (30 mL) and stirred whilst *n*-BuLi (1.6M in hexanes, 35.00 mL, 56.07 mmol) was steadily added at room temperature. The solution was refluxed for 3 days, over which a light brown precipitate formed.[10] The reaction was cooled, the precipitate was allowed to settle and the supernatant was then removed. The solid was suspended in anhydrous THF (25 mL), cooled to 0ºC and anhydrous DMF (5.79 mL, 74.76 mmol) added, the solution was left to stir for 24h. The yellow/brown solution was quenched with H_2O (30 mL) and the reaction was extracted with EtOAc (3 x 50 mL). The combined organics were washed with brine (1 x 50 mL), dried over $MgSO_4$, filtered and concentrated *in vacuo* to give a deep orange oil, which was purified by flash column chromatography (40:60 EtOAc/petrol 40-60), to give **5.10** as a dark yellow solid (2.05 g, 40%), m.p. 187-190℃. δH (400 MHz, $CDCl_3$, 24 °C): 10.66 (2H, s, 1-, 5-C*H*O), 7.67 (2H, d, J = 7.8 Hz, 2-, 6-*H*), 7.25 (2H, d, J = 7.7 Hz, 3-, 7-*H*), 2.75 (12H, s, 4-, 8-N(CH_3)$_2$); δC (100 MHz, $CDCl_3$, 24 °C): 191.0 (1-, 5-*C*HO), 153.6 (4-, 8-*C*), 132.5 (1-, 5-*C*), 130.5 (4a-, 8a-*C*), 126.7 (2-, 6-*C*), 116.7 (3-, 7-*C*), 44.4 (4-, 8-N(*C*H_3)$_2$); ν_{max}/cm^{-1} 2952, 2832, 2864, 2789, 1658 (C=O), 1500, 1477, 1455, 1401, 1364, 1321, 1235, 1185, 1125, 1047, 969, 946, 903, 846, 754, 720; Found: C, 71.19; H, 6.67; N, 10.48%. Calc. for $C_{16}H_{18}N_2O_2$: C, 71.02; H, 6.66; N, 10.36%.

Preparation of 1,1'-(4'',8''-bis(dimethylamino)naphthalene-1'',5''-diyl)bis(2-methylpropan-1-one), 5.12.

In a three-neck flask, 1,5-*bis*(dimethylamino)naphthalene **5.6** (1.00 g, 4.67 mmol) was dissolved in anhydrous hexanes (15 mL) and stirred whilst *n*-BuLi (2.5M in hexanes, 5.60 mL, 14.02 mmol) was steadily added at room temperature. The solution was refluxed for 3 days, over which a light brown precipitate formed.[10] The reaction was cooled, the precipitate was allowed to settle and the supernatant was removed. The solid was suspended in anhydrous THF (15 mL), cooled to 0ºC and isobutyric anhydride (2.32 mL, 14.02 mmol) added, the solution was left to stir for 24h. The yellow/brown solution was quenched with H_2O (30 mL) and the reaction was extracted with EtOAc (3 x 50 mL). The combined organics were washed with brine (1 x 50 mL), dried over $MgSO_4$, filtered and concentrated *in vacuo* to give an oil which was purified by flash column chromatography (20:80 EtOAc/petrol 40-60), to give **5.12** as a brown solid (0.48 g, 29%), m.p. 165-168℃. δH (400 MHz, $CDCl_3$, 24 °C): 7.15-7.26 (4H, m, 2''-, 3''-, 6''-, 7''-*H*), 2.90-3.00 (2H, m, -C*H*$(CH_3)_2$), 2.30-2.88 (12H, v br m, 4''-, 8''-N(C*H*$_3)_2$), 0.80-1.35 (12H, v br m, CH(C*H*$_3)_2$); δC (100 MHz, $CDCl_3$, 24 °C): 209.1 (*C*=O), 150.2 (4'', 8''-*C*), 129.8 (br), 129.7 (br), 125.8 (2''-, 6''-*C*), 116.7 (3'', 7''-*C*), 48.4 & 42.8 (4'', 8''-N(C*H*$_3)_2$), 41.5 (*C*H$(CH_3)_2$), 20.1 & 17.4 (CH(*C*H$_3)_2$); ν_{max}/cm^{-1} 2965, 2940, 2864, 2832, 2789, 1673 (C=O), 1509, 1477, 1377, 1313, 1135, 1015, 974, 842, 818, 721; Found: C, 74.23; H, 8.37; N, 7.69%. Calc. for $C_{22}H_{30}N_2O_2$: C, 74.48; H, 8.46; N, 7.90%.

Preparation of 4-(dimethylamino)-1,5-diformyl-N,N-dimethylnaphthalen-8-aminium trifluoroacetate, 5.15.

Bis aldehyde **5.10** (100 mg, 0.37 mmol) was dissolved in anhydrous diethyl ether (10 mL) and trifluoroacetic acid (6 drops) was added dropwise with a light-coloured precipitate forming immediately. The solution was stirred for a further 2h before the solid was collected by filtration, washed with cold anhydrous diethyl ether and dried under vacuum to give the desired product **5.15** as a pale brown solid (119 mg, 84%), m.p. 152-155℃. δH (400 MHz, d_6-DMSO, 24 °C): 9.21 (2H, br s, 1-, 5-C*H*O), 7.89 (2H, d, J = 7.8 Hz, 2-, 6-*H*), 7.84 (2H, d, J = 7.7 Hz, 3-, 7-*H*), 3.05 (12H, s, 4-, 8-N(CH_3)$_2$); δC (100 MHz, d_6-DMSO, *24* °C): 159.5 (q, $J_{C,F}$ = 32.6 Hz, *C*=O), 150.9 (4-,8-*C*), 131.4 (1-, 5-*C*), 127.9 (4a-, 8a-*C*), 126.8 (2-, 6-*C*), 118.6 (3-, 7-*C*), 115.8 (q, $J_{C,\,F}$ 292 Hz, CF_3), 47.3 (4-, 8-N(*C*H_3)$_2$); δF (376 MHz, d_6-DMSO, 24 °C): -73.93 (CF_3); ν_{max}/cm^{-1} 1669 (C=O), 1500, 1449, 1408, 1356, 1338, 1187, 1168, 1121, 972, 846, 795, 717; Found: C, 56.09; H, 5.14; N, 7.17%. Calc. for $C_{18}H_{19}F_3N_2O_4$: C, 56.25; H, 4.98; N, 7.29%.

Preparation of 5-(dimethylammonio)-6-formyl-2-hydroxy-1,1-dimethyl-1,2-dihydrobenzo[cd]indol-1-ium dichloride, 5.16.

Bis aldehyde **5.10** (100 mg, 0.37 mmol) was dissolved in anhydrous dichloromethane (10 mL) and ethereal hydrochloric acid (2M, 0.55 mL, 1.11 mmol) was added dropwise with a light coloured precipitate forming immediately. The solution was stirred for a further 3h before the solid was collected by filtration, washed with cold anhydrous diethyl ether and dried under vacuum to give the desired product **5.16** as a pale brown solid (100 mg, 79%), m.p. Decomp > 140℃. δH (400 MHz, d_4-Methanol, 24 °C): 8.63 (1H, d, J = 7.8 Hz, 4-*H*), 8.24 (1H, d, J = 7.8

Hz, 8-*H*), 8.18 (1H, d, J = 7.8, 7-*H*), 8.12 (1H, d, J = 7.8 Hz, 3-*H*), 7.14 (1H, s, 2-*H*), 5.86 (1H, s, 6-C(OH)(OCD$_3$)*H*), 3.91 (3H, s, 1-N(C*H*$_3$)), 3.58 (6H, 2 x s, 5-N(C*H*$_3$)$_2$), 3.52 (3H, s, 1-N(C*H*$_3$)); δC (100 MHz, d$_4$-Methanol, 24 °C): 148.2 (8a-*C*), 140.8 (5-*C*), 135.4 (2a-*C*), 134.2 (7-*C*), 133.6 (6-*C*), 130.9 (8b-*C*), 127.3 (4-*C*), 125.9 (3-*C*), 121.4 (5a-*C*), 117.4 (8-*C*), 115.0 (2-*C*), 109.1 (%-*C*(OH)(OCD$_3$)H), 54.9 (1-N(*C*H$_3$)), 57.0 (-O*C*D$_3$), 49.3 (v. br 1-N(*C*H$_3$)), 48.4 (v. br 5-N(*C*H$_3$)$_2$); ν_{max}/cm^{-1} 3513, 3393, 3076, 3008, 2909, 2473, 1656 (C=O), 1628, 1600, 1507, 1459, 1299, 1187, 1138, 1084, 959, 922, 862, 771, 745, 695.

Preparation of 3,3'-Cyano-((4'',8''-bis(dimethylamino)naphthalene-1'',5''-diyl)bis-propenenitrile, 5.19.

Bis aldehyde **5.10** (100 mg, 0.37 mmol), malononitrile (61 mg, 1.11 mmol) and ethylenediamine diacetate (7 mg, 0.04 mmol) were dissolved in anhydrous methanol (5 mL) under nitrogen and refluxed for 2h, during which a precipitate formed. The reaction was cooled and the solid was collected by filtration, washed with cold methanol and dried under vacuum to give the desired product **5.19** as an orange solid (93 mg, 68%), m.p. Decomp > 200℃. δH (400 MHz, CDCl$_3$, 24 °C): 8.69 (2H, s, 3-, 3'-*H*), 7.59 (2H, dd, J = 7.8, 0.9 Hz, 2''-, 6''-*H*), 7.37 (2H, d, J = 7.8 Hz, 3''-, 7''-*H*), 2.72 (12H, s, 4''-, 8''-N(C*H*$_3$)$_2$); δC (100 MHz, CDCl$_3$, *24* °C): 164.0 (3-, 3'-*C*), 153.4 (4''-, 8''-*C*), 131.4 (1''-, 5''-*C*), 129.1 (2''-, 6''-*C*), 125.2 (4a''-, 8a''-*C*), 119.0 (3''-, 7''-*C*), 114.1 (2 x C≡N), 112.7 (2-, 2'-*C*), 45.0 (4''-, 8''-N(*C*H$_3$)$_2$); ν_{max}/cm^{-1} 3043, 2862, 2830, 2788, 2227 (C≡N), 1571, 1505, 1388, 1321, 1202, 1086, 1043, 978, 844, 808, 775, 752, 713; Found: C, 71.85; H, 5.10; N, 22.56%. Calc. for $C_{22}H_{18}N_6$: C, 72.05; H, 4.91; N, 22.92%.

Preparation of Dimethyl 3,3'-(4'',8''-bis(dimethylamino)naphthalene-1'',5''-diyl)(2E,2'E)-bis(2-cyanoacrylate), 5.20.

Bis aldehyde **5.10** (150 mg, 0.56 mmol), methyl cyanoacetate (0.13 mL, 1.39 mmol) and ethylenediamine diacetate (10 mg, 0.06 mmol) were dissolved in anhydrous methanol (10 mL) under nitrogen and refluxed for 3h, during which a precipitate formed. The reaction was cooled and the solid was collected by filtration, washed with cold methanol and dried under vacuum to give the desired product **5.20** as a pale brown/orange solid (187 mg, 78%), m.p. Decomp > 200℃. δH (400 MHz, $CDCl_3$, 24 °C): 9.12 (2H, s, 3-, 3'-*H*), 7.58 (2H, dd, J = 7.8, 1.4 Hz, 2''-, 6''-*H*), 7.30 (2H, d, J = 7.8 Hz, 3''-, 7''-*H*), 3.94 (6H, s, OCH_3), 2.66 (12H, s, 4''-, 8''-N(CH_3)$_2$); δC (100 MHz, $CDCl_3$, 24 °C): 164.0 (*C*=O), 160.3 (3-, 3'-*C*), 153.1 (4''-, 8''-*C*), 131.8 (4a''-, 8a''-*C*), 128.4 (2''-, 6''-*C*), 126.3 (1''-, 5''-*C*), 118.7 (3''-, 7''-*C*), 115.8 (C≡N), 96.9 (2-, 2'-*C*), 53.1 (O*C*H$_3$) 45.0 (4''-, 8''-N(*C*H$_3$)$_2$); ν_{max}/cm^{-1} 2939, 2871, 2838, 2221 (C≡N), 1701 (C=O), 1567, 1505, 1436, 1395, 1340, 1258, 1235, 1198, 1092, 1045, 982, 848, 805, 762, 715; Found: C, 66.51; H, 5.47; N, 13.08%. Calc. for $C_{24}H_{24}N_4O_4$: C, 66.59; H, 5.55; N, 12.95%.

Preparation of Bis-4',8'-dimethylamino-bis-1',5'-(2,2-dimethyl-4,6-dioxo-1,3-dioxan-5-methylidine)naphthalene, 5.23.

Bis aldehyde **5.10** (200 mg, 0.74 mmol) and Meldrum's acid (320 mg, 2.22 mmol) were dissolved in anhydrous methanol (10 mL) under nitrogen and stirred at room temperature for 24h, during which a precipitate formed. The solid was collected by filtration, washed with cold methanol and dried under vacuum to give the desired product **5.23** as an orange solid (190 mg, 49%), m.p. Decomp > 180℃. δH (400 MHz, $CDCl_3$, 24 °C): 8.24 (2H, d, J = 1.3 Hz, 3-*H*), 7.42

(2H, d, J = 7.6 Hz, 3'-, 7'-*H*), 7.33 (2H, dd, J = 7.7, 1.4 Hz, 2'-, 6'-*H*), 3.06 (12H, s, 4'-, 8'-N(C*H*$_3$)$_2$), 1.85 (12H, s, 2-(C*H*$_3$)$_2$); δC (100 MHz, $CDCl_3$, *24* °C): 165.6 & 162.7 (2 x *C*=O), 148.5 (4'-, 8'-*C*), 131.4 (4a'-, 8a'-*C*), 131.2 (3-*C*), 129.7 (1'-, 5'-*C*), 123.9 (2'-, 6'-*C*), 117.9 (3'-, 7'-*C*), 103.7 (2-*C*), 90.8 (5-*C*), 48.7 (4'-, 8'-N(*C*H$_3$)$_2$), 27.0 (2-C(*C*H$_3$)$_2$); ν_{max}/cm^{-1} 2993, 1750, 1729 (C=O), 1636 (C=O), 1617, 1453, 1399, 1373, 1340, 1291, 1211, 1176, 1095, 1000, 978, 944, 844, 700; Found: C, 63.92; H, 6.03; N, 5.41%. Calc. for $C_{28}H_{30}N_2O_8$: C, 64.30; H, 5.74; N, 5.36%.

Spiro-(2''',2'''-dimethyl-4''',6'''-dioxo-1''',3'''-dioxane-5''',3''-1''-methyl-2'',3'',4'',5'',6'',7''-hexahydro-1H-azepino[5,7-f,g]-5-(1',2'-dihydro-1',1'-dimethylbenzo[cd]indolium-2'-yl)-2,2-dimethyl-4,6-dioxo-1,3-dioxan-5-ide, 5.25.

Bis Meldrum's derivative **5.23** (100mg, 0.19 mmol) in MeOH and was left for 7 days at room temperature, resulting in a loss of its strong orange colour and the formation of the white solid. The solution was cooled to maximise precipitation and the solid **5.25** was collected via filtration (95mg, 95%), m.p. Decomp > 220℃. δH (400 MHz, CD_2Cl_2, 24 °C): 7.30 (1H, d, J = 7.6 Hz, 4'-*H*), 7.19 (1H, d, J = 7.6 Hz, 3'-*H*), 7.12 (1H, dd, J = 7.7, 1.6 Hz, 7'-*H*), 6.99 (1H, d, J = 7.8 Hz, 8'-*H*), 6.92 (1H, d, J = 1.5 Hz, 2'-*H*), 3.75-3.85 (4H, m, 2''-, 4''-*H*$_2$), 3.33 (6H, s, 1'-N$^+$(C*H*$_3$)$_2$), 3.11 (3H, s, 1''-NC*H*$_3$), 1.85 (s, 3H, 2'''-C*H*$_3$), 1.77 (s, 3H, 2'''-C*H*$_3$), 1.74 (s, 6H, 2-(C*H*$_3$)$_2$); δC (100 MHz, CD_2Cl_2, 24 °C): 168.9 (4 x *C*=O), 165.3, 150.5, 145.7, 135.9, 130.8 (Ar-*C*$_5$), 127.2 (3'-*C*), 127.0, 125.0 (Ar-*C*$_2$), 120.9 (7'-*C*), 113.7 (4'-*C*), 112.5 (8'-*C*), 105.7 (2'''-*C*), 102.1 (2-*C*), 98.5 (2'-*C*), 69.8 (5-*C*), 64.3 (2''-*C*), 55.4 (3''-*C*), 52.0 (1'-N$^+$(*C*H$_3$)$_2$), 40.9 (4''-*C* & 1''-NCH$_3$), 29.4 & 29.3 (2'''-C(*C*H$_3$)$_2$), 26.3 (2-C(*C*H$_3$)$_2$); ν_{max}/cm^{-1} 1774

(C=O), 1735 (C=O), 1608, 1397, 1367, 1287, 1254, 1179, 1075, 1025, 926, 799, 780; Found: C, 64.42; H, 5.67; N, 5.21%. Calc. for $C_{28}H_{30}N_2O_8$: C, 64.36; H, 5.79; N, 5.36%.

Preparation of 4,8-*Bis*(dimethylamino)-1-naphthaldehyde, 5.11.

1,5-*Bis*(dimethylamino)naphthalene **5.6** (1.00 g, 4.67 mmol) was dissolved in anhydrous hexane (15 mL) and stirred while *n*-BuLi (1.7M in hexanes, 2.75 mL, 4.67 mmol) was steadily added at room temperature. The solution was refluxed for 3 days, over which time a light brown precipitate formed. The solid was suspended in anhydrous THF (15 mL), cooled to 0 ºC and anhydrous DMF (0.43 mL, 5.61 mmol) was added. The solution was left to stir for 24 h. The yellow/brown solution was quenched with H_2O (30 mL) and the reaction was extracted with ethyl acetate (3 x 30 mL). The combined organic layers were washed with brine (30 mL), dried over $MgSO_4$, filtered and concentrated *in vacuo* to give a deep orange oil. Purification by flash column chromatography (40:60 ethyl acetate/petrol 40-60) gave the product **5.11** as a dark orange solid (0.40 g, 35 %), m.p. 45-48℃. δH (400 MHz, $CDCl_3$, 24 °C): 10.62 (1H, s, 1-C*H*O), 7.93 (1H, dd, J = 8.7, 1.4 Hz, 7-*H*), 7.52 (1H, d, J = 7.8 Hz, 2-*H*), 7.42 (1H, t, J = 8.0 Hz, 6-*H*), 7.25 (1H, dd, J = 7.3, 1.4 Hz, 5-*H*), 6.98 (1H, d, J = 7.8 Hz, 3-*H*), 2.89 (6H, s, 4-N(CH_3)$_2$), 2.67 (6H, s, 8-N(CH_3)$_2$); δC (100 MHz, $CDCl_3$, 24 °C): 191.6 (*C*HO), 154.1 (4-*C*), 150.8 (8-*C*), 131.3 (1-*C*), 130.8 (8a-*C*), 130.0 (4a-*C*), 126.0 (2-*C*), 125.8 (6-*C*), 121.1 (7-*C*), 117.9 (5-*C*), 113.3 (3-*C*), 44.9 (2 x N(*C*H$_3$)$_2$); ν_{max}/cm^{-1} 2939, 2864, 2827, 2782, 1666 (C=O), 1599, 1576, 1507, 1451, 1405, 1400, 1358, 1353, 1323, 1202, 1183, 1144, 1080, 1049, 1011, 972, 812, 795, 765, 697. Found: C, 74.14; H, 7.26; H,11.51%. Calc. for $C_{15}H_{18}N_2O$: C, 74.35; H, 7.49; N, 11.56%.

Preparation of 5-(dimethylamino)-2-hydroxy-1,1-dimethyl-1,2-dihydrobenzo[cd]indol-1-ium chloride, 5.28.

Mono-naphthaldehyde **5.11** (360 mg, 1.49 mmol) was dissolved in anhydrous diethyl ether (15 mL) and ethereal hydrochloric acid (1M, 1.49 mL, 1.49 mmol) was added dropwise with immediate formation of a beige precipitate. The solution was stirred for a further 3 h. before the solid was collected by careful filtration under a flow of nitrogen. The solid was washed with cold anhydrous diethyl ether and dried under vacuum to give the desired product **5.28** as a beige solid (362 mg, 87%), m.p. Decomp > 160°C. δH (400 MHz, d_4-METHANOL, 24 °C): 8.64 (1H, d, J = 8.7 Hz, 6-*H*), 8.32 (1H, d, J = 7.8 Hz, 4-*H*), 8.22 (1H, d, J = 7.8 Hz, 8-*H*), 8.08 (1H, t, J = 7.8 Hz, 7-*H*), 7.95 (1H, dd, J = 7.3, 0.9 Hz, 3-*H*), 7.18 (1H, s, 2-*H*), 3.54 (12H, s, 1-, 5-N(CH_3)$_2$); δC (100 MHz, d_4-METHANOL, 24 °C): 145.3 (8a-*C*), 139.1 (5-*C*), 134.1 (2a-*C*), 130.8 (7-*C*), 128.7 (8b-*C*), 123.6 (5a-*C*), 123.0 (3-*C*), 122.7 (4-*C*), 122.3 (6-*C*), 116.9 (8-*C*), 109.1 (2-*C*), 46.1 (1-, 5-N(*C*H$_3$)$_2$); ν_{max}/cm^{-1} 3006, 2827, 2696, 2598, 2447, 1507, 1474, 1427, 1395, 1321, 1283, 1207, 1181, 1159, 1142, 1107, 993, 948, 810, 713, 680.

Preparation of 2-(benzoyloxy)-5-(dimethylamino)-1,1-dimethyl-1,2-dihydrobenzo [cd]indol-1-ium chloride, 5.29.

Mono-naphthaldehyde **5.11** (250 mg, 1.03 mmol) was dissolved in anhydrous diethyl ether (15 mL) and benzoyl chloride (1M, 1.29 mL, 1.29 mmol) was added dropwise with immediate formation of an orange precipitate. The solution was stirred for a further 30 mins before the solid was collected by careful filtration under a flow of nitrogen. The solid was washed with cold anhydrous diethyl ether and dried under vacuum to give the desired product **5.29** as an

orange solid (247 mg, 63%), m.p. Decomp > 85℃. δH (400 MHz, d_2-DCM, 24 °C): 8.99 (1H, d, J = 7.4 Hz, 8-*H*), 8.17 (1H, d, J = 8.5 Hz, 6-*H*), 8.08-8.12 (2H, m, *o*-Ph-*H*), 7.91 (1H, d, J = 0.8 Hz, 2-*H*), 7.70-7.77 (2H, m, *p*-Ph, 7-*H*), 7.65 (1H, dd, J = 7.8, 0.9 Hz, 3-*H*), 7.53 (2H, dd, J = 7.6, 0.8 Hz, *m*-Ph-*H*), 7.15 (1H, d, J = 7.8 Hz, 4-*H*), 4.21 (3H, s, 1-N(C*H*$_3$)), 3.89 (3H, s, 1-N(C*H*$_3$)), 3.07 (6H, s, 5-N(C*H*$_3$)$_2$); δC (100 MHz, d_2-DCM, 24 °C): 165.4 (*C*=O), 152.4 (5-*C*), 145.8 (1-*C*), 135.6 (*p*-Ph-*C*), 130.8 (*o*-Ph-*C*), 129.5 (8b-*C*), 129.4 (*m*-Ph-*C*), 127.8 (7-*C*), 126.9 (*i*-Ph-*C*), 125.9 (6-*C*), 125.6 (5a-*C*), 124.3 (3-*C*), 119.1 (2a-*C*), 117.4 (8-*C*), 115.7 (4-*C*), 100.8 (1-*C*), 56.9 & 49.4 (1-N(*C*H$_3$)$_2$), 44.3 (5-N(C*H*$_3$)$_2$); ν_{max}/cm^{-1} 3341, 3090, 2946, 1606, 1539, 1481, 1407, 1367, 1347, 1293, 1198, 1149, 1090, 1039, 827, 808, 762, 732; Found: C, 69.30; H, 6.18; N, 7.28. Calc. for $C_{22}H_{23}N_2O_2Cl$: C, 69.01; H, 6.06; N, 7.32%.

Preparation of 2-Cyano-3-(4'-,8'-*bis*(dimethylamino)naphthalen-1'-yl)propenenitrile, 5.33.

Mono-naphthaldehyde **5.11** (750 mg, 3.06 mmol), malononitrile (300 mg, 4.59 mmol) and ethylenediamine diacetate (54 mg, 0.3 mmol) were dissolved in anhydrous methanol (10 mL) under nitrogen and refluxed for 24 h. The methanol was removed *in vacuo* to give a deep orange oil which was purified by flash column chromatography (20:80 ethyl acetate/petrol 40-60), to give product **5.33** as an orange solid (649 mg, 72 %), m.p. 105-108℃. δH (400 MHz, CD_2Cl_2, 24 °C): 8.69 (1H, d, J = 0.9 Hz, 3-*H*), 7.99 (1H, dd, J = 8.7, 0.9 Hz, 5'-*H*), 7.48 (1H, t, J = 7.8 Hz, 6'-*H*), 7.44 (1H, dd, J = 7.8, 0.9 Hz, 2'-*H*), 7.37 (1H, dd, J =7.3, 0.9 Hz, 7'-*H*), 7.02 (1H, d, J = 8.2 Hz, 3'-*H*), 2.93 (6H, s, 4'-N(C*H*$_3$)$_2$), 2.66 (6H, s, 8'-N(C*H*$_3$)$_2$); δC (100 MHz, CD_2Cl_2, 24 °C): 165.8 (3-*C*), 154.9 (8'-*C*), 150.2 (4'-*C*), 131.8 (8a'-*C*), 130.1 (4a'-*C*), 128.4 (2'-*C*),

126.2 (6'-*C*), 122.5 (5'-*C*), 122.3 (1'-*C*), 121.9 (8a'-*C*), 120.0 (7'-*C*), 115.4 & 114.0 (2 x *C*≡N), 113.2 (3'-*C*), 73.0 (2-*C*), 45.3 (4'- N(C*H*$_3$)$_2$), 44.8 (8'-N(C*H*$_3$)$_2$); ν_{max}/cm^{-1} 2938, 2864, 2837, 2788, 2218 (C≡N),1574, 1555, 1544, 1507, 1462, 1407, 1375, 1325, 1206, 1195, 1144, 1102, 1076, 1045, 977, 919, 837, 812, 798, 774, 749; Found: C, 74.30; H, 6.34; N, 19.34%. Calc. for $C_{18}H_{18}N_4$: C, 74.46; H, 6.25; N, 19.30%.

Preparation of Methyl (E)-3-(4',8'-bis(dimethylamino)naphthalen-1'-yl)-2-cyanoacrylate, 5.34.

Mono-naphthaldehyde **5.11** (200 mg, 0.88 mmol), methyl cyanoacetate (0.16 mL, 1.44 mmol) and ethylenediamine diacetate (16 mg, 0.09 mmol) were dissolved in anhydrous methanol (10 mL) under nitrogen and refluxed for 5h. The methanol was removed *in vacuo* to give a deep orange oil, which was purified by flash column chromatography (15:85 EtOAc/petrol 40-60), to give **5.34** as an orange solid (120 mg, 42 %), m.p. 80-83℃. δH (400 MHz, CD_2Cl_2, 24 °C): 9.16 (1H, s, 3-*H*), 7.99 (1H, d, J = 8.7 Hz, 5'-*H*), 7.50 (1H, d, J = 7.8 Hz, 2'-*H*), 7.46 (1H, t, J = 7.8 Hz, 6'-*H*), 7.31 (1H, d, J =7.3 Hz, 7'-*H*), 7.02 (1H, d, J = 7.8 Hz, 3'-*H*), 3.92 (3H, s, OC*H*$_3$), 2.92 (6H, s, 4'-N(C*H*$_3$)$_2$), 2.63 (6H, s, 8'-N(C*H*$_3$)$_2$); δC (100 MHz, CD_2Cl_2, 24 °C): 164.7 (*C*=O), 161.7 (3-*C*), 153.8 (4'-*C*), 150.2 (8'-*C*), 131.7 (8a'-*C*), 130.2 (4a'-*C*), 127.8 (2'-*C*), 125.8 (6'-*C*), 123.7 (1'-*C*), 121.8 (5'-*C*), 119.3 (7'-*C*), 116.5 (*C*≡N), 113.5 (3'-*C*), 94.6 (2-*C*), 52.8 (O*C*H$_3$), 45.3 (8'- N(*C*H$_3$)$_2$), 44.9 (4'-N(*C*H$_3$)$_2$); ν_{max}/cm^{-1} 2942, 2864, 2830, 2786, 2219 (C≡N), 1718 (C=O), 1576, 1507, 1265, 1231, 1203, 1090, 760; Found: C, 70.48; H, 6.66; N, 13.07%. Calc. for $C_{19}H_{21}N_3O_2$: C, 70.57; H, 6.55; N, 12.99%.

Preparation of Dimethyl 2-((4',8'-bis(dimethylamino)naphthalen-1'-yl)methylene) malonate, 5.35.

Mono-naphthaldehyde **5.11** (120 mg, 0.53 mmol), dimethyl malonate (0.1 mL, 0.85 mmol) and ethylenediamine diacetate (9 mg, 0.05 mmol) were dissolved in anhydrous methanol (10 mL) under nitrogen and refluxed for 24h. The methanol was removed *in vacuo* to give a deep orange oil, which was purified by flash column chromatography (15:85 EtOAc/petrol 40-60), to give **5.35** as an orange solid (130 mg, 69 %), m.p. 82-85℃. δH (400 MHz, CD_2Cl_2, 24 °C): 8.77 (1H, s, 3-*H*), 7.96 (1H, dd, J = 8.2, 0.9 Hz, 5'-*H*), 7.42 (1H, t, J = 7.3 Hz, 6'-*H*), 7.25 (1H, dd, J = 7.3, 0.9 Hz, 7'-*H*), 7.18 (1H, dd, J =7.8, 1.4 Hz, 2'-*H*), 6.93 (1H, d, J = 7.8 Hz, 3'-*H*), 3.85 (3H, s, OCH_3), 3.61 (3H, s, OCH_3), 2.87 (6H, s, 4'-N(CH_3)$_2$), 2.63 (6H, s, 8'-N(CH_3)$_2$); δC (100 MHz, CD_2Cl_2, 24 °C): 167.7 & 166.0 (2 x *C*=O), 152.4 (4'-*C*), 151.7 (8'-*C*), 150.8 (3-*C*), 131.2 (8a'-*C*), 130.6 (4a'-*C*), 126.4 (2'-*C*), 126.1 (1'-*C*), 125.6 (6'-*C*), 121.0 (5'-*C*), 118.5 (7'-*C*), 118.0 (2-*C*), 113.4 (3'-*C*), 52.7 (O*C*H$_3$), 52.1 (O*C*H$_3$), 45.6 (8'- N(*C*H$_3$)$_2$), 45.0 (4'-N(*C*H$_3$)$_2$); ν_{max}/cm^{-1} 2978, 2946, 2864, 2827, 2778, 1727 (C=O), 1697, 1599, 1578, 1507, 1433, 1362, 1349, 1261, 1224, 1181, 1151, 1069, 974, 939, 918, 814, 775, 708; Found: C, 67.19; H, 6.79; N, 7.53%. Calc. for $C_{20}H_{24}N_2O_4$: C, 67.40; H, 6.79; N, 7.86%.

Preparation of 2-Cyano-3-(4'- dimethylammonio-8'-(dimethylamino)naphthalen-1'-yl)propenenitrile chloride, 5.36.

Dinitrile derivative **5.33** (100 mg, 0.34 mmol) was dissolved in anhydrous diethyl ether (10 mL) and ethereal hydrochloric acid (1M, 0.34 mL, 0.34 mmol) was added dropwise with immediate formation of a yellow precipitate. The solution was stirred for a further 3 h. before

the solid was collected by careful filtration under a flow of nitrogen. The solid was washed with cold anhydrous diethyl ether and dried under vacuum to give the desired product **5.36** as a yellow solid (80 mg, 71%), m.p. 167-170 ℃. δH (400 MHz, CD_2Cl_2, 24 °C): 8.85 (1H, br d, J = 8.2 Hz, 5'-*H*), 8.56 (1H, s, 3-*H*), 7.83 (1H, t, J = 8.0 Hz, 6'-*H*), 7.71 (1H, br d, J = 7.3 Hz, 3'-*H*), 7.60 (1H, d, J = 7.8 Hz, 7'-*H*), 7.54 (1H, d, J = 7.3 Hz, 2'-*H*), 3.33 (6H, s, 4'-$N^+H(CH_3)_2$), 2.71 (6H, s, 8'-$N(CH_3)_2$); δC (100 MHz, CD_2Cl_2, 24 °C): 163.1 (3-*C*), 150.2 (8'-*C*), 142.9 (br, 4'-*C*), 132.2 (8a'-*C*), 130.6 (br 1'-*C*), 129.6 (6'-*C*), 127.7 (4a'-*C*), 126.8 (2'-*C*), 122.2 (7'-*C*), 121.4 (5'-*C*), 118.0 (br 3'-*C*), 114.7 & 113.3 (2 x *C*≡N), 73.4 (2-*C*), 46.8 (4'-$N^+H(CH_3)_2$), 45.4 (8'-$N(CH_3)_2$); ν_{max}/cm^{-1} 3431, 3022, 2973, 2206 (C≡N), 1516, 1509, 1469, 1453, 1434, 1406, 1362, 1326, 1320, 1187, 1147, 1128, 1043, 990, 967, 887, 749, 782, 749, 692, 659; Found: C, 66.04; H, 5.69; N, 16.98. Calc. for $C_{18}H_{19}N_4Cl$: C, 66.15; H, 5.86; N, 17.14%.

Preparation of (E)-1'-(2-cyano-3-methoxy-3-oxoprop-1-en-1-yl)-8'-(dimethylamino)-N,N-dimethylnaphthalen-4'-aminium chloride, 5.37.

Methyl cyanoester **5.34** (120 mg, 0.37 mmol) was dissolved in anhydrous diethyl ether (10 mL) and ethereal hydrochloric acid (1M, 0.37 mL, 0.37 mmol) was added dropwise with a yellow precipitate forming immediately. The solution was stirred for a further 3h before the solid was collected by careful filtration with a nitrogen flow, washed with cold anhydrous diethyl ether and dried under vacuum to give the desired product **5.37** as a yellow solid (80 mg, 60%), m.p. 124-127℃. δH (400 MHz, CD_2Cl_2, 24 °C): 9.00 (1H, s, 3-*H*), 8.90 (1H, br d, J = 8.1 Hz, 5'-*H*), 7.83 (1H, t, J = 7.6 Hz, 6'-*H*), 7.77 (1H, br d, J = 7.8 Hz, 3'-*H*), 7.54 (2H, m, 2'-, 7'-*H*), 3.95 (3H, s, OCH_3), 3.43 (6H, s, 4'-$N^+H(CH_3)_2$), 2.64 (6H, s, 8'-$N(CH_3)_2$); δC (100 MHz, CD_2Cl_2, 24 °C): 163.7 (*C*=O), 158.5 (3-*C*), 150.5 (8'-*C*), 140.3 (4'-*C*), 132.7 (1'-*C*), 131.9 (8a'-*C*), 129.8 (6'-*C*), 127.0 (4a'-*C*), 125.7 (2'-*C*), 121.8 (7'-*C*), 120.2 (5'-*C*), 118.0 (3'-

C), 115.4 (*C*≡N), 95.3 (2-*C*), 53.0 (O*C*H_3), 46.9 (4'-N^+H(C*H*$_3$)$_2$), 45.2 (8'-N(C*H*$_3$)$_2$); ν_{max}/cm^{-1} 2167 (C≡N), 1636 (C=O), 1505, 1459, 1438, 1366, 1269, 1183, 1090, 989, 807, 793, 771; Found: C, 63.10; H, 6.17; N, 11.31. Calc. for $C_{19}H_{22}N_3O_2Cl$: C, 63.42; H, 6.16; N, 11.68%.

Preparation of 5-(dimethylamino)-4-(3-methoxy-2-(methoxycarbonyl)-3-oxoprop-1-en-1-yl)-N,N-dimethylnaphthalen-1-aminium chloride, 5.38.

Di-methyl ester derivative **5.35** (140 mg, 0.39 mmol) was dissolved in anhydrous diethyl ether (10 mL) and ethereal hydrochloric acid (1M, 0.39 mL, 0.39 mmol) was added dropwise with a pale orange/brown precipitate forming immediately. The solution was stirred for a further 2h before the solid was collected by careful filtration with a nitrogen flow, washed with cold anhydrous diethyl ether and dried under vacuum to give the desired product **5.38** as orange solid (67 mg, 79%), m.p. Decomp > 130℃. δH (400 MHz, d_6-DMSO, 24 °C): 8.35 (1H, d, J = 7.8 Hz, Ar-H_1), 8.19 (1H, d, J = 7.8 Hz, Ar-H_1), 7.82 (1H, t, J = 7.3 Hz, 7-*H*), 7.40-7.50 (2H, m, 3-, 4-*H*), 6.23 (1H, d, J = 3.2 Hz, (2-*H*)), 5.25 (1H, d, J = 3.2 Hz, (C*H*(CO_2CH_3)$_2$), 3.83 (3H, s, OC*H*$_3$), 3.76 (6H, s, 1-N^+(C*H*$_3$)$_2$), 3.34 (3H, s, OC*H*$_3$), 3.01 (6H, s, 5-HN^+(C*H*$_3$)$_2$); δC (100 MHz, d_6-DMSO, 24 °C): 167.0 & 166.0 (*C*=O), 147.6 & 147.4 (5-, 8a-*C*), 136.7 (Ar-C_1), 128.5 (7-*C*), 128.1, 124.6, 124.4, 122.2, 120.2, 114.8 (Ar-C_6), 81.7 (2-*C*), 59.4 (1-N^+(*C*H_3)$_2$), 53.7 & 53.1 (2 x O*C*H_3), 52.0 (*C*H(CO_2CH_3)$_2$), 44.6 (5-N^+(*C*H_3)$_2$); ν_{max}/cm^{-1} 3453, 3371, 3028, 2493, 2437, 1742, 1723 (C=O), 1604, 1477, 1442, 1345, 1328, 1254, 1231, 1198, 1177, 1112, 1015, 995, 933, 840, 779, 758; *HRMS* (ESI) calcd for $C_{20}H_{25}N_2O_4$ (M^+): 357.1814, found: 357.1821; *HRMS* (ESI) calcd for $C_{20}H_{26}N_2O_4^{2+}$ (M^{2+}): 179.0946, found:179.0947; Found: C, 55.80; H, 6.16; N, 6.44. Calc. for $C_{20}H_{26}N_2O_4Cl_2$: C, 55.95; H, 6.10; N, 6.52%.

Preparation of 4,8-*Bis*(dimethylamino)-1-naphthaldehyde (^{13}C enriched), 5.41.

1,8-*Bis*(dimethylamino)-1-naphthalene **5.6** (2.88 g, 13.50 mmol) was dissolved in anhydrous hexane (20 mL) and stirred while *n*-BuLi (1.7M in hexanes, 7.94 mL, 13.50 mmol) was steadily added at room temperature. The solution was refluxed for 3 days, over which time a light brown precipitate formed. The solid was suspended in anhydrous THF (20 mL), cooled to 0 ºC and anhydrous (^{13}C=O) DMF (1.00 g, 13.50 mmol) was added. The solution was left to stir for 24 h. The yellow/brown solution was quenched with H_2O (30 mL) and the reaction was extracted with ethyl acetate (3 x 30 mL). The combined organic layers were washed with brine (30 mL), dried over $MgSO_4$, filtered and concentrated *in vacuo* to give a deep orange oil. Purification by flash column chromatography (40:60 ethyl acetate/petrol 40-60) gave the product **5.41** as a dark orange solid (1.22 g, 35 %). δH (400 MHz, $CDCl_3$, 24 °C): 10.41-10.88 (1H, d, J = 186.4 Hz, ^{13}C*H*O), 7.98 (1H, d, J = 8.5 Hz, 7-*H*), 7.55 (1H, dd, J = 7.7, 4.5 Hz, 2-*H*), 7.46 (1H, t, J = 4.4 Hz, 6-*H*), 7.28 (1H, dd, J = 7.4, 1.0 Hz, 5-*H*), 7.00 (1H, d, J = 7.8 Hz, 3-*H*), 2.93 (6H, s, 4-N(C*H*$_3$)$_2$), 2.70 (6H, s, 8-N(C*H*$_3$)$_2$); δC (100 MHz, $CDCl_3$, *24* °C): 191.5 (^{13}*C*HO); HRMS (ESI): Found: 244.1534 ($M+H^+$), $C_{14}{}^{13}CH_{19}N_2O$ requires: 244.1536 ($M+H^+$).

The bis-aldehyde was further isolated as a yellow solid (0.38 g, 10%). δH (400 MHz, $CDCl_3$, 24 °C): 10.44-10.91 (2H, d, J = 187.1 Hz, ^{13}C*H*O), 7.67 (2H, dd, J = 7.8, 4.5 Hz, 2', 6'-*H*), 7.25 (2H, d, J = 7.8 Hz, 3', 7'-*H*), 2.76 (12H, s, 4', 8'-N(C*H*$_3$)$_2$); δC (100 MHz, $CDCl_3$, *24* °C): 191.1 (*C*HO); Found: C, 71.05; H, 6.80; N, 10.17%. Calc. for $C_{14}{}^{13}C_2H_{18}N_2O_2$: C, 71.30; H, 6.66; N, 10.29%.

Preparation of 2-Cyano-3-(4'-,8'-*bis*(dimethylamino)naphthalen-1'-yl)propenenitrile (^{13}C enriched), 5.42.

Enriched naphthaldehyde **5.41** (500 mg, 1.93 mmol), malononitrile (191 mg, 2.90 mmol) and ethylenediamine diacetate (36 mg, 0.20 mmol) were dissolved in anhydrous methanol (10 mL) under nitrogen and refluxed for 24 h. The methanol was removed *in vacuo* to give a deep orange oil which was purified by flash column chromatography (10:90 ethyl acetate/petrol 40-60), to give product **5.42** as an orange solid (360 mg, 64 %). δH (400 MHz, CD_3Cl, 24 °C): 8.50-8.93 (1H, d, J = 172.8 Hz, 3-*H*), 8.01 (1H, d, J = 8.0 Hz, 5'-*H*), 7.44-7.52 (2H, m, 2'-6'-*H*), 7.37 (1H, dd, J =7.3, 1.0 Hz, 7'-*H*), 7.02 (1H, d, J = 7.9 Hz, 3'-*H*), 2.95 (6H, s, 4'-N(CH_3)$_2$), 2.69 (6H, s, 8'-N(CH_3)$_2$); δC (100 MHz, CD_3Cl, 24 °C): 165.3 (3-*C*); *HRMS* (ESI) calcd for $C_{17}{}^{13}CH_{19}N_4$ ($[M+H]^+$): 292.1649, found: 292.1649.

Preparation of 2-Cyano-3-(4'-dimethylammonio-8'-(dimethylamino)naphthalen-1'-yl)propenenitrile chloride (^{13}C enriched), 5.43.

Enriched dinitrile derivative **5.42** (180mg, 0.62 mmol) was dissolved in anhydrous diethyl ether (10 mL) and ethereal hydrochloric acid (1M, 0.62 mL, 0.62 mmol) was added dropwise with immediate formation of a yellow precipitate. The solution was stirred for a further 3 h. before the solid was collected by careful filtration under a flow of nitrogen. The solid was washed with cold anhydrous diethyl ether and dried under vacuum to give the desired product **5.43** as a yellow solid (120 mg, 60%). δH (400 MHz, CD_3Cl, 24 °C): 8.90 (1H, br d, J = 8.2 Hz, 5'-*H*), 8.31-8.75 (1H, d, J = 174.7 Hz, 3-*H*), 7.83 (1H, t, J = 8.0 Hz, 6'-*H*), 7.75 (1H, br d, J = 7.8

Hz, 3'-*H*), 7.58 (1H, d, J = 7.8 Hz, 7'-*H*), 7.54 (1H, m, 2'-*H*), 3.40 (6H, s, 4'-NH(C*H*$_3$)$_2$), 2.71 (6H, s, 8'-N(C*H*$_3$)$_2$); δC (100 MHz, CD_3Cl, 24 °C): 162.5 (3-*C*).

Crystal Data

*Table 5.43. Crystallographic data for **5.8**, **5.10**, **5.12a**, **5.12b**, **5.15** and **5.16**.*

	5.8	**5.10**	**5.12a**	**5.12b**	**5.15**	**5.16**
Formula	$C_{16}H_{18}N_2O_2$	$C_{16}H_{18}N_2O_2$	$C_{22}H_{30}N_2O_2$	$C_{22}H_{30}N_2O_2$	$C_{18}H_{19}F_3N_2O_4$	$C_{16}H_{22}Cl_2N_2O_3$
Formula weight	270.32	270.32	354.48	354.48	384.35	361.25
Crystal system	Triclinic	Monoclinic	Triclinic	Monoclinic	Triclinic	Monoclinic
Space group	*P*-1	$P2_1/c$	*P*-1	$P2_1/c$	*P*-1	$P2_1/c$
***a*[Å]**	8.7039(4)	5.2514(3)	8.7767(3)	13.2495(3)	7.1968(4)	18.9199(9)
***b*[Å]**	9.6406(5)	10.5173(6)	9.6203(3)	20.0128(3)	10.4570(6)	7.4230(4)
***c*[Å]**	17.7773(8)	12.5755(6)	13.1840(4)	7.49379(12)	11.8913(7)	12.1934(6)
***α*[°]**	79.812(4)	90	80.495(2)	90	103.791(5)	90
β [°]	77.968(4)	95.232(5)	79.042(2)	94.6596(16)	90.051(4)	95.572(5)
***γ*[°]**	80.418(4)	90	68.274(3)	90	90.731(5)	90
***V* [Å^3]**	1422.86(12)	691.66(7)	1009.76(6)	1980.48(6)	869.03(9)	1704.38(15)
Z	4	2	2	4	2	4
***ρ* [g cm^{-3}]**	1.262	1.298	1.166	1.189	1.469	1.408
***T* [*K*]**	150.00(10)	150.01(10)	150.01(10)	150.01(10)	150.00(10)	150.01(10)
***λ* (Å)**	0.71073	0.71073	0.71073	0.71073	0.71073	0.71073
***μ* (mm^{-1})**	0.084	0.087	0.074	0.076	0.125	0.397
unique refl.	13235	2901	59803	35689	9488	14009
Refl, I > 2σI	6558	1591	5003	4893	4178	3446
***R*$_1$**	0.0573	0.0494	0.0508	0.0492	0.0556	0.0649
***wR*$_2$**	0.1219	0.1182	0.1434	0.1084	0.1092	0.1721
Δ*ρ*(r) [e Å^{-3}]	0.32/-0.24	0.24/-0.26	0.44/-0.21	0.34/-0.19	0.29/-0.25	0.62/-0.32
Crystallisation Solvent	CH_2Cl_2	CH_2Cl_2	CH_2Cl_2/*n*-hexane	EtOAc *n*-hexane	CH_3CN	CH_3CN/CH_3OH

*Table 5.44. Crystallographic data for **5.19**, **5.20**, **5.23** and **5.25**.*

	5.19	**5.20**	**5.23**	**5.25**
Formula	$C_{22}H_{18}N_6$	$C_{24}H_{24}N_4O_4$	$C_{28}H_{30}N_2O_8$	$C_{28}H_{30}N_2O_8$. CH_3OH
Formula weight	366.42	432.47	522.54	554.58
Crystal system	Monoclinic	Monoclinic	Monoclinic	Triclinic
Space group	$P2_1/n$	$P2_1/n$	$P2_1/n$	P-1
***a*[Å]**	8.38310(10)	7.0648(3)	12.2841(3)	8.2532(6)
***b*[Å]**	5.95530(10)	11.8381(3)	9.5178(2)	9.4964(6)
***c*[Å]**	19.8861(3)	13.3127(4)	22.3033(4)	18.1537(11)
***α*[°]**	90	90	90	77.630(5)
β [°]	93.2110(10)	102.415(3)	98.736(2)	84.033(5)
***γ*[°]**	90	90	90	73.806(6)
***V* [Å^3]**	991.23(3)	1087.36(6)	2577.40(10)	1333.15(16)
Z	2	2	4	2
***ρ* [g cm^{-3}]**	1.228	1.321	1.347	1.302
***T* [*K*]**	150.00(10)	150.01(10)	150.00(10)	150.01(10)
***λ* (Å)**	1.54184	0.71073	1.54184	0.71073
***μ* (mm^{-1})**	0.611	0.092	0.825	0.096
unique refl.	10062	13182	5041*	11364
Refl, I > 2σI	1946	3150	5041*	6108
***R*$_1$**	0.0386	0.0515	0.0714	0.0820
***wR*$_2$**	0.1047	0.1104	0.1784	0.1950
$\Delta\rho$(r) [e Å^{-3}]	0.28/-0.21	0.27/-0.26	0.41/-0.29	1.11/-1.03
Crystallisation Solvent	CH_2Cl_2/*n*-hexane	CH_2Cl_2/*n*-hexane	CH_2Cl_2	CH_3OH

*Table 5.45. Crystallographic data for **5.32-5.37**. Data for **5.36** and **5.37** have been taken for the structures at 150 K.*

	5.32	**5.33**	**5.34**	**5.35**	**5.36**	**5.37**
Formula	$C_{14}H_{15}N_2$. ClH_2O	$C_{18}H_{18}N_4$	$C_{19}H_{21}N_3O_2$	$C_{20}H_{24}N_2O_4$	$C_{18}H_{19}N_4$. $Cl.HO_{0.5}$	$C_{19}H_{22}N_3O_2$. $Cl.HO_{0.5}$
Formula weight	264.74	290.36	323.39	356.41	335.83	368.85
Crystal system	Orthorhombic	Monoclinic	Monoclinic	Monoclinic	Orthorhombic	Orthorhombic
Space group	*Pna*2$_1$	*P*2$_1$/*c*	*P*2$_1$/*c*	*P*2$_1$	*Fdd*2	*Fdd*2
***a*[Å]**	7.0958(8)	20.7770(7)	7.5185(3)	11.0036(5)	44.3599(14)	48.2500(11)
***b*[Å]**	21.837(3)	9.3348(2)	19.7652(6)	7.1553(3)	22.7723(6)	22.7902(6)
***c*[Å]**	8.2661(9)	18.1408(6)	11.8570(3)	11.7448(4)	7.0406(4)	6.66764(17)
***α*[°]**	90	90	90	90	90	90
β [°]	90	114.584(4)	103.387(3)	92.687(4)	90	90
***γ*[°]**	90	90	90	90	90	90
***V* [Å^3]**	1280.8(3)	3199.46(19)	1714.13(10)	923.70(6)	7112.3(5)	7331.9(3)
Z	4	8	4	2	16	16
***ρ* [g cm^{-3}]**	1.373	1.206	1.253	1.281	1.255	1.337
***T* [*K*]**	150.01(10)	150.01(10)	150.00(10)	150.00(10)	150.01(10)	150.00(10)
***λ* (Å)**	1.54184	0.71073	0.71073	0.71073	0.71073	0.71073
***μ* (mm^{-1})**	2.548	0.074	0.083	0.090	0.223	0.229
unique refl.	6456	24059	13061	10212	11234	27649
Refl, I > 2σI	2411	7948	4251	4615	4014	4465
***R*$_1$**	0.0613	0.0637	0.0523	0.0456	0.0411	0.0351
***wR*$_2$**	0.1494	0.1268	0.1103	0.0946	0.0822	0.0753
Δ*ρ*(r) [e Å^{-3}]	0.54/-0.25	0.23/-0.33	0.24/-0.19	0.26/-0.20	0.18/-0.18	0.20/-0.22
Crystallisation Solvent	DCM	CH_2Cl_2	CH_2Cl_2/*n*-hexane	$CHCl_3$	CH_3CN	CH_3CN

References

1 P. C. Bell and J. D. Wallis, *Chem. Commun.*, 1999, **2**, 257–258.

2 N. Mercadal, S. P. Day, A. Jarmyn, M. B. Pitak, S. J. Coles, C. Wilson, G. J. Rees, J. V. Hanna and J. D. Wallis, *CrystEngComm*, 2014, **16**, 8363–8374.

3 D. R. W. Hodgson, A. J. Kirby and N. Feeder, *J. Chem. Soc. Perkin Trans. 1*, 1999, 949–954.

4 P. C. Bell, M. Drameh, N. Hanly and J. D. Wallis, *Acta Crystallogr.*, 2000, **56**, 670–671.

5 A. Lari, M. B. Pitak, S. J. Coles, G. J. Rees, S. P. Day, M. E. Smith, J. V. Hanna and J. D. Wallis, *Org. Biomol. Chem.*, 2012, **10**, 7763–7779.

6 J. O'Leary, X. Formosa, W. Skranc and J. D. Wallis, *Org. Biomol. Chem.*, 2005, **3**, 3273–3283.

7 J. Clayden, C. McCarthy and M. Helliwell, *Chem. Commun.*, 1999, 2059–2060.

8 K. Mlinarić-Majerski, Đ. Škalamera, R. Glaser, L. Cao and L. Isaacs, *Tetrahedron*, 2016, **72**, 1541–1546.

9 P. R. Giles and C. M. Marson, *Dimethylchloromethyleneammonium Chloride*, John Wiley & Sons, Ltd, Chichester, 2001.

10 T. Saeki, A. Toshimitsu and K. Tamao, *J. Organomet. Chem.*, 2003, **686**, 215–222.

11 A. Bondi, *J. Phys. Chem.*, 1964, **68**, 441–451.

12 C. Jelsch, B. Guillot, A. Lagoutte and C. Lecomte, *J. Appl. Crystallogr.*, 2005, **38**, 38–54.

13 R. F. W. Bader, *Atoms in Molecules - A Quantum Theory*, Oxford University Press, Oxford, 1990.

14 J. O'Leary and J. D. Wallis, *Org. Biomol. Chem.*, 2009, **7**, 225–228.

Chapter 6

Structural Models for the Study of the Felkin-Anh Theory

Introduction

Nucleophilic addition to a carbonyl group is one of the most important reactions utilised by synthetic organic chemists,[1–6] allowing for the synthesis of a plethora of functionalities via C-C bond formation. If present, an α-chiral carbon centre has a significant influence on the stereoselectivity of the resultant product, either through 1, 2-asymmetric induction, if the starting material is optically pure, or via diastereoselectivity if the starting material is racemic. The ability to predict and control the manner by which the nucleophilic addition takes place has prompted the proposal of many models.[7]

Cram and Elhafez[8] introduced the first significant model in 1952, which stated: '*In certain non-catalytic reactions of the type shown (Scheme 6.1) that diastereomer will predominate, which could be formed by the approach of the entering group from the least hindered side when the rotational conformation of the C-C bond is such that the double bond is flanked by the two least bulky groups attached to the adjacent asymmetric centre'*. In essence, the rule stated that in the presence of an α-chiral carbon, the attack at the carbonyl group is based on steric hindrance. Cram's model is divided into two rules, dependant on the nature of the α-chiral carbon substituents, the favoured trajectory of the nucleophile and the other reagent present in the reaction. As shown in Scheme 6.1, the generalised ketone **6.1**, with a large (L), medium (M) and small (S) group at the α-carbon, can react via two conformations dependant on two rules: 1) the Cram-chelate rule[9–11] or 2) the Cram rule[8].

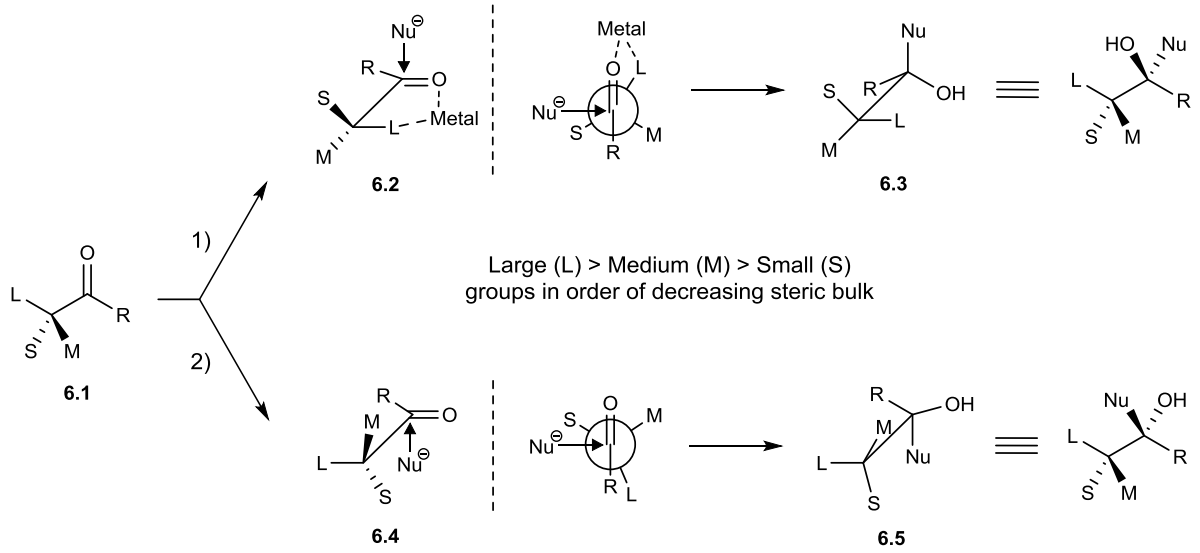

*Scheme 6.49. Reaction of α-chiral ketone **6.1** demonstrating 1) Cram's chelate rule to give **6.3** and 2) Cram's rule to give **6.5**.*

The Cram-chelate rule is obeyed if chelation between the carbonyl group and one of the α-chiral carbon substituents (aided by a metal cation) can occur, locking in the conformation **6.2** and placing the 'S' and 'M' groups on either side of the plane. As a result, the nucleophilic attack proceeds via the smallest substituent 'S', leading to the major product **6.3** (the Cram-chelate product). Since its proposal, this model has been shown to be highly reliable, with numerous examples shown in the literature.[12–18]

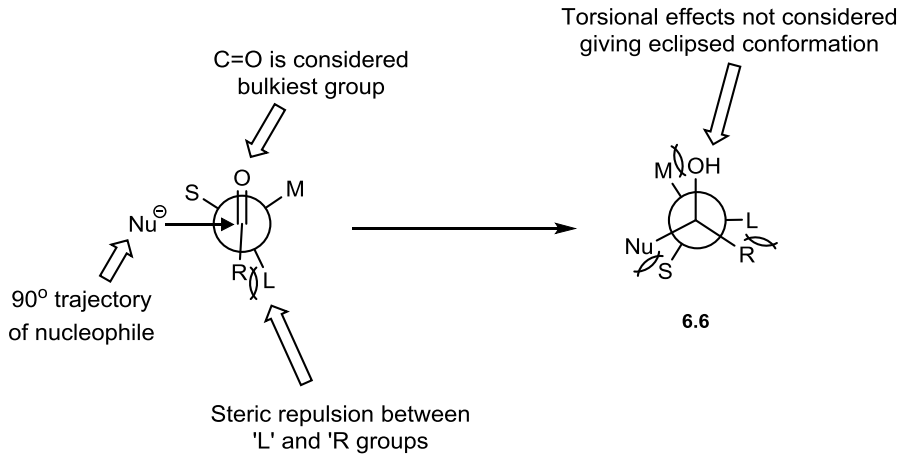

*Scheme 6.50. Summary of the hallmarks of Cram's model, leading to an eclipsed transitional conformation **6.6**.*

The Cram rule approach applies for cases where chelation between one of the α-carbon substituents and the carbonyl group could not occur. Thus, the reactive conformation **6.4** is preferred based upon steric reasoning. However, the carbonyl group in this model is deemed to be the group with the largest steric bulk and therefore substituent 'L' is placed *anti* to it. This overestimated the size of the carbonyl group and would result in an unfavoured steric repulsion between 'L' and 'R', especially in ketones where R ≠ H. In addition, as the carbonyl carbon is rehybridizing under the influence of the approaching nucleophile, the conformation adopts the highly unfavoured eclipsed conformation **6.6**, as shown in Scheme 6.2. Furthermore, the model was found to be inaccurate when one or more of the α-chiral carbon substituents was polar. If this occurs, the most polar group assumed the role of 'L', independent of the steric bulk of the remaining substituents.

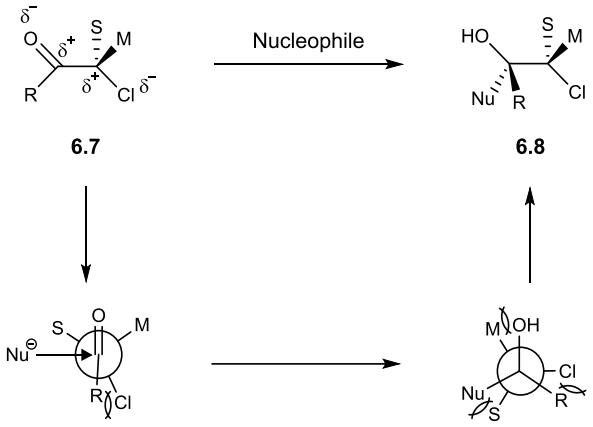

Scheme 6.51. Nucleophilic attack of an α-chloro-ketone according to Cornforth's model.[19]

In 1959, Cornforth *et al.*[19] presented an adapted model based upon Cram's which orientated the most electron-withdrawing group *anti* to the carbonyl group. Using the example of nucleophilic attack of an α-chloro-ketone (**6.7**), he argued that orientation of the chloride group *anti* to the carbonyl group, causes the dipoles of the C=O and C-Cl bonds to lie antiparallel to each other (Scheme 6.3). In turn, this allows for easier polarisation of the carbonyl group, which he states, '*has a marked effect on the energy required to form the transition state with a*

nucleophilic agent' and thus gives hydroxyl **6.8**. The rest of Cornforth's model remained the same as Cram's and thus the problems relating to the steric interactions of the group before the nucleophile's addition persisted.[20]

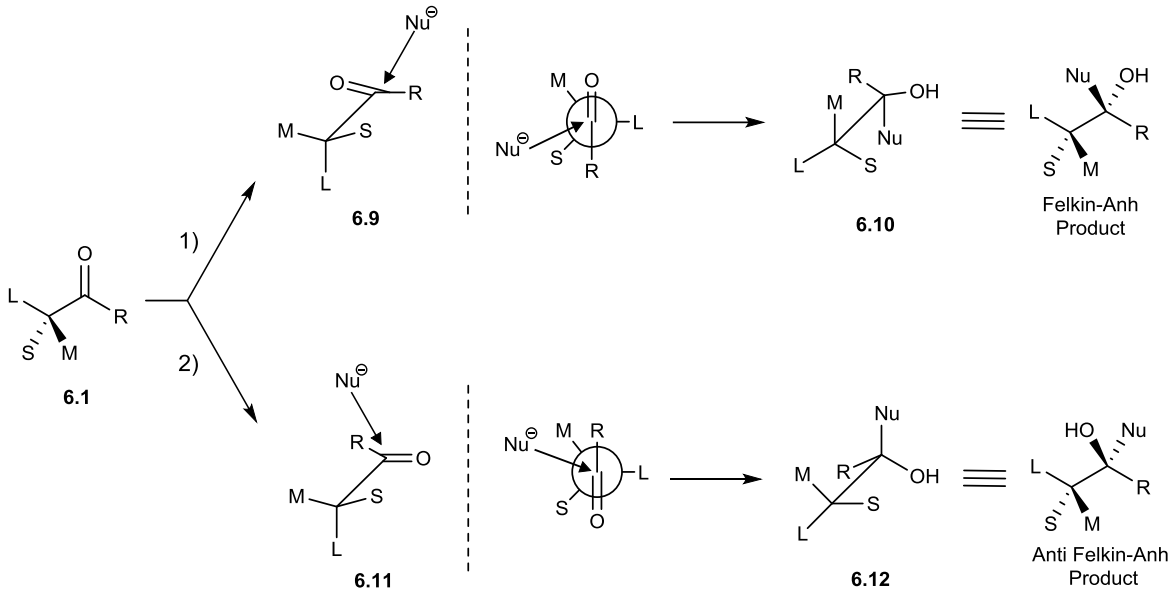

*Scheme 6.52. Nucleophilic attack of α-chiral ketone **6.1** via the two possible conformations (**6.9** and **6.11**), leading to the Felkin-Anh (**6.10**) and anti Felkin-Anh (**6.12**) product.*

Following several important contributions from Felkin,[21] Anh[22] and Eisenstein,[23,24] the Cram rule evolved to become commonly known as the 'Felkin-Anh' model. Key to the progression of the model and its success was that the α-substituent with the largest steric bulk was assigned as 'L', with it being placed orthogonal to the carbonyl group, reducing steric repulsion and generating an approach site for the nucleophile *anti* to the 'L' group. This allowed for two possible conformations (**6.9** and **6.11**), as shown in Scheme 6.4, for the nucleophilic attack. The most energetically favoured conformation was found to be **6.9**, as the trajectory of the nucleophile passed over the smaller 'S' group, resulting in the Felkin-Anh product **6.10**, opposed to passing over the 'M' group (**6.11**) which results in the anti-Felkin-Anh product **6.12**. This idea built successfully on the work of Karabatos,[25–27] which through extensive analysis of the most stable transition states of reactions of this type, states that the nucleophile

must approach the carbonyl carbon via the least-hindered path. Moreover, the Felkin-Anh model conformation means that as the nucleophile is approaching the carbonyl carbon, it passes through a staggered conformation (**6.13**) reducing the steric torsional repulsions (Scheme 6.5), unlike in the Cram rule model (Scheme 6.2).

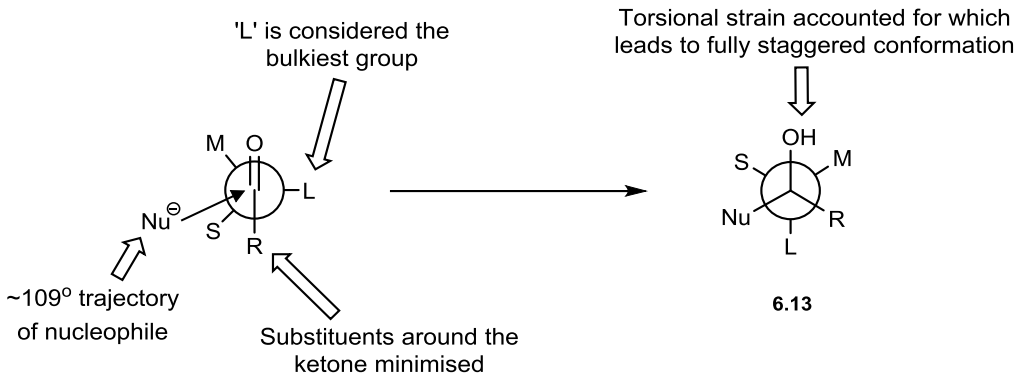

Scheme 6.53. Summary of the hallmarks of the Felkin-Anh model, leading to a preferred staggered transitional conformation ***6.13****.*

The favourability of conformation **6.9** was further reinforced by the works of both Bürgi and Dunitz[28–30] and also Anh and Eisenstein,[31] which demonstrated that the nucleophile prefers not to attack the carbonyl at the previously assumed 90° angle, but instead at an angle of ~109°, an angle that became known as the 'Bürgi-Dunitz angle' (Scheme 6.5 and Figure 6.1).

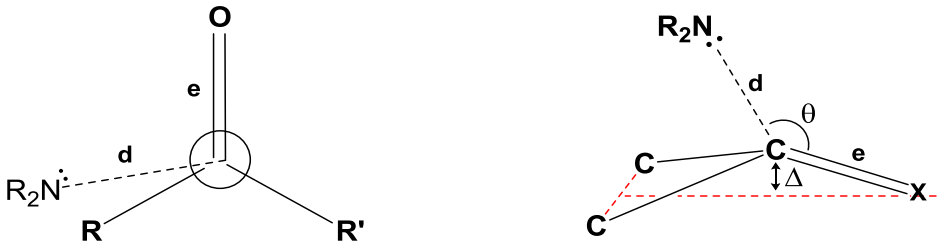

Figure 6.105. Angle of approach (θ) of a nucleophile (R_2N) to an electrophile (C=O), demonstrating the consequential pyramidalisation (Δ) of the electrophile carbon.

The work of Bürgi and Dunitz,[28,29,32] as previously discussed in Chapter 1, utilised the X-ray structural data of six known alkaloids, **6.14-6.19** (Figure 6.2). They identified that each of the structures could be represented as a point on the reaction coordinate along the reaction pathway for nucleophilic addition to a carbonyl group.

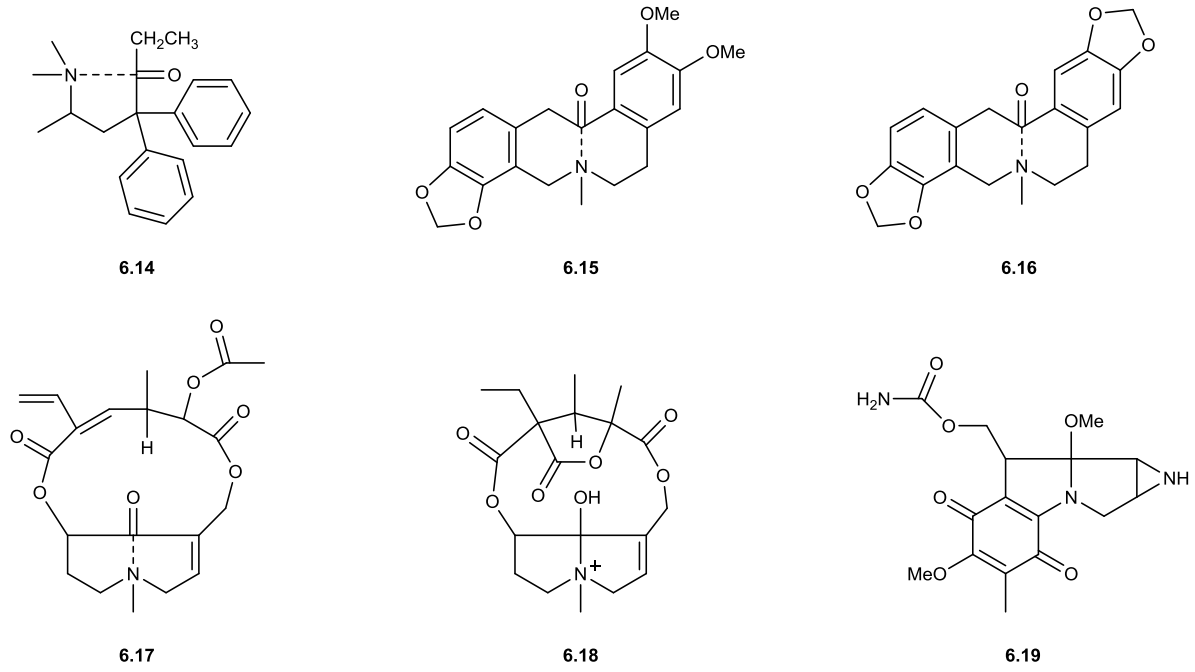

*Figure 6.106. The six alkaloid structures **6.14-6.19** which provided the basis for the work by Bürgi, Dunitz and Shefter.*[28,32]

These structures helped to shape the understanding of how a nucleophile approaches a carbonyl group, leading to the discovery of the Bürgi-Dunitz angle. Furthermore, as the distance between the interacting nucleophile and carbonyl decreased, an increase in pyramidalisation of the carbon from its trigonal plane was observed (Figure 6.1). This is a phenomenon that occurs as the planar trigonal carbonyl begins to become tetrahedral in nature. However, in all of the molecules described in the study, the ketone involved in the interaction or reaction was either in a ring or did not have an α-chiral carbon centre. In fact, no models are reported in the literature that demonstrate both the prearrangement of the α-chiral carbon substituents in tandem with a nucleophile approaching akin to the Bürgi-Dunitz angle.

Herein are described four structural models for the nucleophilic attack on such α-chiral ketones. A series of substituted naphthalenes demonstrating *peri*-interactions have been designed and synthesised in order to mimic a range of co-ordinates along the reaction pathway of nucleophilic attack on a carbonyl group attached to an asymmetrically substituted carbon atom. The molecules are in racemic form. Modification of either the naphthalene skeleton (at the

opposing second set of *peri*-positions) or the nucleophilic moiety will be made, whilst the α-chiral ketone substituents, which contain three substituents of different sizes (**'Small'** = H, **'Medium'** = CH_3 and **'Large'** = Ph) will remain consistent. In each case the molecular structure determined by single crystal X-ray diffraction will be used to observe both the Felkin-Anh orientation and Bürgi-Dunitz effects simultaneously.

Synthesis of the Target Compounds

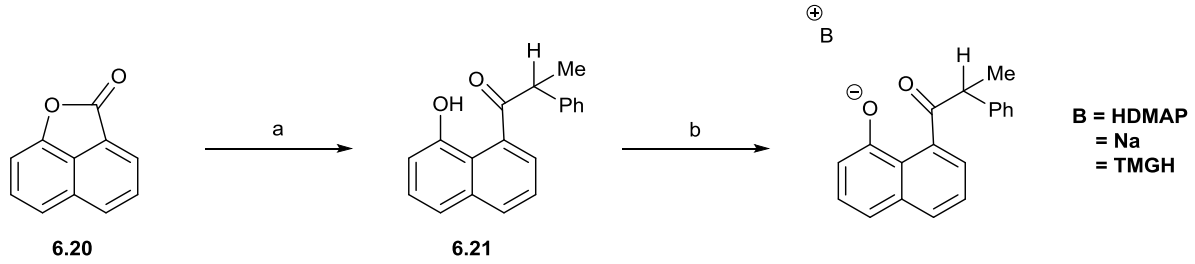

Scheme 6.54. (a) 1-phenylethylmagnesium bromide,[33] THF, -78 to 25 °C; (b) Reaction with a range of bases.

The first target for preparation was the *peri*-hydroxyketone **6.21** (Scheme 6.6). Ring opening of lactone **6.20**[34] by the Grignard reagent 1-phenylethylmagnesium bromide[33] gave the expected ketone **6.21** in a 23% yield. A shift in the ^{13}C NMR signal of the lactone carbonyl from 174.4 to 210 ppm in **6.21,** coupled with ^{1}H NMR signals at 4.65 and 1.63 ppm corresponding to that of the proton α to the carbonyl and the protons of the methyl group respectively, confirm its structure. Despite the ketone **6.21** being a solid at room temperature, exhaustive attempts to grow suitable crystals for structural analysis failed, in each case yielding solvated oils or amorphous powders. The hydroxyl group in **6.21** allows for deprotonation to occur with the potential that the oxyanion salts formed may be more crystalline. The pKa of the hydroxyl group was estimated to be similar to that of a phenolic proton (9.95 in H_2O) and **6.21** was reacted with a series of bases with varying pKa's (Scheme 6.6). Compound **6.21** was reacted with the strong bases 1,1,3,3-tetramethylguanidine (TMG) (pKa 13.6 in DMSO[35]) and sodium hexamethyldisilazide (NaHMDS) Initially, NMR analysis of both reactions revealed notable shifts indicating that a deprotonation had occurred, however NMR analysis of the same samples after 24 hours revealed an almost complete decomposition of the sample. It is important to note that the ketone **21** possesses an α-proton (pKa ~20), which could potentially be targeted by not only the chosen base, but also by the subsequently desired oxyanion across

the *peri*-positions, generating an enolate and a potential site for decomposition to occur (Figure 6.3).

*Figure 6.107. Reaction of **6.21** with a strong base could result in the loss of either acidic proton (red).*

Previous analogous results[36] demonstrate that the weaker base 4-dimethylaminopyridine (DMAP) was not a strong enough base to deprotonate a range of *peri*-hydroxy ketones however, the reaction of **6.21** with DMAP was performed on the basis that if deprotonation did not occur, a hydrogen bonded complex could still allow for structural analysis of the *peri*-hydroxy ketone. Unfortunately, despite yielding a crystalline solid, structural analysis of the product indicated two problems, 1) as previously observed, deprotonation had not taken place, with the DMAP hydrogen bonding to the target hydroxyl proton and 2) the structure contained six crystallographically unique (or 3 pairs of interacting) molecules in the ASU, and two of these were significantly disordered. As a result, the structural model obtained gave poor accuracy with regards to important structural parameters, such as bond lengths and angles, making it unsuitable for use in this study.

In an attempt to prepare a more crystalline hydroxyketone, the target was redesigned to incorporate a phenyl ring *para* to the interacting hydroxyl group (Scheme 6.7). Synthesis of the new target **6.24** began with the bromination of the lactone **6.20** with excess liquid bromine in chloroform, with the desired *mono*-brominated lactone **6.22** isolated as the only major product in a 90% yield. The structure of **6.22** was confirmed by the loss of an aromatic triplet in the ^{1}H NMR spectrum along with the presence of the characteristic two signals for a bromine containing molecular ion in the accurate mass spectrum.

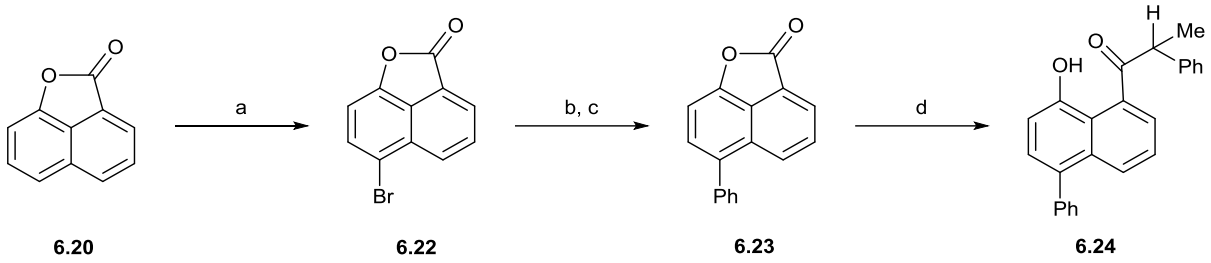

6.20 **6.22** **6.23** **6.24**

Scheme 6.55. (a) Br_2, $CHCl_3$, RT; (b) Phenyl boronic acid, $Pd(PPh_3)_4$ (5 mol%), K_2CO_3, MeOH, reflux; (c) Oxalyl chloride, DCM, RT; (d) 1-phenylethylmagnesium bromide,[33] THF, -78 to RT.

A Suzuki-Miyaura coupling of **6.22** with phenylboronic acid initially seemed to yield no notable organic product when extracted with a range of organic solvents. However, the base (K_2CO_3) required for the catalytic turnover of the palladium catalyst ($Pd(PPh_3)_4$) had hydrolysed the lactone, generating the hydroxy acid **6.22a** most likely as a potassium salt (Scheme 6.8). Acidification of the aqueous portions yielded a milky precipitate which was extracted with ethyl acetate to eventually give a crude yellow solid.

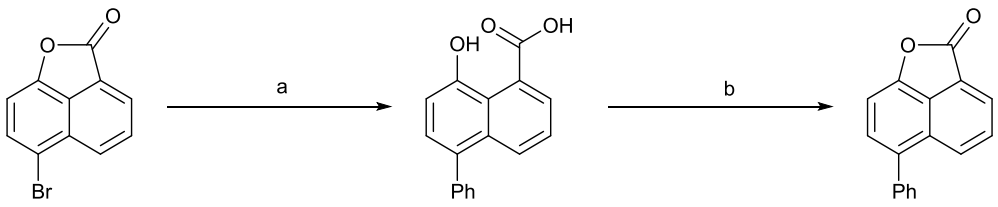

6.22 **6.22a** **6.23**

Scheme 6.56. (a) Phenyl boronic acid, $Pd(PPh_3)_4$ (5 mol%), K_2CO_3, MeOH, reflux; (b) Oxalyl chloride, DCM, RT.

In order to regenerate the *peri*-lactone the crude solid was stirred with excess oxalyl chloride in DCM, generating the reactive acyl chloride intermediate, which underwent *in-situ* cyclisation to give the desired product **6.23** as a crystalline yellow solid in a 30% yield. Regeneration of the lactone was demonstrated by a carbonyl carbon peak at 167.3 ppm in the ^{13}C NMR spectrum, whilst the addition of five aromatic protons in the ^{1}H NMR spectrum indicated a successful incorporation of a new phenyl ring by the Suzuki-Miyaura coupling. The ring opening of phenyl substituted lactone **6.23** was carried out via the same methodology as for lactone **6.20**, giving the desired *peri*-hydroxy ketone **6.24** in a 31% yield. Similarly, a shift in the ^{13}C NMR signal of the lactone carbonyl from 174.4 ppm to 209.0 ppm in **6.24** was observed along with the ^{1}H NMR signals at 1.55 and 4.35 ppm for the methyl and α-protons respectively.

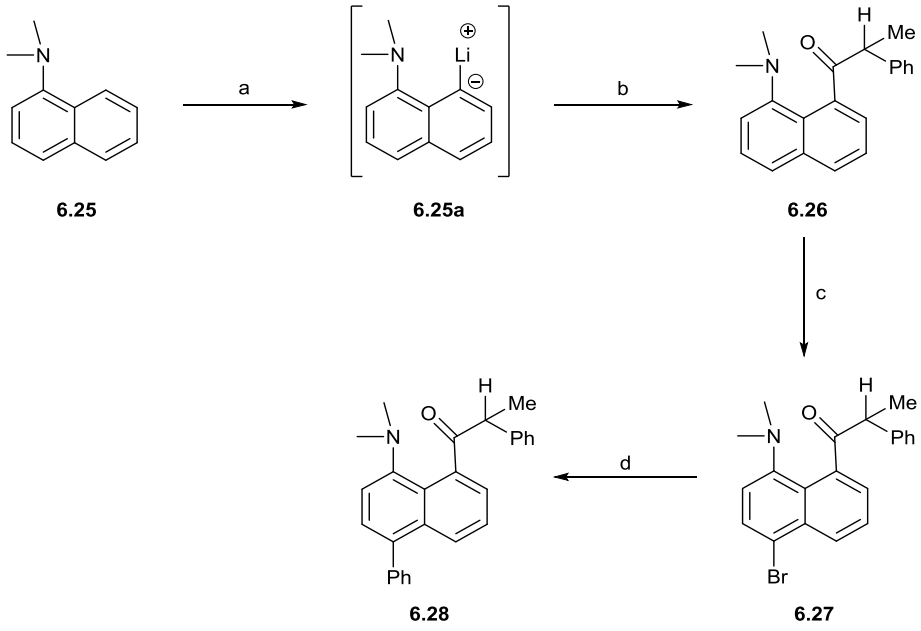

Scheme 6.57. (a) n-BuLi (1.6M), Et_2O, RT; (b) 2-phenylpropanoyl chloride,[37] THF, -78 °C to RT; (c) Br_2, CCl_4, RT; (d) Phenyl boronic acid, $Pd(PPh_3)_4$ (10 mol%), K_2CO_3, DMF, H_2O, reflux.

The synthesis of compound **6.26** with a Me_2N---C=O interaction began with the *peri*-lithiation of 1-dimethylaminonaphthalene **6.25** with *n*-butyl lithium, generating a pale-yellow precipitate of the lithiated salt **6.25a** (Scheme 6.9). The supernatant was removed and the lithiated salt was

reacted with a freshly prepared solution of 2-phenylpropanoyl chloride[37] to give the target ketone **6.26** as a yellow oil in a 46% yield. Despite every effort the oil did not crystallise, thus in a similar fashion to the *peri*-hydroxyl ketone, the target was modified to incorporate a phenyl group *para* to the interacting dimethylamino group. Compound **6.26** was successfully brominated *para* to the dimethylamino group via the slow addition of a solution of bromine in carbon tetrachloride, giving the desired *mono*-substituted product **6.27** as an orange oil in a 50% yield. The structure of **6.27** was confirmed by the loss of an aromatic triplet ^{1}H NMR spectrum. A Suzuki-Miyaura coupling of **6.27** with phenylboronic acid gave the target compound **6.28** as an orange solid in a 65% yield and its structure was confirmed by the introduction of five additional aromatic protons in the ^{1}H NMR spectrum.

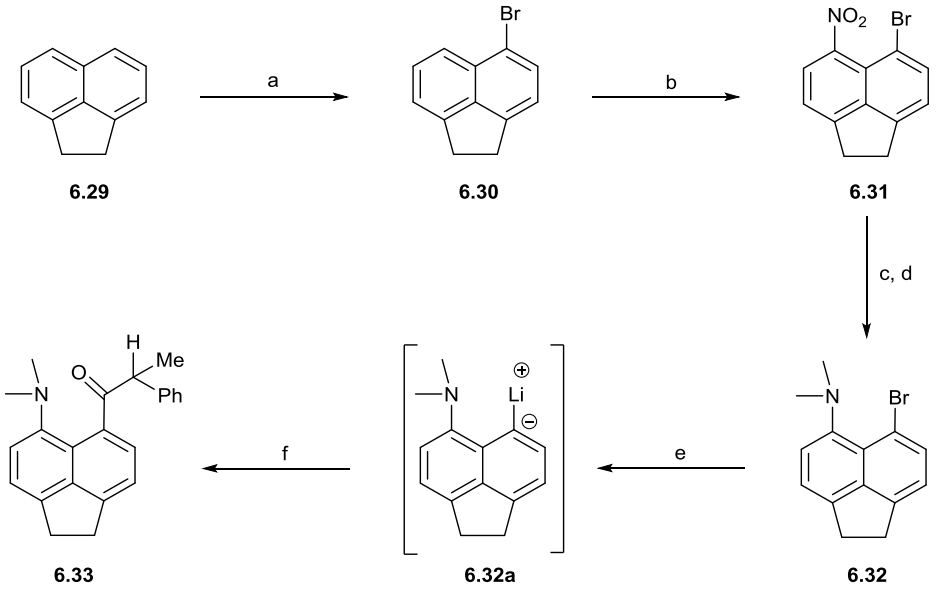

Scheme 6.58. (a) NBS, DMF, RT;[38] (b) Fuming HNO_3, AcOH, RT;[38] (c) Fe, Fe(III)Cl_3, AcOH, EtOH, 100 °C;[39] (d) MeI, K_2CO_3, CH_3CN, 50 °C;[39] (e) n-BuLi (2.5M), THF, -78 to 25 °C; (f) 2-phenylpropanoyl chloride,[37] THF, -78 to 25 °C.

Compound **6.32** which contains an ethylene bridge *para* to the dimethylamino and bromo *peri*-groups was prepared according to known literature procedures[38,39] (Scheme 6.10). To begin, acenaphthene (**6.29**) was *mono*-brominated at the *5*-position *para* to the ethylene bridge with N-bromosuccinimide (**6.30**) before being *peri*-nitrated via the addition of excess fuming nitric acid in acetic acid to give **6.31**.[38] Reduction of the nitro group with iron(III) chloride and iron

powder resulted in the amino compound, which was *N*-dimethylated *in situ* to give **6.32**, following the methods described by Pla *et al.*[39] Following the general methods described for the synthesis of **6.26**, compound **6.32** was *peri*-lithiated with *n*-BuLi at -78 ^{o}C over 3h (**6.32a**) before a freshly prepared solution of 2-phenylpropanoyl chloride[37] was added, resulting in the isolation of the ketone **6.33** as a yellow solid in a 36% yield. The successful addition of the ketone is evidenced by a peak in the ^{13}C NMR spectrum at 208.2 ppm and a stretching frequency of 1686 cm^{-1} in the infrared spectrum.

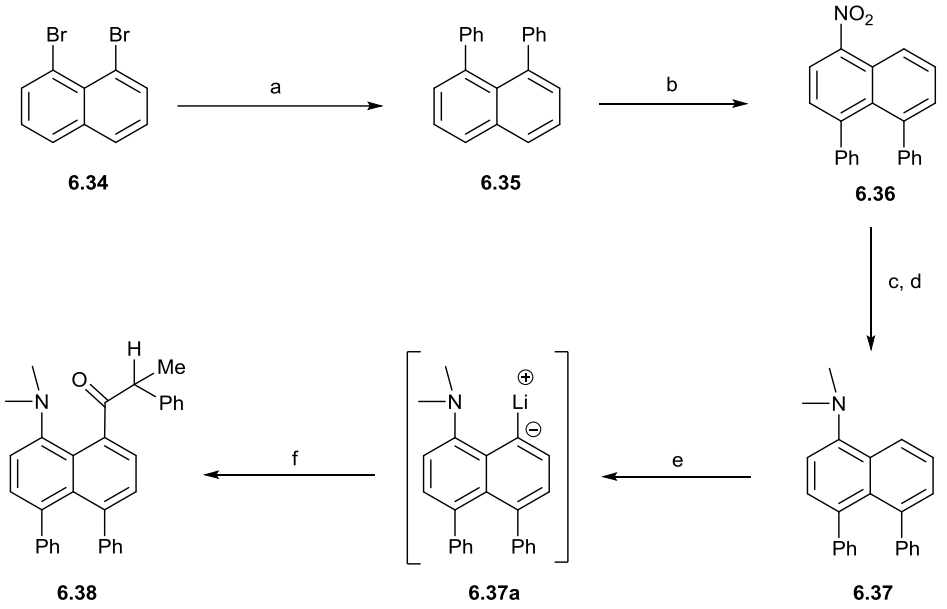

Scheme 6.59. (a) Phenyl boronic acid, Pd(OAc)$_2$ (10 mol%), K$_2$CO$_3$, H$_2$O, DMF, 100 ^{o}C;[40] (b) Conc. HNO$_3$, DCM, 25 ^{o}C;[41] (c) Fe, Fe(III)Cl$_3$, AcOH, EtOH, 100 ^{o}C;[39] (d) MeI, K$_2$CO$_3$, CH$_3$CN, 50 ^{o}C;[39] (e) n-BuLi (2.5M), THF, 80 ^{o}C; (f) 2-phenylpropanoyl chloride,[37] THF, -78 to 25 ^{o}C.

To push the peri-groups in 28 closer together, the 4, 5-diphenyl derivative **6.37** was identified as a target. The synthesis of compound **6.37** was achieved by an adaptation of the methods previously described by Pla *et al.*[39] (Scheme 6.11). However, this synthesis began with the double Suzuki-Miyaura coupling of 1,8-dibromonaphthalene **6.34** with phenylboronic acid[40] to give the fluorescent 1,8-diphenylnaphthalene **6.35**. Nitration of **6.35** as described by House *et al.*[41] resulted in the formation of the *mono*-nitrated naphthalene **6.36**, which was reduced and *N*-dimethylated *in situ* to give the desired 1-dimethylamino-4, 5-diphenyl-naphthalene **6.37**.[39]

Compound **6.37** was *peri*-lithiated with an excess of *n*-butyl lithium in refluxing hexane, generating a grey precipitate of the lithiated salt **6.37a**. The supernatant was removed and the lithiated salt was reacted with a freshly prepared solution of 2-phenylpropanoyl chloride[37] to give the target **6.38** as a 'crispy yellow foam' in a 37% yield. Success of the addition was evidenced by a peak in the ^{13}C NMR spectrum at 203.24 ppm and a stretching frequency of 1675 cm^{-1} in the infrared spectrum corresponding to the carbonyl of the ketone. Recrystallisation of the 'crispy foam' from hexane resulted in the crystallisation of ketone **6.38** as thin hexagonal plates.

Structural Analysis

*Table 6.46. Selected geometric details for the four target compounds **6.24**, **6.28**, **6.33** and **6.38**.*

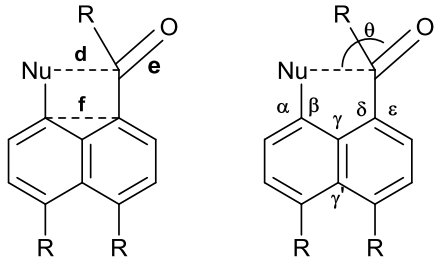

Compound	**d** / Å	**e** / Å	**θ** / º	**f** / Å	**τ**[a] / º	**τ**[b] / º	**Pyr**[c]	**α** / º	**β** / º	**δ** / º	**ε** / º	**γ / γ' / º**
6.24	2.631(2)	1.216(2)	118.5(1)	2.500(3)	-	83.6(2)	0.060(2)	122.4(2)	117.0(2)	124.7(2)	115.8(2)	122.2(2) / 121.9(2)
6.28	2.576(2)	1.221(2)	104.9(1)	2.498(3)	-73.9(2), 52.5(2)	95.0(2)	0.080(2)	122.3(1)	117.7(1)	122.6(1)	117.2(1)	122.3(1) / 121.5(1)
6.33	2.801(2)	1.215(2)	112.3(1)	2.559(2)	-87.7(2), 40.8(2)	96.5(1)	0.056(1)	123.2(1)	117.7(1)	123.7(1)	117.3(1)	127.3(1) / 112.4(1)
6.38	2.490(2)	1.214(2)	103.0(1)	2.462(2)	81.3(2), -45.0(2)	95.2(2)	0.097(2)	122.6(1)	117.5(1)	123.8(1)	116.6(1)	119.6(1) / 124.4(1)

τ^a = torsion angle: C11-N1-C1-C2 & C12-N1-C1-C2, τ^b = torsion angle: O=C-C-C(Ph), [c] Pyr = pyramidality, deviation of carbonyl carbon from the plane of the three neighbouring atoms towards the *peri* O atom.

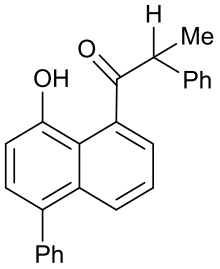

6.24

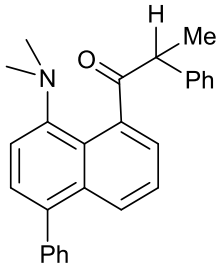

6.28

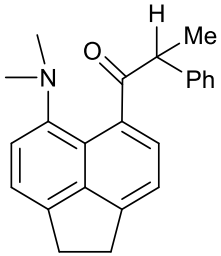

6.33

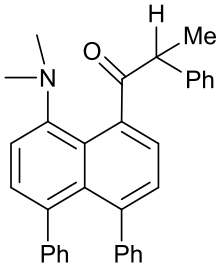

6.38

*Figure 6.108. Structures of the ketones **6.24**, **6.28**, **6.33** and **6.38**.*

To explore how the strength of the nucleophile effected both the Felkin-Anh pre-arrangements and Bürgi-Dunitz angle during the earlier stages of nucleophilic attack on a carbonyl, crystals of the *peri*-hydroxyl and -dimethylamino ketones **6.24** and **6.28** were grown (Figure 6.4). This was achieved via slow evaporation of DCM/$CHCl_3$ (**6.24**) and DCM (**6.28**) solutions and the X-ray crystal structures were determined at 150K and 100K respectively (Figure 6.5). Selected molecular geometry information for the compounds discussed is shown in Table 6.1. In a similar fashion to the *peri*-hydroxyl ketone series discussed in Chapter 2, **6.24** and **6.28** display the expected angular displacements of the two interacting *peri*-groups, resulting in Nu---C=O separations of 2.631(2) and 2.576(2) Å respectively. Bürgi-Dunitz angles of 118.5(1)^o for the former and nearer optimal 104.9(1)^o for the more potent nucleophilic centre in the latter are observed, with both molecules displacing their *peri*-groups marginally to opposite sides of the naphthalene plane. The larger Bürgi-Dunitz angle observed in **6.24** could result from the dimethylamino nucleophile (C(naph)-N(Me_2) bond 1.442(2) Å) sitting 0.083 Å further from the naphthalene ring than the hydroxyl group (C(naph)-O(H) 1.359(2) Å).

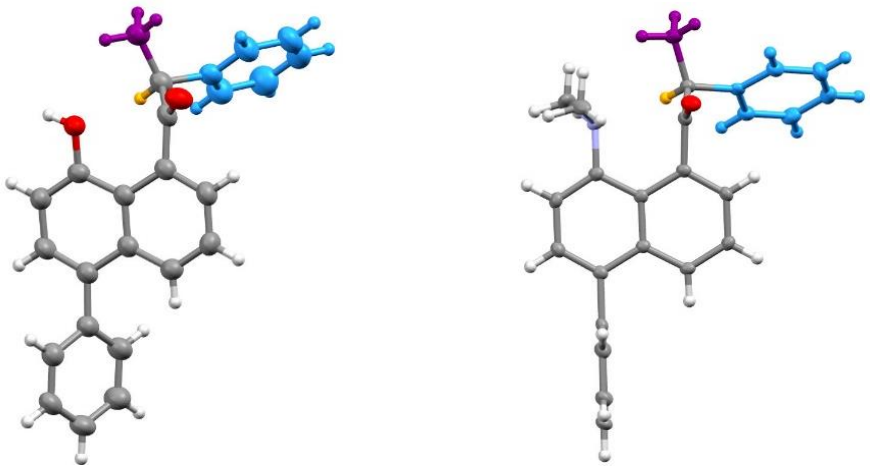

*Figure 6.109. Molecular structures of α-chiral ketones **6.24** (left) and **6.28** (right). The substituents phenyl (blue), methyl (purple) and proton (orange) of the α-carbon have been colour coded.*

The nitrogen atom lone pair of the dimethylamino group is orientated towards the anti-bonding π* orbital of the *peri*-carbon at an angle of 20.6^o to the N---C vector (Figure 6.6). Furthermore,

the two N-methyl groups are positioned either side of the naphthalene plane with C(Me)-N-C-C(H) torsion angles (τ^a) of -73.9(2) and 52.5(2)^o (Figure 6.6). A greater degree of pyramidalisation is observed in **6.28** (0.080(2) Å) compared to **6.24** (0.060(2) Å), as expected due to the increased nucleophilic potency of NMe_2 versus the OH group.

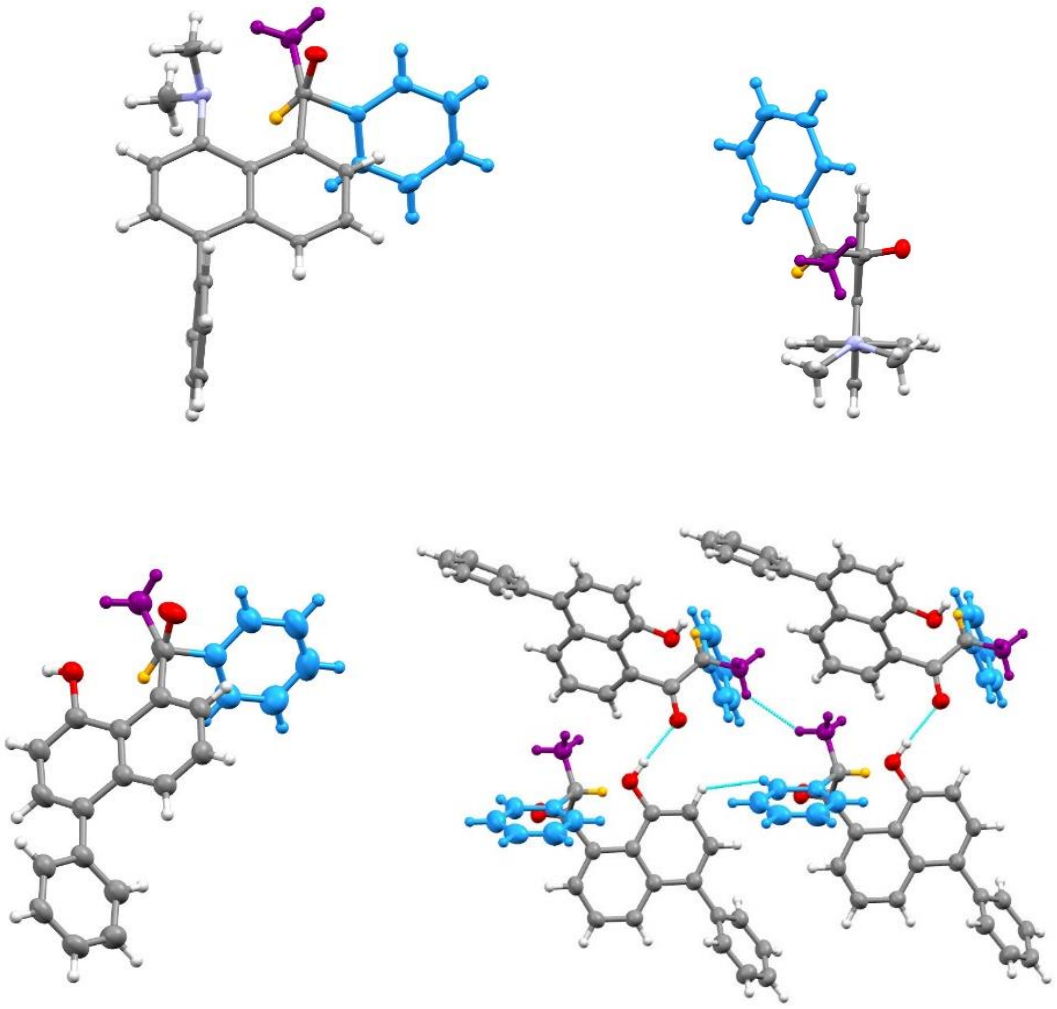

*Figure 6.110. The molecular structure of **6.28** shown with a bird's-eye view (top left) and the Felkin-Anh pre-arrangement (top right). The molecular structure of **6.24** (bottom left) is shown alongside the crystal packing arrangement of **6.24** (bottom right) indicating the hydrogen bonds and close contacts between the atoms. The substituents phenyl (blue), methyl (purple) and proton (orange) of the α-carbon have been colour coded.*

In both compounds **6.24** and **6.28**, the bond from the stereocentre to the *ipso*-carbon of the α-phenyl ring is positioned orthogonal with respect to the carbonyl group (Figure 6.6), with the O=C-C-C(*ipso*) torsion angles (τ^b) of -83.6(2)^o and -95.0(2)^o respectively, demonstrating the expected Felkin-Anh orientation thus clearly supporting that model for nucleophilic attack on

an α-chiral carbonyl group. The phenyl ring *para* to the nucleophile in **6.28** lies almost perpendicular to the best naphthalene plane by 92.3(2)^{o}, minimising the steric repulsions of the two rings, whilst also presenting the phenyl ring face for π-π stacking. The phenyl ring of **6.24,** however, is tilted by only 59.7(3)^{o} with respect to the naphthalene plane, a consequence of minimising the contacts between the ring with other molecules in the packing lattice. The molecules of **6.24** are linked together via hydrogen bonds between hydroxyl and carbonyl groups (O-H---O=C: 1.94 Å). The two shortest intermolecular contacts occur between the methyl group protons and the naphthalene and phenyl '*ortho*' protons (Figure 6.6).

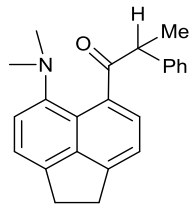

6.33

*Figure 6.111. Structures of the ethylene bridged α-chiral ketone **6.33***

Interactions between the *peri*-groups of such naphthalenes can be influenced by functionalisation at the opposing, second set of *peri*-positions as demonstrated in the previously discussed works of Suzuki and Ishigaki[42] by the installation of a short ethylene bridge. Following the synthesis of the acenaphthene derived *peri*-dimethylamino ketone **6.33** (Figure 6.7), suitable crystals were obtained via slow evaporation of a DCM/hexane solution and the X-ray crystal structure determined at 150 K (Figure 6.8). The strained 5-membered ring (previously shown in Chapter 3) leads to a significant increase in the separation between the interacting *peri*-groups, with a Me_2N---C distance of 2.801(2) Å compared to 2.576(2) Å in the 4-phenyl substituted analogue **6.28**. Moreover, a difference of just under 15^{o} in the *exo*-angles at the ring fusions between the two *peri*-positions (γ and γ') shows how the short bridge has compressed the distance between one set of *peri*-ring carbon atoms and widened the separation between the others (i.e. 127.3(1) vs. 112.4(1)^{o} in **6.33** and 122.3(1) vs.121.5(1)^{o} in **6.28**).

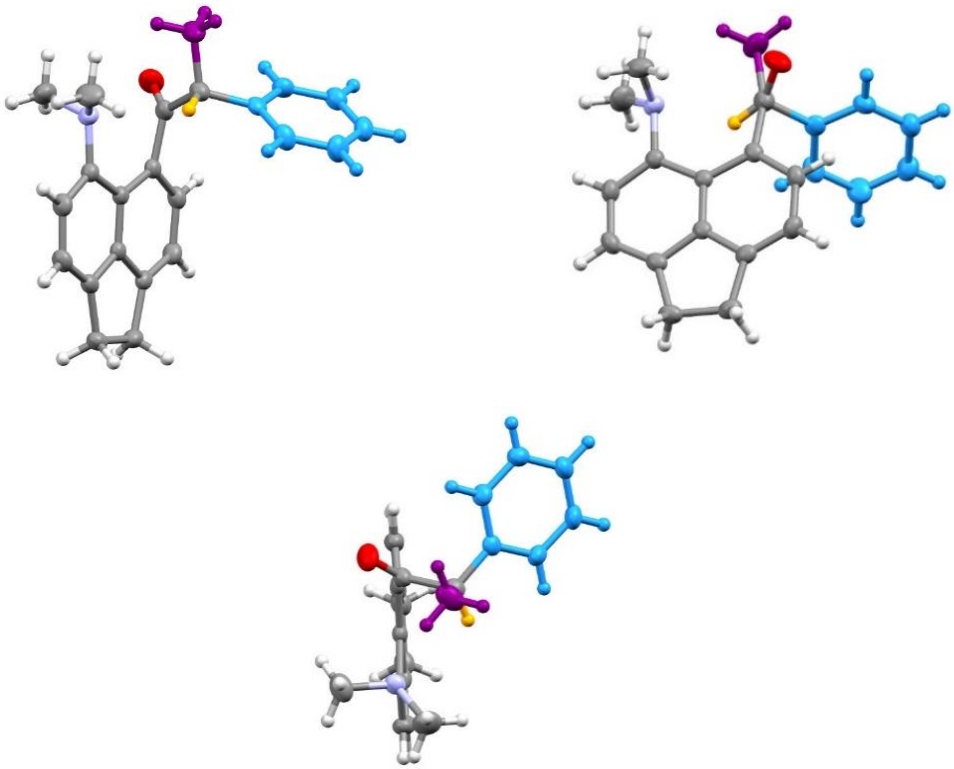

*Figure 6.112. The molecular structure of **6.33** (top left) demonstrating a birds-eye view (bottom middle) and the Felkin-Anh pre-arrangement (right). The substituents phenyl (blue), methyl (purple) and proton (orange) of the α-carbon have been colour coded.*

The *peri*-groups of **6.33** display angular displacements and deviations from the naphthalene plane (to opposite sides) similar to those of **6.28**, with the distance between the two naphthalene *peri*-carbons increasing to 2.559(2) Å in the former compared to 2.498(2) Å in the latter. The increased separation between the *peri*-groups results in the nitrogen lone pair no longer being oriented optimally for interaction with the carbonyl group and instead being found at an angle of 25.3º to the N---C vector. The (H_3)C-N-C-C(H) torsion angles are -87.7(2) and 40.8(2)º, indicate that the nitrogen lone pair are partially conjugated with the aromatic system as opposed to being involved in the *peri*-interaction. As a result, a smaller pyramidalisation of the carbonyl carbon of 0.056(1) Å is observed, similar to that of the weaker OH nucleophile in **6.24**. Despite this, the bond from the stereocentre to the *ipso*-carbon of the α-phenyl ring is still positioned almost orthogonal to the carbonyl group with a torsion angle (τ^b) of -96.5(1)º, and with the

dimethylamino nucleophile approaching along a 112.3(1)^{o} Bürgi-Dunitz trajectory (Figure 6.8).

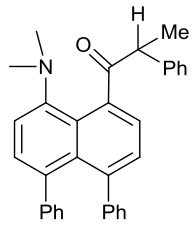

6.38

*Figure 6.113. Structures of the peri-diphenyl α-chiral ketone **6.38***

In contrast to **6.33**, the synthesis of *peri*-diphenyl derivative **6.38** (Figure 6.9) replaced the tethering ethylene bridge with two phenyl rings, causing a repulsion between the two *peri*-phenyl groups. Recrystallisation of **6.38** from *n*-hexane resulted in hexagonal plates and the X-ray structure of one of them was determined at 150 K (Figure 6.10). The two *peri*-phenyl groups are tilted at 69.0(2) and 67.8(2)^{o} in the same direction to the best naphthalene plane, resulting in a widening of the nearby *exo*-angle (γ') to 129.4(1)^{o}. The opposite *exo*-angle (γ) is compressed to 119.6(1)^{o}, with the distance between the two *peri*-naphthalene carbon atoms reducing to 2.462(2) Å. This results in a shortened Me_2N---C distance of 2.490(2) Å, compared to the 4-phenyl analogue **6.28** (2.576(2) Å). As a consequence of the shorter contact, a pyramidalisation of 0.097(2) Å of the carbonyl carbon is observed, the largest seen in the series. The dimethylamino nitrogen lone pair is orientated at 20.4^{o} to the Me_2N---C vector towards the anti-bonding π* orbital, whilst the methyl groups unevenly straddle the naphthalene plane with torsion angles (τ^{a}) of 81.3(2) and -45.0(2)^{o}. This arrangement is partially due to the minimalisation of the H---C contact distances between the *ortho*-naphthalene H and C-methyl protons with one of the N-methyl groups. The two interacting *peri*-atoms of **6.38** deviate from the naphthalene plane by no more than 0.02 Å and demonstrate in-plane angular displacements that are in accordance with those of **6.28** and **6.33**. Meanwhile, the *peri ipso* carbons of the

phenyl groups deviate from the naphthalene plane by 0.110 and 0.152 Å. As is consistent throughout the series, a near orthogonal positioning of the bond from the stereocentre to the *ipso*-carbon of the phenyl ring is observed with a torsion angle (τ^b) of 95.2(2)^o and a Bürgi-Dunitz angle of 103.0(1)^o is observed for the approaching dimethylamino nucleophile (Figure 6.10).

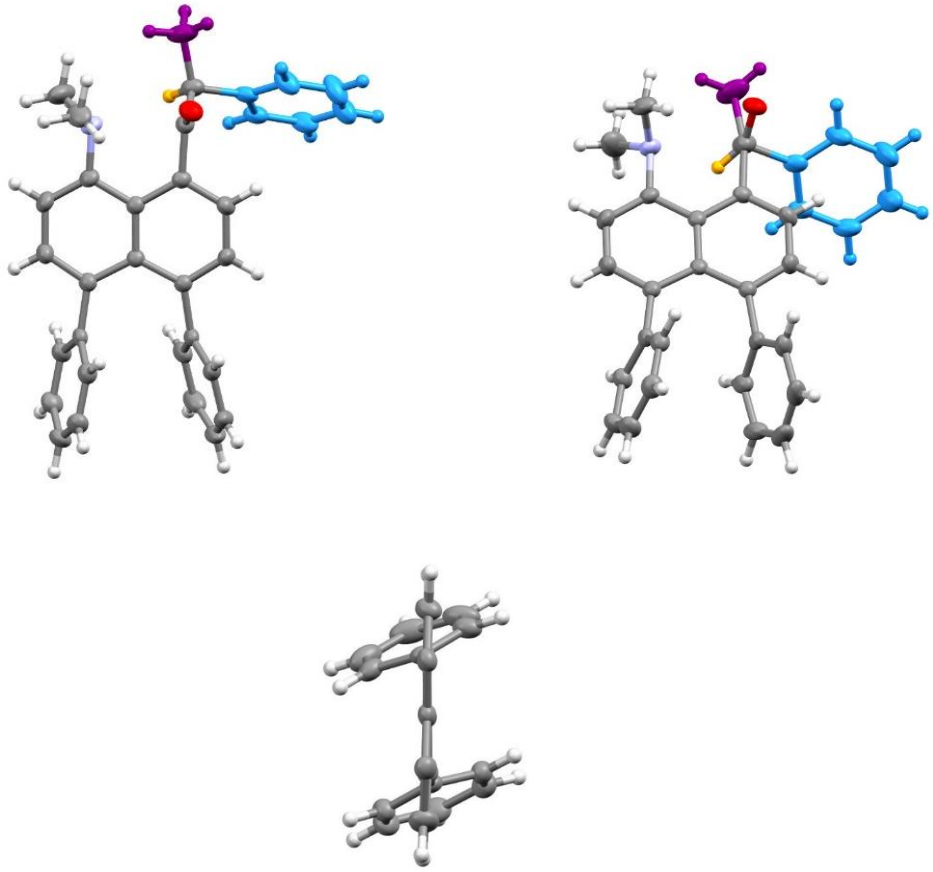

*Figure 6.114. The molecular structure of **6.38** (top left) and the Felkin-Anh pre-arrangement (top right) and a bird's eye view of the tilted phenyl rings (bottom), where the opposite peri-substituents have been omitted. The substituents phenyl (blue), methyl (purple) and proton (orange) of the α-carbon have been colour coded.*

The aim of the series described in this work was to synthesise and obtain structural models which demonstrated the commonly observed Bürgi-Dunitz angle[28,29,32] alongside the rarely observed Felkin-Anh pre-arrangement for nucleophilic attack on an α-chiral carbon atom. In all cases this was successful. Compounds **6.24** and **6.28** allowed for the direct comparison of two nucleophiles which possess different strengths. This was confirmed by the reduction in the

pyramidalisation of the carbonyl carbon when a hydroxyl group was utilised as the nucleophile, but nevertheless, they both displayed satisfactory torsion angles (τ^b) and Bürgi-Dunitz angles, thereby modelling both effects simultaneously. Modification to the naphthalene skeleton in compounds **6.33** and **6.38** created structural models located at very different points on the reactional pathway for nucleophilic addition. When the reactive groups were forced into a closer proximity, **6.38** displayed the greatest degree of pyramidalisation with the shortest interaction distance. When they were pulled apart, the interacting groups of **6.33** began to display signs of a weaker interaction through the orientation of the nucleophile lone pair and the lowest degree of pyramidalisation at the carbonyl carbon in the series. Regardless, both models possessed torsion angles (τ^b) and Bürgi-Dunitz angles parallel to that predicted in the literature. Across the four compounds a clear shift is observed in the ^{13}C NMR carbonyl shifts, with the two longest contacts of **6.24** (209.0 ppm) and **6.33** (208.2 ppm) demonstrating notable downfield shifts compared to that of the shorter contacts of **6.28** (203.7 ppm) and **6.38** (203.4 ppm). Nevertheless, the pyramidalities are all quite small, and there is little difference in the infra-stretches of the carbonyl groups (1673-1675 cm^{-1}) except for the acenaphthene derivative **6.33** which has the longest interaction distance and shows a stronger carbonyl stretch (2.801(2) Å, 1683 cm^{-1}). All four derivatives show the predicted disposition of phenyl, methyl and hydrogen groups relative to the carbonyl group. This provides support for the Felkin-Anh model.

Experimental

General. Solution NMR spectra were measured on a Jeol ECLIPSE ECX or ECZ 400 spectrometer at 400 MHz for ^{1}H and at 100.6 MHz for ^{13}C using $CDCl_3$ as solvent and tetramethylsilane (TMS) as standard unless otherwise stated, and measured in p.p.m. downfield from TMS with coupling constants reported in Hz. IR spectra were recorded on a Perkin Elmer Spectrum 100 FT-IR Spectrometer using Attenuated Total Reflection sampling on solids or oils and are reported in cm^{-1}. Mass spectra were recorded at the EPSRC Mass Spectrometry Centre at the University of Swansea. Chemical analysis data were obtained from Mr Stephen Boyer, London Metropolitan University.

Preparation of 1-(8'-hydroxynaphthalen-1'-yl)-2-phenylpropan-1-one, 6.21.

Lactone[34] **6.20** (2.55 g, 15.00 mmol) was dissolved in anhydrous THF (20 mL) under nitrogen and cooled to -78℃. A solution of 1-phenylethylmagnesium bromide was prepared according to a literature procedure[33] and 15.00 mmol was added steadily to the solution. The reaction was allowed to warm to room temperature and left to stir overnight after which it was treated with water (50 ml). The aqueous solution was washed with EtOAc (3 x 50 mL) and the combined organic layers were washed with H_2O (50 mL), brine (50 mL) and dried over $MgSO_4$. The solvent was removed *in vacuo* to give a crude oil which was purified by flash column chromatography (1:9 EtOAc/petrol 40-60), to give **6.21** as a tan solid (0.95 g, 23%), m.p. 114-117℃. δH (400 MHz, $CDCl_3$, 24 °C): 7.85 (1H, dd, J = 6.8, 2.9 Hz, Ar-H_1), 7.65 (1H, s, O*H*), 7.41 (1H, d, J = 8.1 Hz, 4'-*H*), 7.38 (1H, t, J = 7.6 Hz, 3'-*H*), 7.18-7.30 (7H, m, Ar-H_7), 7.00 (1H, d, J = 7.4 Hz, 2'-*H*), 4.65 (1H, q, J = 6.9 Hz, C*H*), 1.63 (3H, d, J = 6.9 Hz, (C)CH_3); δC (100 MHz, $CDCl_3$, 24 °C): 210.5 (*C*=O), 152.1, 140.6, 136.1, 135.7, 132.2, 128.9, 128.3, 127.9,

127.2, 127.3, 124.5, 121.4 (Ar-*C*$_{12}$), 121.2 (4'-*C*), 113.1 (2'-*C*), 53.0 (*C*H), 19.2 (*C*H$_3$); ν_{max}/cm^{-1} 3270 (br OH), 1677 (C=O), 1582, 1582, 1522, 1451, 1433, 1347, 1280, 1246, 1162, 1135, 1030, 924, 821, 766, 751, 723, 695; *HRMS* (ESI): Found: 259.1118 (M-OH), $C_{19}H_{15}O$ requires: 259.1123 (M-OH).

Preparation of 6-bromo-2H-naphtho[1,8-bc]furan-2-one, 6.22.

Lactone[34] **6.20** (5.00 g, 29.41 mmol) was dissolved in chloroform (350 mL) and stirred whilst liquid bromine (10 mL) was added. The reaction was left to stir for 24h at room temperature before being quenched with sat. sodium thiosulfate solution (250 mL). The organic layer was repeatedly washed with further sodium thiosulfate solution, until no further colour changes were observed, then with H_2O (100 mL) and brine (100 mL) and dried over $MgSO_4$. The solvent was removed *in vacuo* to give a crude yellow solid which was purified by flash column chromatography (5:95 EtOAc/petrol 40-60), to give **6.22** as a pale yellow solid (6.60 g, 90%), m.p. 184-187℃. δH (400 MHz, $CDCl_3$, 24 °C): 8.28 (1H, d, J = 8.2 Hz, 5-*H*), 8.21 (1H, d, J = 6.9 Hz, 3-*H*), 7.91 (1H, dd, J = 8.3, 6.9 Hz, 4-*H*), 7.78 (1H, d, J = 7.8 Hz, 7-*H*), 7.03 (1H, d, J = 7.8 Hz, 8-*H*); δC (100 MHz, $CDCl_3$, 24 °C): 166.3 (*C*=O), 149.5 (8a-*C*), 131.8 & 131.7 (5-, 7-*C*), 130.5 (4-*C*), 130.0 (2a'-*C*), 129.6 (5a-*C*), 127.2 (3-*C*), 121.6 (2a-*C*), 114.4 (6-*C*), 107.3 (8-*C*); ν_{max}/cm^{-1} 1821, 1776 (C=O), 1735, 1638, 1481, 1461, 1436, 1353, 1334, 1228, 1204, 1140, 922, 820, 767, 730, 710; *HRMS* (ESI): Found: 248.9552 (M+H$^+$), $C_{11}H_6BrO_2$ requires: 248.9552 (M+H$^+$).

Preparation of 6-phenyl-2H-naphtho[1,8-bc]furan-2-one, 6.23.

A solution of the bromo-lactone **6.22** (1.00 g, 4.02 mmol) in dry toluene (15 mL) was added under nitrogen to a solution of phenyl boronic acid (0.58 g, 4.82 mmol), potassium carbonate (1.11 g, 8.04 mmol) and tetrakis(triphenylphosphine) palladium (232 mg, 0.2 mmol) in dry MeOH (15 mL). The reaction was heated to reflux for 24h before being cooled and filtered through a pad of celite, washing the pad with H_2O (50 mL) and EtOAc (100mL). The aqueous layer was extracted with EtOAc (2 x 50 mL) and the organics were discarded. The aqueous layer was acidified with conc. HCl, generating a precipitate, which was removed via extraction into EtOAc (3 x 50 mL). The combined organic layers were washed with brine (50 mL) and dried over $MgSO_4$. The solvent was removed *in vacuo* to give a crude yellow solid which was dissolved in dichloromethane (25 mL) and stirred whilst oxalyl chloride (0.52 mL, 6.03 mmol) was added and the reaction stirred for 5h. The solvent was removed *in vacuo* to give a crude yellow solid which was purified by flash column chromatography (5:95 EtOAc/petrol 40-60), to give **6.23** as a yellow solid (300 mg, 30%), m.p. 152-155℃. δH (400 MHz, $CDCl_3$, 24 °C): 8.27 (1H, dd, J = 8.2, 0.3 Hz, 5-*H*), 8.16 (1H, d, J = 7.0 Hz, 3-*H*), 7.80 (1H, dd, J = 8.4, 7.1 Hz, 4-*H*), 7.40-7.60 (6H, m, Ph, 7-*H*), 7.23 (1H, d, J = 7.6 Hz, 8-*H*); δC (100 MHz, $CDCl_3$, 24 °C): 167.3 (*C*=O), 149.5 (8a-*C*), 138.5, 135.1 (Ar-C_2), 131.5 (5-*C*), 129.7 (4-*C* & Ar-C_2), 129.5, 129.3, 128.9, 128.5, 127.9 (Ar-C_6), 126.5 (3-*C*), 121.5 (Ar-C_2), 106.3 (8-*C*); ν_{max}/cm^{-1} 1781 (C=O), 1759, 1636, 1597, 1464, 1440, 1392, 1334, 1306, 1226, 1142, 1064, 931, 834, 766, 738, 706; *HRMS* (ESI): Found: 247.0759 ($M+H^+$), $C_{17}H_{11}O_2$ requires: 247.0755 ($M+H^+$).

Preparation of 1-(8'-hydroxy-5'-phenylnaphthalen-1'-yl)-2-phenylpropan-1-one, 6.24.

Phenyl-lactone **6.23** (700 mg, 2.78 mmol) was dissolved in anhydrous THF (15 mL) under nitrogen and cooled to -78℃. A solution of 1-phenylethylmagnesium bromide was prepared according to a literature procedure[33] and 4.17 mmol were added steadily to the solution. The reaction was allowed to warm to room temperature and left to stir overnight after which it was treated with water (30 ml). The aqueous solution was washed with EtOAc (3 x 30 mL) and the combined organic layers were washed with H_2O (40 mL), brine (40 mL) and dried over $MgSO_4$. The solvent was removed *in vacuo* to give a crude oil which was purified by flash column chromatography (1:9 EtOAc/petrol 40-60), to give **6.24** as an orange solid (300 mg, 31%), m.p. 150-153℃. δH (400 MHz, $CDCl_3$, 24 °C): 8.11 (1H, s, O*H*), 7.71 (1H, dd, J = 8.7, 0.9 Hz, 4'-*H*), 6.90-7.57 (12H, m, Ar-H_{12}), 7.00 (1H, d, J = 7.8 Hz, Ar-H_1), 6.60 (1H, dd, J = 6.9, 0.9 Hz, 2'-*H*), 4.35 (1H, q, J = 6.9 Hz, C*H*), 1.55 (3H, d, J = 6.9 Hz, (C)CH_3); δC (100 MHz, $CDCl_3$, 24 °C): 209.0 (*C*=O), 152.2, 141.6, 131.1, 131.0, 129.5, 129.4, 129.3, 129.0, 128.1, 127.8 (Ar-C_{10}), 127.5 (4'-*C*), 127.1, 126.3, 126.1, 126.0 (Ar-C_4), 125.1 (2'-*C*), 110.8, 110.2 (Ar-C_2), 54.9 (*C*H), 19.0 (*C*H_3); ν_{max}/cm^{-1} 3255 (br OH), 2931, 1673 (C=O), 1584, 1515, 1468, 1444, 1325, 1276, 1246, 1232, 1144, 1021, 943, 827, 762, 697; *HRMS* (ESI): Found: 335.1442 ($M+H^+$), $C_{17}H_{11}O_2$ requires: 335.1436 ($M+H^+$).

Preparation of 1-(8'-(dimethylamino)naphthalen-1'-yl)-2-phenylpropan-1-one, 6.26.

n-BuLi (16.8 ml, 1.6 M in hexane solution, 26.90 mmol) was added to a stirred solution of 1-dimethylaminonaphthalene **6.25** (1.00 g, 5.85 mmol) in dry ether (20 ml) under nitrogen at room temperature and left to stir for 5 days during which time a yellow precipitate formed (**6.25a)**. The solution was carefully removed, and the residual yellow solid was washed several times with dry ether under nitrogen. The solid was dissolved in dry THF (20 ml), cooled to −78 °C and a solution of 2-phenylpropanoyl chloride[37] (6.6 mmol) in THF was added. The mixture was gradually warmed to room temperature and stirred for 16 h, after which it was treated with water (30 ml). The aqueous solution was washed with EtOAc (3 x 30 mL) and the combined organic layers were washed with H_2O (40 mL), brine (40 mL) and dried over $MgSO_4$. The solvent was removed *in vacuo* to give a crude oil which was purified by flash column chromatography (3:97 EtOAc/petrol 40-60), to give **6.26** as a yellow oil (0.81 g, 46%). δH (400 MHz, $CDCl_3$, 24 °C): 7.70 (1H, d, J = 8.1 Hz, 4'-*H*), 7.62 (1H, dd, J = 8.2, 1.0 Hz, Ar-H_1), 7.48 (1H, t, J = 7.6 Hz, 6'-*H*), 7.37 (1H, d, J = 7.2 Hz, Ar-H_1), 7.13 – 7.20 (3H, m, Ar-H_3), 7.11 (1H, t, J = 7.9 Hz, 3'-*H*), 6.92-6.98 (2H, m, Ar-H_2), 6.46 (1H, d, J = 6.9 Hz, 2'-*H*), 4.13 (1H, q, J = 6.8 Hz, C*H*), 2.94 (3H, s, 8-N(CH_3)$_2$), 2.47 (3H, s, 8-N(CH_3)$_2$), 1.64 (3H, d, J = 6.9 Hz, (C)CH_3); δC (100 MHz, $CDCl_3$, 24 °C): 205.1 (*C*=O), 149.9 (8'-*C*), 140.7, 138.0, 134.8, 128.6, 128.1, 128.2, 128.0, 126.6 (Ar-C_{10}), 126.2 (6'-*C*), 125.7 (2'-*C*), 125.0 (Ar-C_1), 124.7 (3'-*C*), 117.5 (Ar-C_1), 54.0 (*C*H), 48.5 (8'-N(*C*H_3)), 43.2 (8'-N(*C*H_3)), 17.3 (*C*H_3); ν_{max}/cm^{-1} 2978, 2939, 2864, 2830, 2789, 1735, 1682 (C=O), 1576, 1464, 1451, 1367, 1250, 1157, 1125, 1019, 935, 829, 773, 697. *HRMS* (ESI): Found: 304.1708 (M+H$^+$), $C_{21}H_{21}NO$ requires: 304.1701 (M+H$^+$).

Preparation of 1-(5'-bromo-8'-(dimethylamino)naphthalen-1'-yl)-2-phenylpropan-1-one, 6.27.

Dimethylamino ketone **6.26** (250 mg, 0.83 mmol) was dissolved in carbon tetrachloride (10 mL) under nitrogen and stirred whilst a solution of liquid bromine (0.74 mmol in 5 mL of CCl_4) was added dropwise over the course of 2h. Once completely added, the reaction was stirred for a further 2h before being quenched with a 1M solution of sodium thiosulfate (10 mL) and a 20% w/v solution of sodium carbonate (10 mL). The aqueous solution was extracted with dichloromethane (3 x 15 mL) and the combined organic layers were washed with H_2O (20 mL), brine (20 mL) and dried over $MgSO_4$. The solvent was removed *in vacuo* to give a crude oil which was purified by flash column chromatography (1:9 EtOAc/petrol 40-60), to give **6.27** as an orange oil (156 mg, 50%). δH (400 MHz, $CDCl_3$, 24 °C): 8.09 (1H, d, J = 8.5 Hz, 4-'*H*), 7.76 (1H, d, J = 8.0 Hz, 6'-*H*), 7.18-7.27 (2H, m, 3'-,7'-*H*), 7.10-7.16 (3H, m, Ar-H_3), 6.87-6.92 (2H, m, Ar-H_2), 6.53 (1H, d, J = 7.0 Hz, 2'-*H*), 4.04 (1H, q, J = 6.9 Hz, C*H*), 2.91 (3H, s, 8'-N(CH_3)), 2.44 (3H, s, 8'-N(CH_3)), 1.62 (3H, d, J = 6.9 Hz, (C)CH_3); δC (100 MHz, $CDCl_3$, 24 °C): 203.9 (*C*=O), 149.8 (8'-*C*), 140.4, 138.4, 132.8 (Ar-C_3), 130.2 (6'-*C*), 129.2, 128.3, 128.1 (Ar-C_4), 127.8 (4'-*C*), 126.8 (Ar-C_1), 126.7 (2'-*C*), 126.5 (3'-*C*), 118.5, 117.8 (Ar-C_2), 54.1 (*C*H), 48.5 (8'-N(*C*H_3)), 43.0 (8'-N(*C*H_3)), 17.2 (*C*H_3); ν_{max}/cm^{-1} 2980, 2939, 2864, 2834, 2788, 1684 (C=O), 1582, 1449, 1367, 1351, 1246, 1133, 1041, 1021, 889, 827, 769, 721, 697; *HRMS* (ESI): Found: 382.0804 ($M+H^+$), $C_{21}H_{21}BrNO$ requires: 382.0807 ($M+H^+$).

Preparation of 1-(8'-(dimethylamino)-5'-phenylnaphthalen-1'-yl)-2-phenylpropan-1-one, 6.28.

Phenyl boronic acid (76 mg, 0.62 mmol), potassium carbonate (145 mg, 1.05 mmol) and tetrakis(triphenylphosphine) palladium (60 mg, 0.06 mmol) were added to a solution of the bromo naphthalene **6.27** (200 mg, 0.52 mmol), in DMF (6 mL) and H_2O (0.5 mL). The orange solution was refluxed for 24h, after which water (30 mL) was added and the reaction was filtered through a pad of celite, washing the pad with ethyl acetate (25 mL). The aqueous layer was washed with ethyl acetate (2 x 25 mL). The combined organics were washed with water (20 mL), brine (20 mL) and dried over $MgSO_4$. The solvent was removed *in vacuo* to give a crude dark brown oil which was purified by flash column chromatography (1:4 EtOAc/petrol 40-60), to give **6.28** as an orange solid (129 mg, 65%), m.p 165-168℃. δH (400 MHz, $CDCl_3$, 24 °C): 7.67 (1H, dd, J = 8.5, 0.8 Hz, 4'-*H*), 7.29-7.45 (7H, m, Ar-H_7), 7.05-7.11 (3H, m, Ar-H_3), 7.00 (1H, dd, J = 8.5, 7.1 Hz, 3'-*H*), 6.87-6.93 (2H, m, Ar-H_2), 6.37 (1H, dd, J = 6.9, 0.7 Hz, 2'-*H*), 4.08 (1H, q, J = 6.8 Hz, C*H*), 2.89 (3H, s, 8'-N(CH_3)), 2.43 (3H, s, 8'-N(CH_3)), 1.56 (3H, d, J = 6.9 Hz, (C)CH_3); δC (100 MHz, $CDCl_3$, 24 °C): 203.7 (*C*=O), 148.3 (8'-*C*), 139.9 (1'-*C*), 139.4, 137.3, 136.1, 131.9, 129.1, 127.3, 126.4, 126.2 (Ar-C_{15}), 125.8 (4'-*C*), 125.7 (Ar-C_1), 124.8 (2'-*C*), 124.2 (3'-*C*), 116.0 (Ar-C_1), 53.0 (*C*H), 47.5 & 42.3 (8'-N(*C*H_3)), 16.4 (*C*H_3); ν_{max}/cm^{-1} 2955, 2818, 1675 (C=O), 1459, 1313, 1258, 1088, 1060, 1021, 948, 855, 795, 775, 721, 704; *HRMS* (ESI): Found: 380.2020 ($M+H^+$), $C_{27}H_{26}NO$ requires: 380.2014 ($M+H^+$).

Preparation of 1-(6'-(dimethylamino)-1',2'-dihydroacenaphthylen-5'-yl)-2-phenylpropan-1-one, 6.33.

Bromo amine[39] **6.32** (0.6 g, 2.17 mmol) was dissolved in anhydrous THF (15 mL) under nitrogen and cooled to -78℃. *n*-BuLi (2.5M in hexanes, 1.3 mL, 3.26 mmol) was steadily added, and the deep red solution was stirred at -78℃ for 3h. A solution of 2-phenylpropanoyl chloride[37] (4.88 mmol) in THF was added at -78 ^{o}C and the reaction was left to warm up to room temperature. After 16 h the resulting solution was quenched with H_2O (10 mL) and stirred for 10min. The aqueous solution was washed with EtOAc (3 x 30 mL) and the combined organic layers were washed with H_2O (40 mL), brine (40 mL) and dried over $MgSO_4$. The solvent was removed *in vacuo* to give a crude brown oil which was purified by flash column chromatography (5:95 EtOAc/petrol 40-60), to give **6.33** as a yellow solid (260 mg, 36%), m.p. 105-108℃. δH (400 MHz, $CDCl_3$, 24 °C): 7.23-7.32 (2H, m, Ar-*H*$_2$), 7.12-7.22 (3H, m, Ar-*H*$_3$), 7.06 (1H, br d, J = 5.3 Hz, Ar-*H*$_2$), 6.96 (1H, d, J = 6.4 Hz, 3'-*H*), 6.52 (1H, br m, 4'-*H*), 4.28 (1H, q, J = 6.9 Hz, C*H*), 3.33 (4H, s, 1'-, 2'-C*H*$_2$), 2.84 (3H, br s, 6'-N(C*H*$_3$)), 2.49 (3H, s, 6'-N(C*H*$_3$)), 1.59 (3H, d, J = 6.9 Hz, (C)C*H*$_3$); δC (100 MHz, $CDCl_3$, 24 °C): 208.2 (*C*=O), 147.1, 147.0, 142.4, 140.9, 140.7, 134.5, 128.5, 128.4 (Ar-*C*$_8$), 127.0 (4'-*C*), 126.8, 126.1, 119.9, 119.3 (Ar-*C*$_4$), 118.7 (3'-*C*), 54.5 (*C*H), 48.3 & 43.7 (br 6'-N(*C*H$_3$)$_2$), 30.7 & 30.0 (1'-, 2'-*C*H$_2$), 17.9 (*C*H$_3$); ν_{max}/cm^{-1} 2976, 2911, 2935, 2821, 2780, 1686 (C=O), 1586, 1492, 1474, 1448, 1364, 1297, 1183, 1151, 1129, 998, 972, 956, 838, 751, 700; *HRMS* (ESI): Found: 330.1847 (M+H$^+$), $C_{17}H_{11}O_2$ requires: 330.1858 (M+H$^+$).

Preparation of 1-(8'-(dimethylamino)-4',5'-diphenylnaphthalen-1'-yl)-2-phenylpropan-1-one, 6.38.

1-Dimethylamino-4,5-diphenylnaphthalene **6.37** (1.2 g, 3.71 mmol), dry hexane (20 mL) and *n*-BuLi (2.5M in hexanes, 5.94 mL, 14.84 mmol) were stirred heated to 80 ^{o}C and the mixture was refluxed for 72 h. The reaction was cooled and the resultant precipitate (**6.37a**) was allowed to settle before removing the supernatant. The residual precipitate was dissolved in tetrahydrofuran (20 mL) and the reaction mixture was cooled to -78 ^{o}C. A solution of 2-phenylpropanoyl chloride[37] (5.57 mmol) in THF was added at -78 ^{o}C, the reaction was left to warm up to room temperature and stirred for 48h. The reaction was quenched with water (100 ml) and extracted with ethyl acetate (3 x 50 mL). The combined organic layers were washed with brine (50 mL), dried over anhydrous $MgSO_4$, filtered and concentrated *in vacuo*. The crude oil was purified by flash column chromatography (5:95 EtOAc/petrol 40-60) to give product **6.38** as a pale yellow solid (630 mg, 37%), m.p. 61-64℃. δH (400 MHz, $CDCl_3$, 24 °C): 7.30-7.40 (2H, m, Ar-*H*$_2$), 7.08-7.20 (3H, m, Ar-*H*$_3$), 6.70-7.02 (13H, m, Ar-*H*$_{13}$), 6.55 (1H, d, J = 7.2 Hz, 2'-*H*), 4.15 (1H, q, J = 6.8 Hz, C*H*), 2.97 (3H, s, 8'-N(C*H*$_3$)), 2.53 (3H, s, 8'-N(C*H*$_3$)), 1.66 (3H, d, J = 6.8 Hz, (C)C*H*$_3$); δC (100 MHz, $CDCl_3$, 24 °C): 203.4 (*C*=O), 149.5 (8'-*C*), 143.0, 142.7, 141.3, 141.2, 138.1, 137.4, 131.4, 130.7, 130.4, 129.5, 128.5, 128.4, 127.5, 127.3, 126.9, 126.0, 125.9 (Ar-*C*$_{18}$), 125.6 (2'-*C*), 116.9 (Ar-*C*$_1$), 54.0 (*C*H), 48.7 & 43.6 (8'-N(*C*H$_3$)$_2$), 17.7 (*C*H$_3$); ν_{max}/cm^{-1} 2981, 2873, 2865, 1675 (C=O), 1490, 1440, 1300, 1138, 1015, 970, 842, 756, 695; *HRMS* (ESI): Found: 456.2343 (M+H$^+$), $C_{33}H_{30}ON$ requires: 456.2327 (M+H$^+$).

Crystal data

*Table 6.47. Crystallographic data for the four target compounds **6.24**, **6.28**, **6.33** and **6.38**.*

	6.24	**6.28**	**6.33**	**6.38**
Formula	$C_{25}H_{20}O_2$	$C_{27}H_{25}NO$	$C_{23}H_{23}NO$	$C_{33}H_{29}NO$
Formula weight	352.41	379.48	329.42	455.57
Crystal system	Monoclinic	Monoclinic	Monoclinic	Monoclinic
Space group	C2/c	$P2_1/n$	$P2_1/c$	$P2_1/c$
***a*[Å]**	15.8973(5)	8.6386(3)	10.4349(2)	15.3621(3)
***b*[Å]**	10.2852(3)	10.9657(3)	13.5670(3)	8.7089(2)
***c*[Å]**	22.3789(8)	21.9706(7)	13.0112(2)	19.0603(4)
***α*[°]**	90	90	90	90
β [°]	98.729(3)	99.992(3)	99.424(2)	95.971(2)
***γ*[°]**	90	90	90	90
***V* [Å^3]**	3616.7(2)	2049.67(11)	1817.14(6)	2536.20(10)
Z	8	4	4	4
***ρ* [g cm^{-3}]**	1.294	1.230	1.204	1.193
***T* [*K*]**	150.01(10)	100.01(10)	150.01(10)	150.01(10)
***λ* (Å)**	1.54184	0.71073	0.71073	0.71073
(mm^{-1})	0.074	0.074	0.073	0.071
unique refl.	3549	4696	4500	5168
Refl, I > 2σI	2602	3516	3511	3862
***R*$_1$**	0.0467	0.0505	0.0441	0.0452
***wR*$_2$**	0.1147	0.1033	0.1045	0.0970
***Δρ*(r) [e Å^{-3}]**	0.210/-0.124	0.259/-0.255	0.238/-0.217	0.167/-0.198
Crystallisation Solvent	CH_2Cl_2/$CHCl_3$	CH_2Cl_2	CH_2Cl_2/*n*-hexane	*n*-hexane

References

1 B. M. Trost and A. H. Weiss, *Adv. Synth. Catal.*, 2009, **351**, 963–983.

2 Y.-L. Liu and X.-T. Lin, *Adv. Synth. Catal.*, 2019, **361**, 876–918.

3 O. Riant and J. Hannedouche, *Org. Biomol. Chem.*, 2007, **5**, 873–888.

4 X.-S. Zhang, K. Chen and Z.-J. Shi, *Chem. Sci.*, 2014, **5**, 2146–2159.

5 S. F. Martin, *Synthesis*, 1979, 633–665.

6 E. L. Eliel and G. Solladie, in *Asymmetric Synthesis Vol. 2*, Academic Press, New York, 1983, pp. 125–199.

7 A. Mengel and O. Reiser, *Chem. Rev.*, 1999, **99**, 1191–1224.

8 D. J. Cram and F. A. A. Elhafez, *J. Am. Chem. Soc.*, 1952, **74**, 5828–5835.

9 M. T. Reetz, B. Raguse and T. Seitz, *Tetrahedron*, 1993, **49**, 8561–8568.

10 M. T. Reetz, M. Hüllmann and T. Seitz, *Angew. Chemie - Int. Ed.*, 1987, **99**, 478–480.

11 M. T. Reetz, *Acc. Chem. Res.*, 1993, **26**, 462–468.

12 X. Chen, E. R. Hortelano, E. L. Eliel and S. V. Frye, *J. Am. Chem. Soc.*, 1992, **114**, 1778–1784.

13 M. T. Reetz and M. Hüllmann, *J. Chem. Soc., Chem. Commun.*, 1986, 1600–1602.

14 X. Chen, E. R. Hortelano, E. L. Eliel and S. V. Frye, *J. Am. Chem. Soc.*, 1990, **112**, 6130–6131.

15 W. D. Samuels, D. A. Nelson and R. T. Hallen, *Tetrahedron Lett.*, 1986, **27**, 3091–3094.

16 W. Clark Still and J. A. Schneider, *Tetrahedron Lett.*, 1980, **21**, 1035–1038.

17 W. Clark Still and J. H. McDonald, *Tetrahedron Lett.*, 1980, **21**, 1031–1034.

18 K. J. Henry, P. A. Grieco and C. T. Jagoe, *Tetrahedron Lett.*, 1992, **33**, 1817–1820.

19 J. W. Cornforth, R. H. Cornforth and K. K. Mathew, *J. Chem. Soc.*, 1959, 112–127.

20 D. A. Evans, S. J. Siska and V. J. Cee, *Angew. Chemie - Int. Ed.*, 2003, **42**, 1761–1765.

21 M. Chérest, H. Felkin and N. Prudent, *Tetrahedron Lett.*, 1968, **9**, 2199–2204.

22 N. T. Anh, *Org. Chem. Synth. React.*, 1980, **88**, 145–162.

23 N. T. Anh and O. Eisenstein, *Tetrahedron Lett.*, 1976, **17**, 155–158.

24 N. T. Anh and O. Eisenstein, *Nouv. J. Chim.*, 1977, **1**, 61–70.

25 G. J. Karabatsos, C. Zioudrou and I. Moustakali, *Tetrahedron Lett.*, 1972, **13**, 5289–

5292.

26 G. J. Karabatsos and T. H. Althuis, *Tetrahedron Lett.*, 1967, **8**, 4911–4914.

27 G. J. Karabatsos, *J. Am. Chem. Soc.*, 1967, **89**, 1367–1371.

28 H. B. Bürgi, J. D. Dunitz and E. Shefter, *J. Am. Chem. Soc.*, 1973, **95**, 5065–5067.

29 H. B. Bürgi, J. D. Dunitz, J. M. Lehn and G. Wipff, *Tetrahedron*, 1974, **30**, 1563–1572.

30 H. B. Bürgi and J. D. Dunitz, *Acc. Chem. Res.*, 1983, **16**, 153–161.

31 N. T. Anh, O. Eisenstein, J. M. Lefour and M. E. Tran Huu Dau, *J. Am. Chem. Soc.*, 1973, **95**, 6146–6147.

32 H. B. Bürgi, J. D. Dunitz and E. Shefter, *Acta Crystallogr.*, 1974, **30**, 1517–1527.

33 A. S. Jones, J. F. Paliga, M. D. Greenhalgh, J. M. Quibell, A. Steven and S. P. Thomas, *Org. Lett.*, 2014, **16**, 5964–5967.

34 A. N. Cammidge and O. Öztürk, *J. Org. Chem.*, 2002, **67**, 7457–7464.

35 K. Kaupmees, A. Trummal and I. Leito, *Croat. Chem. Acta*, 2014, **87**, 385–395.

36 J. C. Bristow, M. A. Addicoat and J. D. Wallis, *CrystEngComm*, 2019, **21**, 1009–1018.

37 D. Wang, N. Zhu, P. Chen, Z. Lin and G. Liu, *J. Am. Chem. Soc.*, 2017, **139**, 15632–15635.

38 L. Liu, C. Zhang and J. Zhao, *Dalton Trans.*, 2014, **43**, 13434–13444.

39 D. Pla, O. Sadek, S. Cadet, B. Mestre-Voegtlé and E. Gras, *Dalton Trans.*, 2015, **44**, 18340–18346.

40 C. F. R. A. C. Lima, J. E. Rodriguez-Borges and L. M. N. B. F. Santos, *Tetrahedron*, 2011, **67**, 689–697.

41 H. O. House and R. W. Bashe, *J. Org. Chem.*, 1967, **32**, 784–791.

42 Y. Ishigaki, T. Shimajiri, T. Takeda, R. Katoono and T. Suzuki, *Chem*, 2018, **4**, 795–806.

Chapter 7

Stabilisation of Triaryl Carbocations in Order to Form Long N-C Bonds

Introduction

The approach of a nucleophilic moiety (i.e. -NMe_2, -OH) toward that of an electrophilic centre (i.e. electron deficient alkenes, carbonyls) based upon a naphthalene scaffold has been extensively explored. Building upon this, we sought to design and synthesise a series of 1, 8-disubstituted naphthalenes which would allow for a positively charged electrophilic species, in this case a carbocation, to be placed *peri* to a nucleophilic dimethylamino group. The nature of the carbocation employed required careful consideration. This is demonstrated by the early work of Dyker *et al.*[1,2] in which they synthesised the two naphthalene based dimethylammonium salts **7.1** and **7.2** shown in Figure 7.1.

7.1 **7.2**

*Figure 7.115. Structures of the two dimethylammonium salts **7.1** and **7.2**.[1,2]*

The naphthalene scaffold and nucleophilic moiety remains constant in both salts **7.1** and **7.2**, however, the N-C bond lengths of the two salts differ dramatically. In tetraphenylborate salt **7.1**, the quaternary carbon is substituted with two alkyl groups and demonstrates a long 1.599(3) Å N-C bond. On the other hand, the two crystallographically unique molecules in tetrafluoroborate salt **7.2** possess much longer N-C bond lengths of 1.719(5) and 1.718(5) Å. This large difference is caused primarily by the substituents α to the N-C bonded quaternary carbon. In both cases a dimethylamino group has bonded to a carbocation. In **7.1** the nitrogen lone pair stabilises a carbocation whose two substituents only have a small positive inductive effect (+I). For **7.2** however, the π systems of the phenyl groups contribute considerable (+M) stabilisation. Alternatively, it can be considered that this π electron density donates into the

antibonding σ* orbital of the long N-C bond, reducing the contribution required from the nitrogen lone pair, weakening the bond. The work of Morimoto *et al*.[3] demonstrates a range of similar isolable triarylcations where the stabilising nucleophilic moiety is not present.

Figure 7.116. Generalised structures of the triarylmethanol (left) and dimethylammonium (right) target compounds.

Utilising this information and further developing it, we set out to synthesise a range of triarylmethanol compounds, from which dehydrated salts would be prepared with the general formula shown in Figure 7.2. The first of the aryl groups is the naphthalene backbone itself, which is attached at one *peri*-position, with the other *peri*-position substituted with a dimethylamino moiety that will remain consistent throughout the investigation. The remaining two α-aryl substituents will be varied. These may be two separate aryl species or a combined unit. The aim is to provide more stabilisation to the carbocation centre from its carbon substituents, so that less donation is needed from the dimethylamino group, so lengthening the N-C bond. In each case the molecular structure determined by single crystal X-ray diffraction will be used to analyse the stabilisation capability of different aryl groups and assess the effect this has on the N-C bond length.

Synthesis of Triarylmethanol Derivatives

Synthesis of the target triarylmethanol compounds began with the *peri*-lithiation of 1-dimethylaminonaphthalene **7.3** with *n*-butyl lithium (Scheme 7.1), generating a pale-yellow precipitate of the lithiated salt **7.3a**.[4] The supernatant was removed and the lithiated salt was dissolved in THF. The solution was cooled to -78 ^{o}C before the addition of methyl chloroformate, with the desired methyl naphthoate **7.4** isolated as a yellow oil in 57% yield. The structure of **7.4** is confirmed by the removal of an aromatic proton signal and addition of a new signal at 3.90 ppm in the ^{1}H NMR spectrum corresponding to the methyl group. Furthermore, signals for the ester carbonyl in the ^{13}C NMR and infrared spectra are shown at 172.1 ppm and 1716 cm^{-1} respectively.

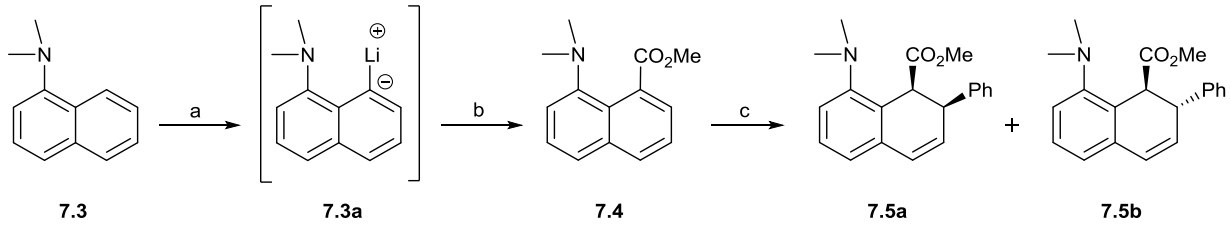

Scheme 7.60. (a) n-BuLi, Et_2O, RT; (b) Methyl chloroformate, THF, -78 ^{o}C to RT; (c) PhLi, THF, -78 ^{o}C to RT.

The reaction of the methoxy ester **7.4** with a range of aryl-lithium compounds was expected to result in the conversion of the ester group to give a triaryl substituted alcohol. However, the addition of an excess of phenyl lithium to a cooled solution of methoxy ester **7.4** in THF did not result in the expected diphenylalcohol. Instead the only notable products isolated from the reaction (besides unreacted starting material) were a mixture of the two diastereoisomers of the *ortho*-(phenyl)substituted, de-aromatised compound **7.5a/7.5b**, where the phenyl group has added to the carbon *ortho* to the ester group. Further purification by flash column chromatography resulted in the separation of one of the isomers, whilst the other remained as a mixture. Crystallisation of the isolated diastereoisomer from DCM yielded crystals suitable for structural determination with the data collected at 150 K. The molecular structure revealed

the compound to be the *cis* isomer **7.5a** as shown in Figure 7.3. The methoxy ester group, due to the *cis* conformation is displaced too far away from the dimethylamino group to partake in an interaction. Isolation and crystallisation of the opposite *trans* isomer may display such an interaction, however attempts to isolate and crystallise it failed. NMR analysis of the purified diastereoisomer confirmed the de-aromatised structure with ^{1}H shifts of 4.17 and 4.49 ppm and ^{13}C shifts of 44.4 and 45.7 ppm for the protons bound to the sp^{3} ring carbons.

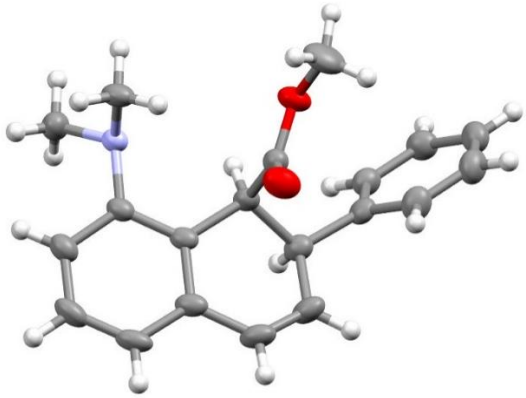

*Figure 7.117. Molecular structure of the isolated diastereoisomer **7.5a**.*

As a result of the desired substitution not taking place, the synthesis was adjusted. Alternatively, the addition of diarylketones to *peri*-lithiated salt **7.3a** was attempted, which following their addition would yield the desired diaryl alcohols directly, reducing the number of synthetic steps (Scheme 7.2). Benzophenone was added to a solution of *peri*-lithiated salt **7.3a** in THF at -78 ^{o}C to give the desired diphenyl alcohol **7.6** in a 76% yield as an off-white solid. The structure of diphenyl alcohol **7.6** was confirmed by the addition of a further 10 aromatic protons in the ^{1}H NMR spectrum, with the tertiary alcohol singlet observed at 11.37 ppm. Moreover, the quaternary *peri*-carbon demonstrates a signal of 83.3 ppm in the ^{13}C NMR spectrum. A sharp signal corresponding to the hydroxyl proton in the ^{1}H NMR is likely the result of a strong hydrogen bond across the *peri*-position to the dimethylamino group. Following the successful synthesis of diphenyl alcohol **7.6**, the *peri*-lithiated salt **7.3a** was successfully reacted with a range of diaryl ketones; 4,4′-dimethoxybenzophenone,

dibenzosuberone, 4-methoxybenzophenone and 4-(dimethylamino)benzophenone, to give the desired aryl alcohols **7.7**-**7.10** in yields ranging from 25% to 48%.

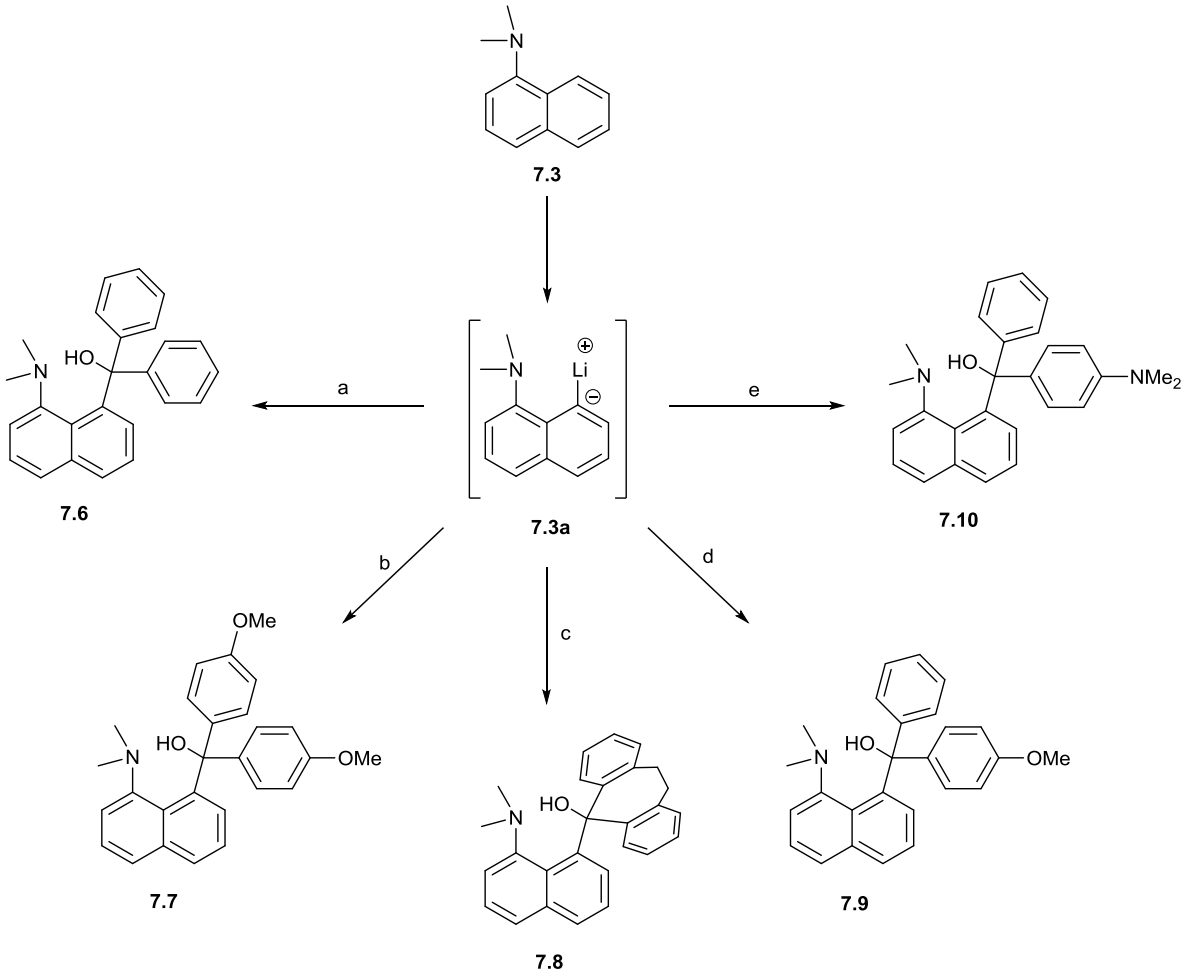

Scheme 7.61. (a) Benzophenone, THF, -78 ºC to RT; (b) 4,4'-dimethoxybenzophenone, THF, -78 ºC to RT; (c) Dibenzosuberone, THF, -78 ºC to RT; (d) 4-methoxybenzophenone, THF, -78 ºC to RT; (e) 4-dimethylaminobenzophenone, THF, -78 ºC to RT.

The structure of di-*para*-methoxy alcohol **7.7** was confirmed by ^{1}H and ^{13}C NMR signals at 3.81 ppm and 55.3 ppm for the *para*-methoxy groups and 11.39 ppm and 82.8 ppm for the hydroxyl proton and the quaternary carbon it is bonded to. The structure of the dibenzosuberol derivative **7.8** was confirmed by signals at 10.26 ppm and 79.2 ppm in the ^{1}H and ^{13}C NMR spectra corresponding to the hydroxyl group and quaternary carbon. A ^{1}H NMR signal at 1.60-2.30 ppm is found for the four protons of the two methylene groups of the 7-membered ring. The structures of the *para mono*-methoxy and *mono*-dimethylamino derivatives **7.9** and **7.10**

were confirmed by ^{1}H NMR signals of 3.78 ppm and 2.91 ppm in corresponding to the O-methyl and N-methyl protons respectively, with ^{13}C NMR signals at 83.0 and 82.9 ppm for the quaternary carbons. In all cases, the appropriate increase in the number of aromatic proton and carbon signals is observed.

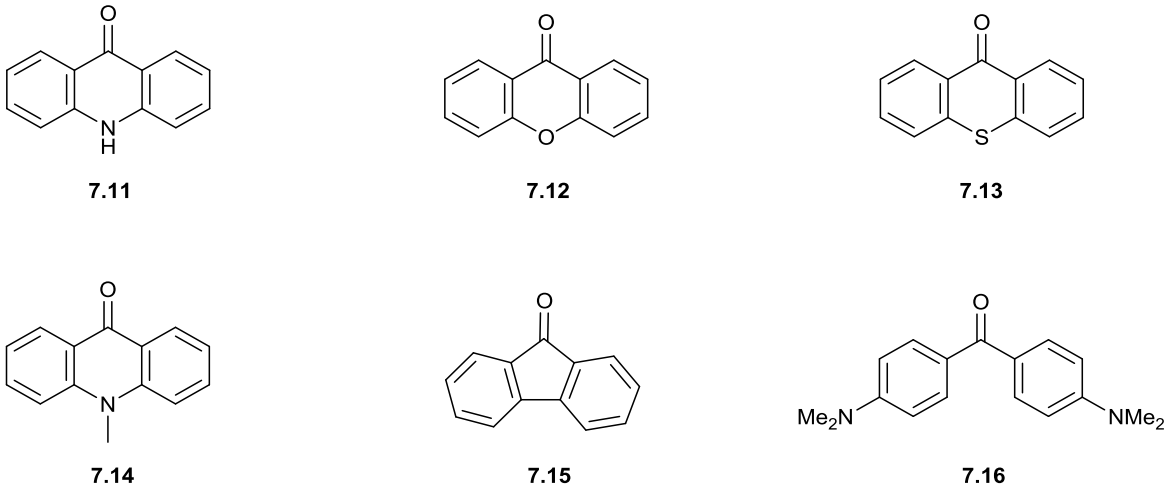

*Figure 7.118. Selection of diarylketones **7.11-7.16** tried in the synthesis of triarylmethanol target compounds.*

The diarylketones **7.11**-**7.16** shown in Figure 7.4 were added to the *peri*-lithiated salt **7.3a** as previously described, however no reaction occurred. This resulted in a crude reaction mixture upon quenching consisting of re-protonated dimethylaminonaphthalene and the diarylketone. Despite an increase to both the reaction time and temperature, no addition took place. The *bis*(4-dimethylaminobenzophenone **7.16** (more commonly known as Michler's ketone) yielded a crude oil which by TLC analysis indicated several new products. However, when the material was purified via flash column chromatography a series of strongly oceanic coloured bands began to form, with each compound eluting from the column as a colourless solution, indicating a reaction between the crude material and either the silica used in the column or a reaction with light. Furthermore, when left in ambient conditions, the crude material began to decompose, developing a darkened colour and an ever more complex TLC signature. As a result, the compound was excluded from the investigation.

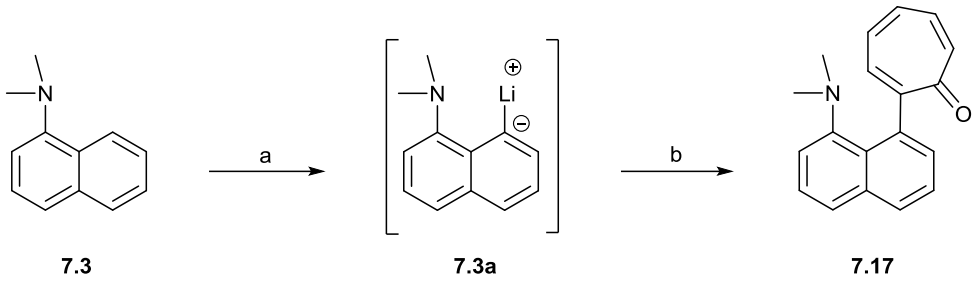

7.3 **7.3a** **7.17**

Scheme 7.62. (a) n-BuLi, Et_2O, RT; (b) Tropone, THF, -78 °C to RT.

Reaction of the *peri*-lithiated salt **7.3a** with tropone did not result in nucleophilic attack at the carbonyl group to give the expected alcohol derivative (Scheme 7.3). Instead, the α-carbon was the site of the nucleophilic attack, which following oxidation of the quaternary proton in the workup, restores the triene of the tropone ring. The product, a deep yellow solid, was the only isolated product in a low yield of 12%. The structure of compound **7.17** is confirmed by the carbonyl stretching frequency of 1567 cm^{-1} and ^{13}C NMR signal of 185.6 ppm. Furthermore, the absence of a peak in the ^{13}C NMR spectrum in the region of 60-110 ppm for the sp^3 quaternary carbon (as in **7.6**-**7.10**) along with no proton signals corresponding to a tertiary proton, confirms the reformation of the triene moiety. The cyclic tri-alkene network presents an interesting structural comparison, whereby in the same molecule, the dimethylamino group can form an attractive interaction between either an alkene (in a Michael type addition) or the carbonyl group.

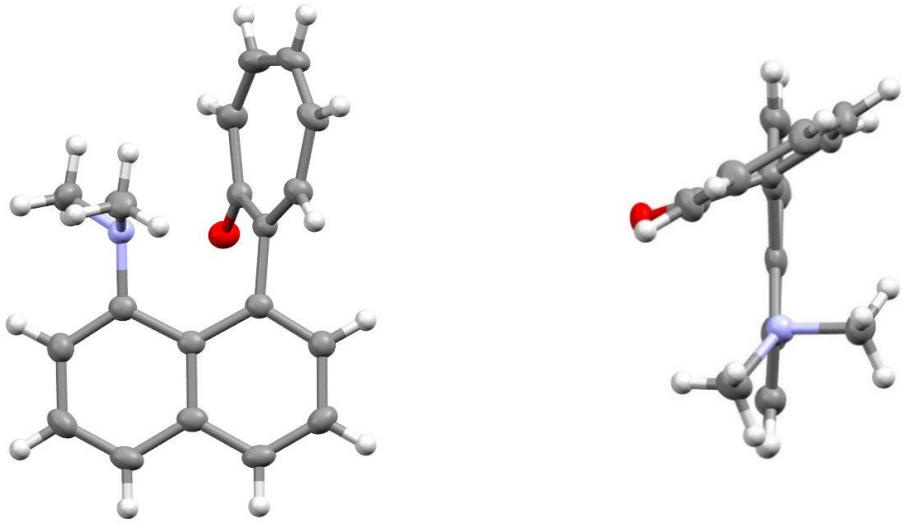

*Figure 7.119. Molecular structure of the α-substituted tropone derivative **7.17** (left) and a birds-eye view (right) demonstrating the orientations of both the dimethylamino and tropone moieties with respect to the naphthalene ring.*

Suitable crystals of the substituted tropone compound **7.17** were grown via slow evaporation of a DCM solution, with the X-ray structure determined at 150 K. As shown in Figure 7.5, the molecular structure of **7.17** demonstrates a close to planar tropone ring substituted at the carbon α to the carbonyl group. The tropone ring is rotated from the idealised naphthalene plane by 67.4(1)^{o} placing the carbonyl of the ring toward the nucleophilic dimethylamino group. This leads to a Me_2N---C=O separation of 2.727(2) Å with the nucleophile approaching the carbonyl at an angle of 94.0(1)^{o}. However, a shorter Me_2N---C=C separation of 2.682(2) Å is observed for the competing interaction, demonstrating a more favourable approach angle of 114.8(1)^{o}. Unlike the majority of structures discussed in the previous chapters, the Me_2N---C=O interaction involves a carbonyl group which is positioned α to the *peri*-connection, giving a 1, 6 interaction that no longer occurs in the same plane as the naphthalene scaffold. Instead, it occurs to one side, with the carbon of the carbonyl group positioned 1.234 Å from the idealised naphthalene plane. The N-methyl groups are unevenly positioned with respect to the naphthalene plane, with torsion angles of -40.4(2) and 90.9(2)^{o} to the *ortho*-carbon of naphthalene plane. This positions the axis of the nucleophilic nitrogen lone pair to lie at an angle of 10.3^{o} to the **N---C**=O vector, whereas it lies at an angle of 24.0^{o} to the **N---C**=C vector,

showing better alignment for the addition to the anti-bonding orbitals of the carbonyl group over the alkene group, despite the slightly elongated interaction distance (Figure 7.6). The *peri*-groups are displaced marginally from the naphthalene plane by no more than 0.17 Å (NMe_2 group), with the expected angular displacements of the nucleophilic moiety toward the retreating electrophile observed.

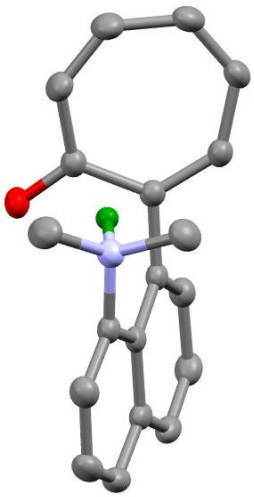

*Figure 7.120. Molecular structure of **7.17** showing the orientation of the nitrogen lone pair (green) more preferably toward the carbonyl group.*

In order to further explore the two competing interactions, it was proposed that the reaction of tropone **7.17** with an acid would lead to protonation of the carbonyl moiety, which typically in compounds of this type[5,6] leads to formation of a long N-C bond across the *peri*-positions. However, following the protonation of the carbonyl group in **7.17**, bond formation could take place at the *peri*-alkene or carbonyl carbons, generating either 5 or 6 membered ring systems.

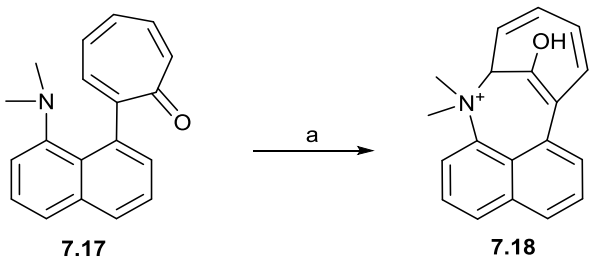

Scheme 7.63. (a) HBF_4, Et_2O, RT.

When reacted with an excess of tetrafluoroboric acid (Scheme 7.4), a dark brown precipitate was isolated under a nitrogen flow in an 83% yield. Spectroscopic analysis of the product confirmed that an N-C bond had formed between the dimethylamino nitrogen and an alkene carbon. However, the data indicates that the N-C bond has been formed at the opposite alkene α-carbon, resulting in the formation of the 7-membered ring in **7.18**. This is supported in the ^{13}C NMR spectrum with shifts of 72.2 ppm for the N-C bonded carbon and 99.9 and 150.9 ppm for the enol carbon atoms. Furthermore, a correlation between both the N-methyl group protons and the C-H peak at 72.2 ppm is observed in the HMBC spectrum. This further proves that a 5-membered ring product (Figure 7.7 (right) has not formed across the *peri*-positions as the N-methyl protons would correlate a carbon which does not carry any hydrogen atoms, which the peak at 72.2 ppm does. Unfortunately, salt **7.18** was found to be extremely hydroscopic, with attempts to crystallise the compound resulting in the isolation of yellow crystals of the starting material **7.17**. As a result, structural data for the compound were not obtained.

*Figure 7.121. Structure of the suggested product **7.18** (left) and the alternate product (right) which cannot be formed due to spectral data.*

Synthesis of Dimethylammonium Salts

In order to generate the desired *peri*-carbocationic species, the hydroxyl groups of the triarylmethanol compounds must be cleaved. This is achievable via the protonation of the hydroxyl group via the addition of an acid, which makes the hydroxyl group more liable to cleavage via dehydration as the resultant cation is stabilised by first its aryl substituents and then the nitrogen lone pair.

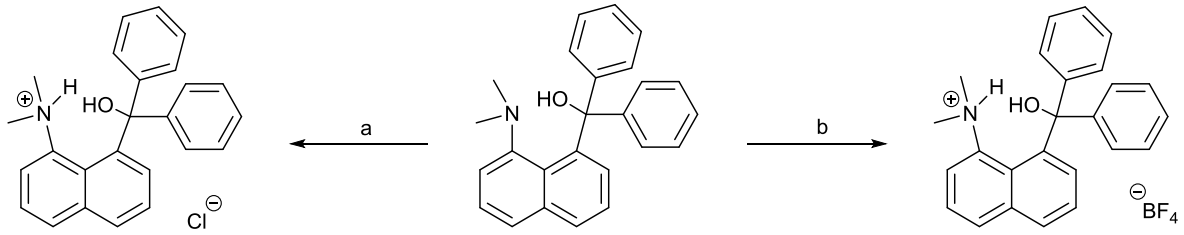

7.19 **7.6** **7.20**

Scheme 7.64. (a) HCl, Et_2O, RT; (b) HBF_4, Et_2O, RT.

Addition of ethereal solutions of hydrochloric acid or tetrafluroroboric acid to solutions of diphenyl alcohol **7.6** in Et_2O at room temperature resulted in the dimethylammonium chloride (**7.19**) or tetrafluoroborate (**7.20**) salts of the diphenyl alcohol (Scheme 7.5). In both cases, a fine white precipitate formed immediately, with **7.19** and **7.20** isolated in 64% and 88% yields respectively. Analysis of both **7.19** and **7.20** by ^{13}C NMR revealed signals of 83.8 and 84.7 ppm respectively for the quaternary *peri*-carbon similar to that of the diphenyl alcohol **7.6** which is found at 83.3 ppm. Crystals of both compounds were successfully obtained via slow evaporation of DCM solutions and the X-ray structures determined at 150 K. The structures confirmed that the dehydration of the hydroxyl group had not occurred in either reaction, with the tetrafluoroborate salt present as a DCM solvate (Figure 7.8). In each case, the oxygen of the hydroxyl group is hydrogen bonded to N(+)-H proton, with the hydroxyl proton hydrogen bonded to the counter anion.

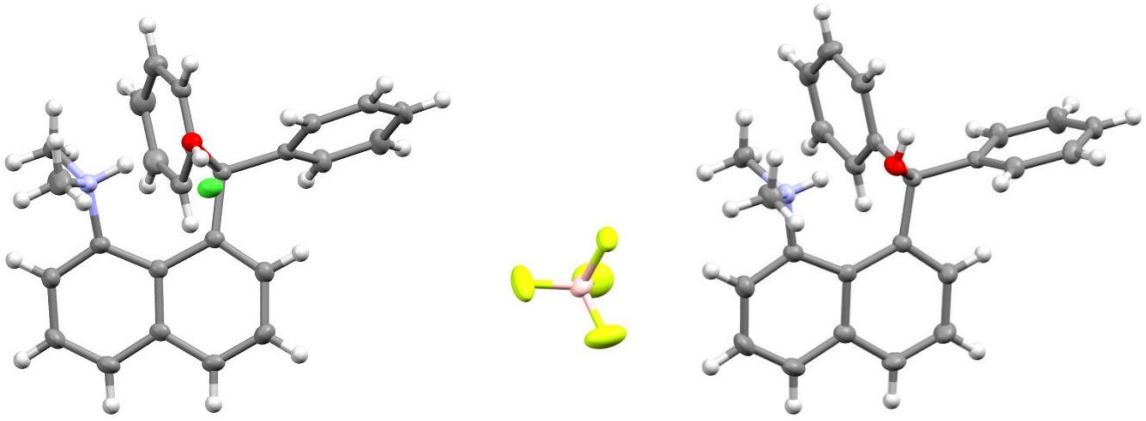

*Figure 7.122. Molecular structures of both the chloride **7.19** and tetrafluoroborate **7.20** diphenyl alcohol salt.*

Diethyl ether as the reaction solvent in the synthesis of **7.19** and **7.20** was altered as a result of its low polarity causing the polar salt to precipitate immediately once the first protonation had occurred, preventing a second protonation at the hydroxyl group. As shown in Scheme 7.6, Dyker *et al*. performed low temperature NMR studies on the formation of the tetrafluoroborate salt **7.2**.[1] They found that the di-cation **7.22** (protonation of both the dimethylamino and hydroxyl group in **7.22**) is generated *in-situ* which results in the formation of a strongly coloured soluble compound. Warming of this solution to above 0 ^{o}C results in the cleavage of the H_2O^+ group, to give the short-lived carbocation **7.23**, which subsequently is stabilised by the *peri*-dimethylamino nitrogen lone pair (freed up by the dissociation of the N-H bond) to give the desired salt **7.2**. It is worth noting that following the cleavage of the H_2O^+, the colour of the solution is dampened, with the crystals of **7.2** being colourless upon isolation.

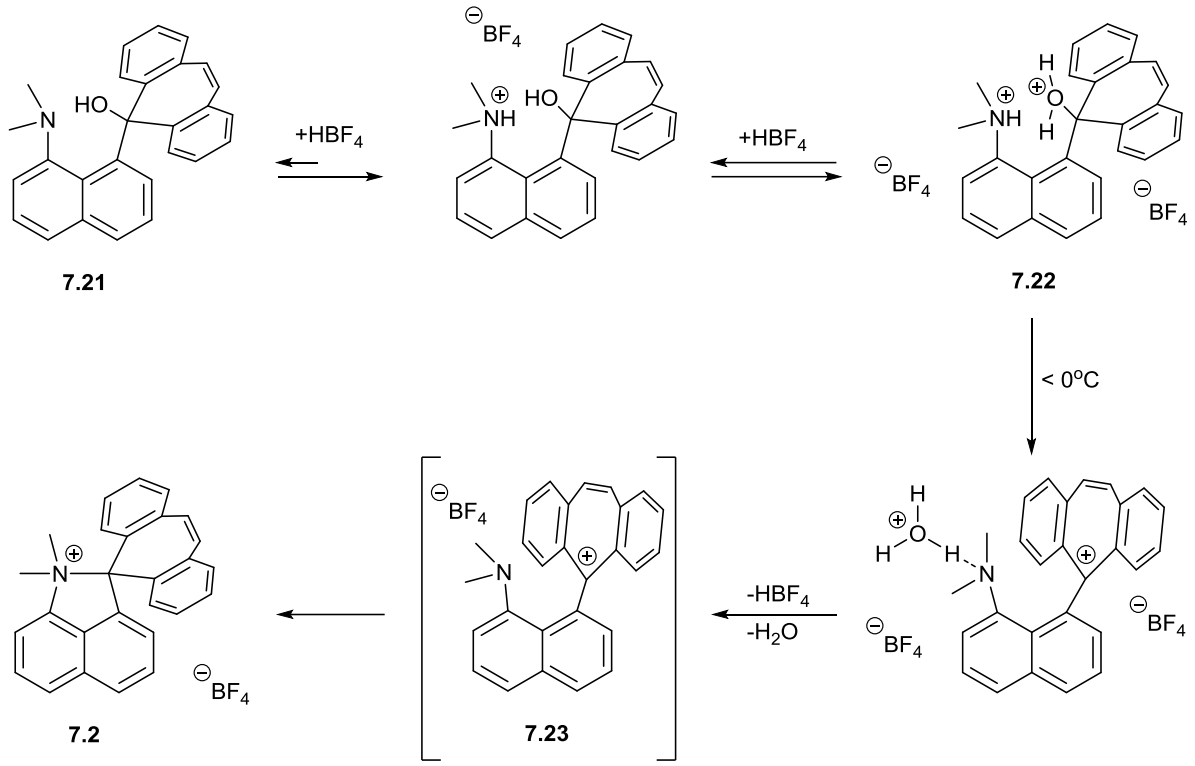

*Scheme 7.65. Reaction mechanism for the dehydration and formation of the dimethylammonium salt **7.2** derived from low temperature NMR studies.*[1]

Following the methods described by Dyker *et al.* an excess of tetrafluoroboric acid was added to a solution of diphenyl alcohol **7.6** this time dissolved in DCM (Scheme 7.7). Immediately upon dropwise addition, a deep red colour formed which if addition was ceased would eventually fade following a few seconds of stirring. Addition of over two equivalents of acid resulted in the colour persisting with it eventually settling at deep orange after 30 mins. The solution was stirred at room temperature for a total of 1h before the stirring was stopped and diethyl ether carefully added to the top of the solution generating a bilayer. The reaction was kept as a bilayer until signs of a precipitate began to form at the interface, at which point the reaction was vigorously stirred and left to do so for 16h. This gave a precipitate which was subsequently isolated as an off-white solid of the dehydrated dimethylammonium compound **7.24** in 88% yield.

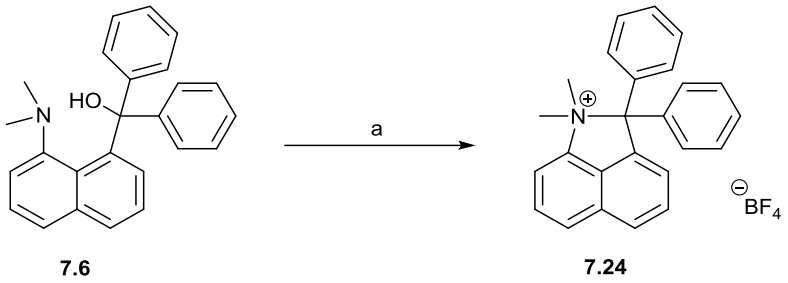

7.6 **7.24**

Scheme 7.66. (a) HBF_4, DCM, RT.

The structure of **7.24** was confirmed by the significant downfield shift in the ^{1}H and ^{13}C NMR signals of the N-methyl groups to 3.18 ppm and 55.8 ppm compared to 2.18 ppm and 47.0 ppm in the diphenyl alcohol **7.6**. This correlates to the formation of a dimethylammonium group and supports N-C bond formation with the *peri*-carbon. Furthermore, the quaternary *peri*-carbon is shifted further downfield to 105.3 ppm (83.3 ppm in **7.6**).

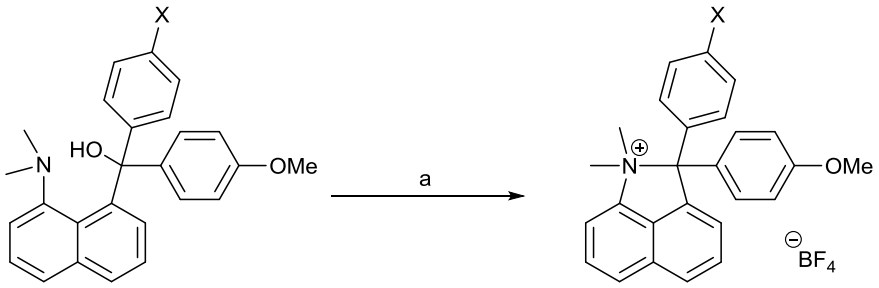

7.7 = OMe
7.9 = H

7.25 = OMe
7.26 = H

Scheme 7.67. (a) HBF_4, DCM, RT.

Reaction of the triaryl alcohols **7.7** and **7.9** with tetrafluoroboric acid by the same method gave the expected dehydrated dimethylammonium compounds **7.25** and **7.26** in yields of 94% and 59% respectively (Scheme 7.8). The colour of both solutions, upon addition of the acid, were found to be luminous red/pink with the colour fading when precipitated to give the two products as pale pink solids. The structure of the dimethoxy salt **7.25** was confirmed with a similar downfield shift in the ^{1}H and ^{13}C NMR signals for N-methyl groups from 2.27 ppm and 47.1 ppm in the alcohol **7.7** to 3.26 ppm and 53.4 ppm in the dimethoxy salt **7.25**. A signal at 106.9

ppm in the ^{13}C NMR further supports the loss of the hydroxyl group. The mono-methoxy salt **7.26** was confirmed in a similar fashion with N-methyl ^{1}H and ^{13}C NMR signals shifted to 3.21/3.38 ppm and 52.4/54.4 ppm from 2.16/2.26 ppm and 46.7/47.0 ppm in the starting alcohol **7.9**.

Dehydration of the dimethylamino triaryl alcohol **7.10**, did not result in the isolation of the desired salt. Despite the reaction proceeding as expected, giving a deep red colour upon acid addition, dilution with diethyl ether did not lead to precipitation, instead forming an orange oil. The oil was separated from the bulk reaction and was washed several times with addition portions of diethyl ether in an attempt to induce crystallisation. This failed and as a result the compound was not pursued.

*Table 7.48. Selected geometric details for the diphenyl (**7.24**), dimethoxy (**7.25**) and Dyker et al (**7.2**) tetrafluoroborate salts.*

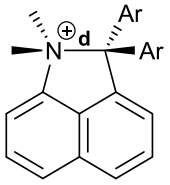

Compound	**d** / Å	**N-C(H$_3$)** / Å	τ^a / °	τ^b / °
7.24	1.653(2)	1.515(2)/1.495(2)	71.9(2)/-57.3(2)	77.9(2)/-39.5(2)
7.25	1.673(2)	1.505(2)/1.513(2)	72.3(2)/-57.0(2)	73.8(2)/-43.8(2)
7.2	1.718(5)	1.499(6)/1.507(6)	63.0(5)/-69.1(5)	63.3(5)/-55.3(5)
	1.719(5)	1.494(6)/1.508(6)	64.5(4)/-66.8(5)	62.4(4)/-56.0(4)

τ^a =C(Ar)-C(*peri*)-C(Ar)-C(H), τ^b = torsion angle: 2 x (H_3)C-N-C-C(H).

Suitable crystals of the two salts **7.24** and **7.25** were grown via slow evaporation of CH_3CN/DCM and DCM/hexane solutions respectively, with X-ray structures determined at 100 K (Figure 7.9). Unfortunately, despite exhaustive efforts, crystals of the mono methoxy salt **26** were not obtained. A selection of geometric data is summarised in Table 7.1 along with the dibenzosuberenone salt **7.2**. The two salts **7.24** and **7.25** differ only by the substitution of two *para*-methoxy groups on the phenyl rings of **7.25**. As a result of their electron donating capabilities, the two methoxy groups increase the electron donation from the phenyl rings into

the anti-bonding orbital of the quaternary carbon of the N-C bond in salt **7.25**, subsequently lowering the contribution required by the nitrogen lone pair to stabilise the carbocation. Consequently, the 1.653(2) Å long N-C bond formed in diphenyl salt **7.24** is shorter than the equivalent bond in the *para*-methoxy salt **7.25** which is found to be 1.673(2) Å. The N-methyl bonds in the two molecules range from 1.495(2)-1.515(2) Å, elongated as a result of the positively charged nitrogen.[7]

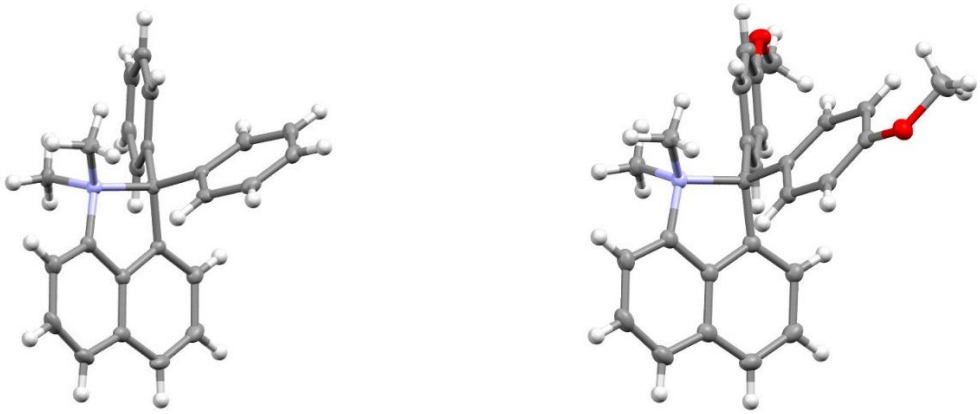

*Figure 7.123. Molecular structures of the diphenyl **7.24** (left) and dimethoxy **7.25** (right) dimethylammonium cations.*

The two *peri*-substituents of the diphenyl salt **7.24** are displaced by 0.2 Å to opposite sides of the idealised naphthalene plane. This results in one of the N-methyl groups being rotated so that it is almost perpendicular to the naphthalene plane, with the same occurring for the phenyl ring anti-periplanar to it. The same observation is made in the methoxy salt **7.25**. As a result of the twist about the N-C bond, the torsional angles of the N-methyl and phenyl groups, with respect to their *ortho*-naphthalene ring carbons, are uneven, unlike dibenzosuberenone salt **7.2** (Figure 7.10 bottom) which show only minor displacements of the *peri*-groups from the idealised naphthalene plane. Therefore, more optimal torsion angles for the N-methyl and suberenone bonds are observed.

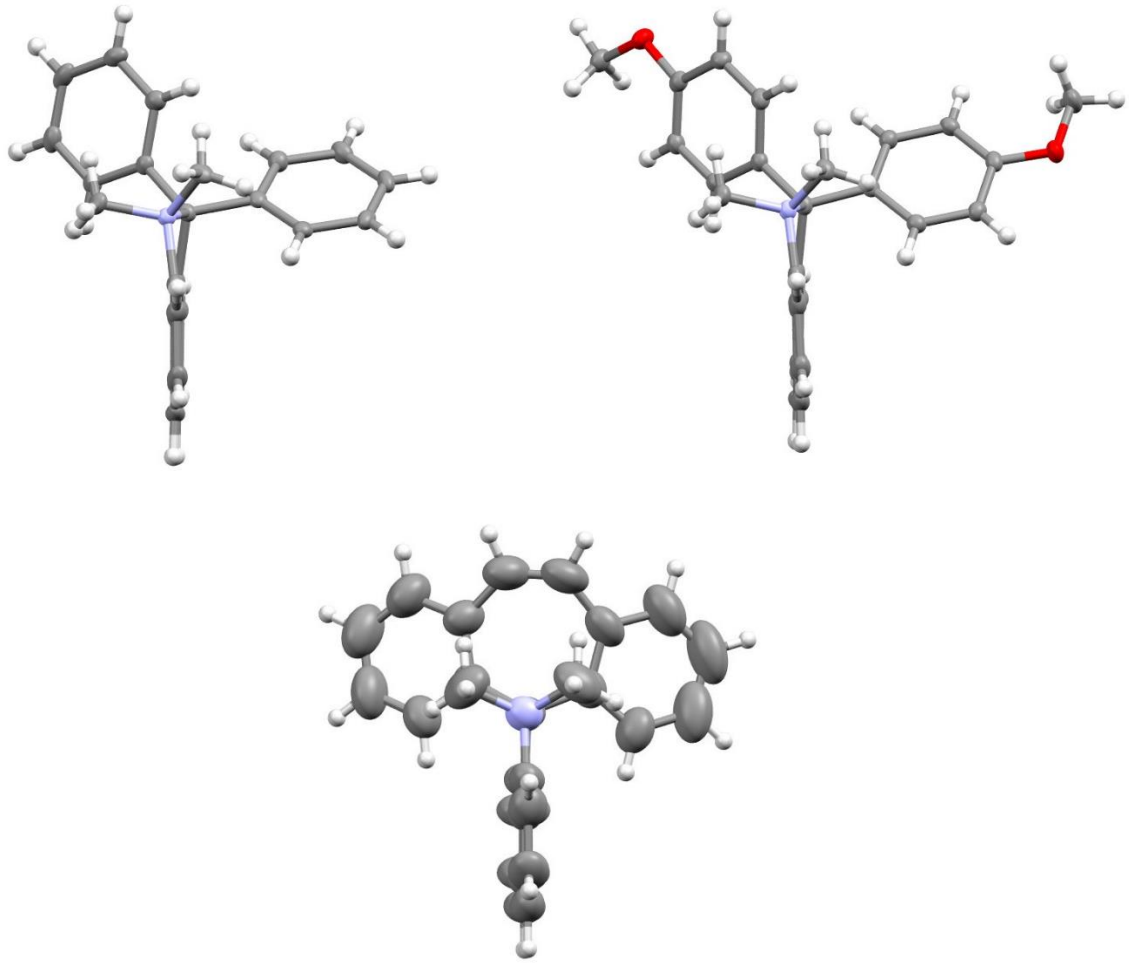

*Figure 7.124. Molecular structures of the diphenyl **7.24** (top left), dimethoxy **7.25** (top right) and Dyker et al **7.2** (bottom) dimethylammonium cations, looking down the naphthalene plane, clearly demonstrating the effect the twist around the N-C bond has on the peri-substituents in **7.24** and **7.25** compared to **7.2**.*

Dropwise addition of tetrafluoroboric acid to a solution of dibenzosuberol **7.8** generated a deep green coloured solution, with a light green precipitate from the reaction after the addition of diethyl ether in 44% yield. The isolated product, however, did not confirm that the expected dehydrated dimethylammonium compound had been synthesised. The N-methyl protons were located in the ^{1}H NMR spectrum as two separate doublets at 3.02 and 2.93 ppm, suggesting the presence of a proton bound to the nitrogen atom. Furthermore, only 12 aromatic protons are accounted for in the spectrum, whilst the starting alcohol possesses 14 aromatic protons. The compound is confirmed as a tetrafluoroborate salt due to the ^{19}F NMR signal of -151.46 ppm and a B-F stretching frequency of 1025 cm^{-1} in the infrared spectrum. However, the ^{13}C NMR

spectrum demonstrates no signal corresponding to a quaternary carbon in the 60-110 ppm range. Crystals of the unknown compound were grown via slow evaporation from a DCM/hexane solution and the structure determined at 100 K.

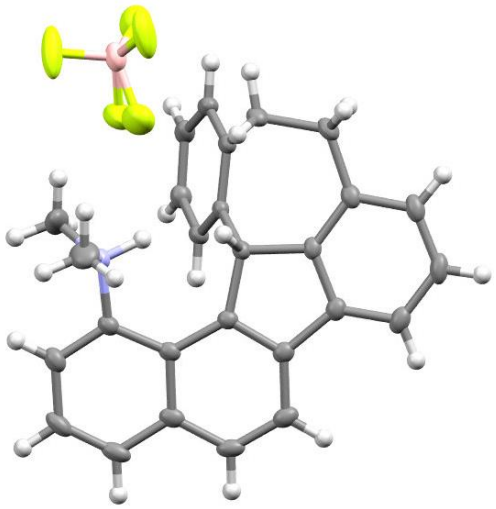

*Figure 7.125. Molecular structure of the 6-ring system of salt **7.28**.*

As shown in Figure 7.11, the isolated salt has not generated a long N-C bond across the *peri*-positions, but instead formed a new 5-membered ring linking the *ortho*-carbons of the naphthalene ring and one of the benzene rings. This generates a 6-ringed system, in which the naphthalene, newly formed 5-membered and one of the benzene rings lie in almost the same plane, with the remaining benzosuberone moiety orientated almost perpendicular to it at an angle between 109-114º. A proposed mechanism for the generation of the salt **7.28** is shown in Scheme 7.9.

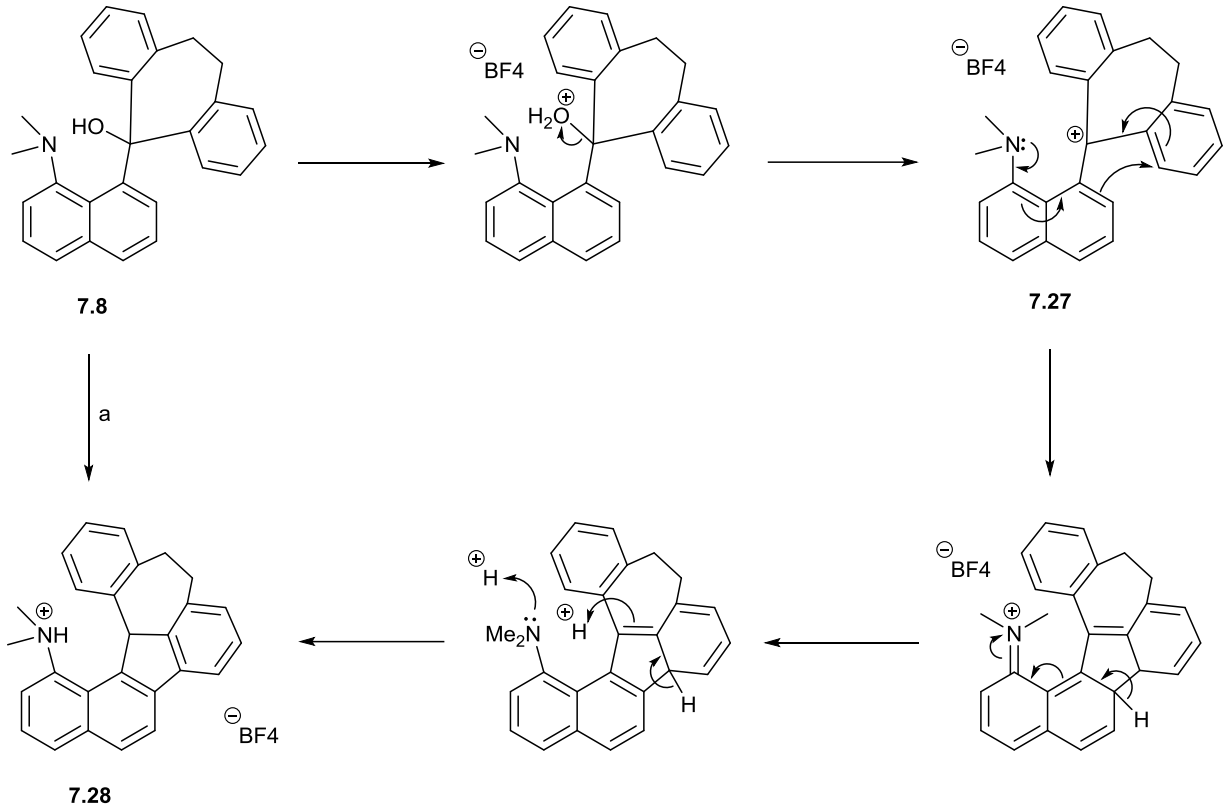

*Scheme 7.68. A proposed mechanism for the generation of the 6-ringed system **7.28**. (a) HBF_4, DCM, RT.*

Following the formation of the carbocation **7.27** via dehydration of the alcohol, addition of the *ortho*-carbons of the naphthalene and benzene rings is driven by the free nitrogen lone pair. The aromaticity of the naphthalene ring is then restored, removing the dimethylaminium cation. Rearrangement of the *ortho*-benzene ring proton rearomatises the ring, resulting in a tertiary carbon centre. The free dimethylamino group, not required in the stabilisation of any carbocation centres is thus protonated due to the highly acidic environment. The rearrangement of the cationic species **7.27** in this fashion, compared to the dibenzosuberenone derivative **7.2** could be a result of the reduced aryl stabilisation to the carbocation **7.27** due to the removal of the ethene bridge in **7.2** for the ethylene bridge of **7.27**. Alternatively, the increased flexibility of the fused system could allow for a better optimised orientation of the benzene and naphthalene *ortho*-carbons, facilitating the rearrangement.

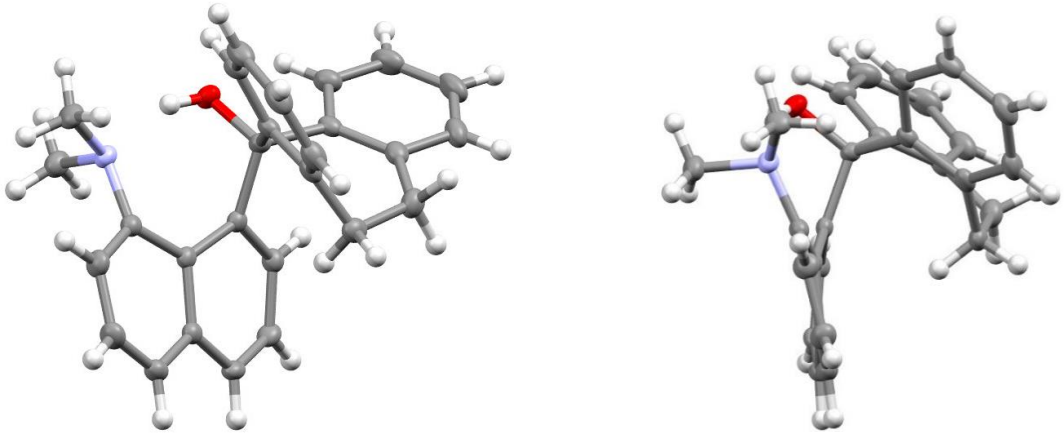

*Figure 7.126. Molecular structure of dibenzosuberol **7.8** (left) and the twisting observed in the naphthalene ring (right).*

Crystals of the starting material, the dibenzosuberol adduct **7.8**, were grown via the slow evaporation of a DCM/hexanes solution and the structure determined at 150K (Figure 7.12). In order for the dimethylamino group to form a hydrogen bond with the *peri*-tertiary alcohol, both of the *peri*-carbons are forced significantly to opposite sides of the best naphthalene plane by 0.702 Å (NMe_2) and 0.855 Å (C(OH)(Ar)), resulting in a severe twist in the naphthalene skeleton. As a consequence of the flexible ethylene bridge in the fused aryl system, the group is able orientated almost perpendicular to the plane, with the benzene ring closest the naphthalene displaced away due to the flexibility of the bridge. This generates a short contact between on of the ethylene bridge protons and the naphthalene ring of 2.36 Å. Looking at the structure of the dibenzosuberol **7.8** it is clear that the size and flexibility of the fused aryl system has allowed for greater reactional freedom, than the more rigid fused aryl system of **7.21**, facilitating the ring fusion observed in the synthesis of **7.28**. The multi-ringed system of **7.28** may not be of use in this investigation, but if separated giving enantiopure samples it could be used as a potential chiral base. Furthermore, modifications to either the ring system (e.g. via substitution) or the dimethylamino moiety could lead to the development of a series of chiral bases with differing properties/uses.

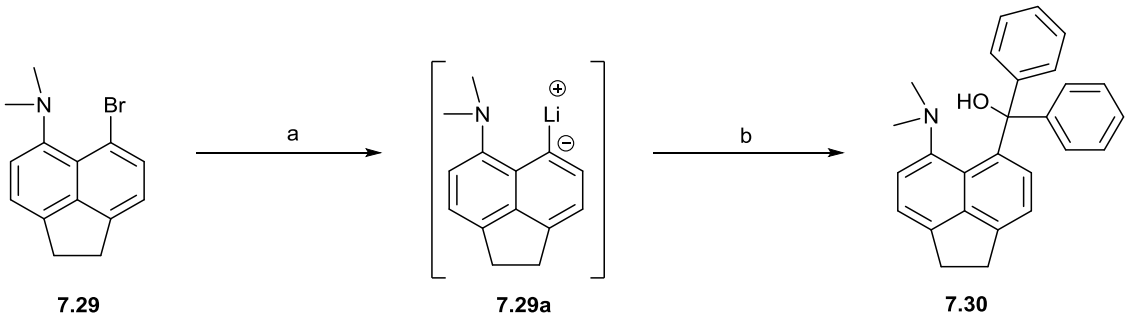

7.29 **7.29a** **7.30**

Scheme 7.69. (a) n-BuLi, THF, -78 °C; (b) Benzophenone, -78 °C to RT.

Previously we have demonstrated how the short ethylene bridge across one set of *peri*-positions in acenaphthene can pull apart groups substituted at the opposite *peri*-positions. This widens the *exo*-angle and increases the distance between the *peri*-groups (Chapter 3). Utilising this approach, the acenaphthene diphenyl alcohol derivative **7.30** was designed and targeted, with the final target being the dehydrated salt akin to **7.24** and **7.25**. Synthesis began with the *peri*-lithiation of the bromo amine **7.29**[8] (synthesis of **7.29** previously described in Chapter 3 as **3.36**) with *n*-BuLi at -78 °C over 3h, which resulted in a deep red solution of the *peri*-lithiated compound **7.29a**. The addition of an excess of benzophenone resulted in the isolation of the desired bridged diphenyl alcohol **7.30** as a brown solid in 64% yield (Scheme 7.10). The structure of **7.30**, like its unsubstituted analogue **7.6**, was confirmed by the addition of 10 aromatic protons in the ^{1}H NMR spectrum, with the tertiary alcohol singlet observed at 11.41 ppm. Whilst the quaternary *peri*-carbon demonstrates a signal of 82.7 ppm in the ^{13}C NMR spectrum.

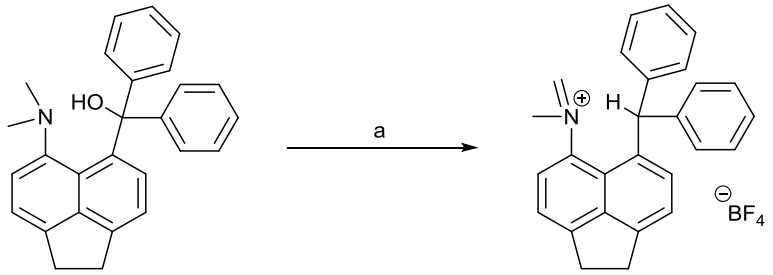

7.30 **7.31**

Scheme 7.70. (a) HBF_4, DCM, RT.

Tetrafluoroboric acid was added dropwise to a solution of acenaphthene alcohol **7.30** generating a deep blue/green coloured solution (Scheme 7.11). The reaction was layered with diethyl ether and subsequently stirred for a further 16h, resulting in the precipitate of a light green solid that was isolated in an 84% yield. Analysis of the product by ^{1}H NMR revealed that the desired dehydrated salt had not been synthesised. Akin to the acenaphthene derivatives studied in Chapter 3, a hydride from one of the N-methyl groups of the nucleophile had been transferred to the *peri*-carbon, quenching the carbocation and resulting in the formation of an iminium cation. Signals in the ^{1}H NMR spectrum of 6.42 ppm for the methylene protons of the iminium cation demonstrate this, with the methylene ^{13}C NMR signal found at 172.1 ppm. Furthermore, the tertiary *peri*-proton is located as a singlet at 5.68 ppm resulting in the *peri*-carbon shifting to 54.0 ppm.

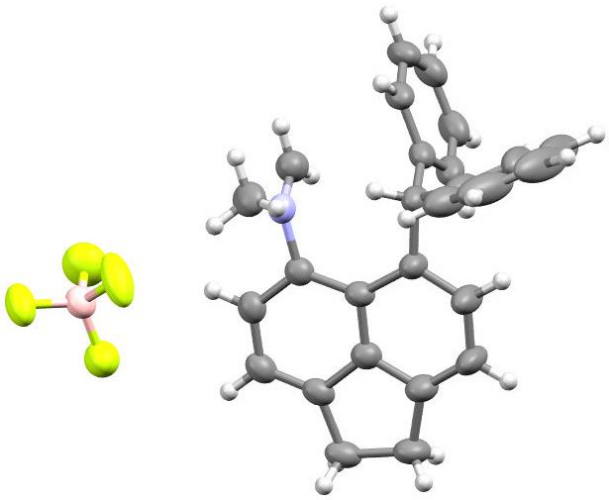

*Figure 7.127. Molecular structure of the acenaphthene iminium salt **7.31**.*

Crystals of the iminium cation **7.31** were obtained from a DCM/hexanes solution and their structure determined at 150 K (Figure 7.13). Unfortunately, the asymmetric unit possesses four individual cation-anion pairs, with two sets of the molecule pairs demonstrating disorder. The structure is therefore inaccurate with respect to obtaining accurate measurements (i.e. bond distances and angles). The data does however allow for the confirmation of the structure of the

iminium cation **7.31**, with the two N-C bonds lengths (excluding the N-C(Ar)) differing significantly from each other; N=C 1.251-1.264 Å / N-C 1.480-1.488 Å. Moreover, the average sum of the bond angles at the nitrogen atoms in the four cations is 359.8^{o} corresponding to a planar conformation. In all cases the acenaphthene has induced a widening of the *exo*-angle between the opposite *peri*-positions, with wide N---C contact distances in the range of *ca.* 3.0 Å. Like the examples shown in Chapter 3, the widening of this distance has allowed for a greater degree of rotation for the dimethylamino group. Couple this with the increased potency of the electrophile in these cases (the carbocation) and it is not surprising that the distance is too large for the nitrogen lone pair to provide stabilisation, thus resulting in the transfer of the hydride to generate the more adequately stabilised iminium cation, rather than the tertiary cation.

Following the example set by Dyker *et al*, we set out to investigated whether similarly stabilised carbocations could generate long N-C bonds and whether an increase in the stabilisation to the carbon of the N-C bond could isolate an earlier point in the bond formation process. The two salts **7.24** and **7.25** demonstrate this idea successfully, whereby the increased electron donation provided by the methoxy groups of **7.25** increased the N-C bond length by 0.02 Å compared to diphenyl **7.24**. Interesting, other examples proceeded via alternate reacton pathways upon the generation of similar carbocations. For example; the dibenzosuberone reacted via a ring coupling between the benzene and naphthalene rings to give **7.28**, unlike that of the reported dibenzosuberenone **7.2**. This gave an interesting 6-ringed hydrocarbon chiral system which could potentially be employed as a chiral base. The acenaphthene derivative **7.30** resulted in a proton transfer to the carbocation, with the interaction distance between the *peri*-groups too large for the nitrogen lone to provide stabilisation, instead generating iminium cation **7.31**.

Experimental

General. Solution NMR spectra were measured on a Jeol ECLIPSE ECX or ECZ 400 spectrometer at 400 MHz for ^{1}H and at 100.6 MHz for ^{13}C using $CDCl_3$ as solvent and tetramethylsilane (TMS) as standard unless otherwise stated, and measured in p.p.m. downfield from TMS with coupling constants reported in Hz. IR spectra were recorded on a Perkin Elmer Spectrum 100 FT-IR Spectrometer using Attenuated Total Reflection sampling on solids or oils and are reported in cm^{-1}. Mass spectra were recorded at the EPSRC Mass Spectrometry Centre at the University of Swansea. Chemical analysis data were obtained from Mr Stephen Boyer, London Metropolitan University.

Preparation of methyl 8-(dimethylamino)-1-naphthoate, 7.4.

n-BuLi (16.8 ml, 1.6 M in hexane solution, 26.90 mmol) was added to a stirred solution of 1-dimethylaminonaphthalene (1.00 g, 5.85 mmol) in dry ether (10 ml) under nitrogen at room temperature and left to stir for 5 days during which time a yellow precipitate formed. The solution was carefully removed, and the yellow solid was washed several times with dry ether under nitrogen. The solid was dissolved in dry THF (10 ml), cooled to −78°C and methyl chloroformate (0.45 mL, 5.85 mmol) was added. The mixture was gradually warmed to room temperature and stirred for 2 h. A small portion of methanol (3 mL) was added to the reaction before the solvent was removed *in vacuo* and the resultant crude material purified by flash column chromatography (20:80 ethyl acetate/petrol 40-60) to give **7.4** as a yellow oil (0.77 g, 57%). δH (400 MHz, $CDCl_3$, 24 °C): 7.86 (1H, dd, J = 7.8, 1.8 Hz, Ar-*H*$_1$), 7.66 (1H, dd, J = 8.2, 1.4 Hz, Ar-*H*$_1$), 7.37-7.52 (4H, m, Ar-*H*$_4$), 3.90 (3H, s, OC*H*$_3$), 2.66 (6H, s, N(C*H*$_3$)$_2$); δC (100 MHz, $CDCl_3$, *24* °C): 172.1 (*C*=O), 150.7 (8-*C*), 135.0, 131.1, 129.5, 128.2, 126.7, 125.4,

125.3, 125.2, 119.5 (Ar-*C*$_9$), 52.1 (O*C*H$_3$), 46.2 (N(*C*H$_3$)$_2$); ν_{max}/cm^{-1} 2942, 2860, 2827, 2784, 1716 (C=O), 1504, 1466, 1449, 1429, 1375, 1340, 1269, 1194, 1161, 1142, 1082, 1012, 831, 808, 732; HRMS (ESI): Found: 230.1188 (M+H$^+$) $C_{14}H_{15}NO_2$ requires: 230.1181 (M+H$^+$).

Preparation of methyl (1R,2R)-8-(dimethylamino)-2-phenyl-1,2-dihydronaphthalene-1-carboxylate, 7.5a.

Phenyl lithium (8.8 ml, 1.8 M in dibutyl ether solution, 15.72 mmol) was added to a stirred solution of the methyl ester **7.4** (0.90 g, 3.93 mmol) in dry THF (20 ml) under nitrogen at -78℃ and left to stir for 1 h before the reaction was warmed to room temperature and stirred for a further 16 h. The reaction was quenched with water (50 mL) and the aqueous solution was washed with EtOAc (3 x 30 mL) and the combined organic layers were washed with H_2O (40 mL), brine (40 mL) and dried over $MgSO_4$. The solvent was removed *in vacuo* and the resultant crude material was purified by flash column chromatography (10:90 ethyl acetate/petrol 40-60) to give **7.5a** as an off white solid (189 mg, 16%), m.p. 55-58℃. δH (400 MHz, $CDCl_3$, 24 °C): 7.22-7.38 (6H, m, Ar-*H*$_6$), 7.11 (1H, dd, J = 8.1, 1.1 Hz, Ar-*H*$_1$), 6.96 (1H, dd, J = 7.4, 0.8 Hz, Ar-*H*$_1$), 6.67 (1H, dd, J = 9.7, 3.1 Hz, 3-*H*), 6.06 (1H, dd, J = 9.7, 2.2 Hz, 4-*H*), 4.49 (1H, d, J = 8.1 Hz, 1-*H*), 4.17 (1H, m, 2-*H*), 3.20 (3H, s, OC*H*$_3$), 2.55 (6H, s, N(C*H*$_3$)$_2$); δC (100 MHz, $CDCl_3$, *24* °C): 172.0 (*C*=O), 152.4 (8-*C*), 149.5 (Ar-*C*$_1$), 129.4 (3-*C*), 128.7 (4-*C*), 128.5, 128.4, 128.3, 128.2, 127.9, 126.9, 123.2, 120.6 (Ar-*C*$_8$), 51.0 (O*C*H$_3$), 45.7 (1-*C*), 45.5 (N(*C*H$_3$)$_2$), 44.4 (2-*C*); ν_{max}/cm^{-1} 3034, 2989, 2890, 2860, 2830, 2788, 1733 (C=O), 1586, 1472, 1451, 1433, 1351, 1164, 1041, 1013, 989, 922, 812, 754, 704; HRMS (ESI): Found: 308.1651 (M+H$^+$), $C_{20}H_{21}NO_2$ requires: 308.1650 (M+H$^+$).

Preparation of (8'-(dimethylamino)naphthalen-1'-yl)diphenylmethanol, 7.6.

n-BuLi (16.8 ml, 1.6 M in hexane solution, 26.90 mmol) was added to a stirred solution of 1-dimethylaminonaphthalene (1.00 g, 5.85 mmol) in dry ether (10 ml) under nitrogen at room temperature and left to stir for 5 days during which time a yellow precipitate formed. The solution was carefully removed, and the yellow solid was washed several times with dry ether under nitrogen. The solid was dissolved in dry THF (10 ml), cooled to −78°C and benzophenone (1.27 g, 6.97 mmol) was added. The mixture was gradually warmed to room temperature and stirred for 16 h, after which it was treated with water (30 ml). The aqueous solution was washed with EtOAc (3 x 30 mL) and the combined organic layers were washed with H_2O (40 mL), brine (40 mL) and dried over $MgSO_4$. The solvent was removed *in vacuo* and the resultant crude material purified by flash column chromatography (10:90 ethyl acetate/petrol 40-60) to give **7.6** as an off white solid (1.45 g, 76%), m.p. 148-151℃. δH (400 MHz, $CDCl_3$, 24 °C): 11.37 (1H, s, O*H*), 7.75-7.85 (2H, m, Ar-*H*$_2$), 7.42-7.47 (2H, m, Ar-*H*$_2$), 7.15-7.26 (11H, m, Ar-*H*$_{11}$), 6.92 (1H, dd, J = 7.4, 1.4 Hz, Ar-*H*), 2.18 (6H, s, N(C*H*$_3$)$_2$); δC (100 MHz, $CDCl_3$, *24* °C): 150.0, 149.3, 143.5, 137.4, 131.8, 129.8, 129.7, 129.5, 128.6, 127.7, 126.6, 125.4, 124.3, 122.2 (Ar-C_{22}), 83.3 (*C*(Ph)$_2$(OH)), 47.0 (N(*C*H$_3$)$_2$); ν_{max}/cm^{-1} 2607 (OH), 1483, 1444, 1170, 1041, 833, 760, 698; HRMS (ESI): Found: 354.1853 (M+H$^+$) 336.1764 (M - OH), $C_{25}H_{24}NO$ requires: 354.1858 (M+H$^+$), 336.1752 (M – OH).

Preparation of 1-(hydroxydiphenylmethyl)-N,N-dimethylnaphthalen-8-aminium chloride, 7.19.

Diphenyl alcohol **7.6** (100 mg, 0.28 mmol), was dissolved in Et_2O (10 mL) and stirred whilst ethereal hydrochloric acid (2.0 M, 0.76 mL, 1.56 mmol) was added dropwise. A fine white precipitate formed and was isolated under a nitrogen stream and washed with portions of cold anhydrous diethyl ether. The precipitate was thoroughly dried *in vacuo* to give **7.19** as a white solid (70 mg, 64%), m.p. 137-141℃. δH (400 MHz, $CDCl_3$, 24 °C): 7.87 (1H, d, J = 6.8 Hz, Ar-H_1), 7.80 (1H, d, J = 7.3 Hz, Ar-H_1), 7.87 (2H, m, Ar-H_2), 7.48 (2H, m, 6-, 7-*H*), 7.13-7.35 (11H, m, Ar-H_{11}), 6.96 (1H, d, J = 8.2 Hz, 2-*H*), 2.33 (6H, s, N(CH_3)$_2$); δC (100 MHz, $CDCl_3$, *24* °C): 149.0 (8-*C*), 137.5 (Ar-C_1), 132.5 (2-*C*), 130.7, 130.4, 128.9, 128.6, 128.1, 127.2 (Ar-C_{16}), 125.6 (6-*C*), 124.8 (Ar-C_1), 122.2 (7-*C*), 83.8 *C*(Ph)$_2$(OH)), 47.5 (N(*C*H$_3$)$_2$); ν_{max}/cm^{-1} 2775, 2614, 1487, 1459, 1444, 1349, 1330, 1172, 1155, 1030, 998, 831, 758, 698.

Preparation of 1-(hydroxydiphenylmethyl)-N,N-dimethylnaphthalen-8-aminium tetrafluoroborate, 7.20.

Diphenyl alcohol **7.6** (200 mg, 0.56 mmol), was dissolved in anhydrous diethyl ether (5 mL) and stirred whilst tetrafluoroboric acid diethyl ether complex (0.08 mL, 0.56 mmol) was added dropwise. A fine white precipitate formed and was isolated under a nitrogen stream and washed with portions of cold anhydrous diethyl ether. The precipitate was thoroughly dried *in vacuo* to give **7.20** as a white solid (180 mg, 72%), m.p. 162-165℃. δH (400 MHz, $CDCl_3$, 24 °C): 8.03 (1H, dd, J = 8.2, 1.1 Hz, 5-*H*), 7.93 (1H, dd, J = 8.2, 1.3 Hz, 4-*H*), 7.76 (1H, dd, J = 7.8, 1.3 Hz, 7-*H*), 7.61 (1H, t, J = 7.8 Hz, 6-*H*), 7.24-7.35 (7H, m, 3-, Ph-H_6), 7.08-7.13 (4H, m,

Ph-*H*$_4$), 6.98 (1H, dd, J = 7.4, 1.3 Hz, 2-*H*), 2.67 (6H, s, N(C*H*$_3$)$_2$); δC (100 MHz, $CDCl_3$, 24 °C): 145.1, 139.3, 137.6, 136.8 (Ar-*C*$_5$), 133.4 (2-*C*), 133.1 (5-*C*), 131.6 (4-*C*), 128.7 (Ph-*C*$_4$), 128.6 (Ph-*C*$_2$), 128.4 (Ph-*C*$_4$), 126.0 (6-*C*), 125.4 (3-*C*), 124.9 (Ar-*C*$_1$), 122.2 (7-*C*), 84.7 (*C*(Ph)$_2$(OH)), 47.3 (N(*C*H$_3$)$_2$); δF (376 MHz, $CDCl_3$, 24 °C): -149.83 ($^-BF_4$); ν_{max}/cm^{-1} 3403, 3025, 1492, 1448, 1338, 1094, 1071 (br B-F), 978, 829, 764, 702; Found: C, 67.98; H, 5.45; N, 3.18. Calc. for $C_{25}H_{24}NOBF_4$: C, 68.05; H, 5.48; N, 3.17%.

Preparation of 1,1-dimethyl-2,2-diphenyl-1,2-dihydrobenzo[cd]indol-1-ium tetrafluoroborate, 7.24.

Diphenyl alcohol **7.6** (175 mg, 0.49 mmol) was dissolved in dichloromethane (5 mL) and stirred whilst Tetrafluoroboric acid diethyl ether complex (0.40 mL, 2.94 mmol) was added dropwise. After stirring for 1h at room temperature, stirring was ceased and diethyl ether (20 mL) was slowly added generating a bilayer, the bilayers were combined gradually generating a precipitate and stirring was continued for another 16h. The precipitate was filtered, washed with further portions of diethyl ether (20 mL) and dried *in vacuo* to give **7.24** as an off white solid (185 mg, 88%), m.p. decomp, >150℃. δH (400 MHz, CD_3CN, 24 °C): 8.12 (1H, dd, J = 5.8, 3.1 Hz, 6'-*H*), 8.03 (1H, d, J = 8.4 Hz, 5'-*H*), 7.84-7.88 (2H, m, 7'-, 8'-*H*), 7.73 (1H, dd, J = 8.4, 7.2 Hz, 4'-*H*), 7.40-7.55 (10H, m, Ph-H$_{10}$), 7.37 (1H, d, J = 7.20 Hz, 3'-*H*), 3.18 (6H, s, N(C*H*$_3$)$_2$); δC (100 MHz, CD_3CN, 24 °C): 147.4 (8a'-*C*), 135.2, 133.6, 132.3, 131.6, 131.3, 131.0, 130.5 (Ar-*C*$_{15}$), 130.2 (7'-*C*), 129.9 (Ar-*C*$_1$), 128.9 (6'-*C*), 127.3 (5'-*C*), 125.9 (3'-*C*), 116.0 (8'-*C*), 105.3 (*C*Ph$_2$), 55.8 (N(*C*H$_3$)$_2$); δF (376 MHz, CD_3CN, 24 °C): -151.55 ($^-BF_4$); ν_{max}/cm^{-1} 1492, 1463, 1449, 1049, 1026 (br B-F), 825, 760, 704; HRMS (ESI): Found: 336.1748 (M^+), $C_{25}H_{22}N^+$ requires: 336.1752 (M^+).

Preparation of (8'-(dimethylamino)naphthalen-1'-yl)bis(4-methoxyphenyl)methanol, 7.7.

n-BuLi (13.45 ml, 2.0 M in hexane solution, 26.90 mmol) was added to a stirred solution of 1-dimethylaminonaphthalene (1.00 g, 5.85 mmol) in dry ether (10 ml) under nitrogen at room temperature and left to stir for 5 days during which time a yellow precipitate formed. The solution was carefully removed, and the yellow solid was washed several times with dry ether under nitrogen. The solid was dissolved in dry THF (10 ml), cooled to −78°C and 4,4′-dimethoxybenzophenone (1.70 g, 7.02 mmol) was added. The mixture was gradually warmed to room temperature and stirred for 16 h, after which it was treated with water (30 ml). The aqueous solution was washed with EtOAc (3 x 30 mL) and the combined organic layers were washed with H_2O (40 mL), brine (40 mL) and dried over $MgSO_4$. The solvent was removed *in vacuo* and the resultant crude material was purified by flash column chromatography (20:80 ethyl acetate/petrol 40-60) to give **7.7** as a pale yellow solid (1.16 g, 48%), m.p. 192-195°C. δH (400 MHz, $CDCl_3$, 24 °C): 11.39 (1H, s, O*H*), 7.83 (1H, dd, J = 6.4, 3.2 Hz, 5'-*H*), 7.79 (1H, d, J = 7.3 Hz, 4'-*H*), 7.42-7.50 (2H, m, 6'-, 7'-*H*), 7.24 (1H, t, J = 7.3 Hz, 3'-*H*), 7.15 (4H, d, J = 8.7 Hz, 2-*H*), 7.00 (1H, dd, J = 7.8, 1.4 Hz, 2'-*H*), 7.15 (4H, d, J = 9.2 Hz, 3-*H*), 3.81 (6H, s, OCH_3), 2.27 (6H, s, N(CH_3)$_2$); δC (100 MHz, $CDCl_3$, *24* °C): 158.2 (4-*C*), 149.4 (8a'-*C*), 144.0, 142.7, 137.4 (Ar-C_3), 131.7 (1'-*C*), 129.9 (Ar-C_1), 129.7 (4'-*C*), 129.6 (2-*C*), 129.5 (5'-*C*), 125.4 (Ar-C_1), 124.2 (3'-*C*), 122.2 (Ar-C_1), 113.0 (3-*C*), 82.8 (C(Ph)$_2$(OH)), 55.3 (OCH_3), 47.1 (N(CH_3)$_2$); ν_{max}/cm^{-1} 2942, 2834, 2640 (OH), 1733, 1602, 1505, 1451, 1295, 1246, 1170, 1105, 1030, 833, 818, 777; HRMS (ESI): Found: 414.2076 (M+H$^+$) 396.1982 (M-OH), $C_{27}H_{28}NO_3$ requires: 414.2069 (M+H$^+$), 396.1964 (M–OH).

Preparation of 2,2-bis(4-methoxyphenyl)-1,1-dimethyl-1,2-dihydrobenzo[cd]indol-1-ium tetrafluoroborate, 7.25.

Dimethoxy aryl alcohol **7.7** (200 mg, 0.48 mmol) was dissolved in dichloromethane (5 mL) and stirred whilst Tetrafluoroboric acid diethyl ether complex (0.33 mL, 2.42 mmol) was added dropwise. After stirring for 1h at room temperature, stirring was ceased and diethyl ether (20 mL) was slowly added generating a bilayer, the bilayers were combined gradually generating a precipitate and stirring was continued for another 16h. The precipitate was filtered, washed with further portions of diethyl ether (20 mL) and dried *in vacuo* to give **7.25** as a pink solid (221 mg, 94%), m.p. 149-152℃. δH (400 MHz, $CDCl_3$, 24 °C): 8.09 (1H, d, J = 7.4 Hz, 8'-*H*), 8.04 (1H, d, J = 8.4 Hz, 6'-*H*), 7.98 (1H, d, J = 8.1 Hz, 5'-*H*), 7.86 (1H, t, J = 7.7 Hz, 7'-*H*), 7.74 (1H, dd, J = 8.2, 7.1 Hz, 4'-*H*), 7.36 (4H, d, J = 8.9 Hz, 2-*H*), 7.29 (1H, d, J = 7.0 Hz, 3'-*H*), 6.94 (1H, d, J = 9.2 Hz, 3-*H*), 3.83 (6H, s, OCH_3), 3.26 (6H, s, N(CH_3)$_2$); δC (100 MHz, $CDCl_3$, 24 °C): 161.8 (4-*C*), 146.1 (8a'-*C*), 137.8 (2a'-*C*), 132.3 (5a'-*C*), 131.8 (2-*C*), 130.3 (4'-*C*), 129.8 (7'-*C*), 127.9 (2a''-*C*), 127.7 (6'-*C*), 126.3 (5'-*C*), 125.5 (1-*C*), 124.6 (3'-*C*), 116.2 (8'-*C*), 115.0 (3-*C*), 106.9 (*C*(Ar)$_3$), 55.9 (O*C*H$_3$), 53.4 (N(*C*H$_3$)$_2$); δF (376 MHz, $CDCl_3$, 24 °C): -151.73 ($^-BF_4$); ν_{max}/cm^{-1} 1604, 1578, 1509, 1459, 1444, 1302, 1258, 1183, 1053, 1019 (br B-F), 857, 818, 777, 764, 678; HRMS (ESI): Found: 396.1952 (M^+), $C_{27}H_{26}N^+O_2$ requires: 396.1964 (M^+).

Preparation of 5-(8'-dimethylamino-1'-naphthyl)-5-hydroxy-5H-dibenzo[a,d]cycloheptane, 7.8.

n-BuLi (16.15 ml, 2.5 M in hexane solution, 40.35 mmol) was added to a stirred solution of 1-dimethylaminonaphthalene (1.50 g, 8.77 mmol) in dry ether (20 ml) under nitrogen at room temperature and left to stir for 5 days during which time a yellow precipitate formed. The solution was carefully removed, and the yellow solid was washed several times with dry ether under nitrogen. The solid was dissolved in dry THF (20 ml), cooled to −78°C and dibenzosuberone (1.9 mL, 10.53 mmol) was added. The mixture was gradually warmed to room temperature and stirred for 16 h, after which it was treated with water (30 ml). The aqueous solution was washed with EtOAc (3 x 30 mL) and the combined organic layers were washed with H_2O (40 mL), brine (40 mL) and dried over $MgSO_4$. The solvent was removed *in vacuo* and the resultant crude material was purified by flash column chromatography (20:80 EtOAc/petrol 40-60) to give **7.8** as an off white solid (1.25 g, 38%), m.p. 173-176℃. δH (400 MHz, $CDCl_3$, 24 °C): 10.26 (1H, s, O*H*), 8.16 (2H, d, J = 7.9, 0.9 Hz, 3'-*H*), 7.70 (1H, dd, J = 6.3, 3.0 Hz, Ar-H_1), 7.64 (1H, dd, J = 8.0, 0.8 Hz, Ar-H_1), 7.12-7.32 (6H, m, Ar-H_6), 7.06 (2H, t, J = 7.3 Hz, Ar-H_2), 6.80 (2H, d, J = 7.4 Hz, Ar-H_2), 2.40 (6H, s, N(CH_3)$_2$), 1.60-2.30 (4H, m, 1-, 2-*H*); δC (100 MHz, $CDCl_3$, 24 °C): 151.1 (8'-*C*), 146.4, 142.7, 136.9, 136.8 (Ar-C_4), 130.2, 129.6, 128.4, 128.2 (Ar-C_4), 127.3, 126.9, 125.8, 125.6, 125.2, 124.9, 118.7 (Ar-C_7), 79.2 (*C*(Ph)$_2$(OH)), 47.8 (8'-N(CH_3)$_2$), 31.6 (1-, 2-*C*); ν_{max}/cm^{-1} 2993, 2944, 2879, 2850, 2830, 2788, 1476, 1453, 1366, 1282, 1161, 1038, 989, 825, 775, 752, 740; HRMS (ESI): Found: 380.2017 (M+H$^+$) 362.1918 (M-OH), $C_{27}H_{26}NO$ requires: 380.2014 (M+H$^+$), 362.1909 (M–OH).

Preparation of N,N-dimethyl-11,15b-dihydro-10H-benzo[a]benzo[4,5]cyclohepta[1,2,3-jk]fluoren-8'-aminium tetrafluoroborate, 7.28.

Aryl alcohol **7.8** (300 mg, 0.79 mmol) was dissolved in dichloromethane (5 mL) and stirred whilst Tetrafluoroboric acid diethyl ether complex (0.54 mL, 3.96 mmol) was added dropwise. After stirring for 1h at room temperature, stirring was ceased and diethyl ether (20 mL) was slowly added generating a bilayer, the bilayers were combined gradually generating a precipitate and stirring was continued for another 16h. The precipitate was filtered, washed with further portions of diethyl ether (20 mL) and dried *in vacuo* to give **7.28** as a green solid (155 mg, 44%), m.p. Decomposed >220℃. δH (400 MHz, CD_3CN, 24 °C): 7.55-7.62 (2H, m, Ar-H_2), 7.42-7.50 (2H, m, Ar-H_2), 7.36-7.39 (1H, m, Ar-H_1), 7.25-7.33 (2H, m, Ar-H_2), 7.16 (1H, d, J = 8.1 Hz, Ar-H_1), 6.96 (1H, t, J = 7.8 Hz, Ar-H_1), 6.67-6.75 (2H, m, Ar-H_2), 6.56 (1H, dd, J = 9.3, 2.2 Hz, Ar-H_1), 4.87 (1H, s, C*H*), 2.90-3.57 (4H, m, CH_2-CH_2), 3.02 (3H, d, J = 5.3 Hz, HN^+CH_3), 2.37 (3H, d, J = 5.3 Hz, HN^+CH_3); δC (100 MHz, CD_3CN, 24 °C): 146.0, 144.9, 143.6, 141.2, 139.2, 138.9, 138.3, 135.1, 133.7, 133.0, 131.6, 131.4, 131.3, 130.8, 129.6, 129.5, 128.3, 127.9, 127.6, 126.7, 122.3, 119.9 (Ar-C_{22}), 52.1 (HN+CH_3), 52.0 (*C*H), 44.7 (HN+CH_3), 35.6 & 34.2 (CH_2-CH_2); δF (376 MHz, CD_3CN, 24 °C): -151.46 ($^-BF_4$); ν_{max}/cm^{-1} 3175, 1472, 1457, 1395, 1341, 1025 (br B-F), 848, 836, 758; HRMS (ESI): Found: 362.1922 (M^+), $C_{27}H_{24}N$ requires: 362.1909 (M^+).

Preparation of (8'-(dimethylamino)naphthalen-1'-yl)(4-methoxyphenyl) (phenyl)methanol, 7.9.

n-BuLi (13.45 ml, 2.0 M in hexane solution, 26.90 mmol) was added to a stirred solution of 1-dimethylaminonaphthalene (1.00 g, 5.85 mmol) in dry ether (10 ml) under nitrogen at room temperature and left to stir for 5 days during which time a yellow precipitate formed. The solution was carefully removed, and the yellow solid was washed several times with dry ether under nitrogen. The solid was dissolved in dry THF (10 ml), cooled to −78°C and 4-methoxybenzophenone (1.49 g, 7.02 mmol) was added. The mixture was gradually warmed to room temperature and stirred for 16 h, after which it was treated with water (30 ml). The aqueous solution was washed with EtOAc (3 x 30 mL) and the combined organic layers were washed with H_2O (40 mL), brine (40 mL) and dried over $MgSO_4$. The solvent was removed *in vacuo* and the resultant crude material was purified by flash column chromatography (20:80 ethyl acetate/petrol 40-60) to give **7.9** as a white solid (0.56 g, 25%), m.p. 151-154℃. δH (400 MHz, $CDCl_3$, 24 °C): 11.36 (1H, s, O*H*), 7.81 (1H, t, J = 4.9 Hz, 6'-*H*), 7.77 (1H, dd, J = 8.0, 1.4 Hz, 4'-*H*), 7.42-7.48 (2H, m, 5'-, 7'-*H*), 7.17-7.25 (6H, m, 2''-, 3''-, 4''-, 3'-*H*), 7.11 (2H, d, J = 8.7 Hz, 2-*H*), 6.94 (1H, dd, J = 7.4, 1.4 Hz, 2'-*H*), 6.79 (2H, d, J = 8.9 Hz, 3-*H*), 3.78 (3H, s, OCH_3), 2.26 (3H, s, N-CH_3), 2.16 (3H, s, N-CH_3); δC (100 MHz, $CDCl_3$, *24* °C): 158.1 (4-*C*), 150.2 (Ar-C_1), 149.2 (8'-*C*), 143.6 (Ar-C_1), 142.2 (1-*C*), 137.3 (Ar-C_1), 131.6 (2'-*C*), 129.7 (Ar-C_1), 129.6 & 129.4 (4'-, 6'-, 2-*C*), 128.4 & 127.6 (2''-, 3''-*C*), 126.4, 125.2, 124.1, 122.0 (Ar-C_4), 112.8 (3-*C*), 83.0 *C*$(Ar)_3$(OH), 55.2 (OCH_3), 47.0 & 46.7 (N(CH_3)$_2$); ν_{max}/cm^{-1} 2944, 2898, 2827, 2495 (OH), 1604, 1582, 1505, 1489, 1448, 1369, 1302, 1246, 1172, 1030, 890, 825, 807, 780, 764;

Preparation of 2'-(4-methoxyphenyl)-1,1-dimethyl-2-phenyl-1,2-dihydrobenzo[cd]indol-1'-ium tetrafluoroborate, 7.26.

Aryl alcohol **7.9** (100 mg, 0.26 mmol) was dissolved in dichloromethane (5 mL) and stirred whilst tetrafluoroboric acid diethyl ether complex (0.17 mL, 1.31 mmol) was added dropwise. After stirring for 1h at room temperature, stirring was ceased and diethyl ether (20 mL) was slowly added generating a bilayer, the bilayers were combined gradually generating a precipitate and stirring was continued for another 16h. The precipitate was filtered, washed with further portions of diethyl ether (20 mL) and dried *in vacuo* to give **7.26** as a pink solid (70 mg, 59%), m.p. 148-151℃. δH (400 MHz, $CDCl_3$, 24 °C): 8.11 (1H, d, J = 7.3 Hz, 8'-*H*), 8.04 (1H, d, J = 8.7 Hz, 6'-*H*), 7.98 (1H, d, J = 8.2 Hz, 5'-*H*), 7.87 (1H, t, J = 7.8 Hz, 7'-*H*), 7.74 (1H, t, J = 7.3 Hz, 4'-*H*), 7.34-7.49 (7H, m, 2''-, 3''-, 4''-, 2-*H*), 7.30 (1H, d, J = 6.9 Hz, 3'-*H*), 6.98 (1H, d, J = 8.2 Hz, *3-H*), 3.85 (3H, s, OCH_3), 3.38 (3H, s, N^+-CH_3), 3.21 (3H, s, N^+-CH_3); δC (100 MHz, $CDCl_3$, 24 °C): 161.6 (4-*C*), 145.9 (8a'-*C*), 137.3, 134.3, 132.0 (Ar-C_3), 131.7 (2-*C*), 131.0 (Ar-C_1), 130.0 (4'-*C*), 129.5 (7'-*C*), 129.5 & 129.4 (2''-, 3''-, 4''-*C*), 127.5 (6'-*C*), 127.4 (Ar-C_1), 126.1 (5'-*C*), 124.4 (Ar-C_1), 124.3 (3'-*C*), 115.7 (8'-*C*), 114.8 (3-*C*), 105.1 ($C(Ar)_3$), 55.6 (OCH_3), 54.4 & 52.4 ($N^+(CH_3)_2$); ν_{max}/cm^{-1} 1600, 1576, 1507, 1455, 1302, 1258, 1187, 1054, 1034 (br B-F), 851, 829, 788, 769, 734, 708 684.

Preparation of (8'-(dimethylamino)naphthalen-1'-yl)(4-(dimethylamino)phenyl) (phenyl)methanol, 7.10.

n-BuLi (16.15 ml, 2.5 M in hexane solution, 40.35 mmol) was added to a stirred solution of 1-dimethylaminonaphthalene (1.50 g, 8.77 mmol) in dry ether (15 ml) under nitrogen at room temperature and left to stir for 5 days during which time a yellow precipitate formed. The solution was carefully removed, and the yellow solid was washed several times with dry ether under nitrogen. The solid was dissolved in dry THF (20 ml), cooled to −78°C and 4-dimethylaminobenzophenone (2.37 g, 10.52 mmol) was added. The mixture was gradually warmed to room temperature and stirred for 16 h, after which it was treated with water (30 ml). The aqueous solution was washed with EtOAc (3 x 30 mL) and the combined organic layers were washed with H_2O (40 mL), brine (40 mL) and dried over $MgSO_4$. The solvent was removed *in vacuo* and the resultant crude material was purified by flash column chromatography (30:70 ethyl acetate/petrol 40-60) to give **7.10** as a white solid (1.51 g, 43%). δH (400 MHz, $CDCl_3$, 24 °C): 11.29 (1H, s, O*H*), 7.80 (1H, dd, J = 5.5, 4.0 Hz, 6'-*H*), 7.75 (1H, dd, J = 8.0, 1.4 Hz, 4'-*H*), 7.42-7.46 (2H, m, 5'-, 7'-*H*), 7.17-7.25 (6H, m, 2''-, 3''-, 4''-, 3'-*H*), 7.05 (2H, d, J = 8.8 Hz, 2-*H*), 6.98 (1H, dd, J = 7.4, 1.4 Hz, 2'-*H*), 6.63 (2H, d, J = 9.0 Hz, 3-*H*), 2.91 (6H, s, 4-N(CH_3)$_2$), 2.27 (3H, s, 8'-N-CH_3), 2.15 (3H, s, 8'-N-CH_3); δC (100 MHz, $CDCl_3$, *24* °C): 150.6 (Ar-C_1), 149.3 (8'-*C*), 149.1 (4-*C*), 144.0, 138.0, 137.3 (Ar-C_3), 131.6 (2'-*C*), 129.8 (Ar-C_1), 129.4 (4'-*C*), 129.3 (6'-*C*), 129.1 (2-*C*), 128.4 & 127.5 (2''-, 3''-*C*), 126.2, 125.1, 124.1, 121.9 (Ar-C_4), 111.7 (3-*C*), 82.9 *C*(Ar)$_3$(OH), 47.1 & 46.6 (8'-N(*C*H$_3$)$_2$), 40.6 (4-N(*C*H$_3$)$_2$);

Preparation of 2-(8'-(dimethylamino)naphthalen-1'-yl)cyclohepta-2,4,6-trien-1-one, 7.17.

n-BuLi (11.1 mL, 1.6 M in hexane solution, 17.75 mmol) was added to a stirred solution of 1-dimethylaminonaphthalene (0.66 g, 3.86 mmol) in dry ether (10 ml) under nitrogen at room temperature and left to stir for 5 days during which time a yellow precipitate formed. The solution was carefully removed, and the yellow solid was washed several times with dry ether under nitrogen. The solid was dissolved in dry THF (10 ml), cooled to −78 °C and tropone (0.45 mL, 4.63 mmol) was added. The mixture was gradually warmed to room temperature and stirred for 16 h, after which it was treated with water (30 ml). The aqueous solution was washed with EtOAc (3 x 30 mL) and the combined organic layers were washed with H_2O (40 mL), brine (40 mL) and dried over $MgSO_4$. The solvent was removed *in vacuo* and the resultant crude material was purified by flash column chromatography (30:70 EtOAc/petrol 40-60) to give **7.17** as a yellow solid (0.13 g, 12%), m.p. 160-163℃. δH (400 MHz, $CDCl_3$, 24 °C): 7.81 (1H, dd, J = 8.2, 0.9 Hz, 4'-*H*), 7.63 (1H, dd, J = 8.2, 0.9 Hz, 5'-*H*), 7.47 (1H, dd, J = 8.2, 6.9 Hz, 3'-*H*), 7.39 (1H, t, J = 7.8 Hz, 6'-*H*), 7.29 (1H, dd, J = 6.9, 1.4 Hz, 2'-*H*), 7.16-7.26 (2H, m, *Tropone*-, 7'-*H*), 6.86-7.09 (3H, m, Tropone-H_3), 6.75 (1H, dd, J = 10.5, 7.8 Hz, Tropone-H_1), 2.47 & 2.07 (6H, s, N(CH_3)$_2$); δC (100 MHz, $CDCl_3$, 24 °C): 185.6 (1-*C*=O), 158.1 (Ar-C_1), 150.1 (8'-*C*), 137.7, 137.5, 135.2, 134.2, 133.8, 130.5 (Ar-C_6), 129.1 (4'-*C*), 128.6 (2'-*C*), 127.8, 127.4, 125.8, 125.7, 125.5 (Ar-C_5), 118.4 (7'-*C*), 47.1 & 40.4 (8'-N(CH_3)$_2$); ν_{max}/cm^{-1} 2857, 2782, 1625, 1567 (C=O), 1507, 1459, 1371, 1258, 1217, 1026, 915, 831, 777, 695; HRMS (ESI): Found: 276.1386 ($M+H^+$), $C_{19}H_{18}NO$ requires: 276.1388 ($M+H^+$).

Preparation of 1,1-Dimethyl-2,7-dihydro-(2,7-hydroxymetheno)-naphtho(1,8-bcd)azecinium tetrafluoroborate, 7.18.

Tropone derivative **7.17** (50 mg, 0.18 mmol) was dissolved in anhydrous dichloromethane (5 mL) and stirred whilst Tetrafluoroboric acid diethyl ether complex (0.12 mL, 0.91 mmol) was added dropwise. After stirring for 24h at room temperature, anhydrous diethyl ether (20 mL) was added generating a precipitate and stirring was continued for another 1h. The precipitate was carefully filtered under a nitrogen flow, washed with further portions of anhydrous diethyl ether (20 mL) and dried *in vacuo* to give **7.18** as a dark brown solid (98 mg, 83%), m.p. 120-123℃. δH (400 MHz, d_6-Acetone, 24 °C): 8.95 (1H, d, J = 7.8 Hz, 8-*H*), 8.25 (1H, d, J = 7.8 Hz, 13-*H*), 8.17 (1H, d, J = 8.5 Hz, 11-*H*), 7.96 (1H, d, J = 8.2 Hz, 10-*H*), 7.77 (1H, t, J = 7.8 Hz, 12-*H*), 7.70 (1H, t, J = 7.8 Hz, 9-*H*), 7.10 (1H, d, J = 11.4 Hz, 6-*H*), 7.00 (1H, dd, J = 11.7, 5.3 Hz, 5-*H*), 6.36 (1H, dd, J = 9.6, 5.5 Hz, 4-*H*), 6.05 (1H, app t, J = 7.3 Hz, 3-*H*), 4.12 (3H, s, 1-N(CH_3)$_2$), 3.96 (1H, d, J = 6.6 Hz, 2-*H*), 3.65 (3H, s, 1-N(CH_3)$_2$); δC (100 MHz, d_6-Acetone, *24* °C): 150.9 (14-*C*), 136.7 (13a-*C*), 134.3 (10a-*C*), 134.0 (5-*C*), 131.5 (11-*C*), 129.1 (6-*C*), 128.3 (9-*C*), 126.9 (10-*C*), 126.5 (8-*C*), 125.8 (12-*C*), 125.1 (4-*C*), 124.3 (7a-*C*), 122.9 (3-*C*), 120.1 (7a'-*C*), 118.6 (13-*C*), 99.9 (14-*C*), 72.2 (2-*C*), 58.5 & 49.9 (1-N+(*C*H_3)$_2$); δF (376 MHz, d_6-Acetone, 24 °C): -149.83 ($^-BF_4$); ν_{max}/cm^{-1} 3539, 3240, 3054, 1627, 1470, 1444, 1356, 1330, 1276, 1019 (br B-F), 957, 829, 764.

Preparation of (6-(dimethylamino)-1,2-dihydroacenaphthylen-5-yl)diphenylmethanol, 7.30.

Bromo amine[8] (0.5 g, 1.81 mmol) was dissolved in anhydrous THF (15 mL) under nitrogen and cooled to -78℃. *n*-BuLi (1.7 mL, 1.6M in hexanes, 2.72 mmol) was steadily added, and the deep red solution was stirred at -78℃ for 3h. Benzophenone (0.66 g, 3.62 mmol) was added and the reaction was allowed to warm to room temperature. After 16 h. the reaction was quenched with H_2O (10 mL) and stirred for 10min. The aqueous solution was washed with EtOAc (3 x 30 mL) and the combined organic layers were washed with H_2O (40 mL), brine (40 mL) and dried over $MgSO_4$. The solvent was removed *in vacuo* to give a crude deep orange oil which was purified by flash column chromatography (15:85 EtOAc/petrol 40-60), to give **7.30** as a brown solid (0.44 g, 64%), m.p. 193-196℃. δH (400 MHz, $CDCl_3$, 24 °C): 11.41 (1H, s, O*H*), 7.42 (1H, d, J = 7.3 Hz, 7-*H*), 7.28 (1H, d, J = 7.6 Hz, 8-*H*), 7.15-7.27 (10H, m, Ph-*H*$_{10}$), 7.02 (1H, d, J = 7.4 Hz, 3-*H*), 6.80 (1H, d, J = 7.4 Hz, *4*-*H*), 3.36 (4H, m, 1-, 2-*H*), 2.20 (6H, s, N(C*H*$_3$)$_2$); δC (100 MHz, $CDCl_3$, *24* °C): 150.1, 146.4, 146.2 (Ar-*C*$_3$), 145.7 (6-*C*), 142.4, 140.4 (Ar-*C*$_2$), 132.5 (4-*C*), 128.7, 127.7 (Ar-*C*$_2$), 126.6 (*Para*-*C*), 123.8 (7-*C*), 119.8 (8-*C*), 118.2 (3-*C*), 82.7 (*C*(Ph)$_2$(OH)), 46.9 (N(C*H*$_3$)$_2$), 30.0 & 29.8 (1-, 2-*C*); ν_{max}/cm^{-1} 2920, 2901, 2632, 1615, 1483, 1444, 1425, 1323, 1176, 1125, 1041, 967, 848, 762, 698; HRMS (ESI): Found: 380.2016 (M+H$^+$) 362.1923 (M-OH), $C_{27}H_{25}NO$ requires: 380.2014 (M+H$^+$), 362.1909 (M–OH).

Preparation of 6-benzhydryl-N-methyl-N-methylene-1,2-dihydroacenaphthylen-5-aminium tetrafluoroborate, 7.31.

Acenaphthene diphenyl alcohol **7.30** (100 mg, 0.81 mmol) was dissolved in dichloromethane (5 mL) and stirred whilst Tetrafluoroboric acid diethyl ether complex (0.30 mL, 4.04 mmol) was added dropwise. After stirring for 1h at room temperature, stirring was ceased and diethyl ether (20 mL) was slowly added generating a bilayer, the bilayers were combined gradually generating a precipitate and stirring was continued for another 16h. The precipitate was filtered, washed with further portions of diethyl ether (20 mL) and dried *in vacuo* to give **7.31** as a green solid (100 mg, 84%), m.p. 177-180℃. δH (400 MHz, $CDCl_3$, 24 °C): 8.15 (1H, d, J = 6.9 Hz, N^+CH_2), 7.69 (1H, d, J = 7.3 Hz, Ar-*H1*), 7.23-7.41 (7H, m, Ar-*H7*), 7.16 (1H, d, J = 7.3 Hz, Ar-*H1*), 7.05 (1H, d, J = 7.8 Hz, Ar-*H1*), 7.05 (2H, d, J = 6.9 Hz, Ar-*H2*), 6.90 (2H, d, J = 6.9 Hz, Ar-*H2*), 6.42 (1H, d, J = 6.9 Hz, N^+CH_2), 5.68 (1H, s, C*H*), 4.34 (3H, s, N(+)CH_3), 3.46 (4H, m, 1-, 2-*H*); δC (100 MHz, $CDCl_3$, *24* °C): 172.1 (CH_2), 151.9, 146.9, 146.8, 144.4, 142.7, 142.0, 141.6, 141.3, 135.0, 134.1, 132.1, 130.2, 130.0, 129.9, 129.5, 128.9, 128.6, 128.3, 127.9, 127.2, 125.3, 122.4, 121.3, 119.9 (Ar-C_{24}), 54.0 (*C*H), 53.5 (N(+)*C*H_3), 30.5 & 30.1 (1-, 2-*C*); δF (376 MHz, $CDCl_3$, 24 °C): -150.90 ($^-BF_4$); ν_{max}/cm^{-1} 3024, 1606, 1492, 1466, 1448, 1045, 1030 (br B-F), 846, 758, 736, 702; HRMS (ESI): Found: 362.1906 (M^+), $C_{27}H_{24}N^+$ requires: 362.1909 (M^+).

Crystal Data

*Table 7.49. Crystallographic data for the ortho phenyl **7.5a**, dimethylammonium alcohol salts **7.19** and **7.20**, dehydrated dimethylammonium salts **7.24** and **7.25**, dibenzosuberol **7.8**, dimethylammonium ringed system **7.28**, tropone **7.17** and the acenaphthene dimethylamminium salt **7.31**.*

	7.5a	**7.19**	**7.20**	**7.24**	**7.25**	**7.8**	**7.28**	**7.17**	**7.31**
Formula	$C_{20}H_{21}NO_2$	$C_{25}H_{24}NO.Cl$	$C_{25}H_{24}NO.BF_4.CH_2Cl_2$	$C_{25}H_{22}N.BF_4$	$C_{27}H_{26}NO_2.BF_4$	$C_{27}H_{25}NO$	$C_{27}H_{24}N.BF_4$	$C_{19}H_{17}NO$	$C_{27}H_{24}N.BF_4$
Formula weight	307.38	389.90	526.19	423.24	483.30	379.48	449.28	275.33	449.28
Crystal system	Monoclinic	Monoclinic	Triclinic	Orthorhombic	Triclinic	Monoclinic	Monoclinic	Monoclinic	Triclinic
Space group	$P2_1/n$	$P2_1/n$	P-1	$Pbca$	P-1	$P2_1/n$	$P2_1/n$	$P2_1/n$	P-1
***a*[Å]**	7.9050(5)	11.6622(3)	12.1224(4)	16.6385(6)	9.3788(3)	8.2571(2)	8.2075(3)	7.0423(2)	11.6577(5)
***b*[Å]**	28.0033(17)	12.6184(4)	13.1959(5)	13.1233(4)	11.1291(4)	15.8381(3)	12.3404(4)	15.4445(4)	18.4867(7)
***c*[Å]**	7.9355(6)	14.1387(4)	16.3995(7)	18.4248(6)	12.0845(4)	15.1192(4)	20.9528(6)	13.2297(3)	22.8840(10)
***α*[°]**	90	90	87.849(3)	90	107.690(3)	90	90	90	67.937(4)
β [°]	110.179(8)	91.927(3)	89.903(3)	90	103.244(3)	97.836(2)	94.948(3)	92.962(2)	87.518(4)
***γ*[°]**	90	90	70.736(3)	90	91.680(3)	90	90	90	84.831(3)
***V* [Å^3]**	1648.8(2)	2079.45(10)	2474.57(17)	4023.1(2)	1163.07(7)	1958.78(8)	2114.27(12)	1437.00(6)	4551.8(3)
Z	4	4	4	8	2	4	4	4	8
***ρ* [g cm^{-3}]**	1.238	1.245	1.412	1.398	1.380	1.287	1.411	1.273	1.311
***T* [*K*]**	150.00(10)	150.01(10)	150.01(10)	100.02(10)	100.01(10)	150.01(10)	100.01(10)	150.01(10)	150.00(10)
***λ* (Å)**	0.71073	0.71073	0.71073	0.71073	1.54184	0.71073	0.71073	1.54184	1.54184
***μ* (mm^{-1})**	0.080	0.199	0.313	0.106	0.904	0.077	0.106	0.611	0.817
unique refl.	3433	10499	25101	13588	17748	23822	30012	7164	39928
Refl, I > 2σI	2749	4761	11320	4706	4524	4850	5245	2814	15853
***R*$_1$**	0.0483	0.0426	0.0604	0.0512	0.0388	0.0484	0.0463	0.0406	0.1034
***wR*$_2$**	0.1213	0.0884	0.1443	0.1073	0.1028	0.1022	0.1082	0.1023	0.3147
***Δρ*(r) [e Å^{-3}]**	0.17/-0.18	0.34/-0.25	0.91/-0.95	0.51/-0.42	0.47/-0.30	0.24/-0.28	0.46/-0.45	0.21/-0.22	2.05/-0.62
Crystallisation Solvent	CH_2Cl_2	CH_2Cl_2	CH_2Cl_2	CH_3CN/CH_2Cl_2	CH_2Cl_2/*n*-hexane	CH_2Cl_2/*n*-hexane	CH_2Cl_2/*n*-hexane	CH_2Cl_2	CH_2Cl_2/*n*-hexane

References

1 G. Dyker, M. Hagel, G. Henkel and M. Köckerling, *European J. Org. Chem.*, 2008, 3095–3101.

2 G. Dyker, M. Hagel, G. Henkel, M. Köckerling, C. Näther, S. Petersen and G. P. Schiemenz, *Naturforsch. J. Chem. Sci.*, 2001, **56**, 1109–1116.

3 K. Morimoto and Y. Murakami, *Appl. Opt.*, 1969, **8**, 50–54.

4 J. Betz, F. Hampel and W. Bauer, *J. Chem. Soc.*, 2001, 1876–1879.

5 A. Lari, M. B. Pitak, S. J. Coles, G. J. Rees, S. P. Day, M. E. Smith, J. V. Hanna and J. D. Wallis, *Org. Biomol. Chem.*, 2012, **10**, 7763–7779.

6 N. Mercadal, S. P. Day, A. Jarmyn, M. B. Pitak, S. J. Coles, C. Wilson, G. J. Rees, J. V. Hanna and J. D. Wallis, *CrystEngComm*, 2014, **16**, 8363–8374.

7 H. Bock and N. Nagel, *Naturforsch. B.*, 1998, 792–804.

8 D. Pla, O. Sadek, S. Cadet, B. Mestre-Voegtlé and E. Gras, *Dalton Trans.*, 2015, **44**, 18340–18346.

Chapter 8

Conclusions and Future Work

Conclusion and Future Work

A primary focus of the work carried out in this thesis aimed to 'study new systems based on *peri*-naphthalene to gain structural information on systems with Me_2N---C contacts in the range of 1.65-2.41 Å, in particular by installing substituents at the opposite, unsubstituted second set of *peri*-positions.' The work summarised in chapters 3-5 successfully addressed this target.

Firstly, in chapter 3, the effect of substituting the naphthalene skeleton for that of acenaphthene, thus positioning a short ethylene bridge opposite to the Me_2N---C *peri*-contact was demonstrated. The effects of this short bridge in some structural models demonstrated the expected result, whereby the distance between the two interacting opposite *peri*-substituents was increased compared to the respective naphthalene derivatives. However, beyond a certain separation distance and in the presence of a more electrophilic *peri*-alkene, the increased rotational freedom of the groups allowed for a type 2 *tert*-amino effect reaction. This reaction led to the synthesis of several multi-ringed azepines. A similar trend was also observed with a range of 4, 5-disubstitiuted fluorene derivatives (a bridged biphenyl). Extension of this work, to explore alternative bridging systems was attempted briefly but was not successful and remains an area open to future research.

The work of chapter 4 investigated the opposite of that in chapter 3, whereby a *peri*-repulsion was generated between groups at the opposite *peri*-positions. In all cases, the repulsion led to a reduction in the N---C distance, resulting in a short contact of 2.359(2) Å in the ethenedinitrile derivative **4.16** and the formation of a long N-C bond of 1.672(1) Å when one nitrile was replaced by an ester group in **4.18**. Modification of the two groups involved in the *peri*-repulsion remains unexplored, with the potential to functionalise the phenyl rings available or alter the groups entirely, for example two bulky alkyl groups.

Chapter 5 introduced a symmetrical naphthalene system with the same set of N---C(alkene) *peri*-interactions at both positions. Generally, the N---C distances increased throughout the series compared to the corresponding systems with just one set of interactions and no second set of *peri* groups. When the alkene terminated in a cyclic diester in **5.23,** a long N-C bond (1.676(4) Å) formed at one *peri* site and a N---C contact of 2.615(4) Å remained at the other. Further systems, in which one electrophile group was omitted, led to salts demonstrating a *peri* Me_2N^+H---H repulsion, and generating compounds with N-C bonds in the range of 1.7-2.1 Å. Of particular importance is the ethenedintrile derivative **5.36**, which undergoes a reversible structural change in the solid-state under cooling, which was carefully mapped by extensive X-ray diffraction. As well as this, preliminary charge density X-ray crystallography and solid-state NMR have been performed. The body of work thus far on this extraordinary system has allowed for a greater insight into the long N-C bond, however additional studies could develop this further. These could take place in the form of variable temperature infrared spectroscopy, whereby the relevant stretching frequencies of the bonds of interest could be followed over a temperature range. Furthermore, the effect of pressure on the crystal lattice during collection could be explored, to see if this would adjust the Me_2N---C separation. An accurate survey of the charge density between the two groups is in progress and should be coupled to calculations of the lattice energy. Further solid-state NMR studies with compounds where both peri atoms are isotopically labelled (^{15}N, ^{13}C) would be interesting to see at what separation magnetic coupling can be observed between the two nuclei. Furthermore, Schiemenz's suggestion that the $^{1}H/^{13}C$ coupling in the N-methyl groups might be correlated with degree of bond formation could also be investigated. With regards to all the compounds in the series, simple modifications to the existing structural models, for example; generating a range of alternate salts (tetrafluoroborate, bromide or fluoride) or alteration of the nucleophile (diethylamino or aziridino) could be explored.

In addition to studying new systems based on *peri*-naphthalene, a significant amount of work was performed in the modification of either the nucleophilic or electrophilic centres. In chapter 2, a hydroxyl group was employed as the nucleophilic moiety, focusing on the more nucleophilic oxyanion form. This resulted in the first *peri*-interactions between naphtholate oxyanions and electrophilic double bonds in the form of tetramethylguanidine crystalline salts with O---C contacts in the range: 2.558(2)–2.618(2) Å. The next step for this work would be to reduce one of the naphthalene's rings, so that the oxyanion was attached to a sp^3 centre, and thus be more nucleophilic, though the alignment of the anion and the electrophile would depend on the conformation of the fused cyclohexane ring. The work of chapter 7 investigated structures where a dimethylamino group reacted with a range of stabilised carbocation centres across the *peri*-positions on naphthalene to form long N-C bonds (1.653(2)-1.673(2) Å). In some cases, interesting and unexpected fused multi-ringed systems were produced.

Finally, utilising the information obtained in chapters 2-4 a structural investigation was performed with four structures which demonstrate the Felkin-Anh model for nucleophilic attack of a carbon centre adjacent to a chiral centre (-CH(Ph)Me), showing both the expected conformation of the two groups involved in the reaction, and also showing a small increase in the pyramidality of the attacked carbon with increasing nucleophilicity of the attacking species.

The data produced in this thesis, along with published material, allowed the construction of a correlation between the formation of a N-C bond with the breaking of an alkene in the Michael reaction between a dimethylamino group and a $CH=C(CN)_2$ group. This provides an important comparison to calculation. No attempt to search for alternative polymorphs or solvates of the compounds made. However, for those compounds where the interactions were in the range 1.6-2.3 Å, should be subjected to a range of studies of crystallisations at higher temperatures and in different solvents, since often new crystalline forms can be found, and are likely to have

slightly different Me_2N---C distances than the original polymorph, and thus provide further data to study the correlation between bond forming and breaking.